MITOCHONDRIAL METABOLISM IN ISCHEMIC HEART DISEASE

EDITED BY: Shijun Wang, Jian Wu, Lei-Lei Ma, Yang Li and Haiyang Tang

PUBLISHED IN: Frontiers in Cardiovascular Medicine

frontiers Research Topics

Frontiers eBook Copyright Statement

The copyright in the text of individual articles in this eBook is the property of their respective authors or their respective institutions or funders. The copyright in graphics and images within each article may be subject to copyright of other parties. In both cases this is subject to a license granted to Frontiers.

The compilation of articles constituting this eBook is the property of Frontiers.

Each article within this eBook, and the eBook itself, are published under the most recent version of the Creative Commons CC-BY licence. The version current at the date of publication of this eBook is CC-BY 4.0. If the CC-BY licence is updated, the licence granted by Frontiers is automatically updated to the new version.

When exercising any right under the CC-BY licence, Frontiers must be attributed as the original publisher of the article or eBook, as applicable.

Authors have the responsibility of ensuring that any graphics or other materials which are the property of others may be included in the CC-BY licence, but this should be checked before relying on the CC-BY licence to reproduce those materials. Any copyright notices relating to those materials must be complied with.

Copyright and source acknowledgement notices may not be removed and must be displayed in any copy, derivative work or partial copy which includes the elements in question.

All copyright, and all rights therein, are protected by national and international copyright laws. The above represents a summary only. For further information please read Frontiers' Conditions for Website Use and Copyright Statement, and the applicable CC-BY licence.

ISSN 1664-8714
ISBN 978-2-88976-620-8
DOI 10.3389/978-2-88976-620-8

About Frontiers

Frontiers is more than just an open-access publisher of scholarly articles: it is a pioneering approach to the world of academia, radically improving the way scholarly research is managed. The grand vision of Frontiers is a world where all people have an equal opportunity to seek, share and generate knowledge. Frontiers provides immediate and permanent online open access to all its publications, but this alone is not enough to realize our grand goals.

Frontiers Journal Series

The Frontiers Journal Series is a multi-tier and interdisciplinary set of open-access, online journals, promising a paradigm shift from the current review, selection and dissemination processes in academic publishing. All Frontiers journals are driven by researchers for researchers; therefore, they constitute a service to the scholarly community. At the same time, the Frontiers Journal Series operates on a revolutionary invention, the tiered publishing system, initially addressing specific communities of scholars, and gradually climbing up to broader public understanding, thus serving the interests of the lay society, too.

Dedication to Quality

Each Frontiers article is a landmark of the highest quality, thanks to genuinely collaborative interactions between authors and review editors, who include some of the world's best academicians. Research must be certified by peers before entering a stream of knowledge that may eventually reach the public - and shape society; therefore, Frontiers only applies the most rigorous and unbiased reviews.
Frontiers revolutionizes research publishing by freely delivering the most outstanding research, evaluated with no bias from both the academic and social point of view. By applying the most advanced information technologies, Frontiers is catapulting scholarly publishing into a new generation.

What are Frontiers Research Topics?

Frontiers Research Topics are very popular trademarks of the Frontiers Journals Series: they are collections of at least ten articles, all centered on a particular subject. With their unique mix of varied contributions from Original Research to Review Articles, Frontiers Research Topics unify the most influential researchers, the latest key findings and historical advances in a hot research area! Find out more on how to host your own Frontiers Research Topic or contribute to one as an author by contacting the Frontiers Editorial Office: frontiersin.org/about/contact

MITOCHONDRIAL METABOLISM IN ISCHEMIC HEART DISEASE

Topic Editors:
Shijun Wang, Fudan University, China
Jian Wu, Fudan University, China
Lei-Lei Ma, Fudan University, China
Yang Li, Stanford University, United States
Haiyang Tang, University of Arizona, United States

Citation: Wang, S., Wu, J., Ma, L.-L., Li, Y., Tang, H., eds. (2022). Mitochondrial Metabolism in Ischemic Heart Disease. Lausanne: Frontiers Media SA.
doi: 10.3389/978-2-88976-620-8

Table of Contents

05 ***Editorial: Mitochondrial Metabolism in Ischemic Heart Disease***
Lei Yang, Shijun Wang, Jian Wu, Lei-Lei Ma, Yang Li and Haiyang Tang

08 ***Endothelial GABBR2 Regulates Post-ischemic Angiogenesis by Inhibiting the Glycolysis Pathway***
Hongze Zhang, Hong Zhou, Jianying Yuan, Yong Nan and Jingquan Liu

17 ***Advances in Cardiotoxicity Induced by Altered Mitochondrial Dynamics and Mitophagy***
Yiyuan Yin and Haitao Shen

31 ***Role of the Mitochondrial Protein Import Machinery and Protein Processing in Heart Disease***
Fujie Zhao and Ming-Hui Zou

52 ***Association of Lectin-Like Oxidized Low-Density Lipoprotein Receptor-1 With Angiotensin II Type 1 Receptor Impacts Mitochondrial Quality Control, Offering Promise for the Treatment of Vascular Senescence***
Yoshihiro Uchikado, Yoshiyuki Ikeda, Yuichi Sasaki, Masaaki Iwabayashi, Yuichi Akasaki and Mitsuru Ohishi

72 ***New Insights Into the Role of Mitochondria Quality Control in Ischemic Heart Disease***
Yanguo Xin, Xiaodong Zhang, Jingye Li, Hui Gao, Jiayu Li, Junli Li, Wenyu Hu and Hongwei Li

88 ***Ketone Body Metabolism in the Ischemic Heart***
Stephen C. Kolwicz Jr

99 ***Mitochondrial Metabolism in Myocardial Remodeling and Mechanical Unloading: Implications for Ischemic Heart Disease***
Min Jiang, Xiaoye Xie, Feng Cao and Yabin Wang

116 ***Cardioprotective Effects of n-3 Polyunsaturated Fatty Acids: Orchestration of mRNA Expression, Protein Phosphorylation, and Lipid Metabolism in Pressure Overload Hearts***
Xiang Li, Weijiang Tan, Shuang Zheng, Junjie Zhang, Caiyi Zhu, Chun Cai, Honghua Chen, Chenqi Yang, Le Kang, Zhanhong Pan, W. Glen Pyle, Peter H. Backx, Yunzeng Zou and Feng Hua Yang

133 ***Regulation of Mitochondrial Dynamics by Aerobic Exercise in Cardiovascular Diseases***
Changping Gu, Jie Yan, Liang Zhao, Guanghan Wu and Yue-lan Wang

140 ***Mitochondria in Pathological Cardiac Hypertrophy Research and Therapy***
Dan Yang, Han-Qing Liu, Fang-Yuan Liu, Zhen Guo, Peng An, Ming-Yu Wang, Zheng Yang, Di Fan and Qi-Zhu Tang

152 ***Mitochondrial DNA Depletion Syndrome and Its Associated Cardiac Disease***
Haiying Wang, Yijun Han, Shenwei Li, Yunan Chen, Yafen Chen, Jing Wang, Yuqing Zhang, Yawen Zhang, Jingsuo Wang, Yong Xia and Jinxiang Yuan

168 ***Programmed Exercise Attenuates Familial Hypertrophic Cardiomyopathy in Transgenic E22K Mice* via *Inhibition of PKC-α/NFAT Pathway***
Haiying Wang, Yuedong Lin, Ran Zhang, Yafen Chen, Wei Ji, Shenwei Li, Li Wang, Rubin Tan and Jinxiang Yuan

180 ***Exercise-Generated β-Aminoisobutyric Acid (BAIBA) Reduces Cardiomyocyte Metabolic Stress and Apoptosis Caused by Mitochondrial Dysfunction Through the miR-208b/AMPK Pathway***
Yanan Yu, Wewei Chen, Ming Yu, Jinsha Liu, Huan Sun and Ping Yang

196 ***Dioscin Alleviates Cardiac Dysfunction in Acute Myocardial Infarction* via *Rescuing Mitochondrial Malfunction***
Tianyu Shen, Dayin Lyu, Mengping Zhang, Hui Shang and Qiulun Lu

204 ***Melatonin Engineered Adipose-Derived Biomimetic Nanovesicles Regulate Mitochondrial Functions and Promote Myocardial Repair in Myocardial Infarction***
Yang Zhang, Ning Yang, Xu Huang, Yan Zhu, Shan Gao, Zhongyang Liu, Feng Cao and Yabin Wang

215 ***Profilin 2 and Endothelial Exosomal Profilin 2 Promote Angiogenesis and Myocardial Infarction Repair in Mice***
Zhenkun Li, Xueyun Huo, Keyan Chen, Fenghua Yang, Weijiang Tan, Qi Zhang, Haixu Yu, Changlong Li, Deshan Zhou, Hao Chen, Baoquan Zhao, Yuan Wang, Zhenwen Chen and Xiaoyan Du

230 ***NEU1 Regulates Mitochondrial Energy Metabolism and Oxidative Stress Post-myocardial Infarction in Mice* via *the SIRT1/PGC-1 Alpha Axis***
Zhen Guo, Di Fan, Fang-Yuan Liu, Shu-Qing Ma, Peng An, Dan Yang, Min-Yu Wang, Zheng Yang and Qi-Zhu Tang

frontiers | Frontiers in Cardiovascular Medicine

EDITORIAL
published: 27 June 2022
doi: 10.3389/fcvm.2022.961580

Editorial: Mitochondrial Metabolism in Ischemic Heart Disease

Lei Yang[1], *Shijun Wang*[2], *Jian Wu*[2], *Lei-Lei Ma*[3], *Yang Li*[4] *and Haiyang Tang*[5,6]*

[1] College of Veterinary Medicine, Northwest A&F University, Xianyang, China, [2] Shanghai Institute of Cardiovascular Diseases, Zhongshan Hospital and Institutes of Biomedical Sciences, Fudan University, Shanghai, China, [3] Department of Cardiology, Zhongshan Hospital, Fudan University, Shanghai, China, [4] Department of Ophthalmology, Stanford University, Palo Alto, CA, United States, [5] State Key Laboratory of Respiratory Disease, National Clinical Research Center for Respiratory Disease, Guangzhou, China, [6] Guangdong Key Laboratory of Vascular Disease, Guangzhou Institute of Respiratory Health, The First Affiliated Hospital of Guangzhou Medical University, Guangzhou, China

Keywords: mitochondria, heart failure, oxidative stress, cell metabolism, ischemia—reperfusion

OPEN ACCESS

Edited and reviewed by:
Ichiro Manabe,
Chiba University, Japan

***Correspondence:**
Haiyang Tang
tanghy2008@yahoo.com

Specialty section:
This article was submitted to Cardiovascular Metabolism, a section of the journal Frontiers in Cardiovascular Medicine

Received: *04 June 2022*
Accepted: *07 June 2022*
Published: *27 June 2022*

Citation:
Yang L, Wang S, Wu J, Ma L-L, Li Y and Tang H (2022) Editorial: Mitochondrial Metabolism in Ischemic Heart Disease. Front. Cardiovasc. Med. 9:961580. doi: 10.3389/fcvm.2022.961580

Editorial on the Research Topic

Mitochondrial Metabolism in Ischemic Heart Disease

Ischemic heart disease (IHD) is the single greatest cause of mortality worldwide and the most common underlying cause of heart failure (HF) (1). The major causes of IHD include atherosclerosis-related narrowing or obstruction of the vascular lumen, myocardial ischemia, and hypoxia/necrosis caused by coronary artery spasm. Despite existing treatments and interventions such as drug therapy, left ventricular assist device, artificial heart, and heart transplantation, the progression of HF caused by IHD is essentially irreversible (2, 3). Underlying the pathogenic mechanisms of IHD lacks comprehensively understanding and the investigations on the novel targets and signaling pathways involved in the development and progression of IHD are urgently needed.

Mitochondria are critical in the energy production of cardiomyocytes, generating 90% of adenosine triphosphate (ATP) for cardiac energy support. Moreover, mitochondria are the main sites for generating oxidative phosphorylation (OXPHOS), which is the primary energy source for maintaining normal heart contractile function (4). Mitochondria are not only the power plants of the cardiomyocytes, but also is the centers of signal transmission (5, 6), and they are closely connected with cell activities such as apoptosis (7), reactive oxygen species (ROS) generation (8), and lipid metabolism (9). Nevertheless, how aberrant regulation of mitochondria functions as an antecedent indicator of IHD and its restoration by pharmaceutical or non-pharmaceutical intervention is yet to elucidate.

Recent reports including the studies under this Research Topic have borne out claims that mitochondrial dysfunction is highly associated with IHD. Contributing factors to mitochondrial disorder in IHD include mitophagy disorder, ROS exacerbation and mitochondria-related inflammation. Xin et al. reported that mitochondria are important organelles involved in energy production of cardiomyocytes, mitochondrial disorder results in the pathogenesis of IHD.

Oxidative stress, caused by excessive ROS, is a crucial pathophysiological mechanism of myocardial infarction (MI), through impairment of cell function and vitality. ROS are byproducts of the mitochondrial synthesis of ATP. When mitochondrial function declines, more ROS are produced, resulting in the development of MI (10). Shen et al. found that dioscin, a natural product, alleviated cardiac dysfunction and remodeling post-MI by maintaining the Kreb's cycle and restraining mitochondrial ROS accumulation to improve mitochondrial quality control. Hence, restoring mitochondrial function may be an effective therapeutic strategy for IHD. Zhang et al. constructed novel biomimetic adipose-derived stem cells (ADSC)-derived nanovesicles

(ADSC NVs) and consisted engineered ADSC NVs with melatonin (Mel) to form a novel Mel@NVs delivery system. The Mel@NVs alleviated mitochondrial dysfunction and promoted myocardial repair by ameliorating excessive ROS generation, promoting microvascular formation, and attenuating cardiac fibrosis. Therefore, targeting anti-ROS production would be a new therapeutic strategy for IHD.

Mitophagy is a kind of autophagy that removes damaged or dysfunctional mitochondria to prevent excessive accumulation of ROS. Mitochondria maintain the stability of mitochondrial dynamics through mitophagy, which is the basis of maintaining mitochondrial homeostasis and ensuring mitochondrial function. Proper functioning of this machinery is essential for maintaining a healthy cardiovascular system (11, 12). Uchikado et al. indicated oxidized low-density lipoprotein (ox-LDL) induces mitochondrial fission, leading to mitochondrial dysfunction and senescence through the association of lectin-like oxidized low-density lipoprotein scavenger receptor-1 (LOX-1) and angiotensin II type 1 receptor (AT1R), which activates the CRAF/MEK/ERK pathway. Furthermore, AT1R inhibition suppresses dynamin-related protein 1 (Drp1) activation and induces Rab9-dependent alternative autophagy through the CRAF/MEK/ERK axis in human vascular smooth muscle cells (VSMCs). Inhibition of AT1R also ameliorates cellular senescence by regulating mitochondrial dynamics, which may provide new ideas for the treatment of IHD.

As the second most energy-consuming organ of the body, the heart needs cardiomyocytes to produce a large amount of ATP to maintain normal functions, and most of the energy generated by cardiomyocytes comes from mitochondrial metabolism. In IHD, insufficient oxygen supply and mitochondrial dysfunction lead to reduced ATP production, making glycolysis as a more prominent source of energy (13). In this Research Topic collection, Jiang et al. summarized the role of abnormal mitochondrial metabolism in IHD progression and the current understanding of shutting down mechanotransduction to improve mitochondrial dysfunction and HF. Although increasing numbers of mechanical circulatory support (MCS) devices have been applied in clinical practice to alter myocardial energy metabolism, more research is

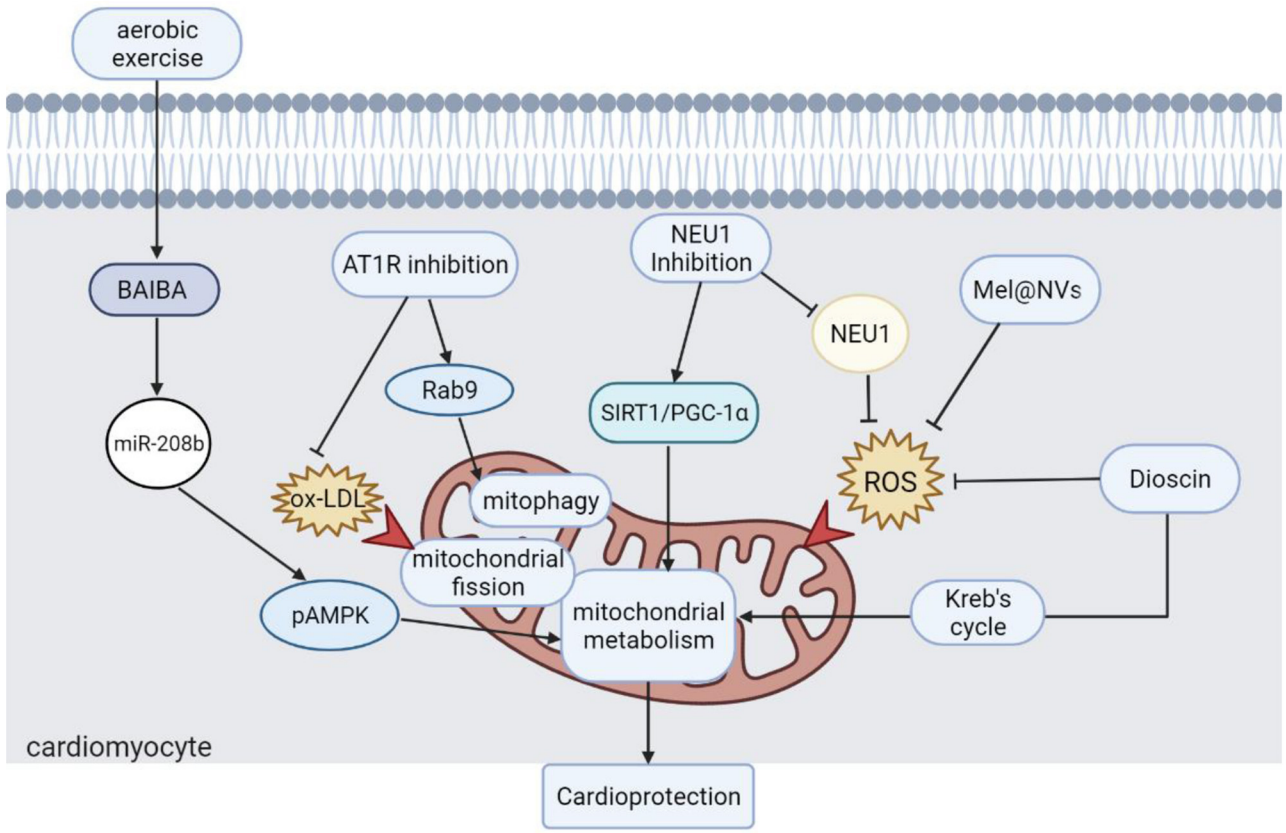

FIGURE 1 | Strategies for mitochondria-targeted IHD therapy. Moderate aerobic exercise is an effective strategy to protect heart function. Different approaches to restore mitochondrial dynamics, autophagy, and metabolism are effective strategies for the treatment of IHD. Scavenging ROS accumulation is also one of the ways to restore mitochondrial function, which also plays a positive role in the recovery of cardiac function. BAIBA, β-Aminoisobutyric Acid; pAMPK, AMPK phosphorylation; AT1R, angiotensin II type 1 receptor; ox-LDL, oxidized low-density lipoprotein; Drp1, dynamin-related protein 1; NEU1, neuraminidase 1; SIRT1, sirtuin-1; PGC-1α, peroxisome proliferator-activated receptor γ coactivator α; Mel@NVs, melatonin engineered NVs; ROS: reactive oxygen species.

needed to clarify its benefits on cardiac function and long-term prognosis. Guo et al. also found that cardiomyocyte-specific Neuraminidase1 (NEU1) deficiency alleviated MI-induced myocardial remodeling, oxidative stress, and mitochondrial metabolism disorder by regulating the sirtuin-1/peroxisome proliferator-activated receptor γ coactivator α (SIRT1/PGC-1α) signaling pathway. Cardiomyocyte-specific NEU1 inhibition provides a new direction for treatment after MI. Inhibitors of NEU1 may be a novel treatment option for IHD by ameliorating mitochondrial metabolism.

Moderate aerobic exercise is known to have a beneficial effect on cardiac function in HF (14). Cardiometabolic disorders in patients with HF can be partially recovered through exercise because of improved mitochondrial quality control, bioenergetics and cardiac function (15). Gu et al. in Research Topic, discussed the mechanism of aerobic exercise in maintaining normal mitochondrial function and improving cardiovascular disease. Mitofusin 2 (MFN2) and optic atrophy 1 (OPA1), which are beneficial to mitochondrial fusion and biogenesis, can be elevated by aerobic exercise. Drp1-induced mitochondrial fission can be inhibited by aerobic exercise in cardiovascular diseases. Regular aerobic exercise can reduce mitochondrial fission, enhance mitochondrial fusion, and improve mitochondrial autophagy or biogenesis, thus benefiting human health. Moreover, Yu et al. found exercise-generated β-Aminoisobutyric Acid (BAIBA) effectively improved both cardiac function and energy metabolism and reduced apoptosis in rats with HF after MI. BAIBA increased AMP-activated protein kinase (AMPK) phosphorylation through the expression of miR-208b and reduced apoptosis in H_2O_2-induced H_9C_2 cells, reshaping the energy metabolism of rats with HF and improving mitochondrial dysfunction. BAIBA has potential as an alternative to exercise therapy or synergistically with exercise therapy in the treatment of IHD.

In conclusion, this Research Topic discusses the role of mitochondria in the process of IHD and provides some strategies for mitochondria- targeted IHD therapy (**Figure 1**). Restoration of mitochondrial dynamics and metabolism is effective in alleviating experimental MI and HF, and further clinical trials are needed to confirm these strategies. Natural or artificial compounds that ameliorate excess ROS could reduce mitochondrial dysfunction and alleviate cardiac dysfunction, which may provide a novel treatment for IHD in the future. In addition, moderate aerobic exercise shows promise in restoring heart function in IHD, and maintaining regular exercise is also an effective strategy for preventing IHD.

AUTHOR CONTRIBUTIONS

LY draft the manuscript with input from SW, JW, L-LM, YL, and HT. All authors contributed to the article and approved the submitted version.

FUNDING

This work was supported in parts by National Key Research and Development Program of China (2019YFE0119400) and Natural Science Foundation of China (81970052 and 82170057).

REFERENCES

1. Nowbar AN, Gitto M, Howard JP, Francis DP, Al-Lamee R. Mortality from ischemic heart disease. *Circ Cardiovasc Qual Outcomes.* (2019) 12:e005375. doi: 10.1161/CIRCOUTCOMES.118.005375
2. Braunwald E. The war against heart failure: the Lancet lecture. *Lancet.* (2015) 385:812–24. doi: 10.1016/S0140-6736(14)61889-4
3. Owens AT, Brozena SC, Jessup M. New management strategies in heart failure. *Circ Res.* (2016) 118:480–95. doi: 10.1161/CIRCRESAHA.115.306567
4. Neubauer S. The failing heart–an engine out of fuel. *N Engl J Med.* (2007) 356:1140–51. doi: 10.1056/NEJMra063052
5. Kuang S, Sun L, Zhang X, Liao X, Rees TW, Zeng L, et al. A mitochondrion-localized two-photon photosensitizer generating carbon radicals against hypoxic tumors. *Angew Chem Int Ed Engl.* (2020) 59:20697–703. doi: 10.1002/anie.202009888
6. Roth KG, Mambetsariev I, Kulkarni P, Salgia R. The mitochondrion as an emerging therapeutic target in cancer. *Trends Mol Med.* (2020) 26:119–34. doi: 10.1016/j.molmed.2019.06.009
7. Jeong SY, Seol DW. The role of mitochondria in apoptosis. *BMB Rep.* (2008) 41:11–22. doi: 10.5483/BMBRep.2008.41.1.011
8. Cadenas S. Mitochondrial uncoupling, ROS generation and cardioprotection. *Biochim Biophys Acta Bioenerg.* (2018) 1859:940–50. doi: 10.1016/j.bbabio.2018.05.019
9. Bartel K, Pein H, Popper B, Schmitt S, Janaki-Raman S, Schulze A, et al. Connecting lysosomes and mitochondria - a novel role for lipid metabolism in cancer cell death. *Cell Commun Signal.* (2019) 17:87. doi: 10.1186/s12964-019-0399-2
10. Zorov DB, Juhaszova M, Sollott SJ. Mitochondrial reactive oxygen species (ROS) and ROS-induced ROS release. *Physiol Rev.* (2014) 94:909–50. doi: 10.1152/physrev.00026.2013
11. Dorn DG II. Evolving concepts of mitochondrial dynamics. *Annu Rev Physiol.* (2019) 81:1–17. doi: 10.1146/annurev-physiol-020518-114358
12. Forte M, Schirone L, Ameri P, Basso C, Catalucci D, Modica J, et al. The role of mitochondrial dynamics in cardiovascular diseases. *Br J Pharmacol.* (2021) 178:2060–76. doi: 10.1111/bph.15068
13. Essop MF, Opie LH. Metabolic therapy for heart failure. *Eur Heart J.* (2004) 25:1765–8. doi: 10.1016/j.ehj.2004.08.019
14. Cattadori G, Segurini C, Picozzi A, Padeletti L, Anzà C. exercise and heart failure: an update. *ESC Heart Fail.* (2018) 5:222–32. doi: 10.1002/ehf2.12225
15. Campos JC, Queliconi BB, Bozi LHM, Bechara LRG, Dourado PMM, Andres AM, et al. Exercise reestablishes autophagic flux and mitochondrial quality control in heart failure. *Autophagy.* (2017) 13:1304–17. doi: 10.1080/15548627.2017.1325062

Conflict of Interest: The authors declare that the research was conducted in the absence of any commercial or financial relationships that could be construed as a potential conflict of interest.

Publisher's Note: All claims expressed in this article are solely those of the authors and do not necessarily represent those of their affiliated organizations, or those of the publisher, the editors and the reviewers. Any product that may be evaluated in this article, or claim that may be made by its manufacturer, is not guaranteed or endorsed by the publisher.

Copyright © 2022 Yang, Wang, Wu, Ma, Li and Tang. This is an open-access article distributed under the terms of the Creative Commons Attribution License (CC BY). The use, distribution or reproduction in other forums is permitted, provided the original author(s) and the copyright owner(s) are credited and that the original publication in this journal is cited, in accordance with accepted academic practice. No use, distribution or reproduction is permitted which does not comply with these terms.

frontiers in Cardiovascular Medicine

ORIGINAL RESEARCH
published: 04 August 2021
doi: 10.3389/fcvm.2021.696578

Endothelial GABBR2 Regulates Post-ischemic Angiogenesis by Inhibiting the Glycolysis Pathway

Hongze Zhang[1], *Hong Zhou*[1], *Jianying Yuan*[1], *Yong Nan*[1] *and Jingquan Liu*[2,3*†]

[1] Department of Emergency Medicine and Critical Care, Shanghai Songjiang District Central Hospital, Songjiang Hospital Affiliated to Shanghai Jiaotong University School of Medicine (Preparatory Stage), Shanghai, China, [2] Department of Intensive Care Unit, Zhejiang Provincial People's Hospital, Hangzhou, China, [3] Department of Intensive Care Unit, People's Hospital of Hangzhou Medicine College, Hangzhou, China

OPEN ACCESS

Edited by:
Lei-Lei Ma,
Fudan University, China

Reviewed by:
Zengyong Qiao,
Shanghai Jiao Tong University Affiliated Sixth People's Hospital South Campus, China
Rui Lu,
Stanford University, United States

***Correspondence:**
Jingquan Liu
jing_quan_liu@163.com

†Present address:
Jingquan Liu,
Zhejiang Provincial People's Hospital,
Hangzhou, China

Specialty section:
This article was submitted to Cardiovascular Metabolism, a section of the journal Frontiers in Cardiovascular Medicine

Received: 17 April 2021
Accepted: 15 June 2021
Published: 04 August 2021

Citation:
Zhang H, Zhou H, Yuan J, Nan Y and Liu J (2021) Endothelial GABBR2 Regulates Post-ischemic Angiogenesis by Inhibiting the Glycolysis Pathway. Front. Cardiovasc. Med. 8:696578. doi: 10.3389/fcvm.2021.696578

Purpose: Angiogenesis post-ischemia plays an essential role in preventing ischemic damage to tissue by improving the blood recovery. Determining the regulatory mechanism of ischemic angiogenesis, therefore, could provide effective therapeutics for ischemic injury.

Materials and Methods: The RNA sequencing (RNA-seq) database was used to predict the association of gamma-aminobutyric acid type B receptor subunit 2 (GABBR2) with endothelial-specific expression. The role of GABBR2 in angiogenesis was verified *in vitro* by downregulating GABBR2 in human umbilical vein endothelial cells (HUVECs) with lentiviral vectors. Besides, the *in vivo* effect of GABBR2 on the blood recovery of an ischemic hindlimb was demonstrated by establishing a hindlimb ischemia model in normal and GABBR2 adenoviral vector-infected mice. Then, the mobilization of endothelial progenitor cells (EPCs) in peripheral blood post-ischemia was determined by flow cytometry. Finally, the XF analyzer and Western blot were used to determine the effect of GABBR2 on endothelial metabolism.

Results: The RNA-seq results indicated a strong association between GABBR2 and endothelial revascularization, and the upregulation of GABBR2 was detected in both hypoxia-treated HUVECs and ischemic mouse hindlimb. Hypoxia treatment for 6 h increased the proliferation, migration, and tube formation of HUVECs, which were inhibited by GABBR2 knockdown. Additionally, GABBR2 downregulation significantly decreased the blood flow recovery of mouse ischemic hindlimb. The expressions of the EPC markers $CD34^+$ and $CD133^+$ significantly decreased in the peripheral blood in hindlimb post-ischemia. Mechanically, glycolysis-dominated metabolism of HUVECs was compromised by GABBR2 knockdown. Evidences of the decreased expressions of HKII, PFKFB3, and PKM1 also supported the compromised glycolysis induced by GABBR2 downregulation.

Conclusion: Our study demonstrated that GABBR2 regulated angiogenesis post-ischemia by inhibiting the glycolysis pathway.

Keywords: GABBR2, angiogenesis, glycolysis, endothelial (dys)function, ischemic injury

INTRODUCTION

The rapid and timely reestablishment of blood vessels in response to injury or in pathological conditions ensures the efficient supply of oxygen and nutrients, which are essential for the protection of tissues from ischemic injury. Peripheral arterial diseases (PADs) are associated with dysfunctional collateral circulation and are linked to a high risk of cardiovascular events, specifically stroke and myocardial infarction (1). Illustrating the mechanism of endothelial cell (EC) angiogenesis could provide therapeutic targets in ameliorating the development of cardiovascular events.

Current studies majorly focus on the growth factors, receptors, signaling molecules, and others involved in the process of angiogenesis, but no significant efficacy or specificity was revealed so far. Recent findings have demonstrated that pathological angiogenesis and EC dysfunction are accompanied by EC-specific metabolic alterations. Targeting EC metabolism is therefore emerging as a novel therapeutic strategy (2–4). The switch of ECs from quiescence to growth metabolically demands that 85% ATP is produced glycolytically (3, 5, 6). Even though glucose oxidative metabolism produces 34 molecules of ATP, ECs still preferentially utilize glycolysis instead of oxidative metabolism. As glycolytic regulators, 6-phosphofructo-2-kinase/fructose-2,6-bisphosphatase 3 (PFKFB3) and hexokinase2 (HK2) are rate-limiting enzymes that regulate EC angiogenesis by modulating glycolytic metabolism. Silencing of the glycolytic regulators PFKFB3 and HK2 inhibited the atrial development and branching of mouse skin and the proliferation of filopodia in the retinal vasculature (5, 7). The reasons for glycolysis-dependent metabolism might lie in ECs bathing in oxygen needing anaerobic metabolism to protect themselves from oxidative stress. The stored oxygen is diffused to perivascular cells. In addition, glycolysis yields fewer but faster ATP, which is necessary for the angiogenesis of ECs in hypoxic tissues.

Gamma-aminobutyric acid (GABA) receptors are heterodimeric G-protein-coupled receptors comprising the GABAB1 and GABAB2 subunits (GABBR2) (8). Gamma-aminobutyric acid receptors are located mainly in the central nervous system (CNS) and retina. Additionally, GABA receptors have also been detected in peripheral tissues and are shown to modulate intracellular calcium concentration (9, 10). These receptors can inhibit the release of many neurotransmitters, such as dopamine, serotonin, and acetylcholine, *via* G-protein-dependent inhibition of neuronal voltage-gated Ca^{2+} channels. Functional GABA receptors are implicated in various disorders, including cognitive impairments, nociception, anxiety, depression, and epilepsy (11, 12). Gamma-aminobutyric acid is a neurotrophic factor that plays an important role in embryonic development of the nervous system by promoting the proliferation, migration, and differentiation of embryonic neural cells and neural crest cells (13, 14). Additionally, GABA receptors regulate intracellular signaling by inhibiting adenylyl cyclase activity (15). Here, we found a potential of GABBR2 in regulating EC function. Then, the effect of GABBR2 on angiogenesis capacity was established by downregulating GABBR2 *in vivo* and *in vitro*. Our present results illustrated that GABBR2 knockdown inhibited the angiogenesis process post-ischemia by regulation of the glycolysis-dominant metabolism.

MATERIALS AND METHODS

Animals

Adult C57BL/6J male mice (weighing 20–22 g), obtained from Shanghai Research Center for Model Organisms, were used in this study. Care and all animal experiments were performed in accordance with institutional guidelines. Mice were housed at room temperature under a 12:12 light/dark cycle with free access to water and standard laboratory mouse chow.

Murine Hindlimb Ischemia Model

The fur in the hindlimb of adult C57BL/6J male mice were removed after anesthetized by intraperitoneal injection of pentobarbital sodium (40 mg/kg body weight). Then, the skin of the left hindlimb was dissected and the femoral artery exposed. Ischemia of the hindlimb was induced by ligation and excision of the femoral artery at middle and two terminals.

Perfusion Recovery Detection

Blood flow recovery in the ischemic hindlimb was analyzed by laser Doppler perfusion imaging (PeriScan PIM 3 System, Perimed, Stockholm, Sweden) on days 1, 3, 5, 7, and 10. In detail, the mice were anesthetized by intraperitoneal injection of pentobarbital sodium and placed on 37°C heating plate, and then the hindquarters were imaged by laser Doppler imaging. Blood flow recovery was calculated as the perfusion ratio of ischemic limbs vs. non-ischemic limbs.

Cell Culture

Human umbilical vein endothelial cells (HUVECs) were obtained from Cell Bank of Chinese Academy of Science (Shanghai, China) and cultured in Dulbecco's modified Eagle's medium (DMEM) with 10% fetal bovine serum (FBS) at 37°C in a humidified incubator with 21% O_2 and 5% CO_2. Hypoxia treatment was performed by culturing the cells in an incubator with 1% O_2 and 5% CO_2. For GABBR2 knockdown in HUVECs, the lentiviral vectors were infected for at least 12 h, then the medium was replaced with a virus-free medium.

Tubule Formation Assay and CCK-8 Assay

The angiogenic effect of HUVECs was quantified by tubule formation assay in Matrigel (cat no. 354234, Corning, Corning, NY, USA). The Matrigel solution was thawed overnight at 4°C, and then 200 μl thawed Matrigel was transferred and plated onto a 24-well plate per well. After incubating for 30 min at 37°C, 10^4 HUVECs were resuspended with endothelial cell basal medium (ECM-2, Lonza, Basel, Switzerland) and then seeded onto the Matrigel. After 6 h, the tube formation status was imaged by a microscope (Nikon TE2000, Nikon, Tokyo, Japan). For the CCK-8 assay, Cell Counting Kit-8 (Weiao Co., Shanghai, China) was used for the assessment of cellular proliferation.

Flow Cytometry Assay

To assess the endothelial progenitor cell (EPC) levels mobilized post-ischemic injury, peripheral blood samples were harvested at

day 7 post-hindlimb ischemia in mice. Erythrocyte lysis buffer (BD Biosciences, Franklin Lakes, NJ, USA) was used to lyse red blood cells in a shaker at room temperature for 10 min. After fixing with 4% paraformaldehyde, the cells were stained with the antibodies CD34-FITC (11-0349-42, eBioscience, San Diego, CA, USA) and CD133-PE (12-1331-82, eBioscience). Stained cells were then analyzed on a FACScan flow cytometer (Becton Dickinson, Franklin Lakes, NJ, USA).

Adenoviral Vector Construction and Transfection

The AAV9–GABBR2–shRNA–zsgreen vector was used in this study for the downregulation of GABBR2 expression in mouse hindlimb. Adenovirus was injected intramuscularly according to the manufacturer's instruction. Of Ad.GABBR2 or Ad.Null, 5×10^9 plaque-forming units (PFU) in 100 μl of phosphate-buffered saline (PBS) was injected into the gastrocnemius muscle of mice 4 weeks before surgery, respectively.

Western Blot

Cultured cells and tissue from mouse hindlimb were lysed on ice with RIPA buffer (Sigma-Aldrich, St. Louis, MO, USA) containing protease inhibitor cocktail (ThermoFisher Scientific, Waltham, MA, USA) and PhosSTOP (ThermoFisher Scientific) for at least 30 min. After centrifugation at 12,000 rpm for 10 min at 4°C, supernatant fractions were collected and analyzed by sodium dodecyl sulfate polyacrylamide gel electrophoresis (SDS-PAGE) and immunoblotting. The following antibodies were obtained from Cell Signaling (Danvers, MA, USA): GABA(B)R2 antibody (#3839, 1:1,000), Hexokinase II (HKII) antibody (#2867, 1:1,000), and pyruvate kinase muscle 1 (PKM1) antibody (#7067, 1:1,000). Vascular endothelial growth factor (VEGF) antibody (#65373, 1:1,000), anti-PFKFB3 (ab181861, 1/1,000–1/10,000), and anti-CD31 (ab76533, 1/5,000–1/20,000) were obtained from Abcam (MitoSciences-Abcam, Eugene, OR, USA). Horseradish peroxidase (HRP)-conjugated monoclonal mouse anti-beta actin (KC-5A08, 1:5,000) was obtained from KangChen Bio-tech Co. (Shanghai, China).

Bioenergetics Assay of ECAR Changes

The extracellular acidification rates (ECARs) of the HUVECs in different groups were analyzed using an XFe96 extracellular flux analyzer (Seahorse Bioscience, Billerica, MA, USA). The optimal seeding density of HUVECs ranges from 10,000 to 60,000 cells per well and gives confluency of approx. 95% overnight in a 96-well seahorse culture plate. ECAR was determined by adding glucose (10 mM), oligomycin A (1 μM), and 2-deoxy-D-glucose (1 M).

Immunofluorescent Staining

The quadriceps femoris muscles of wild-type (WT) and GABBR2 knockdown (KD) ischemic limbs were harvested and embedded with OCT. Then, the embedded tissues were sectioned at 8 μm. After fixation and blocking, the sections were incubated with goat anti-mouse CD31 antibody (1:200, NOVUS Biologicals, Littleton, CO, USA). Alexa Fluor 549 donkey anti-goat secondary antibody (1:150, ThermoFisher Scientific) was used for fluorescence imaging.

EdU Staining Assay

The effect of GABBR2 on the proliferative abilities of HUVECs was detected by using the BeyoClick EdU Cell Proliferation Kit with Alexa Fluor 488 (Beyotime, Jiangsu, China). In detail, 100 μM 5-ethynyl-2′-deoxyuridine (EdU) solution was added to the medium and incubated with HUVECs for 2 h. The divided cells stained with green represented EdU-positive cells.

Statistical Analyses

Statistical analyses were performed using one-way ANOVA with Tukey's correction using GraphPad 8.0 software. Statistical results were shown as the mean ± standard error of the mean (SEM). Every experiment was repeated at least three times.

RESULTS

GABBR2 Was Closely Related to Endothelial Angiogenesis and Upregulated by Hypoxia Treatment

The RNA sequencing (RNA-seq) data from the Human Protein Atlas (https://www.proteinatlas.org/) predicted an endothelial-specific expression of GABBR2 (**Figure 1A**). We therefore speculated that GABBR2 might play an important role in the regulation of angiogenesis. To obtain the genes involved in angiogenesis, we resorted to the publicly available ANGIOGENES database of RNA-seq (http://angiogenes.uni-frankfurt.de), identifying 14,153 genes whose transcription was dynamically modulated during VEGF stimulation (12 h) of HUVECs. Gamma-aminobutyric acid type B receptor subunit 2 was one of the genes closely related to physical or pathological angiogenesis (**Figure 1B**). Hypoxia was a driver that regulates angiogenesis and vascular remodeling (16). To explore the effect of hypoxia on the regulation of GABBR2, we cultured HUVECs under the condition of 1% oxygen for 0, 6, 12, and 24 h. The results in **Figures 1C,D** demonstrated a significantly enhanced expression of GABBR2 in HUVECs after hypoxia treatment. Furthermore, to determine the role of GABBR2 in mouse vascular ECs, we performed a hindlimb ischemia model and detected the expression of GABBR2 in the ischemic hindlimb muscle at different time points. The results also showed a markedly upregulated expression of GABBR2 in hindlimb post-ischemia (**Figures 1E,F**). The above results indicated that GABBR2 might play an important role in regulating the angiogenesis of ECs post-hypoxia or ischemia.

GABBR2 Downregulation Regulated the Angiogenesis of HUVECs With or Without Hypoxia Treatment

Human umbilical vein endothelial cells were used to further demonstrate the role of GABBR2 in angiogenesis. We

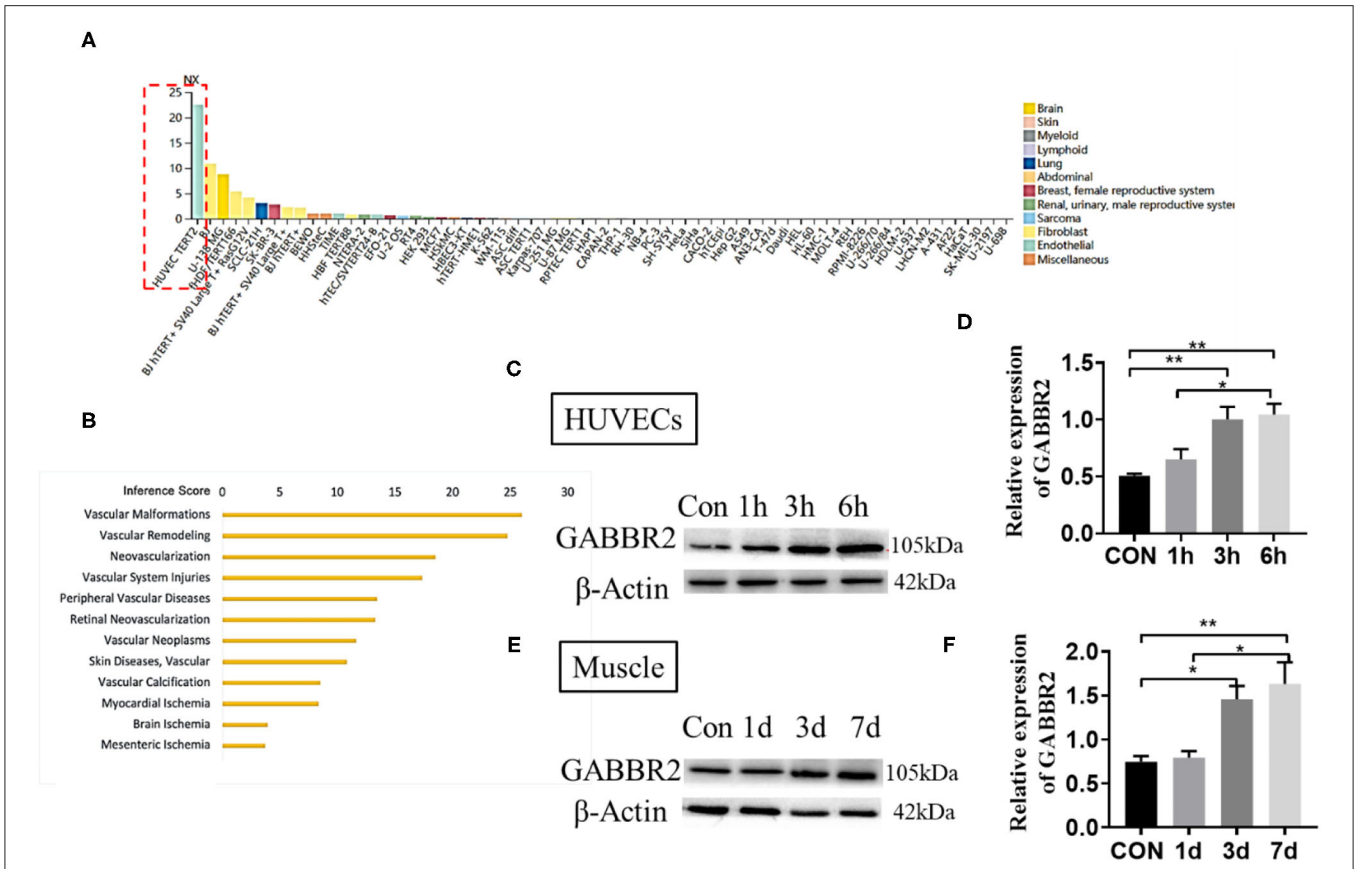

FIGURE 1 | Gamma-aminobutyric acid type B receptor subunit 2 (GABBR2) expression increased in hypoxia-treated endothelial cells *in vitro* and mouse ischemic hindlimb *in vivo*. **(A)** Prediction of an endothelial-specific expression of GABBR2 by RNA-seq data. **(B)** Re-speculation of the role of GABBR2 in angiogenesis. **(C,D)** Expression changes of GABBR2 in human umbilical vein endothelial cells (HUVECs) after hypoxia treatment for 1, 3, and 6 h. **(E,F)** Expression changes of GABBR2 in the muscle of mouse ischemic hindlimb on days 1, 3, and 7. $^{*}p < 0.05$; $^{**}p < 0.01$.

constructed the lentivirus-mediated GABBR2 downregulation in HUVECs and analyzed the proliferation and migration capacity. The results showed that about 90% of the GABBR2 expression was downregulated after lentivirus transfection (**Figure 2A**). The CCK-8 assay results showed that GABBR2 knockdown significantly inhibited the proliferation of HUVECs under normoxia, which could be further inhibited after 6 h of hypoxic treatment (**Figure 2B**). Besides, the EdU staining assay demonstrated that GABBR2 knockdown significantly decreased the ratio of EdU-positive cells under normoxia and hypoxia (**Figure 2C**). Then, the migration capacity was calculated as the average wound healing distance; promotion of endothelial migration was detected after hypoxia treatment, which could be eliminated by GABBR2 knockdown (**Figure 2D**). Since angiogenesis capacity could be evaluated by a tube-like construction formation in Matrigel, we then assessed the effect of GABBR2 knockdown on the formation of capillary-like tubes. As shown in **Figure 2E**, GABBR2 knockdown significantly inhibited the capillary-like tube formation in HUVECs.

GABBR2 Knockdown Inhibited the Blood Flow Recovery in Ischemic Mouse Hindlimb

Adenovirus encoding a constitutively inactive form of GABBR2 was injected in mouse hindlimb by multipoint for 4 weeks (**Figure 3A**). The Western blot results demonstrated that the expression of GABBR2 was downregulated by about 80% in the muscle of mouse hindlimb (**Figure 3B**). To determine the role of GABBR2 knockdown in angiogenesis and blood flow recovery, a hindlimb ischemia model was established in normal and GABBR2-downregulated mice. The blood flow recovery status on days 1, 3, 5, 7, and 10 was evaluated by laser Doppler imaging post-ischemia. The results indicated that GABBR2 downregulation significantly abrogated the blood flow recovery by 3.84, 1.98, and 2.13 times on days 5, 7, and 10, respectively (**Figures 3C,D**). To further prove the inhibitory effect of GABBR2 knockdown on the angiogenesis of mouse ischemic hindlimb, we determined the expression of VEGF and platelet endothelial cell adhesion molecule-1 (PECAM-1/CD31) in WT and GABBR2-downregulated hindlimbs. The

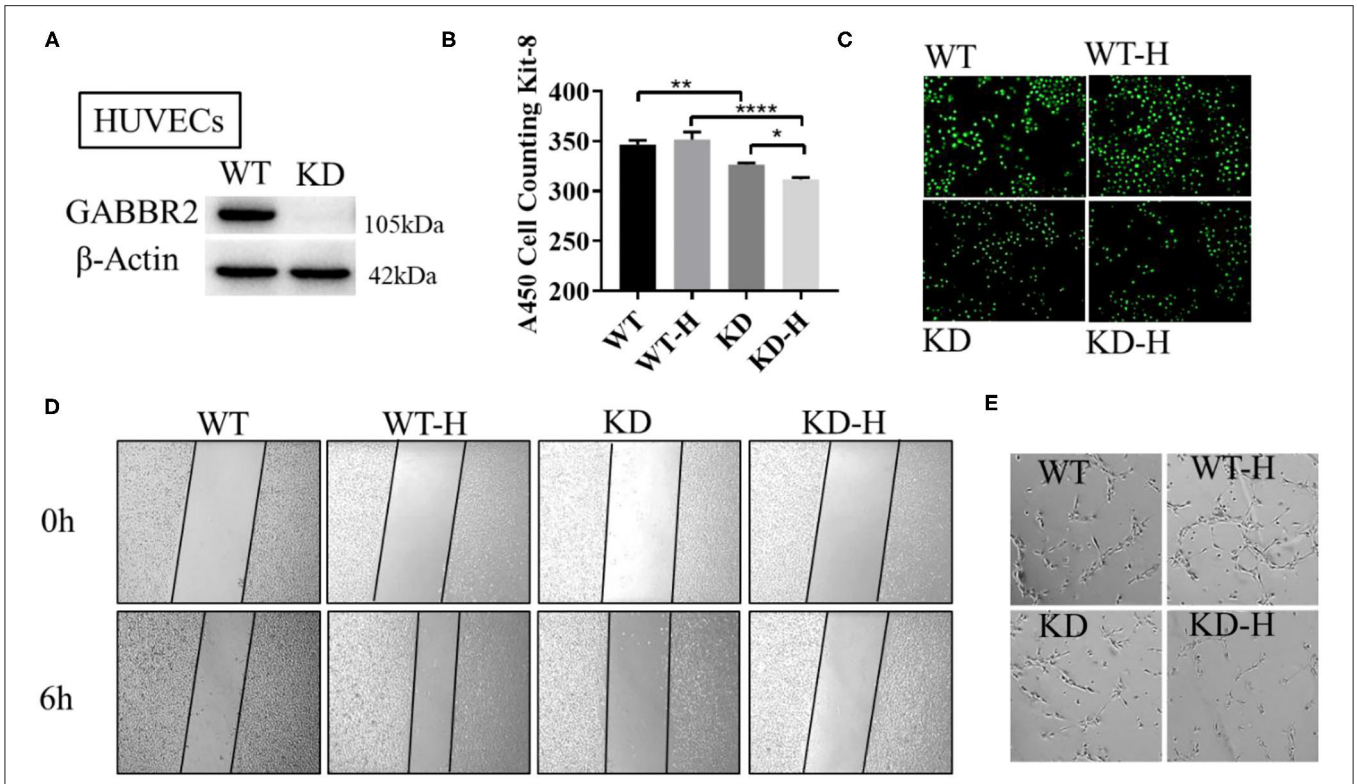

FIGURE 2 | Effect of gamma-aminobutyric acid type B receptor subunit 2 (GABBR2) knockdown on the proliferation, migration, and angiogenesis of human umbilical vein endothelial cells (HUVECs). **(A)** Downregulation of GABBR2 in HUVECs by lentivirus transfection. **(B)** Cellular proliferation changes induced by 6 h of hypoxic treatment in normal and GABBR2-downregulated HUVECs. **(C)** EdU staining induced by 6 h of hypoxic treatment in normal and GABBR2-downregulated HUVECs. **(D)** Wound healing distance changes induced by 6 h of hypoxic treatment in normal and GABBR2-downregulated HUVECs. **(E)** Tube-like construction formation induced by 6 h of hypoxic treatment in normal and GABBR2 downregulated HUVECs. $^{*}p < 0.05$; $^{**}p < 0.01$; $^{****}p < 0.0001$.

results indicated that the upregulation of VEGF and CD31 induced by ischemia was inhibited by GABBR2 knockdown (**Figure 3E**). Immunofluorescent staining of CD31 in WT and GABBR2-downregulated hindlimbs showed consistent results in that GABBR2 knockdown decreased CD31 expression in ischemic hindlimb (**Figure 3F**). Overall, these evidences demonstrated that GABBR2 is an important regulator in promoting angiogenesis post-ischemia.

GABBR2 Knockdown Decreased the Mobilization of EPCs in Peripheral Blood Post-ischemia

CD34 and CD133 are the most commonly used EPC markers expressed in early and mature vascular ECs that play an important role in EPC proliferation and differentiation, therefore serving as a powerful pan-endothelial marker (17, 18). To determine the mobilization of EPCs, we collected peripheral blood from normal and ischemic mice with or without GABBR2–shRNA transfection. Then, we analyzed CD34- or CD133-positive cells and CD34/CD133 double-positive cells by using flow cytometry. The data showed that ischemia increased the ratio of CD34 and CD133 double-positive cells in peripheral blood from 2.45 to 7.17%, which was significantly blunted by GABBR2 knockdown (**Figures 4A–D**). These results implied that ischemia-induced mobilization of EPCs in peripheral blood was markedly inhibited by GABBR2 downregulation.

GABBR2 Knockdown Inhibited the Angiogenesis of HUVECs by Regulating the Glycolysis Pathway

It was reported that ECs rely on glycolysis to participate in vessel sprouting (3). To analyze the effect of GABBR2 downregulation on cellular energetics, lentivirus-mediated GABBR2 knockdown in HUVECs was used in our study. Since hypoxia promotes glycolysis, we detected the metabolic changes of HUVECs under normoxic and hypoxic conditions by assessing the ECAR. The results showed that hypoxia treatment remarkably increased the ECARs of HUVECs. However, GABBR2 downregulation inhibited the glycolysis levels of HUVECs under hypoxic condition (**Figure 5A**). Furthermore, total ATP generation was evaluated in HUVECs with different GABBR2 expressions. The results demonstrated that GABBR2 knockdown significantly decreased cellular ATP production (**Figure 5B**). HKII, PFKFB3, and PKM1 are three key enzymes responsible for glycolysis. Our results indicated that the expressions of these enzymes were enhanced by hypoxia treatment, which were significantly

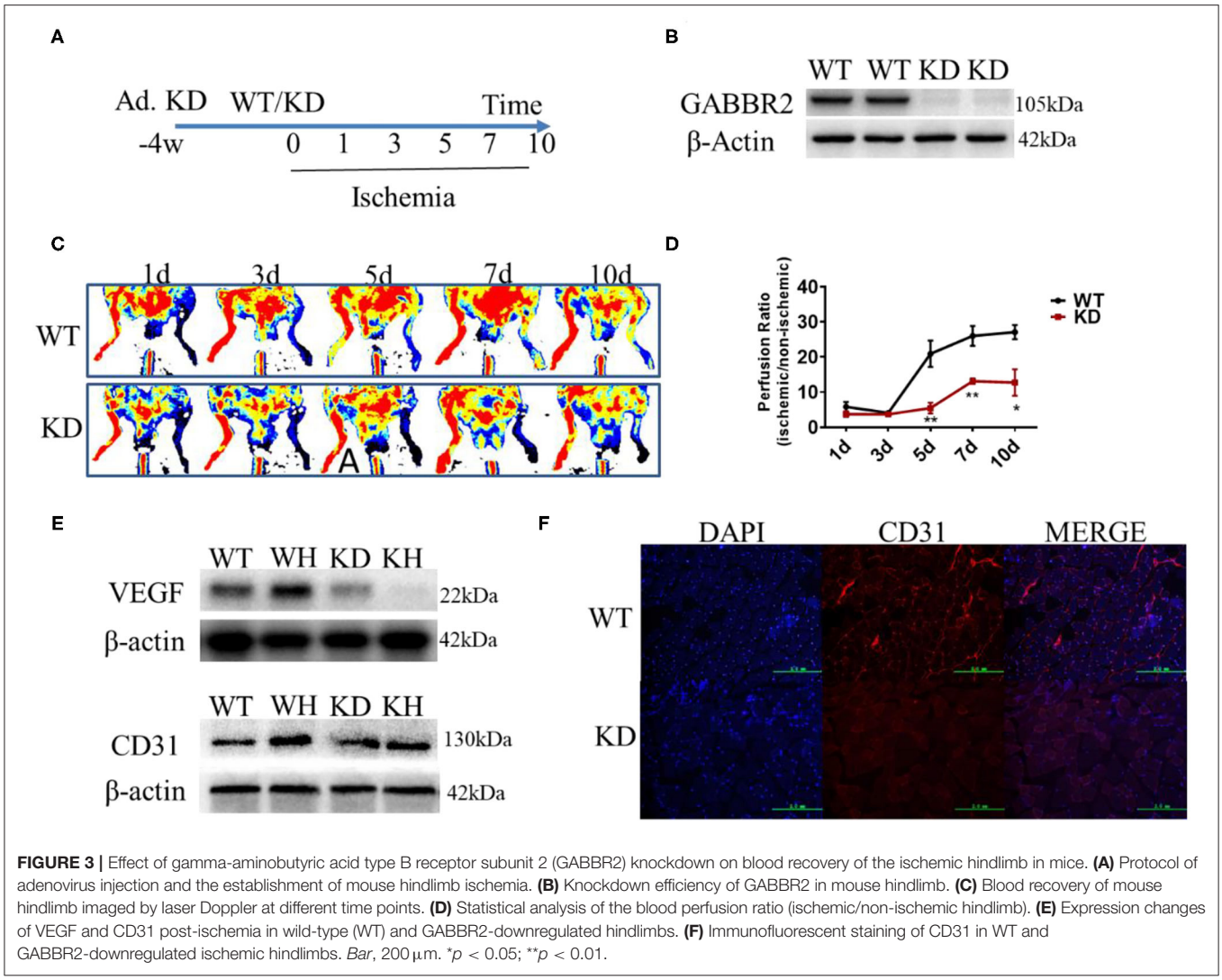

FIGURE 3 | Effect of gamma-aminobutyric acid type B receptor subunit 2 (GABBR2) knockdown on blood recovery of the ischemic hindlimb in mice. **(A)** Protocol of adenovirus injection and the establishment of mouse hindlimb ischemia. **(B)** Knockdown efficiency of GABBR2 in mouse hindlimb. **(C)** Blood recovery of mouse hindlimb imaged by laser Doppler at different time points. **(D)** Statistical analysis of the blood perfusion ratio (ischemic/non-ischemic hindlimb). **(E)** Expression changes of VEGF and CD31 post-ischemia in wild-type (WT) and GABBR2-downregulated hindlimbs. **(F)** Immunofluorescent staining of CD31 in WT and GABBR2-downregulated ischemic hindlimbs. *Bar*, 200 μm. $^{*}p < 0.05$; $^{**}p < 0.01$.

downregulated by GABBR2 downregulation under normoxic or hypoxic condition (**Figures 5C–E**). The above results indicated that the inhibitory effect of GABBR2 knockdown on glycolysis capacity could be responsible for the damaged angiogenesis post-ischemia.

DISCUSSION

The present study demonstrated that the upregulation of GABBR2 induced by hypoxia or ischemia plays an important role in the proliferation, migration, and angiogenesis of HUVECs, which were further proven by the compromised blood recovery in GABBR2-downregulated ischemic hindlimb of mice. Besides, the mobilization of $CD34^{+}/CD133^{+}$ cells in peripheral blood was inhibited by hindlimb GABBR2 knockdown in mice. Mechanically, GABBR2 downregulation inhibited the glycolysis capacity of HUVECs by downregulating the expression of glycolysis-associated enzymes. Gamma-aminobutyric acid type B receptor subunit 2 was reported to implicate in a number of neuronal disorders, including cognitive impairments, nociception, anxiety, and depression (19–21). In the neuronal pathophysiology of many CNS diseases and disorders, GABBR2 regulates intracellular signaling by G protein-coupled receptors to activate adenylyl cyclase. However, our study indicated that the critical role of GABBR2 in the process of EC angiogenesis might be attributed to the regulation of the glycolysis pathway. Our results provide a new horizon and mechanism for post-ischemic angiogenesis, which could be a potential therapeutic target of metabolism regulation.

Several modes of vessel formation have been identified, including sprouting angiogenesis, vasculogenesis, and arteriogenesis. Vasculogenesis is defined as the process in which angioblasts differentiate into ECs in the developing mammalian embryo. Subsequent sprouting angiogenesis ensures the expansion of the vascular network. Then, pericytes or vascular smooth muscle cells cover ECs to provide stability and control perfusion, which is known as arteriogenesis (22). In other words, angiogenesis refers to the formation of new blood vessels

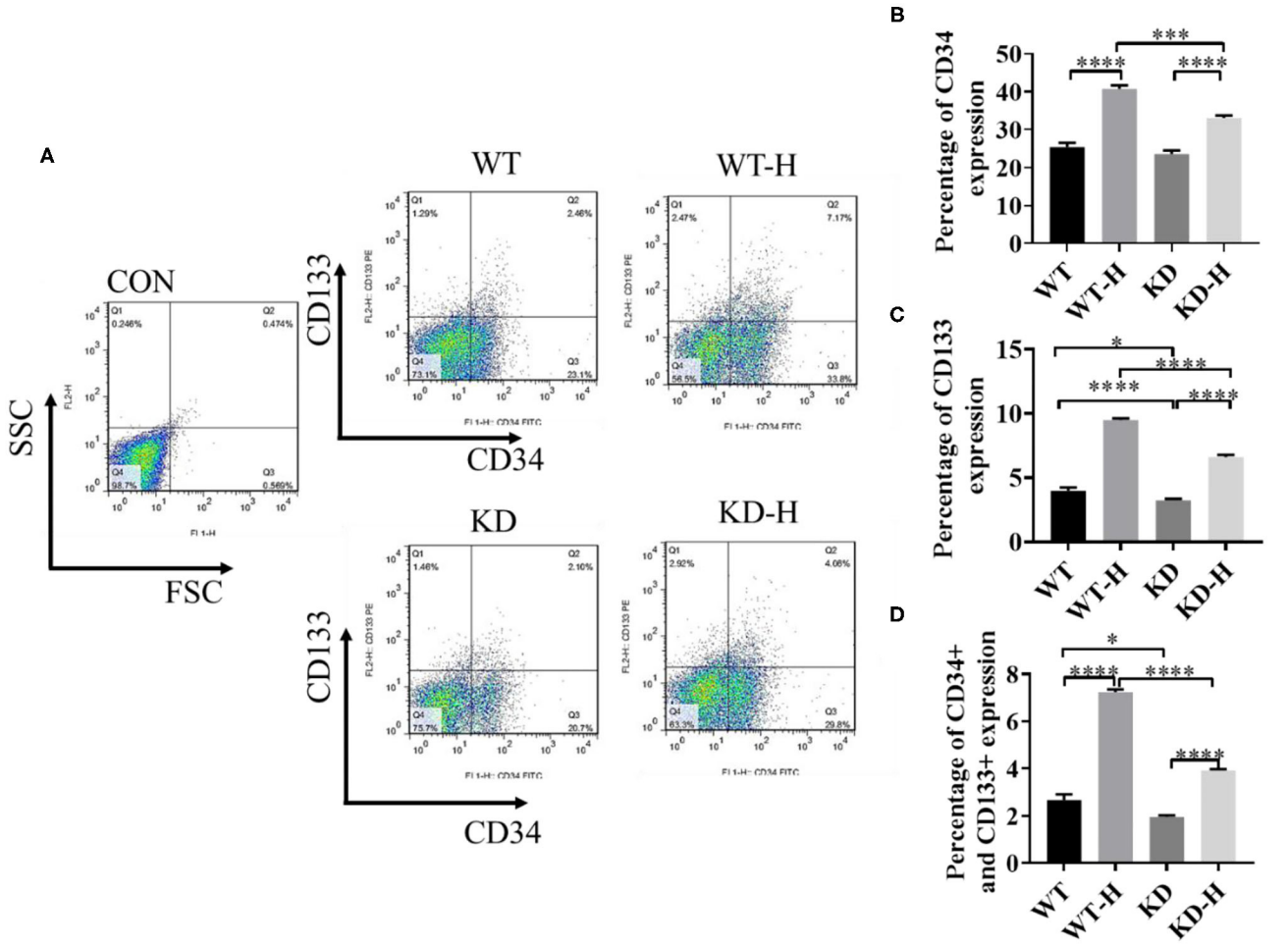

FIGURE 4 | Effect of gamma-aminobutyric acid type B receptor subunit 2 (GABBR2) knockdown on endothelial progenitor cell (EPC) mobilization in peripheral blood in hindlimb post-ischemia. **(A)** Representative images of $CD34^+/CD133^+$ cells in the peripheral blood of mice analyzed by flow cytometry. *WT*, normal mice; *KD*, GABBR2-downregulated mice; *WT-H*, wild-type (WT) mice with hindlimb ischemia; *KD-H*, GABBR2 knockdown (KD) mice with hindlimb ischemia. **(B)** Ratio of $CD34^+$ cells in the peripheral blood of normal and ischemic mice. **(C)** Ratio of $CD133^+$ cells in the peripheral blood of normal and ischemic mice. **(D)** Ratio of $CD34^+$ and $CD133^+$ cells in the peripheral blood of normal and ischemic mice. $^*p < 0.05$; $^{***}p < 0.001$; $^{****}p < 0.0001$.

from preexisting vessels, which was intensively explored in our study. Given the complexity of angiogenesis, the pro-angiogenic factors that play a predominant role in angiogenesis, such as VEGF and CD31, were detected in our study. Our results showed that the expressions of VEGF and CD31 were activated by hypoxia, which was consistent with the enhanced angiogenesis in the ischemic hindlimb. However, GABBR2 knockdown inhibited VEGF and CD31 expressions, as well as post-ischemic angiogenesis in the hindlimb. Taken together, we conclude that the blood recovery of the ischemic hindlimb in mice was majorly regulated by the mode of angiogenesis, which was further modulated by GABBR2.

The repair of healthy adult vessels or the expansion of pathological vessels can be aided by the recruitment of bone marrow-derived cells and/or EPCs to the vascular wall (23, 24). Mobilization of EPCs might represent an effective means to augment the resident population of ECs (25). Different cytokines and growth factors stimulate bone marrow-derived EPCs to circulate in adult peripheral blood, participating in angiogenesis. Vascular endothelial growth factor is an important cytokine for EPC mobilization from the bone marrow into the peripheral circulation (26, 27). In our study, an increased expression of VEGF was observed in the ischemic hindlimb and, accordingly, a significantly enhanced EPC mobilization in peripheral blood. Gamma-aminobutyric acid type B receptor subunit 2 knockdown inhibited VEGF expression and EPC mobilization. The evidences from our study indicated that GABBR2 knockdown blunted EPC mobilization by inhibiting VEGF expression.

Despite the 36 mol of ATP from glucose oxidation vs. 2 mol of ATP from aerobic glycolysis, ECs generate ATP mainly from glycolysis. Furthermore, the switch of ECs from quiescence to vessel branching accelerates aerobic glycolysis (5, 28, 29). Moreover, a hypoxic environment in the hindlimb favors the glycolysis pathway, whereas glycolysis-dominant metabolism

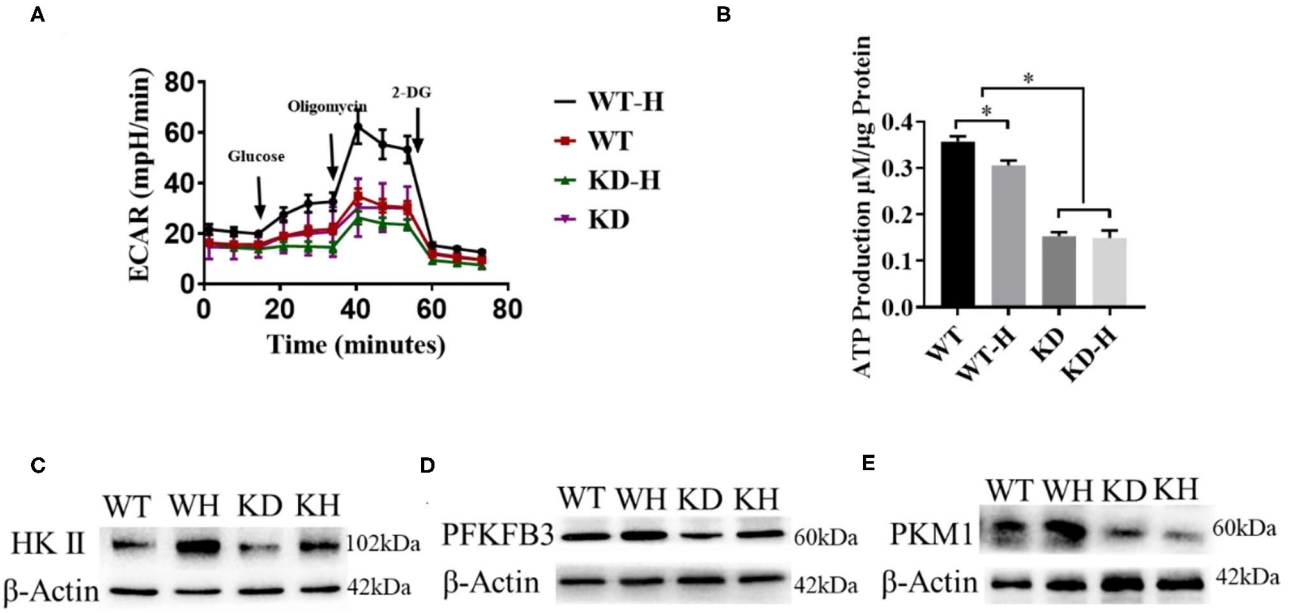

FIGURE 5 | Effect of gamma-aminobutyric acid type B receptor subunit 2 (GABBR2) knockdown on the glycolysis capacity of human umbilical vein endothelial cells (HUVECs) after hypoxia treatment. **(A)** Extracellular acidification rate (ECAR) changes induced by 6 h of hypoxic treatment in normal and GABBR2-downregulated HUVECs. *WT*, normal mice; *KD*, GABBR2-downregulated mice; *WT-H*, wild-type (WT) mice with hindlimb ischemia; *KD-H*, GABBR2 knockdown (KD) mice with hindlimb ischemia. **(B)** ATP production changes induced by 6 h of hypoxic treatment in normal and GABBR2-downregulated HUVECs. **(C–E)** Expression changes of HKII, PFKFB3, and PKM1 induced by 6 h of hypoxic treatment in normal and GABBR2-downregulated HUVECs. $^*p < 0.05$.

also makes ECs more hypoxia-resistant. In our study, the stimulation of glycolysis by hypoxia was accompanied by the upregulation of GABBR2, indicating the potential connection between glycolysis and GABBR2. Given the above fact, the regulating mode of GABBR2 in glycolysis warrants further exploration. The study of De Bock and colleagues reported that the pro-angiogenic molecule VEGF stimulates the expression of the glycolysis activator PFKFB3 (5). Intriguingly, our study demonstrated that VEGF production was induced by hypoxia, but inhibited by GABBR2 knockdown. Consistent with this result, the expressions of the glycolysis activators, namely, HKII, PFKFB3, and PKM1, were upregulated by hypoxia, but downregulated by GABBR2 knockdown. In brief, we conclude that GABBR2 regulated the glycolysis pathway by controlling the secretion of pro-angiogenic molecules.

Human umbilical vein endothelial cell metabolism plays an important role in the formation of new vessels. The importance of metabolism could be described as the engine in a car and the angiogenic signals as the driver. Once metabolism is compromised, new vessel formation was inhibited regardless of EC angiogenic signals (2). The division and migration of ECs for the formation of new vessels demand a large amount of energy. Endothelial cells highly rely on glycolysis instead of oxidative metabolism for ATP production, most of which is produced by the conversion of glucose into lactate (5, 29, 30). Our results indicated that the glycolysis of ECs was further stimulated by hypoxia treatment, which was evidenced by the significantly increased ECARs. Combined with the profile of the glycolysis-dominated metabolism, enhanced glycolysis post-hypoxia was demonstrated. This reaction, however, was inhibited by GABBR2 knockdown with or without hypoxia treatment. The compromised glycolysis metabolism was further illustrated by the decreased expressions of the catalyzing enzymes participating in the metabolic pathway. Our present study indicated that GABBR2 might be a potential therapeutic target in modulating EC metabolism and the process of ischemia in PADs.

DATA AVAILABILITY STATEMENT

The datasets presented in this study can be found in online repositories. The names of the repository/repositories and accession number(s) can be found below: https://www.proteinatlas.org/ENSG00000136928-GABBR2/cell.

ETHICS STATEMENT

The animal study was reviewed and approved by Hangzhou Medicine College.

AUTHOR CONTRIBUTIONS

HZha and JL contributed to the study design. HZha and HZho collected the data. JY and YN performed statistical analysis and conducted the literature search. HZha interpreted the data. HZha, HZho, JY, YN, and JL prepared the manuscript. JL helped with fund collection. All authors contributed to the article and approved the submitted version.

FUNDING

This project was supported by The General Project Funds from the Health Department of Zhejiang Province (grant nos. 2018KY210, 2019RC118).

SUPPLEMENTARY MATERIAL

The Supplementary Material for this article can be found online at: https://www.frontiersin.org/articles/10.3389/fcvm.2021.696578/full#supplementary-material

REFERENCES

1. Mascarenhas JV, Albayati MA, Shearman CP, Jude EB. Peripheral arterial disease. *Endocrinol Metab Clin North Am.* (2014) 43:149–66. doi: 10.1016/j.ecl.2013.09.003
2. Potente M, Carmeliet P. The link between angiogenesis and endothelial metabolism. *Annu Rev Physiol.* (2017) 79:43–66. doi: 10.1146/annurev-physiol-021115-105134
3. De Bock K, Georgiadou M, Carmeliet P. Role of endothelial cell metabolism in vessel sprouting. *Cell Metab.* (2013) 18:634–47. doi: 10.1016/j.cmet.2013.08.001
4. Eelen G, de Zeeuw P, Treps L, Harjes U, Wong BW, Carmeliet P. Endothelial cell metabolism. *Physiol Rev.* (2018) 98:3–58. doi: 10.1152/physrev.00001.2017
5. De Bock K, Georgiadou M, Schoors S, Kuchnio A, Wong BW, Cantelmo AR, et al. Role of PFKFB3-driven glycolysis in vessel sprouting. *Cell.* (2013) 154:651–63. doi: 10.1016/j.cell.2013.06.037
6. Ghesquiere B, Wong BW, Kuchnio A, Carmeliet P. Metabolism of stromal and immune cells in health and disease. *Nature.* (2014) 511:167–76. doi: 10.1038/nature13312
7. Yu P, Wilhelm K, Dubrac A, Tung JK, Alves TC, Fang JS, et al. FGF-dependent metabolic control of vascular development. *Nature.* (2017) 545:224–8. doi: 10.1038/nature 22322
8. Fritzius T, Bettler B. The organizing principle of GABAB receptor complexes: physiological and pharmacological implications. *Basic Clin Pharmacol.* (2020) 126:25–34. doi: 10.1111/bcpt.13241
9. Zhou Z, Sun H, Li X, Li Y, Zhao S, Zhang D, et al. local GABAergic system is functionally expressed in human fallopian tube. *Biochem Biophys Res Commun.* (2010) 398:237–41. doi: 10.1016/j.bbrc.2010.06.066
10. Mizuta K, Mizuta F, Xu D, Masaki E, Panettieri RJ, Emala CW. Gi-coupled gamma-aminobutyric acid-B receptors cross-regulate phospholipase C and calcium in airway smooth muscle. *Am J Respir Cell Mol Biol.* (2011) 45:1232–8. doi: 10.1165/rcmb.2011-0088OC
11. Bettler B, Kaupmann K, Mosbacher J, Gassmann M. Molecular structure and physiological functions of GABA(B) receptors. *Physiol Rev.* (2004) 84:835–67. doi: 10.1152/physrev.00036.2003
12. Lujan R, Ciruela F. GABAB receptors-associated proteins: potential drug targets in neurological disorders? *Curr Drug Targets.* (2012) 13:129–44. doi: 10.2174/138945012798868425
13. Watanabe M, Maemura K, Kanbara K, Tamayama T, Hayasaki H. GABA and GABA receptors in the central nervous system and other organs. *Int Rev Cytol.* (2002) 213:1–47. doi: 10.1016/S0074-7696(02)13011-7
14. Fiszman ML, Schousboe A. Role of calcium and kinases on the neurotrophic effect induced by gamma-aminobutyric acid. *J Neurosci Res.* (2004) 76:435–41. doi: 10.1002/jnr.20062
15. Padgett CL, Slesinger PA. GABAB receptor coupling to G-proteins and ion channels. *Adv Pharmacol.* (2010) 58:123–47. doi: 10.1016/S1054-3589(10)58006-2
16. Semenza GL. Hypoxia-inducible factor 1 and cardiovascular disease. *Annu Rev Physiol.* (2014) 76:39–56. doi: 10.1146/annurev-physiol-021113-170322
17. Fritzenwanger M, Lorenz F, Jung C, Fabris M, Thude H, Barz D, et al. Differential number of CD34+, CD133+ and CD34+/CD133+ cells in peripheral blood of patients with congestive heart failure. *Eur J Med Res.* (2009) 14:113–7. doi: 10.1186/2047-783X-14-3-113
18. Golab-Janowska M, Paczkowska E, Machalinski B, Kotlega D, Meller A, Safranow K, et al. Elevated inflammatory parameter levels negatively impact populations of circulating stem cells (CD133+), early endothelial progenitor cells (CD133+/VEGFR2+), and fibroblast growth factor in stroke patients. *Curr Neurovasc Res.* (2019) 16:19–26. doi: 10.2174/1567202616666190129164906
19. Blein S, Hawrot E, Barlow P. The metabotropic GABA receptor: molecular insights and their functional consequences. *Cell Mol Life Sci.* (2000) 57:635–50. doi: 10.1007/PL00000725
20. Philpott AL, Fitzgerald PB, Bailey NW, Churchyard A, Georgiou-Karistianis N, Cummins TD, et al. GABBR2 gene variant modifies pathophysiology in Huntington's disease. *Neurosci Lett.* (2016) 620:8–13. doi: 10.1016/j.neulet.2016.03.038
21. Samanta D, Zarate YA. Widening phenotypic spectrum of GABBR2 mutation. *Acta Neurol Belg.* (2019) 119:493–6. doi: 10.1007/s13760-019-01088-5
22. Carmeliet P, Jain RK. Molecular mechanisms and clinical applications of angiogenesis. *Nature.* (2011) 473:298–307. doi: 10.1038/nature10144
23. Del PN, Pignataro F. The role of endothelial progenitors in the repair of vascular damage in systemic sclerosis. *Front Immunol.* (2018) 9:1383. doi: 10.3389/fimmu.2018.01383
24. Kirton JP, Xu Q. Endothelial precursors in vascular repair. *Microvasc Res.* (2010) 79:193–9. doi: 10.1016/j.mvr.2010.02.009
25. Verloop RE, Koolwijk P, van Zonneveld AJ, van Hinsbergh VW. Proteases and receptors in the recruitment of endothelial progenitor cells in neovascularization. *Eur Cytokine Netw.* (2009) 20:207–19. doi: 10.1684/ecn.2009.0174
26. Liu ZJ, Velazquez OC. Hyperoxia, endothelial progenitor cell mobilization, and diabetic wound healing. *Antioxid Redox Signal.* (2008) 10:1869–82. doi: 10.1089/ars.2008.2121
27. Sun R, Huang J, Sun B. Mobilization of endothelial progenitor cells in sepsis. *Inflamm Res.* (2020) 69:1–9. doi: 10.1007/s00011-019-01299-9
28. Krutzfeldt A, Spahr R, Mertens S, Siegmund B, Piper HM. Metabolism of exogenous substrates by coronary endothelial cells in culture. *J Mol Cell Cardiol.* (1990) 22:1393–404. doi: 10.1016/0022-2828(90)90984-A
29. Culic O, Gruwel ML, Schrader J. Energy turnover of vascular endothelial cells. *Am J Physiol.* (1997) 273:C205–13. doi: 10.1152/ajpcell.1997.273.1.C205
30. Rohlenova K, Veys K, Miranda-Santos I, De Bock K, Carmeliet P. Endothelial cell metabolism in health and disease. *Trends Cell Biol.* (2018) 28:224–36. doi: 10.1016/j.tcb.2017.10.010

Conflict of Interest: The authors declare that the research was conducted in the absence of any commercial or financial relationships that could be construed as a potential conflict of interest.

Publisher's Note: All claims expressed in this article are solely those of the authors and do not necessarily represent those of their affiliated organizations, or those of the publisher, the editors and the reviewers. Any product that may be evaluated in this article, or claim that may be made by its manufacturer, is not guaranteed or endorsed by the publisher.

Copyright © 2021 Zhang, Zhou, Yuan, Nan and Liu. This is an open-access article distributed under the terms of the Creative Commons Attribution License (CC BY). The use, distribution or reproduction in other forums is permitted, provided the original author(s) and the copyright owner(s) are credited and that the original publication in this journal is cited, in accordance with accepted academic practice. No use, distribution or reproduction is permitted which does not comply with these terms.

frontiers in Cardiovascular Medicine

REVIEW
published: 20 September 2021
doi: 10.3389/fcvm.2021.739095

Advances in Cardiotoxicity Induced by Altered Mitochondrial Dynamics and Mitophagy

*Yiyuan Yin and Haitao Shen**

Department of Emergency Medicine, ShengJing Hospital of China Medical University, Shenyang, China

Mitochondria are the most abundant organelles in cardiac cells, and are essential to maintain the normal cardiac function, which requires mitochondrial dynamics and mitophagy to ensure the stability of mitochondrial quantity and quality. When mitochondria are affected by continuous injury factors, the balance between mitochondrial dynamics and mitophagy is broken. Aging and damaged mitochondria cannot be completely removed in cardiac cells, resulting in energy supply disorder and accumulation of toxic substances in cardiac cells, resulting in cardiac damage and cardiotoxicity. This paper summarizes the specific underlying mechanisms by which various adverse factors interfere with mitochondrial dynamics and mitophagy to produce cardiotoxicity and emphasizes the crucial role of oxidative stress in mitophagy. This review aims to provide fresh ideas for the prevention and treatment of cardiotoxicity induced by altered mitochondrial dynamics and mitophagy.

Keywords: mitochondrial dynamics, cardiotoxicity, mitophagy, mitochondrial fission, mitochondrial fusion

OPEN ACCESS

Edited by:
Haiyang Tang,
University of Arizona, United States

Reviewed by:
Pritesh Jain,
University of California, San Diego, United States
Stephen C. Kolwicz Jr,
Ursinus College, United States

****Correspondence:***
Haitao Shen
shenht@sj-hospital.org

Specialty section:
This article was submitted to Cardiovascular Metabolism, a section of the journal Frontiers in Cardiovascular Medicine

Received: *10 July 2021*
Accepted: *27 August 2021*
Published: *20 September 2021*

Citation:
Yin Y and Shen H (2021) Advances in Cardiotoxicity Induced by Altered Mitochondrial Dynamics and Mitophagy. Front. Cardiovasc. Med. 8:739095. doi: 10.3389/fcvm.2021.739095

INTRODUCTION

As the body's "power plant," heart is the body's largest oxygen and energy consumption organ. Therefore, mitochondria, as the core organelles of oxidative phosphorylation, play an important role in maintaining cardiac homeostasis. Under normal conditions, cardiac cells regulate the dynamic balance of mitochondria through a variety of signal pathways, remove damaged mitochondria through the process of mitochondrial fission, fusion and autophagy, and maintain the normal cardiac function. However, injury factors such as hypoxia, oxidative stress, poisoning, and hyperglycemia can cause abnormalities in mitochondrial dynamics and mitophagy, resulting in cardiotoxicity. Therefore, interventional treatment for different injury factors is of great significance for improving cardiotoxicity induced by altered mitochondrial dynamics and mitophagy.

CONCEPT OF MITOCHONDRIAL DYNAMICS AND MITOPHAGY

Mitochondria are critical organelles of eclectic cells and can reach 25–35% of cell volume (1–3). They have a phospholipid bimolecular membrane structure and play a crucial role in maintaining normal functionality in cells and metabolizing steady state. Moreover, they are also the primary locations for the oxidative metabolism of cells. Also, mitochondria have a mediated effect on cell proliferation or apoptosis, regulation of nuclear gene expression,

and innate immunity (4, 5). Under normal physiological conditions, mitochondria produce ATP through the tricarboxylic acid cycle to meet the energy needs of the heart (6–8). It is not only the power plant of the cell, but also the center of signal transmission including calcium homeostasis (9, 10), which ensure the normal operation of the mitochondrial electron transport chain to maintain the normal cardiac function (11, 12). In the electron transport chain, premature leakage of electrons will lead to the production of physiological reactive oxygen species (ROS), and a small amount of ROS can be decomposed by superoxide dismutase (SOD) and glutathione (GSH) in the mitochondria (9, 10, 13). When the mitochondria is in an abnormal state, the tricarboxylic acid cycle and calcium homeostasis are destroyed, and the mitochondrial membrane potential dissipation in turn leads to the disorder of the electron transport chain and the accumulation of ROS (14, 15). The original mitochondrial quality of cardiac cells cannot maintain the normal function of cardiac cells, resulting in cardiac dysfunction and cardiotoxicity (6, 16, 17).

Although mitochondria are usually described as independent organelles, they actually form a dynamic equilibrium network maintained by mitochondrial dynamics, which is essential for maintaining normal cell metabolism. In mitochondrial structures, the outer mitochondrial membranes (OMM) comprises a relatively smooth lipid double layer, and the inner mitochondrial membrane (IMM) folds inwards to form a structure called argon (18). The fission of membranes and outer membranes in mitochondria is a critical event in mitochondrial fission; it is a process that divides a single mitochondrion into two mitochondria, guided by a dynamin-related protein 1 (DRP1) (19). Mitochondrial fusion is divided into outer membrane fusion and endometrial fusion, the balance of which determines the connectivity of the network (20).

Mitophagy is the process that identifies damaged mitochondria in cells, which in turn binds to autophagy-related proteins to create autophagic small bodies. These bodies are degraded by fusion with lysosomes (21). Generally, mitochondria are abundant in cardiac cells, making the cardiac cells more sensitive to alterations in mitochondrial functionality (22). Under normal circumstances, a certain mitophagy level promptly removes damage to aging mitochondria and metabolic toxic substances, promotes mitochondrial renewal, and ensures the survival of cells (23–25).

THE PHYSIOLOGICAL STATE OF MITOCHONDRIAL DYNAMICS AND MITOPHAGY

Cardiotoxicity is caused by altered mitochondrial dynamics and mitophagy (26, 27). The cardiac cells can remove dysfunctional mitochondria through mitochondrial fission, fusion, and autophagy. The process has a direct regulatory effect on the quantity and quality of the cardiac mitochondria. Thus, it ensures the stability of the inner environment of cardiac cells (28–32). Under normal physiological conditions, mitochondria are constantly updated to sustain healthy cardiac functionality. Moreover, it can promote the formation of new mitochondria and maintain the cardiac continuous contraction. At this stage, the cardiac can promptly remove damaged mitochondria through fission, fusion, and autophagy, and facilitate the recovery of effective cellular components, such as proteins, deoxyribonucleic acid (DNA), etc., to ensure the normal metabolism of updated cells, thus compensate to ensure the nominal function of mitochondria to maintain the cardiac continuous contraction state (33).

It is generally believed that fission and fusion are carried out at the same time and are dynamically balanced, and fission is often regarded as a prerequisite for mitophagy (34–37). Parkin, the key protein of mitophagy, can induce ubiquitination or degradation of MFN1/2, thereby inhibiting mitochondrial fusion (38, 39). The significance of mitophagy for fusion is that when damaged mitochondria fuse with healthy mitochondria, a larger damaged mitochondria will be formed, which can activate mitophagy and maintain mitochondrial homeostasis (34, 40–42). In mitochondrial fission, fusion and mitophagy, mitochondrial autophagy plays a central role (34).

Mitochondrial Fission

Mitochondrial fission is divided into the fission of membranes and outer membranes in mitochondria and is regulated by DRP1 (43, 44). DRP1 is classified as a homologous protein of guanosine triphosphate (GTP) hydrolyzed enzyme (GTPase) power protein. It has an active role in endocytosis and is a key regulatory factor in mitochondrial fission, primarily located in cell pulp (20, 45, 46).

The serine 637 (S637) phosphorylation of DRP1 inhibits the translocation of mitochondria DRP1 and its GTPase activity. Meanwhile, serine 616 (S616) phosphorylation elevates the DRP1 activity, which splits the mitochondria. During the fission process, mitochondrial fission 1 (FIS1) protein, mitochondrial fission factor (MFF), 49 kDa mitochondrial dynamic protein (MiD49), and 51 kDa mitochondrial kinetic protein (MiD51) induce DRP1 phosphorylation to recruit DRP1 into the mitochondrial outer membrane. Afterward, the DRP1 oligopoly reaction at the fission point of the OMM self-assembles to create a spiral structure. It forms a cleavage ring that shrinks and shears the mitochondrial outer and inner membranes and breaking the mitochondria (47–54). Notably, FIS1 is distributed throughout the outer membrane, while MFF is dotted, showing a stronger interaction with DRP1 than FIS1. FIS1 and MFF can independently promote the collection and oligopoly of the mitochondrial outer membrane, yet, MFF plays a more critical role. Besides, in the absence of MFF and FIS1, MiD49 and MiD51 can recruit DRP1 to the mitochondria (49).

Furthermore, cyclase-associated protein (CAP) are recently discovered split-promoting proteins that induce the oligomerization of DRP1 and the expression of FIS1, which promotes DRP1-mediated mitochondrial fission (55).

Mitochondrial Fusion

Mitochondrial fusion is divided into outer membrane fusion and endometrial fusion. It is regulated by a variety of proteins, including mitofusin (MFN) in the outer membrane of mitochondria and optic atrophy protein 1 (OPA1) (44,

45, 49, 51, 56–61). Among them, mitofusin 1 (MFN1) and mitofusin 2 (MFN2) regulate mitochondrial outer membrane fusion. MFN1 positioned mitochondria and MFN2 positioned mitochondria and endoplasmic reticulum. MFN1 and MFN2 form a stable homologous dimer through their GTPase domain. Next, hydrolyzed GTP and the outer membrane of the two mitochondria are combined and fused, which is critical for outer membrane fusion (49, 52, 54, 56).

The OPA1 regulates the fusion of the IMM. OPA1 is treated with mitochondrial processing peptide (MPP) enzyme to produce a long-form OPA1 (L-OPA1) of membrane binding, and then positioned as intermembrane space AAA (i-AAA) protease in the membrane of the mitochondria IMM peptide enzymes and mitochondrial AAA (m-AAA) protease are further cut into short -form OPA1 (S-OPA1). Afterward, the mitochondrial membranes are arranged into two layers of film while maintaining the fidelity of the mitochondrial crucible structure and promoting endometrial fusion (49, 58, 62).

Mitophagy

Mitophagy is an autophagy process that is regulated by several mechanisms and protein molecules. However, it is different than ordinary autophagy and is highly selective (63, 64). Presently, three major pathways can induce and activate mitophagy: PTEN-induced kinase 1 (PINK1)-Parkin signaling pathway, BCL2 interacting protein 3 (BNIP3)/NIP3-like protein X (NIX) pathway, and the FUN14 domain containing 1 (FUNDC1) signaling pathway. Out of the three, the PINK1-Parkin signaling pathway is the most characteristic and significant autophagy pathway (65–67). In mitophagy, different pathways cooperate and coordinate to sustain the normal functionality in cells.

The PINK1-Parkin Signaling Pathway

PINK1 is a mitochondrial serine-threonine protein kinase. When the mitochondrial membrane potential decreases, the PINK1-Parkin signaling pathway PINK1 aggregates in the mitochondrial membrane's outer membrane and activates Parkin on damaged mitochondria (68–76). Generally, PINK1 is less expressed. It enters the mitochondria, anchors the mitochondrial intima through the mediation of outer membrane-related proteins. Under external stimulation or pathological conditions, mitochondrial depolarization can cause PINK1 translocation to mitochondria's outer membrane. Afterward, it catalyzes ubiquitin phosphorylation to activate the Parkin receptor binding Parkin and initiate mitophagy (30, 70, 77–85). Moreover, the PINK1-Parkin pathway is also the primary mechanism of Zinc induced mitophagy (86).

BNIP3/NIX Pathway

BNIP3 (also known as NIX) is a member of the Bcl-2 protein family. It is a form of a mitochondrial outer membrane protein with a biphasic effect. The phosphorylation of their microtubule-associated protein 1A/1B-light chain 3 (LC3)-interacting region (LIR) binds to LC3-phosphatidylethanolamine conjugate light chain 3 (LC3II), which is involved in mitophagy and plays a significant role in myocardial mitochondrial regeneration (24, 87–89). The hypoxia inducible factor 1 subunit alpha (HIF-1α) can bind to the BNIP3 promoter to induce BNIP3, and BNIP3 expression can also promote PINK1 translocation, and then induce mitophagy (90). Reportedly, the cardiac dual-specificity phosphatase-1 (DUSP1) also induces BNIP3 expression and promotes mitophagy (91).

FUNDC1 Signaling Pathway

The FUNDC1 is a highly conserved mitochondrial outer membrane protein. Similar to BNIP3/NIX, it directly interacts with LC3 through the N end, mediating hypoxia-induced mitophagy, which is widely expressed in various cells, tissues, and organs, particularly heart (63, 79, 88, 90, 92, 93). Under normal oxygen conditions, FUNDC1 phosphorylated by semi refined carrageenan (SRC) kinases and Casein kinase II (CK2) decreases their affinity to LC3, which effectively inhibits mitophagy. FUNDC1 was dephosphorylated by serine 13-position phosphatase, such as PGAM family member 5 (PGAM5), triggering its association with LC3, thereby enhancing mitophagy (23, 88, 93).

Biogenesis

Mitochondrial biogenesis is also considered to be an important factor in maintaining mitochondrial homeostasis. It is a complex process involving the synthesis of mitochondrial inner and outer membranes and mitochondrial-encoded proteins, the synthesis and input of mitochondrial-encoded proteins, and the replication of mitochondrial DNA (mtDNA) (94–97), which is mainly regulated by PPARG Coactivator 1 Alpha (PGC-1α) and Nuclear Respiratory Factor 1 (NRF1), and can be defined as "the process of producing new components of the mitochondrial network" (98–100). Some scholars evaluate the biogenesis of mitochondria by measuring the rate of mitochondrial protein synthesis. Mitochondrial biogenesis and mitophagy coordinately regulate the molecular mechanism of mitochondrial homeostasis (101–104). On the one hand, the process of mitochondrial biogenesis is accompanied by mitophagy, on the other hand, abnormal mitophagy can feedback and inhibit mitochondrial biogenesis, and the PGC-1α-NRF1-FUNDC1 pathway plays a key role in it, cooperating to maintain the quality and quantity of mitochondria (96, 97, 105, 106).

THE PATHOPHYSIOLOGICAL STATE OF MITOCHONDRIAL DYNAMICS AND MITOPHAGY

When cardiac cells are stimulated by mechanical traction, ischemia-reperfusion injury, and oxidative stress, they can cause changes in the shape, structure and function of the heart (107–110). Multiple signal pathways are activated when the heart is stimulated by pathogenic factors, such as mitogen-activated protein kinase signaling pathway, calcineurin (CaN) signaling pathways, protein kinase A signaling pathways and angiotensin type I receptors cause calcium homeostasis to be destroyed and calcium overload, which ultimately leads to cardiac pathophysiological changes (111–114). When excessive or continuous stress acts on the heart, the mitochondrial

energy metabolism function and quality control system are seriously disturbed, which exceeds the self-regulation range of mitochondrial dynamics and mitophagy. On the one hand, it causes the energy metabolism of cardiac cells to become impaired, on the other hand, the mtDNA and ROS released by damaged mitochondria accumulate to reach a toxic concentration, which together lead to cardiotoxicity (25, 66, 115–117), the process of cardiotoxicity caused by different injury factors is shown in **Figure 1**. Cardiotoxicity refers to cardiac damage caused by excessive accumulation of endogenous or exogenous substances to reach a toxic concentration (118). Generally speaking, cardiotoxicity can cause cardiac electrophysiological dysfunction or myocardial damage (119). Moreover, mitochondrial dynamics play a vital role in the onset of nervous system diseases, implying that mitochondrial dynamics disorders may have damaging effects on cardiac neuronal cells (120).

In addition, among smoking and obesity people, the cardiovascular morbidity has increased significantly (121–126). It has been reported that smoking and obesity can cause abnormal mitochondrial dynamics and mitophagy (127–131). Therefore, smoking and obesity may also lead to mitochondrial damage, which in turn causes cardiac dysfunction, leading to cardiotoxicity.

Hypoxia

Generally, hypoxia refers to any kind of physiological oxygen deficiency or tissue oxygen demand deficiency state and the integration of local responses defines hypoxia as a paradigm of reactions affecting the entire body (86, 132, 133). Studies have shown that inhibiting the breathing of rats caused obvious cardiotoxicity (79, 134–138).

Mitochondrial Fission, Fusion, and Hypoxia

During mitochondrial fission, lack of oxygen can increase the production of 4-hydroxyethyl ether (4-HNE) to promote the S616 phosphorylation of DRP1 to induce mitochondrial fission. Besides, in the presence of histone deacetylase 6 (HDAC6), hypoxia can promote mitochondrial fusion by inducing the binding of HDAC6 with MFN2, causing mitochondrial dysfunction (139–141).

Mitophagy and Hypoxia

Hypoxia can be specifically activated by FUNDC1; under normal conditions, FUNDC1 is highly conserved and stable in mitochondria's outer membrane. During hypoxia, it is FUNDC1 dephosphorylated by 13 phosphatases (such as PGAM5) of serine, triggering its binding to LC3 and improving mitophagy activity. It removes damaged mitochondria (23, 79, 88, 92, 93, 142–144). Hypoxia can activate poly (ADP-ribose) polymerase (PARP), promoting mitophagy by regulating mitochondrial membrane potential and inducing cardiomyocyte apoptosis, ROS is central for PARP mediated mitochondrial membrane potential ($\Delta\Psi$m) decline, and inhibited PARP can reduce the production after injury (80). Moreover, the activation of FUNDC1 is vital in platelet aggregation. Past studies have demonstrated that lacking the FUNDC1 gene can make the mitochondrial function of blood platelet disordered. In long-term hypoxia, it will eventually form a microthrombus and lead to cardiac microvascular structure destruction (79, 145).

Oxidative Stress

Oxidative stress (OS) is a state of imbalance between oxidation and antioxidant effect in the body. It produces several destructive products, such as ROS, which has an adverse impact on the body and is often considered to be a crucial factor that leads to aging and disease (146, 147). OS is caused by the imbalance between ROS and endogenous antioxidants in response to injury, which can lead to cardiotoxicity (148). ROS is a collective common term that includes highly oxidative radicals such as hydroxyl (OH-) and superoxide (O2•-) radicals, and non-radical species such as hydrogen peroxide (H2O2) (149–151). Antioxidants in the mitochondria, such as superoxide dismutase (SOD) and glutathione (GSH), will rapidly degrade or sequester O2·-, thereby reducing reactivity (152–154). Due to the high concentration of mitochondria in myocardial tissue, reduced mitochondrial antioxidant capacity results in cardiac dysfunction (155–157). In addition, ROS is involved in a series of vascular diseases associated with the functional properties of the endothelial cell barrier (158–160).

Reportedly, ROS can significantly promote the activity of DRP1 to increase the mitochondrial fission frequency, resulting in mitochondrial dysfunction. Oxidative stress can significantly increase the expression of WD repeat domain 26 (WDR26) protein, which is a critical medium for PINK1-Parkin signaling pathways to induce cell mitophagy and depolarize mitochondria by elevating the mitochondrial membrane potential, causing PINK1 to transpose, which in turn catalyzes ubiquitin phosphorylation to activate the Parkin receptor (70, 78–80, 161). Parkin is dependent on p53, it triggers mitophagy through autophagy small body lysosome pathways and then degrades through autophagy-lysosome pathways. Moreover, oxidative stress could also lead to an extended opening time for mitochondrial permeability transition pore (mPTP), releasing apoptosis factors such as cytochrome c into the matrix, damaging cells (162–164). Meanwhile, ROS activates multiple inflammatory pathways such as NLR family pyrin domain containing 3 (NLRP3)-mediated inflammatory responses. And the inhibition of mitophagy further aggravates these inflammatory responses and exacerbates damage (165). During myocardial ischemic re-perfusion injury (MIRI), the cell ischemia hypoxia activates PINK1/Parkin-mediated mitophagy and then removes the defective mitochondria. Afterward, restores the intracellular steady-state to offset the damage inflicted by hypoxia. In the case where Parkin is lacking, it will further aggravate ischemia re-perfusion damage and inflict damage to the heart (78, 166–170). Uncoupling protein 2 (UCP2) and vitamin D interferes with abnormal mitophagy to protect the damaged cardiac from ischemic re-injection (171, 172). Moreover, oxidative stress reactions can also activate mitophagy through BNIP3/NIX and ROS promotes BNIP3 expression by activating the HIF-1α, which subsequentially induces mitophagy (89, 90). Reportedly, the oxidative stress response is a crucial cause of mitophagy disorders in diabetic

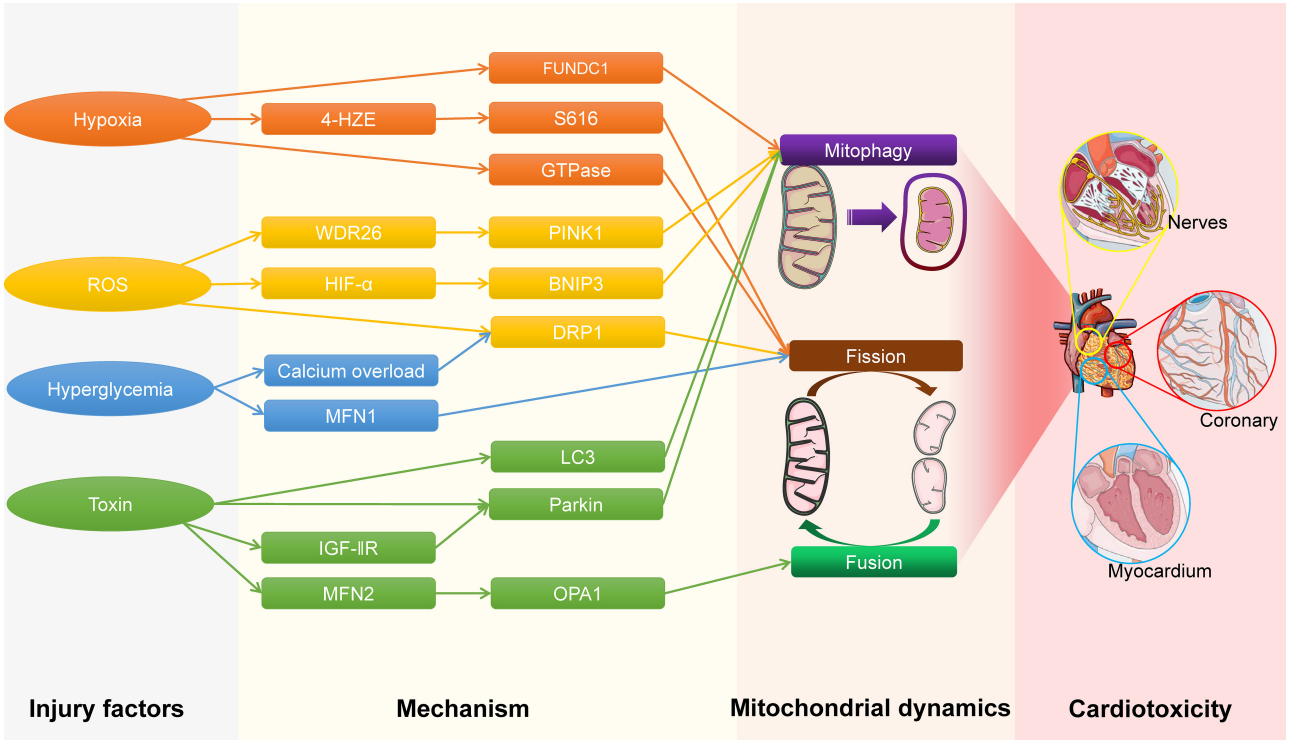

FIGURE 1 | The process of cardiotoxicity caused by different injury factors.

patients (24). In addition, membrane associated Ring-CH-Type Finger 5 (MARCHF5) and cellular communication network factor 1 (CCN1/Cyr61) are protein molecules located in the mitochondrial outer membrane, these proteins also play a vital role in the autophagy process of mitochondria, reducing expression during oxidative stress, and further inhibits mitophagy (173, 174).

Hyperglycemia

Studies have shown that hyperglycemia can increase the opening of mPTP by causing mitochondrial rupture and stimulating the generation of ROS, leading to the release of cytochrome c into the cytoplasm to activate the NLRP3 inflammasome (175–177). Subsequently, NLRP3 activates downstream nuclear factors to cause the release of inflammatory factors such as TNF-α and IL-6 further promotes the occurrence of inflammation, which well-explains the pathogenesis of diabetic cardiomyopathy (178–180).

Hyperglycemia causes calcium overload by activating the ORAI calcium release-activated calcium modulator 1 (ORAI1) channel-mediated Ca^{2+} internal flow pathway. It would induce S616 phosphorylation to further advance the expression of DRP1 and inhibit the MFN1 gene expression, as well as promote mitochondria fission, resulting in mitochondrial dysfunction (53, 181, 182). Moreover, protein kinase A activity is significantly inhibited at low glucose levels, enhancing the positioning capacity of DRP1 on the outer membrane of the mitochondria, which significantly increases the rate of mitochondrial fission (183). Past studies have established that hunger or reduced insulin signals are a strong trigger for autophagy (92, 184, 185). Hyperglycemia can induce myocardial mitochondria division but inhibit mitophagy, causing the accumulation of functionally impaired mitochondria (57, 186, 187). Additionally, DRP1 and ROS have mutually reinforcing associations (188). As a result, oxidative stress reactions increase and ROS accumulates during hyperglycemia conditions, which further damages cardiac cells (24, 189).

Poisoning

Poisoning refers to the systemic damage caused by the poisoning amount of harmful substances after entering the human body. Cardiotoxicity caused by drugs is divided into type I cardiotoxicity and type II cardiotoxicity (190–193). Among them, type I cardiotoxicity is associated with irreversible cardiac cell injury and is typically caused by anthracyclines and conventional chemotherapeutic agents, such as doxorubicin (DOX), daunorubicin, taxane and so on (194–196). Type II cardiotoxicity, associated with reversible myocardial dysfunction, is generally caused by biologicals and targeted drugs, such as trastuzumab, pertuzumab, azidothymidine, sumatinib, cloflupine, and cocaine, ethanol, etc (197, 198). The above-mentioned drugs can cause cardiotoxicity by interfering with mitochondrial dynamics and mitophagy, and ROS plays an important role in this process (26, 199–202). Studies have shown that anthracyclines such as doxorubicin and daunorubicin accumulate in the heart by binding to cardiolipin in the inner mitochondrial membrane (198). Anthracyclines binds with high

affinity to the mitochondrial phospholipid cardiolipin, inhibits its function, stimulates ROS production, inhibits oxidative phosphorylation, and causes mitochondrial DNA damage. These events result in mitochondrial defects, leading to the opening of mPTP and the activation of cell death pathways, which precipitate myocardial dysfunction (27, 203, 204). In addition, recent experimental studies have found mitochondrial iron accumulation following doxorubicin to be the mediator of doxorubicin cardiotoxicity from redox cycling and oxidative injury. ABCB8, a mitochondrial transport protein facilitates the export of iron from the mitochondria. Doxorubicin reduces ABCB8 transporter in the mitochondria. Overexpression of ABCB8 protein or administration of dexrazoxane, an iron chelator reverses the anthracycline-induced mitochondrial iron overload and oxidative injury. It has been reported that the expression of TNF-α and IL-6 in the myocardial tissue and H9C2 cells treated with DOX increased significantly (1, 198, 205–208). Taxane further inhibits mitophagy by interfering with the normal microtubular transport function in the cardiomyocytes (26, 153, 198).

Unlike anthracyclines, trastuzumab induced left ventricular dysfunction (LVD) and congestive heart failure (CHF) are mostly reversible upon its discontinuation. At a molecular level, trastuzumab binds to the extracellular domain 4 of HER2 receptor, which prevents HER2 dimerization, activation and downstream signaling (190, 194–196). It may induce the occurrence of oxidative stress, which can also lead to the opening of mPTP and the activation of cell death pathways, leading to cardiac dysfunction (192, 209, 210). There are reports that drugs that cause type II cardiotoxicity can also enhance anthracycline cardiotoxicity, such as azidothymidine and rosiglitazone (193, 198, 211). In addition, there are some antidepressants and excessive metal elements, such as cloflupine, cocaine, antimony, mercury and so on (197, 212).

Mitochondrial Fission, Fusion and Poisoning

Poisoning can change the mitochondrial dynamically regulated protein expression. On the one hand, poisoning induces the expression of MFN2 and OPA1 in the cardiac tissue, which increases the mitochondrial length and organelle aspect ratio and excessive mitochondrial fusion. As a result, the activity of mitochondrial respiratory chains is reduced, which leads to severe cell defects (213–215). On the other hand, poisoning promotes apoptosis by promoting DRP1 phosphorylation, subsequentially leading to the fission of mitochondria in cardiac cells (216).

Mitophagy and Poisoning

Doxorubicin (DOX), organophosphorus, nicotine, excessive alcohol, and other toxic substances can also inhibit the expression of Parkin, deteriorate the mitophagy ability of cardiac cells, damage mitochondria, and destroyed substances in cardiac cells will continue to accumulate, causing cardiac damage (26, 217, 218). Moreover, the decrease of mitophagy can lead to excessive ROS in cardiac cells, further promote the release of cytochrome c and cysteine aspartate protease, disrupt the stability of mitochondria DNA, inhibit the activity of respiratory electron-transport chain, and reduce both oxygen utilization and consumption. It can even initiate mitochondrial apoptosis and induce mitochondrial damage (26, 88, 219–224). Parkin overexpression increases mitophagy, which aggravates cell death through poisoning. And, Parkin knockdown has the opposite effect (225, 226). DOX can also dysregulate the cytosolic and mitochondrial signaling axes, which leads to mitophagy destruction and arrhythmias, causing impaired mitochondrial clearance, the accumulation of dysfunctional mitochondria, ROS overload, and a lack of Adenosine triphosphate (ATP). Meanwhile, DOX can also phosphorylate BNIP3 and then inhibit mitophagy, which is closely related to the mitochondrial sirtuins (SIRT3-SIRT4) pathway (26, 27, 150, 206, 207, 221, 225, 227, 228). Recently, it was reported that excessive DOX can also significantly induce elevated insulin-like growth factor-II receptor (IGF-IIR) expression, IGF-IIR induces myocardial hypertrophy and cardiomyocyte death in a paracrine/autocrine manner. Concurrently, IGF-IIR can further promote mitophagy by inducing Parkin expression and cause cardiac damage (28, 229, 230).

THERAPEUTIC APPLICATION OF MITOCHONDRIAL DYNAMICS AND MITOPHAGY

Mitochondrial dynamics and mitophagy play an important role in cardiotoxicity, so they can be regarded as potential therapeutic targets. Cardiotoxicity can be treated, or its progress can be delayed by promoting or inhibiting mitochondrial dynamics and mitophagy, thus maintaining the functional stability of mitochondria and reducing cell damage under the influence of injury factors (**Table 1**).

Hypoxia preconditioning induced FUNDC1-dependent activation of mitophagy and decreased I/R-induced cardiac injury (79). Shaftaside is a natural flavonoid. Shaftaside and MYLS22 can effectively inhibit the expression of DRP1 and OPA1 to inhibit mitochondrial fission and reduce the cardiotoxicity induced by hypoxia, oxidative stress, hyperglycemia and poisoning (231). In healthy and MIRI rat cardiomyocytes, Zn and salidroside can activate mitophagy by up-regulating the expression of PINK1/Parkin, clear damaged mitochondria, and maintain normal cardiac function (86, 232–234). Myocardial mitochondrial function adapts to stress during acute exercise and manifests as significant upregulation of the mitophagy-related protein BNIP3, which stimulates mitophagy and minimizes myocardial injury. Melatonin and acute exercise preconditioning can activate the expression of PINK1 and BNIP3, respectively, to enhance mitophagy and decreased ROS-induced cardiac injury (235–242). Metformin can inhibit mitochondrial fission by the activation of MFN1 and the inhibition of DRP1, which decreased hyperglycemia -induced cardiotoxicity (176, 243–247).

CONCLUSIONS AND PROSPECTS

Mitochondrial dynamics and mitophagy are decisive factors for maintaining the homeostasis of the cardiac cell environment

TABLE 1 | Therapeutic application of mitochondrial dynamics and mitophagy.

Injury factors	Key protein	Representative interventions	Mechanisms	Effects to cardiotoxicity
Hypoxia	FUNDC1	Hypoxia preconditioning	Mitophagy	Protection
Hypoxia	DRP1	Schaftoside	Fission	Protection
OS	PINK1	Zine, Melatonin	Mitophagy	Protection
OS	BNIP3	Acute exercise	Mitophagy	Protection
OS	DRP1	Melatonin	Fission	Protection
Hyperglycemia	DRP1	Metformin	Fission	Protection
Hyperglycemia	MFN1	Metformin	Fission	Protection
Anthracyclines poisoning	BNIP3	Acute exercise	Mitophagy	Protection
Organophosphate poisoning	Parkin	Salidroside	Mitophagy	Protection
Nicotine poisoning	OPA1	MYLS22	Fusion	Protection

and ensuring the normal function of the cardiac. Hypoxia, hyperglycemia, and oxidative stress mainly interfere with mitochondrial fission and mitophagy to cause cardiotoxicity, while poisoning mainly interferes with mitochondrial fusion and mitophagy to cause cardiotoxicity. In view of different injury factors, taking different representative interventions to maintain the normal mitochondrial dynamics and mitophagy is of great significance for the prevention and treatment of cardiotoxicity. However, whether different therapeutic effects can be achieved through different routes of administration requires further research. Therefore, the exploration, regulation, and monitoring of the balance point in mitochondrial dynamics is crucial for preventing external injury factors from inducing cardiotoxicity. However, at the advent, the specific mechanism of action of mitochondrial dynamics and mitophagy in the process of cardiotoxicity is yet to be established. Extensive empirical studies are needed to study, confirm, and provide a theoretical basis for mitochondrial dynamics-induced cardiotoxicity, which would help prevent various causes of cardiotoxicity.

AUTHOR CONTRIBUTIONS

HS and YY contributed to conception and design of the study. YY wrote the first draft of the manuscript. All authors contributed to the article and approved the submitted version.

FUNDING

This study was funded by Science Foundation of Liaoning Education Department (FWZR2020012), 345 Talent Project of Shengjing Hospital, Science and Technology Department of Liaoning Province (2020JH2/10300126).

REFERENCES

1. Varricchi G, Ameri P, Cadeddu C, Ghigo A, Madonna R, Marone G, et al. Antineoplastic drug-induced cardiotoxicity: a redox perspective. *Front Physiol.* (2018) 9:167. doi: 10.3389/fphys.2018.00167
2. Luo Y, Ma J, Lu W. The significance of mitochondrial dysfunction in cancer. *Int J Mol Sci.* (2020) 21:5598. doi: 10.3390/ijms21165598
3. Vasquez-Trincado C, Garcia-Carvajal I, Pennanen C, Parra V, Hill JA, Rothermel BA, et al. Mitochondrial dynamics, mitophagy and cardiovascular disease. *J Physiol.* (2016) 594:509–25. doi: 10.1113/JP271301
4. Lazarou M. Keeping the immune system in check: a role for mitophagy. *Immunol Cell Biol.* (2015) 93:3–10. doi: 10.1038/icb.2014.75
5. Galluzzi L, Vitale I, Aaronson SA, Abrams JM, Adam D, Agostinis P, et al. Molecular mechanisms of cell death: recommendations of the nomenclature committee on cell death 2018. *Cell Death Differ.* (2018) 25:486–541. doi: 10.1038/s41418-017-0012-4
6. Appiah Kubi G, Pei D. Cell-penetrating and mitochondrion-targeting molecules. *Meth Enzymol.* (2020) 641:311–28. doi: 10.1016/bs.mie.2020.04.044
7. Bajpai P, Darra A, Agrawal A. Microbe-mitochondrion crosstalk and health: an emerging paradigm. *Mitochondrion.* (2018) 39:20–5. doi: 10.1016/j.mito.2017.08.008
8. Biner O, Schick T, Ganguin AA, von Ballmoos C. Towards a synthetic mitochondrion. *Chimia.* (2018) 72:291–6. doi: 10.2533/chimia.2018.291
9. Kuang S, Sun L, Zhang X, Liao X, Rees TW, Zeng L, et al. A mitochondrion-localized two-photon photosensitizer generating carbon radicals against hypoxic tumors. *Angew Chem Int Ed Engl.* (2020) 59:20697–703. doi: 10.1002/anie.202009888
10. Roth KG, Mambetsariev I, Kulkarni P, Salgia R. The mitochondrion as an emerging therapeutic target in cancer. *Trends Mol Med.* (2020) 26:119–34. doi: 10.1016/j.molmed.2019.06.009
11. Yang X, Zhang D, Li J, Ji W, Yang N, Gu S, et al. A mitochondrion-targeting Mn(ii)-terpyridine complex for two-photon photodynamic therapy. *Chem Commun.* (2020) 56:9032–5. doi: 10.1039/D0CC02051F
12. Zhuang Y, Li L, Feng L, Wang S, Su H, Liu H, et al. Mitochondrion-targeted selenium nanoparticles enhance reactive oxygen species-mediated cell death. *Nanoscale.* (2020) 12:1389–96. doi: 10.1039/C9NR09039H
13. Hampl V, Cepička I, Eliáš M. Was the mitochondrion necessary to start eukaryogenesis? *Trends Microbiol.* (2019) 27:96–104. doi: 10.1016/j.tim.2018.10.005
14. Chan DC. Mitochondrial dynamics and its involvement in disease. *Annu Rev Pathol.* (2020) 15:235–59. doi: 10.1146/annurev-pathmechdis-012419-032711
15. Zimorski V, Rauch C, van Hellemond JJ, Tielens AGM, Martin WF. The mitochondrion of euglena gracilis. *Adv Exp Med Biol.* (2017) 979:19–37. doi: 10.1007/978-3-319-54910-1_2
16. Annesley SJ, Fisher PR. Mitochondria in health and disease. *Cells.* (2019) 8:680. doi: 10.3390/cells8070680
17. Yang Y, Li T, Li Z, Liu N, Yan Y, Liu B. Role of mitophagy in cardiovascular disease. *Aging Dis.* (2020) 11:419–37. doi: 10.14336/AD.2019.0518

18. Shah M, Chacko LA, Joseph JP, Ananthanarayanan V. Mitochondrial dynamics, positioning and function mediated by cytoskeletal interactions. *Cell Mol Life Sci.* (2021) doi: 10.1007/s00018-021-03762-5
19. Xian H, Liou YC. Functions of outer mitochondrial membrane proteins: mediating the crosstalk between mitochondrial dynamics and mitophagy. *Cell Death Differ.* (2021) 28:827–42. doi: 10.1038/s41418-020-00657-z
20. Fenton AR, Jongens TA, Holzbaur ELF. Mitochondrial dynamics: shaping and remodeling an organelle network. *Curr Opin Cell Biol.* (2021) 68:28–36. doi: 10.1016/j.ceb.2020.08.014
21. Martinet W, Schrijvers DM, Timmermans JP, Bult H. Interactions between cell death induced by statins and 7-ketocholesterol in rabbit aorta smooth muscle cells. *Br J Pharmacol.* (2008) 154:1236–46. doi: 10.1038/bjp.2008.181
22. Morales CR, Pedrozo Z, Lavandero S, Hill JA. Oxidative stress and autophagy in cardiovascular homeostasis. *Antioxid Redox Signal.* (2014) 20:507–18. doi: 10.1089/ars.2013.5359
23. Davidson SM, Adameová A, Barile L, Cabrera-Fuentes HA, Lazou A, Pagliaro P, et al. Mitochondrial and mitochondrial-independent pathways of myocardial cell death during ischaemia and reperfusion injury. *J Cell Mol Med.* (2020) 24:3795–806. doi: 10.1111/jcmm.15127
24. Qiu Z, Ming H, Lei S, Zhou B, Zhao B, Yu Y, et al. Roles of HDAC3-orchestrated circadian clock gene oscillations in diabetic rats following myocardial ischaemia/reperfusion injury. *Cell Death Dis.* (2021) 12:43. doi: 10.1038/s41419-020-03295-y
25. Wang Y, Zhang C, Shen Z, Kou R, Xie K, Song F. Activation of PINK1-Parkin-dependent mitophagy in Tri-ortho-cresyl phosphate-treated Neuro2a cells. *Chem Biol Int.* (2019) 308:70–79. doi: 10.1016/j.cbi.2019.05.025
26. Bartlett JJ, Trivedi PC, Pulinilkunnil T. Autophagic dysregulation in doxorubicin cardiomyopathy. *J Mol Cell Cardiol.* (2017) 104:1–8. doi: 10.1016/j.yjmcc.2017.01.007
27. Koleini N, Kardami E. Autophagy and mitophagy in the context of doxorubicin-induced cardiotoxicity. *Oncotarget.* (2017) 8:46663–80. doi: 10.18632/oncotarget.16944
28. Pandey S, Kuo W-W, Shen C-Y, Yeh Y-L, Ho T-J, Chen R-J, et al. Insulin-like growth factor II receptor-α is a novel stress-inducible contributor to cardiac damage underpinning doxorubicin-induced oxidative stress and perturbed mitochondrial autophagy. *Am J Physiol Cell Physiol.* (2019) 317:C235–43. doi: 10.1152/ajpcell.00079.2019
29. Xin T, Lu C. Irisin activates opa1-induced mitophagy to protect cardiomyocytes against apoptosis following myocardial infarction. *Aging.* (2020) 12:4474–88. doi: 10.18632/aging.102899
30. Guan L, Che Z, Meng X, Yu Y, Li M, Yu Z, et al. MCU Up-regulation contributes to myocardial ischemia-reperfusion injury through calpain/OPA-1–mediated mitochondrial fusion/mitophagy inhibition. *J Cell Mol Med.* (2019) 23:7830–43. doi: 10.1111/jcmm.14662
31. Wang S, Wang L, Qin X, Turdi S, Sun D, Culver B, et al. ALDH2 contributes to melatonin-induced protection against APP/PS1 mutation-prompted cardiac anomalies through cGAS-STING-TBK1-mediated regulation of mitophagy. *Sig Transd Targ Ther.* (2020) 5:119. doi: 10.1038/s41392-020-0171-5
32. Hu Y, Wang X, Li Q, Pan Y, Xu L. Salvianolic acid B alleviates myocardial ischemic injury by promoting mitophagy and inhibiting activation of the NLRP3 inflammasome. *Mol Med Rep.* (2020) 22:5199–208. doi: 10.3892/mmr.2020.11589
33. Chiao YA, Kolwicz SC, Basisty N, Gagnidze A, Zhang J, Gu H, et al. Rapamycin transiently induces mitochondrial remodeling to reprogram energy metabolism in old hearts. *Aging.* (2016) 8:314–27. doi: 10.18632/aging.100881
34. Xie LL, Shi F, Tan Z, Li Y, Bode AM, Cao Y. Mitochondrial network structure homeostasis and cell death. *Cancer Sci.* (2018) 109:3686–94. doi: 10.1111/cas.13830
35. Bhargava P, Schnellmann RG. Mitochondrial energetics in the kidney. *Nat Rev Nephrol.* (2017) 13:629–46. doi: 10.1038/nrneph.2017.107
36. Chiurazzi M, Di Maro M, Cozzolino M, Colantuoni A. Mitochondrial dynamics and microglia as new targets in metabolism regulation. *Int J Mol Sci.* (2020) 21:3450. doi: 10.3390/ijms21103450
37. Ding M, Liu C, Shi R, Yu M, Zeng K, Kang J, et al. Mitochondrial fusion promoter restores mitochondrial dynamics balance and ameliorates diabetic cardiomyopathy in an optic atrophy 1-dependent way. *Acta Physiol.* (2020) 229:e13428. doi: 10.1111/apha.13428
38. Michurina SS, Stafeev IS, Menshikov MY, Parfyonova YV. Mitochondrial dynamics keep balance of nutrient combustion in thermogenic adipocytes. *Mitochondrion.* (2021) 59:157–68. doi: 10.1016/j.mito.2021.05.001
39. Simula L, Nazio F, Campello S. The mitochondrial dynamics in cancer and immune-surveillance. *Semin Cancer Biol.* (2017) 47:29–42. doi: 10.1016/j.semcancer.2017.06.007
40. Zhong X, Cui P, Cai Y, Wang L, He X, Long P, et al. Mitochondrial dynamics is critical for the full pluripotency and embryonic developmental potential of pluripotent stem cells. *Cell Metab.* (2019) 29:979–92.e4. doi: 10.1016/j.cmet.2018.11.007
41. Serasinghe MN, Chipuk JE. *Mitochondrial fission in human diseases. Handb Exp Pharmacol.* (2017) 240:159–88. doi: 10.1007/164_2016_38
42. Wang Y, Liu HH, Cao YT, Zhang LL, Huang F, Yi C. The role of mitochondrial dynamics and mitophagy in carcinogenesis, metastasis and therapy. *Front Cell Dev Biol.* (2020) 8:413. doi: 10.3389/fcell.2020.00413
43. Houzelle A, Jörgensen JA, Schaart G, Daemen S, van Polanen N, Fealy CE, et al. Human skeletal muscle mitochondrial dynamics in relation to oxidative capacity and insulin sensitivity. *Diabetologia.* (2021) 64:424–36. doi: 10.1007/s00125-020-05335-w
44. Nomura R, Sato T, Sato Y, Medin JA, Kushimoto S, Yanagisawa T. Azidothymidine-triphosphate impairs mitochondrial dynamics by disrupting the quality control system. *Redox Biol.* (2017) 13:407–17. doi: 10.1016/j.redox.2017.06.011
45. Lam HYP, Chen CC, Chen TT, Chang KC, Wu WJ, Yang TH, et al. Mitochondrial dynamics in angiostrongylus cantonensis-infected mouse brain. *Parasitol Int.* (2021) 80:102231. doi: 10.1016/j.parint.2020.102231
46. Zhu H, Toan S, Mui D, Zhou H. Mitochondrial quality surveillance as a therapeutic target in myocardial infarction. *Acta Physiol.* (2021) 231:e13590. doi: 10.1111/apha.13590
47. McLean FH, Campbell FM, Langston RF, Sergi D, Resch C, Grant C, et al. A high-fat diet induces rapid changes in the mouse hypothalamic proteome. *Nutr Metab.* (2019) 16:26. doi: 10.1186/s12986-019-0352-9
48. Lu Y, Chen L, Ye J, Chen C, Zhou Y, Li K, et al. Surgery/Anesthesia disturbs mitochondrial fission/fusion dynamics in the brain of aged mice with postoperative delirium. *Aging.* (2020) 12:844–65. doi: 10.18632/aging.102659
49. Li R, Toan S, Zhou H. Role of mitochondrial quality control in the pathogenesis of nonalcoholic fatty liver disease. *Aging.* (2020) 12:6467–85. doi: 10.18632/aging.102972
50. Liu X, Zhao X, Li X, Lv S, Ma R, Qi Y, et al. PM(2.5) triggered apoptosis in lung epithelial cells through the mitochondrial apoptotic way mediated by a ROS-DRP1-mitochondrial fission axis. *J Hazard Mater.* (2020) 397:122608. doi: 10.1016/j.jhazmat.2020.122608
51. Wang Z, White A, Wang X, Ko J, Choudhary G, Lange T, et al. Mitochondrial fission mediated cigarette smoke-induced pulmonary endothelial injury. *Am J Respir Cell Mol Biol.* (2020) 63:637–51. doi: 10.1165/rcmb.2020-0008OC
52. Yu R, Lendahl U, Nistér M, Zhao J. Regulation of mammalian mitochondrial dynamics: opportunities and challenges. *Front Endocrinol.* (2020) 11:374. doi: 10.3389/fendo.2020.00374
53. Wu QR, Zheng DL, Liu PM, Yang H, Li LA, Kuang SJ, et al. High glucose induces Drp1-mediated mitochondrial fission via the orai1 calcium channel to participate in diabetic cardiomyocyte hypertrophy. *Cell Death Dis.* (2021) 12:216. doi: 10.1038/s41419-021-03502-4
54. Wu L, Kang Z, Qiao N, Wang C, Tang Z. Cu-induced mitochondrial dysfunction is mediated by abnormal mitochondrial fission through oxidative stress in primary chicken embryo hepatocytes. *J Trace Elem Med Biol.* (2021) 65:126721. doi: 10.1016/j.jtemb.2021.126721
55. Shang X, Zhang Y, Xu J, Li M, Wang X, Yu R. SRV2 promotes mitochondrial fission and Mst1-Drp1 signaling in LPS-induced septic cardiomyopathy. *Aging.* (2020) 12:1417–32. doi: 10.18632/aging.102691
56. Han H, Tan J, Wang R, Wan H, He Y, Yan X, et al. PINK1 phosphorylates Drp1(S616) to regulate mitophagy-independent mitochondrial dynamics. *EMBO Rep.* (2020) 21:e48686. doi: 10.15252/embr.201948686
57. Saotome M, Ikoma T, Hasan P, Maekawa Y. Cardiac insulin resistance in heart failure: the role of mitochondrial dynamics. *Int J Mol Sci.* (2019) 20:3552. doi: 10.3390/ijms20143552

58. Han H, Li X, Guo Y, Zheng M, Xue T, Wang L. Plant sterol ester of α-linolenic acid ameliorates high-fat diet-induced nonalcoholic fatty liver disease in mice: association with regulating mitochondrial dysfunction and oxidative stress via activating AMPK signaling. *Food Funct.* (2021) 12:2171–88. doi: 10.1039/D0FO02623A
59. Gao S, Hu J. Mitochondrial fusion: the machineries in and out. *Trends Cell Biol.* (2021) 31:62–74. doi: 10.1016/j.tcb.2020.09.008
60. Di Nottia M, Verrigni D, Torraco A, Rizza T, Bertini E, Carrozzo R. Mitochondrial dynamics: molecular mechanisms, related primary mitochondrial disorders and therapeutic approaches. *Genes.* (2021) 12:247. doi: 10.3390/genes12020247
61. Sessions DT, Kashatus DF. Mitochondrial dynamics in cancer stem cells. *Cell Mol Life Sci*. (2021) 78:3803–16. doi: 10.1007/s00018-021-03773-2
62. Wang L, Huang X, Dai T, Xie J, Lv QX, Hou Y, et al. The role of mitochondrial dynamics in the TiO(2) nanotube-accelerated osteogenic differentiation of MC3T3-E1 cells. *Biochem Biophys Res Commun.* (2021) 535:33–8. doi: 10.1016/j.bbrc.2020.12.025
63. Xiao Y, Chen W, Zhong Z, Ding L, Bai H, Chen H, et al. Electroacupuncture preconditioning attenuates myocardial ischemia-reperfusion injury by inhibiting mitophagy mediated by the mTORC1-ULK1-FUNDC1 pathway. *Biomed Pharmacother.* (2020) 127:110148. doi: 10.1016/j.biopha.2020.110148
64. Yu W, Gao B, Li N, Wang J, Qiu C, Zhang G, et al. Sirt3 deficiency exacerbates diabetic cardiac dysfunction: role of Foxo3A-Parkin-mediated mitophagy. *Biochim Biophys Acta Mol Basis Dis.* (2017) 1863:1973–83. doi: 10.1016/j.bbadis.2016.10.021
65. Gottlieb RA, Andres AM, Sin J, Taylor DP. Untangling autophagy measurements: all fluxed up. *Circ Res.* (2015) 116:504–14. doi: 10.1161/CIRCRESAHA.116.303787
66. Yang X, Pan W, Xu G, Chen L. Mitophagy: a crucial modulator in the pathogenesis of chronic diseases. *Clin Chim Acta.* (2020) 502:245–54. doi: 10.1016/j.cca.2019.11.008
67. Bi W, Jia J, Pang R, Nie C, Han J, Ding Z, et al. Thyroid hormone postconditioning protects hearts from ischemia/reperfusion through reinforcing mitophagy. *Biomed Pharmacother.* (2019) 118:109220. doi: 10.1016/j.biopha.2019.109220
68. Li G, Yang J, Yang C, Zhu M, Jin Y, McNutt MA, et al. PTENalpha regulates mitophagy and maintains mitochondrial quality control. *Autophagy.* (2018) 14:1742–60. doi: 10.1080/15548627.2018.1489477
69. Yang KC, Ma X, Liu H, Murphy J, Barger PM, Mann DL, et al. Tumor necrosis factor receptor-associated factor 2 mediates mitochondrial autophagy. *Circ Heart Fail.* (2015) 8:75–87. doi: 10.1161/CIRCHEARTFAILURE.114.001635
70. Feng Y, Zhao J, Hou H, Zhang H, Jiao Y, Wang J, et al. WDR26 promotes mitophagy of cardiomyocytes induced by hypoxia through Parkin translocation. *Acta Biochim Biophys Sin.* (2016) 48:1075–84. doi: 10.1093/abbs/gmw104
71. Huang C, Andres AM, Ratliff EP, Hernandez G, Lee P, Gottlieb RA. Preconditioning involves selective mitophagy mediated by Parkin and p62/SQSTM1. *PLoS ONE.* (2011) 6:e20975. doi: 10.1371/journal.pone.0020975
72. Piquereau J, Godin R, Deschenes S, Bessi VL, Mofarrahi M, Hussain SN, et al. Protective role of PARK2/Parkin in sepsis-induced cardiac contractile and mitochondrial dysfunction. *Autophagy.* (2013) 9:1837–51. doi: 10.4161/auto.26502
73. Li J, Shi W, Zhang J, Ren L. To explore the protective mechanism of PTEN-Induced Kinase 1 (PINK1)/parkin mitophagy-mediated extract of periplaneta americana on lipopolysaccharide-induced cardiomyocyte injury. *Med Sci Monitor.* (2019) 25:1383–91. doi: 10.12659/MSM.912980
74. Yang CN, Kok SH, Wang HW, Chang JZ, Lai EH, Shun CT, et al. Simvastatin alleviates bone resorption in apical periodontitis possibly by inhibition of mitophagy-related osteoblast apoptosis. *Int Endod J.* (2019) 52:676–88. doi: 10.1111/iej.13055
75. Monier S, Samadi M, Prunet C, Denance M, Laubriet A, Athias A, et al. Impairment of the cytotoxic and oxidative activities of 7β-hydroxycholesterol and 7-ketocholesterol by esterification with oleate. *Biochem Biophys Res Commun.* (2003) 303:814–24. doi: 10.1016/S0006-291X(03)00412-1
76. Lazarova D, Semkova S, Zlateva G, Tatsuya H, Aoki I, Bakalova R. Quantum sensors to track total redox-status and oxidative stress in cells and tissues using electron-paramagnetic resonance, magnetic resonance imaging, optical imaging. *Anal Chem.* (2021) 93:2828–37. doi: 10.1021/acs.analchem.0c04116
77. Andres AM, Hernandez G, Lee P, Huang C, Ratliff EP, Sin J, et al. Mitophagy is required for acute cardioprotection by simvastatin. *Antioxid Redox Signal.* (2014) 21:1960–73. doi: 10.1089/ars.2013.5416
78. Gottlieb RA, Pourpirali S. Lost in translation: miRNAs and mRNAs in ischemic preconditioning and ischemia/reperfusion injury. *J Mol Cell Cardiol.* (2016) 95:70–7. doi: 10.1016/j.yjmcc.2015.11.011
79. Zhang W, Siraj S, Zhang R, Chen Q. Mitophagy receptor FUNDC1 regulates mitochondrial homeostasis and protects the heart from I/R injury. *Autophagy.* (2017) 13:1080–1. doi: 10.1080/15548627.2017.1300224
80. Cao S, Sun Y, Wang W, Wang B, Zhang Q, Pan C, et al. Poly (ADP-ribose) polymerase inhibition protects against myocardial ischaemia/reperfusion injury via suppressing mitophagy. *J Cell Mol Med.* (2019) 23:6897–906. doi: 10.1111/jcmm.14573
81. Feng Y, Madungwe NB, da Cruz Junho CV, Bopassa JC. Activation of G protein-coupled oestrogen receptor 1 at the onset of reperfusion protects the myocardium against ischemia/reperfusion injury by reducing mitochondrial dysfunction and mitophagy. *Br J Pharmacol.* (2017) 174:4329–44. doi: 10.1111/bph.14033
82. Lu W, Sun J, Yoon JS, Zhang Y, Zheng L, Murphy E, et al. Mitochondrial protein PGAM5 regulates mitophagic protection against cell necroptosis. *PLoS ONE.* (2016) 11:e0147792. doi: 10.1371/journal.pone.0147792
83. Fan H, He Z, Huang H, Zhuang H, Liu H, Liu X, et al. Mitochondrial quality control in cardiomyocytes: a critical role in the progression of cardiovascular diseases. *Front Physiol.* (2020) 11:252. doi: 10.3389/fphys.2020.00252
84. Xiao D, Chang W, Ding W, Wang Y, Fa H, Wang J. Enhanced mitophagy mediated by the YAP/Parkin pathway protects against DOX-induced cardiotoxicity. *Toxicol Lett.* (2020) 330:96–107. doi: 10.1016/j.toxlet.2020.05.015
85. Xiong W, Hua J, Liu Z, Cai W, Bai Y, Zhan Q, et al. PTEN induced putative kinase 1 (PINK1) alleviates angiotensin II-induced cardiac injury by ameliorating mitochondrial dysfunction. *Int J Cardiol.* (2018) 266:198–205. doi: 10.1016/j.ijcard.2018.03.054
86. Bian X, Teng T, Zhao H, Qin J, Qiao Z, Sun Y, et al. Zinc prevents mitochondrial superoxide generation by inducing mitophagy in the setting of hypoxia/reoxygenation in cardiac cells. *Free Radic Res.* (2018) 52:80–91. doi: 10.1080/10715762.2017.1414949
87. Lee Y, Kwon I, Jang Y, Cosio-Lima L, Barrington P. Endurance exercise attenuates doxorubicin-induced cardiotoxicity. *Med Sci Sports Exercise.* (2020) 52:25–36. doi: 10.1249/MSS.0000000000002094
88. Zhou H, Zhu P, Wang J, Zhu H, Ren J, Chen Y. Pathogenesis of cardiac ischemia reperfusion injury is associated with CK2α-disturbed mitochondrial homeostasis via suppression of FUNDC1-related mitophagy. *Cell Death Different.* (2018) 25:1080–93. doi: 10.1038/s41418-018-0086-7
89. Zhu N, Li J, Li Y, Zhang Y, Du Q, Hao P, et al. Berberine protects against simulated ischemia/reperfusion injury-induced H9C2 cardiomyocytes apoptosis *In Vitro* and myocardial ischemia/reperfusion-induced apoptosis *In Vivo* by regulating the mitophagy-mediated HIF-1alpha/BNIP3 pathway. *Front Pharmacol.* (2020) 11:367. doi: 10.3389/fphar.2020.00367
90. Kubli DA, Gustafsson ÅB. Unbreak my heart: targeting mitochondrial autophagy in diabetic cardiomyopathy. *Antioxid Redox Sig.* (2015) 22:1527–44. doi: 10.1089/ars.2015.6322
91. Jin Q, Li R, Hu N, Xin T, Zhu P, Hu S, et al. DUSP1 alleviates cardiac ischemia/reperfusion injury by suppressing the Mff-required mitochondrial fission and Bnip3-related mitophagy via the JNK pathways. *Redox Biol.* (2018) 14:576–87. doi: 10.1016/j.redox.2017.11.004
92. Li W, Yin L, Sun X, Wu J, Dong Z, Hu K, et al. Alpha-lipoic acid protects against pressure overload-induced heart failure via ALDH2-dependent Nrf1-FUNDC1 signaling. *Cell Death Dis.* (2020) 11:599. doi: 10.1038/s41419-020-02805-2
93. Zhang W, Chen C, Wang J, Liu L, He Y, Chen Q. Mitophagy in cardiomyocytes and in platelets: a major mechanism of

cardioprotection against ischemia/reperfusion injury. *Physiology.* (2018) 33:86–98. doi: 10.1152/physiol.00030.2017
94. Fontecha-Barriuso M, Martin-Sanchez D, Martinez-Moreno JM, Monsalve M, Ramos AM, Sanchez-Niño MD, et al. The role of PGC-1α and mitochondrial biogenesis in kidney diseases. *Biomolecules.* (2020) 10:347. doi: 10.3390/biom10020347
95. Li Y, Feng YF, Liu XT, Li YC, Zhu HM, Sun MR, et al. Songorine promotes cardiac mitochondrial biogenesis via Nrf2 induction during sepsis. *Redox Biol.* (2021) 38:101771. doi: 10.1016/j.redox.2020.101771
96. Liu L, Li Y, Wang J, Zhang D, Wu H, Li W, et al. Mitophagy receptor FUNDC1 is regulated by PGC-1α/NRF1 to fine tune mitochondrial homeostasis. *EMBO Rep.* (2021) 22:e50629. doi: 10.15252/embr.202050629
97. Nishida Y, Nawaz A, Kado T, Takikawa A, Igarashi Y, Onogi Y, et al. Astaxanthin stimulates mitochondrial biogenesis in insulin resistant muscle via activation of AMPK pathway. *J Cachexia Sarcopenia Muscle.* (2020) 11:241–258. doi: 10.1002/jcsm.12530
98. Bishop DJ, Botella J, Genders AJ, Lee MJ, Saner NJ, Kuang J, et al. High-intensity exercise and mitochondrial biogenesis: current controversies and future research directions. *Physiology.* (2019) 34:56–70. doi: 10.1152/physiol.00038.2018
99. Fanibunda SE, Deb S, Maniyadath B, Tiwari P, Ghai U, Gupta S, et al. Serotonin regulates mitochondrial biogenesis and function in rodent cortical neurons via the 5-HT(2A) receptor and SIRT1-PGC-1α axis. *Proc Natl Acad Sci USA.* (2019) 116:11028–37. doi: 10.1073/pnas.1821332116
100. Krämer L, Groh C, Herrmann JM. The proteasome: friend and foe of mitochondrial biogenesis. *FEBS Lett.* (2021) 595:1223–38. doi: 10.1002/1873-3468.14010
101. Bouchez C, Devin A. Mitochondrial biogenesis and mitochondrial reactive oxygen species (ROS): a complex relationship regulated by the cAMP/PKA signaling pathway. *Cells.* (2019) 8:287. doi: 10.3390/cells8040287
102. English AM, Schuler MH, Xiao T, Kornmann B, Shaw JM, Hughes AL. ER-mitochondria contacts promote mitochondrial-derived compartment biogenesis. *J Cell Biol.* (2020) 219:e202002144. doi: 10.1083/jcb.202002144
103. Blanco FJ, Fernández-Moreno M. Mitochondrial biogenesis: a potential therapeutic target for osteoarthritis. *Osteoarthr Cartil.* (2020) 28:1003–6. doi: 10.1016/j.joca.2020.03.018
104. Sheremet NL, Andreeva NA, Shmel'kova MS, Tsigankova PG. [Mitochondrial biogenesis in hereditary optic neuropathies]. *Vestn Oftalmol.* (2019) 135:85–91. doi: 10.17116/oftalma201913505185
105. Tang JX, Thompson K, Taylor RW, Oláhová M. Mitochondrial OXPHOS biogenesis: co-regulation of protein synthesis, import, assembly pathways. *Int J Mol Sci.* (2020) 21:3820. doi: 10.3390/ijms21113820
106. Simmons EC, Scholpa NE, Schnellmann RG. Mitochondrial biogenesis as a therapeutic target for traumatic and neurodegenerative CNS diseases. *Exp Neurol.* (2020) 329:113309. doi: 10.1016/j.expneurol.2020.113309
107. Brunello E, Fusi L, Ghisleni A, Park-Holohan SJ, Ovejero JG, Narayanan T, et al. Myosin filament-based regulation of the dynamics of contraction in heart muscle. *Proc Natl Acad Sci USA.* (2020) 117:8177–86. doi: 10.1073/pnas.1920632117
108. Corbin EA, Vite A, Peyster EG, Bhoopalam M, Brandimarto J, Wang X, et al. Tunable and reversible substrate stiffness reveals a dynamic mechanosensitivity of cardiomyocytes. *ACS Appl Mater Interfaces.* (2019) 11:20603–14. doi: 10.1021/acsami.9b02446
109. Datta Chaudhuri R, Banik A, Mandal B, Sarkar S. Cardiac-specific overexpression of HIF-1α during acute myocardial infarction ameliorates cardiomyocyte apoptosis via differential regulation of hypoxia-inducible pro-apoptotic and anti-oxidative genes. *Biochem Biophys Res Commun.* (2021) 537:100–8. doi: 10.1016/j.bbrc.2020.12.084
110. Dias PP, Capila RF, do Couto NF, Estrada D, Gadelha FR, Radi R, et al. Cardiomyocyte oxidants production may signal to T. Cruzi intracellular development. *PLoS Negl Trop Dis.* (2017) 11:e0005852. doi: 10.1371/journal.pntd.0005852
111. Haque ZK, Wang DZ. How cardiomyocytes sense pathophysiological stresses for cardiac remodeling. *Cell Mol Life Sci.* (2017) 74:983–1000. doi: 10.1007/s00018-016-2373-0
112. Huang TH, Yip HK, Sun CK, Chen YL, Yang CC, Lee FY. P-cresyl sulfate causes mitochondrial hyperfusion in H9C2 cardiomyoblasts. *J Cell Mol Med.* (2020) 24:8379–90. doi: 10.1111/jcmm.15303
113. Kang H, Liu J, Sun A, Liu X, Fan Y, Deng X. Vascular smooth muscle cell glycocalyx mediates shear stress-induced contractile responses via a Rho kinase (ROCK)-myosin light chain phosphatase (MLCP) pathway. *Sci Rep.* (2017) 7:42092. doi: 10.1038/srep42092
114. Ling SSM, Chen YT, Wang J, Richards AM, Liew OW. Ankyrin repeat domain 1 protein: a functionally pleiotropic protein with cardiac biomarker potential. *Int J Mol Sci.* (2017) 18. doi: 10.3390/ijms18071362
115. Zhou J, Xi C, Wang W, Fu X, Jinqiang L, Qiu Y, et al. Triptolide-induced oxidative stress involved with Nrf2 contribute to cardiomyocyte apoptosis through mitochondrial dependent pathways. *Toxicol Lett.* (2014) 230:454–66. doi: 10.1016/j.toxlet.2014.08.017
116. Zhou H, Zhang Y, Hu S, Shi C, Zhu P, Ma Q, et al. Melatonin protects cardiac microvasculature against ischemia/reperfusion injury via suppression of mitochondrial fission-VDAC1-HK2-mPTP-mitophagy axis. *J Pineal Res.* (2017) 63:e12413. doi: 10.1111/jpi.12413
117. Yu W, Sun S, Xu H, Li C, Ren J, Zhang Y. TBC1D15/RAB7-regulated mitochondria-lysosome interaction confers cardioprotection against acute myocardial infarction-induced cardiac injury. *Theranostics.* (2020) 10:11244–63. doi: 10.7150/thno.46883
118. Farías JG, Molina VM, Carrasco RA, Zepeda AB, Figueroa E, Letelier P, et al. Antioxidant therapeutic strategies for cardiovascular conditions associated with oxidative stress. *Nutrients.* (2017) 9:966. doi: 10.3390/nu9090966
119. Mancilla TR, Iskra B, Aune GJ. Doxorubicin-induced cardiomyopathy in children. *Compr Physiol.* (2019) 9:905–31. doi: 10.1002/cphy.c180017
120. Bar-Yosef T, Damri O, Agam G. Dual role of autophagy in diseases of the central nervous system. *Front Cell Neurosci.* (2019) 13:196. doi: 10.3389/fncel.2019.00196
121. Axelrod CL, King WT, Davuluri G, Noland RC, Hall J, Hull M, et al. BAM15-mediated mitochondrial uncoupling protects against obesity and improves glycemic control. *EMBO Mol Med.* (2020) 12:e12088. doi: 10.15252/emmm.202012088
122. Blignaut M, Espach Y, van Vuuren M, Dhanabalan K, Huisamen B. Revisiting the cardiotoxic effect of chloroquine. *Cardiovasc Drugs Ther.* (2019) 33:1–11. doi: 10.1007/s10557-018-06847-9
123. Dai J, Liang K, Zhao S, Jia W, Liu Y, Wu H, et al. Chemoproteomics reveals baicalin activates hepatic CPT1 to ameliorate diet-induced obesity and hepatic steatosis. *Proc Natl Acad Sci USA.* (2018) 115:E5896–905. doi: 10.1073/pnas.1801745115
124. Araya J, Tsubouchi K, Sato N, Ito S, Minagawa S, Hara H, et al. PRKN-regulated mitophagy and cellular senescence during COPD pathogenesis. *Autophagy.* (2019) 15:510–26. doi: 10.1080/15548627.2018.1532259
125. Barish R, Lynce F, Unger K, Barac A. Management of cardiovascular disease in women with breast cancer. *Circulation.* (2019) 139:1110–20. doi: 10.1161/CIRCULATIONAHA.118.039371
126. Findlay SG, Gill JH, Plummer R, DeSantis C, Plummer C. Chronic cardiovascular toxicity in the older oncology patient population. *J Geriatr Oncol.* (2019) 10:685–9. doi: 10.1016/j.jgo.2019.01.018
127. Kaboré EG, Guenancia C, Vaz-Luis I, Di Meglio A, Pistilli B, Coutant C, et al. Association of body mass index and cardiotoxicity related to anthracyclines and trastuzumab in early breast cancer: French CANTO cohort study. *PLoS Med.* (2019) 16:e1002989. doi: 10.1371/journal.pmed.1002989
128. Kalkhoran SB, Hernandez-Resendiz S, Ong SG, Ramachandra CJA, Hausenloy DJ. Mitochondrial shaping proteins as novel treatment targets for cardiomyopathies. *Cond Med.* (2020) 3:216–26.
129. Kosalka P, Johnson C, Turek M, Sulpher J, Law A, Botros J, et al. Effect of obesity, dyslipidemia, and diabetes on trastuzumab-related cardiotoxicity in breast cancer. *Curr Oncol.* (2019) 26:e314–21. doi: 10.3747/co.26.4823
130. Tan L, Su X, Li X, Li H, Hu B. Correlation of HER2 codon 655 polymorphism with cardiotoxicity risk in Chinese HER2-positive breast cancer patients undergoing epirubicin/cyclophosphamide followed by docetaxel plus trastuzumab adjuvant chemotherapy. *Int J Clin Exp Pathol.* (2020) 13:286–94.
131. Yao RQ, Ren C, Xia ZF, Yao YM. Organelle-specific autophagy in inflammatory diseases: a potential therapeutic target underlying the quality control of multiple organelles. *Autophagy.* (2021) 17:385–401. doi: 10.1080/15548627.2020.1725377

132. Xie Q, Li S, Gao Y, Jin L, Dai C, Song J. Ergosterol attenuates isoproterenol-induced myocardial cardiotoxicity. *Cardiovasc Toxicol.* (2020) 20:500–6. doi: 10.1007/s12012-020-09574-6
133. FrangeŽ R, Šuput D, Molgó J, Benoit E. Ostreolysin a/pleurotolysin b and equinatoxins: structure, function and pathophysiological effects of these pore-forming proteins. *Toxins.* (2017) 9:128. doi: 10.3390/toxins9040128
134. Zhou H, Fu LX, Li L, Chen YY, Zhu HQ, Zhou JL, et al. The epigallocatechin gallate derivative Y6 reduces the cardiotoxicity and enhances the efficacy of daunorubicin against human hepatocellular carcinoma by inhibiting carbonyl reductase 1 expression. *J Ethnopharmacol.* (2020) 261:113118. doi: 10.1016/j.jep.2020.113118
135. Yang F, Zhao LN, Sun Y, Chen Z. Levosimendan as a new force in the treatment of sepsis-induced cardiomyopathy: mechanism and clinical application. *J Int Med Res.* (2019) 47:1817–28. doi: 10.1177/0300060519837103
136. Song Y, Xu C, Liu J, Li Y, Wang H, Shan D, et al. Heterodimerization with 5-HT(2B)R is indispensable for β(2)AR-Mediated cardioprotection. *Circ Res.* (2021) 128:262–77. doi: 10.1161/CIRCRESAHA.120.317011
137. Yu X, Ruan Y, Shen T, Qiu Q, Yan M, Sun S, et al. Dexrazoxane protects cardiomyocyte from doxorubicin-induced apoptosis by modulating miR-17-5p. *Biomed Res Int.* (2020) 2020:5107193. doi: 10.1155/2020/5107193
138. Cypher AD, Consiglio J, Bagatto B. Hypoxia exacerbates the cardiotoxic effect of the polycyclic aromatic hydrocarbon, phenanthrene in Danio rerio. *Chemosphere.* (2017) 183:574–81. doi: 10.1016/j.chemosphere.2017.05.109
139. Zhao Y, Wang B, Zhang J, He D, Zhang Q, Pan C, et al. ALDH2 (aldehyde dehydrogenase 2) protects against hypoxia-induced pulmonary hypertension. *Arterioscler Thromb Vasc Biol.* (2019) 39:2303–19. doi: 10.1161/ATVBAHA.119.312946
140. Zhang D, Liu Y, Tang Y, Wang X, Li Z, Li R, et al. Increased mitochondrial fission is critical for hypoxia-induced pancreatic beta cell death. *PLoS ONE.* (2018) 13:e0197266. doi: 10.1371/journal.pone.0197266
141. Nishimura A, Shimauchi T, Tanaka T, Shimoda K, Toyama T, Kitajima N, et al. Hypoxia-induced interaction of filamin with Drp1 causes mitochondrial hyperfission-associated myocardial senescence. *Sci Signal.* (2018) 11:eaat5185. doi: 10.1126/scisignal.aat5185
142. Kuang Y, Ma K, Zhou C, Ding P, Zhu Y, Chen Q, et al. Structural basis for the phosphorylation of FUNDC1 LIR as a molecular switch of mitophagy. *Autophagy.* (2016) 12:2363–73. doi: 10.1080/15548627.2016.1238552
143. Lv M, Wang C, Li F, Peng J, Wen B, Gong Q, et al. Structural insights into the recognition of phosphorylated FUNDC1 by LC3B in mitophagy. *Protein Cell.* (2016) 8:25–38. doi: 10.1007/s13238-016-0328-8
144. Hao P, Liu Y, Guo H, Zhang Z, Chen Q, Hao G, et al. Prolylcarboxypeptidase mitigates myocardial ischemia/reperfusion injury by stabilizing mitophagy. *Front Cell Dev Biol.* (2020) 8:584933. doi: 10.3389/fcell.2020.584933
145. Zhou H, Li D, Zhu P, Hu S, Hu N, Ma S, et al. Melatonin suppresses platelet activation and function against cardiac ischemia/reperfusion injury via PPARγ/FUNDC1/mitophagy pathways. *J Pineal Res.* (2017) 63:e12438. doi: 10.1111/jpi.12438
146. Paradies G, Paradies V, Ruggiero FM, Petrosillo G. Mitochondrial bioenergetics and cardiolipin alterations in myocardial ischemia-reperfusion injury: implications for pharmacological cardioprotection. *Am J Physiol Heart Circ Physiol.* (2018) 315:H1341–52. doi: 10.1152/ajpheart.00028.2018
147. Hernandez-Resendiz S, Prunier F, Girao H, Dorn G, Hausenloy DJ, E-Action CC. Targeting mitochondrial fusion and fission proteins for cardioprotection. *J Cell Mol Med.* (2020) 24:6571–85. doi: 10.1111/jcmm.15384
148. Songbo M, Lang H, Xinyong C, Bin X, Ping Z, Liang S. Oxidative stress injury in doxorubicin-induced cardiotoxicity. *Toxicol Lett.* (2019) 307:41–8. doi: 10.1016/j.toxlet.2019.02.013
149. Chen T, Deng Z, Zhao R, Shen H, Li W. SYKT alleviates doxorubicin-induced cardiotoxicity via modulating ROS-Mediated p53 and MAPK signal pathways. *Evid Based Compl Alternat Med.* (2018) 2018:2581031. doi: 10.1155/2018/2581031
150. He L, Liu F, Li J. Mitochondrial sirtuins and Doxorubicin-induced cardiotoxicity. *Cardiovasc Toxicol.* (2021) 21:179–91. doi: 10.1007/s12012-020-09626-x
151. Kurauchi K, Nishikawa T, Miyahara E, Okamoto Y, Kawano Y. Role of metabolites of cyclophosphamide in cardiotoxicity. *BMC Res Notes.* (2017) 10:406. doi: 10.1186/s13104-017-2726-2
152. Long G, Chen H, Wu M, Li Y, Gao L, Huang S, et al. Antianemia drug roxadustat (FG-4592) protects against doxorubicin-induced cardiotoxicity by targeting antiapoptotic and antioxidative pathways. *Front Pharmacol.* (2020) 11:1191. doi: 10.3389/fphar.2020.01191
153. Lu J, Li J, Hu Y, Guo Z, Sun D, Wang P, et al. Chrysophanol protects against doxorubicin-induced cardiotoxicity by suppressing cellular PARylation. *Acta Pharm Sin B.* (2019) 9:782–93. doi: 10.1016/j.apsb.2018.10.008
154. Russo M, Guida F, Paparo L, Trinchese G, Aitoro R, Avagliano C, et al. The novel butyrate derivative phenylalanine-butyramide protects from doxorubicin-induced cardiotoxicity. *Eur J Heart Fail.* (2019) 21:519–28. doi: 10.1002/ejhf.1439
155. Wei S, Ma W, Li X, Jiang C, Sun T, Li Y, et al. Involvement of ROS/NLRP3 inflammasome signaling pathway in doxorubicin-induced cardiotoxicity. *Cardiovasc Toxicol.* (2020) 20:507–19. doi: 10.1007/s12012-020-09576-4
156. Yarmohammadi F, Rezaee R, Karimi G. Natural compounds against doxorubicin-induced cardiotoxicity: a review on the involvement of Nrf2/ARE signaling pathway. *Phytother Res.* (2021) 35 1163–75. doi: 10.1002/ptr.6882
157. Zhao L, Qi Y, Xu L, Tao X, Han X, Yin L, et al. MicroRNA-140-5p aggravates doxorubicin-induced cardiotoxicity by promoting myocardial oxidative stress via targeting Nrf2 and Sirt2. *Redox Biol.* (2018) 15:284–96. doi: 10.1016/j.redox.2017.12.013
158. Barnes PJ. Oxidative stress-based therapeutics in COPD. *Redox Biol.* (2020) 33:101544. doi: 10.1016/j.redox.2020.101544
159. Cano Sanchez M, Lancel S, Boulanger E, Neviere R. Targeting oxidative stress and mitochondrial dysfunction in the treatment of impaired wound healing: a systematic review. *Antioxidants.* (2018) 7:98. doi: 10.3390/antiox7080098
160. Datta S, Cano M, Ebrahimi K, Wang L, Handa JT. The impact of oxidative stress and inflammation on RPE degeneration in non-neovascular AMD. *Prog Retin Eye Res.* (2017) 60:201–18. doi: 10.1016/j.preteyeres.2017.03.002
161. Yin J, Guo J, Zhang Q, Cui L, Zhang L, Zhang T, et al. Doxorubicin-induced mitophagy and mitochondrial damage is associated with dysregulation of the PINK1/parkin pathway. *Toxicol In Vitro.* (2018) 51:1–10. doi: 10.1016/j.tiv.2018.05.001
162. Penna C, Perrelli MG, Pagliaro P. Mitochondrial pathways, permeability transition pore, and redox signaling in cardioprotection: therapeutic implications. *Antioxid Redox Signal.* (2013) 18:556–99. doi: 10.1089/ars.2011.4459
163. Chen Z, Wu D, Li L, Chen L. Apelin/APJ system: a novel therapeutic target for myocardial ischemia/reperfusion injury. *DNA Cell Biol.* (2016) 35:766–75. doi: 10.1089/dna.2016.3391
164. Tian Y, Lv W, Lu C, Zhao X, Zhang C, Song H. LATS2 promotes cardiomyocyte H9C2 cells apoptosis via the Prx3-Mfn2-mitophagy pathways. *J Recept Signal Transduct Res.* (2019) 39:470–8. doi: 10.1080/10799893.2019.1701031
165. Gottlieb RA, Mentzer Jr RM, Linton PJ. Impaired mitophagy at the heart of injury. *Autophagy.* (2011) 7:1573–4. doi: 10.4161/auto.7.12.18175
166. Miller BA, Cheung JY. TRPM2 protects against tissue damage following oxidative stress and ischaemia-reperfusion. *J Physiol.* (2016) 594:4181–91. doi: 10.1113/JP270934
167. Tang L, Li Y-p, Hu J, Chen A-h, Mo Y. Dexpramipexole attenuates myocardial ischemia/reperfusion injury through upregulation of mitophagy. *Eur J Pharmacol.* (2021) 899:173962. doi: 10.1016/j.ejphar.2021.173962
168. Wu MY, Yiang GT, Liao WT, Tsai AP, Cheng YL, Cheng PW, et al. Current mechanistic concepts in ischemia and reperfusion injury. *Cell Physiol Biochem.* (2018) 46:1650–67. doi: 10.1159/000489241
169. Tang W, Lin D, Chen M, Li Z, Zhang W, Hu W, et al. PTEN-mediated mitophagy and APE1 overexpression protects against cardiac hypoxia/reoxygenation injury. *In Vitro Cell Dev Biol Animal.* (2019) 55:741–8. doi: 10.1007/s11626-019-00389-6
170. Zhou H, Zhu P, Guo J, Hu N, Wang S, Li D, et al. Ripk3 induces mitochondrial apoptosis via inhibition of FUNDC1 mitophagy in cardiac IR injury. *Redox Biology.* (2017) 13::498–507. doi: 10.1016/j.redox.2017.07.007

171. Wu H, Ye M, Liu D, Yang J, Ding Jw, Zhang J, et al. UCP2 protect the heart from myocardial ischemia/reperfusion injury via induction of mitochondrial autophagy. *J Cell Biochem.* (2019) 120:15455–66. doi: 10.1002/jcb.28812
172. Lee TL, Lee M-H, Chen Y-C, Lee Y-C, Lai T-C, et al. Vitamin D attenuates ischemia/reperfusion-induced cardiac injury by reducing mitochondrial fission and mitophagy. *Front Pharmacol.* (2020) 11:604700. doi: 10.3389/fphar.2020.604700
173. Li Q, Yu Z, Xiao D, Wang Y, Zhao L, An Y, et al. Baicalein inhibits mitochondrial apoptosis induced by oxidative stress in cardiomyocytes by stabilizing MARCH5 expression. *J Cell Mol Med.* (2020) 24:2040–51. doi: 10.1111/jcmm.14903
174. Su B-C, Hsu P-L, Mo F-E. CCN1 triggers adaptive autophagy in cardiomyocytes to curb its apoptotic activities. *J Cell Commun Sig.* (2019) 14:93–100. doi: 10.1007/s12079-019-00534-6
175. Chaurasia SS, Lim RR, Parikh BH, Wey YS, Tun BB, Wong TY, et al. The NLRP3 inflammasome may contribute to pathologic neovascularization in the advanced stages of diabetic retinopathy. *Sci Rep.* (2018) 8:2847. doi: 10.1038/s41598-018-21198-z
176. Ding S, Xu S, Ma Y, Liu G, Jang H, Fang J. Modulatory mechanisms of the NLRP3 inflammasomes in diabetes. *Biomolecules.* (2019) 9:850. doi: 10.3390/biom9120850
177. Hou Y, Lin S, Qiu J, Sun W, Dong M, Xiang Y, et al. NLRP3 inflammasome negatively regulates podocyte autophagy in diabetic nephropathy. *Biochem Biophys Res Commun.* (2020) 521:791–8. doi: 10.1016/j.bbrc.2019.10.194
178. Li DX, Wang CN, Wang Y, Ye CL, Jiang L, Zhu XY, et al. NLRP3 inflammasome-dependent pyroptosis and apoptosis in hippocampus neurons mediates depressive-like behavior in diabetic mice. *Behav Brain Res.* (2020) 391:112684. doi: 10.1016/j.bbr.2020.112684
179. Wan Z, Fan Y, Liu X, Xue J, Han Z, Zhu C, et al. NLRP3 inflammasome promotes diabetes-induced endothelial inflammation and atherosclerosis. *Diabetes Metab Syndr Obes.* (2019) 12:1931–42. doi: 10.2147/DMSO.S222053
180. Wang J, Shen X, Liu J, Chen W, Wu F, Wu W, et al. High glucose mediates NLRP3 inflammasome activation via upregulation of ELF3 expression. *Cell Death Dis.* (2020) 11:383. doi: 10.1038/s41419-020-2598-6
181. Hao Y, Liu HM, Wei X, Gong X, Lu ZY, Huang ZH. Diallyl trisulfide attenuates hyperglycemia-induced endothelial apoptosis by inhibition of Drp1-mediated mitochondrial fission. *Acta Diabetol.* (2019) 56:1177–89. doi: 10.1007/s00592-019-01366-x
182. Wu G, Xiong Q, Wei X, Wang Y, Hu X, He G, et al. Mitochondrial unfolded protein response gene CLPP changes mitochondrial dynamics and affects mitochondrial function. *PeerJ.* (2019) 7:e7209. doi: 10.7717/peerj.7209
183. Zheng F, Jia B, Dong F, Liu L, Rasul F, He J, et al. Glucose starvation induces mitochondrial fragmentation depending on the dynamin GTPase Dnm1/Drp1 in fission yeast. *J Biol Chem.* (2019) 294:17725–34. doi: 10.1074/jbc.RA119.010185
184. Rohrbach S, Aslam M, Niemann B, Schulz R. Impact of caloric restriction on myocardial ischaemia/reperfusion injury and new therapeutic options to mimic its effects. *Br J Pharmacol.* (2014) 171:2964–92. doi: 10.1111/bph.12650
185. Yu LM, Dong X, Xue XD, Xu S, Zhang X, Xu YL, et al. Melatonin attenuates diabetic cardiomyopathy and reduces myocardial vulnerability to ischemia-reperfusion injury by improving mitochondrial quality control: Role of SIRT6. *J Pineal Res.* (2020) 70:e12698. doi: 10.1111/jpi.12698
186. Kobayashi S, Zhao F, Zhang Z, Kobayashi T, Huang Y, Shi B, et al. Mitochondrial fission and mitophagy coordinately restrict high glucose toxicity in cardiomyocytes. *Front Physiol.* (2020) 11:604069. doi: 10.3389/fphys.2020.604069
187. Nishida K, Otsu K. Sterile inflammation and degradation systems in heart failure. *Circ J.* (2017) 81:622–8. doi: 10.1253/circj.CJ-17-0261
188. Hu L, Ding M, Tang D, Gao E, Li C, Wang K, et al. Targeting mitochondrial dynamics by regulating Mfn2 for therapeutic intervention in diabetic cardiomyopathy. *Theranostics.* (2019) 9:3687–706. doi: 10.7150/thno.33684
189. Xu X, Kobayashi S, Chen K, Timm D, Volden P, Huang Y, et al. Diminished autophagy limits cardiac injury in mouse models of type 1 diabetes. *J Biol Chem.* (2013) 288:18077–92. doi: 10.1074/jbc.M113.474650
190. Ewer MS, Ewer SM. Cardiotoxicity of anticancer treatments. *Nat Rev Cardiol.* (2015) 12:547–58. doi: 10.1038/nrcardio.2015.65
191. Ferdinandy P, Baczkó I, Bencsik P, Giricz Z, Görbe A, Pacher P, et al. Definition of hidden drug cardiotoxicity: paradigm change in cardiac safety testing and its clinical implications. *Eur Heart J.* (2019) 40:1771–77. doi: 10.1093/eurheartj/ehy365
192. Jain D, Aronow W. Cardiotoxicity of cancer chemotherapy in clinical practice. *Hosp Pract 1995.* (2019) 47:6–15. doi: 10.1080/21548331.2018.1530831
193. Nicolazzi MA, Carnicelli A, Fuorlo M, Scaldaferri A, Masetti R, Landolfi R, et al. Anthracycline and trastuzumab-induced cardiotoxicity in breast cancer. *Eur Rev Med Pharmacol Sci.* (2018) 22:2175–85. doi: 10.26355/eurrev_201804_14752
194. Bhagat A, Kleinerman ES. Anthracycline-induced cardiotoxicity: causes, mechanisms, and prevention. *Adv Exp Med Biol.* (2020) 1257:181–92. doi: 10.1007/978-3-030-43032-0_15
195. Cardinale D, Colombo A, Bacchiani G, Tedeschi I, Meroni CA, Veglia F, et al. Early detection of anthracycline cardiotoxicity and improvement with heart failure therapy. *Circulation.* (2015) 131:1981–8. doi: 10.1161/CIRCULATIONAHA.114.013777
196. Curigliano G, Cardinale D, Dent S, Criscitiello C, Aseyev O, Lenihan D, et al. Cardiotoxicity of anticancer treatments: epidemiology, detection, and management. *CA Cancer J Clin.* (2016) 66:309–25. doi: 10.3322/caac.21341
197. Shabalala S, Muller CJF, Louw J, Johnson R. Polyphenols, autophagy and doxorubicin-induced cardiotoxicity. *Life Sci.* (2017) 180:160–70. doi: 10.1016/j.lfs.2017.05.003
198. Varga ZV, Ferdinandy P, Liaudet L, Pacher P. Drug-induced mitochondrial dysfunction and cardiotoxicity. *Am J Physiol Heart Circ Physiol.* (2015) 309:H1453–67. doi: 10.1152/ajpheart.00554.2015
199. Burridge PW, Li YF, Matsa E, Wu H, Ong SG, Sharma A, et al. Human induced pluripotent stem cell-derived cardiomyocytes recapitulate the predilection of breast cancer patients to doxorubicin-induced cardiotoxicity. *Nat Med.* (2016) 22:547–56. doi: 10.1038/nm.4087
200. Gorini S, De Angelis A, Berrino L, Malara N, Rosano G, Ferraro E. Chemotherapeutic drugs and mitochondrial dysfunction: focus on doxorubicin, trastuzumab, and sunitinib. *Oxid Med Cell Longev.* (2018) 2018:7582730. doi: 10.1155/2018/7582730
201. Hantson P. Mechanisms of toxic cardiomyopathy. *Clin Toxicol.* (2019) 57:1–9. doi: 10.1080/15563650.2018.1497172
202. Henriksen PA. Anthracycline cardiotoxicity: an update on mechanisms, monitoring and prevention. *Heart.* (2018) 104:971–77. doi: 10.1136/heartjnl-2017-312103
203. Prathumsap N, Shinlapawittayatorn K, Chattipakorn SC, Chattipakorn N. Effects of doxorubicin on the heart: from molecular mechanisms to intervention strategies. *Eur J Pharmacol.* (2020) 866:172818. doi: 10.1016/j.ejphar.2019.172818
204. Tadokoro T, Ikeda M, Ide T, Deguchi H, Ikeda S, Okabe K, et al. Mitochondria-dependent ferroptosis plays a pivotal role in doxorubicin cardiotoxicity. *JCI Insight.* (2020) 5:e132747. doi: 10.1172/jci.insight.132747
205. Timm KN, Tyler DJ. The role of AMPK activation for cardioprotection in doxorubicin-induced cardiotoxicity. *Cardiovasc Drugs Ther.* (2020) 34:255–69. doi: 10.1007/s10557-020-06941-x
206. Wallace KB, Sardão VA, Oliveira PJ. Mitochondrial determinants of doxorubicin-induced cardiomyopathy. *Circ Res.* (2020) 126:926–41. doi: 10.1161/CIRCRESAHA.119.314681
207. Wang P, Wang L, Lu J, Hu Y, Wang Q, Li Z, et al. SESN2 protects against doxorubicin-induced cardiomyopathy via rescuing mitophagy and improving mitochondrial function. *J Mol Cell Cardiol.* (2019) 133:125–37. doi: 10.1016/j.yjmcc.2019.06.005
208. Wenningmann N, Knapp M, Ande A, Vaidya TR, Ait-Oudhia S. Insights into doxorubicin-induced cardiotoxicity: molecular mechanisms, preventive strategies, early monitoring. *Mol Pharmacol.* (2019) 96:219–32. doi: 10.1124/mol.119.115725

209. Herrmann J. Adverse cardiac effects of cancer therapies: cardiotoxicity and arrhythmia. *Nat Rev Cardiol.* (2020) 17:474–502. doi: 10.1038/s41569-020-0348-1
210. Jerusalem G, Lancellotti P, Kim SB. HER2+ breast cancer treatment and cardiotoxicity: monitoring and management. *Breast Cancer Res Treat.* (2019) 177:237–50. doi: 10.1007/s10549-019-05303-y
211. Zakaria ZZ, Benslimane FM, Nasrallah GK, Shurbaji S, Younes NN, Mraiche F, et al. Using zebrafish for investigating the molecular mechanisms of drug-induced cardiotoxicity. *Biomed Res Int.* (2018) 2018:1642684. doi: 10.1155/2018/1642684
212. Rudy Y. In silico pipeline for drug cardiotoxicity assessment. *Circ Res.* (2020) 126:965–7. doi: 10.1161/CIRCRESAHA.120.316901
213. Abdullah CS, Alam S, Aishwarya R, Miriyala S, Bhuiyan MAN, Panchatcharam M, et al. Doxorubicin-induced cardiomyopathy associated with inhibition of autophagic degradation process and defects in mitochondrial respiration. *Sci Rep.* (2019) 9(1). doi: 10.1038/s41598-018-37862-3
214. Zhou L, Li R, Liu C, Sun T, Htet Aung LH, Chen C, et al. Foxo3a inhibits mitochondrial fission and protects against doxorubicin-induced cardiotoxicity by suppressing MIEF2. *Free Radic Biol Med.* (2017) 104:360–70. doi: 10.1016/j.freeradbiomed.2017.01.037
215. Pillai VB, Kanwal A, Fang YH, Sharp WW, Samant S, Arbiser J, et al. Honokiol, an activator of Sirtuin-3 (SIRT3) preserves mitochondria and protects the heart from doxorubicin-induced cardiomyopathy in mice. *Oncotarget.* (2017) 8:34082–98. doi: 10.18632/oncotarget.16133
216. Du J, Hang P, Pan Y, Feng B, Zheng Y, Chen T, et al. Inhibition of miR-23a attenuates doxorubicin-induced mitochondria-dependent cardiomyocyte apoptosis by targeting the PGC-1α/Drp1 pathway. *Toxicol Appl Pharmacol.* (2019) 369:73–81. doi: 10.1016/j.taap.2019.02.016
217. Jia G, Meng Z, Liu C, Ma X, Gao J, Liu J, et al. Nicotine induces cardiac toxicity through blocking mitophagic clearance in young adult rat. *Life Sciences.* (2020) 257:118084. doi: 10.1016/j.lfs.2020.118084
218. Wang S, Ren J. Role of autophagy and regulatory mechanisms in alcoholic cardiomyopathy. *Bio Biophys Acta.* (2018) 1864:2003–9. doi: 10.1016/j.bbadis.2018.03.016
219. Saito T, Nah J, Oka SI, Mukai R, Monden Y, Maejima Y, et al. An alternative mitophagy pathway mediated by Rab9 protects the heart against ischemia. *J Clin Invest.* (2019) 129:802–19. doi: 10.1172/JCI122035
220. Zhang X, Li Z-L, Eirin A, Ebrahimi B, Pawar AS, Zhu X-Y, et al. Cardiac metabolic alterations in hypertensive obese pigs. *Hypertension.* (2015) 66:430–6. doi: 10.1161/HYPERTENSIONAHA.115.05478
221. Mancilla TR, Davis LR, Aune GJ. Doxorubicin-induced p53 interferes with mitophagy in cardiac fibroblasts. *PLoS ONE.* (2020) 15:e0238856. doi: 10.1371/journal.pone.0238856
222. Gharanei M, Hussain A, Janneh O, Maddock H. Attenuation of doxorubicin-induced cardiotoxicity by mdivi-1: a mitochondrial division/mitophagy inhibitor. *PLoS ONE.* (2013) 8:e77713. doi: 10.1371/journal.pone.0077713
223. Nordgren KKS, Wallace KB. Disruption of the Keap1/Nrf2-antioxidant response system after chronic doxorubicin exposure *In Vivo*. *Cardiovasc Toxicol.* (2020) 20:557–70. doi: 10.1007/s12012-020-09581-7
224. Dhingra A, Jayas R, Afshar P, Guberman M, Maddaford G, Gerstein J, et al. Ellagic acid antagonizes Bnip3-mediated mitochondrial injury and necrotic cell death of cardiac myocytes. *Free Radic Biol Med.* (2017) 112:411–22. doi: 10.1016/j.freeradbiomed.2017.08.010
225. Catanzaro MP, Weiner A, Kaminaris A, Li C, Cai F, Zhao F, et al. Doxorubicin-induced cardiomyocyte death is mediated by unchecked mitochondrial fission and mitophagy. *FASEB J.* (2019) 33:11096–108. doi: 10.1096/fj.201802663R
226. Yang M, Wang S, Fu S, Wu NN, Xu X, Sun S, et al. Deletion of the E3 ubiquitin ligase, Parkin, exacerbates chronic alcohol intake-induced cardiomyopathy through an ambra1-dependent mechanism. *Bri J Pharmacol.* (2021) 178:964–82. doi: 10.1111/bph.15340
227. Wang P, Lan R, Guo Z, Cai S, Wang J, Wang Q, et al. Histone demethylase JMJD3 mediated doxorubicin-induced cardiomyopathy by suppressing SESN2 expression. *Front Cell Dev Biol.* (2020) 8:548605. doi: 10.3389/fcell.2020.548605
228. Liu X, Zhang S, An L, Wu J, Hu X, Lai S, et al. Loss of Rubicon ameliorates doxorubicin-induced cardiotoxicity through enhancement of mitochondrial quality. *Int J Cardiol.* (2019) 296:129–35. doi: 10.1016/j.ijcard.2019.07.074
229. Huang CY, Kuo WW, Ho TJ, Chiang SF, Pai PY, Lin JY, et al. Rab9-dependent autophagy is required for the IGF-IIR triggering mitophagy to eliminate damaged mitochondria. *J Cell Physiol.* (2018) 233:7080–91. doi: 10.1002/jcp.26346
230. Huang C-Y, Lai C-H, Kuo C-H, Chiang S-F, Pai P-Y, Lin J-Y, et al. Inhibition of ERK-Drp1 signaling and mitochondria fragmentation alleviates IGF-IIR-induced mitochondria dysfunction during heart failure. *J Mol Cell Cardiol.* (2018) 122:58–68. doi: 10.1016/j.yjmcc.2018.08.006
231. Zhou K, Wu J, Chen J, Zhou Y, Chen X, Wu Q, et al. Schaftoside ameliorates oxygen glucose deprivation-induced inflammation associated with the TLR4/Myd88/Drp1-related mitochondrial fission in BV2 microglia cells. *J Pharmacol Sci.* (2019) 139:15–22. doi: 10.1016/j.jphs.2018.10.012
232. Gu C, Li L, Huang Y, Qian D, Liu W, Zhang C, et al. Salidroside ameliorates mitochondria-dependent neuronal apoptosis after spinal cord ischemia-reperfusion injury partially through inhibiting oxidative stress and promoting mitophagy. *Oxid Med Cell Longev.* (2020) 2020:3549704. doi: 10.1155/2020/3549704
233. Li R, Chen J. Salidroside protects dopaminergic neurons by enhancing PINK1/parkin-mediated mitophagy. *Oxid Med Cell Longev.* (2019) 2019:9341018. doi: 10.1155/2019/9341018
234. Zhang Z, Xu T, Chen J, Shao Z, Wang K, Yan Y, et al. Parkin-mediated mitophagy as a potential therapeutic target for intervertebral disc degeneration. *Cell Death Dis.* (2018) 9:980. doi: 10.1038/s41419-018-1024-9
235. Yuan Y, Pan SS. Parkin mediates mitophagy to participate in cardioprotection induced by late exercise preconditioning but bnip3 does not. *J Cardiovasc Pharmacol.* (2018) 71:303–16. doi: 10.1097/FJC.0000000000000572
236. Li H, Miao W, Ma J, Xv Z, Bo H, Li J, et al. Acute exercise-induced mitochondrial stress triggers an inflammatory response in the myocardium via NLRP3 inflammasome activation with mitophagy. *Oxid Med Cell Longev.* (2016) 2016:1987149. doi: 10.1155/2016/1987149
237. Cao S, Shrestha S, Li J, Yu X, Chen J, Yan F, et al. Melatonin-mediated mitophagy protects against early brain injury after subarachnoid hemorrhage through inhibition of NLRP3 inflammasome activation. *Sci Rep.* (2017) 7:2417. doi: 10.1038/s41598-017-02679-z
238. Dhanabalan K, Mzezewa S, Huisamen B, Lochner A. Mitochondrial oxidative phosphorylation function and mitophagy in ischaemic/reperfused hearts from control and high-fat diet rats: effects of long-term melatonin treatment. *Cardiovasc Drugs Ther.* (2020) 34:799–811. doi: 10.1007/s10557-020-06997-9
239. Han YS, Kim SM, Lee JH, Jung SK, Noh H, Lee SH. Melatonin protects chronic kidney disease mesenchymal stem cells against senescence via PrP(C) -dependent enhancement of the mitochondrial function. *J Pineal Res.* (2019) 66:e12535. doi: 10.1111/jpi.12535
240. Kang JW, Hong JM, Lee SM. Melatonin enhances mitophagy and mitochondrial biogenesis in rats with carbon tetrachloride-induced liver fibrosis. *J Pineal Res.* (2016) 60:383–93. doi: 10.1111/jpi.12319
241. Liu Y, Yan J, Sun C, Li G, Li S, Zhang L, et al. Ameliorating mitochondrial dysfunction restores carbon ion-induced cognitive deficits via co-activation of NRF2 and PINK1 signaling pathway. *Redox Biol.* (2018) 17:143–57. doi: 10.1016/j.redox.2018.04.012
242. Onphachanh X, Lee HJ, Lim JR, Jung YH, Kim JS, Chae CW, et al. Enhancement of high glucose-induced PINK1 expression by melatonin stimulates neuronal cell survival: involvement of MT(2)/Akt/NF-κB pathway. *J Pineal Res.* (2017) 63:e12427. doi: 10.1111/jpi.12427
243. Wang Q, Zhang M, Torres G, Wu S, Ouyang C, Xie Z, et al. Metformin suppresses diabetes-accelerated atherosclerosis via the

inhibition of drp1-mediated mitochondrial fission. *Diabetes.* (2017) 66:193–205. doi: 10.2337/db16-0915

244. de Marañón AM, Canet F, Abad-Jiménez Z, Jover A, Morillas C, Rocha M, et al. Does metformin modulate mitochondrial dynamics and function in type 2 diabetic patients? *Antioxid Redox Signal.* (2021) 35:377–85. doi: 10.1089/ars.2021.0019
245. Hu Y, Chen H, Zhang L, Lin X, Li X, Zhuang H, et al. The AMPK-MFN2 axis regulates MAM dynamics and autophagy induced by energy stresses. *Autophagy.* (2021) 17:1142–56. doi: 10.1080/15548627.2020.1749490
246. Izzo A, Nitti M, Mollo N, Paladino S, Procaccini C, Faicchia D, et al. Metformin restores the mitochondrial network and reverses mitochondrial dysfunction in down syndrome cells. *Hum Mol Genet.* (2017) 26:1056–69. doi: 10.1093/hmg/ddx016
247. Mollo N, Nitti M, Zerillo L, Faicchia D, Micillo T, Accarino R, et al. Pioglitazone improves mitochondrial organization and bioenergetics in down syndrome cells. *Front Genet.* (2019) 10:606. doi: 10.3389/fgene.2019.00606

Conflict of Interest: The authors declare that the research was conducted in the absence of any commercial or financial relationships that could be construed as a potential conflict of interest.

Publisher's Note: All claims expressed in this article are solely those of the authors and do not necessarily represent those of their affiliated organizations, or those of the publisher, the editors and the reviewers. Any product that may be evaluated in this article, or claim that may be made by its manufacturer, is not guaranteed or endorsed by the publisher.

Copyright © 2021 Yin and Shen. This is an open-access article distributed under the terms of the Creative Commons Attribution License (CC BY). The use, distribution or reproduction in other forums is permitted, provided the original author(s) and the copyright owner(s) are credited and that the original publication in this journal is cited, in accordance with accepted academic practice. No use, distribution or reproduction is permitted which does not comply with these terms.

frontiers in Cardiovascular Medicine

REVIEW
published: 28 September 2021
doi: 10.3389/fcvm.2021.749756

Role of the Mitochondrial Protein Import Machinery and Protein Processing in Heart Disease

*Fujie Zhao and Ming-Hui Zou**

Center for Molecular and Translational Medicine, Georgia State University, Atlanta, GA, United States

Mitochondria are essential organelles for cellular energy production, metabolic homeostasis, calcium homeostasis, cell proliferation, and apoptosis. About 99% of mammalian mitochondrial proteins are encoded by the nuclear genome, synthesized as precursors in the cytosol, and imported into mitochondria by mitochondrial protein import machinery. Mitochondrial protein import systems function not only as independent units for protein translocation, but also are deeply integrated into a functional network of mitochondrial bioenergetics, protein quality control, mitochondrial dynamics and morphology, and interaction with other organelles. Mitochondrial protein import deficiency is linked to various diseases, including cardiovascular disease. In this review, we describe an emerging class of protein or genetic variations of components of the mitochondrial import machinery involved in heart disease. The major protein import pathways, including the presequence pathway (TIM23 pathway), the carrier pathway (TIM22 pathway), and the mitochondrial intermembrane space import and assembly machinery, related translocases, proteinases, and chaperones, are discussed here. This review highlights the importance of mitochondrial import machinery in heart disease, which deserves considerable attention, and further studies are urgently needed. Ultimately, this knowledge may be critical for the development of therapeutic strategies in heart disease.

Keywords: mitochondrial protein import machinery, heart disease, TOM complex, TIM23 complex, TIM22 complex, CHCHD4 (MIA40)

OPEN ACCESS

Edited by:
Shijun Wang,
Fudan University, China

Reviewed by:
Piotr Bragoszewski,
Nencki Institute of Experimental Biology (PAS), Poland
Xin Jie Chen,
Upstate Medical University, United States

***Correspondence:**
Ming-Hui Zou
mzou@gsu.edu

Specialty section:
This article was submitted to Cardiovascular Metabolism, a section of the journal Frontiers in Cardiovascular Medicine

Received: *29 July 2021*
Accepted: *26 August 2021*
Published: *28 September 2021*

Citation:
Zhao F and Zou M-H (2021) Role of the Mitochondrial Protein Import Machinery and Protein Processing in Heart Disease. Front. Cardiovasc. Med. 8:749756. doi: 10.3389/fcvm.2021.749756

INTRODUCTION

Mitochondria are vital for energy production in eukaryotic cells, generating cellular ATP through oxidative phosphorylation (OXPHOS) (1). Importantly, mitochondria are also crucial for numerous metabolic pathways, maintenance of calcium homeostasis, and regulation of cell proliferation and apoptosis (2). However, only 13 proteins involved in OXPHOS are encoded by the mitochondrial genome in mammals. About 99%—more than 1,500—mammalian mitochondrial proteins are encoded by the nuclear genome, synthesized as precursors in the cytosol, and need to be imported into mitochondria by mitochondrial protein import machinery (3). To date, six translocases of the mitochondrial protein import machinery have been discovered. The TOM complex serves as the entry gate for most precursors at the outer membrane (OM); the TIM22 and TIM23 complexes at the inner membrane (IM) are responsible for the insertion of carrier precursors into the IM and the translocation of presequence-carrying precursors into the mitochondrial matrix or IM individually; the mitochondrial intermembrane space (IMS) import

and assembly machinery (MIA) complex mediates the import of cysteine-rich proteins to the IMS; the SAM and MIM complexes are responsible for insertion of β-barrel proteins and α-helical proteins, respectively, into the OM (**Figure 1** and **Table 1**) (3). The dynamic interaction and cooperation of these mitochondrial protein import pathways enable cells to respond to environmental stress and energy demands rapidly and with plasticity. Further, mitochondrial protein import pathways function not only as independent units for protein translocation, but also are deeply integrated into a functional network of mitochondrial bioenergetics, protein quality control, mitochondrial dynamics and morphology, and interaction with other organelles (4). Mitochondrial protein import deficiency is linked to various diseases, including neuropathies, myopathies, neurodegenerative diseases, cancer, and cardiovascular disorders (5, 6). The heart is a high-energy–requiring organ that depends heavily on mitochondrial activity and the efficient import of mitochondrial proteins. However, in heart disease, the roles of the mitochondrial protein import machinery have not been well-studied. Here, we summarize the current knowledge on mitochondrial protein import in heart disease for the first time. This review highlights the importance of the mitochondrial import machinery in heart disease, which deserves considerable attention, and further studies are urgently needed. Ultimately, this knowledge may be critical for the development of therapeutic strategies in heart disease.

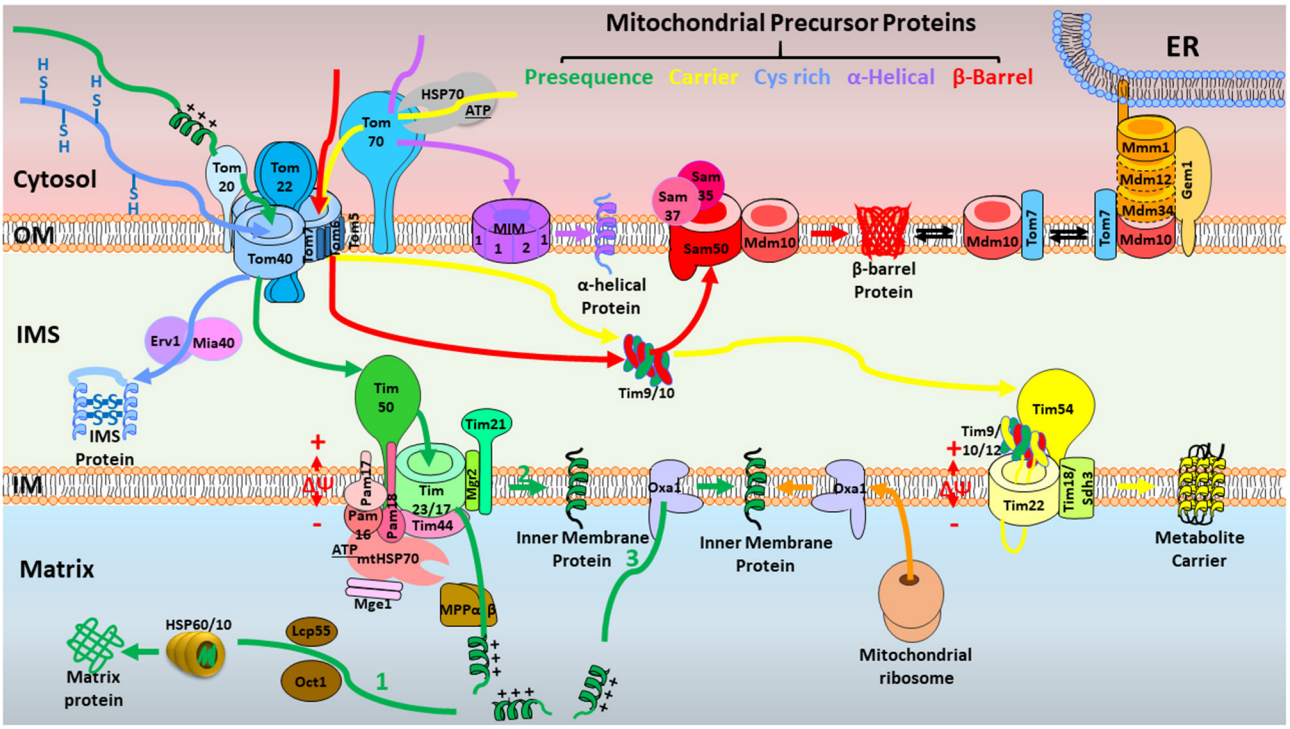

FIGURE 1 | Overview of the major mitochondrial protein import pathways in yeast. First, the presequence pathway transports presequence-carrying cleavable preproteins to the mitochondrial matrix (1) or IM (2, 3) (in green). Presequence-carrying precursors to the mitochondrial matrix (1) are typically recognized by TOM at the OM, passage the IM through TIM23, and are driven into the matrix assisted by PAM. $\Delta\psi$ across the IM is essential for the entry of presequences into the matrix. The presequences are cleaved by MPP, and additional proteolytic processing occurs by intermediate cleaving peptidases. Presequence-carrying precursors that integrate into IM follow two distinct routes. IM proteins are either directly laterally released from the TIM23 complex (2) or transported into the matrix first followed by further insertion into the IM with the help of Oxa1 (3). Oxa1 also is responsible for insertion of IM proteins synthesized on mitochondrial ribosomes. Second, in the carrier pathway for the import of precursor proteins without a cleavable presequence, yet with internal targeting signals into the IM (in yellow), carrier precursors are accompanied by cytosolic chaperones, delivered to the Tom70 receptor of the TOM complex, bound by small TIM chaperones in the IMS, and eventually integrated into the IM by the TIM22 complex in a $\Delta\psi$-dependent manner. Third, in the MIA pathway for cysteine-rich proteins to the IMS (in blue), the precursors are kept in a reduced state in the cytosol, imported by the TOM complex, oxidized by the MIA machinery, and stay in an oxidized state in the IMS. Fourth, in the SAM complex for β-barrel proteins to the OM (in red), the precursors of β-barrel proteins are imported by the TOM complex at the OM, bound to small TIM chaperones in the IMS, and inserted into the OM by the SAM complex. Fifth, some proteins with α-helical transmembrane segments are inserted into the OM by the MIM complex (in purple). Typically, the Tom40 channel is not involved in this route, but Tom70 is indispensable. In addition, ERMES is a complex that connects ER and mitochondrial OM, facilitating the dynamic substrate exchange between ER and mitochondrion. Mdm10 is a protein with dual localization in SAM and ERMES. OM, outer membrane; IM, inner membrane; IMS, intermembrane space; TOM, the translocase of the outer membrane; TIM23, the inner membrane translocase TIM23; PAM, presequence translocase-associated motor; $\Delta\psi$, membrane potential; MPP, mitochondrial processing peptidase; Oxa1, oxidase assembly protein 1; TIM22, the carrier translocase of the inner membrane TIM22; MIA, mitochondrial intermembrane space import and assembly machinery; SAM, sorting and assembly machinery; MIM, mitochondrial import complex; ERMES, endoplasmic reticulum (ER)–mitochondria encounter structure.

TABLE 1 | Components of mitochondrial import machinery in fungi and mammals.

Complex	Fungi (protein/gene name)	Mammals (protein/gene name)
TOM	Tom20/TOM20	Tom20/TOMM20
	Tom22/TOM22	Tom22/TOMM22
	Tom70/TOM70	Tom70/TOMM70
	Tom40/TOM40	Tom40/TOMM40
	Tom5/TOM5	Tom5/TOMM5
	Tom6/TOM6	Tom6/TOMM6
	Tom7/TOM7	Tom7/TOMM7
TIM22	Tim22/TIM22	Tim22/TIMM22
	Tim9/TIM9	Tim9/TIMM9
	Tim10/TIM10	Tim10a/TIMM10A
	Tim12/TIM12	Tim10b/TIMM10B
	Tim54/TIM54	
	Tim18/TIM18	
	Sdh3/SDH3	
		AGK/AGK
		Tim29/TIMM29
TIM23	Tim50/TIM50	Tim50/TIMM50
	Tim23/TIM23	Tim23/TIMM23
	Tim17/TIM17	Tim17a/TIMM17A
		Tim17b/TIMM17B
	Tim21/TIM21	Tim21/TIMM21
PAM	Tim44/TIM44	Tim44/TIMM44
	mtHsp70/SSC1	Mortalin/HSPA9
	(Pam16/Tim16)/(PAM16/TIM16)	(Tim16/Magmas)/(PAM16/MAGMAS)
	(Pam18/Tim14)/(PAM18/TIM14)	(DnaJC15/MCJ)/DNAJC15
		(DnaJC19/Tim14)/DNAJC19
	(Mge1/GrpE)/GRE1	mtGrpE/GRPEL1
	Pam17/PAM17	
OXA	Oxa1/OXA1	Oxa1/OXA1L
Matrix	(Mas1/β-MPP)/MAS1	β-MPP/PMPCB
	(Mas2/α-MPP)/MAS2	α-MPP/PMPCA
	MIP/OCT1	MIP/MIPEP
	Hsp60/HSP60	Hsp60/HSPD1
	Hsp10/HSP10	Hsp10/HSPE1
	mtHsp70/SSC1	mtHsp70/GRP75
	(Mge1/GrpE)/GRE1	mtGrpE/GRPEL1
MIA	Mia40/MIA40	Mia40/CHCHD4
	Erv1/ERV1	ALR/GFER
		AIF/AIFM1
SAM	Sam50/SAM50	Sam50/SAMM50
	Sam35/SAM35	Metaxin-1/MTX1
	Or	Metaxin-2/MTX2
	Sam37/SAM37	Metaxin-3/MTX3
	Mdm10/MDM10	
Soluble IMS TIMs	Tim9/TIM9	Tim9/TIMM9
	Tim10/TIM10	Tim10a/TIMM10A
	Tim8/TIM8	Tim10b/TIMM10B
	Tim13/TIM13	Tim8a/TIMM8A
		Tim8b/TIMM8B
		Tim13/TIMM13
Cytosolic chaperones	Hsp70/(SSB1 or SSB2)	Hsc70/HSPA8
		Hsp90 alpha/HSP90A
		Tom34/TOMM34
		AIP/AIP

OVERVIEW OF MITOCHONDRIAL PROTEIN IMPORT MACHINERY (IN YEAST)

Presequence Pathway to the Mitochondrial Matrix and IM

The presequence pathway is the best characterized pathway, responsible for the import of ∼60% of all mitochondrial proteins (7). The precursor proteins in this pathway carry a cleavable N-terminal presequence that functions as a targeting signal (7–9). This unique feature of the pathway distinguishes it from all the others, where the precursor proteins do not have cleavable presequences, but possess different kinds of internal targeting signals. **Presequence-carrying precursors to the mitochondrial matrix** are typically recognized by the translocase of the outer membrane (TOM) (9–11), passaged through the IM by the translocase of the inner membrane (TIM23) (12–16), and driven into the matrix assisted by the presequence translocase-associated motor (PAM) (**Figure 1**) (17–24). The membrane potential ($\Delta\psi$) across the IM is essential for the activation of the TIM23 channel and the translocation of presequences into the matrix (25–28). The presequences are cleaved by the mitochondrial processing peptidase (MPP) (3, 29–31), and additional proteolytic processing occurs by intermediate cleaving peptidases (7, 32–34). **Presequence-carrying precursors that integrate into the IM** follow two distinct routes (**Figure 1**). IM proteins are either directly released laterally from the TIM23 complex (35–37) or transported first into the matrix, followed by further insertion into the IM with the help of the oxidase assembly protein 1 (Oxa1) insertase (38–41). Oxa1 also is responsible for insertion of IM proteins synthesized on mitochondrial ribosomes (42).

The presequences are located at the N-termini of preproteins and typically consist of ∼15–50 amino acids. An essential characteristic of mitochondrial presequences is the formation of an amphipathic α-helix that is specifically recognized by mitochondrial import receptors and other mitochondrial import components during preprotein translocation by TOM, TIM23, and PAM (3).

The TOM complex is the main gate for precursors entering mitochondria. The TOM complex is composed of Tom20, Tom22, and Tom70 as receptors, β-barrel protein Tom40 forming the channel, and three small associated proteins, Tom5, Tom6, and Tom7 (11, 43–45). Tom20 and Tom22 function cooperatively as the receptors for presequence-carrying precursors (9, 10, 46). Tom70 mainly functions as the receptor for preproteins with internal targeting sequences, such as carrier precursors (47–52). Presequence-carrying precursors cross the Tom40 channel as linear polypeptide chains (44, 45, 53–57), and interact with the tail of the Tom22 receptor in the IMS (57). Tom22 has presequence binding sites on both the cytoplasmic and IMS sides of the OM. The exact roles of the three small subunits, Tom5, Tom6, and Tom7, have not been well-clarified. It has been proposed that they are not essential for TOM functions but are involved in the assembly and stability of the TOM complex (58–61).

The TIM23 complex translocates cleavable preproteins into mitochondrial matrix or IM. Tim50, Tim23, Tim17, and Tim21

compose the main elements of the TIM23 complex (12, 13, 16, 62–65). Tim50 functions as a presequence receptor that binds preproteins emerging in the IMS (63) and a channel blocker that closes out the TIM23 channel in the absence of preproteins (25, 66–69). Tim23 and associated partner Tim17 form the channel (16, 25, 28, 64, 70, 71). Tim21, Tim50, and Tim23 expose domains to the IMS that transiently connect the TOM and TIM23 complexes to facilitate the preprotein transfer (16, 67, 72–74). Additionally, Tim21 also physically links the TIM23 complex to the respiratory chain III-IV supercomplex [*bc*1 complex and cytochrome *c* oxidase (COX)] (65, 75, 76). Tim21 thus plays a dual role in TOM-TIM23 transfer and the recruitment of respiratory chain complexes. A small membrane protein, Mgr2, functions as a lateral gatekeeper for preproteins that are sorted into the IM (35, 76). The $\Delta\psi$ across the IM is crucial for translocation of the presequences through the Tim23 channel, which is negative at the matrix side and positive at the IMS side of the IM, whereas presequences are mostly positively charged. Two roles have been assigned to $\Delta\psi$: activation of TIM23 channel (25) and an electrophoretic effect that drives the import of presequences (77, 78).

PAM. The $\Delta\psi$ is a prerequisite for translocation of the presequence across the TIM23 channel. Nevertheless, it is not sufficient to import the entire protein into the matrix. PAM is necessary for the translocation of matrix proteins. The core of PAM is formed by the molecular chaperone mitochondrial 70 kDa heat shock protein (mtHsp70) (17, 18) and its co-chaperones (Tim44, Mge1, Pam16, Pam17, and Pam18) (16, 21, 79, 80). mtHsp70 binds the unfolded polypeptide chain and drives its translocation into the matrix in an ATP-dependent manner (17, 18). The peripheral membrane protein Tim44 is a docking site for mtHsp70 at the TIM23 complex (21). Mge1 (also known as mitochondrial GrpE) stimulates the release of ADP from mtHsp70 (81). Pam16, Pam17, and Pam18 are three membrane-associated co-chaperones. Pam18 (also termed Tim14) is a J-type co-chaperone that stimulates the ATPase activity of mtHsp70 (82, 83). The J-related Pam16 (Tim16) forms a complex with Pam18 and functions as a negative regulator (82–86). Pam17 mediates the organization of the TIM23–PAM interaction (79, 87).

MPP. Once arriving in the matrix, the presequences of both IM-sorted and matrix-targeted precursors are removed by a heterodimeric enzyme, MPP (3, 29–31, 88). Additional proteases, the intermediate cleaving peptidase (Icp55) (7, 89) and the octapeptidyl aminopeptidase (Oct1, also termed mitochondrial intermediate peptidase, MIP) (90, 91), can remove destabilizing N-terminal amino acid residues of the imported proteins. mtHSP70 and other chaperones, like the HSP60–HSP10 chaperonin complex, further assist proteins folding into their active forms (92). The clipped presequence peptides undergo subsequent degradation by the matrix peptidasome, termed presequence protease (PreP) or Cym1 (93, 94).

OXA translocase is vital for exporting proteins from the mitochondrial matrix into the IM. OXA has three different roles. (1) Proteins encoded by the mitochondrial genome are exported into the IM by Oxa1 (42, 95–97). (2) Some presequence-carrying proteins imported into the matrix *via* the TOM-TIM23 machinery are exported into the IM *via* Oxa1. This import-export pathway is termed conservative sorting of nuclear-encoded IM proteins (38–41, 98–100). (3) Oxa1 is also vital for the assembly of the carrier translocase TIM22 (38, 101).

Carrier Pathway Into the IM

The carrier pathway is the second mitochondrial protein import pathway to be discovered, and is responsible for importing precursor proteins without a cleavable presequence, yet with different kinds of internal targeting signals (3, 102–104). The carrier precursors are accompanied by cytosolic chaperones, such as the HSP70 and HSP90 classes in the cytosol, directly delivered to the Tom70 receptor of the TOM complex (47, 105, 106), and then bound by small TIM chaperones in the IMS (107–110) and eventually integrated into the IM by the carrier translocase of the IM (TIM22) complex in a $\Delta\psi$-dependent manner (**Figure 1**) (109, 111–116).

Chaperone-guided transport of carrier precursors (including chaperones in the cytosol and IMS). The carrier import pathway uses the same mitochondrial entry gate as the presequence pathway, the TOM complex. However, the mechanisms of translocation differ significantly. The involvement of cytosolic (47, 105, 106) and mitochondrial IMS chaperones, which is crucial to prevent aggregation of the hydrophobic carrier precursors in the aqueous environment, is the main feature distinguishing this from the presequence pathway. Chaperones of the Hsp70 and Hsp90 classes directly participate in delivering the precursors to Tom70 (47, 105, 106). The receptor Tom70 possesses two distinct binding sites, one for the precursor and another for a chaperone (47, 49, 117), ATP is needed to release the precursor proteins from the cytosolic chaperones (47, 48). Upon binding to Tom70, the carrier precursors are transferred to the central receptor Tom22, followed by insertion into the Tom40 channel in a loop conformation (118, 119), and transferred to small TIM chaperones in the IMS (107–110). These small TIM heterohexameric chaperone complexes, like the Tim9-Tim10 complex (120, 121) and the homologous Tim8-Tim13 complex (122), bind to the precursor proteins and transfer them through the aqueous IMS to IM.

Insertion of carrier precursors into the IM. The TIM22 complex consists of the receptor-like protein Tim54, the channel-forming protein Tim22, the Tim9-Tim10-Tim12 chaperone complex, and the Tim18-Sdh3 module. The majority of Tim54 domain is exposed to the IMS and probably functions as the binding site for the Tim9-Tim10-Tim12 complex (123, 124). The Tim9-Tim10-Tim12 complex is a modified form of the IMS chaperone, docking onto the TIM22 complex (123, 125). Carrier precursors are inserted into the Tim22 channel in a $\Delta\psi$-dependent manner (115). The Tim18-Sdh3 module is involved in the assembly of the TIM22 complex (126, 127). The carrier precursors are first bound to the Tim9–Tim10–Tim12 chaperone complex on the surface of the translocase. Upon activation of the Tim22 channel ($\Delta\psi$-dependent), the precursors are inserted into the translocase, probably in a loop structure. Finally, the proteins are laterally released into the lipid phase of the IM.

MIA Complex

Many IMS proteins contain internal targeting signals and characteristic cysteine motifs. In the cytosol, the precursors are kept in a reduced and unfolded state (128). Upon import by the TOM complex (60), they are oxidized by the MIA machinery, and stay in the IMS in an oxidized state (**Figure 1**). The MIA system consists of two main components: the oxidoreductase Mia40 and the sulfhydryl oxidase Erv1 (129–133).

Mia40 serves as a receptor and protein disulfide carrier. Most IMS proteins are synthesized without cleavable presequences but contain cysteine motifs. Unlike presequence-carrying precursors and carrier precursors, none of the Tom receptors is necessary for the import of MIA substrates (60, 61). Instead, upon passage through the Tom40 channel (60), Mia40 functions as a receptor on the IMS side of the Tom40 channel (133–138). It recognizes an internal signal of the precursor proteins, typically consisting of a hydrophobic element flanked by a cysteine residue (133, 139, 140). Mia40 binds to precursors *via* hydrophobic interaction and catalyzes the formation of disulfide bonds in imported proteins (133, 138). The disulfide bonds facilitate the conformational stabilization and assembly of many IMS proteins.

Erv1 cooperates with Mia40 in a disulfide relay. Mia40 does not form disulfide bonds *de novo*. Disulfide bonds are generated by Erv1 and transferred to Mia40 by the formation of transient intermolecular disulfide bonds (141). Mia40 then transfers the disulfides onto the imported protein. Upon transfer of disulfide bonds to proteins, cysteines of Mia40 become reduced and are re-oxidized by Erv1. Electrons originating from the oxidation of imported proteins flow in the opposite direction. They flow from Mia40 to Erv1 and then to O_2 or cytochrome *c* of the respiratory chain (141–144). In addition to most IMS proteins, some IM and matrix proteins are also MIA-system–dependent (28, 71, 113, 114, 145).

Sorting Pathways of Mitochondrial OM Proteins

All the mitochondrial OM proteins are imported from the cytosol. The membrane contains two different types of integral protein: β-barrel proteins, which are integrated into the membrane by multiple transmembrane β-strands, and α-helical proteins, which are membrane-anchored by one or more α-helical transmembrane segments.

Sorting and Assembly Machinery for β-Barrel Proteins. The precursors of β-barrel proteins initially pass through the TOM complex at the OM (146), then bind to small TIM chaperones in the IMS (110), like the carrier precursors, to avoid aggregation (**Figure 1**). Subsequent insertion of the β-barrel proteins into the OM is performed by the SAM complex, which consists of a membrane-integrated protein, Sam50 (Tob55), and two peripheral membrane proteins exposed to the cytosol, Sam35 and Sam37 (147–149). Folding of the β-barrel proteins occurs at Sam50-Sam35, followed by lateral release into the lipid phase of the OM (148, 150, 151). Sam37 directly interacts with Tom22, coupling the TOM and SAM complexes into a transient supercomplex that promotes the efficient transfer of precursor proteins (54, 152).

OM Insertion of α-Helical Proteins. The main α-helical proteins are classified as signal-anchored proteins (containing an α-helical transmembrane segment at the N-terminus), tail-anchored proteins (containing an α-helical transmembrane segment at the C-terminus), and polytopic (multi-spanning) OM proteins. α-helical OM proteins are imported *via* distinct routes that do not involve the Tom40 channel, in contrast to most mitochondrial proteins. The insertion of some signal-anchored and polytopic OM proteins is performed by the MIM complex (153–156), which consists of multiple copies of Mim1 and one copy of Mim2, both of which are small single-spanning OM proteins (**Figure 1**) (157, 158). Tom70 is required for the insertion of some polytopic proteins into MIM (155, 156). In the case of tail-anchored proteins and some multi-spanning proteins, import is aided by the lipid composition of the membrane, and no proteinaceous machinery has been identified (159–162). However, the exact mechanism for sorting and insertion of α-helical outer membrane proteins is only partially understood, and further studies are urgently needed.

INTEGRATION OF MITOCHONDRIAL PROTEIN IMPORT INTO FUNCTIONAL NETWORKS

Mitochondrial protein import pathways not only function as independent units for protein translocation, but also are deeply integrated into a functional network of mitochondrial bioenergetics, protein quality control, mitochondrial dynamics and morphology, and interaction with other organelles.

The protein import activity serves as a sensor for the fitness and quality of mitochondria. The protein import activity is determined by the energetic state ($\Delta\psi$, ATP levels) and protein homeostasis of mitochondria. Both the translocation of precursor proteins through the TIM23 complex and the TIM22 complex require the $\Delta\psi$ (25, 77, 78, 113, 115, 116). The ATP-dependent chaperones play essential roles in delivering carrier precursors to Tom70 receptor (47, 48), driving presequence precursor translocation to the matrix (17, 18) and folding in the matrix (92). Impairment of respiratory chain activity, reduction of ATP levels, and accumulation of misfolded proteins or reactive oxygen species (ROS) in the matrix (163) will directly affect the import-driving activity of the translocases. The protein import activity of mitochondria is thus a sensitive indicator of their energetic state and fitness.

Mitochondrial protein import machinery and respiratory chain assembly. Both the insertion of mitochondrial-encoded proteins from the matrix into the IM and the import of nuclear-encoded precursors from the cytosol into mitochondria rely heavily on the mitochondrial protein import machinery. Increased mitochondrial ROS levels generated by the respiratory chain contribute to decreased mitochondrial translation efficiency (164). In addition, the TIM23 complex forms supercomplexes with respiratory complexes III and IV as

well as with the ADP/ATP carrier. These interactions of the TIM23 complex facilitate protein import under energy-limiting conditions (65, 75, 165) and can also promote the assembly of respiratory complexes (166–168). The respiratory chain complexes also function as assembly platforms for some PAM subunits (75).

Mitochondrial protein import machinery associated with protein quality control, specifically in the following aspects: (1) Mitochondrial unfolded protein response (UPR^{mt}): the stress-activated transcription factor ATFS-1 contains a mitochondrial presequence and a nuclear localization signal. In healthy mitochondria, ATFS-1 is imported into the mitochondrial matrix and degraded by the LON AAA+ protease. When mitochondrial import is mildly impaired, ATFS-1 is translocated into the nucleus, where it functions as a transcription factor and induces expression of mitochondrial chaperones, proteases, and other elements to promote recovery of impaired mitochondria (169–171). (2) Unfolded protein response activated by mistargeted mitochondrial proteins (UPR [am]): upon mild damage to mitochondrial protein import, some mitochondrial precursors fail to enter mitochondria and accumulate in the cytosol, thus triggering mitochondrial Precursor Over-accumulation Stress (mPOS). This is followed by a stress response termed UPR [am] that reduces cytosolic protein synthesis and increases proteasome activity to clear the mistargeted proteins from the cytosol (172, 173). (3) PTEN-induced kinase 1 (PINK1)/Parkin-induced mitophagy: in healthy conditions, PINK1 is imported into the IM by the presequence pathway and processed by MPP and the presenilin-associated rhomboid-like protease PARL, following the retrotranslocation into the cytosol and degradation by the proteasome (174, 175). Upon severe damage to mitochondrial protein import, PINK1 remains at the OM bound to the TOM complex, where it phosphorylates ubiquitin and the E3 ubiquitin ligase Parkin, triggering the removal of damaged mitochondria by mitophagy (176, 177). (4) Mitochondria as guardian in the cytosol (MAGIC): in certain conditions, some aggregation-prone or misfolded cytosolic proteins may be imported into mitochondria for further degradation. This process is termed MAGIC, suggesting a crucial role of mitochondria in cytosolic proteostasis (178). (5) Proteolysis of mitochondrial proteins: upon removal of the presequence by MPP, destabilizing N-terminal amino acid residues of the imported proteins can be further removed by the intermediate cleaving peptidase Icp55 (which removes a single amino acid) or the mitochondrial intermediate peptidase Oct1 (which removes an octapeptide) (7, 34). The matrix AAA+ proteases, CLPXP and LON, degrade misfolded proteins and prevent protein aggregation in the matrix (179–182). The IM contains two AAA+ proteases: the i-AAA protease removes misfolded proteins from the IM, IMS, and OM (183–185), whereas the m-AAA protease degrades proteins from the matrix and IM (186, 187). Thus, the process of mitochondrial protein import is connected to protein turnover and quality control.

Mitochondrial protein import machinery connected to mitochondrial membrane architecture and dynamics. The mitochondrial contact site and cristae organizing system (MICOS) is a large protein complex enriched at crista junctions of the IM (188–190). It is crucial for the maintenance of inner membrane cristae organization and is embedded into an interactional network with protein translocases, including TOM, SAM, and MIA. Thus, it provides a dynamic link between protein import, mitochondrial membrane dynamics, and membrane contact sites (136, 188, 189, 191).

The inner-membrane fusion protein optic atrophy (OPA1) is an example of how protein import and processing are connected to mitochondrial membrane dynamics. OPA1 is first processed by matrix MPP, generating a long isoform, and further processed by different IM proteases, AAA+ protease, or OMA1 in mammals and Pcp1 in yeast, yielding a short isoform (192–195). The balance between long OPA1 and the short isoform is essential for membrane fusion and fission, which is modulated by stress and mitochondrial energetic state. Thus, the processing of imported mitochondrial protein is linked to mitochondrial fragmentation, mitophagy, or even cell death.

Endoplasmic reticulum–mitochondria encounter structure (ERMES). ERMES is a multi-subunit protein complex that connects the endoplasmic reticulum and mitochondrial OM, mainly formed by the MDM complex (196, 197). Other molecules, such as voltage-dependent anion-selective channel (VDAC) (198), TOM70 (199, 200), and inositol trisphosphate (inositol 1,4,5-trisphosphate) receptors (194) also play crucial roles in forming ER-mitochondria contact sites. The outer membrane protein Mdm10 is a subunit of both SAM and MDM complexes (196). The shuttling of Mdm10 between SAM and MDM is regulated by the small protein Tom7 (58, 196, 197, 201). Therefore, TOM, SAM, and ERMES are linked as a functional network, involved in the maintenance of mitochondrial morphology and the transport of lipids and calcium (202–205).

MITOCHONDRIAL PROTEIN IMPORT MACHINERY AND HEART DISEASE

Mitochondrial dynamics have become a key topic in the field of heart disease. However, only limited studies investigated the involvement of mitochondrial protein import machinery in these diseases (Summarized in **Table 2**). Moreover, most of these studies were related to the presequence pathway, which undertakes the import of ∼60% of all mitochondrial proteins.

Presequence Pathway Associated With Heart Disease

TOM Complex in Heart Disease

Tom20 is an essential receptor subunit of the TOM complex that recognizes mitochondrial precursor proteins with cleavable N-terminal presequences. Tom20 expression was reduced by ischemic insults (206, 207), and showed a cardioprotective role against ischemia/reperfusion (I/R) injury through enhancing the mitochondrial import of PKCepsilon (PKCε) in an HSP90-dependent manner (208). PKCε, a member of the serine/threonine kinase family, has been demonstrated to play a protective role against cardiac I/R injury (208, 216, 293). Additionally, calcium homeostasis, which is closely related to

TABLE 2 | Reported proteins or genes in mitochondrial protein import machinery associated with heart disease.

Protein/gene name	Import pathway/role	Associated disease/stress or physiological process	Expression or function in disease	References
Tom20/ TOMM20	TOM complex/ Receptor	Myocardial I/R injury; Cardiac calcium overload	Decreased level of Tom20 protein upon myocardial I/R injury; Potential regulator of cardiac calcium homeostasis.	(206–210)
Tom22/ TOMM22	TOM complex/ Receptor	Cardiac calcium homeostasis; Cardiac aldosterone synthesis; Chronic hypoxia	Receptor for mitoBK_{Ca}; Promoting the synthesis of cardiac aldosterone; Increased level of Tom22 mRNA in chronically hypoxic rat hearts.	(211–215)
Tom70/ TOMM70	TOM complex/ Receptor	Cardiac hypertrophy; Myocardial I/R injury; Myocardial infarction; Diabetic cardiomyopathy; Heart failure	Decreased level of Tom70 protein in hypertrophic and diabetic hearts, upon I/R injury or post-MI; Altered phosphorylation level of Tom70 in rat hearts with heart failure.	(216–228)
Tom40/ TOMM40	TOM complex/ Channel	Cardiovascular-related traits; Cardiac arrhythmia; Heat stress-induced apoptosis; Cardiac aging	TOMM40/APOE locus was associated with the main risk factors for cardiovascular disease; Homozygous deletion of TOMM40 in mammals was lethal; Heterozygous TOMM40 knockdown mice with ECG alteration; Upregulated Tom40 associated with heat stress-induced cardiomyocyte apoptosis; Reduced expression of Tom40 in hearts of old DCM patients.	(214, 215, 229–238)
Tom5/ TOMM5	TOM complex/ Assisted protein	Lipoprotein-associated phospholipase A2 activity	Correlated with increased activity of lipoprotein-associated phospholipase A2.	(239)
Tim50/ TIMM50	TIM23 complex/ Receptor	Cardiovascular developmental defects; DCM and cardiac hypertrophy	Loss of Tim50 impaired cardiac development in zebrafish embryos; Tim50 deficiency exacerbated cardiac hypertrophy in mice; Downregulated expression of Tim50 in human DCM hearts and in murine hypertrophic hearts.	(240, 241)
Tim23/ TIMM23	TIM23 complex/ Channel	Myocardial H/R or I/R injury; DCM	Reduced Tim23 expression level in hearts of patients with DCM, upon H/R or I/R injury.	(207, 238, 242–244)
mtHSP70/ GRP75	TOM-TIM23 pathway/ PAM	Myocardial H/R injury; Diabetic cardiomyopathy; Chronic AF	Decreased expression of mtHSP70 upon H/R injury, in IFM of T1DM hearts and SSM of T2DM hearts; Increased expression of mtHSP70 in human hearts with chronic AF.	(245–249)
Tim14/ DNAJC19	TOM-TIM23 pathway/ IM cochaperone	DCMA syndrome	Mutations in DNAJC19 were related to DCMA syndrome, a novel autosomal recessive syndrome characterized by early-onset DCM, non-progressive cerebellar ataxia, testicular dysgenesis, growth failure, mild developmental delay, and 3-methylglutaconic aciduria.	(250–255)
MAGMAS/ MAGMAS	TOM-TIM23 pathway/ IM cochaperone	Early death due to heart failure	Two patients from a family with MAGMAS mutation died at 2 years of age of heart failure.	(256)
HSP90/ HSP90A	TOM-TIM23 pathway/ Cytosolic chaperone	Myocardial I/R injury	HSP90 played a beneficial role against myocardial I/R injury.	(208, 217, 257–262)
HSP60/HSPD1 and HSP10/HSPE1	TOM-TIM23 pathway/ MM chaperones	DCM; Myocardial I/R injury; chronic AF; Early death due to heart failure	Cardiac-specific HSP60 deficiency in mice led to DCM; HSP10 overexpression protected against myocardial I/R injury; Both HSP60 and HSP10 were upregulated in human hearts with chronic AF; A girl with HSP60 deficiency died at 2 days of age of heart failure.	(263–266)
MPPα/ PMPCA	TOM-TIM23 pathway/ MPP	PMPCA gene mutation-associated multisystem impairments; Myocardial I/R injury	PMPCA mutants had multisystem impairments, including developmental delay, severe hypotonia, ataxia, lactic acidemia, severe hypertrophic left ventricular cardiomyopathy; Downregulation of MPPα was beneficial to cardiomyocytes during I/R injury.	(258, 267)
MIP/ MIPEP	TOM-TIM23 pathway/ MPP	COXPD31/Eldomery–Sutton syndrome	Mutations in the MIPEP gene caused COXPD31/Eldomery–Sutton syndrome, a recessive disorder with developmental delay, cardiomyopathy, cataracts, hypotonia, left ventricular non-compaction, variable seizures.	(268)
Lon Protease/ LONP1	TOM-TIM23 pathway/ MM Protease	High-fat diet stress; Cardiac hypertrophy; Hypoxia insults; Cardiac aging; Friedreich's ataxia	Lon seemed beneficial to cardiomyocytes upon high-fat diet and hypertrophic stresses but harmful to cardiomyocytes upon hypoxia insults; In aged hearts, Lon expression increased, but proteolytic efficiency declined; In cardiac-specific frataxin-deletion mice, Lon expression and activity were increased in the heart.	(269–276)
YME1L/ YME1L1	TOM-TIM23 pathway/ MM Protease	DCM and heart failure; Experimental autoimmune myocarditis; Myocardial infarction	Cardiac-specific ablation of YME1L in mice led to DCM and heart failure; YME1L was also crucial for the progression of experimental autoimmune myocarditis to DCM and the therapeutic efficacy of mesenchymal stem cells in myocardial infarction.	(195, 277–279)

(Continued)

TABLE 2 | Continued

Protein/gene name	Import pathway/role	Associated disease/stress or physiological process	Expression or function in disease	References
CLPP/ CLPP	TOM-TIM23 pathway/ MM Protease	DARS2-deficiency–related mitochondrial cardiomyopathy	Loss of CLPP in the heart could alleviate DARS2-deficiency–induced mitochondrial cardiomyopathy.	(280)
AGK/ AGK	TIM22 complex	Sengers syndrome	Mutations in the AGK gene led to Sengers syndrome, an autosomal recessive mitochondrial disorder characterized by hypertrophic cardiomyopathy, congenital cataracts, skeletal myopathy, exercise intolerance, and lactic acidosis.	(281–286)
Tim8a/ TIMM8A	small TIM chaperone in IMS	Myocardial I/R injury	Downregulation of Tim8a was related to the protective role of SB216763 treatment in myocardial I/R stress.	(258)
ALR/ GFER	CHCHD4 Mia40 complex	Cardiac development delay	Inhibition of ALR activity or expression in zebrafish embryos led to retarded cardiac development.	(287)
AIF/ AIFM1	CHCHD4 Mia40 complex	Prenatal ventriculomegaly; Childhood cardiomyopathy; Ischemic cardiomyopathy; DCM	Mutations in the AIFM1 gene led to early prenatal ventriculomegaly and childhood cardiomyopathy; Muscle-specific loss of AIF in mouse led to severe DCM; Harlequin (Hq) mice with AIF deficiency displayed more severe ischemic damage than wild-type hearts.	(288–292)

I/R, ischemia/reperfusion; mitoBK$_{Ca}$, mitochondrial large conductance voltage and Ca [2+]-dependent K [+] channel; MI, myocardial infarction; DCM, dilated cardiomyopathy; H/R, hypoxia/reoxygenation; AF, atrial fibrillation; IFM, interfibrillar mitochondria; SSM, subsarcolemmal mitochondria; T1DM, type 1 diabetes mellitus; T2DM, type 2 diabetes mellitus; MM, mitochondrial matrix; DNAJC19, DNAJ Homolog, subfamily C, member 19; IM, inner membrane; DCMA, dilated cardiomyopathy with ataxia; MPP$_{\alpha}$, Mitochondrial processing peptidase subunit alpha; MIP, mitochondrial intermediate peptidase; CLPP, mitochondrial ATP-dependent Clp proteolytic subunit; AGK, acylglycerol kinase; ALR, FAD-linked sulfhydryl oxidase ALR; AIF, apoptosis-inducing factor.

cardiac health, is influenced by Tom20. For example, Wattamon recently reported that the protective role of fibroblast growth factor 2 (FGF-2) against calcium overload was partially mediated by mitochondrial connexin 43 (Cx43) (introduced below), probably in a Tom20-dependent manner (209). Cx43 was imported into mitochondria *via* a Tom20-dependent pathway (257). In another study, Tom20 was reported to be responsible for the direct insertion of VDAC, a protein crucial in regulating cardiac calcium homeostasis (210) through mitochondrial permeability transition pore (mPTP) (294) and mitochondria-associated endoplasmic reticulum membranes (MAMs), into the OM of heart mitochondria in rats (295). Thus, Tom20 could be a crucial adaptor of cardiac calcium homeostasis in a Cx43- or VDAC-associated manner.

Tom22 serves as the central receptor for both presequence precursors and carrier precursors. Furthermore, it is also the key factor linking the TOM and SAM complex to a supercomplex by interaction with Sam37, which promotes the efficient transfer of β-barrel precursors. Tom22 was recently identified as a potential receptor for cardiac mitochondrial large conductance voltage and Ca^{2+}-dependent K [+] (mitoBK$_{Ca}$) channels, facilitating the import of mitoBK$_{Ca}$ *via* the presequence pathway (211). Tom22 deficiency might induce cardiomyocyte dysfunction by interfering with cardiac mitochondrial Ca^{2+} import (211). Additionally, Tom22 has been reported as a potential regulator of heart function through assisting the synthesis of cardiac aldosterone in mitochondria (212). Finally, in chronically hypoxic rat hearts, the level of Tom22 mRNA was increased in cardiac ventricles (213), suggesting a potential role of Tom22 in ischemic heart disease.

Tom40, encoded by the TOMM40 gene, forms the main protein-conducting channel of the TOM complex. Previous studies indicated TOMM40 was genetically associated with cardiovascular-related traits (214, 215, 229, 230). Several genome-wide association studies (GWAS) have identified that the TOMM40/APOE locus was strongly associated with low-density lipoprotein cholesterol [rs157580 (231)], high-density lipoprotein cholesterol [rs2075650, (232), rs157581 (233)], high-sensitivity C-reactive protein [rs2075650 (234)], type 2 diabetes [rs157580 (231)], or metabolic syndrome (235). Additionally, experimental evidence showed that homozygous deletion of TOMM40 in mammals was lethal, and heterozygous TOMM40 knockdown mice were found to have cardiac arrhythmia that deteriorated with age (236). Upregulated Tom40 transcription was reported associated with heat stress-induced apoptosis of rat cardiomyocytes (237). Moreover, expression of Tom40 and Tim23 was reduced only in older dilated cardiomyopathy (DCM) patients but not in younger DCM patients, suggesting age-related alterations of these proteins (238).

Small Tom Proteins (Tom5, Tom6, and Tom7). An allele of TOMM5 (the gene encoding Tom5) intronic variant (rs57578064) was correlated with a significant increase in lipoprotein-associated phospholipase A2 activity, which is associated with increased risk of cardiovascular events (239). Tom7 deficit in endothelial cells particularly damaged formation of the cerebrovascular network, but not cardiac vasculature, in zebrafish and mice (296).

TIM23 Complex in Heart Disease

Tim23, the channel-forming protein of the TIM23 complex, responsible for the translocation of presequence precursors into mitochondrial matrix or IM, was reduced by hypoxia/reoxygenation (H/R) or I/R (207, 242, 243). Restoring expression of Tim23 by various treatments seemed protective (207, 242, 243) against H/R or I/R injuries. However, a controversial study from Bian showed that the protective role of zinc against I/R injury was mediated by enhanced mitophagy, accompanied by downregulation of Tom20 and Tim23 expression (244). In addition, another study reported the association of decreased Tim23 expression in patients with DCM (238).

Tim50 is the receptor of the TIM23 complex that recognizes presequence carrying proteins. Guo et al. demonstrated that the loss of Tim50 during early zebrafish embryonic development caused neurodegeneration, cardiovascular defects (dysmorphic heart, reduced heartbeat, and decreased circulating blood), and impaired motility. These pathological changes might result from increased cell death, which was mediated by mitochondrial membrane permeabilization and acceleration of cytochrome *c* release (240). Tang et al. further identified that Tim50 was downregulated in both human DCM heart and transverse aortic constriction (TAC)-induced murine hypertrophic heart (241). Meanwhile, global Tim50 knockout mice showed more severe cardiac hypertrophy than wild-type mice, which was alleviated by cardiac-specific overexpression of Tim50 *via* reducing ROS accumulation and ASK1 activity (241).

The Presequence-Pathway–Associated Chaperones in Heart Disease

mtHSP70 (also known as GRP75/ mortalin/ PBP74) is an essential ATP-dependent chaperone of the PAM complex. It drives the translocation of preproteins into the matrix in the membrane-bound motor form and exhibits typical chaperone activity to prevent protein misfolding and aggregation in the soluble form. *In vitro* studies, mtHSP70 was identified as a cardioprotective chaperone against H/R-induced oxidative stress (245, 246), potentially *via* increased import of nuclear genome-encoded antioxidant defense proteins, such as DJ-1 (246). Expression of mtHSP70 was significantly decreased in the interfibrillar mitochondria (IFM) of type 1 diabetes mellitus (T1DM) (247) and the subsarcolemmal mitochondria (SSM) of type 2 diabetes mellitus (T2DM) (248). Cardiac-specific mtHSP70 overexpression restored cardiac function and nuclear-encoded mitochondrial protein import, contributing to a beneficial impact on proteome signature and enhanced mitochondrial function during T2DM (248). Further, mtHSP70 expression was increased in myocardial samples from patients with chronic atrial fibrillation, which suggested an adaptive heat shock response to restore cellular homeostasis (249).

HSP60 and HSP10 are mitochondrial matrix chaperones, playing pivotal roles in implementing protein folding and preventing protein aggregation. Cardiac-specific HSP60 deficiency in mice led to DCM, heart failure, and lethality. Interestingly, the import of preproteins into mitochondria was unaffected by HSP60 deficiency. However, the imported proteins processed by HSP60 underwent further degradation, suggesting lower stability of those proteins (263). HSP10 showed a similar cardioprotective role in I/R-induced myocyte death (264). Both the beneficial roles of HSP60 and HSP10 in cardiomyocytes were related to the preserved function of Complex I and Complex II. Clinical evidence found upregulated expression of both mitochondrial HSP60 and HSP10 in myocardial samples from patients with chronic atrial fibrillation (265). Agsteribbe et al. reported a single case of a girl who had facial dysmorphic features and breathing difficulties upon birth and died at 2 days of age of heart failure (266). The post-mortem examination revealed that the amount of mitochondrial HSP60 was only about 1/5 of the normal level (266).

Tim14 (encoded by DNAJC19), human homolog to yeast Pam18/Tim14, is a mitochondrial IM co-chaperone of the TIM23 complex. Mutations in DNAJC19 were related to DCM and cerebellar ataxia (DCMA) syndrome, a novel autosomal recessive syndrome characterized by early-onset DCM with conduction defects, non-progressive cerebellar ataxia, testicular dysgenesis, growth failure, mild developmental delay, and 3-methylglutaconic aciduria, with or without sensorineural hearing loss and basal ganglia lesions (250–255). The pathogenic mechanism of DCMA was associated with protein import inefficiency and cardiolipin remodeling. Experimental evidence suggested DNAJC19 forms a complex with prohibitins (PHBs). Furthermore, the loss of PHB/DNAJC19 complexes affected cardiolipin acylation and led to the accumulation of cardiolipin species with altered acyl chains (297).

MAGMAS (mitochondria-associated granulocyte macrophage colony stimulating factor signaling molecule), also termed PAM16/Tim16, forms a stable subcomplex with J-protein Pam18 or DnaJC19. It tethers to the TIM23 complex in yeast and humans (298). Cybel et al. reported that two patients from a family with MAGMAS mutation died at 2 years of age of heart failure (256).

HSP90, a chaperone mainly located in the cytoplasm, also played a beneficial role against I/R injury (258, 259) through translocation of PKCε, (208, 217) Cx43, (257, 260) AKT, (261), and Pim1/Lon (262) into mitochondria, potentially *via* the HSP-TOM mitochondrial import pathway.

The Presequence-Pathway–Associated Proteinases and Peptidases in Heart Disease

Mitochondrial Lon Protease is crucial for the clearance of oxidized or misfolded proteins in the matrix. It played a beneficial role in improving cardiac metabolic flexibility *via* degradation of pyruvate dehydrogenase kinase 4 in mice fed a high-fat diet (269). Moreover, it was also verified to enhance cardiac function *via* improving mitochondrial respiration capacity in pressure overload-induced heart failure in mice (270). However, it seemed harmful to cardiomyocytes upon hypoxia insults, which was associated with enhanced ROS production (271, 272) and accelerated degradation of phosphorylated complex IV subunits (273). In murine heart, mitochondrial Lon protease levels rose with age, but proteolytic efficiency and adaptation to stress were compromised in older animals (274, 275). Mitochondrial Lon protease was also found to be involved in Friedreich's

ataxia (FRDA), a rare hereditary neurodegenerative disease characterized by progressive ataxia and cardiomyopathy due to mitochondrial frataxin defect. In cardiac-specific frataxin-deletion mice, a progressive increase in mitochondrial Lon and ClpP protease expression and activity were found in the heart, accompanied by the loss of mitochondrial Fe–S proteins (276).

YME1L. As we mentioned above, the balance between long OPA1 (L-OPA1) and short OPA1 (S-OPA1), which is crucial for mitochondrial fusion and fission, is modulated by two mitochondrial proteases, OMA1 and the AAA+ protease YME1L. Cardiac-specific ablation of YME1L in mice led to DCM and heart failure *via* activated OMA1 and accelerated OPA1 proteolysis, which triggered mitochondrial fragmentation and altered cardiac metabolism (195). Moreover, cardiac function and mitochondrial morphology were rescued by Oma1 deletion by preventing OPA1 cleavage (195). The regulation of YME1L in mitochondrial fusion *via* OPA1 proteolysis was further verified in experimental autoimmune myocarditis animals (277) and YME1L-overexpressing or deficit cells (278). Furthermore, it was related to the therapeutic efficacy of mesenchymal stem cells for myocardial infarction (279).

MPPα. MPP is a dimeric protease in the matrix that removes N-terminal presequences and consists of MPPα and MPPβ. Mugdha reported that a patient with mutations in the PMPCA gene, which encodes MPPα, had multisystem impairments, including developmental delay, severe hypotonia, ataxia, lactic acidemia, and severe hypertrophic left ventricular cardiomyopathy and died at 14 months from respiratory failure (267). This phenotype may be related to reduced MPPα levels and impaired processing of frataxin and other mitochondrial proteins. Downregulation of MPPα was found linked to the protective role of GSK inhibitor SB216763 in I/R injury (258).

MIP/Oct1. Upon removal of the presequence by MPP, some mitochondrial precursor proteins undergo secondary processing carried out by the mitochondrial intermediate peptidase MIP/Oct1 or intermediate cleaving peptidase Icp55/XPNPEP3 to remove destabilizing N-terminal amino acid residues of the imported proteins. Mutations in the MIPEP gene, which encodes MIP, causes COXPD31/Eldomery–Sutton syndrome with developmental delay, cardiomyopathy, left ventricular non-compaction, hypotonia, and infantile death (268).

CLPP (mitochondrial ATP-dependent Clp proteolytic subunit), a mitochondrial matrix proteinase, has a central role in protein homeostasis. Loss of CLPP in the heart was found to alleviate mitochondrial cardiomyopathy induced by DARS2 deficiency, potentially mediated by increased *de novo* synthesis of individual OXPHOS subunits, without affecting the mammalian UPR [mt] (280).

Carrier Pathway Involved in Heart Disease

Tom70 mainly serves as the receptor for hydrophobic precursors without a cleavable presequence, such as carrier precursors. Tom70 protein was downregulated in hypertrophic heart of animals and humans, which was associated with increased oxidative stress. Furthermore, upregulation of Tom70 provided cardiomyocytes with full resistance to diverse pro-hypertrophic insults (218). Tom70 expression was also reduced by I/R insult in cardiomyocytes (219–222). Supplementation of Tom70 significantly attenuated I/R injury by promoting translocation of PKCε (216, 217) [to increase the expression of KATP channel pore-forming subunit Kir6.2 (223), augment mitochondrial respiratory capacity, and modulate cardiac glucose metabolism (224)], MICU1 (to reduce mitochondrial Ca^{2+} overload), (222) and PINK1 (associated with mitophagy) (221, 225) into mitochondria. Increased expression of PGC-1α/Tom70 was also involved in melatonin-induced cardiac protection against post-myocardial infarction, which was associated with inhibited mitochondrial impairment and reduced ROS generation (219, 220). In the hearts of diabetic db/db mice, Tom70 expression was suppressed. Reconstitution of Tom70 protected against diabetic cardiomyopathy through its antioxidant and antiapoptotic properties (226). Moreover, in aging hearts of diabetic db/db mice, only the expression of mitochondrial membrane proteins like Tom70 and VDAC, but not respiratory enzymes, could be increased by short-term exercise (227). Further, phosphoproteome mapping in a rat model of heart failure revealed phosphorylation of several import machinery proteins (Tom70, HSP90, and Tim8a), suggesting that the modification of mitochondrial protein import was involved in heart failure (228).

AGK (acylglycerol kinase). AGK is a mitochondrial lipid kinase that was recently identified as a subunit of the TIM22 complex. It plays an indispensable role in the import and assembly of mitochondrial carrier proteins in the IM (299). It has been shown that loss-of-function mutations in the AGK gene cause Sengers syndrome (281–286), an autosomal recessive mitochondrial disorder characterized by hypertrophic cardiomyopathy, congenital cataracts, skeletal myopathy, exercise intolerance, and lactic acidosis. Loss of AGK led to destabilized TIM22 complex; defects in the biogenesis of carrier substrates (such as adenine nucleotide translocator); lower complex I, III, and IV activities; perturbed tricarboxylic acid (TCA) cycle; and higher citrate synthase activity (300).

Tim8a (Tim8a/DDP1 and Tim8b/DDP2 are human homologs of yeast Tim8) is a small TIM chaperone in the IMS. Tim8a expression in ischemic rat heart was downregulated by treatment with GSK inhibitor SB216763, which showed a protective effect against I/R stress (258), suggesting a potential role of Tim8a in ischemic heart disease.

MIA Machinery Related to Heart Disease

FAD-linked sulfhydryl oxidase ALR is the human homolog of yeast Erv1. The interaction between Mia40 and Erv1/ALR facilitates the import of the small Tim proteins and cysteine-rich proteins. Inhibition of ALR activity by MitoBloCK-6 or a translation initiation codon (ATG) morpholino targeted to ALR in zebrafish embryos led to retarded cardiac development and impaired cardiac function (287).

Apoptosis-Inducing Factor (AIF) was initially characterized as a pro-apoptotic factor. It translocates from the mitochondrial IMS to the nucleus in the presence of apoptotic insults. It is also critical for the mitochondrial import and maturation of CHCHD4 (in human)/Mia40 (in yeast) (301–303). Mutations of the AIF-encoding gene AIFM1 led to early prenatal

ventriculomegaly (288) and childhood cardiomyopathy (289), accompanied by respiratory chain complex I and IV deficiency. Global loss of AIF in mice during embryogenesis resulted in embryonic growth retardation and death during mid-gestation. Muscle-specific loss of AIF in mice led to severe DCM and skeletal muscle atrophy, associated with a significant defect in respiratory chain complex I activity (290). The Harlequin (Hq) mice, a genetic model with an 80% reduction in mitochondrial AIF, displayed more severe ischemic damage than wild-type hearts after acute I/R injury (291, 292).

Other Molecules Involved in Heart Disease by Impacting Mitochondrial Protein Import Efficiency or Altering Mitochondrial Protein Translocation

Cardiolipin (CL) is a unique phospholipid that is localized and synthesized in mitochondrial IM. CL plays a central role in many biological processes, such as mitochondrial biogenesis, protein import, morphology and mitophagy, oxidative phosphorylation, and apoptosis (304–306). Defective remodeling of CL due to genetic mutations of TAZ-1 causes Barth syndrome, a rare, X-linked recessive, infantile-onset debilitating disorder characterized by early-onset cardiomyopathy, skeletal myopathy, growth delay, and neutropenia (304–309). The molecular mechanisms were partially mediated by impaired mitochondrial import machinery. CL was verified to play a central role in the structural integrity and functions of mitochondrial translocases, such as TOM Complex (44, 310), TIM22 Complex, and TIM23 Complex (26, 311, 312).

Connexin 43 (Cx43) is the predominant protein forming gap junctions and non-junctional hemichannels in ventricular cardiomyocytes and is also localized at the IM of cardiomyocyte mitochondria (313–315). The translocation of Cx43 to the IM was TOM-HSP90–dependent and was enhanced by ischemic preconditioning (IP). The beneficial role of mitochondrial Cx43 in I/R stress was associated with its regulation of mitochondrial potassium influx and ROS production (257, 313–315). The cardioprotection of IP was abolished by genetic ablation of Cx43, blockade of mitochondrial Cx43 import, or age-related loss of mitochondrial Cx43 (257, 316–318).

PINK1 is imported into the mitochondrial matrix in healthy conditions, followed by retrotranslocation into cytosol and degradation by the proteasome. Perturbation of this process causes mitophagy, which plays a vital role in the quality control of mitochondria in heart disease. Given that it has been well-studied and summarized in many other reviews (319, 320), we do not discuss it here in detail.

NDUFB10, an accessory subunit of complex I, is a substrate of the MIA machinery (CHCHD4/ Mia40) for oxidation-dependent protein import into the mitochondrial IMS. Mutation of cysteine 107 of NDUFB10 impaired its mitochondrial import *via* CHCHD4 and resulted in complex I assembly defect, led to fatal infantile lactic acidosis and cardiomyopathy in a single-case report of an infant (321).

In addition, some other proteins also showed a protective effect against I/R or H/R stress through enhancing their translocation from the cytosol to the mitochondria; these include α-crystallin B (cryAB, the major small heat shock protein in cardiomyocytes) *via* VDAC-Tom20 (322) and DJ-1 *via* mtHSP70 (246, 323–325).

Other Conditions That Affect Mitochondrial Protein Import Efficiency in Heart Disease

According to their subcellular spatial arrangement in cardiomyocytes, mitochondria are classified into three groups: subsarcolemmal mitochondria (SSM) existing below the cell membrane, interfibrillar mitochondria (IFM) residing in rows between the myofibrils, and perinuclear mitochondria located at the nuclear poles. Mitochondrial subpopulations vary in structure and function and appear to be influenced disparately in different cardiac pathologies, including I/R, heart failure, aging, exercise, and diabetes mellitus. According to recent studies, the mitochondrial import machinery in IFM of T1DM hearts (247, 326) and SSM of T2DM hearts (248, 327) were more susceptible to inefficiency. Further, many studies reported the downregulation of mitochondrial import-machinery components in heart disease, such as heart failure, DCM, ischemic cardiomyopathy, diabetic cardiomyopathy, etc. Supplements of corresponding components could partially recover cardiac function.

However, some studies pointed out an enhancement of mitochondrial protein import in aging animals. Craig et al. found mitochondria from senescent animals exhibited a higher import rate of precursors into the matrix than mitochondria from young animals (328). Later studies showed that, although expression of some key import machinery components was upregulated in the aging heart, import efficiency was compromised (238). The mechanism and significance need to be determined in future studies.

In addition, the import rate of matrix-localized proteins was found to be increased in heart of hyperthyroid animals or by T3 treatment (329–332), which was partially mediated by elevated levels of the OM receptor Tom20 and mtHSP70. Meanwhile, the proteolysis of matrix proteins was unaffected.

CONCLUSION

Mitochondrial import machinery pathways are involved in various heart diseases, including heart failure, DCM, hypertrophic cardiomyopathy, ischemic cardiomyopathy, and diabetic cardiomyopathy. Mutants of genes encoding components of the mitochondrial import machinery in humans or genetic deficiency of those genes in animals usually cause severe mitochondrial cardiomyopathy and are lethal, highlighting the critical role of mitochondrial import machinery in heart disease. However, compared with neurodegenerative diseases, in which the functions of mitochondrial import machinery are relatively well-studied and established, research in heart disease is still fairly limited. Although many studies

detected some components of mitochondrial import machinery, most studies simply regarded those components as indicators of mitochondrial content to evaluate mitochondrial biogenesis or mitophagy. The function of mitochondrial import machinery was highly neglected. Actually, even from the perspective of mitochondrial biogenesis or mitophagy, under different stimuli, import machinery components are able to adapt to diverse cellular functions, which are not always proportional to mitochondrial quantity.

Furthermore, our current understanding of mitochondrial import machinery in heart disease is still widely based on experimental evidence from yeast. Nevertheless, recent research in higher eukaryotes has identified more complex and diverse functions in some conserved components of mitochondrial import machinery. Furthermore, with the development of high-throughput sequencing in genomics, transcriptomics, proteomics, and metabolomics, more and more novel import machinery components have been revealed in mammals. The roles of mitochondrial import machinery in heart disease deserve considerable attention, and future studies are urgently needed.

AUTHOR CONTRIBUTIONS

FZ devised the original idea of the work, searched the literature, and wrote the manuscript. M-HZ edited the manuscript. All authors made significant contributions to this work and approved it for publication.

FUNDING

M-HZ's lab was supported by funding from the following agencies: National Heart, Lung, and Blood Institute (HL079584, HL080499, HL089920, HL110488, HL128014, HL132500, HL137371, and HL142287) and National Cancer Institute (CA213022). M-HZ is the Eminent Scholar in Molecular and Translational Medicine of the Georgia Research Alliance.

ACKNOWLEDGMENTS

We thank Jian Li for literature search. Yang Wu for the language editing and optimization. Donghong Zhang, Zhixue Liu, and Ping Song for critical reading of the manuscript.

REFERENCES

1. Dennerlein S, Wang C, Rehling P. Plasticity of mitochondrial translation. *Trends Cell Biol.* (2017) 27:712–21. doi: 10.1016/j.tcb.2017.05.004
2. Schmidt O, Harbauer AB, Rao S, Eyrich B, Zahedi RP, Stojanovski D, et al. Regulation of mitochondrial protein import by cytosolic kinases. *Cell.* (2011) 144:227–39. doi: 10.1016/j.cell.2010.12.015
3. Wiedemann N, Pfanner N. Mitochondrial machineries for protein import and assembly. *Annu Rev Biochem.* (2017) 86:685–714. doi: 10.1146/annurev-biochem-060815-014352
4. Pfanner N, Warscheid B, Wiedemann N. Mitochondrial proteins: from biogenesis to functional networks. *Nat Rev Mol Cell Biol.* (2019) 20:267–84. doi: 10.1038/s41580-018-0092-0
5. Nicolas E, Tricarico R, Savage M, Golemis EA, Hall MJ. Disease-associated genetic variation in human mitochondrial protein import. *Am J Hum Genet.* (2019) 104:784–801. doi: 10.1016/j.ajhg.2019.03.019
6. Jackson TD, Palmer CS, Stojanovski D. Mitochondrial diseases caused by dysfunctional mitochondrial protein import. *Biochem Soc Trans.* (2018) 46:1225–38. doi: 10.1042/BST20180239
7. Vogtle FN, Wortelkamp S, Zahedi RP, Becker D, Leidhold C, Gevaert K, et al. Global analysis of the mitochondrial N-proteome identifies a processing peptidase critical for protein stability. *Cell.* (2009) 139:428–39. doi: 10.1016/j.cell.2009.07.045
8. Roise D, Horvath SJ, Tomich JM, Richards JH, Schatz G. A chemically synthesized pre-sequence of an imported mitochondrial protein can form an amphiphilic helix and perturb natural and artificial phospholipid bilayers. *EMBO J.* (1986) 5:1327–34. doi: 10.1002/j.1460-2075.1986.tb04363.x
9. Abe Y, Shodai T, Muto T, Mihara K, Torii H, Nishikawa S, et al. Structural basis of presequence recognition by the mitochondrial protein import receptor Tom20. *Cell.* (2000) 100:551–60. doi: 10.1016/S0092-8674(00)80691-1
10. van Wilpe S, Ryan MT, Hill K, Maarse AC, Meisinger C, Brix J, et al. Tom22 is a multifunctional organizer of the mitochondrial preprotein translocase. *Nature.* (1999) 401:485–9. doi: 10.1038/46802
11. Mokranjac D, Neupert W. Cell biology: architecture of a protein entry gate. *Nature.* (2015) 528:201–2. doi: 10.1038/nature16318
12. Lohret TA, Jensen RE, Kinnally KW. Tim23, a protein import component of the mitochondrial inner membrane, is required for normal activity of the multiple conductance channel, MCC. *J Cell Biol.* (1997) 137:377–86. doi: 10.1083/jcb.137.2.377
13. Bauer MF, Sirrenberg C, Neupert W, Brunner M. Role of Tim23 as voltage sensor and presequence receptor in protein import into mitochondria. *Cell.* (1996) 87:33–41. doi: 10.1016/S0092-8674(00)81320-3
14. Dekker PJ, Keil P, Rassow J, Maarse AC, Pfanner N, Meijer M. Identification of MIM23, a putative component of the protein import machinery of the mitochondrial inner membrane. *FEBS Lett.* (1993) 330:66–70. doi: 10.1016/0014-5793(93)80921-G
15. Demishtein-Zohary K, Marom M, Neupert W, Mokranjac D, Azem A. GxxxG motifs hold the TIM23 complex together. *FEBS J.* (2015) 282:2178–86. doi: 10.1111/febs.13266
16. Chacinska A, Lind M, Frazier AE, Dudek J, Meisinger C, Geissler A, et al. Mitochondrial presequence translocase: switching between TOM tethering and motor recruitment involves Tim21 and Tim17. *Cell.* (2005) 120:817–29. doi: 10.1016/j.cell.2005.01.011
17. Kang PJ, Ostermann J, Shilling J, Neupert W, Craig EA, Pfanner N. Requirement for hsp70 in the mitochondrial matrix for translocation and folding of precursor proteins. *Nature.* (1990) 348:137–43. doi: 10.1038/348137a0
18. Horst M, Oppliger W, Rospert S, Schonfeld HJ, Schatz G, Azem A. Sequential action of two hsp70 complexes during protein import into mitochondria. *EMBO J.* (1997) 16:1842–9. doi: 10.1093/emboj/16.8.1842
19. Demishtein-Zohary K, Gunsel U, Marom M, Banerjee R, Neupert W, Azem A, et al. Role of Tim17 in coupling the import motor to the translocation channel of the mitochondrial presequence translocase. *Elife.* (2017) 6:22696. doi: 10.7554/eLife.22696
20. Ting SY, Yan NL, Schilke BA, Craig EA. Dual interaction of scaffold protein Tim44 of mitochondrial import motor with channel-forming translocase subunit Tim23. *Elife.* (2017) 6:23609. doi: 10.7554/eLife.23609
21. Banerjee R, Gladkova C, Mapa K, Witte G, Mokranjac D. Protein translocation channel of mitochondrial inner membrane and matrix-exposed import motor communicate via two-domain coupling protein. *Elife.* (2015) 4:e11897. doi: 10.7554/eLife.11897
22. Sikor M, Mapa K, von Voithenberg LV, Mokranjac D, Lamb DC. Real-time observation of the conformational dynamics of mitochondrial Hsp70 by spFRET. *EMBO J.* (2013) 32:1639–49. doi: 10.1038/emboj.2013.89
23. Schendzielorz AB, Schulz C, Lytovchenko O, Clancy A, Guiard B, Ieva R, et al. Two distinct membrane potential-dependent steps drive

mitochondrial matrix protein translocation. *J Cell Biol.* (2017) 216:83–92. doi: 10.1083/jcb.201607066
24. Schulz C, Rehling P. Remodelling of the active presequence translocase drives motor-dependent mitochondrial protein translocation. *Nat Commun.* (2014) 5:4349. doi: 10.1038/ncomms5349
25. Truscott KN, Kovermann P, Geissler A, Merlin A, Meijer M, Driessen AJ, et al. A presequence- and voltage-sensitive channel of the mitochondrial preprotein translocase formed by Tim23. *Nat Struct Biol.* (2001) 8:1074–82. doi: 10.1038/nsb726
26. Malhotra K, Modak A, Nangia S, Daman TH, Gunsel U, Robinson VL, et al. Cardiolipin mediates membrane and channel interactions of the mitochondrial TIM23 protein import complex receptor Tim50. *Sci Adv.* (2017) 3:e1700532. doi: 10.1126/sciadv.1700532
27. Denkert N, Schendzielorz AB, Barbot M, Versemann L, Richter F, Rehling P, et al. Cation selectivity of the presequence translocase channel Tim23 is crucial for efficient protein import. *Elife.* (2017) 6:28324. doi: 10.7554/eLife.28324
28. Ramesh A, Peleh V, Martinez-Caballero S, Wollweber F, Sommer F, van der Laan M, et al. A disulfide bond in the TIM23 complex is crucial for voltage gating and mitochondrial protein import. *J Cell Biol.* (2016) 214:417–31. doi: 10.1083/jcb.201602074
29. Hawlitschek G, Schneider H, Schmidt B, Tropschug M, Hartl FU, Neupert W. Mitochondrial protein import: identification of processing peptidase and of PEP, a processing enhancing protein. *Cell.* (1988) 53:795–806. doi: 10.1016/0092-8674(88)90096-7
30. Neupert W. A perspective on transport of proteins into mitochondria: a myriad of open questions. *J Mol Biol.* (2015) 427:1135–58. doi: 10.1016/j.jmb.2015.02.001
31. Fukasawa Y, Tsuji J, Fu SC, Tomii K, Horton P, Imai K. MitoFates: improved prediction of mitochondrial targeting sequences and their cleavage sites. *Mol Cell Proteomics.* (2015) 14:1113–26. doi: 10.1074/mcp.M114.043083
32. Varshavsky A. The N-end rule pathway and regulation by proteolysis. *Protein Sci.* (2011) 20:1298–345. doi: 10.1002/pro.666
33. Veling MT, Reidenbach AG, Freiberger EC, Kwiecien NW, Hutchins PD, Drahnak MJ, et al. Multi-omic mitoprotease profiling defines a role for Oct1p in coenzyme Q production. *Mol Cell.* (2017) 68:970–77 e11. doi: 10.1016/j.molcel.2017.11.023
34. Vogtle FN, Prinz C, Kellermann J, Lottspeich F, Pfanner N, Meisinger C. Mitochondrial protein turnover: role of the precursor intermediate peptidase Oct1 in protein stabilization. *Mol Biol Cell.* (2011) 22:2135–43. doi: 10.1091/mbc.e11-02-0169
35. Ieva R, Schrempp SG, Opalinski L, Wollweber F, Hoss P, Heisswolf AK, et al. Mgr2 functions as lateral gatekeeper for preprotein sorting in the mitochondrial inner membrane. *Mol Cell.* (2014) 56:641–52. doi: 10.1016/j.molcel.2014.10.010
36. Matta SK, Kumar A, D'Silva P. Mgr2 regulates mitochondrial preprotein import by associating with channel-forming Tim23 subunit. *Mol Biol Cell.* (2020) 31:1112–23. doi: 10.1091/mbc.E19-12-0677
37. Schendzielorz AB, Bragoszewski P, Naumenko N, Gomkale R, Schulz C, Guiard B, et al. Motor recruitment to the TIM23 channel's lateral gate restricts polypeptide release into the inner membrane. *Nat Commun.* (2018) 9:4028. doi: 10.1038/s41467-018-06492-8
38. Stiller SB, Hopker J, Oeljeklaus S, Schutze C, Schrempp SG, Vent-Schmidt J, et al. Mitochondrial OXA translocase plays a major role in biogenesis of inner-membrane proteins. *Cell Metab.* (2016) 23:901–8. doi: 10.1016/j.cmet.2016.04.005
39. Park K, Botelho SC, Hong J, Osterberg M, Kim H. Dissecting stop transfer vs. conservative sorting pathways for mitochondrial inner membrane proteins in vivo. *J Biol Chem.* (2013) 288:1521–32. doi: 10.1074/jbc.M112.409748
40. Bohnert M, Rehling P, Guiard B, Herrmann JM, Pfanner N, van der Laan M. Cooperation of stop-transfer and conservative sorting mechanisms in mitochondrial protein transport. *Curr Biol.* (2010) 20:1227–32. doi: 10.1016/j.cub.2010.05.058
41. Herrmann JM, Neupert W, Stuart RA. Insertion into the mitochondrial inner membrane of a polytopic protein, the nuclear-encoded Oxa1p. *EMBO J.* (1997) 16:2217–26. doi: 10.1093/emboj/16.9.2217
42. Hell K, Neupert W, Stuart RA. Oxa1p acts as a general membrane insertion machinery for proteins encoded by mitochondrial DNA. *EMBO J.* (2001) 20:1281–8. doi: 10.1093/emboj/20.6.1281
43. Kiebler M, Pfaller R, Sollner T, Griffiths G, Horstmann H, Pfanner N, et al. Identification of a mitochondrial receptor complex required for recognition and membrane insertion of precursor proteins. *Nature.* (1990) 348:610–6. doi: 10.1038/348610a0
44. Hill K, Model K, Ryan MT, Dietmeier K, Martin F, Wagner R, et al. Tom40 forms the hydrophilic channel of the mitochondrial import pore for preproteins [see comment]. *Nature.* (1998) 395:516–21. doi: 10.1038/26780
45. Shiota T, Imai K, Qiu J, Hewitt VL, Tan K, Shen HH, et al. Molecular architecture of the active mitochondrial protein gate. *Science.* (2015) 349:1544–8. doi: 10.1126/science.aac6428
46. Yamano K, Yatsukawa Y, Esaki M, Hobbs AE, Jensen RE, Endo T. Tom20 and Tom22 share the common signal recognition pathway in mitochondrial protein import. *J Biol Chem.* (2008) 283:3799–807. doi: 10.1074/jbc.M708339200
47. Young JC, Hoogenraad NJ, Hartl FU. Molecular chaperones Hsp90 and Hsp70 deliver preproteins to the mitochondrial import receptor Tom70. *Cell.* (2003) 112:41–50. doi: 10.1016/S0092-8674(02)01250-3
48. Bhangoo MK, Tzankov S, Fan AC, Dejgaard K, Thomas DY, Young JC. Multiple 40-kDa heat-shock protein chaperones function in Tom70-dependent mitochondrial import. *Mol Biol Cell.* (2007) 18:3414–28. doi: 10.1091/mbc.e07-01-0088
49. Wu Y, Sha B. Crystal structure of yeast mitochondrial outer membrane translocon member Tom70p. *Nat Struct Mol Biol.* (2006) 13:589–93. doi: 10.1038/nsmb1106
50. Backes S, Hess S, Boos F, Woellhaf MW, Godel S, Jung M, et al. Tom70 enhances mitochondrial preprotein import efficiency by binding to internal targeting sequences. *J Cell Biol.* (2018) 217:1369–82. doi: 10.1083/jcb.201708044
51. Melin J, Kilisch M, Neumann P, Lytovchenko O, Gomkale R, Schendzielorz A, et al. A presequence-binding groove in Tom70 supports import of Mdl1 into mitochondria. *Biochim Biophys Acta.* (2015) 1853:1850–9. doi: 10.1016/j.bbamcr.2015.04.021
52. Yamamoto H, Fukui K, Takahashi H, Kitamura S, Shiota T, Terao K, et al. Roles of Tom70 in import of presequence-containing mitochondrial proteins. *J Biol Chem.* (2009) 284:31635–46. doi: 10.1074/jbc.M109.041756
53. Bayrhuber M, Meins T, Habeck M, Becker S, Giller K, Villinger S, et al. Structure of the human voltage-dependent anion channel. *Proc Natl Acad Sci USA.* (2008) 105:15370–5. doi: 10.1073/pnas.0808115105
54. Qiu J, Wenz LS, Zerbes RM, Oeljeklaus S, Bohnert M, Stroud DA, et al. Coupling of mitochondrial import and export translocases by receptor-mediated supercomplex formation. *Cell.* (2013) 154:596–608. doi: 10.1016/j.cell.2013.06.033
55. Lackey SW, Taylor RD, Go NE, Wong A, Sherman EL, Nargang FE. Evidence supporting the 19 beta-strand model for Tom40 from cysteine scanning and protease site accessibility studies. *J Biol Chem.* (2014) 289:21640–50. doi: 10.1074/jbc.M114.578765
56. Esaki M, Kanamori T, Nishikawa S, Shin I, Schultz PG, Endo T. Tom40 protein import channel binds to non-native proteins and prevents their aggregation. *Nat Struct Biol.* (2003) 10:988–94. doi: 10.1038/nsb1008
57. Melin J, Schulz C, Wrobel L, Bernhard O, Chacinska A, Jahn O, et al. Presequence recognition by the tom40 channel contributes to precursor translocation into the mitochondrial matrix. *Mol Cell Biol.* (2014) 34:3473–85. doi: 10.1128/MCB.00433-14
58. Yamano K, Tanaka-Yamano S, Endo T. Tom7 regulates Mdm10-mediated assembly of the mitochondrial import channel protein Tom40. *J Biol Chem.* (2010) 285:41222–31. doi: 10.1074/jbc.M110.163238
59. Dietmeier K, Honlinger A, Bomer U, Dekker PJ, Eckerskorn C, Lottspeich F, et al. Tom5 functionally links mitochondrial preprotein receptors to the general import pore. *Nature.* (1997) 388:195–200. doi: 10.1038/40663
60. Gornicka A, Bragoszewski P, Chroscicki P, Wenz LS, Schulz C, Rehling P, et al. discrete pathway for the transfer of intermembrane space proteins across the outer membrane of mitochondria. *Mol Biol Cell.* (2014) 25:3999–4009. doi: 10.1091/mbc.e14-06-1155
61. Kurz M, Martin H, Rassow J, Pfanner N, Ryan MT. Biogenesis of Tim proteins of the mitochondrial carrier import pathway: differential targeting

mechanisms and crossing over with the main import pathway. *Mol Biol Cell.* (1999) 10:2461–74. doi: 10.1091/mbc.10.7.2461
62. Schulz C, Schendzielorz A, Rehling P. Unlocking the presequence import pathway. *Trends Cell Biol.* (2015) 25:265–75. doi: 10.1016/j.tcb.2014.12.001
63. Rahman B, Kawano S, Yunoki-Esaki K, Anzai T, Endo T, NMR. analyses on the interactions of the yeast Tim50 C-terminal region with the presequence and Tim50 core domain. *FEBS Lett.* (2014) 588:678–84. doi: 10.1016/j.febslet.2013.12.037
64. Martinez-Caballero S, Grigoriev SM, Herrmann JM, Campo ML, Kinnally KW. Tim17p regulates the twin pore structure and voltage gating of the mitochondrial protein import complex TIM23. *J Biol Chem.* (2007) 282:3584–93. doi: 10.1074/jbc.M607551200
65. van der Laan M, Wiedemann N, Mick DU, Guiard B, Rehling P, Pfanner N, et al. role for Tim21 in membrane-potential-dependent preprotein sorting in mitochondria. *Curr Biol.* (2006) 16:2271–6. doi: 10.1016/j.cub.2006.10.025
66. Meinecke M, Wagner R, Kovermann P, Guiard B, Mick DU, Hutu DP, et al. Tim50 maintains the permeability barrier of the mitochondrial inner membrane. *Science.* (2006) 312:1523–6. doi: 10.1126/science.1127628
67. Tamura Y, Harada Y, Shiota T, Yamano K, Watanabe K, Yokota M, et al. Tim23-Tim50 pair coordinates functions of translocators and motor proteins in mitochondrial protein import. *J Cell Biol.* (2009) 184:129–41. doi: 10.1083/jcb.200808068
68. Mokranjac D, Sichting M, Popov-Celeketic D, Mapa K, Gevorkyan-Airapetov L, Zohary K, et al. Role of Tim50 in the transfer of precursor proteins from the outer to the inner membrane of mitochondria. *Mol Biol Cell.* (2009) 20:1400–7. doi: 10.1091/mbc.e08-09-0934
69. Gevorkyan-Airapetov L, Zohary K, Popov-Celeketic D, Mapa K, Hell K, Neupert W, et al. Interaction of Tim23 with Tim50 is essential for protein translocation by the mitochondrial TIM23 complex. *J Biol Chem.* (2009) 284:4865–72. doi: 10.1074/jbc.M807041200
70. Rainbolt TK, Atanassova N, Genereux JC, Wiseman RL. Stress-regulated translational attenuation adapts mitochondrial protein import through Tim17A degradation. *Cell Metab.* (2013) 18:908–19. doi: 10.1016/j.cmet.2013.11.006
71. Wrobel L, Sokol AM, Chojnacka M, Chacinska A. The presence of disulfide bonds reveals an evolutionarily conserved mechanism involved in mitochondrial protein translocase assembly. *Sci Rep.* (2016) 6:27484. doi: 10.1038/srep27484
72. Lytovchenko O, Melin J, Schulz C, Kilisch M, Hutu DP, Rehling P. Signal recognition initiates reorganization of the presequence translocase during protein import. *EMBO J.* (2013) 32:886–98. doi: 10.1038/emboj.2013.23
73. Mokranjac D, Popov-Celeketic D, Hell K, Neupert W. Role of Tim21 in mitochondrial translocation contact sites. *J Biol Chem.* (2005) 280:23437–40. doi: 10.1074/jbc.C500135200
74. Albrecht R, Rehling P, Chacinska A, Brix J, Cadamuro SA, Volkmer R, et al. The Tim21 binding domain connects the preprotein translocases of both mitochondrial membranes. *EMBO Rep.* (2006) 7:1233–8. doi: 10.1038/sj.embor.7400828
75. Wiedemann N, van der Laan M, Hutu DP, Rehling P, Pfanner N. Sorting switch of mitochondrial presequence translocase involves coupling of motor module to respiratory chain. *J Cell Biol.* (2007) 179:1115–22. doi: 10.1083/jcb.200709087
76. Gebert M, Schrempp SG, Mehnert CS, Heisswolf AK, Oeljeklaus S, Ieva R, et al. Mgr2 promotes coupling of the mitochondrial presequence translocase to partner complexes. *J Cell Biol.* (2012) 197:595–604. doi: 10.1083/jcb.201110047
77. Martin J, Mahlke K, Pfanner N. Role of an energized inner membrane in mitochondrial protein import. Delta psi drives the movement of presequences. *J Biol Chem.* (1991) 266:18051–7. doi: 10.1016/S0021-9258(18)55235-2
78. Turakhiya U, von der Malsburg K, Gold VAM, Guiard B, Chacinska A, van der Laan M, et al. Protein import by the mitochondrial presequence translocase in the absence of a membrane potential. *J Mol Biol.* (2016) 428:1041–52. doi: 10.1016/j.jmb.2016.01.020
79. Popov-Celeketic D, Mapa K, Neupert W, Mokranjac D. Active remodelling of the TIM23 complex during translocation of preproteins into mitochondria. *EMBO J.* (2008) 27:1469–80. doi: 10.1038/emboj.2008.79
80. Ting SY, Schilke BA, Hayashi M, Craig EA. Architecture of the TIM23 inner mitochondrial translocon and interactions with the matrix import motor. *J Biol Chem.* (2014) 289:28689–96. doi: 10.1074/jbc.M114.588152
81. Dekker PJ, Pfanner N. Role of mitochondrial GrpE and phosphate in the ATPase cycle of matrix Hsp70. *J Mol Biol.* (1997) 270:321–7. doi: 10.1006/jmbi.1997.1131
82. Mokranjac D, Bourenkov G, Hell K, Neupert W, Groll M. Structure and function of Tim14 and Tim16, the J and J-like components of the mitochondrial protein import motor. *EMBO J.* (2006) 25:4675–85. doi: 10.1038/sj.emboj.7601334
83. D'Silva PR, Schilke B, Hayashi M, Craig EA. Interaction of the J-protein heterodimer Pam18/Pam16 of the mitochondrial import motor with the translocon of the inner membrane. *Mol Biol Cell.* (2008) 19:424–32. doi: 10.1091/mbc.e07-08-0748
84. Kozany C, Mokranjac D, Sichting M, Neupert W, Hell K. The J domain-related cochaperone Tim16 is a constituent of the mitochondrial TIM23 preprotein translocase. *Nat Struct Mol Biol.* (2004) 11:234–41. doi: 10.1038/nsmb734
85. Frazier AE, Dudek J, Guiard B, Voos W, Li Y, Lind M, et al. Pam16 has an essential role in the mitochondrial protein import motor. *Nat Struct Mol Biol.* (2004) 11:226–33. doi: 10.1038/nsmb735
86. Li Y, Dudek J, Guiard B, Pfanner N, Rehling P, Voos W. The presequence translocase-associated protein import motor of mitochondria. Pam16 functions in an antagonistic manner to Pam18. *J Biol Chem.* (2004) 279:38047–54. doi: 10.1074/jbc.M404319200
87. van der Laan M, Chacinska A, Lind M, Perschil I, Sickmann A, Meyer HE, et al. Pam17 is required for architecture and translocation activity of the mitochondrial protein import motor. *Mol Cell Biol.* (2005) 25:7449–58. doi: 10.1128/MCB.25.17.7449-7458.2005
88. Taylor AB, Smith BS, Kitada S, Kojima K, Miyaura H, Otwinowski Z, et al. Crystal structures of mitochondrial processing peptidase reveal the mode for specific cleavage of import signal sequences. *Structure.* (2001) 9:615–25. doi: 10.1016/S0969-2126(01)00621-9
89. Naamati A, Regev-Rudzki N, Galperin S, Lill R, Pines O. Dual targeting of Nfs1 and discovery of its novel processing enzyme, Icp55. *J Biol Chem.* (2009) 284:30200–8. doi: 10.1074/jbc.M109.034694
90. Gakh O, Cavadini P, Isaya G. Mitochondrial processing peptidases. *Biochim Biophys Acta.* (2002) 1592:63–77. doi: 10.1016/S0167-4889(02)00265-3
91. Koppen M, Langer T. Protein degradation within mitochondria: versatile activities of AAA proteases and other peptidases. *Crit Rev Biochem Mol Biol.* (2007) 42:221–42. doi: 10.1080/10409230701380452
92. Ostermann J, Horwich AL, Neupert W, Hartl FU. Protein folding in mitochondria requires complex formation with hsp60 and ATP hydrolysis. *Nature.* (1989) 341:125–30. doi: 10.1038/341125a0
93. Johnson KA, Bhushan S, Stahl A, Hallberg BM, Frohn A, Glaser E, et al. The closed structure of presequence protease PreP forms a unique 10,000 Angstroms3 chamber for proteolysis. *EMBO J.* (2006) 25:1977–86. doi: 10.1038/sj.emboj.7601080
94. Mossmann D, Vogtle FN, Taskin AA, Teixeira PF, Ring J, Burkhart JM, et al. Amyloid-beta peptide induces mitochondrial dysfunction by inhibition of preprotein maturation. *Cell Metab.* (2014) 20:662–9. doi: 10.1016/j.cmet.2014.07.024
95. He S, Fox TD. Membrane translocation of mitochondrially coded Cox2p: distinct requirements for export of N and C termini and dependence on the conserved protein Oxa1p. *Mol Biol Cell.* (1997) 8:1449–60. doi: 10.1091/mbc.8.8.1449
96. Pfeffer S, Woellhaf MW, Herrmann JM, Forster F. Organization of the mitochondrial translation machinery studied in situ by cryoelectron tomography. *Nat Commun.* (2015) 6:6019. doi: 10.1038/ncomms7019
97. Ott M, Herrmann JM. Co-translational membrane insertion of mitochondrially encoded proteins. *Biochim Biophys Acta.* (2010) 1803:767–75. doi: 10.1016/j.bbamcr.2009.11.010
98. Hell K, Herrmann JM, Pratje E, Neupert W, Stuart RA. Oxa1p, an essential component of the N-tail protein export machinery in mitochondria. *Proc Natl Acad Sci USA.* (1998) 95:2250–5. doi: 10.1073/pnas.95.5.2250
99. Hartl FU, Schmidt B, Wachter E, Weiss H, Neupert W. Transport into mitochondria and intramitochondrial sorting of the Fe/S

protein of ubiquinol-cytochrome c reductase. *Cell.* (1986) 47:939–51. doi: 10.1016/0092-8674(86)90809-3
100. Rojo EE, Stuart RA, Neupert W. Conservative sorting of F0-ATPase subunit 9: export from matrix requires delta pH across inner membrane and matrix ATP. *EMBO J.* (1995) 14:3445–51. doi: 10.1002/j.1460-2075.1995.tb07350.x
101. Hildenbeutel M, Theis M, Geier M, Haferkamp I, Neuhaus HE, Herrmann JM, et al. The membrane insertase Oxa1 is required for efficient import of carrier proteins into mitochondria. *J Mol Biol.* (2012) 423:590–9. doi: 10.1016/j.jmb.2012.07.018
102. Hansen KG, Herrmann JM. Transport of proteins into mitochondria. *Protein J.* (2019) 38:330–42. doi: 10.1007/s10930-019-09819-6
103. Endres M, Neupert W, Brunner M. Transport of the ADP/ATP carrier of mitochondria from the TOM complex to the TIM2254 complex. *EMBO J.* (1999) 18:3214–21. doi: 10.1093/emboj/18.12.3214
104. Brix J, Rudiger S, Bukau B, Schneider-Mergener J, Pfanner N. Distribution of binding sequences for the mitochondrial import receptors Tom20, Tom22, and Tom70 in a presequence-carrying preprotein and a non-cleavable preprotein. *J Biol Chem.* (1999) 274:16522–30. doi: 10.1074/jbc.274.23.16522
105. Faou P, Hoogenraad NJ. Tom34: a cytosolic cochaperone of the Hsp90/Hsp70 protein complex involved in mitochondrial protein import. *Biochim Biophys Acta.* (2012) 1823:348–57. doi: 10.1016/j.bbamcr.2011.12.001
106. Gava LM, Goncalves DC, Borges JC, Ramos CH. Stoichiometry and thermodynamics of the interaction between the C-terminus of human 90kDa heat shock protein Hsp90 and the mitochondrial translocase of outer membrane Tom70. *Arch Biochem Biophys.* (2011) 513:119–25. doi: 10.1016/j.abb.2011.06.015
107. Baker MJ, Webb CT, Stroud DA, Palmer CS, Frazier AE, Guiard B, et al. Structural and functional requirements for activity of the Tim9-Tim10 complex in mitochondrial protein import. *Mol Biol Cell.* (2009) 20:769–79. doi: 10.1091/mbc.e08-09-0903
108. Koehler CM, Merchant S, Oppliger W, Schmid K, Jarosch E, Dolfini L, et al. Tim9p, an essential partner subunit of Tim10p for the import of mitochondrial carrier proteins. *EMBO J.* (1998) 17:6477–86. doi: 10.1093/emboj/17.22.6477
109. Sirrenberg C, Endres M, Folsch H, Stuart RA, Neupert W, Brunner M. Carrier protein import into mitochondria mediated by the intermembrane proteins Tim10/Mrs11 and Tim12/Mrs5. *Nature.* (1998) 391:912–5. doi: 10.1038/36136
110. Weinhaupl K, Lindau C, Hessel A, Wang Y, Schutze C, Jores T, et al. Structural basis of membrane protein chaperoning through the mitochondrial intermembrane space. *Cell.* (2018) 175:1365–79 e25. doi: 10.1016/j.cell.2018.10.039
111. Sirrenberg C, Bauer MF, Guiard B, Neupert W, Brunner M. Import of carrier proteins into the mitochondrial inner membrane mediated by Tim22. *Nature.* (1996) 384:582–5. doi: 10.1038/384582a0
112. Koehler CM, Jarosch E, Tokatlidis K, Schmid K, Schweyen RJ, Schatz G. Import of mitochondrial carriers mediated by essential proteins of the intermembrane space. *Science.* (1998) 279:369–73. doi: 10.1126/science.279.5349.369
113. Okamoto H, Miyagawa A, Shiota T, Tamura Y, Endo T. Intramolecular disulfide bond of Tim22 protein maintains integrity of the TIM22 complex in the mitochondrial inner membrane. *J Biol Chem.* (2014) 289:4827–38. doi: 10.1074/jbc.M113.543264
114. Wrobel L, Trojanowska A, Sztolsztener ME, Chacinska A. Mitochondrial protein import: Mia40 facilitates Tim22 translocation into the inner membrane of mitochondria. *Mol Biol Cell.* (2013) 24:543–54. doi: 10.1091/mbc.e12-09-0649
115. Rehling P, Model K, Brandner K, Kovermann P, Sickmann A, Meyer HE, et al. Protein insertion into the mitochondrial inner membrane by a twin-pore translocase. *Science.* (2003) 299:1747–51. doi: 10.1126/science.1080945
116. Kerscher O, Holder J, Srinivasan M, Leung RS, Jensen RE. The Tim54p-Tim22p complex mediates insertion of proteins into the mitochondrial inner membrane. *J Cell Biol.* (1997) 139:1663–75. doi: 10.1083/jcb.139.7.1663
117. Li J, Qian X, Hu J, Sha B. Molecular chaperone Hsp70/Hsp90 prepares the mitochondrial outer membrane translocon receptor Tom71 for preprotein loading. *J Biol Chem.* (2009) 284:23852–9. doi: 10.1074/jbc.M109.023986
118. Wiedemann N, Pfanner N, Ryan MT. The three modules of ADP/ATP carrier cooperate in receptor recruitment and translocation into mitochondria. *EMBO J.* (2001) 20:951–60. doi: 10.1093/emboj/20.5.951
119. Curran SP, Leuenberger D, Schmidt E, Koehler CM. The role of the Tim8p-Tim13p complex in a conserved import pathway for mitochondrial polytopic inner membrane proteins. *J Cell Biol.* (2002) 158:1017–27. doi: 10.1083/jcb.200205124
120. Webb CT, Gorman MA, Lazarou M, Ryan MT, Gulbis JM. Crystal structure of the mitochondrial chaperone TIM910 reveals a six-bladed alpha-propeller. *Mol Cell.* (2006) 21:123–33. doi: 10.1016/j.molcel.2005.11.010
121. Curran SP, Leuenberger D, Oppliger W, Koehler CM. The Tim9p-Tim10p complex binds to the transmembrane domains of the ADP/ATP carrier. *EMBO J.* (2002) 21:942–53. doi: 10.1093/emboj/21.5.942
122. Davis AJ, Alder NN, Jensen RE, Johnson AE. The Tim9p/10p and Tim8p/13p complexes bind to specific sites on Tim23p during mitochondrial protein import. *Mol Biol Cell.* (2007) 18:475–86. doi: 10.1091/mbc.e06-06-0546
123. Gebert N, Chacinska A, Wagner K, Guiard B, Koehler CM, Rehling P, et al. Assembly of the three small Tim proteins precedes docking to the mitochondrial carrier translocase. *EMBO Rep.* (2008) 9:548–54. doi: 10.1038/embor.2008.49
124. Wagner K, Gebert N, Guiard B, Brandner K, Truscott KN, Wiedemann N, et al. The assembly pathway of the mitochondrial carrier translocase involves four preprotein translocases. *Mol Cell Biol.* (2008) 28:4251–60. doi: 10.1128/MCB.02216-07
125. Lionaki E, de Marcos Lousa C, Baud C, Vougioukalaki M, Panayotou G, Tokatlidis K. The essential function of Tim12 in vivo is ensured by the assembly interactions of its C-terminal domain. *J Biol Chem.* (2008) 283:15747–53. doi: 10.1074/jbc.M800350200
126. Gebert N, Gebert M, Oeljeklaus S, von der Malsburg K, Stroud DA, Kulawiak B, et al. Dual function of Sdh3 in the respiratory chain and TIM22 protein translocase of the mitochondrial inner membrane. *Mol Cell.* (2011) 44:811–8. doi: 10.1016/j.molcel.2011.09.025
127. Kulawiak B, Hopker J, Gebert M, Guiard B, Wiedemann N, Gebert N. The mitochondrial protein import machinery has multiple connections to the respiratory chain. *Biochim Biophys Acta.* (2013) 1827:612–26. doi: 10.1016/j.bbabio.2012.12.004
128. Durigon R, Wang Q, Ceh Pavia E, Grant CM, Lu H. Cytosolic thioredoxin system facilitates the import of mitochondrial small Tim proteins. *EMBO Rep.* (2012) 13:916–22. doi: 10.1038/embor.2012.116
129. Allen S, Balabanidou V, Sideris DP, Lisowsky T, Tokatlidis K. Erv1 mediates the Mia40-dependent protein import pathway and provides a functional link to the respiratory chain by shuttling electrons to cytochrome c. *J Mol Biol.* (2005) 353:937–44. doi: 10.1016/j.jmb.2005.08.049
130. Mesecke N, Terziyska N, Kozany C, Baumann F, Neupert W, Hell K, et al. disulfide relay system in the intermembrane space of mitochondria that mediates protein import. *Cell.* (2005) 121:1059–69. doi: 10.1016/j.cell.2005.04.011
131. Hell K. The Erv1-Mia40 disulfide relay system in the intermembrane space of mitochondria. *Biochim Biophys Acta.* (2008) 1783:601–9. doi: 10.1016/j.bbamcr.2007.12.005
132. Rissler M, Wiedemann N, Pfannschmidt S, Gabriel K, Guiard B, Pfanner N, et al. The essential mitochondrial protein Erv1 cooperates with Mia40 in biogenesis of intermembrane space proteins. *J Mol Biol.* (2005) 353:485–92. doi: 10.1016/j.jmb.2005.08.051
133. Chacinska A, Pfannschmidt S, Wiedemann N, Kozjak V, Sanjuan Szklarz LK, Schulze-Specking A, et al. Essential role of Mia40 in import and assembly of mitochondrial intermembrane space proteins. *EMBO J.* (2004) 23:3735–46. doi: 10.1038/sj.emboj.7600389
134. Terziyska N, Grumbt B, Kozany C, Hell K. Structural and functional roles of the conserved cysteine residues of the redox-regulated import receptor Mia40 in the intermembrane space of mitochondria. *J Biol Chem.* (2009) 284:1353–63. doi: 10.1074/jbc.M805035200
135. Banci L, Bertini I, Cefaro C, Cenacchi L, Ciofi-Baffoni S, Felli IC, et al. Molecular chaperone function of Mia40 triggers consecutive induced folding steps of the substrate in mitochondrial protein import. *Proc Natl Acad Sci USA.* (2010) 107:20190–5. doi: 10.1073/pnas.1010095107
136. von der Malsburg K, Muller JM, Bohnert M, Oeljeklaus S, Kwiatkowska P, Becker T, et al. Dual role of mitofilin in mitochondrial

membrane organization and protein biogenesis. *Dev Cell.* (2011) 21:694–707. doi: 10.1016/j.devcel.2011.08.026
137. Weckbecker D, Longen S, Riemer J, Herrmann JM. Atp23 biogenesis reveals a chaperone-like folding activity of Mia40 in the IMS of mitochondria. *EMBO J.* (2012) 31:4348–58. doi: 10.1038/emboj.2012.263
138. Peleh V, Cordat E, Herrmann JM. Mia40 is a trans-site receptor that drives protein import into the mitochondrial intermembrane space by hydrophobic substrate binding. *Elife.* (2016) 5:16177. doi: 10.7554/eLife.16177
139. Milenkovic D, Ramming T, Muller JM, Wenz LS, Gebert N, Schulze-Specking A, et al. Identification of the signal directing Tim9 and Tim10 into the intermembrane space of mitochondria. *Mol Biol Cell.* (2009) 20:2530–9. doi: 10.1091/mbc.e08-11-1108
140. Sideris DP, Petrakis N, Katrakili N, Mikropoulou D, Gallo A, Ciofi-Baffoni S, et al. A novel intermembrane space-targeting signal docks cysteines onto Mia40 during mitochondrial oxidative folding. *J Cell Biol.* (2009) 187:1007–22. doi: 10.1083/jcb.200905134
141. Bien M, Longen S, Wagener N, Chwalla I, Herrmann JM, Riemer J. Mitochondrial disulfide bond formation is driven by intersubunit electron transfer in Erv1 and proofread by glutathione. *Mol Cell.* (2010) 37:516–28. doi: 10.1016/j.molcel.2010.01.017
142. Bihlmaier K, Mesecke N, Terziyska N, Bien M, Hell K, Herrmann JM. The disulfide relay system of mitochondria is connected to the respiratory chain. *J Cell Biol.* (2007) 179:389–95. doi: 10.1083/jcb.200707123
143. Dabir DV, Leverich EP, Kim SK, Tsai FD, Hirasawa M, Knaff DB, et al. role for cytochrome c and cytochrome c peroxidase in electron shuttling from Erv1. *EMBO J.* (2007) 26:4801–11. doi: 10.1038/sj.emboj.7601909
144. Kawano S, Yamano K, Naoe M, Momose T, Terao K, Nishikawa S, et al. Structural basis of yeast Tim40/Mia40 as an oxidative translocator in the mitochondrial intermembrane space. *Proc Natl Acad Sci USA.* (2009) 106:14403–7. doi: 10.1073/pnas.0901793106
145. Longen S, Woellhaf MW, Petrungaro C, Riemer J, Herrmann JM. The disulfide relay of the intermembrane space oxidizes the ribosomal subunit mrp10 on its transit into the mitochondrial matrix. *Dev Cell.* (2014) 28:30–42. doi: 10.1016/j.devcel.2013.11.007
146. Jores T, Klinger A, Gross LE, Kawano S, Flinner N, Duchardt-Ferner E, et al. Characterization of the targeting signal in mitochondrial beta-barrel proteins. *Nat Commun.* (2016) 7:12036. doi: 10.1038/ncomms 12036
147. Klein A, Israel L, Lackey SW, Nargang FE, Imhof A, Baumeister W, et al. Characterization of the insertase for beta-barrel proteins of the outer mitochondrial membrane. *J Cell Biol.* (2012) 199:599–611. doi: 10.1083/jcb.201207161
148. Wiedemann N, Kozjak V, Chacinska A, Schonfisch B, Rospert S, Ryan MT, et al. Machinery for protein sorting and assembly in the mitochondrial outer membrane. *Nature.* (2003) 424:565–71. doi: 10.1038/nature01753
149. Paschen SA, Waizenegger T, Stan T, Preuss M, Cyrklaff M, Hell K, et al. Evolutionary conservation of biogenesis of beta-barrel membrane proteins. *Nature.* (2003) 426:862–6. doi: 10.1038/nature02208
150. Hohr AIC, Lindau C, Wirth C, Qiu J, Stroud DA, Kutik S, et al. Membrane protein insertion through a mitochondrial beta-barrel gate. *Science.* (2018) 359:aah6834. doi: 10.1126/science.aah6834
151. Kutik S, Stojanovski D, Becker L, Becker T, Meinecke M, Kruger V, et al. Dissecting membrane insertion of mitochondrial beta-barrel proteins. *Cell.* (2008) 132:1011–24. doi: 10.1016/j.cell.2008.01.028
152. Wenz LS, Ellenrieder L, Qiu J, Bohnert M, Zufall N, van der Laan M, et al. Sam37 is crucial for formation of the mitochondrial TOM-SAM supercomplex, thereby promoting beta-barrel biogenesis. *J Cell Biol.* (2015) 210:1047–54. doi: 10.1083/jcb.201504119
153. Popov-Celeketic J, Waizenegger T, Rapaport D. Mim1 functions in an oligomeric form to facilitate the integration of Tom20 into the mitochondrial outer membrane. *J Mol Biol.* (2008) 376:671–80. doi: 10.1016/j.jmb.2007.12.006
154. Hulett JM, Lueder F, Chan NC, Perry AJ, Wolynec P, Likic VA, et al. The transmembrane segment of Tom20 is recognized by Mim1 for docking to the mitochondrial TOM complex. *J Mol Biol.* (2008) 376:694–704. doi: 10.1016/j.jmb.2007.12.021
155. Papic D, Krumpe K, Dukanovic J, Dimmer KS, Rapaport D. Multispan mitochondrial outer membrane protein Ugo1 follows a unique Mim1-dependent import pathway. *J Cell Biol.* (2011) 194:397–405. doi: 10.1083/jcb.201102041
156. Becker T, Wenz LS, Kruger V, Lehmann W, Muller JM, Goroncy L, et al. The mitochondrial import protein Mim1 promotes biogenesis of multispanning outer membrane proteins. *J Cell Biol.* (2011) 194:387–95. doi: 10.1083/jcb.201102044
157. Kruger V, Becker T, Becker L, Montilla-Martinez M, Ellenrieder L, Vogtle FN, et al. Identification of new channels by systematic analysis of the mitochondrial outer membrane. *J Cell Biol.* (2017) 216:3485–95. doi: 10.1083/jcb.201706043
158. Dimmer KS, Papic D, Schumann B, Sperl D, Krumpe K, Walther DM, et al. A crucial role for Mim2 in the biogenesis of mitochondrial outer membrane proteins. *J Cell Sci.* (2012) 125:3464–73. doi: 10.1242/jcs.103804
159. Gupta A, Becker T. Mechanisms and pathways of mitochondrial outer membrane protein biogenesis. *Biochim Biophys Acta Bioenerg.* (2021) 1862:148323. doi: 10.1016/j.bbabio.2020.148323
160. Keskin A, Akdogan E, Dunn CD. Evidence for amino acid snorkeling from a high-resolution, *in vivo* analysis of Fis1 tail-anchor insertion at the mitochondrial outer membrane. *Genetics.* (2017) 205:691–705. doi: 10.1534/genetics.116.196428
161. Vogtle FN, Keller M, Taskin AA, Horvath SE, Guan XL, Prinz C, et al. The fusogenic lipid phosphatidic acid promotes the biogenesis of mitochondrial outer membrane protein Ugo1. *J Cell Biol.* (2015) 210:951–60. doi: 10.1083/jcb.201506085
162. Sauerwald J, Jores T, Eisenberg-Bord M, Chuartzman SG, Schuldiner M, Rapaport D. Genome-wide screens in saccharomyces cerevisiae highlight a role for cardiolipin in biogenesis of mitochondrial outer membrane multispan proteins. *Mol Cell Biol.* (2015) 35:3200–11. doi: 10.1128/MCB.00107-15
163. Haynes CM, Ron D. The mitochondrial UPR - protecting organelle protein homeostasis. *J Cell Sci.* (2010) 123:3849–55. doi: 10.1242/jcs.075119
164. Topf U, Suppanz I, Samluk L, Wrobel L, Boser A, Sakowska P, et al. Quantitative proteomics identifies redox switches for global translation modulation by mitochondrially produced reactive oxygen species. *Nat Commun.* (2018) 9:324. doi: 10.1038/s41467-017-02694-8
165. Mehnert CS, Rampelt H, Gebert M, Oeljeklaus S, Schrempp SG, Kochbeck L, et al. The mitochondrial ADP/ATP carrier associates with the inner membrane presequence translocase in a stoichiometric manner. *J Biol Chem.* (2014) 289:27352–62. doi: 10.1074/jbc.M114.556498
166. Dennerlein S, Oeljeklaus S, Jans D, Hellwig C, Bareth B, Jakobs S, et al. MITRAC7 acts as a COX1-specific chaperone and reveals a checkpoint during cytochrome c oxidase assembly. *Cell Rep.* (2015) 12:1644–55. doi: 10.1016/j.celrep.2015.08.009
167. Mick DU, Dennerlein S, Wiese H, Reinhold R, Pacheu-Grau D, Lorenzi I, et al. MITRAC links mitochondrial protein translocation to respiratory-chain assembly and translational regulation. *Cell.* (2012) 151:1528–41. doi: 10.1016/j.cell.2012.11.053
168. Richter-Dennerlein R, Oeljeklaus S, Lorenzi I, Ronsor C, Bareth B, Schendzielorz AB, et al. Mitochondrial protein synthesis adapts to influx of nuclear-encoded protein. *Cell.* (2016) 167:471–83 e10. doi: 10.1016/j.cell.2016.09.003
169. Shpilka T, Haynes CM. The mitochondrial UPR: mechanisms, physiological functions and implications in ageing. *Nat Rev Mol Cell Biol.* (2018) 19:109–20. doi: 10.1038/nrm.2017.110
170. Nargund AM, Pellegrino MW, Fiorese CJ, Baker BM, Haynes CM. Mitochondrial import efficiency of ATFS-1 regulates mitochondrial UPR activation. *Science.* (2012) 337:587–90. doi: 10.1126/science.1223560
171. Rolland SG, Schneid S, Schwarz M, Rackles E, Fischer C, Haeussler S, et al. Compromised mitochondrial protein import acts as a signal for UPR(mt). *Cell Rep.* (2019) 28:1659–69 e5. doi: 10.1016/j.celrep.2019.07.049
172. Wrobel L, Topf U, Bragoszewski P, Wiese S, Sztolsztener ME, Oeljeklaus S, et al. Mistargeted mitochondrial proteins activate a proteostatic response in the cytosol. *Nature.* (2015) 524:485–8. doi: 10.1038/nature14951
173. Wang X, Chen XJ. A cytosolic network suppressing mitochondria-mediated proteostatic stress and cell death. *Nature.* (2015) 524:481–4. doi: 10.1038/nature14859
174. Jin SM, Lazarou M, Wang C, Kane LA, Narendra DP, Youle RJ. Mitochondrial membrane potential regulates PINK1 import

and proteolytic destabilization by PARL. *J Cell Biol.* (2010) 191:933–42. doi: 10.1083/jcb.201008084
175. Yamano K, Youle RJ. PINK1 is degraded through the N-end rule pathway. *Autophagy.* (2013) 9:1758–69. doi: 10.4161/auto.24633
176. Lazarou M, Jin SM, Kane LA, Youle RJ. Role of PINK1 binding to the TOM complex and alternate intracellular membranes in recruitment and activation of the E3 ligase Parkin. *Dev Cell.* (2012) 22:320–33. doi: 10.1016/j.devcel.2011.12.014
177. Kane LA, Lazarou M, Fogel AI Li Y, Yamano K, Sarraf SA, Banerjee S, et al. PINK1 phosphorylates ubiquitin to activate Parkin E3 ubiquitin ligase activity. *J Cell Biol.* (2014) 205:143–53. doi: 10.1083/jcb.201402104
178. Ruan L, Zhou C, Jin E, Kucharavy A, Zhang Y, Wen Z, et al. Cytosolic proteostasis through importing of misfolded proteins into mitochondria. *Nature.* (2017) 543:443–46. doi: 10.1038/nature21695
179. Wagner I, Arlt H, van Dyck L, Langer T, Neupert W. Molecular chaperones cooperate with PIM1 protease in the degradation of misfolded proteins in mitochondria. *EMBO J.* (1994) 13:5135–45. doi: 10.1002/j.1460-2075.1994.tb06843.x
180. Kang SG, Dimitrova MN, Ortega J, Ginsburg A, Maurizi MR. Human mitochondrial ClpP is a stable heptamer that assembles into a tetradecamer in the presence of ClpX. *J Biol Chem.* (2005) 280:35424–32. doi: 10.1074/jbc.M507240200
181. Bender T, Lewrenz I, Franken S, Baitzel C, Voos W. Mitochondrial enzymes are protected from stress-induced aggregation by mitochondrial chaperones and the Pim1/LON protease. *Mol Biol Cell.* (2011) 22:541–54. doi: 10.1091/mbc.e10-08-0718
182. Fischer F, Langer JD, Osiewacz HD. Identification of potential mitochondrial CLPXP protease interactors and substrates suggests its central role in energy metabolism. *Sci Rep.* (2015) 5:18375. doi: 10.1038/srep18375
183. Ohba Y, MacVicar T, Langer T. Regulation of mitochondrial plasticity by the i-AAA protease YME1L. *Biol Chem.* (2020) 401:877–90. doi: 10.1515/hsz-2020-0120
184. Baker MJ, Mooga VP, Guiard B, Langer T, Ryan MT, Stojanovski D. Impaired folding of the mitochondrial small TIM chaperones induces clearance by the i-AAA protease. *J Mol Biol.* (2012) 424:227–39. doi: 10.1016/j.jmb.2012.09.019
185. Wu X, Li L, Jiang H. Mitochondrial inner-membrane protease Yme1 degrades outer-membrane proteins Tom22 and Om45. *J Cell Biol.* (2018) 217:139–49. doi: 10.1083/jcb.201702125
186. Deshwal S, Fiedler KU, Langer T. Mitochondrial proteases: multifaceted regulators of mitochondrial plasticity. *Annu Rev Biochem.* (2020) 89:501–28. doi: 10.1146/annurev-biochem-062917-012739
187. Opalinska M, Janska H. AAA proteases: guardians of mitochondrial function and homeostasis. *Cells.* (2018) 7:100163. doi: 10.3390/cells7100163
188. Hoppins S, Collins SR, Cassidy-Stone A, Hummel E, Devay RM, Lackner LL, et al. A mitochondrial-focused genetic interaction map reveals a scaffold-like complex required for inner membrane organization in mitochondria. *J Cell Biol.* (2011) 195:323–40. doi: 10.1083/jcb.201107053
189. Harner M, Korner C, Walther D, Mokranjac D, Kaesmacher J, Welsch U, et al. The mitochondrial contact site complex, a determinant of mitochondrial architecture. *EMBO J.* (2011) 30:4356–70. doi: 10.1038/emboj.2011.379
190. Pfanner N, van der Laan M, Amati P, Capaldi RA, Caudy AA, Chacinska A, et al. Uniform nomenclature for the mitochondrial contact site and cristae organizing system. *J Cell Biol.* (2014) 204:1083–6. doi: 10.1083/jcb.201401006
191. Bohnert M, Wenz LS, Zerbes RM, Horvath SE, Stroud DA, von der Malsburg K, et al. Role of mitochondrial inner membrane organizing system in protein biogenesis of the mitochondrial outer membrane. *Mol Biol Cell.* (2012) 23:3948–56. doi: 10.1091/mbc.e12-04-0295
192. Ehses S, Raschke I, Mancuso G, Bernacchia A, Geimer S, Tondera D, et al. Regulation of OPA1 processing and mitochondrial fusion by m-AAA protease isoenzymes and OMA1. *J Cell Biol.* (2009) 187:1023–36. doi: 10.1083/jcb.200906084
193. Ishihara N, Fujita Y, Oka T, Mihara K. Regulation of mitochondrial morphology through proteolytic cleavage of OPA1. *EMBO J.* (2006) 25:2966–77. doi: 10.1038/sj.emboj.7601184
194. Anand R, Wai T, Baker MJ, Kladt N, Schauss AC, Rugarli E, et al. The i-AAA protease YME1L and OMA1 cleave OPA1 to balance mitochondrial fusion and fission. *J Cell Biol.* (2014) 204:919–29. doi: 10.1083/jcb.201308006
195. Wai T, Garcia-Prieto J, Baker MJ, Merkwirth C, Benit P, Rustin P, et al. Imbalanced OPA1 processing and mitochondrial fragmentation cause heart failure in mice. *Science.* (2015) 350:aad0116. doi: 10.1126/science.aad0116
196. Ellenrieder L, Opalinski L, Becker L, Kruger V, Mirus O, Straub SP, et al. Separating mitochondrial protein assembly and endoplasmic reticulum tethering by selective coupling of Mdm10. *Nat Commun.* (2016) 7:13021. doi: 10.1038/ncomms13021
197. Stroud DA, Oeljeklaus S, Wiese S, Bohnert M, Lewandrowski U, Sickmann A, et al. Composition and topology of the endoplasmic reticulum-mitochondria encounter structure. *J Mol Biol.* (2011) 413:743–50. doi: 10.1016/j.jmb.2011.09.012
198. Muller CS, Bildl W, Haupt A, Ellenrieder L, Becker T, Hunte C, et al. Cryo-slicing blue native-mass spectrometry (csBN-MS), a novel technology for high resolution complexome profiling. *Mol Cell Proteomics.* (2016) 15:669–81. doi: 10.1074/mcp.M115.054080
199. Elbaz-Alon Y, Eisenberg-Bord M, Shinder V, Stiller SB, Shimoni E, Wiedemann N, et al. Lam6 regulates the extent of contacts between organelles. *Cell Rep.* (2015) 12:7–14. doi: 10.1016/j.celrep.2015.06.022
200. Murley A, Sarsam RD, Toulmay A, Yamada J, Prinz WA, Nunnari J. Ltc1 is an ER-localized sterol transporter and a component of ER-mitochondria and ER-vacuole contacts. *J Cell Biol.* (2015) 209:539–48. doi: 10.1083/jcb.201502033
201. Meisinger C, Wiedemann N, Rissler M, Strub A, Milenkovic D, Schonfisch B, et al. Mitochondrial protein sorting: differentiation of beta-barrel assembly by Tom7-mediated segregation of Mdm10. *J Biol Chem.* (2006) 281:22819–26. doi: 10.1074/jbc.M602679200
202. Kornmann B, Currie E, Collins SR, Schuldiner M, Nunnari J, Weissman JS, et al. An ER-mitochondria tethering complex revealed by a synthetic biology screen. *Science.* (2009) 325:477–81. doi: 10.1126/science.1175088
203. Meisinger C, Rissler M, Chacinska A, Szklarz LK, Milenkovic D, Kozjak V, et al. The mitochondrial morphology protein Mdm10 functions in assembly of the preprotein translocase of the outer membrane. *Dev Cell.* (2004) 7:61–71. doi: 10.1016/j.devcel.2004.06.003
204. Yamano K, Tanaka-Yamano S, Endo T. Mdm10 as a dynamic constituent of the TOB/SAM complex directs coordinated assembly of Tom40. *EMBO Rep.* (2010) 11:187–93. doi: 10.1038/embor.2009.283
205. Flinner N, Ellenrieder L, Stiller SB, Becker T, Schleiff E, Mirus O. Mdm10 is an ancient eukaryotic porin co-occurring with the ERMES complex. *Biochim Biophys Acta.* (2013) 1833:3314–25. doi: 10.1016/j.bbamcr.2013.10.006
206. Boengler K, Gres P, Cabestrero A, Ruiz-Meana M, Garcia-Dorado D, Heusch G, et al. Prevention of the ischemia-induced decrease in mitochondrial Tom20 content by ischemic preconditioning. *J Mol Cell Cardiol.* (2006) 41:426–30. doi: 10.1016/j.yjmcc.2006.05.015
207. Feng R, Cai M, Wang X, Zhang J, Tian Z. Early aerobic exercise combined with hydrogen-rich saline as preconditioning protects myocardial injury induced by acute myocardial infarction in rats. *Appl Biochem Biotechnol.* (2019) 187:663–76. doi: 10.1007/s12010-018-2841-0
208. Budas GR, Churchill EN, Disatnik MH, Sun L, Mochly-Rosen D. Mitochondrial import of PKCepsilon is mediated by HSP90: a role in cardioprotection from ischaemia and reperfusion injury. *Cardiovasc Res.* (2010) 88:83–92. doi: 10.1093/cvr/cvq154
209. Srisakuldee W, Makazan Z, Nickel BE, Zhang F, Thliveris JA, Pasumarthi KB, et al. The FGF-2-triggered protection of cardiac subsarcolemmal mitochondria from calcium overload is mitochondrial connexin 43-dependent. *Cardiovasc Res.* (2014) 103:72–80. doi: 10.1093/cvr/cvu066
210. Paillard M, Tubbs E, Thiebaut PA, Gomez L, Fauconnier J, Da Silva CC, et al. Depressing mitochondria-reticulum interactions protects cardiomyocytes from lethal hypoxia-reoxygenation injury. *Circulation.* (2013) 128:1555–65. doi: 10.1161/CIRCULATIONAHA.113.001225
211. Zhang J, Li M, Zhang Z, Zhu R, Olcese R, Stefani E, et al. The mitochondrial BKCa channel cardiac interactome reveals BKCa association with the mitochondrial import receptor subunit Tom22, and the adenine nucleotide translocator. *Mitochondrion.* (2017) 33:84–101. doi: 10.1016/j.mito.2016.08.017
212. Bose HS, Whittal RM, Marshall B, Rajapaksha M, Wang NP, Bose M, et al. A novel mitochondrial complex of aldosterone synthase, steroidogenic acute regulatory protein, and Tom22 synthesizes aldosterone in the rat heart. *J Pharmacol Exp Ther.* (2021) 377:108–20. doi: 10.1124/jpet.120.000365

213. Benak D, Sotakova-Kasparova D, Neckar J, Kolar F, Hlavackova M. Selection of optimal reference genes for gene expression studies in chronically hypoxic rat heart. *Mol Cell Biochem.* (2019) 461:15–22. doi: 10.1007/s11010-019-03584-x
214. Middelberg RP, Ferreira MA, Henders AK, Heath AC, Madden PA, Montgomery GW, et al. Genetic variants in LPL, OASL and TOMM40/APOE-C1-C2-C4 genes are associated with multiple cardiovascular-related traits. *BMC Med Genet.* (2011) 12:123. doi: 10.1186/1471-2350-12-123
215. Jeemon P, Pettigrew K, Sainsbury C, Prabhakaran D, Padmanabhan S. Implications of discoveries from genome-wide association studies in current cardiovascular practice. *World J Cardiol.* (2011) 3:230–47. doi: 10.4330/wjc.v3.i7.230
216. Yang Z, Sun W, Hu K. Molecular mechanism underlying adenosine receptor-mediated mitochondrial targeting of protein kinase C. *Biochim Biophys Acta.* (2012) 1823:950–8. doi: 10.1016/j.bbamcr.2011.12.012
217. Kang C, Qin J, Osei W, Hu K. Regulation of protein kinase C-epsilon and its age-dependence. *Biochem Biophys Res Commun.* (2017) 482:1201–06. doi: 10.1016/j.bbrc.2016.12.012
218. Li J, Qi M, Li C, Shi D, Zhang D, Xie D, et al. Tom70 serves as a molecular switch to determine pathological cardiac hypertrophy. *Cell Res.* (2014) 24:977–93. doi: 10.1038/cr.2014.94
219. Pei HF, Hou JN, Wei FP, Xue Q, Zhang F, Peng CF, et al. Melatonin attenuates postmyocardial infarction injury *via* increasing Tom70 expression. *J Pineal Res.* (2017) 62:12371. doi: 10.1111/jpi.12371
220. Lochner A, Marais E, Huisamen B. Melatonin and cardioprotection against ischaemia/reperfusion injury: what's new? A review. *J Pineal Res.* (2018) 65:e12490. doi: 10.1111/jpi.12490
221. Kato H, Lu Q, Rapaport D, Kozjak-Pavlovic V. Tom70 is essential for PINK1 import into mitochondria. *PLoS ONE.* (2013) 8:e58435. doi: 10.1371/journal.pone.0058435
222. Xue Q, Pei H, Liu Q, Zhao M, Sun J, Gao E, et al. MICU1 protects against myocardial ischemia/reperfusion injury and its control by the importer receptor Tom70. *Cell Death Dis.* (2017) 8:e2923. doi: 10.1038/cddis.2017.280
223. Garg V, Hu K. Protein kinase C isoform-dependent modulation of ATP-sensitive K+ channels in mitochondrial inner membrane. *Am J Physiol Heart Circ Physiol.* (2007) 293:H322–32. doi: 10.1152/ajpheart.01035.2006
224. Mayr M, Liem D, Zhang J, Li X, Avliyakulov NK, Yang JI, et al. Proteomic and metabolomic analysis of cardioprotection: Interplay between protein kinase C epsilon and delta in regulating glucose metabolism of murine hearts. *J Mol Cell Cardiol.* (2009) 46:268–77. doi: 10.1016/j.yjmcc.2008.10.008
225. Yuan Y, Pan SS. Parkin mediates mitophagy to participate in cardioprotection induced by late exercise preconditioning but Bnip3 does not. *J Cardiovasc Pharmacol.* (2018) 71:303–16. doi: 10.1097/FJC.0000000000000572
226. Wang P, Wang D, Yang Y, Hou J, Wan J, Ran F, et al. Tom70 protects against diabetic cardiomyopathy through its antioxidant and antiapoptotic properties. *Hypertens Res.* (2020) 43:1047–56. doi: 10.1038/s41440-020-0518-x
227. Botta A, Laher I, Beam J, Decoffe D, Brown K, Halder S, et al. Short term exercise induces PGC-1alpha, ameliorates inflammation and increases mitochondrial membrane proteins but fails to increase respiratory enzymes in aging diabetic hearts. *PLoS ONE.* (2013) 8:e70248. doi: 10.1371/journal.pone.0070248
228. Giorgianni F, Usman Khan M, Weber KT, Gerling IC, Beranova-Giorgianni S. Phosphoproteome mapping of cardiomyocyte mitochondria in a rat model of heart failure. *Mol Cell Biochem.* (2014) 389:159–67. doi: 10.1007/s11010-013-1937-7
229. Palmer ND, Kahali B, Kuppa A, Chen Y, Du X, Feitosa MF, et al. Allele specific variation at APOE increases non-alcoholic fatty liver disease and obesity but decreases risk of Alzheimer's disease and myocardial infarction. *Hum Mol Genet.* (2021) 2021:ddab096. doi: 10.1093/hmg/ddab096
230. Talmud PJ, Drenos F, Shah S, Shah T, Palmen J, Verzilli C, et al. Gene-centric association signals for lipids and apolipoproteins identified via the HumanCVD BeadChip. *Am J Hum Genet.* (2009) 85:628–42. doi: 10.1016/j.ajhg.2009.10.014
231. Kong X, Zhao Q, Xing X, Zhang B, Zhang X, Hong J, et al. Genetic variants associated with lipid profiles in Chinese patients with type 2 diabetes. *PLoS ONE.* (2015) 10:e0135145. doi: 10.1371/journal.pone.0135145
232. Abe S, Tokoro F, Matsuoka R, Arai M, Noda T, Watanabe S, et al. Association of genetic variants with dyslipidemia. *Mol Med Rep.* (2015) 12:5429–36. doi: 10.3892/mmr.2015.4081
233. Park S, Kang S. A minor allele of the haplotype located in the 19q13 loci is associated with a decreased risk of hyper-LDL-cholesterolemia, and a balanced diet and high protein intake can reduce the risk. *Lipids Health Dis.* (2020) 19:178. doi: 10.1186/s12944-020-01352-1
234. Christiansen MK, Larsen SB, Nyegaard M, Neergaard-Petersen S, Ajjan R, Wurtz M, et al. Coronary artery disease-associated genetic variants and biomarkers of inflammation. *PLoS ONE.* (2017) 12:e0180365. doi: 10.1371/journal.pone.0180365
235. Kraja AT, Chasman DI, North KE, Reiner AP, Yanek LR, Kilpelainen TO, et al. Pleiotropic genes for metabolic syndrome and inflammation. *Mol Genet Metab.* (2014) 112:317–38. doi: 10.1016/j.ymgme.2014.04.007
236. Zeh R. *Neurological and Molecular Biological Characterisation of the Mutant Mouse Line Tom40*. Munich: Technische Universität München. (2013).
237. Wang X, Wang S, Liu W, Wang T, Wang J, Gao X, et al. Epigenetic upregulation of miR-126 induced by heat stress contributes to apoptosis of rat cardiomyocytes by promoting Tomm40 transcription. *J Mol Cell Cardiol.* (2019) 129:39–48. doi: 10.1016/j.yjmcc.2018.10.005
238. Barcena ML, Pozdniakova S, Haritonow N, Breiter P, Kuhl AA, Milting H, et al. Dilated cardiomyopathy impairs mitochondrial biogenesis and promotes inflammation in an age- and sex-dependent manner. *Aging.* (2020) 12:24117–33. doi: 10.18632/aging.202283
239. Yeo A, Li L, Warren L, Aponte J, Fraser D, King K, et al. Pharmacogenetic meta-analysis of baseline risk factors, pharmacodynamic, efficacy and tolerability endpoints from two large global cardiovascular outcomes trials for darapladib. *PLoS ONE.* (2017) 12:e0182115. doi: 10.1371/journal.pone.0182115
240. Guo Y, Cheong N, Zhang Z, De Rose R, Deng Y, Farber SA, et al. Tim50, a component of the mitochondrial translocator, regulates mitochondrial integrity and cell death. *J Biol Chem.* (2004) 279:24813–25. doi: 10.1074/jbc.M402049200
241. Tang K, Zhao Y, Li H, Zhu M, Li W, Liu W, et al. Translocase of inner membrane 50 functions as a novel protective regulator of pathological cardiac hypertrophy. *J Am Heart Assoc.* (2017) 6:4346. doi: 10.1161/JAHA.116.004346
242. Zhang XX, Wu XS, Mi SH, Fang SJ, Liu S, Xin Y, et al. Neuregulin-1 promotes mitochondrial biogenesis, attenuates mitochondrial dysfunction, and prevents hypoxia/reoxygenation injury in neonatal cardiomyocytes. *Cell Biochem Funct.* (2020) 38:549–57. doi: 10.1002/cbf.3503
243. Schubert C, Raparelli V, Westphal C, Dworatzek E, Petrov G, Kararigas G, et al. Reduction of apoptosis and preservation of mitochondrial integrity under ischemia/reperfusion injury is mediated by estrogen receptor beta. *Biol Sex Differ.* (2016) 7:53. doi: 10.1186/s13293-016-0104-8
244. Bian X, Teng T, Zhao H, Qin J, Qiao Z, Sun Y, et al. Zinc prevents mitochondrial superoxide generation by inducing mitophagy in the setting of hypoxia/reoxygenation in cardiac cells. *Free Radic Res.* (2018) 52:80–91. doi: 10.1080/10715762.2017.1414949
245. Williamson CL, Dabkowski ER, Dillmann WH, Hollander JM. Mitochondria protection from hypoxia/reoxygenation injury with mitochondria heat shock protein 70 overexpression. *Am J Physiol Heart Circ Physiol.* (2008) 294:H249–56. doi: 10.1152/ajpheart.00775.2007
246. Zhou TT, Wang XY, Huang J, Deng YZ, Qiu LJ, Liu HY, et al. Mitochondrial translocation of DJ-1 is mediated by Grp75: implication in cardioprotection of resveratrol against hypoxia/reoxygenation-induced oxidative stress. *J Cardiovasc Pharmacol.* (2020) 75:305–13. doi: 10.1097/FJC.0000000000000805
247. Baseler WA, Dabkowski ER, Williamson CL, Croston TL, Thapa D, Powell MJ, et al. Proteomic alterations of distinct mitochondrial subpopulations in the type 1 diabetic heart: contribution of protein import dysfunction. *Am J Physiol Regul Integr Comp Physiol.* (2011) 300:R186–200. doi: 10.1152/ajpregu.00423.2010
248. Shepherd DL, Hathaway QA, Nichols CE, Durr AJ, Pinti MV, Hughes KM, et al. Mitochondrial proteome disruption in the diabetic heart

through targeted epigenetic regulation at the mitochondrial heat shock protein 70 (mtHsp70) nuclear locus. *J Mol Cell Cardiol.* (2018) 119:104–15. doi: 10.1016/j.yjmcc.2018.04.016
249. Kirmanoglou K, Hannekum A, Schafler AE. Expression of mortalin in patients with chronic atrial fibrillation. *Basic Res Cardiol.* (2004) 99:404–8. doi: 10.1007/s00395-004-0477-4
250. Davey KM, Parboosingh JS, McLeod DR, Chan A, Casey R, Ferreira P, et al. Mutation of DNAJC19, a human homologue of yeast inner mitochondrial membrane co-chaperones, causes DCMA syndrome, a novel autosomal recessive Barth syndrome-like condition. *J Med Genet.* (2006) 43:385–93. doi: 10.1136/jmg.2005.036657
251. Ojala T, Polinati P, Manninen T, Hiippala A, Rajantie J, Karikoski R, et al. New mutation of mitochondrial DNAJC19 causing dilated and noncompaction cardiomyopathy, anemia, ataxia, and male genital anomalies. *Pediatr Res.* (2012) 72:432–7. doi: 10.1038/pr.2012.92
252. Ucar SK, Mayr JA, Feichtinger RG, Canda E, Coker M, Wortmann SB. Previously unreported biallelic mutation in DNAJC19: are sensorineural hearing loss and basal ganglia lesions additional features of dilated cardiomyopathy and ataxia (DCMA) syndrome? *JIMD Rep.* (2017) 35:39–45. doi: 10.1007/8904_2016_23
253. Al Teneiji A, Siriwardena K, George K, Mital S, Mercimek-Mahmutoglu S. Progressive cerebellar atrophy and a novel homozygous pathogenic DNAJC19 variant as a cause of dilated cardiomyopathy ataxia syndrome. *Pediatr Neurol.* (2016) 62:58–61. doi: 10.1016/j.pediatrneurol.2016.03.020
254. Sparkes R, Patton D, Bernier F. Cardiac features of a novel autosomal recessive dilated cardiomyopathic syndrome due to defective importation of mitochondrial protein. *Cardiol Young.* (2007) 17:215–7. doi: 10.1017/S1047951107000042
255. Vasilescu C, Ojala TH, Brilhante V, Ojanen S, Hinterding HM, Palin E, et al. Genetic basis of severe childhood-onset cardiomyopathies. *J Am Coll Cardiol.* (2018) 72:2324–38. doi: 10.1016/j.jacc.2018.08.2171
256. Mehawej C, Delahodde A, Legeai-Mallet L, Delague V, Kaci N, Desvignes JP, et al. The impairment of MAGMAS function in human is responsible for a severe skeletal dysplasia. *PLoS Genet.* (2014) 10:e1004311. doi: 10.1371/journal.pgen.1004311
257. Rodriguez-Sinovas A, Boengler K, Cabestrero A, Gres P, Morente M, Ruiz-Meana M, et al. Translocation of connexin 43 to the inner mitochondrial membrane of cardiomyocytes through the heat shock protein 90-dependent TOM pathway and its importance for cardioprotection. *Circ Res.* (2006) 99:93–101. doi: 10.1161/01.RES.0000230315.56904.de
258. Nguyen T, Wong R, Wang G, Gucek M, Steenbergen C, Murphy E. Acute inhibition of GSK causes mitochondrial remodeling. *Am J Physiol Heart Circ Physiol.* (2012) 302:H2439–45. doi: 10.1152/ajpheart.00033.2012
259. Small BA, Lu Y, Hsu AK, Gross GJ, Gross ER. Morphine reduces myocardial infarct size *via* heat shock protein 90 in rodents. *Biomed Res Int.* (2015) 2015:129612. doi: 10.1155/2015/129612
260. Tu RH Li QJ, Huang Z, He Y, Meng JJ, Zheng HL, Zeng ZY, et al. Novel functional role of heat shock protein 90 in mitochondrial connexin 43-mediated hypoxic postconditioning. *Cell Physiol Biochem.* (2017) 44:982–97. doi: 10.1159/000485399
261. Barksdale KA, Bijur GN. The basal flux of Akt in the mitochondria is mediated by heat shock protein 90. *J Neurochem.* (2009) 108:1289–99. doi: 10.1111/j.1471-4159.2009.05878.x
262. Borillo GA, Mason M, Quijada P, Volkers M, Cottage C, McGregor M, et al. Pim-1 kinase protects mitochondrial integrity in cardiomyocytes. *Circ Res.* (2010) 106:1265–74. doi: 10.1161/CIRCRESAHA.109.212035
263. Fan F, Duan Y, Yang F, Trexler C, Wang H, Huang L, et al. Deletion of heat shock protein 60 in adult mouse cardiomyocytes perturbs mitochondrial protein homeostasis and causes heart failure. *Cell Death Differ.* (2020) 27:587–600. doi: 10.1038/s41418-019-0374-x
264. Lin KM, Hollander JM, Kao VY, Lin B, Macpherson L, Dillmann WH. Myocyte protection by 10 kD heat shock protein (Hsp10) involves the mobile loop and attenuation of the Ras GTP-ase pathway. *FASEB J.* (2004) 18:1004–6. doi: 10.1096/fj.03-0348fje
265. Schafler AE, Kirmanoglou K, Pecher P, Hannekum A, Schumacher B. Overexpression of heat shock protein 60/10 in myocardium of patients with chronic atrial fibrillation. *Ann Thorac Surg.* (2002) 74:767–70. doi: 10.1016/S0003-4975(02)03830-4
266. Agsteribbe E, Huckriede A, Veenhuis M, Ruiters MH, Niezen-Koning KE, Skjeldal OH, et al. A fatal, systemic mitochondrial disease with decreased mitochondrial enzyme activities, abnormal ultrastructure of the mitochondria and deficiency of heat shock protein 60. *Biochem Biophys Res Commun.* (1993) 193:146–54. doi: 10.1006/bbrc.1993.1602
267. Joshi M, Anselm I, Shi J, Bale TA, Towne M, Schmitz-Abe K, et al. Mutations in the substrate binding glycine-rich loop of the mitochondrial processing peptidase-alpha protein (PMPCA) cause a severe mitochondrial disease. *Cold Spring Harb Mol Case Stud.* (2016) 2:a000786. doi: 10.1101/mcs.a000786
268. Eldomery MK, Akdemir ZC, Vogtle FN, Charng WL, Mulica P, Rosenfeld JA, et al. MIPEP recessive variants cause a syndrome of left ventricular non-compaction, hypotonia, and infantile death. *Genome Med.* (2016) 8:106. doi: 10.1186/s13073-016-0360-6
269. Crewe C, Schafer C, Lee I, Kinter M, Szweda LI. Regulation of pyruvate dehydrogenase kinase 4 in the heart through degradation by the lon protease in response to mitochondrial substrate availability. *J Biol Chem.* (2017) 292:305–12. doi: 10.1074/jbc.M116.754127
270. Hoshino A, Okawa Y, Ariyoshi M, Kaimoto S, Uchihashi M, Fukai K, et al. Oxidative post-translational modifications develop LONP1 dysfunction in pressure overload heart failure. *Circ Heart Fail.* (2014) 7:500–9. doi: 10.1161/CIRCHEARTFAILURE.113.001062
271. Zhan R, Guo W, Gao X, Liu X, Xu K, Tang B. Real-time *in situ* monitoring of Lon and Caspase-3 for assessing the state of cardiomyocytes under hypoxic conditions *via* a novel Au-Se fluorescent nanoprobe. *Biosens Bioelectron.* (2021) 176:112965. doi: 10.1016/j.bios.2021.112965
272. Kuo CY, Chiu YC, Lee AY, Hwang TL. Mitochondrial Lon protease controls ROS-dependent apoptosis in cardiomyocyte under hypoxia. *Mitochondrion.* (2015) 23:7–16. doi: 10.1016/j.mito.2015.04.004
273. Sepuri NBV, Angireddy R, Srinivasan S, Guha M, Spear J, Lu B, et al. Mitochondrial LON protease-dependent degradation of cytochrome c oxidase subunits under hypoxia and myocardial ischemia. *Biochim Biophys Acta Bioenerg.* (2017) 1858:519–28. doi: 10.1016/j.bbabio.2017.04.003
274. Pomatto LCD, Cline M, Woodward N, Pakbin P, Sioutas C, Morgan TE, et al. Aging attenuates redox adaptive homeostasis and proteostasis in female mice exposed to traffic-derived nanoparticles ("vehicular smog"). *Free Radic Biol Med.* (2018) 121:86–97. doi: 10.1016/j.freeradbiomed.2018.04.574
275. Delaval E, Perichon M, Friguet B. Age-related impairment of mitochondrial matrix aconitase and ATP-stimulated protease in rat liver and heart. *Eur J Biochem.* (2004) 271:4559–64. doi: 10.1111/j.1432-1033.2004.04422.x
276. Guillon B, Bulteau AL, Wattenhofer-Donze M, Schmucker S, Friguet B, Puccio H, et al. Frataxin deficiency causes upregulation of mitochondrial Lon and ClpP proteases and severe loss of mitochondrial Fe-S proteins. *FEBS J.* (2009) 276:1036–47. doi: 10.1111/j.1742-4658.2008.06847.x
277. Wu B, Li J, Ni H, Zhuang X, Qi Z, Chen Q, et al. TLR4 activation promotes the progression of experimental autoimmune myocarditis to dilated cardiomyopathy by inducing mitochondrial dynamic imbalance. *Oxid Med Cell Longev.* (2018) 2018:3181278. doi: 10.1155/2018/3181278
278. Hu Y, Xu Y, Chen W, Qiu Z. Stomatin-like protein-2: a potential target to treat mitochondrial cardiomyopathy. *Heart Lung Circ.* (2021) 5:74. doi: 10.1016/j.hlc.2021.05.074
279. Zhao Y, Zhu J, Zhang N, Liu Q, Wang Y, Hu X, et al. GDF11 enhances therapeutic efficacy of mesenchymal stem cells for myocardial infarction via YME1L-mediated OPA1 processing. *Stem Cells Transl Med.* (2020) 9:1257–71. doi: 10.1002/sctm.20-0005
280. Seiferling D, Szczepanowska K, Becker C, Senft K, Hermans S, Maiti P, et al. Loss of CLPP alleviates mitochondrial cardiomyopathy without affecting the mammalian UPRmt. *EMBO Rep.* (2016) 17:953–64. doi: 10.15252/embr.201642077
281. Mayr JA, Haack TB, Graf E, Zimmermann FA, Wieland T, Haberberger B, et al. Lack of the mitochondrial protein acylglycerol kinase causes Sengers syndrome. *Am J Hum Genet.* (2012) 90:314–20. doi: 10.1016/j.ajhg.2011.12.005
282. Allali S, Dorboz I, Samaan S, Slama A, Rambaud C, Boespflug-Tanguy O, et al. Mutation in the AGK gene in two siblings with unusual Sengers syndrome. *Metab Brain Dis.* (2017) 32:2149–54. doi: 10.1007/s11011-017-0101-6

283. Khatter S, Puri RD, Bijarnia-Mahay S, Aggarwal M, Ramprasad V, Saxena R, et al. Sengers syndrome in Asian Indians–two novel mutations and variant phenotype-genotype correlation. *Transl Sci Rare Dis.* (2017) 2:157–64. doi: 10.3233/TRD-170017
284. Haghighi A, Haack TB, Atiq M, Mottaghi H, Haghighi-Kakhki H, Bashir RA, et al. Sengers syndrome: six novel AGK mutations in seven new families and review of the phenotypic and mutational spectrum of 29 patients. *Orphanet J Rare Dis.* (2014) 9:119. doi: 10.1186/s13023-014-0119-3
285. Kang Y, Stroud DA, Baker MJ, De Souza DP, Frazier AE, Liem M, et al. Sengers syndrome-associated mitochondrial acylglycerol kinase is a subunit of the human TIM22 protein import complex. *Mol Cell.* (2017) 67:457–70 e5. doi: 10.1016/j.molcel.2017.06.014
286. Kor D, Yilmaz B, Horoz O, Ceylaner G, Sizmaz S, Demir F. Two novel mutations in the AGK gene: two case reports with Sengers syndrome. *Gene Technol.* (2016) 5:2. doi: 10.4172/2329-6682.1000140
287. Dabir DV, Hasson SA, Setoguchi K, Johnson ME, Wongkongkathep P, Douglas CJ, et al. A small molecule inhibitor of redox-regulated protein translocation into mitochondria. *Dev Cell.* (2013) 25:81–92. doi: 10.1016/j.devcel.2013.03.006
288. Berger I, Ben-Neriah Z, Dor-Wolman T, Shaag A, Saada A, Zenvirt S, et al. Early prenatal ventriculomegaly due to an AIFM1 mutation identified by linkage analysis and whole exome sequencing. *Mol Genet Metab.* (2011) 104:517–20. doi: 10.1016/j.ymgme.2011.09.020
289. Heimer G, Eyal E, Zhu X, Ruzzo EK, Marek-Yagel D, Sagiv D, et al. Mutations in AIFM1 cause an X-linked childhood cerebellar ataxia partially responsive to riboflavin. *Eur J Paediatr Neurol.* (2018) 22:93–101. doi: 10.1016/j.ejpn.2017.09.004
290. Joza N, Oudit GY, Brown D, Benit P, Kassiri Z, Vahsen N, et al. Muscle-specific loss of apoptosis-inducing factor leads to mitochondrial dysfunction, skeletal muscle atrophy, and dilated cardiomyopathy. *Mol Cell Biol.* (2005) 25:10261–72. doi: 10.1128/MCB.25.23.10261-10272.2005
291. van Empel VP, Bertrand AT, van der Nagel R, Kostin S, Doevendans PA, Crijns HJ, et al. Downregulation of apoptosis-inducing factor in harlequin mutant mice sensitizes the myocardium to oxidative stress-related cell death and pressure overload-induced decompensation. *Circ Res.* (2005) 96:e92–e101. doi: 10.1161/01.RES.0000172081.30327.28
292. Xu A, Szczepanek K, Hu Y, Lesnefsky EJ, Chen Q. Cardioprotection by modulation of mitochondrial respiration during ischemia-reperfusion: role of apoptosis-inducing factor. *Biochem Biophys Res Commun.* (2013) 435:627–33. doi: 10.1016/j.bbrc.2013.05.033
293. Chen L, Shi D, Guo M. The roles of PKC-delta and PKC-epsilon in myocardial ischemia/reperfusion injury. *Pharmacol Res.* (2021) 170:105716. doi: 10.1016/j.phrs.2021.105716
294. Javadov S, Karmazyn M, Escobales N. Mitochondrial permeability transition pore opening as a promising therapeutic target in cardiac diseases. *J Pharmacol Exp Ther.* (2009) 330:670–8. doi: 10.1124/jpet.109.153213
295. Schleiff E, Silvius JR, Shore GC. Direct membrane insertion of voltage-dependent anion-selective channel protein catalyzed by mitochondrial Tom20. *J Cell Biol.* (1999) 145:973–8. doi: 10.1083/jcb.145.5.973
296. Shi D, Qi M, Zhou L, Li X, Ni L, Li C, et al. Endothelial mitochondrial preprotein translocase Tomm7-Rac1 signaling axis dominates cerebrovascular network homeostasis. *Arterioscler Thromb Vasc Biol.* (2018) 38:2665–77. doi: 10.1161/ATVBAHA.118.311538
297. Richter-Dennerlein R, Korwitz A, Haag M, Tatsuta T, Dargazanli S, Baker M, et al. DNAJC19, a mitochondrial cochaperone associated with cardiomyopathy, forms a complex with prohibitins to regulate cardiolipin remodeling. *Cell Metab.* (2014) 20:158–71. doi: 10.1016/j.cmet.2014.04.016
298. Sinha D, Joshi N, Chittoor B, Samji P, D'Silva P. Role of Magmas in protein transport and human mitochondria biogenesis. *Hum Mol Genet.* (2010) 19:1248–62. doi: 10.1093/hmg/ddq002
299. Vukotic M, Nolte H, Konig T, Saita S, Ananjew M, Kruger M, et al. Acylglycerol kinase mutated in sengers syndrome is a subunit of the TIM22 protein translocase in mitochondria. *Mol Cell.* (2017) 67:471–83 e7. doi: 10.1016/j.molcel.2017.06.013
300. Siriwardena K, Mackay N, Levandovskiy V, Blaser S, Raiman J, Kantor PF, et al. Mitochondrial citrate synthase crystals: novel finding in Sengers syndrome caused by acylglycerol kinase (AGK) mutations. *Mol Genet Metab.* (2013) 108:40–50. doi: 10.1016/j.ymgme.2012.11.282
301. Hangen E, Feraud O, Lachkar S, Mou H, Doti N, Fimia GM, et al. Interaction between AIF and CHCHD4 regulates respiratory chain biogenesis. *Mol Cell.* (2015) 58:1001–14. doi: 10.1016/j.molcel.2015.04.020
302. Meyer K, Buettner S, Ghezzi D, Zeviani M, Bano D, Nicotera P. Loss of apoptosis-inducing factor critically affects MIA40 function. *Cell Death Dis.* (2015) 6:e1814. doi: 10.1038/cddis.2015.170
303. Modjtahedi N, Kroemer G. CHCHD4 links AIF to the biogenesis of respiratory chain complex I. *Mol Cell Oncol.* (2016) 3:e1074332. doi: 10.1080/23723556.2015.1074332
304. Bertero E, Kutschka I, Maack C, Dudek J. Cardiolipin remodeling in Barth syndrome and other hereditary cardiomyopathies. *Biochim Biophys Acta Mol Basis Dis.* (2020) 1866:165803. doi: 10.1016/j.bbadis.2020.165803
305. Monteiro JP, Oliveira PJ, Jurado AS. Mitochondrial membrane lipid remodeling in pathophysiology: a new target for diet and therapeutic interventions. *Prog Lipid Res.* (2013) 52:513–28. doi: 10.1016/j.plipres.2013.06.002
306. Paradies G, Paradies V, Ruggiero FM, Petrosillo G. Role of cardiolipin in mitochondrial function and dynamics in health and disease: molecular and pharmacological aspects. *Cells.* (2019) 8:70728. doi: 10.3390/cells8070728
307. Brandner K, Mick DU, Frazier AE, Taylor RD, Meisinger C, Rehling P. Taz1, an outer mitochondrial membrane protein, affects stability and assembly of inner membrane protein complexes: implications for Barth Syndrome. *Mol Biol Cell.* (2005) 16:5202–14. doi: 10.1091/mbc.e05-03-0256
308. Sabbah HN. Barth syndrome cardiomyopathy: targeting the mitochondria with elamipretide. *Heart Fail Rev.* (2021) 26:237–53. doi: 10.1007/s10741-020-10031-3
309. Vreken P, Valianpour F, Nijtmans LG, Grivell LA, Plecko B, Wanders RJ, et al. Defective remodeling of cardiolipin and phosphatidylglycerol in Barth syndrome. *Biochem Biophys Res Commun.* (2000) 279:378–82. doi: 10.1006/bbrc.2000.3952
310. Gebert N, Joshi AS, Kutik S, Becker T, McKenzie M, Guan XL, et al. Mitochondrial cardiolipin involved in outer-membrane protein biogenesis: implications for Barth syndrome. *Curr Biol.* (2009) 19:2133–9. doi: 10.1016/j.cub.2009.10.074
311. Kutik S, Rissler M, Guan XL, Guiard B, Shui G, Gebert N, et al. The translocator maintenance protein Tam41 is required for mitochondrial cardiolipin biosynthesis. *J Cell Biol.* (2008) 183:1213–21. doi: 10.1083/jcb.200806048
312. Tamura Y, Harada Y, Yamano K, Watanabe K, Ishikawa D, Ohshima C, et al. Identification of Tam41 maintaining integrity of the TIM23 protein translocator complex in mitochondria. *J Cell Biol.* (2006) 174:631–7. doi: 10.1083/jcb.200603087
313. Boengler K, Schulz R. Connexin 43 and mitochondria in cardiovascular health and disease. *Adv Exp Med Biol.* (2017) 982:227–46. doi: 10.1007/978-3-319-55330-6_12
314. Michela P, Velia V, Aldo P, Ada P. Role of connexin 43 in cardiovascular diseases. *Eur J Pharmacol.* (2015) 768:71–6. doi: 10.1016/j.ejphar.2015.10.030
315. Wang M, Smith K, Yu Q, Miller C, Singh K, Sen CK. Mitochondrial connexin 43 in sex-dependent myocardial responses and estrogen-mediated cardiac protection following acute ischemia/reperfusion injury. *Basic Res Cardiol.* (2019) 115:1. doi: 10.1007/s00395-019-0759-5
316. Boengler K, Konietzka I, Buechert A, Heinen Y, Garcia-Dorado D, Heusch G, et al. Loss of ischemic preconditioning's cardioprotection in aged mouse hearts is associated with reduced gap junctional and mitochondrial levels of connexin 43. *Am J Physiol Heart Circ Physiol.* (2007) 292:H1764–9. doi: 10.1152/ajpheart.01071.2006
317. Schulz R, Boengler K, Totzeck A, Luo Y, Garcia-Dorado D, Heusch G. Connexin 43 in ischemic pre- and postconditioning. *Heart Fail Rev.* (2007) 12:261–6. doi: 10.1007/s10741-007-9032-3
318. Ruiz-Meana M, Rodriguez-Sinovas A, Cabestrero A, Boengler K, Heusch G, Garcia-Dorado D. Mitochondrial connexin43 as a new player in the pathophysiology of myocardial ischaemia-reperfusion injury. *Cardiovasc Res.* (2008) 77:325–33. doi: 10.1093/cvr/cvm062
319. Saito T, Sadoshima J. Molecular mechanisms of mitochondrial autophagy/mitophagy in the heart. *Circ Res.* (2015) 116:1477–90. doi: 10.1161/CIRCRESAHA.116.303790

320. Mukherjee UA, Ong SB, Ong SG, Hausenloy DJ. Parkinson's disease proteins: novel mitochondrial targets for cardioprotection. *Pharmacol Ther.* (2015) 156:34–43. doi: 10.1016/j.pharmthera.2015.10.005
321. Friederich MW, Erdogan AJ, Coughlin CR, Elos MT, Jiang H, O'Rourke CP, et al. Mutations in the accessory subunit NDUFB10 result in isolated complex I deficiency and illustrate the critical role of intermembrane space import for complex I holoenzyme assembly. *Hum Mol Genet.* (2017) 26:702–16. doi: 10.1093/hmg/ddw431
322. Chis R, Sharma P, Bousette N, Miyake T, Wilson A, Backx PH, et al. alpha-Crystallin B prevents apoptosis after H2O2 exposure in mouse neonatal cardiomyocytes. *Am J Physiol Heart Circ Physiol.* (2012) 303:H967–78. doi: 10.1152/ajpheart.00040.2012
323. Zhang Y, Li XR, Zhao L, Duan GL, Xiao L, Chen HP. DJ-1 preserving mitochondrial complex I activity plays a critical role in resveratrol-mediated cardioprotection against hypoxia/reoxygenation-induced oxidative stress. *Biomed Pharmacother.* (2018) 98:545–52. doi: 10.1016/j.biopha.2017.12.094
324. Deng YZ, Xiao L, Zhao L, Qiu LJ, Ma ZX, Xu XW, et al. Molecular mechanism underlying hypoxic preconditioning-promoted mitochondrial translocation of DJ-1 in hypoxia/reoxygenation H9c2 cells. *Molecules.* (2019) 25:10071. doi: 10.3390/molecules25010071
325. Ding H, Xu XW, Wang H, Xiao L, Zhao L, Duan GL, et al. DJ-1 plays an obligatory role in the cardioprotection of delayed hypoxic preconditioning against hypoxia/reoxygenation-induced oxidative stress through maintaining mitochondrial complex I activity. *Cell Biochem Funct.* (2018) 36:147–54. doi: 10.1002/cbf.3326
326. Baseler WA, Dabkowski ER, Jagannathan R, Thapa D, Nichols CE, Shepherd DL, et al. Reversal of mitochondrial proteomic loss in Type 1 diabetic heart with overexpression of phospholipid hydroperoxide glutathione peroxidase. *Am J Physiol Regul Integr Comp Physiol.* (2013) 304:R553–65. doi: 10.1152/ajpregu.00249.2012
327. Dabkowski ER, Baseler WA, Williamson CL, Powell M, Razunguzwa TT, Frisbee JC, et al. Mitochondrial dysfunction in the type 2 diabetic heart is associated with alterations in spatially distinct mitochondrial proteomes. *Am J Physiol Heart Circ Physiol.* (2010) 299:H529–40. doi: 10.1152/ajpheart.00267.2010
328. Craig EE, Hood DA. Influence of aging on protein import into cardiac mitochondria. *Am J Physiol.* (1997) 272:H2983–8. doi: 10.1152/ajpheart.1997.272.6.H2983
329. Schneider JJ, Hood DA. Effect of thyroid hormone on mtHsp70 expression, mitochondrial import and processing in cardiac muscle. *J Endocrinol.* (2000) 165:9–17. doi: 10.1677/joe.0.1650009
330. Marin-Garcia J. Thyroid hormone and myocardial mitochondrial biogenesis. *Vascul Pharmacol.* (2010) 52:120–30. doi: 10.1016/j.vph.2009.10.008
331. Craig EE, Chesley A, Hood DA. Thyroid hormone modifies mitochondrial phenotype by increasing protein import without altering degradation. *Am J Physiol.* (1998) 275:C1508–15. doi: 10.1152/ajpcell.1998.275.6.C1508
332. Colavecchia M, Christie LN, Kanwar YS, Hood DA. Functional consequences of thyroid hormone-induced changes in the mitochondrial protein import pathway. *Am J Physiol Endocrinol Metab.* (2003) 284:E29–35. doi: 10.1152/ajpendo.00294.2002

Conflict of Interest: The authors declare that the research was conducted in the absence of any commercial or financial relationships that could be construed as a potential conflict of interest.

Publisher's Note: All claims expressed in this article are solely those of the authors and do not necessarily represent those of their affiliated organizations, or those of the publisher, the editors and the reviewers. Any product that may be evaluated in this article, or claim that may be made by its manufacturer, is not guaranteed or endorsed by the publisher.

Copyright © 2021 Zhao and Zou. This is an open-access article distributed under the terms of the Creative Commons Attribution License (CC BY). The use, distribution or reproduction in other forums is permitted, provided the original author(s) and the copyright owner(s) are credited and that the original publication in this journal is cited, in accordance with accepted academic practice. No use, distribution or reproduction is permitted which does not comply with these terms.

frontiers in Cardiovascular Medicine

ORIGINAL RESEARCH
published: 17 November 2021
doi: 10.3389/fcvm.2021.788655

Association of Lectin-Like Oxidized Low-Density Lipoprotein Receptor-1 With Angiotensin II Type 1 Receptor Impacts Mitochondrial Quality Control, Offering Promise for the Treatment of Vascular Senescence

Yoshihiro Uchikado, Yoshiyuki Ikeda, Yuichi Sasaki, Masaaki Iwabayashi, Yuichi Akasaki and Mitsuru Ohishi*

Department of Cardiovascular Medicine and Hypertension, Graduate School of Medical and Dental Sciences Kagoshima University, Kagoshima, Japan

OPEN ACCESS

Edited by:
Haiyang Tang,
University of Arizona, United States

Reviewed by:
Silvana Balzan,
Italian National Research Council, Italy
Tamara Saez,
University of Alberta, Canada

***Correspondence:**
Yoshiyuki Ikeda
alltezza@m2.kufm.kagoshima-u.ac.jp

Specialty section:
This article was submitted to Cardiovascular Metabolism, a section of the journal Frontiers in Cardiovascular Medicine

Received: *03 October 2021*
Accepted: *26 October 2021*
Published: *17 November 2021*

Citation:
Uchikado Y, Ikeda Y, Sasaki Y, Iwabayashi M, Akasaki Y and Ohishi M (2021) Association of Lectin-Like Oxidized Low-Density Lipoprotein Receptor-1 With Angiotensin II Type 1 Receptor Impacts Mitochondrial Quality Control, Offering Promise for the Treatment of Vascular Senescence. Front. Cardiovasc. Med. 8:788655. doi: 10.3389/fcvm.2021.788655

Lectin-like oxidized low-density lipoprotein (ox-LDL) causes vascular senescence and atherosclerosis. It has been reported that ox-LDL scavenger receptor-1 (LOX-1) is associated with the angiotensin II type 1 receptor (AT1R). While mitochondria play a crucial role in the development of vascular senescence and atherosclerosis, they also undergo quality control through mitochondrial dynamics and autophagy. The aim of this study was to investigate (1) whether LOX-1 associates with AT1R, (2) if this regulates mitochondrial quality control, and (3) whether AT1R inhibition using Candesartan might ameliorate ox-LDL-induced vascular senescence. We performed *in vitro* and *in vivo* experiments using vascular smooth muscle cells (VSMCs), and C57BL/6 and apolipoprotein E-deficient (ApoE KO) mice. Administration of oxidized low-density lipoprotein (ox-LDL) to VSMCs induced mitochondrial dysfunction and cellular senescence accompanied by excessive mitochondrial fission, due to the activation of fission factor Drp1, which was derived from the activation of the Raf/MEK/ERK pathway. Administration of either Drp1 inhibitor, mdivi-1, or AT1R blocker candesartan attenuated these alterations. Electron microscopy and immunohistochemistry of the co-localization of LAMP2 with TOMM20 signal showed that AT1R inhibition also increased mitochondrial autophagy, but this was not affected by Atg7 deficiency. Conversely, AT1R inhibition increased the co-localization of LAMP2 with Rab9 signal. Moreover, AT1R inhibition-induced mitochondrial autophagy was abolished by Rab9 deficiency, suggesting that AT1R signaling modulated mitochondrial autophagy derived from Rab9-dependent alternative autophagy. Inhibition of the Raf/MEK/ERK pathway also decreased the excessive mitochondrial fission, and Rab9-dependent mitochondrial autophagy, suggesting that AT1R signaling followed the Raf/MEK/ERK axis modulated both mitochondrial dynamics and autophagy. The degree of mitochondrial dysfunction, reactive oxygen species production, vascular senescence, atherosclerosis, and the number of fragmented mitochondria accompanied by Drp1 activation were all higher

in ApoE KO mice than in C57BL/6 mice. These detrimental alterations were successfully restored, and mitochondrial autophagy was upregulated with the administration of candesartan to ApoE KO mice. The association of LOX-1 with AT1R was found to play a crucial role in regulating mitochondrial quality control, as cellular/vascular senescence is induced by ox-LDL, and AT1R inhibition improves the adverse effects of ox-LDL.

Keywords: mitochondrial dynamics, dynamin-related protein 1, mitochondrial autophagy, angiotensin II type 1 receptor, oxidized low-density lipoprotein, senescence

INTRODUCTION

Hyperlipidemia is a major risk factor for atherosclerosis and senescence, and is reportedly related to cardiovascular disease (CVD), including coronary artery disease (1). There is increasing evidence that statins are effective for the primary and secondary prevention of CVD from a large clinical trial (2, 3). However, the incidence of CVD adverse events remains as high as 45%, even with statin treatment (4). Moreover, plaque progression is observed in one of three patients with lower levels of low-density lipoprotein (LDL) cholesterol (<70 mg/dl) in coronary artery lesions (5). Thus, the prevention of atherosclerotic CVD has a residual risk that is insufficient even if lipids are sufficiently lowered. Lectin-like ox-LDL scavenger receptor-1 (LOX-1) is a major receptor for ox-LDL and plays a crucial role in the genesis of reactive oxygen species (ROS) in vascular smooth muscle cells (VSMCs). It has recently been reported that LOX-1 associates with angiotensin II (Ang II) type 1 receptor (AT1R) and activates its downstream signal ERK in human umbilical vein endothelial cells (6, 7). The renin-angiotensin system (RAS), the main regulatory system for blood pressure, has been widely documented as being involved in the pathogenesis of several disease states, including CVD. RAS signaling was found to accelerate arterial senescence and arteriosclerosis in human VSMCs and an atherosclerotic apolipoprotein E-deficient (ApoE KO) mouse model (8, 9). Therefore, the treatment using AT1R blocker (ARB) based on the concept of association with LOX-1 and AT1R may have the potential to solve residual risk from lipid-lowering therapies in CVD patients. Indeed, several experimental and clinical studies revealed that ARB therapy combined with statin reduced atherosclerotic plaque of ApoE KO mice and improved clinical symptom and cardiac function in patients with CVD (10, 11).

Mitochondria, however, produce adenosine triphosphate (ATP), which generates ROS as a byproduct of ATP synthesis, and as their function declines, they yield more ROS, resulting in the development of vascular senescence and atherosclerosis. Thus, mitochondrial quality should be strictly controlled, as it can critically impact cellular viability and eventually an individuals' life. Mitochondria have a self-maintenance system to dynamically change their morphology, so-called mitochondrial dynamics (fission and fusion), and impaired mitochondria are eliminated through autophagy. Mitochondrial fission generates small spherical mitochondria, whereas fusion redistributes tubular or elongated mitochondria. Fusion is a mechanism that allows intact mitochondria to complement a damaged unit and share components, thereby maintaining metabolic efficiency. However, fission could isolate an altered subset of mitochondria and induce mitochondrial autophagy to eliminate damaged cells (12). Mitochondrial fission and fusion processes in mammals are mediated by several small GTPases, including dynamin-related protein 1 (Drp1), mitofusin 1 (Mfn1), mitofusin 2 (Mfn2), and optic atrophy 1 (Opa1) (13–15).

A previous study reported that AT1R KO mice had preserved mitochondrial function, leading to longevity (16). However, there are few reports on the relationship between the recovery of mitochondrial function from the effects AT1R inhibition and mitochondrial quality control through mitochondrial dynamics and autophagy. While the administration of ox-LDL decreased mitochondrial function in HL-1 cells, there is no report that this mitochondrial dysfunction is ameliorated by AT1R inhibition in terms of mitochondrial dynamics and autophagy (17). Therefore, we hypothesized that (1) the association of LOX-1 and AT1R is involved in mitochondrial quality control through mitochondrial dynamics and autophagy, and (2) AT1R inhibition using ARB, Candesartan, may ameliorate ox-LDL-mediated senescence, leading to atherosclerosis.

MATERIALS AND METHODS

Cell Culture and Treatment

Human aortic smooth muscle cells were purchased from LONZA (Portsmouth, NH, USA) and cultured in smooth muscle basal medium-2 (Lonza, Cat #CC-3181) supplemented with SMC growth medium (Lonza, Cat #CC-4149), as described previously (18). Prior to stimulation, the cells were starved in 0.5 % FBS-containing medium for 16 h. The cells were treated with 20 μmol/L ox-LDL (Thermo Fisher Scientific, Cat #L34357). Time of the exposure to ox-LDL was 24 h for assessment of senescence in immunoblot (detections of p53 and p21) and in Senescence-associated β-galactosidase (SA-β gal) staining, 12 h for mitochondrial autophagy in immunohistochemistry, and 3 h for other experiments. The following inhibitors were used:

Abbreviations: LOX-1, lectin-like oxidized low-density lipoprotein scavenger receptor-1; AT1R, angiotensin II type 1 receptor; VSMCs, vascular smooth muscle cells; ApoE KO, apolipoprotein E deficient; ox-LDL, oxidized low-density lipoprotein; CVD, cardiovascular disease; ROS, reactive oxygen species; ATP, adenosine triphosphate; Drp1, dynamin-related protein 1; Mfn1, mitofusin 1; Mfn2, mitofusin 2; Opa1, Optic-atrophy 1; Candesartan, Candesartan cilexetil; DMSO, dimethyl sulfoxide; SA-β gal, Senescence-associated β-galactosidase; SEM, standard error of the mean; ARB, angiotensin II type 1 receptor blocker; Ang II, angiotensin II; EM, electron microscopy; RAS, renin-angiotensin system; EBA, Extraction Buffer A; PBS, phosphate-buffered saline.

20 μmol/L Mdivi-1 (Sigma, Cat #M0199), Drp1 inhibitor; 10 μmol/L candesartan cilexetil (Candesartan) (Sigma-Aldrich, Cat #SML0245), ARB; 10 μmol/L Dabrafenib (Selleck, Cat #S2807), RAF inhibitor; 2 μmol/L PD184352 (Selleck, Cat #S1020), MEK inhibitor; 2 μmol/L SCH772984 (Selleck, Cat #S7101), ERK inhibitor. For the inhibition experiments, cells were treated with each inhibitor for 1 h following the addition of ox-LDL. Control cells were exposed to the same amount of dimethyl sulfoxide (DMSO). The dose of Candesartan was based on the previous report (19).

Animal Models

This study was conducted in compliance with the protocol reviewed by the Institutional Animal Care and Use Committee and was approved by the Faculty of Medicine at Kagoshima University. All animal experiments followed the recommendations in the guidelines for animal experimentation at research institutes (Ministry of Education, Culture, Sports, Science and Technology, Japan), the guidelines for animal experimentation at institutes (Ministry of Health, Labor and Welfare, Japan), and the guidelines for proper conduct of animal experimentation (Science Council of Japan). In this experiment, we used only male mice, housed in groups of one to three per cage. Mice had free access to water and food during the experimental period and were maintained at room temperature (25 ± 2°C) under a standard 12/12 h light-dark cycle. For comparison of C57BL/6 and ApoE KO mice, ∼35-week-old mice were used. To suppress mitochondrial fission, ApoE KO mice that were ∼30 weeks old were administered either mdivi-1 (1.2 mg/kg) or with the same amount of DMSO by intraperitoneal injection for 4 weeks. To check the role of AT1R inhibition, ApoE KO mice at 16 weeks of age were administered either candesartan (10 mg/kg) or the same amount of DMSO by intraperitoneal injection for 8 weeks. Body weight and food intake were measured weekly after the injection. Systolic and diastolic blood pressure and heart rate of mouse were measured by MK-2000, a computer-controlled tail-cuff system (Muromachi Kikai).

Tissue Preparation

All mice were sacrificed with an overdose of sodium pentobarbital (100 mg/kg) by intraperitoneal injection. ATP production, H_2O_2 measurement, and senescence-associated β-galactosidase (SA-β gal) staining were performed in a single mouse. For ATP production and H_2O_2 measurement, we isolated the mitochondrial fraction from vessels immediately after removal of aorta samples from the ascending aorta to the bifurcation of the common iliac artery. For SA-β gal staining, the aortic trees were removed and cut longitudinally from the ascending aorta to the abdominal aorta. We performed immunohistochemical analysis, Masson's trichrome staining and immunoblot analysis for the same mouse. For Masson's trichrome staining and immunohistochemical analysis, ascending aortas were fixed in 4% paraformaldehyde phosphate buffer solution, embedded in paraffin, and sectioned into 4 μm tissue sections. For immunoblot analysis, the remaining aorta samples from the ascending aorta to the bifurcation of the common iliac artery were rinsed with phosphate-buffered saline (PBS) and stored at −80°C.

Immunoblot Analysis

Immunoblot analysis was performed in accordance with a previous report (18, 20). The primary antibodies used were as follows: Drp1 (1:1000, BD Biosciences, Cat #611112, RRID:AB_398423), Phospho-Drp1 ser616 (1:200, Cell Signaling Technology, Cat #4494, RRID:AB_11178659), Phospho-Drp1 ser637 (1:200, Cell Signaling Technology, Cat #4867, RRID:AB_10622027; 1:500, Abcam, Cat #ab193216), Opa1 (1:1000, BD Biosciences, Cat #612606, RRID:AB_399888), Mfn1 (1:1000, Abcam, Cat #ab57602, RRID:AB_2142624), Mfn2 (1:500, Sigma-Aldrich, Cat #M6319, RRID:AB_477221), COX IV (1:1000, Cell Signaling Technology, Cat #4844, RRID:AB_2085427), p53 (1:1000, Abcam, Cat #ab131442, RRID:AB_11155283; 1:200, Santa Cruz Biotechnology, Cat # sc-99, RRID:AB_628086), p21 (1:2000, Abcam, Cat #ab109199, RRID:AB_10861551), ERK1/2 (1:500, Santa Cruz Biotechnology, Cat #sc-514302, RRID:AB_2571739), Phospho-ERK1/2 (1:500, Santa Cruz Biotechnology, Cat #sc-7383, RRID:AB_627545), MEK1/2 (1:500, Santa Cruz Biotechnology, Cat #sc-81504, RRID:AB_1126111), Phospho-MEK1/2 (1:500, Santa Cruz Biotechnology, Cat #sc-81503, RRID:AB_1126112), CRAF (1:1000, Cell Signaling Technology, Cat #9422, RRID:AB_390808), Phospho-CRAF ser338 (1:500, Cell Signaling Technology, Cat #9427, RRID:AB_2067317), β-actin (1:1000, Santa Cruz Biotechnology, Cat #sc-47778 HRP, RRID:AB_2714189), and α-tubulin (1:1000, Sigma-Aldrich, Cat #T6199, RRID:AB_477583). The secondary antibodies used were as follows: goat anti-rabbit antibody (1:4000, Bio-Rad, Cat #170-6515, RRID:AB_11125142) or goat anti-mouse antibody (1:2000, Santa Cruz Biotechnology, Cat #sc-516102, RRID:AB_2687626). Bands were visualized using ECL Prime western blotting Detection Reagent (Amersham, Cat #RPN2232) and detected with Lumino Graph II (ATTO).

Confocal Immunohistochemistry

Immunostaining *in vivo* and *in vitro* was performed as described previously (18, 21). The samples were stained with primary and secondary antibodies as follows: anti-Rab9 mouse monoclonal antibody (1:100, Abcam, Cat #ab2810, RRID:AB_303323), anti-LAMP2 rabbit polyclonal antibody (1:100, Sigma, Cat #L0668, RRID:AB_477154), anti-LAMP2 mouse monoclonal antibody (1:100, Abcam, Cat #ab25631, RRID:AB_470709), anti-TOMM20 rabbit monoclonal antibody (1:100, Abcam, Cat #ab186734, RRID:AB_2716623), anti- LC3B rabbit polyclonal antibody (1:100, Abcam, Cat #ab51520, RRID:AB_881429), Alexa Fluor 488-conjugated goat anti-rabbit IgG (1:100, Abcam, Cat #ab150081, RRID:AB_2734747), and Alexa Fluor 594-conjugated goat anti-mouse IgG (1:100, Abcam, Cat #ab150120, RRID:AB_2631447). Fluorescence images were obtained using an LSM700 confocal laser scanning microscope (Zeiss, Cat #LSM700, RRID:SCR_017377). Pearson's correlation coefficient was calculated to quantify the colocalization correlation of the

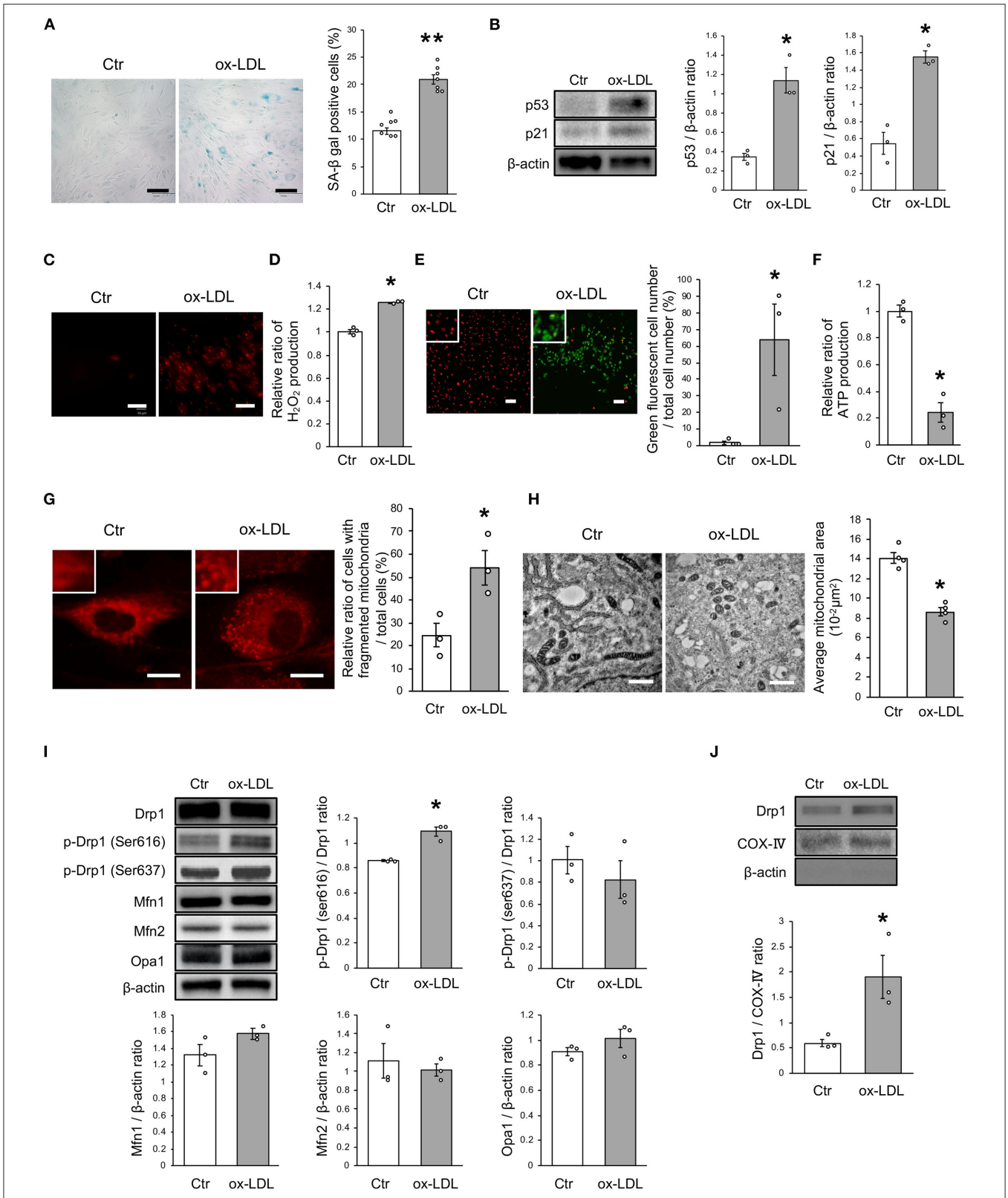

FIGURE 1 | Ox-LDL treatment induced mitochondrial fission, ROS production, mitochondrial dysfunction, and cellular senescence. **(A)** Representative images and quantitative analysis of SA-β gal staining of cells treated with ox-LDL or the control. Scale bar = 100 μm. $^{**}P < 0.01$ vs. Ctr ($n = 7$ per group). **(B)** Immunoblots and

(Continued)

FIGURE 1 | quantitative analysis of p53, p21, and β-actin in cells treated with ox-LDL or the control. *$P < 0.05$ vs. Ctr ($n = 3$ per group). **(C)** Representative images of MitoSox Red in cells treated with ox-LDL or the control. Scale bar = 100 μm. **(D)** Relative mitochondrial H_2O_2 production in cells treated with ox-LDL or the control. *$P < 0.05$ vs. Ctr ($n = 3$ per group). **(E)** Representative images and quantitative analysis of JC-1 staining in cells treated with ox-LDL or the control. Scale bar = 100 μm. *$P < 0.05$ vs. Ctr ($n = 3$ per group). **(F)** Relative mitochondrial ATP production in cells treated with ox-LDL or the control. *$P < 0.05$ vs. Ctr ($n = 3$ per group). **(G)** Representative images of Mitotracker Red in cells treated with ox-LDL or control. Scale bar = 10 μm. *$P < 0.05$ vs. Ctr ($n = 3$ per group). **(H)** Electron microscopic images and quantitative analysis of mitochondria and average mitochondrial areas in cells treated with ox-LDL or the control. Scale bar = 1 μm. *$P < 0.05$ vs. Ctr ($n = 4$ per group). **(I)** Immunoblots and quantitative analysis for Drp1, p-Drp1 (Ser616), p-Drp1 (Ser637), Mfn1, Mfn2, Opa1, and β-actin in cells with ox-LDL or the control. *$P < 0.05$ vs. Ctr ($n = 3$ per group). **(J)** Immunoblots and quantitative analysis for Drp1, COX IV, and β-actin in mitochondrial fractions of cells treated with ox-LDL or the control. *$P < 0.05$ vs. Ctr ($n = 3$ per group). All data are presented as the mean ± SEM. Statistical analysis were conducted by Wilcoxon rank sum test **(B,D-J)** and Student's *t*-test **(A)**.

intensity distributions between the two channels, as previously described (22). We performed independent *in-vitro* experiments three times.

SA-β Gal Staining

SA-β gal activity in VSMCs was evaluated using the SA-β gal staining kit (Cell Signaling Technology, Cat #9860), according to the manufacturer's protocol. SA-β gal activity *in vitro* was assessed using β galactosidase staining solution (pH 6.0): 930 μl Staining solution, 10 μl solution A, 10 μl solution B, 50 μl DMF containing with 1 mg X-gal. Briefly, cells were washed with PBS and fixed with Fixative solution. Then they were stained with β galactosidase staining solution for 12 h at 37°C. SA-β gal positive cells were quantitatively determined within at least 200 cells that were counted in no less than four random fields using a microscope (Keyence, Cat #BZ X-710, RRID:SCR_017202). As described previously, SA-β gal activity *in vivo* was assessed using SA-β gal solution: 1 mg/ml X-Gal (Invitrogen, Cat #15520034), 1 mol/L $MgCl_2$, 2% NP-40, 100 mmol/L potassium ferrocyanide (II), 100 mmol/L potassium ferrocyanide (III), and 40 mmol/L citric acid/sodium phosphate buffer (pH 6.0) (18). Briefly, after washing the harvested aortic trees from the ascending aorta to the abdominal aorta with PBS, they were stained with SA-β gal solution for 24 h at 37°C. The samples were then washed three times with PBS and fixed with 4% paraformaldehyde. Images were captured using a digital camera (Nikon, Cat #D810). SA-β gal positive area were quantified using ImageJ FIJI (National Institutes of Health, RRID:SCR_003070).

Evaluation of Mitochondrial Reactive Oxygen Species and Membrane Potential Measurements

The methods for evaluation of mitochondrial reactive oxygen species and membrane potential measurements have been described previously (21). Briefly, intracellular mitochondrial ROS generation was measured using the MitoSox™ Red mitochondrial superoxide indicator (Invitrogen, Cat #M36008) under a microscope (Keyence, Cat #BZ-X710, RRID:SCR_017202). To evaluate mitochondrial membrane potential, the state of the mitochondrial membrane potential was visualized using MitoPT®JC-1 (ImmunoChemistry Technologies, Cat #924) with red and green fluorescence indicating polarized and depolarized mitochondria. Depolarized mitochondria were evaluated by counting the number of green fluorescent cells in at least 150 cells in each experiment.

Mitotracker Staining

After administration of either ox-LDL treated with or without each inhibitor, or control vehicle to VSMCs as described above, the cells were stained with MitoTracker Red FM (Invitrogen, Cat #M22425), according to the manufacturer's protocol. Fluorescence images of live cells were acquired using a LSM700 confocal laser scanning microscope. The method for evaluating mitochondrial morphology has been described previously (21). More than 20 cells were chosen randomly in each experiment, and the percentage of cells with fragmented mitochondria was calculated.

Mitochondrial Isolation

Mitochondrial fractions of VSMCs or isolated mouse aortas were purified using a different mitochondrial isolation kit (Thermo Fisher Scientific, Cat #89874; Sigma-Aldrich, Cat #MITOISO1), according to the manufacture's instruction. Briefly, *in vitro* experiment, cells were collected by cell scraper and then centrifuge at 850 × g for 2 min at 4°C. After removing supernatant samples were added several reagents and incubated according to the instruction. Then, samples were centrifuged at 700 × g for 5 min at 4°C. Supernatant were then centrifuged at 12,000 × g for 15 min at 4°C. After removing supernatant, the pellets were washed with 500 μl of Mitochondria Isolation Reagent C, and centrifuged again at 12,000 × g for 5 min at 4°C. The pellets contained mitochondria fraction. *In vivo* experiment, after washing the harvested aortic trees with Extraction Buffer A (EBA) [50 mmol/L HEPES, 1 mol/L mannitol, 350 mmol/L sucrose, 5 mmol/L EGTA], they were cut thinly and incubated in EBA containing 0.25 mg/ml trypsin on ice for 3 min. Then, removed supernatant and added 8 volumes of EBA containing 0.25 mg/ml trypsin for 20 min. After adding albumin solution and remove supernatant, samples were added eight volumes of EBA containing 0.25 mg/ml trypsin and homogenized. Homogenates were centrifuged at 600 × *g* for 5 min at 4°C. Supernatant were then centrifuged at 11,000 × *g* for 10 min at 4°C. The pellets were mitochondrial fractions. Regardless of *in vitro* or *vivo* experiments, performed all the isolation procedure at 4°C with ice-cold solutions.

H_2O_2 Measurement and ATP Production

Mitochondrial fractions of cells and tissues were prepared as described above. H_2O_2 production was measured using an Amplex Red H_2O_2 assay kit (Invitrogen, Cat #A22188), according to the manufacturer's recommendations. ATP production was quantified using an ATP Bioluminescent Assay

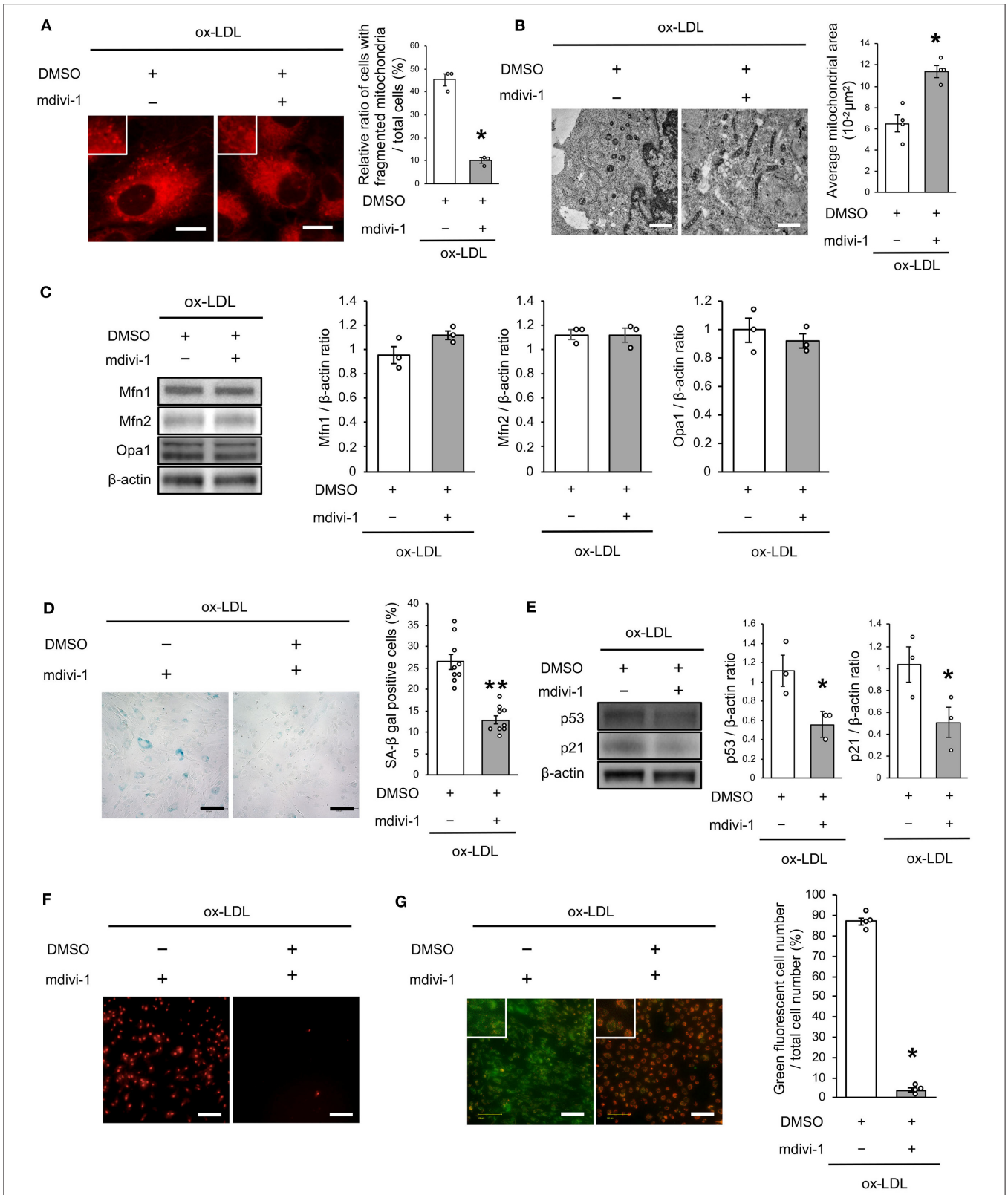

FIGURE 2 | Mdivi-1 treatment retarded excessive mitochondrial fission, ROS production, mitochondrial dysfunction and cellular senescence, which were induced by ox-LDL. **(A)** Representative images and quantitative analysis of Mito-tracker Red in ox-LDL-treated cells with mdivi-1 or the control vehicle. Scale bar = 10 μm.

(Continued)

FIGURE 2 | *$P < 0.05$ vs. ox-LDL with the control ($n = 3$ per group). **(B)** Electron microscopic images and quantitative analysis of mitochondria and average mitochondrial areas in ox-LDL-treated cells with mdivi-1 or the control. Scale bar = 1 μm. *$P < 0.05$ vs. ox-LDL with the control ($n = 4$ per group). **(C)** Immunoblots and quantitative analysis for Mfn1, Mfn2, Opa1, and β-actin in ox-LDL-treated cells with mdivi-1 or the control ($n = 3$ per group). **(D)** Representative images and quantitative analysis of SA-β gal staining of ox-LDL-treated cells with mdivi-1 or the control. **$P < 0.01$ vs. ox-LDL with the control ($n = 9$ per group). **(E)** Immunoblots and quantitative analysis for p53, p21, and β-actin in ox-LDL-treated cells with mdivi-1 or the control. *$P < 0.05$ vs. ox-LDL with the control ($n = 3$ per group). **(F)** Representative images of MitoSox Red in ox-LDL-treated cells with mdivi-1 or the control. Scale bar = 100 μm. **(G)** Representative images and quantitative analysis of JC-1 staining in ox-LDL-treated cells with mdivi-1 or the control. Scale bar = 100 μm. *$P < 0.05$ vs. ox-LDL with the control ($n = 3$ per group). All data are presented as the mean ± SEM. Statistical analysis were conducted by Wilcoxon rank sum test **(A-C,E,G)** and Student's *t*-test **(D)**.

kit (Sigma-Aldrich, Cat #213-579-1), according to a previously described method (21).

Masson's Trichrome Staining

We used 4 mice per group in comparison of C57BL/6 and ApoE KO mice, 3 mice per group in that of ApoE KO mice treated with mdivi-1 or the control, and 3 mice per group in that of ApoE KO mice treated with Candesartan or the control. Mice aorta samples were fixed as described above, and Masson's trichrome staining was used to visualize the state of fibrosis. Interstitial fibrosis was quantified using ImageJ FIJI (National Institutes of Health, RRID:SCR_003070).

Transmission Electron Microscopy Analysis

The method of creating samples for EM has been described previously (21). Sections of the samples were observed using a HITACHI H-7650 transmission electron microscope (HITACHI).

Evaluation of Average Mitochondrial Area

The number of mitochondria in each experiment was determined within at least 50 mitochondria, as assessed using EM. Mitochondria were randomly selected from no less than three independent experiments. The average mitochondrial area was calculated from the number of mitochondria and the total area of the mitochondria using ImageJ FIJI.

Evaluation of Mitochondrial Autophagy

In vitro experiment, the cells of each group were quantitatively determined within at least 15 cells, counted in no less than three independent experiments assessed using EM. *In vivo* experiment, 600 μm^2 of the aorta of each mouse was observed in a random fashion. The number of mitochondria engulfed by autophagosomes was counted using the EM. Three samples were assessed per group.

Small Interfering RNA Transfection

For ERK1, ERK2, and Rab9 RNA knockdown, cells were transfected with ERK1, ERK2, Rab9, or control siRNA (Santa Cruz, Cat #sc-29307, sc-35335, sc-44065, sc-37007) using the siRNA transfection reagent (Santa Cruz, Cat #sc-29528), according to the manufacturer's protocol. For siRNA targeting *Atg7*, we transfected cells with *Atg7* or control (Thermo Fisher Scientific, Cat #s20650, #4390843) using the Lipofectamine RNAiMAX transfection reagent (Invitrogen™, 13778150), according to the manufacturer's protocol. Efficient knockdowns of ERK1, ERK2, Rab9, and *Atg7* were confirmed by immunoblotting (**Supplementary Figures 1A-D**).

Statistical Analysis

All data are presented as mean ± standard error of the mean (SEM). For datasets with a small sample size ($n = 3$–5) or a biased distribution, the results were assessed statistically for significant differences by non-parametric statistical analysis using Wilcoxon rank sum test. Otherwise, statistical significance was assessed using Student's *t*-test. All statistical analyses were performed using the JMP Pro 15 (SAS Institute). Statistical significance was set at $P < 0.05$.

RESULTS

ox-LDL Induced Mitochondrial Fission, ROS Production, Mitochondrial Dysfunction, and Cellular Senescence

First, we investigated the effects of ox-LDL on cellular senescence. ox-LDL was found to increase the ratio of SA-β gal positive cells (**Figure 1A**). The expression of p53 and p21 was also higher in VSMCs treated with ox-LDL (**Figure 1B**), suggesting that ox-LDL induces cellular senescence. We then evaluated oxidative stress and mitochondrial function. The intensity of MitoSox Red fluorescence and H_2O_2 production were found to be higher in ox-LDL-treated cells (**Figures 1C,D**). Mitochondrial membrane potential and ATP production were lower in ox-LDL-treated cells (**Figures 1E,F**), suggesting that ox-LDL decreased mitochondrial function and increased ROS production. To assess whether ox-LDL modulates mitochondrial dynamics in VSMCs, we performed MitoTracker Red and electron microscopic analyses. Administration of ox-LDL increased the ratio of cells with fragmented mitochondria (**Figure 1G**). Both fused and small spherical mitochondria without ox-LDL were identified (**Figure 1H**). However, most of the mitochondria treated with ox-LDL showed a small spherical shape (**Figure 1H**). These results indicated that ox-LDL forced mitochondrial fission. We consequently investigated how mitochondrial fission was regulated in response to ox-LDL. Immunoblot analysis revealed that ox-LDL induced phosphorylation of Drp1 at serine 616, which is the activating form of Drp1 and the primary regulator of mitochondrial fission, but it did not modulate other mitochondrial dynamics factors, such as Mfn1, Mfn2, and Opa1, which induced mitochondrial fusion (**Figure 1I**). Although Drp1 is localized primarily in the cytosol, ox-LDL assembles Drp1 to mitochondria (**Figure 1J**). These results suggest that ox-LDL induces mitochondrial fission through Drp1 activation and

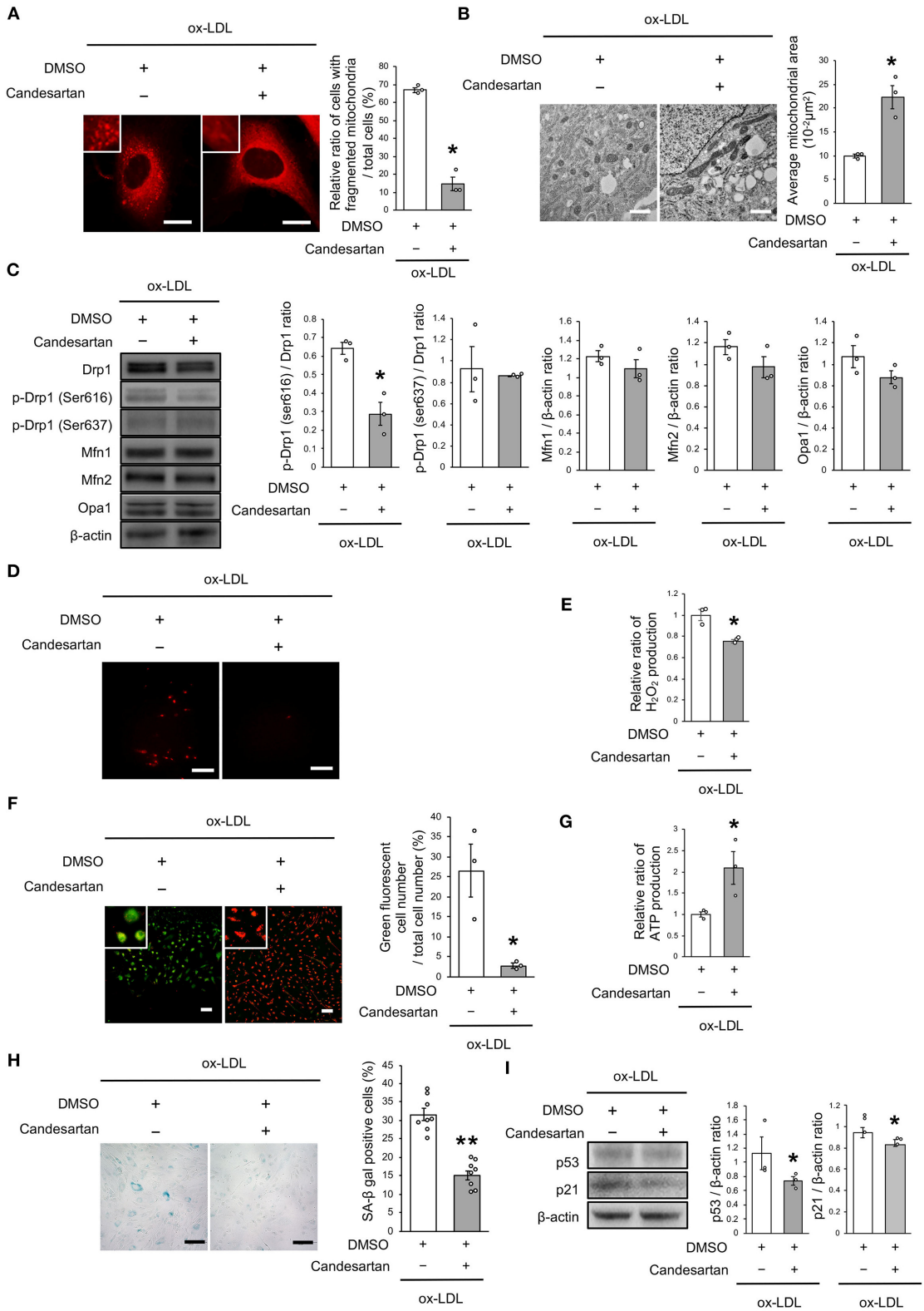

FIGURE 3 | AT1R inhibition retarded excessive mitochondrial fission, ROS production, mitochondrial dysfunction, and cellular senescence, which are induced by ox-LDL. **(A)** Representative images and quantitative analysis of Mitotracker Red in ox-LDL-treated cells with Candesartan or the control vehicle. Scale bar = 10 μm.

(Continued)

FIGURE 3 | *$P < 0.05$ vs. ox-LDL with the control ($n = 3$ per group). **(B)** Electron microscopic images and quantitative analysis of mitochondria and average mitochondrial areas in Candesartan-treated vs. vehicle-treated cells with ox-LDL. *$P < 0.05$ vs. ox-LDL with the control ($n = 3$ per group). **(C)** Immunoblots and quantitative analysis for Drp1, p-Drp1 (Ser616), p-Drp1 (Ser637), Mfn1, Mfn2, Opa1, and β-actin in ox-LDL treated cells with Candesartan or the control. *$P < 0.05$ vs. ox-LDL with the control ($n = 3$ per group). **(D)** Representative images of MitoSox Red in ox-LDL-treated cells with Candesartan or the control vehicle. **(E)** Relative mitochondrial H_2O_2 production in ox-LDL-treated cells with Candesartan or the control. *$P < 0.05$ vs. ox-LDL with control vehicle ($n = 3$ per group). **(F)** Representative images and quantitative analysis of JC-1 staining in ox-LDL-treated cells with Candesartan or the control. Scale bar = 100 μm. *$P < 0.05$ vs. ox-LDL with the control ($n = 3$ per group). **(G)** Relative mitochondrial ATP production in ox-LDL-treated cells with Candesartan or the control. *$P < 0.05$ vs. ox-LDL with the control. ($n = 3$ per group). **(H)** Representative images and quantitative analysis of SA-β gal staining of ox-LDL-treated cells with Candesartan or the control. Scale bar = 100 μm. **$P < 0.01$ vs. ox-LDL with the control ($n = 8$ per group). **(I)** Immunoblots and quantitative analysis for p53, p21, and β-actin in cells with Candesartan or the control under ox-LDL treatment. *$P < 0.05$ vs. ox-LDL with the control ($n = 3$ per group). All data are presented as the mean ± SEM. Statistical analysis were conducted by Wilcoxon rank sum test **(A-C,E-G,I)** and Student's *t*-test **(H)**.

may cause ROS production, mitochondrial dysfunction, and cellular senescence.

Drp1 Inhibition Retarded Excessive Mitochondrial Fission, Mitochondrial Dysfunction, ROS Production, and Cellular Senescence

To investigate whether ox-LDL-induced mitochondrial fission causes mitochondrial dysfunction, increased ROS production, and cellular senescence, we used mdivi-1, a small molecule that selectively inhibits the assembly of Drp1 to mitochondria. Mdivi-1 treatment decreased the ratio of cells with fragmented mitochondria induced by ox-LDL (**Figure 2A**). Moreover, mdivi-1 suppressed ox-LDL-mediated excessive mitochondrial fission and induced mitochondrial fusion (**Figure 2B**). However, mdivi-1 did not regulate mitochondrial fusion factors, such as Mfn1, Mfn2, and Opa1 (**Figure 2C**), indicating that mdivi-1 successfully restored mitochondrial fission by inhibiting Drp1. Under these conditions, mdivi-1 decreased the ratio of SA-β gal positive cells and the expression of p53 and p21 in VSMCs treated with ox-LDL (**Figures 2D,E**). The intensity of MitoSox Red fluorescence was lower in mdivi-1-treated cells than in untreated cells (**Figure 2F**). Furthermore, the administration of ox-LDL treated with mdivi-1 improved the mitochondrial membrane potential (**Figure 2G**). These results suggest that excessive mitochondrial fission is restored by Drp1 inhibition, mitochondrial dysfunction, ROS production, and cellular senescence.

Receptor Association of LOX-1/AT1R Regulates Mitochondrial Dynamics

We next investigated whether the receptor association of LOX-1 with AT1R is involved in regulating mitochondrial dynamics using candesartan, an ARB. As shown in **Figure 3A**, AT1R inhibition decreased the ratio of cells with fragmented mitochondria (**Figure 3A**). Moreover, both fused and small spherical mitochondria were observed in VSMCs treated with candesartan (**Figure 3B**). Ox-LDL-induced Drp1 phosphorylation at Ser616 was also decreased by AT1R inhibition, but AT1R inhibition did not modulate other mitochondrial dynamics factors (**Figure 3C**). The intensity of MitoSox Red fluorescence and H_2O_2 production was lower in ARB-treated cells than in untreated cells (**Figures 3D,E**). Moreover, the administration of ox-LDL treated with ARB improved mitochondrial membrane potential and increased ATP production (**Figures 3F,G**). Furthermore, ARB decreased the ratio of SA-β gal positive cells and the expression of p53 and p21 in VSMCs treated with ox-LDL (**Figures 3H,I**). These results suggest that AT1R inhibition improved the imbalance of excessive mitochondrial fission and restored ROS production, mitochondrial dysfunction, and cellular senescence.

ox-LDL Induced Drp1 Activation via the CRAF/MEK/ERK Pathway

The mechanism of ox-LDL-induced mitochondrial fission was then investigated. Ox-LDL was found to activate CRAF/MEK/ERK, which is downstream of AT1R (**Figure 4A**). We consequently investigated whether CRAF, MEK, or ERK modulated Drp1 activation using inhibition experiments. The results showed that Dabrafenib, a RAF inhibitor, inactivated MEK, ERK, and Drp1 (**Figure 4B**). MEK inhibition using PD184352 inactivated ERK and Drp1, but not CRAF (**Figure 4C**). ERK inhibition using SCH772984 also inactivated Drp1, but not CRAF (**Figure 4D**). Knockdowns of ERK1 or ERK2 did not modulate activation of MEK (**Figure 4E** and **Supplementary Figures 1A,B**). The CRAF/MEK/ERK pathway was found to play a role in activating Drp1 (**Figures 4D,E**), while ARB decreased ox-LDL-induced CRAF/MEK/ERK activation (**Figure 4F**). These results suggest that ox-LDL activates Drp1 through CRAF/MEK/ERK signaling, and this is downstream of AT1R.

AT1R Inhibition Induced Mitochondrial Autophagy Derived From Rab9-Dependent Alternative Autophagy

As dysfunctional mitochondria are eliminated through autophagy, which is generally believed to require mitochondrial fission, we investigated whether AT1R inhibition regulates mitochondrial autophagy. Electron microscopic analysis showed that mitochondrial autophagy increased in ox-LDL and ARB-treated cells (**Figure 5A**). Under ox-LDL treatment, immunohistochemistry analysis showed that the colocalization of mitochondrial protein TOMM20 and LAMP2, which is a marker of autolysosomes, was higher in ARB-treated cells than in untreated cells (**Figure 5B**). These results suggest that AT1R inhibition promotes mitochondrial autophagy. In contrast, ARB treatment did not change the colocalization of LAMP2 with LC3, which is a hallmark of autophagy (**Figure 5C**). Recent studies have revealed the existence of at least two forms of

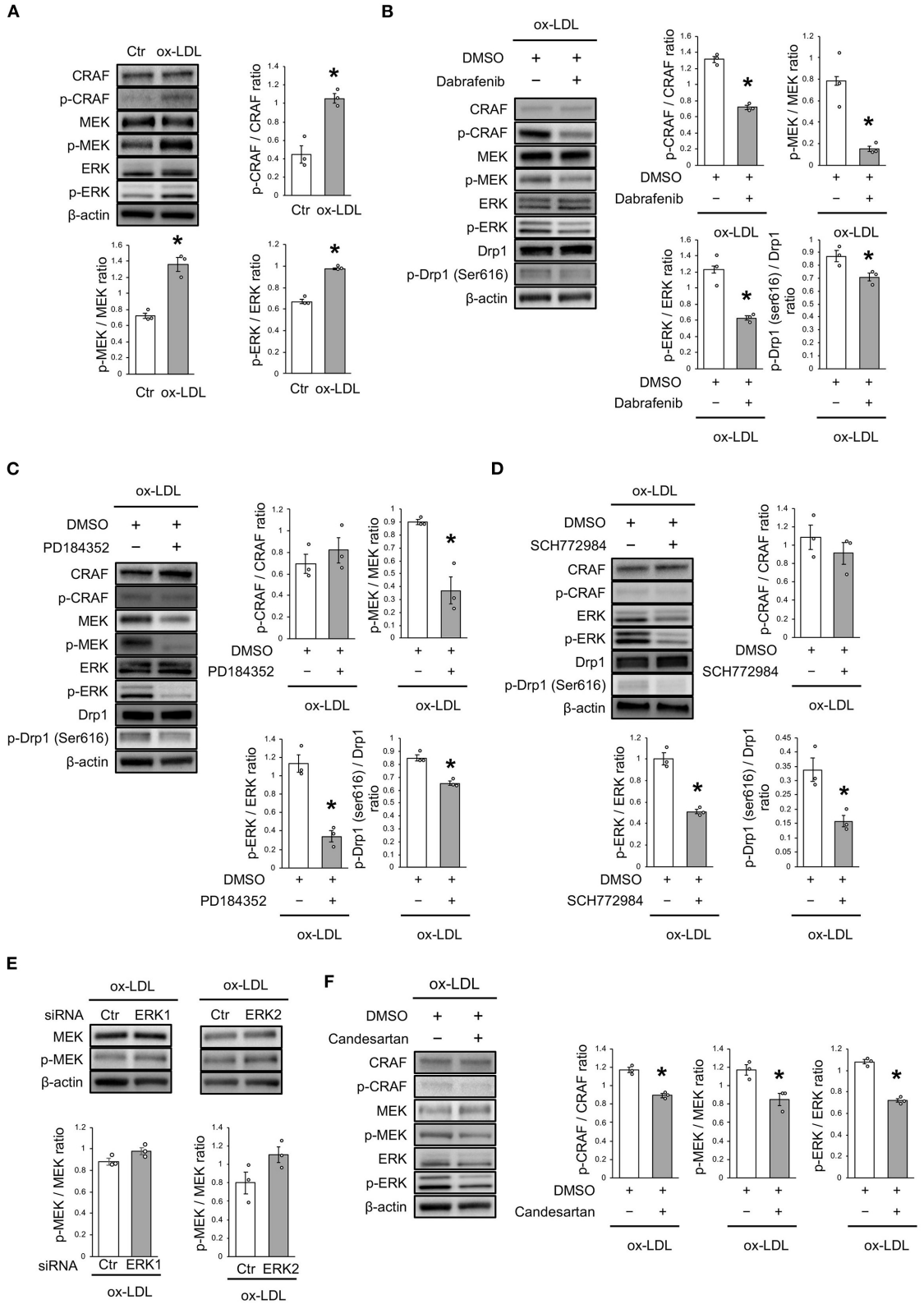

FIGURE 4 | ox-LDL induced Drp1 activation through AT1R and the CRAF/MEK/ERK pathway. **(A)** Immunoblots and quantitative analysis for CRAF, p-CRAF, MEK, p-MEK, ERK, p-ERK, and β-actin in cells with ox-LDL or the control. *$P < 0.05$ vs. the control ($n = 3$ per group). **(B)** Immunoblots and quantitative analysis for CRAF,

(Continued)

FIGURE 4 | p-CRAF, MEK, p-MEK, ERK, p-ERK, Drp1, p-Drp1 (Ser616), and β-actin in Dabrafenib-treated vs. control cells with ox-LDL. *$P < 0.05$ vs. ox-LDL with the control ($n = 3$ per group). **(C)** Immunoblots and quantitative analysis for CRAF, p-CRAF, MEK, p-MEK, ERK, p-ERK, Drp1, p-Drp1 (Ser616), and β-actin in PD184352-treated vs. control cells with ox-LDL. *$P < 0.05$ vs. ox-LDL with the control ($n = 3$ per group). **(D)** Immunoblots and quantitative analysis for CRAF, p-CRAF, MEK, p-MEK, ERK, p-ERK, Drp1, p-Drp1 (Ser616), and β-actin in SCH772984-treated vs. the control cells with ox-LDL. *$P < 0.05$ vs. ox-LDL without SCH772984 ($n = 3$ per group). **(E)** Immunoblots and quantitative analysis for CRAF, p-CRAF, MEK, p-MEK, ERK, p-ERK, and β-actin in Candesartan-treated vs. control cells with ox-LDL. *$P < 0.05$ vs. ox-LDL with the control ($n = 3$ per group). All data are presented as the mean ± SEM. Statistical analysis were conducted by Wilcoxon rank sum test **(A-F)**.

autophagy. One is LC3- and *Atg7*-dependent autophagy, which is also considered to be conventional autophagy. The other is called alternative autophagy, does not require the use of LC3 or *Atg7* but does require the membrane trafficking protein Rab9 (23). To examine whether mitochondrial autophagy is related to conventional autophagy or alternative autophagy, we examined the colocalization of LAMP2 with Rab9 using double-staining immunohistochemistry. The colocalization of LAMP2 with Rab9 staining was also significantly increased in ox-LDL-treated cells with ARB (**Figure 5D**). In addition, the colocalization of TOMM20 with LAMP2 induced by AT1R inhibition was not affected by *Atg7* knockdown, but by Rab9 knockdown in ox-LDL-treated cells (**Figures 5E,F**). Furthermore, Rab9 knockdown increased the ratio of SA-β gal positive cells in ox-LDL-treated cells with candesartan, indicating that AT1R inhibition induces mitochondrial autophagy through Rab9 (**Supplementary Figure 1E**). These results suggest that AT1R inhibition induces mitochondrial autophagy derived from Rab9-dependent alternative autophagy, leading to the suppression of cellular senescence by maintaining mitochondrial quality control.

Rab9-Dependent Mitochondrial Autophagy Was Not Affected by ERK Inhibition but by MEK Inhibition

We further analyzed whether CRAF/MEK/ERK is involved in AT1R inhibition-mediated mitochondrial autophagy derived from Rab9-dependent alternative autophagy. ERK inhibition did not affect the colocalization of LAMP2 and TOMM20 (**Figure 6A**), whereas MEK inhibition increased the colocalization of LAMP2 with either TOMM20 or Rab9 (**Figures 6B,C**), indicating that AT1R inhibition-induced mitochondrial autophagy is mediated by the AT1R/CRAF/MEK pathway.

Drp1 Inhibition Improved the Imbalance of Mitochondrial Dynamics and Vascular Senescence in ApoE KO Mice

We investigated the relationship between vascular senescence and mitochondrial dynamics in C57BL/6 and ApoE KO mice. Body weight, heart rate, and blood pressure were not found to differ between C57BL/6 and ApoE KO mice (**Table 1**). EM revealed that ApoE KO mice forced mitochondrial dynamics resulting in excessive fission when compared to C57BL/6 mice (**Figure 7A**). Immunoblot analysis indicated that the arterial expression of Drp1 phosphorylation at serine 616 was higher in ApoE KO mice than in C57BL/6 mice, but other mitochondrial dynamics factors were not significantly different between the two groups (**Figure 7B**). ATP production was lower and H_2O_2 production was higher in ApoE KO mice than in C57BL/6 mice, suggesting that ApoE KO mice had reduced mitochondrial function and increased oxidative stress in the arteries (**Figures 7C,D**). Arterial fibrosis, was assessed using Masson's trichrome staining, and was found to have increased in ApoE KO mice when compared with that in C57BL/6 mice (**Figure 7E**). The ratio of arterial senescence assessed by SA-β gal staining was greater in ApoE KO mice than in C57BL/6 mice (**Figure 7F**). Immunoblot analysis showed that the expression of p21 and p53 was higher in ApoE KO mice than in C57BL/6 mice (**Figure 7G**). These results indicate that arterial senescence is facilitated in ApoE-KO mice. Next, we investigated ApoE KO mice treated with mdivi-1 to investigate whether the inhibition of mitochondrial fission retarded vascular senescence. Food intake during the experiment, body weight, heart rate, and blood pressure were not different between ApoE KO mice treated with mdivi-1 and the control vehicle (**Table 2**). EM analysis revealed that excessive mitochondrial fission was reduced in ApoE KO mice treated with mdivi-1 compared to those treated with the control vehicle (**Figure 7H**). Immunoblot analysis showed that the administration of mdivi-1 did not significantly change the expression of mitochondrial fusion factors (**Figure 7I**). The ratio of the arterial fibrosis and senescence area, assessed using Masson trichrome analysis and SA-β gal staining, respectively, were lower in ApoE KO mice administered mdivi-1 than in those treated with the control vehicle (**Figures 7J,K**). These results suggest that excessive mitochondrial fission through Drp1 activation promotes arterial senescence in ApoE KO mice.

AT1R Inhibition Improved the Imbalance of Mitochondrial Dynamics and Induced Rab9-Dependent Mitochondrial Autophagy, Leading to Anti-vascular Senescence

Finally, we investigated whether AT1R inhibition attenuated vascular senescence by regulating mitochondrial dynamics and mitochondrial autophagy in ApoE KO mice. Food intake during the experiment, body weight, heart rate, and blood pressure were not different between ApoE KO mice treated with candesartan or the control vehicle (**Table 3**). EM revealed that excessive mitochondrial fission was reduced in ApoE KO mice treated with candesartan when compared to that in the control mice (**Figure 8A**). The arterial expression of Drp1 phosphorylation at serine 616 was lower in ApoE KO mice treated with candesartan when compared to that in the control mice. Other

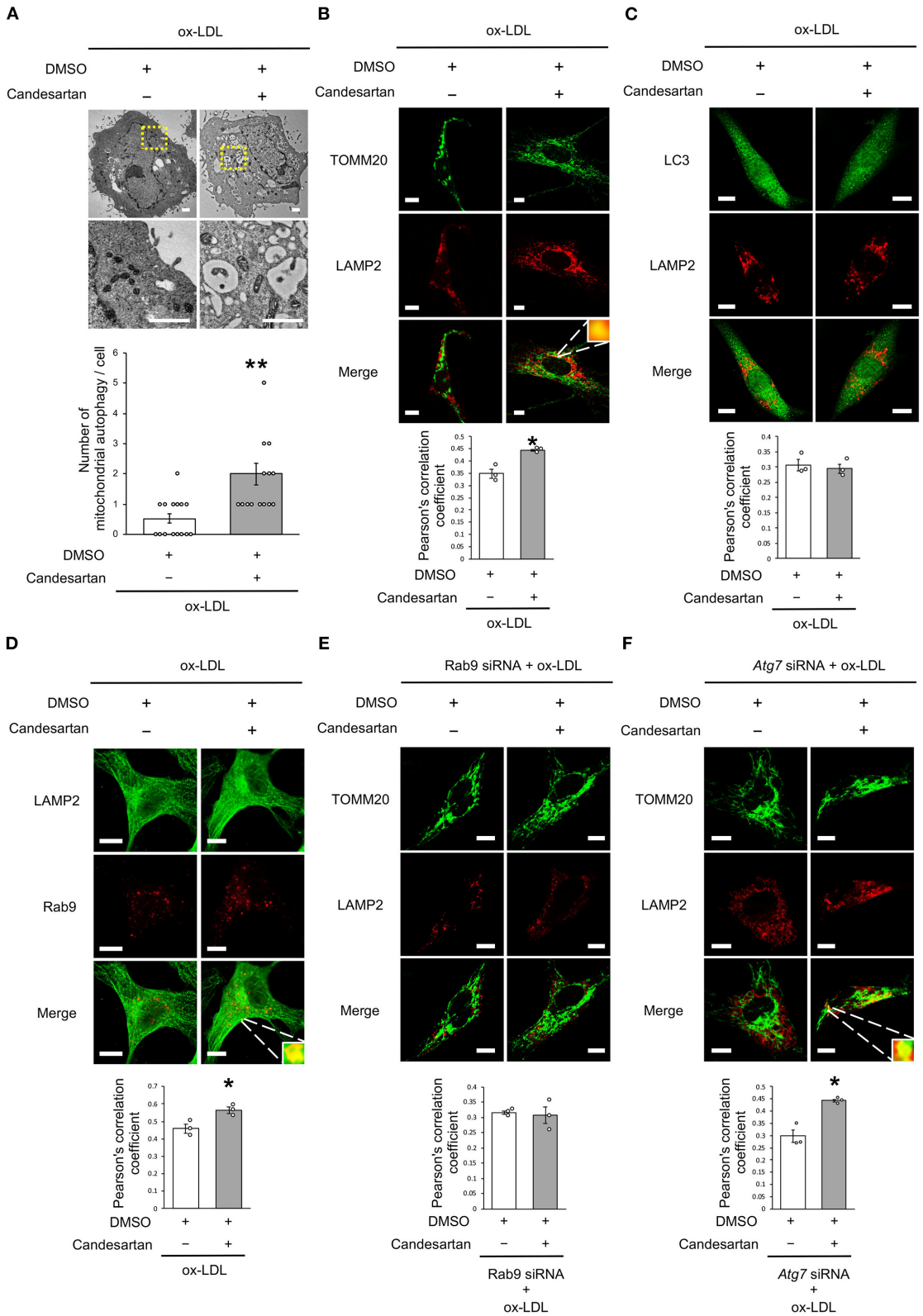

FIGURE 5 | AT1R inhibition induced mitochondrial autophagy derived from Rab9-dependent alternative autophagy with ox-LDL treatment. **(A)** Electron microscopic images and quantitative analysis of the number of mitochondrial autophagy in Candesartan-treated vs. the control cells with ox-LDL. Scale bar = 1 μm. $^{**}P < 0.01$ vs.

(Continued)

FIGURE 5 | ox-LDL with the control ($n = 15$ per group). **(B)** Representative images and quantitative analysis of TOMM20 (green) and LAMP2 (red) immunohistochemistry in Candesartan-treated vs. control cells with ox-LDL. Scale bar = 10 μm. *$P < 0.05$ vs. ox-LDL with the control ($n = 3$ per group). **(C)** Representative images and quantitative analysis of LC3 (green) and LAMP2 (red) immunohistochemistry in Candesartan-treated vs. control vehicle-treated cells with ox-LDL ($n = 3$ per group). Scale bar = 10 μm. **(D)** Representative images and quantitative analysis of LAMP2 (green) and Rab9 (red) immunohistochemistry in Candesartan-treated vs. control cells with ox-LDL. Scale bar = 10 μm. *$P < 0.05$ vs. ox-LDL with the control ($n = 3$ per group). **(E)** Representative images and quantitative analysis of TOMM20 (green) and LAMP2 (red) immunohistochemistry in Candesartan-treated vs. control cells transfected with siRab9 under ox-LDL treatment. Scale bar = 10 μm. ($n = 3$ per group). **(F)** Representative images and quantitative analysis of TOMM20 (green) and LAMP2 (red) immunohistochemistry in Candesartan-treated vs. control cells transfected with si*Atg7* under ox-LDL treatment. Scale bar = 10 μm. *$P < 0.05$ when compared with control vehicle-treated cells transfected with si*Atg7* under ox-LDL treatment ($n = 3$ per group). All data are presented as the mean ± SEM. Statistical analysis were conducted by Wilcoxon rank sum test **(B,C,E,F)** and Student's *t*-test **(A)**.

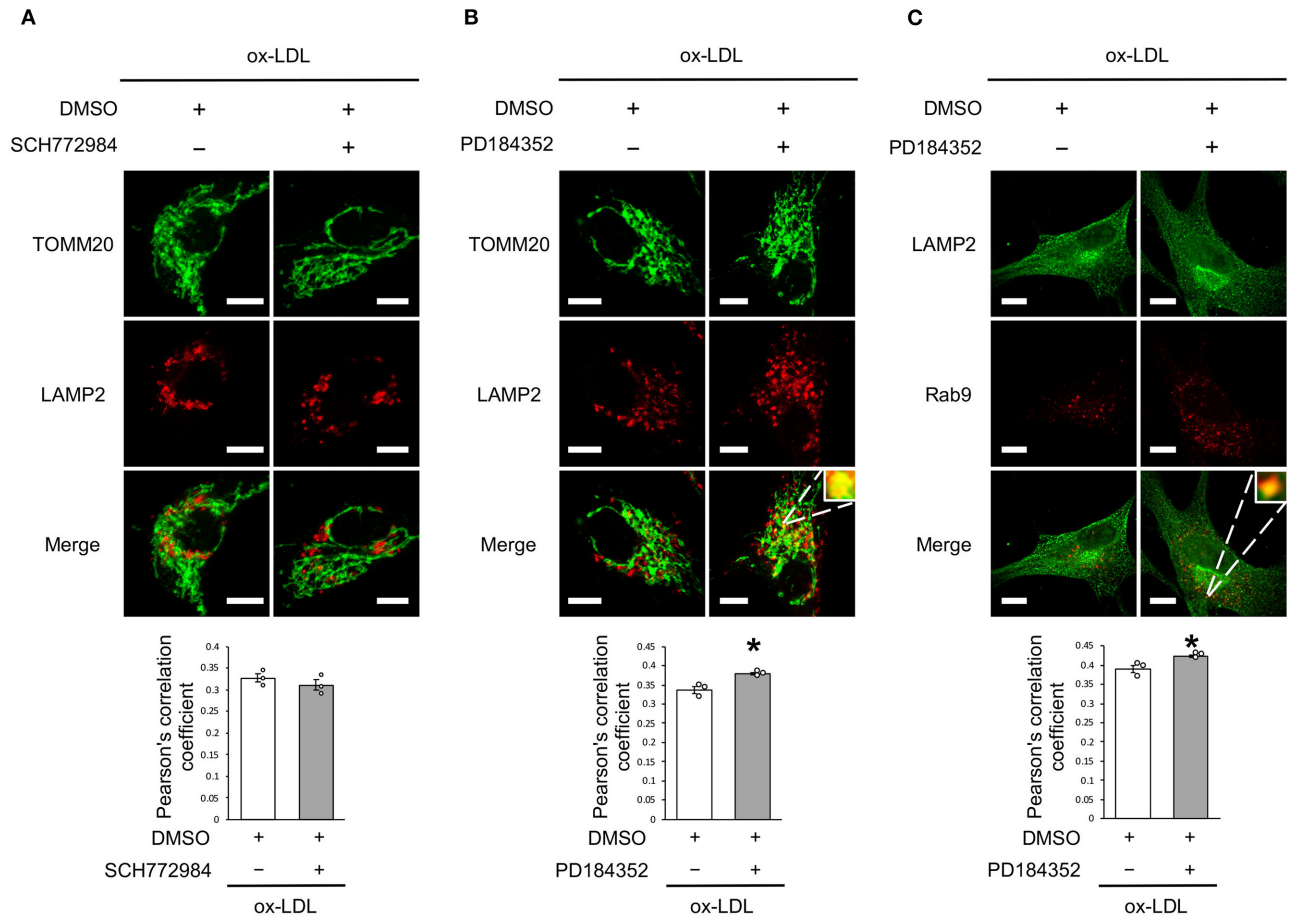

FIGURE 6 | Rab9-dependent mitochondrial autophagy was not affected by ERK inhibition but was affected by MEK inhibition. **(A)** Representative images and quantitative analysis of TOMM20 (green) and LAMP2 (red) immunohistochemistry in SCH772984-treated vs. control vehicle-treated cells with ox-LDL. Scale bar = 10 μm. ($n = 3$ per group). **(B)** Representative images and quantitative analysis of TOMM20 (green) and LAMP2 (red) immunohistochemistry in PD184352-treated vs. control vehicle-treated cells with ox-LDL. Scale bar = 10 μm. *$P < 0.05$ when compared with ox-LDL with the control ($n = 3$ per group). **(C)** Representative images and quantitative analysis of LAMP2 (green) and Rab9 (red) immunohistochemistry in PD184352-treated vs. control cells with ox-LDL. Scale bar = 10 μm. *$P < 0.05$ when compared with ox-LDL with the control ($n = 3$ per group). All data are presented as the mean ± SEM. Statistical analysis were conducted by Wilcoxon rank sum test **(A-C)**.

mitochondrial dynamics factors were not significantly different between the two groups (**Figure 8B**). H_2O_2 production was lower and ATP production was higher in ApoE KO mice administered candesartan (**Figures 8C,D**). The ratio of arterial fibrosis and the senescence area were also lower in ApoE KO mice administered with candesartan when compared with the control (**Figures 8E,F**). Immunoblot analysis showed that the expression of p53 and p21 was lower in ApoE KO mice treated with candesartan (**Figure 8G**). To examine mitochondrial autophagy induced by AT1R inhibition, we performed EM and immunohistochemistry. The number of autophagy-engulfing mitochondria was higher in ApoE KO mice administered with

TABLE 1 | Body weight, heart rate, and blood pressure of the C57BL/6 and ApoE KO mice.

	C57BL/6 (n = 18)	ApoE KO (n = 15)	*P*-value
BW (g)	32.8 ± 0.7	32.1 ± 0.5	N.S.
HR (bpm)	705 ± 11	668 ± 13	N.S.
BP (mmHg)	107 ± 4/63 ± 3	116 ± 5/71 ± 4	N.S.

All values are presented as the mean and SD. BW, body weight; HR, heart rate; BP, blood pressure.

candesartan when compared to the control (**Figure 8H**). The colocalization of LAMP2 with Rab9 or TOMM20 was also higher in ApoE KO mice treated with the ARB when compared with the control (**Figures 8I,J**). Taken together, AT1R inhibition was found to contribute to improved mitochondrial quality control through the suppression of excessive mitochondrial fission and the induction of Rab9-dependent mitochondrial autophagy, causing anti-arterial senescence in ApoE KO mice.

DISCUSSION

Our findings indicate that AT1R inhibition attenuates excessive mitochondrial fission that is induced by ox-LDL and thus augments mitochondrial autophagy, which is crucial for maintaining mitochondrial quality control and the effect of anti-senescence. In human VSMCs exposed to ox-LDL, AT1R inhibition suppresses Drp1 activation through the CRAF/MEK/ERK pathway, which is downstream of the AT1R signal, and did not induce conventional *Atg7*/LC3-dependent autophagy but Rab9-dependent alternative autophagy. The administration of candesartan to ApoE KO mice retarded excessive mitochondrial fission and induced Rab9-dependent alternative autophagy, resulting in anti-vascular senescence.

Regardless of mitochondrial dynamics, there were some reports of mitochondrial fission induced by ox-LDL or a high-fat diet in various cells or animals. Treatment with ox-LDL induces excessive mitochondrial fission in rat annulus fibrosus cells (24) and the hearts of high-fat-fed C57BL/6 mice showed mitochondrial fission (17). As shown in **Figure 4**, ox-LDL activated CRAF, MEK, and ERK. Either inhibition of CRAF, MEK, or ERK inactivated the phosphorylation of Drp1 at serine 616 induced by ox-LDL. Furthermore, AT1R inhibition suppressed the activation of CRAF, MEK, ERK, and Drp1 induced by ox-LDL. These results revealed that ox-LDL activated Drp1 through AT1R and CRAF/MEK/ERK pathway. It has been reported that Drp1 may be involved in this cascade in various cells. Ang II activates Drp1 through MEK/ERK signaling by interacting with protein kinase Cδ in rat VSMCs (25). Another study has reported that the high-mobility group box-1 activated phosphorylation of Drp1 at serine 616 through ERK in rat pulmonary artery SMCs (26). Ox-LDL was also reported to activate RAF/MEK/ERK, one of the most well-defined pathways in cancer biology, in rat VSMCs (27, 28). The signals indicated by these reports are consistent with the cascade of Drp1 activation in human VSMCs. As mentioned previously, ox-LDL upregulated ERK through receptor association with LOX-1 and AT1R (9). However, it had not been previously reported that AT1R and its downstream signal are involved in ox-LDL-induced mitochondrial fission, as we revealed in this investigation. Furthermore, there are no previous reports indicating that the association of LOX-1 and AT1R plays a role in regulating mitochondrial dynamics.

Many researchers have reported that mitochondrial fission adversely affects atherosclerosis, various cell types, and diseases. Drp1 inhibition attenuates VSMC proliferation and reduces ROS production (25). Anoxia reoxygenation activated phosphorylation of Drp1 at serine 616, which facilitated cardiomyocyte death in HL-1 cells, but was attenuated by the inhibition of cyclin dependent kinase 1 and protein kinase Cδ (29). HIF-1α activation in human pulmonary artery SMCs leads to mitochondrial fission by cyclin B1/CDK1-dependent phosphorylation of Drp1 at serine 616, resulting in pulmonary artery remodeling (30). Conversely, there are some reports that suppressing mitochondrial fission improves mitochondrial conditions. Prior to the administration of mdivi-1 to an ischemia reperfusion murine model, it had inhibited mitochondrial fission, which prevented the opening of the mitochondrial permeability transition pore and decreased infarct size (31). However, excessive suppression of fission has been reported as an adverse effect. Cardiomyocyte-specific ablation of Drp1 mice resulted in the accumulation of damaged mitochondria and left ventricular dysfunction, and finally death within 13 weeks. Under ischemia reperfusion conditions, mice treated with a high dose of mdivi-1 showed a greater degree of myocardial damage than the control mice (32). This is because excessive inhibition of mitochondrial fission suppresses mitochondrial autophagy, leading to the accumulation of damaged mitochondria. Indeed, we also found that ox-LDL treated with a high concentration of mdivi-1 increased p53 expression when compared to that in the control (data not shown). Given these results, it may be important to maintain an optimal balance between mitochondrial fission and fusion.

There have been some reports on the relationship between RAS signaling and autophagy in various cells and animals. However, all these studies have shown that Ang II induced conventional autophagy and its inhibition by AT1R inhibition provided beneficial protective effects on the cardiovascular system. In addition, there have been no reports examining the relationship between RAS signaling and alternative autophagy. Ang II increased LC3-II expression in rat VSMCs, resulting in decreased apoptosis (33). Another study revealed that Ang II induced LC3-depenent autophagy through AT1R/RhoA/Rho kinase, leading to hypertrophy, and ARB reduced autophagy (34). In human umbilical vein endothelial cells, Ang II induces *Atg5*-dependent autophagy via AT1R and decreases nitric oxide production, leading to dysfunction of human umbilical vein endothelial cells (35). For mitochondrial autophagy, one study reported that the renovascular hypertension model for domestic pigs improved left ventricular hypertrophy by reducing the myocardial LC3-II/LC3-I ratio and colocalization of Parkin

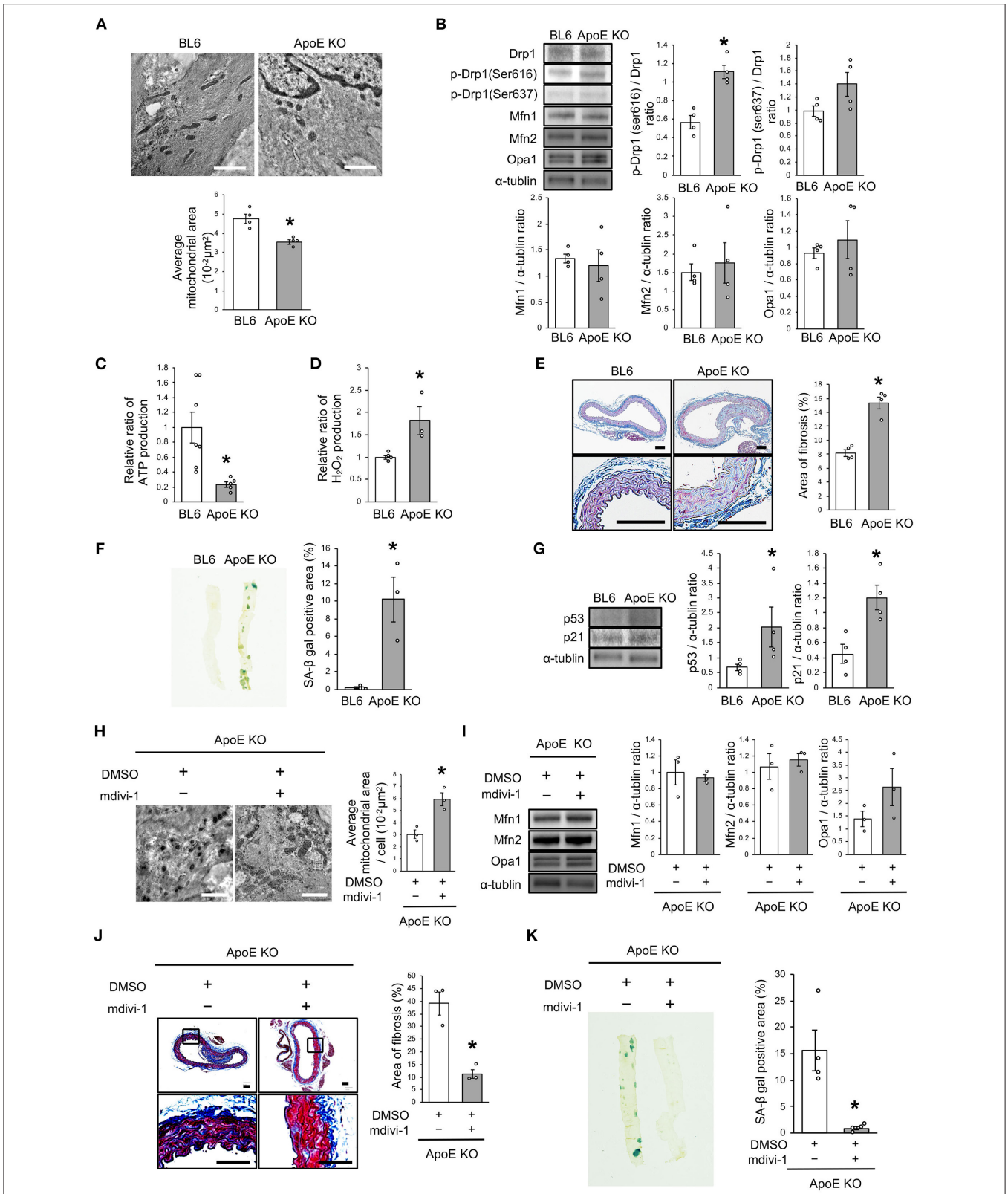

FIGURE 7 | Drp1 inhibition improved the imbalance of excessive mitochondrial fission and vascular senescence in ApoE KO mice. **(A)** Electron microscopic images and quantitative analysis of mitochondria and average mitochondrial areas in C57BL/6 and ApoE KO mice. Scale bar = 1 μm. *$P < 0.05$ vs. C57BL/6 ($n = 4$ per

(Continued)

FIGURE 7 | group). **(B)** Immunoblots and quantitative analysis for Drp1, p-Drp1 (Ser616), p-Drp1 (Ser637), Mfn1, Mfn2, Opa1, and α-tublin in C57BL/6 and ApoE KO mice. *$P < 0.05$ vs. C57BL/6 ($n = 4$ per group). **(C)** Relative mitochondrial ATP production in C57BL/6 and ApoE KO mice. *$P < 0.05$ vs. C57BL/6 (C57BL/6; $n = 7$, ApoE KO mice; $n = 5$). **(D)** Relative mitochondrial H_2O_2 production in C57BL/6 and ApoE KO mice. *$P < 0.05$ vs. C57BL/6 ($n = 4$ per group). **(E)** Representative images and quantitative analysis of Masson's trichrome staining in C57BL/6 and ApoE KO mice. Scale bar = 100 μm. *$P < 0.05$ vs. C57BL/6 ($n = 4$ per group). **(F)** Representative images and quantitative analysis of SA-β gal staining of arteries in C57BL/6 and ApoE KO mice. *$P < 0.05$ vs. C57BL/6 ($n = 3$ per group). **(G)** Immunoblots and quantitative analysis for p53, p21, and α-tublin in C57BL/6 and ApoE KO mice. *$P < 0.05$ vs. C57BL/6 ($n = 4$ per group). **(H)** Electron microscopic images and quantitative analysis of mitochondria and average mitochondrial areas in ApoE KO mice treated with mdivi-1 or the control. Scale bar = 1 μm. *$P < 0.05$ vs. ApoE KO mice with the control ($n = 3$ per group). **(I)** Immunoblots and quantitative analysis for Mfn1, Mfn2, Opa1, and α-tublin in ApoE KO mice treated with mdivi-1 or the control, ($n = 3$ per group). **(J)** Representative images and quantitative analysis of Masson's trichrome staining in ApoE KO mice treated with mdivi-1 or the control. Scale bar = 100 μm. *$P < 0.05$ vs. ApoE KO mice with the control ($n = 3$ per group). **(K)** Representative images and quantitative analysis of SA-β gal staining of the arteries in ApoE KO mice treated with mdivi-1 or the control. *$P < 0.05$ vs. ApoE KO mice with the control ($n = 3$ per group). All data are presented as the mean ± SEM. Statistical analysis were conducted by Wilcoxon rank sum test **(A,B,D-K)** and Student's *t*-test **(C)**.

TABLE 2 | Body weight, food intake, heart rate, and blood pressure of ApoE KO mice administered with mdivi-1 or the control vehicle.

	ApoE KO + control vehicle ($n = 7$)	ApoE KO + mdivi-1 ($n = 7$)	*P*-value
BW (g)	31.9 ± 1.3	31.4 ± 2.5	N.S.
FI (g/day)	3.7 ± 0.3	3.7 ± 0.4	N.S.
HR (bpm)	692 ± 35	657 ± 72	N.S.
BP (mmHg)	113 ± 18/76 ± 9	118 ± 16/72 ± 22	N.S.

All values are presented as the mean and SD. BW, body weight; FI, food intake; HR, heart rate; BP, blood pressure.

TABLE 3 | Body weight, food intake, heart rate, and blood pressure of ApoE KO mice administered with Candesartan or the control vehicle.

	ApoE KO + control vehicle ($n = 13$)	ApoE KO + Candesartan ($n = 14$)	*P*-value
BW (g)	29.3 ± 1.7	28.7 ± 2.5	N.S.
FI (g/day)	3.9 ± 0.2	4.0 ± 0.3	N.S.
HR (bpm)	680 ± 41	707 ± 15	N.S.
BP (mmHg)	117 ± 17/77 ± 13	113 ± 13/74 ± 17	N.S.

All values are presented as the mean and SD. BW, body weight; FI, food intake; HR, heart rate; BP, blood pressure.

and Tomm20, suggesting that ARB suppressed LC3-dependent mitochondrial autophagy (36).

There are two forms of autophagy, as mentioned above: LC3-dependent autophagy and Rab9-dependent autophagy (21, 23, 37). Since we have recently demonstrated that Rab9-dependent alternative autophagy causes estrogen-mediated mitochondrial autophagy through the SIRT1/LKB1/AMPK/Ulk1 pathway (21), we examined which type of autophagy AT1R-induced mitochondrial autophagy contributes to. As shown in **Figure 5**, the colocalization of LAMP2-Rab9 signals and the number of autophagosome-engulfed mitochondria in VSMCs was increased by AT1R inhibition treated with ox-LDL. It is noteworthy that this phenotype was affected by the knockdown of Rab9 and was not diminished after the silencing of *Atg7*, which is essential for inducing LC3-dependent conventional autophagy, suggesting that AT1R inhibition in VSMCs exposed to ox-LDL induces *Atg7*-independent and Rab9-dependent alternative autophagy. One study reported that ox-LDL treatment increased with the colocalization of LC3-TOMM20 and this colocalization was decreased by 3-methyladenine treatment, an inhibitor of conventional autophagy, suggesting that ox-LDL induced LC3-dependent mitochondrial autophagy. However, ox-LDL reduces mitochondrial function and generates ROS. This is because mitochondria impaired by ox-LDL cannot be eliminated by ox-LDL-mediated physiological mitochondrial autophagy (38). Since AT1R inhibition attenuated mitochondrial dysfunction and ROS production, AT1R inhibition regulated mitochondrial autophagy derived from Rab9-dependent alternative autophagy is crucial to sustain mitochondrial quality control in VSMCs.

Although it is generally believed that mitochondrial autophagy requires fission, we revealed that AT1R inhibition simultaneously induces mitochondrial fusion and mitochondrial autophagy. This is because AT1R inhibition did not physiologically suppress mitochondrial fission in our experiment. Indeed, as assessed by EM and Mitotracker, AT1R inhibition did not force the proportion of the cells to have excessive mitochondrial fusion, but decreased the number of cells with excessive mitochondrial fission induced by ox-LDL. Moreover, it has been reported that the amount of mitochondrial autophagy decreases with hepatocyte-specific deletion in Drp1 mice, whereas mitochondrial autophagy occurs in Drp1-Opa1 double knockout mice, indicating that fission is not necessarily required for the induction of mitochondrial autophagy (39). A previous study reported that either statin or ARB had a mild inhibitory effect on LOX-1 expression, and the combination of statin and ARB inhibited LOX-1 completely in the arteries of ApoE KO mice fed a high fat diet (10). Given this report and our findings, AT1R inhibition using ARB is the potential key therapy and combined use of statin with ARB could facilitate to improve residual risk from lipid-lowering therapies through mitochondrial quality control in CVD patients.

Here, we have revealed for the first time that AT1R inhibition attenuates cellular senescence by regulating mitochondrial dynamics and inducing Rab9-dependent alternative autophagy through the CRAF/MEK/ERK axis in terms of mitochondrial quality control in human VSMCs (**Figure 9**). We hope that these findings will help to retard vascular senescence and contribute to the development of a method by which to reduce residual risk of CVD.

FIGURE 8 | AT1R inhibition improved the imbalance of excessive mitochondrial fission and induced Rab9-dependent mitochondrial autophagy, leading to anti-vascular senescence. **(A)** Electron microscopic images and quantitative analysis of mitochondria and average mitochondrial areas in ApoE KO mice treated with

(Continued)

FIGURE 8 | Candesartan or the control. Scale bar = 1 μm. *$P < 0.05$ vs. ApoE KO mice with the control ($n = 3$ per group). **(B)** Immunoblots and quantitative analysis for Drp1, p-Drp1 (Ser616), p-Drp1 (Ser637), Mfn1, Mfn2, Opa1, and α-tublin in ApoE KO mice treated with Candesartan or the control. *$P < 0.05$ vs. ApoE KO mice with vehicle ($n = 3$ per group). **(C)** Relative mitochondrial H_2O_2 production in ApoE KO mice treated with Candesartan or the control. *$P < 0.05$ vs. ApoE KO mice with the control ($n = 3$ per group). **(D)** Relative mitochondrial ATP production in ApoE KO mice treated with Candesartan or the control. *$P < 0.05$ vs. ApoE KO mice with the control (ApoE KO mice with Candesartan; $n = 5$, ApoE KO mice with the control; $n = 3$). **(E)** Representative images and quantitative analysis of Masson's trichrome staining in ApoE KO mice treated with Candesartan or the control. Scale bar = 100 μm. *$P < 0.05$ vs. ApoE KO mice with the control ($n = 3$ per group). **(F)** Representative images and quantitative analysis of SA-β gal staining of arteries in ApoE KO mice treated with Candesartan or the control. *$P < 0.05$ vs. ApoE KO mice with the control vehicle (ApoE KO mice with Candesartan; $n = 3$, ApoE KO mice with the control; $n = 4$). **(G)** Immunoblots and quantitative analysis for p53, p21, and β-actin in ApoE KO mice with Candesartan or the control. *$P < 0.05$ vs. ApoE KO mice with the control ($n = 3$ per group). **(H)** Electron microscopic images of mitochondrial autophagy in ApoE KO mice treated with Candesartan or the control. Scale bar = 1 μm. **$P < 0.01$ vs. ApoE KO mice with the control ($n = 14$ per group). **(I)** Representative images of TOMM20 (green) and LAMP2 (red) immunohistochemistry in ApoE KO mice treated with Candesartan or the control. Scale bar = 10 μm. *$P < 0.05$ vs. ApoE KO mice with the control ($n = 3$ per group). **(J)** Representative images and quantitative analysis of LAMP2 (green) and Rab9 (red) immunohistochemistry in the ApoE KO mice treated with Candesartan or the control. Scale bar = 10 μm. *$P < 0.05$ vs. ApoE KO mice with the control ($n = 3$ per group). All Data are presented as the mean ± SEM. Statistical analysis were conducted by Wilcoxon rank sum test **(A-G,I,J)** and Student's *t*-test **(H)**.

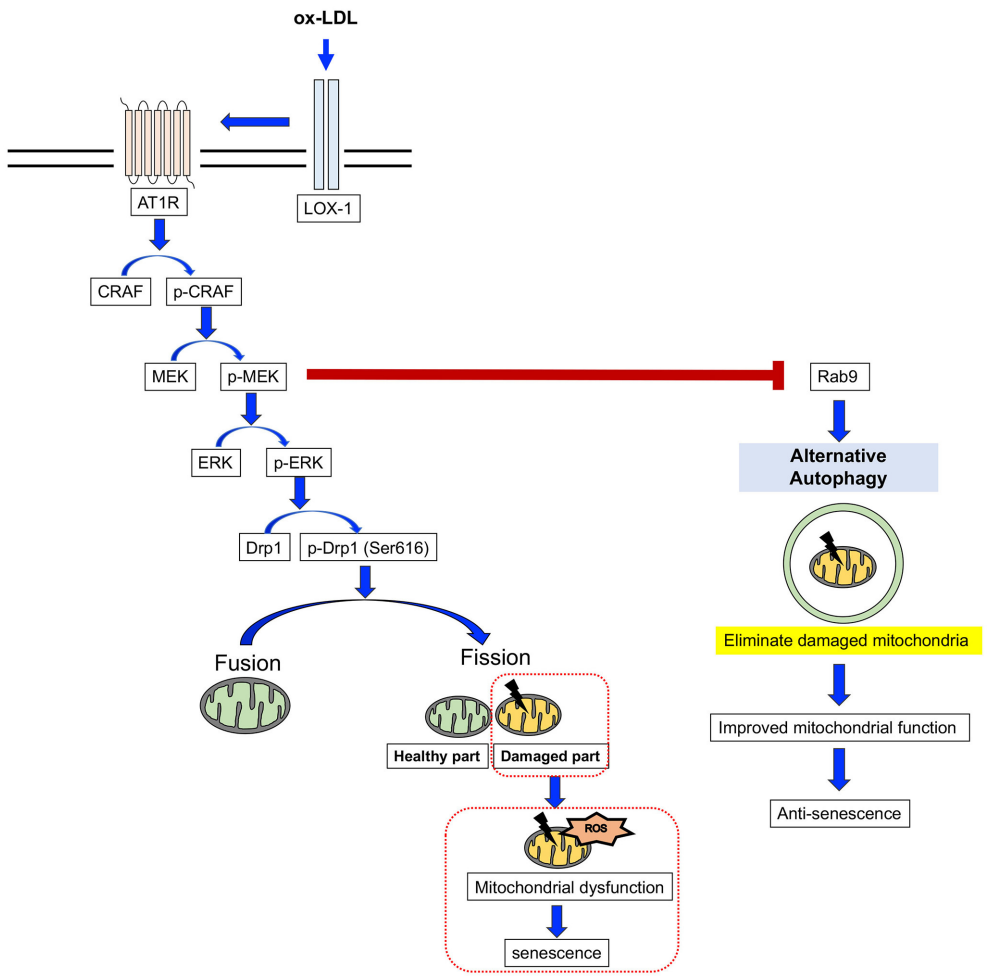

FIGURE 9 | The mechanism for the AT1R inhibition of anti-senescence through mitochondrial quality control. ox-LDL induced mitochondrial fission through the association of LOX-1 and AT1R and the CRAF/MEK/ERK pathway, resulting in mitochondrial dysfunction and senescence. AT1R inhibition attenuated senescence by suppression of this cascade and induced Rab9-dependent alternative autophagy through the CRAF/MEK axis and aspects of the mitochondrial quality control process in human VSMCs.

Limitations

Despite the promising nature of our results, there were some acknowledged limitations in this study. First, we did not conduct *in vivo* experiments for arterial-specific loss of function of Rab9 or Drp1 conditional knockout mice. Second, we did not determine the precise mechanisms of mitochondrial autophagy induced by AT1R inhibition. In particular, in the future we should aim to determine how

Rab9-dependent alternative autophagy recognizes impaired mitochondria in a PINK1-Parkin pathway-independent manner. Further studies are thus required to confirm the role of mitochondrial autophagy.

DATA AVAILABILITY STATEMENT

The raw data supporting the conclusions of this article will be made available by the authors, without undue reservation.

ETHICS STATEMENT

The animal study was reviewed and approved by The Faculty of Medicine at Kagoshima University.

AUTHOR CONTRIBUTIONS

YU performed most of the experiments, analyzed the data, interpreted the results, and wrote the manuscript. YI designed the study, interpreted the results, and edited the manuscript. YS and MI performed the experiments and analyzed the data. YA provided project resources. MO designed and supervised the study, interpreted the results, and provided the project resources. All authors have approved the submitted version of the manuscript.

FUNDING

This work was supported by the Japan Society for the Promotion of Science KAKENHI (Grant Nos. JP19K07891 and JP21K15649).

ACKNOWLEDGMENTS

We thank Ms. Ayako Shiokawa and Ms. Aya Yanagi for their excellent technical assistance and all the staff members of the Institute of Laboratory Animal Science, Kagoshima University (Frontier Science Research Center), who maintained the animals in good condition. We also thank the Joint Research Laboratory, Kagoshima University Graduate School of Medical and Dental Science for the use of their facilities. We would also like to thank Editage for English language editing.

SUPPLEMENTARY MATERIAL

The Supplementary Material for this article can be found online at: https://www.frontiersin.org/articles/10.3389/fcvm.2021.788655/full#supplementary-material

REFERENCES

1. Matthews C, Gorenne I, Scott S, Figg N, Kirkpatrick P, Ritchie A, et al. Vascular smooth muscle cells undergo telomere-based senescence in human atherosclerosis: effects of telomerase and oxidative stress. *Circ Res*. (2006) 99:156–64. doi: 10.1161/01.RES.0000233315.38086.bc
2. Rosenson RS. Statins: can the new generation make an impression? *Expert Opin Emerg Drugs*. (2004) 9:269–79. doi: 10.1517/14728214.9.2.269
3. LaRosa JC, Grundy SM, Waters DD, Shear C, Barter P, Fruchart JC, et al. Intensive lipid lowering with atorvastatin in patients with stable coronary disease. *N Engl J Med*. (2005) 352:1425–35. doi: 10.1056/NEJMoa050461
4. Ridker PM, Danielson E, Fonseca FA, Genest J, Gotto AM Jr, Kastelein JJ, et al. Rosuvastatin to prevent vascular events in men and women with elevated C-reactive protein. *N Engl J Med*. (2008) 359:2195–207. doi: 10.1056/NEJMoa0807646
5. Nicholls SJ, Ballantyne CM, Barter PJ, Chapman MJ, Erbel RM, Libby P, et al. Effect of two intensive statin regimens on progression of coronary disease. *N Engl J Med*. (2011) 365:2078–87. doi: 10.1056/NEJMoa1110874
6. Wang X, Phillips MI, Mehta JL. LOX-1 and angiotensin receptors, and their interplay. *Cardiovasc Drugs Ther*. (2011) 25:401–17. doi: 10.1007/s10557-011-6331-7
7. Yamamoto K, Kakino A, Takeshita H, Hayashi N, Li L, Nakano A, et al. Oxidized LDL (oxLDL) activates the angiotensin II type 1 receptor by binding to the lectin-like oxLDL receptor. *FASEB J*. (2015) 29:3342–56. doi: 10.1096/fj.15-271627
8. Kunieda T, Minamino T, Nishi J, Tateno K, Oyama T, Katsuno T, et al. Angiotensin II induces premature senescence of vascular smooth muscle cells and accelerates the development of atherosclerosis via a p21-dependent pathway. *Circulation*. (2006) 114:953–60. doi: 10.1161/CIRCULATIONAHA.106.626606
9. Min LJ, Mogi M, Iwanami J, Li JM, Sakata A, Fujita T, et al. Cross-talk between aldosterone and angiotensin II in vascular smooth muscle cell senescence. *Cardiovasc Res*. (2007) 76:506–16. doi: 10.1016/j.cardiores.2007.07.008
10. Chen J, Li D, Schaefer R, Mehta JL. Cross-talk between dyslipidemia and renin-angiotensin system and the role of LOX-1 and MAPK in atherogenesis studies with the combined use of rosuvastatin and candesartan. *Atherosclerosis*. (2006) 184:295–301. doi: 10.1016/j.atherosclerosis.2005.04.016
11. Ito Y, Maejima Y, Tamura N, Shiheido-Watanabe Y, Konishi M, Ashikaga T, et al. Synergistic effect of combined HMG-CoA reductase inhibitor and angiotensin-II receptor blocker therapy in patients with chronic heart failure: the HF-COSTAR trial. *Circ J*. (2011) 75:589–95. doi: 10.1253/circj.CJ-10-0804
12. Ikeda Y, Shirakabe A, Brady C, Zablocki D, Ohishi M, Sadoshima J. Molecular mechanisms mediating mitochondrial dynamics and mitophagy and their functional roles in the cardiovascular system. *J Mol Cell Cardiol*. (2015) 78:116–22. doi: 10.1016/j.yjmcc.2014.09.019
13. Frank S, Gaume B, Bergmann-Leitner ES, Leitner WW, Robert EG, Catez F, et al. The role of dynamin-related protein 1, a mediator of mitochondrial fission, in apoptosis. *Dev Cell*. (2001) 1:515–25. doi: 10.1016/S1534-5807(01)00055-7
14. Santel A, Fuller MT. Control of mitochondrial morphology by a human mitofusin. *J Cell Sci*. (2001) 114:867–74. doi: 10.1242/jcs.114.5.867
15. Cipolat S, Martins de Brito O, Dal Zilio B, Scorrano L. OPA1 requires mitofusin 1 to promote mitochondrial fusion. *Proc Natl Acad Sci USA*. (2004) 101:15927–32. doi: 10.1073/pnas.0407043101
16. Benigni A, Corna D, Zoja C, Sonzogni A, Latini R, Salio M, et al. Disruption of the Ang II type 1 receptor promotes longevity in mice. *J Clin Invest*. (2009) 119:524–30. doi: 10.1172/JCI36703
17. Zheng P, Ding Y, Lu F, Liu N, Wu H, Bian Z, et al. Atorvastatin reverses high cholesterol-induced cardiac remodelling and regulates mitochondrial quality-control in a cholesterol-independent manner: An experimental study. *Clin Exp Pharmacol Physiol*. (2021) 48:1150–61. doi: 10.1111/1440-1681.13507
18. Sasaki Y, Ikeda Y, Miyauchi T, Uchikado Y, Akasaki Y, Ohishi M. Estrogen-SIRT1 axis plays a pivotal role in protecting arteries against menopause-induced senescence and atherosclerosis. *J Atheroscler Thromb*. (2020) 27:47–59. doi: 10.5551/jat.47993

19. Shao JQ, Iwashita N, Du H, Wang YT, Wang YY, Zhao M, et al. Angiotensin II receptor blocker provides pancreatic β-cell protection independent of blood pressure lowering in diabetic db/db mice. *Acta Pharmacol Sin*. (2007) 28:246–57. doi: 10.1111/j.1745-7254.2007.00492.x
20. Yang HJ, Kong B, Shuai W, Zhang J, Huang H. MD1 deletion exaggerates cardiomyocyte autophagy induced by heart failure with preserved ejection fraction through ROS/MAPK signalling pathway. *J Cell Mol Med*. (2020) 24:9300–12. doi: 10.1111/jcmm.15579
21. Sasaki Y, Ikeda Y, Uchikado Y, Akasaki Y, Sadoshima J, Ohishi M. Estrogen plays a crucial role in Rab9-dependent mitochondrial autophagy, delaying arterial senescence. *J Am Heart Assoc*. (2021) 10:e019310. doi: 10.1161/JAHA.120.019310
22. Zinchuk V, Zinchuk O, Okada T. Quantitative colocalization analysis of multicolor confocal immunofluorescence microscopy images: pushing pixels to explore biological phenomena. *Acta Histochem Cytochem*. (2007) 40:101–11. doi: 10.1267/ahc.07002
23. Nishida Y, Arakawa S, Fujitani K, Yamaguchi H, Mizuta T, Kanaseki T, et al. Discovery of Atg5/Atg7-independent alternative macroautophagy. *Nature*. (2009) 461:654–8. doi: 10.1038/nature08455
24. Wu W, Jing D, Huang X, Yang W, Shao Z. Drp1-mediated mitochondrial fission is involved in oxidized low-density lipoprotein-induced AF cell apoptosis. *J Orthop Res*. (2021) 39:1496–504. doi: 10.1002/jor.24828
25. Lim S, Lee SY, Seo HH, Ham O, Lee C, Park JH, et al. Regulation of mitochondrial morphology by positive feedback interaction between PKCδ and Drp1 in vascular smooth muscle cell. *J Cell Biochem*. (2015) 116:648–60. doi: 10.1002/jcb.25016
26. Feng W, Wang J, Yan X, Zhang Q, Chai L, Wang Q, et al. ERK/Drp1-dependent mitochondrial fission contributes to HMGB1-induced autophagy in pulmonary arterial hypertension. *Cell Prolif*. (2021) 54:e13048. doi: 10.1111/cpr.13048
27. Yang CM, Chien CS, Hsiao LD, Pan SL, Wang CC, Chiu CT, et al. Mitogenic effect of oxidized low-density lipoprotein on vascular smooth muscle cells mediated by activation of Raf/MEK/MAPK pathway. *Br J Pharmacol*. (2001) 132:1531–41. doi: 10.1038/sj.bjp.0703976
28. McCubrey JA, Steelman LS, Chappell WH, Abrams SL, Wong EW, Chang F, et al. Roles of the Raf/MEK/ERK pathway in cell growth, malignant transformation and drug resistance. *Biochim Biophys Acta*. (2007) 1773:1263–84. doi: 10.1016/j.bbamcr.2006.10.001
29. Zaja I, Bai X, Liu Y, Kikuchi C, Dosenovic S, Yan Y, et al. Cdk1, PKCδ and calcineurin-mediated Drp1 pathway contributes to mitochondrial fission-induced cardiomyocyte death. *Biochem Biophys Res Commun*. (2014) 453:710–21. doi: 10.1016/j.bbrc.2014.09.144
30. Marsboom G, Toth PT, Ryan JJ, Hong Z, Wu X, Fang YH, et al. Dynamin-related protein 1 (DRP1)-mediated mitochondrial mitotic fission permits hyperproliferation of vascular smooth muscle cells and offers a novel therapeutic target in pulmonary hypertension. *Circ Res*. (2012) 110:1484–97. doi: 10.1161/CIRCRESAHA.111.263848
31. Ong SB, Subrayan S, Lim SY, Yellon DM, Davidson SM, Hausenloy DJ. Inhibiting mitochondrial fission protects the heart against ischemia/reperfusion injury. *Circulation*. (2010) 121:2012–22. doi: 10.1161/CIRCULATIONAHA.109.906610
32. Ikeda Y, Shirakabe A, Maejima Y, Zhai P, Sciarretta S, Toli J, et al. Endogenous Drp1 mediates mitochondrial autophagy and protects the heart against energy stress. *Circ Res*. (2015) 116:264–78. doi: 10.1161/CIRCRESAHA.116.303356
33. Lu J, Shan J, Liu N, Ding Y, Wang P. Tanshinone IIA can inhibit angiotensin II-induced proliferation and autophagy of vascular smooth muscle cells via regulating the MAPK signaling pathway. *Biol Pharm Bull*. (2019) 42:1783–8. doi: 10.1248/bpb.b19-00053
34. Mondaca-Ruff D, Riquelme JA, Quiroga C, Norambuena-Soto I, Sanhueza-Olivares F, Villar-Fincheira P, et al. Angiotensin II-regulated autophagy is required for vascular smooth muscle cell hypertrophy. *Front Pharmacol*. (2019) 9:1553. doi: 10.3389/fphar.2018.01553
35. Liu D, Sun WP, Chen JW, Jiang Y, Xue R, Wang LH, et al. Autophagy contributes to angiotensin II induced dysfunction of HUVECs. *Clin Exp Hypertens*. (2021) 43:462–73. doi: 10.1080/10641963.2021.1901110
36. Zhang X, Li ZL, Crane JA, Jordan KL, Pawar AS, Textor SC, et al. Valsartan regulates myocardial autophagy and mitochondrial turnover in experimental hypertension. *Hypertension*. (2014) 64:87–93. doi: 10.1161/HYPERTENSIONAHA.113.02151
37. Saito T, Nah J, Oka SI, Mukai R, Monden Y, Maejima Y, et al. An alternative mitophagy pathway mediated by Rab9 protects the heart against ischemia. *J Clin Invest*. (2019) 129:802-19. doi: 10.1172/JCI122035
38. Swiader A, Nahapetyan H, Faccini J, D'Angelo R, Mucher E, Elbaz M, et al. Mitophagy acts as a safeguard mechanism against human vascular smooth muscle cell apoptosis induced by atherogenic lipids. *Oncotarget*. (2016) 7:28821–35. doi: 10.18632/oncotarget.8936
39. Yamada T, Murata D, Adachi Y, Itoh K, Kameoka S, Igarashi A, et al. Mitochondrial stasis reveals p62-mediated ubiquitination in parkin-independent mitophagy and mitigates nonalcoholic fatty liver disease. *Cell Metab*. (2018) 28:588–604.e5. doi: 10.1016/j.cmet.2018.06.014

Conflict of Interest: YI is a member of the Editorial Team of *Frontiers in Cardiovascular Medicine*, and MO is a member of the Editorial Team of *Circulation Journal*.

The remaining authors declare that the research was conducted in the absence of any commercial or financial relationships that could be construed as a potential conflict of interest.

Publisher's Note: All claims expressed in this article are solely those of the authors and do not necessarily represent those of their affiliated organizations, or those of the publisher, the editors and the reviewers. Any product that may be evaluated in this article, or claim that may be made by its manufacturer, is not guaranteed or endorsed by the publisher.

Copyright © 2021 Uchikado, Ikeda, Sasaki, Iwabayashi, Akasaki and Ohishi. This is an open-access article distributed under the terms of the Creative Commons Attribution License (CC BY). The use, distribution or reproduction in other forums is permitted, provided the original author(s) and the copyright owner(s) are credited and that the original publication in this journal is cited, in accordance with accepted academic practice. No use, distribution or reproduction is permitted which does not comply with these terms.

frontiers in Cardiovascular Medicine

MINI REVIEW
published: 26 November 2021
doi: 10.3389/fcvm.2021.774619

New Insights Into the Role of Mitochondria Quality Control in Ischemic Heart Disease

Yanguo Xin[1†], Xiaodong Zhang[2,3†], Jingye Li[1], Hui Gao[1], Jiayu Li[1], Junli Li[4], Wenyu Hu[5] and Hongwei Li[1,6,7*]*

[1] Department of Cardiology, Cardiovascular Center, Beijing Friendship Hospital, Capital Medical University, Beijing, China, [2] General Surgery Department, Beijing Friendship Hospital, Capital Medical University, Beijing, China, [3] National Clinical Research Center for Digestive Diseases, Beijing, China, [4] Laboratory of Heart Valve Disease, West China Hospital, Sichuan University, Chengdu, China, [5] Department of Cardiology, The First Affiliated Hospital of China Medical University, Shenyang, China, [6] Beijing Key Laboratory of Metabolic Disorder Related Cardiovascular Disease, Beijing, China, [7] Department of Geriatrics, Cardiovascular Center, Beijing Friendship Hospital, Capital Medical University, Beijing, China

OPEN ACCESS

Edited by:
Jian Wu,
Fudan University, China

Reviewed by:
Xu Chen,
University of Mississippi Medical Center, United States
Yasuhiro Maejima,
Tokyo Medical and Dental University, Japan

***Correspondence:**
Hongwei Li
lhw19656@sina.com
Wenyu Hu
huwen0320@163.com

[†] These authors have contributed equally to this work

Specialty section:
This article was submitted to Cardiovascular Metabolism, a section of the journal Frontiers in Cardiovascular Medicine

Received: 12 September 2021
Accepted: 09 November 2021
Published: 26 November 2021

Citation:
Xin Y, Zhang X, Li J, Gao H, Li J, Li J, Hu W and Li H (2021) New Insights Into the Role of Mitochondria Quality Control in Ischemic Heart Disease. Front. Cardiovasc. Med. 8:774619. doi: 10.3389/fcvm.2021.774619

IHD is a significant cause of mortality and morbidity worldwide. In the acute phase, it's demonstrated as myocardial infarction and ischemia-reperfusion injury, while in the chronic stage, the ischemic heart is mainly characterised by adverse myocardial remodelling. Although interventions such as thrombolysis and percutaneous coronary intervention could reduce the death risk of these patients, the underlying cellular and molecular mechanisms need more exploration. Mitochondria are crucial to maintain the physiological function of the heart. During IHD, mitochondrial dysfunction results in the pathogenesis of ischemic heart disease. Ischemia drives mitochondrial damage not only due to energy deprivation, but also to other aspects such as mitochondrial dynamics, mitochondria-related inflammation, etc. Given the critical roles of mitochondrial quality control in the pathological process of ischemic heart disease, in this review, we will summarise the efforts in targeting mitochondria (such as mitophagy, mtROS, and mitochondria-related inflammation) on IHD. In addition, we will briefly revisit the emerging therapeutic targets in this field.

Keywords: mitochondria, myocardial infarction, metabolism, remodelling, inflammation

INTRODUCTION

AMI is myocardial necrosis due to acute obstruction of a coronary artery or induced hypoperfusion of myocardial tissue, which is attributed to millions of deaths worldwide every year. The longer duration of ischemia usually leads to much more severe myocardial damage. Therefore, timely reestablishment of blood flow is the critical factor for rescuing the ischemic tissue. However, another form of strike, called IRI is also responsible for local damage (1, 2) (**Figure 1**). According to previous evidence, IRI describes tissue ischemia with inadequate oxygen supply after successful reperfusion of the culprit artery. Currently, there are no efficient strategies to prevent the damage caused by IRI (3). Thus, more explorations of the underlying molecular mechanisms are urgent to foster the identification of novel agents to improve outcomes following MI or IRI.

Adverse myocardial remodelling is a significant feature of acute myocardial infarction, characterised by various gradual changes of left ventricular morphology, such as infarcted zone

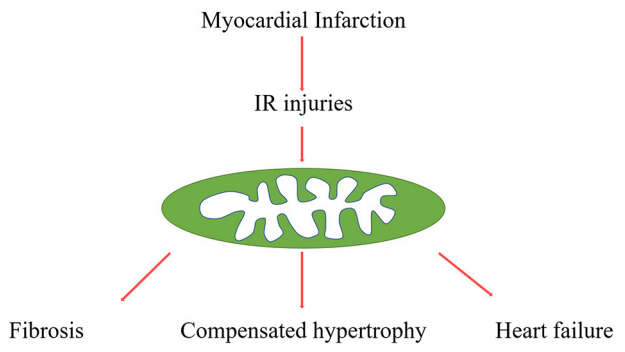

FIGURE 1 | Procedures from myocardial infarction to post-infarction remodelling. Myocardial infarction and reperfusion attributed mitochondria damage, mitochondria function, and structure disorders are involved in various pathophysiological processes, such as cardiac fibrosis, compensated hypertrophy, and final heart failure.

expansion and chamber dilatation. HF is the end stage of myocardial remodelling after AMI. It's diagnosed in ∼13% of patients at 30 days and 20–30% at 1 year after discharge for MI (4, 5) (**Figure 1**). In addition, accumulated evidence indicated that myocardial inflammation and myocardial fibroblasts play critical roles in the process of cardiac repairment after AMI, but excessive inflammation and fibrosis also lead to cardiac remodelling (6, 7). Cardiac fibrosis has been an independent risk factor in HF, which attributed HF patients to sudden cardiac death and increased overall mortality independently of the ejection fraction (8). Although various studies focus on the underlying mechanisms of this pathological process, there are still many unsolved problems in this field, and there are no effective strategies to reverse this process.

Mitochondria is the energy house of cardiomyocytes, generating ATP to maintain normal heart contractile function (9). Mitochondria metabolic dysfunction is a key characteristic of ischemic heart disease. In addition, with more studies focusing on mitochondria, it's reported that mitochondria is not only an energy organelle, but also closely connected with apoptosis (10), ROS generation (11–13), lipid metabolism (14–16), and inflammation (17). All these mechanisms contribute to acute phase and post-infarction remodelling (18). In this review, we discuss the roles of mitochondria in the pathological of ischemic heart disease and the potential in translating mito-protective strategies into the clinical setting.

MITOCHONDRIAL REMODELLING IN ISCHEMIC HEART DISEASE

Mitochondrial remodelling in ischemic heart disease includes structural and metabolic changes, both of which are identified to play key roles through each stage of the pathogenesis of ischemic heart disease. In cardiomyocytes, mitochondria are highly dynamic organelles, in response to environmental or metabolic changes, they underwent continuous fission, fusion and cristae remodelling (**Figure 2**). Fusion is an essential dynamic process to maintain the equilibration of matrix metabolites, intact mtDNA, and even membrane components (19–21). In reverse, mitochondrial fission exerts the function to segregate dysfunctional mitochondria to clean damaged proteins and mtDNA (19, 22). These mitochondrial activities are strictly regulated by a group of GTPases related to the dynamin family (23). Through the control of these proteins, mitochondria can maintain a dynamic fission-fusion balance to exert physiological functions. The structural disequilibrium is closely related to acute and chronic heart diseases, involving various molecular mechanisms (discussed in the following parts).

The double-membrane mitochondria mediate OXPHOS, coupling the substrate oxidation to ATP generation, which is also known as the electron transport chain, ETC (24, 25). Mitochondrial energy remodelling is a key characteristic of myocardial ischemia. In the early ischemia stage, FAO, the main metabolic way of heart, increases slightly and provides 60–90% of cardiac ATP production. In addition, the rapid depletion of oxygen switches mitochondria metabolism to glycolysis (26), resulting in pyruvate and lactate accumulation, followed by intracellular acidification. After reperfusion, the restoration of oxygen may initiate the burst of ROS, resulting in severe intracellular damage. ROS, combined with calcium overload, will trigger the opening of the mPTP. Despite various researches on this topic, the exact molecular composition of mPTP is still controversial (**Figure 3**). Previous evidence indicated that mPTP includes ANT, VDAC, CyPD and PiC (27, 28), but genetic ablation of these proteins revealed that they are the regulators but not the pore of mPT (29, 30). Mitochondrial F_1F_0 ATP synthase is known to form dimers in the inner mitochondrial membrane (31, 32). Some studies indicated that the ablation of the main membrane-embedded component of ATP synthase, c-subunit, resulted in no change of the sensitivity of mPT (33, 34), however, other evidence found that c-subunit knockout lead to attenuate mPT (35, 36). Previous studies found that mitochondrial F_1F_0 ATP synthase dimers were essential to form the inner mitochondrial membrane channel, maintaining their physical function (37, 38). However, Nelli et al. found that ATP synthase monomer is sufficient, and dimer formation is not required, for mPTP activity (39). Anyway, despite the controversial components of mPTP, current evidence indicated that mPTP opening could lead to the depolarization of mitochondrial membrane potential followed by cell death. Upon heart failure, FAO and mitochondrial OXPHOS decrease, resulting in cardiac ATP behind the requirement. Although the slight increase of glucose uptake and glycolysis could exert a compensatory response, this upregulation is insufficient to restore ATP production (40–42). Accumulating evidence suggest that mitochondrial respiration disturbance is a potential contributory factor to ischemic heart disease due to its generation of ROS (43). Mitochondrial remodelling participates in many regulating processes in ischemic heart disease, which will be discussed in the following parts.

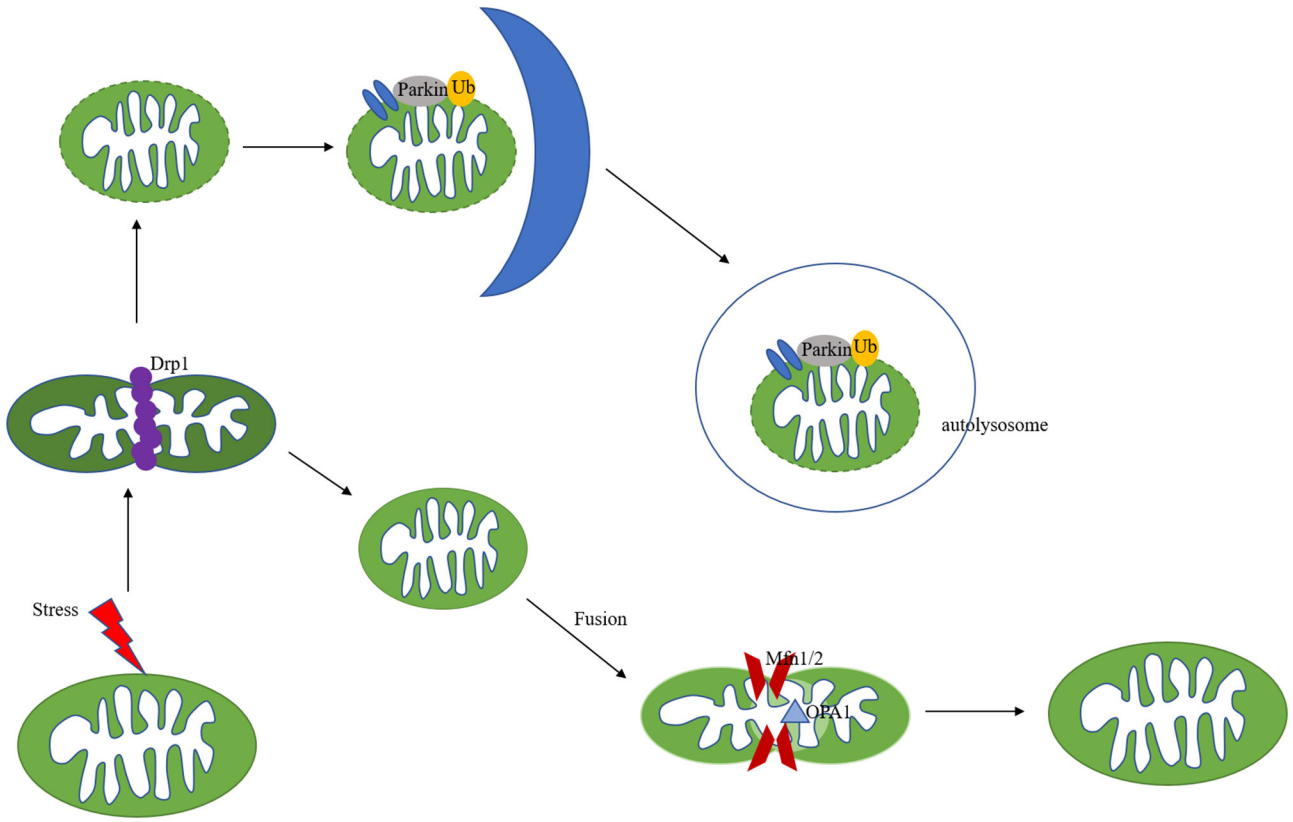

FIGURE 2 | Mechanisms of mitochondria dynamics and mitophagy. Mitochondria are highly dynamic organelles undergoing coordinated cycles of fission and fusion. A series of GTPase-related proteins are involved in the dynamic process. Drp1 is the main regulator of mitochondrial fission, and Mfn1/2, combined with OPA1 regulate the fusion process. After mitochondrial fission, the mitochondrial fragments could be cleared out via PINK/Parkin-mediated mitophagy pathway.

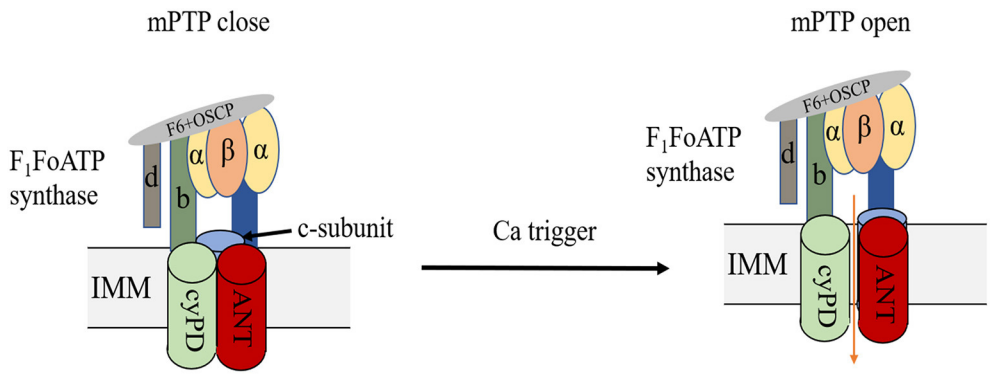

FIGURE 3 | Structure of mPTP. mPTP is a non-specific and -selective channel composed of multiple proteins, which is voltage-dependent and spans cytoplasm, OMM, IMM, and mitochondrial matrix. F_1F_0 (F)-ATP synthase is the main component of the pore and that the regulatory molecule CypD is a protein modulator of the mPTP.

MITOCHONDRIA MITOPHAGY IN ISCHEMIC HEART DISEASE

Mitophagy is a specific subtype of autophagy, which is also an important mitochondria quality control system to maintain mitochondrial homeostasis (44, 45). The mechanisms of mitophagy induced by mitochondrial stress are complicated (**Figure 2**). Mitophagy impairment causes the accumulation of defective organelles, leading to cell and tissue damage. Previous studies focused on autophagosome-mediated mitophagy via LC3 adapters. Recently, many studies have investigated a PINK/Parkin pathway involved in mitophagy. PINK and Parkin

were first reported as genetic factors of Parkinson's disease (46). PINK is a mitochondrial serine/threonine-protein kinase and Parkin is a cytosolic E3-ubiquitin ligase (47, 48). Under physical conditions, PINK is transported to the inner mitochondrial membrane and cleaved by MPP. The auto-phosphorylation of PINK recruited Parkin translocation to the mitochondrial surface (49, 50). Pathological stresses cause mitochondrial membrane depolarization and reduce the cleavage of PINK. Accumulated PINK could be self-phosphorylated and activated, recruiting Parkin to damaged mitochondria and triggering its E3 ligase activity (51, 52). PINK could also phosphorylate ubiquitin (Ub), forming poly-Ub chains on dysfunctional mitochondria. Parkin would be activated by PINK after binding with phospho-Ub, amplifying mitophagy signals (53). Parkin could polyubiquitinate its substrates, such as VDAC1 and Mfn1/2, leading to their degradation by the proteasomes (54, 55), followed by mitochondria fission and mitophagy (**Figure 2**). PINK-Parkin pathway also interferes with other mitochondrial quality control mechanisms, mitochondrial fusion, and fission play an essential role in mitophagy, mediating by dynamics-related proteins (the fission and fusion proteins) (56). Mitochondrial fission results in small fragmented mitochondria while fusion forms the elongated interconnected network. Mitochondria are divided into polarised and depolarised daughter mitochondria. Mitochondrial fission is usually considered as the prerequisite for the occurrence of mitophagy. Drp1 knockout disrupts mitochondria fission, promotes elongated mitochondria, and inhibits mitophagy, which aggravates cardiac dysfunction during IR injury (57). Fission inhibition resulted in the progression of cardiac injury due to impaired mitophagy, in addition, overexpression of Drp1 could promote mitophagy-mediated cell death (58, 59). Song et al. reported that Drp1 ablation interrupts mitochondrial fission and increases the activation of Parkin-mediated mitophagy, and Parkin deletion in Drp1-knockout mice rescues heart function and alleviates cardiac remodelling (60). NR4A1 could aggravate IR injury via increasing mitochondrial fission through Drp1 translocation and mitophagy suppression, NR4A1 ablation could protect against pathological fission and mitochondrial dysfunction. Novel therapeutic targeting the balance among NR4A1, fission, and mitophagy may improve cardiac function following IR injury (61).

In addition to increased mitochondrial fission during I/R injury, the decreased mitochondrial fusion promoted mitochondrial fragmentation, resulting in cardiac cell death and dysfunction. Mitochondrial fusion, mediated by mitofusin 1/2 and OPA1, could prevent damaged mitochondria from fusing with healthy ones. The dynamin-related protein OPA1, located on the inner mitochondrial membrane, protects against apoptosis by preventing the release of cytochrome c from the mitochondria (62). Chen et al. found that OPA1 decreased in samples from human hearts with ischemic cardiomyopathy (63). Increased ROS reduced the expression of OPA1 and aggravated cardiomyocytes apoptosis in response to I/R injury (64). OPA1 overexpression protected cardiomyocytes against hypoxia-induced damage and enhanced cell viability by inducing mitophagy (65), and melatonin could attenuate IRI via improving mitophagy and activating the AMPK-OPA1 signalling pathway (66). Additionally, Lichun et al. (67) found that increased expression of MCU induced calpain activation, down-regulating OPA1 and leading to myocardial IRI.

Current evidence indicated that impaired mitophagy participated in cardiac IRI. PTENα deficiency could disrupt mitophagy and lead to the accumulation of damaged mitochondria, followed by the higher risk of IR injury (68). WDR26 is a scaffolding protein that was found to increase after cardiac ischemia. Increasing the expression of WDR26 could increase mitochondria potential, thereby inhibit cardiomyocyte apoptosis via promoting Parkin-mediated mitophagy (69). Many agents such as antioxidants from grapes were reported to exert protection against IR injury by promoting the PINK/Parkin pathway (70, 71). Zinc ion also demonstrated cardiac protection from IR injury via promoting PINK-dependent mitophagy through the MAPK/ERK pathway, the activation of PINK/Parkin-dependent mitophagy could significantly decrease mitochondrial superoxide generation and oxidative stress (72). Cardiac Drp1 heterozygous knockout mice suffer disturbed mitophagy and are more susceptible to IR injury (57). FUNDC1 is a mitophagy receptor after hypoxia (73), exerting a protective property in cardiac IR injury. A decrease of FUNDC1 could increase ROS levels and promote apoptosis, leading to an increase in cardiac IR injury via MAPK/ERK-CREB pathway. Restoration of FUNDC1 levels could reduce myocardial infarct size (74). In addition, platelet activation and thrombosis formation is the key step in cardiac ischemia (75). Platelet-specific FUNDC1 ablation induces worse cardiac damage via mitophagy interruption and platelet activation (76, 77).

In addition to Parkin, there are several other ubiquitin E3 ligases, such as SMURF1, SIAH1, Gp78 also involve in mitophagy regulation (78, 79). All these factors could generate ubiquitin chains after being located on the mitochondrial surface, followed by the recruitment of autophagy adaptors such as optineurin, nuclear dot protein 52, and p62. These adaptors interact directly with LC3, anchoring Ub-tagged mitochondria into autophagosomes. PINK1 ubiquitin kinase mediates optineurin, nuclear dot protein 52 recruitment on damaged mitochondria, stimulating mitophagy. The serine/threonine-protein kinase TBK1 modulates the phosphorylation status of the adaptors, followed by their increasing binding affinity to Ub chains, and promoting mitochondrial removal (80–82). Choong et al. (83) reported that damaged mitochondria could release into extracellular space in free naked form or in membrane-surrounded vesicles. Mitochondrial stress may enhance this extracellular release process. Extracellular mitochondrial release acts as an alternative pathway to PRKN-dependent and independent mitophagy to help with the clearance of damaged mitochondria.

Macrophages are the most heterogeneous immune cell population, which could be activated by a variety of cytokines. A recent work examining macrophage transcriptome in the mice heart post- MI showed a robust reprogramming of mitochondrial genes, suggesting that mitochondrial function may lie at the heart of macrophage function and cardiac remodelling. Another primary function of macrophages is to eliminate unwanted

material through phagocytosis (84). Nicolás-Ávila et al. (85) identified a non-canonical route of elimination of abnormal mitochondria from cardiomyocytes in vesiculated structures (exophers). The exophers is then taken up and processed by macrophages surround cardiomyocytes through the phagocytic receptor Mertk. In cardiac stress such as AMI and hypertrophy, failure to eliminate mitochondria-laden exophers results in activation of the inflammasome and autophagy arrest, ultimately compromising mitochondrial fitness.

Cardiac remodelling is also a canonical pathological process after myocardial infarction, characterised with a large number of cardiomyocytes undergoing cell death. To maintain normal cardiac output, surviving cardiomyocytes will increase in cellular size, mass, and volume. In addition to cardiomyocytes, cardiac fibroblasts are also activated to secret components of the ECM, which promotes the differentiation to myofibroblasts and exert increased migratory, proliferative and secretory properties (86). BNIP3 is an apoptosis-inducing protein, Diwan et al. (87) and Dorn et al. (88) reported that BNIP3 ablation in unstressed mice reveals no essential function, but BNIP3 specific knockout mice suffered reduced apoptosis and cardiac remodelling after myocardial infarction. It is possible that BNIP3 regulates mitochondrial quality through mitophagy under baseline conditions. However, during cardiac injury, BNIP3 may act as a death promoter. Pingjun and colleagues found that RIPK3 mediated cardiomyocyte necroptosis via AMPK/Parkin-mitophagy axis in post-MI heart failure (89). Moshi et al. (90) found that conditional ablation of Drp1 in mouse embryonic fibroblasts promoted mPTP-mediated mitophagy. In summary, mitophagy is indispensable for physiological mitochondrial function, interruption of which may reduce mitochondrial dysfunction both in ischemia and post-ischemic reperfusion.

MITOCHONDRIAL ROS IN ISCHEMIC HEART DISEASE

It's undoubtful that ROS is a toxic product of aerobic metabolism, involving in various physiological and pathological processes (91, 92). Mitochondria is the major cellular source of ROS. On the one hand, mitochondria consume more than 95% of the oxygen to generate the energy required to sustain life (93). During ischemia, oxygen transported to mitochondrial ETC reduced sharply, after blood restoration bring back oxygen, an electron back-up primer the soluble ubiquinone component of the ETC (especially complex I and complex III) to generate oxygen free radicals. On the other hand, NADPH oxidase was another source of ROS. NADPH oxidase could not deal with the superfluous ROS, causing damage to DNA, proteins, lipids or modulate cellular signalling pathways (**Figure 4**).

Increased ROS levels could activate various second message pathways, such as the ERK, P38, protein kinase C, and PI3-kinase pathways (94–96). Zorov et al. reported that mtROS could dissipate the mitochondrial membrane potential and lead to mPTP opening (97). In the following study, Aon et al. (98) demonstrated that during ischemia-reperfusion injury, excessive ROS from ETC could activate the inner mitochondrial anion channel, causing the release of ROS into the cytoplasm and simultaneous dissipation of the membrane potential. As mentioned above, Nox is another important source of ROS. Braunersreuther et al. reported that in Nox1/Nox2 knockout mice, myocardial infarct size was significantly smaller than that in wild-type mice subjected to IR (30 min of ischemia and 24 h of reperfusion), the underlying pathways include Akt/ERK in Nox1-knockout mice and STAT3/ERK in Nox2-knockout mice (99). Matsushima et al. (100) aimed to figure out the role of Nox-4 in mediating IR injury and they found that Nox-4 knockout mice suffered reduced ROS production and attenuation of the infarct size after IR via the HIF-1α/PPARα pathway.

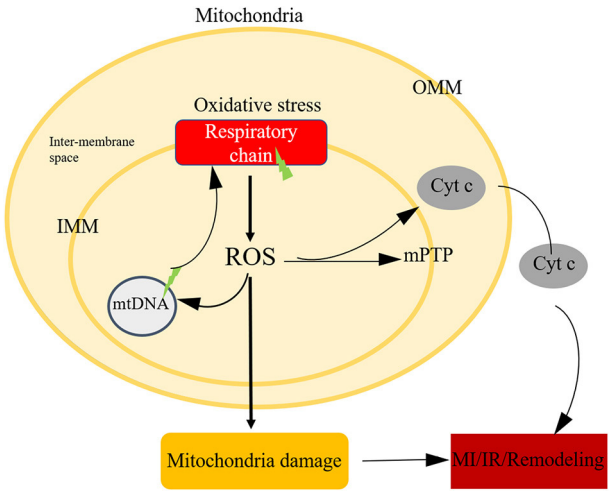

FIGURE 4 | Mitochondria oxidative stress in ischemic heart disease. Mitochondria is the main source of ROS, after oxidative stress, the respiratory chain could generate ROS, the imbalance level of ROS could attribute to mtDNA damage, initiate the open of mPTP, leading to cell death.

In addition to the harmful aspects, redox signalling also contributes to protective or adaptive responses during IR injury (101, 102). Many potential signal pathways have been reported in this process, HIF signalling is one of the most important ones. During ischemia, cardiomyocyte energy metabolism switches from FAO to glycolysis, under control of HIF, followed by the activated expression of several glycolytic genes (103–105). In addition, it's reported that oxidative stress following IR injury is neutralised by the CNC -bZIP transcription factor Nrf2, which could regulate intracellular redox homeostasis. With the accumulation of intracellular oxidants, the levels of Nrf2 increased in the nucleus, binding to ARE in the upstream regulatory regions of genes encoding detoxification and antioxidant enzymes, enhancing their transcription. This has been shown to protect the heart from IR injury (106, 107). Recently, some studies investigated that MAOs, including MAO-A and MAO-B, is another source of ROS. Located on the OMM, MAOs could generate O_2 and H_2O_2 (108). During IR injury, the increased activity of the MAO-A isoform significantly deteriorated myocardial injury (109, 110) and promoted the cardiac remodelling (110).

Cardiac fibrosis is a significant feature of adverse cardiac remodelling after myocardial infarction, sustained fibrosis could result in myocardial stiffness, decrease of heart function, and increased risk of arrhythmias (111). After myocardial infarction, cardiac fibroblasts transform to a proinflammatory state, secreting cytokines and MMPs, later post-MI phase, fibroblasts transform to anti-inflammatory phenotype and generate ECM (112). It's reported that ROS is an important regulator of MMPs, the increased levels of ROS could increase the activity of MMPs, decrease tissue inhibitors of MMPs and increase collagen synthesis (113, 114). *In vitro* tests indicated that ROS could decrease collagen synthesis and increase transcriptional and posttranslational levels of MMPs (115, 116). *In vivo*, mice receiving ROS scavengers after MI could preserve left ventricular function via decreasing the activity of MMPs (117, 118). The evidence indicated that MMPs are key regulators in the process that ROS influences cardiac fibrosis. Gpx is an antioxidant enzyme, which could scavenge H_2O_2, meanwhile prevent the formation of other kinds of toxic radicals. Gpx transgenic mice presented improved heart function via attenuating apoptosis, fibrosis, and decreasing MMP-9 activation after MI (119). Some studies also identified the effect of mitochondrial oxidative stress on remote myocardium after MI. Overexpression of Prx3, a mitochondrial antioxidant enzyme, could inhibit cardiac remodelling and failure (120). Cardiolipin inhibition could prevent adverse cardiac remodelling in the non-infarcted MI border zone via the restoration of ETC and reduced ROS (121). In addition, another study demonstrated that increased lipid peroxidation products could be detected in post-MI heart failure (122). These studies indicated that mitochondrial oxidative stress is an important factor regulating ischemic heart disease.

MITOCHONDRIA-RELATED INFLAMMATION IN ISCHEMIC HEART DISEASE

Current evidence demonstrated that inflammatory cell recruitment, together with the activation of innate and adaptive immune reactions, are the features of MI and IR injury (123, 124). Inflammation is an important component of tissue repair. However, recent studies suggested that excessive inflammation-related processes contributed to poor outcomes. In a steady-state, leukocytes and macrophages are the most prevalent subset in adult mouse hearts. After MI, B-, and T-cells were recruited to myocardium, leading to their increase of 5–10-folds. Circulating blood monocytes migrate into the infarcted heart and differentiate into macrophages. Many signalling pathways have been identified to be involved in mediating inflammation in acute and chronic myocardial injury. In this section, we mainly focused on the relationship between mitochondria and inflammation during cardiac injury (**Figure 5**).

The inflammasome is a cytoplasmic multiprotein complex that contributes to the release of mature cytokines during the innate immune response. Inflammasome could recognise PAMPs or host-derived DAMPs, recruiting, and activating the pro-inflammatory protease caspase-1. NLRP3 inflammasome consists of NLRP3, ASC, and caspase-1 proteins, which play important roles in the pathophysiology of MI. Mitochondrial events and NLRP3 inflammasome activation are tightly bounded. The NLRP3 inflammasome could induce mitochondrial damage via mtROS (125), decreased production of mtROS could effectively inhibit the activation of NLRP3 inflammasome (126). In addition, the insufficiency of damaged mitochondria clearance due to disturbed mitophagy flow would strengthen the activation of the NLRP3 inflammasome. mtDNA is a potential pro-inflammatory trigger for immune cells and is widely accepted as a member of DAMPs (127). Kiichi et al. (128) indicated that mtDNA released into cytoplasm might activate NLRP3 inflammasome, mitophagy could clear damaged mitochondria, followed by the inhibition of NLRP3 inflammasome. Depleting the autophagic proteins LC3B and beclin 1 increased the activation of caspase-1along with secretion of IL-1 β and IL-18. Calcium homeostasis is a critical factor for maintaining mitochondrial function. NLRP3 stimulators (such as ATP) may result in calcium inflow and lead to mitochondrial damage, followed by an increase of mtROS and depletion of mitochondrial membrane potential (129). cGAS/STING is another reported cytosolic mtDNA-sensing pathway, when mitochondria damage leads to the release of fragmented mtDNA into the cytosol, cGAS activates STING, followed by the activation of TBK1, resulting in the translation of interferon genes (130). The inflammatory process initiated by mtDNA is a critical mechanism of ischemic heart disease.

Emerging evidence suggests that macrophage function is closely associated with its mitochondrial metabolism (131, 132). Changes in mitochondrial function have been observed in activated macrophages. In pro-inflammatory macrophages, impairment of TCA flux leads to the accumulation of metabolic intermediates such as succinate and malate (133), overload of succinate is linked to abnormal ROS production (134). The generation of αKG from glutaminolysis is important for alternative M2 activation of macrophages via JMJD3-dependent epigenetic reprogramming of M2 genes (135). Shuang et al. (136) reported a new mechanism of macrophage in the process of myocardial repair after MI, in which efferocytosis increased the level of cellular fatty acids, the increased fatty acids fueled mitochondrial respiration and activated an NAD^+-dependent signal transduction cascade, and this process is positive for wound healing. In 2015, Xu et al. (137) reported that the NOTCH signalling pathway is involved in mitochondrial metabolism remodelling, resulting in mtROS generation and pro-inflammatory gene expressions, such as TNF α and IL-1β.

There are other participants reported to be related to the mitochondria-related inflammation process. Mst1 is a stress-activated, pro-apoptotic kinase, Jing et al. (138) reported that the SRV2 deletion inactivated the Mst1-mROS signalling pathway in cardiomyocytes, which could regulate the inflammation and oxidative stress. Another regulator of inflammatory process-S100a8/a9 caused cell death in the early stage of IR injury via mitochondrial respiratory dysfunction (139). Mechanistically, S100a8/a9 downregulated NDUF gene expression which will inhibit the activity of mitochondrial complex I via Toll-like

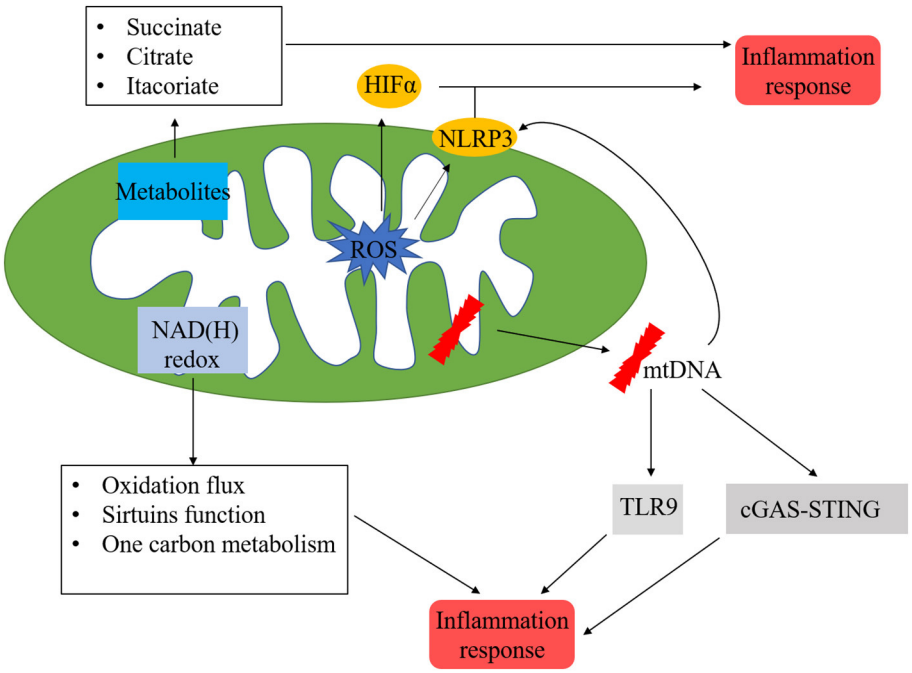

FIGURE 5 | Mitochondria-related inflammation in ischemic heart disease. Many factors in mitochondria could initiate mitochondria-related inflammation, ROS from mitochondrial respiratory chain could directly activate HIFα and NLRP3, which are vital regulators in inflammation process. In addition, metabolites from mitochondria, such as succinate, citrate, and itacoriate also cause inflammation. mtROS could lead to mtDNA damage, which trigger the inflammation response via NLRP3, cGAS/STING, and TLR9 pathways. NAD(H) redox is another initiator of inflammation response via the regulation of oxidation flux, sirtuins function, and one carbon metabolism.

receptor 4/Erk–mediated Pparg coactivator 1 alpha/nuclear respiratory factor 1 signalling suppression.

MITOCHONDRIAL PROTEIN POST-TRANSLATIONAL MODIFICATION IN ISCHEMIC HEART DISEASE

PTMs are alterations of proteins occurring after the translational process catalysed by numerous enzymes. Protein PTMs are important in various physiological and cellular processes, such as differentiation (140), protein degradation (141), gene expression (142, 143). PTMs of proteins have been identified to affect mitochondrial quality control, leading to the exacerbation, or alleviation of ischemic heart disease (144–146) (**Figure 2**).

Protein phosphorylation plays a critical regulatory role in cardiomyocytes via mediating protein activation or deactivation. Phosphorylation of mitochondrial proteins is vital to maintain mitochondrial function. Phosphorylation of mitochondrial complex IV subunit mediated its physical function in myocardial mitochondria. During IR injury, protein kinase A-dependent phosphorylation of complex IV increased and resulted in a decrease of its activity, followed by an increase in ROS production (147, 148). The STAT3 is a key regulator of mitochondrial metabolism via the interaction with mitochondrial proteins. In ischemic conditions, STAT3 phosphorylation improved mitochondrial function via preserving mitochondrial complex I, preventing mPTP opening with the result of infarction area reduction (149–151).

In eukaryotic cells, the UPS is a primary system of protein degradation. The ubiquitination occurred via ubiquitin-binding its COOH group with the target protein (152, 153). Ubiquitination has been widely accepted as one of the major ways of protein degradation to maintain mitochondrial quality. As we presented previously, PINK/Parkin-mediated mitophagy is a critical pathway for mitochondrial quality control. Parkin is an E3 ligase, which can ubiquitinate several mitochondrial outer membrane proteins via E3 ligase activity to recruit the p62 protein. CypD ubiquitinated by Parkin could inhibit mPTP opening, alleviating myocardial injury (154). In the process of heart remodelling after IR injury, exogenous ubiquitin supplement could reduce caspase-9 expression in the mitochondrial death pathway, increasing mitochondrial production, reducing infarct area, and finally restoring heart function (155). Wangxing et al. (156) demonstrated that leptin-overexpressing hMSCs into the infarcted heart could improve cardiac function. Further mechanical exploration indicated that leptin restored mitochondrial respiratory function via enhancing OPA1 expression by inhibiting the activity of OMA1, a mitochondrial protease. In addition, phosphorylation of GSK3 is a prerequisite for ubiquitination-depended degradation of OMA1 and attenuation of long-OPA1 cleavage.

SUMO is a member of the large family of ubiquitin-like proteins. SUMOylation is a classic ubiquitination-like PTMs,

linking the SUMO protein to the lysine residue of the substrate protein (157). In heart IR injury, the binding of SUMO with Drp1 increased to form a complex, increasing the acidification of the complex could maintain mitochondrial quality and improve cardiac function (158). Another deSUMOylation-related enzyme, SENP3 could alleviate IR injury via the inhibition of Drp1 localisation in the mitochondria (159). Acetylation is one of the major PTMs in cell biology, SIRT3 and SIRT5 are sirtuins found in mitochondria. Angela et al. reported that SIRT3 could reduce the activity of CypD, inhibiting the opening of mPTP. Increasing SIRT3 expression in the failing heart could improve cardiac function (160). Studies showed that decreased expression of SIRT3 in heart increased susceptibility to IR injury (161, 162). In addition, SIRT1 was also found to be involved in cardiac IR injury, study found that increased expression of SIRT1 could restore left ventricular function during the construction of myocardial IR models (163). Zhao et al. invested the role of HDACs inhibition in myocardial IR injury and found that HDACs inhibition protected the heart against I/R injury (164). Moreover, SIRT5 (–/–) mouse hearts are more tendentious to suffer IRI due to the increase of lysine succinylation followed by the accumulation of mitochondrial ROS, and mtROS scavenged by SDH inhibition could reverse this process (165). Accordingly, the exploration of the interaction of PTMs in ischemic heart disease by modulating mitochondrial quality control has a bright future to investigate novel therapeutic targets.

MiRNAs are short non-coding RNA binding to the 3' UTR sequences and regulating targeted gene expression either by mRNA degradation or translational repression (166). Mitochondria contain miRNAs that are termed as mitomiRs in several species and cell types (167). MitomiRs target either mitochondrial or nuclear proteincoding mRNAs, thereby influencing mitochondrial metabolism and dynamics through regulation of the main mitochondrial pathways, such as OXPHOS, ETC components, TCA cycle (168). Overexpression of miRNA-34a in AMI patients' serum enhances cardiomyocyte apoptosis by down-regulating mitochondrial anti-apoptotic protein aldehyde dehydrogenase 2 (169). miRNA-1 could enter mitochondria and regulate mitochondrial ETC via targeting proteins in ETC networks, while increased miRNA-1 expression has been found in the remote myocardium of AMI patients (170). Mitochondrial miRNA-762 regulates cardiomyocyte apoptosis via impairing the core subunit of mitochondrial complex I (171). In addition, lncRNAs are also a heterogeneous class of transcripts involved in the epigenetic regulation of gene and genome activity (172, 173). Recent data indicated that lncRNAs localised to mitochondria, regulating mitochondrial function (174–176). Circulating levels of mitochondrial lncRNA LIPCAR were downregulated early after AMI and upregulated during later stages and were associated with adverse cardiac remodelling and death (175). In addition to lncRNAs, growing evidence also reports that circRNAs are involved in the regulation of the mitochondrial dynamics and cardiomyocyte apoptosis. Kun et al. (177) found that MFACR regulated mitochondrial fission and apoptosis in the heart by targeting and downregulation of miR-652-3p. To sum up, mitochondrial non-coding RNAs are involved in the pathogenesis of myocardial infarction via regulating various pathways.

TARGETED THERAPIES

Early reperfusion of occluded coronary arteries is the most effective strategy of AMI over the past decades. However, there is no effective therapy for reperfusion injury and alleviation of cardiac remodellin. Therefore, with a growing understanding of the molecular mechanisms of ischemia, IR injury, and chronic remodelling, we may develop more novel therapeutic targets to protect the heart from IHD and improve clinical outcomes of these patients. Considering numerous studies in this field, we only discussed the agents involved in mitochondrial targets in animal studies or clinical trials.

Over decades, mtROS is one of the most popular targets of heart protection. A reduced generation or increased scavenge of mtROS have been reported to increase outcomes. MitoQ is the first mitochondria-targeted antioxidant, which is bioavailable orally without toxicity detected. Rat received MitoQ for 2 weeks suffered reduced oxidative stress and resisted heart ischemia-reperfusion injury (178). SS-31 is a kind of small artificial peptides with therapeutic potential due to its antioxidant properties (179–181), in rat tests, SS-31 could attenuate the strike of ischemia and reperfusion via reducing MI size (180, 182, 183). SODs are metal-containing antioxidant enzymes, protecting cells from damage by converting superoxide radicals to H_2O_2 and O_2. Mito-specific SOD mimetics exert protection under oxidative stress (184). Clinical trials of SS-31 in patients with heart failure and acute myocardial infarction have been tested, although the myocardial infarct size did not show an improvement, it showed acceptable safety and tolerability (185, 186). Cerrato's group two analogues of SS-31 (mtCPP-1 and mtgCPP) and reported greater efficiency and antioxidant capacity than SS-31 (187, 188). In an animal model of post-infarction heart failure, activation of ALDH2 with Alda-1 improves the clinical outcomes via the decrease of reactive aldehydes (189).

mPTP is a mitochondria voltage- and Ca2+-dependent high-conductance channel. Piot et al. exerted a clinical trial that included 58 patients who suffered acute ST-elevation myocardial infarction to receive cyclosporine immediately before undergoing PCI, it came out that cyclosporine could decrease the infarct size to some extent (190). Currently, some larger clinical trials are ongoing to test the effect of mPTP inhibition on short- and long-term patients' outcomes. Trehalose is a small molecule from mushrooms, which could activate mitophagy. Studies indicated that administration of trehalose for 4 weeks could reverse cardiac remodelling and fibrosis in MI model mice (191, 192). Spermidine is another natural compound that activates autophagy. In the MI rat model, oral supplementation of spermidine is inversely associated with all-cause mortality and MI risk via enhancement of mitochondrial respiration (193). In addition, Jing et al. reported that spermidine supplement improved MI-induced cardiac dysfunction through AMPK/mTOR mediated autophagic flux (194). Mdivi-1 is an inhibitor of mitochondria-related fission protein-Drp1, which is proved to reduce infarct size, rescue cardiac function in the IRI

mouse model (195). In addition, mdivi-1 treatment ameliorated IRI via the inhibition of connexin 43 loss and suppression of MMP3 (196). UPR^{mt} is critical to maintain mitochondrial proteostasis under cellular stress, UPR^{mt} induced by oligomycin or doxycycline has been identified to reduce MI size in mice models (197). The expression of AMPK increased in failing heart, metformin is considered as a pharmacological activator of AMPK, which could reduce cardiac infarct size and improve heart contractibility in a rat MI model. Artificial compounds targeting AMPK have been designed, Abbott lab generated an artificial agent, named A769662, which could reduce infarct size in rats via specific activating AMPK on β subunit (198, 199).

Although various experimental studies developed effective cardioprotective strategies, there are few successful clinical translations. And this has been attributed to different factors: firstly, there are no effective delivery systems for agents to carry out their functions. Secondly, animal models are different from patients with ischemic heart disease, which usually also suffered from other co-morbidities such as hypertension, diabetes. Recently, some clinical agents such as DPP-4 and SGLT2 have been identified to protect cardiomyocytes from IRI damage via mitochondrial function preservation. GLP-1 is an incretin hormone with cardioprotective capacities and was markedly increased in acute myocardial infarction. In physical conditions, GLP-1 could be degraded by DPP-4, Sebastian et al. (200) found that DPP-4 inhibitor could maintain the serum concentration of GLP-1, increasing AMPK activity and mitochondrial respiratory capacity of non-infarcted tissues. In addition, GLP-1 agonist, liraglutide could reduce cardiac infarct size, protected cardiomyocytes from injury and preserved contractile function via suppressing ROS generation, NADPH oxidase and proinflammatory signals (201). SGLT-2 inhibitors are a new generation of anti-diabetic agents, which have been recommended in cardio-protection (202). Various studies proved that SGLT-2 inhibitors could ameliorate cardiac remodelling and increase mitochondrial function (203, 204). Another type of anti-diabetic agent, metformin is also reported to exert cardio-protection by restoring mitochondria function and dynamics in cardiac I/R injury (205). Some natural agents or analogues such as taurine, fisetin, and humanin also exert cardio-protection against IRI by reducing mitochondrial dysfunction (206–208). In summary, despite there is much evidence supporting the targeting of mitochondria as a therapy strategy in IHD, more efforts are needed to promote the basic to clinical translation.

CONCLUSIONS

Mitochondrial homeostasis is critical for the maintain of the mitochondria network. In this review, we summarised the advances supporting the view that mitochondrial disorder is a major contributor to cardiac injury, IRI, as well as chronic remodelling. Mitophagy disorder, increased mtROS, mitochondria-related inflammation and post-translation of mitochondrial proteins are considered contributory factors to mitochondrial dysfunction in ischemic heart disease. Accordingly, many targeted modulations involved in mitochondrial quality control provide great chances for the design of novel therapies. Although there are no drugs with successful clinical transformation, which are directly targeted mitochondria-related mechanisms, many regulatory proteins or peptides and miRNAs possess significant potential.

AUTHOR CONTRIBUTIONS

YX, JinL, HG, and JuL contributed to the first and second version of the manuscript. XZ and HL contributed to the second version. HL supervised the project. JiaL made great contribution to our revision manuscript and provided helpful opinions. All authors contributed to the article and approved the submitted version.

FUNDING

This work was supported by Beijing Natural Science Foundation (No.7214219); Natural Science Foundation of Liao Ning Province (2019-MS-386).

REFERENCES

1. Dorweiler B, Pruefer D, Andrasi TB, Maksan SM, Schmiedt W, Neufang A, et al. Ischemia-reperfusion injury: pathophysiology and clinical implications. *Eur J Trauma Emerg Surg.* (2007) 33:600–12. doi: 10.1007/s00068-007-7152-z
2. Murphy E, Steenbergen C. Mechanisms underlying acute protection from cardiac ischemia-reperfusion injury. *Physiol Rev.* (2008) 88:581–609. doi: 10.1152/physrev.00024.2007
3. Heusch G, Gersh BJ. The pathophysiology of acute myocardial infarction and strategies of protection beyond reperfusion: a continual challenge. *Eur Heart J.* (2017) 38:774–84. doi: 10.1093/eurheartj/ehw224
4. Hung J, Teng TH, Finn J, Knuiman M, Briffa T, Stewart S, et al. Trends from 1996 to 2007 in incidence and mortality outcomes of heart failure after acute myocardial infarction: a population-based study of 20,812 patients with first acute myocardial infarction in Western Australia. *J Am Heart Assoc.* (2013) 2:e000172. doi: 10.1161/JAHA.113.000172
5. Sulo G, Igland J, Vollset SE, Nygård O, Ebbing M, Sulo E, et al. Heart failure complicating acute myocardial infarction; burden and timing of occurrence: a nation-wide analysis including 86 771 patients from the cardiovascular disease in Norway (CVDNOR) Project. *J Am Heart Assoc.* (2016) 5:e002667. doi: 10.1161/JAHA.115.002667
6. Kaneko H, Anzai T, Takahashi T, Kohno T, Shimoda M, Sasaki A, et al. Role of vascular endothelial growth factor-A in development of abdominal aortic aneurysm. *Cardiovasc Res.* (2011) 91:358–67. doi: 10.1093/cvr/cvr080
7. Hara H, Takeda N, Komuro I. Pathophysiology and therapeutic potential of cardiac fibrosis. *Inflamm Regen.* (2017) 37:13. doi: 10.1186/s41232-017-0046-5
8. Gulati A, Jabbour A, Ismail TF, Guha K, Khwaja J, Raza S, et al. Association of fibrosis with mortality and sudden cardiac death in patients with nonischemic dilated cardiomyopathy. *JAMA.* (2013) 309:896–908. doi: 10.1001/jama.2013.1363
9. Neubauer S. The failing heart–an engine out of fuel. *N Engl J Med.* (2007) 356:1140–51. doi: 10.1056/NEJMra063052
10. Jeong SY, Seol DW. The role of mitochondria in apoptosis. *BMB Rep.* (2008) 41:11–22. doi: 10.5483/BMBRep.2008.41.1.011
11. Yang Y, Karakhanova S, Hartwig W, D'Haese JG, Philippov PP, Werner J, et al. Mitochondria and mitochondrial ROS in cancer: novel targets for anticancer therapy. *J Cell Physiol.* (2016) 231:2570–81. doi: 10.1002/jcp.25349

12. Zorov DB, Juhaszova M, Sollott SJ. Mitochondrial reactive oxygen species (ROS) and ROS-induced ROS release. *Physiol Rev.* (2014) 94:909–50. doi: 10.1152/physrev.00026.2013
13. Cadenas S. Mitochondrial uncoupling, ROS generation and cardioprotection. *Biochim Biophys Acta Bioenerg.* (2018) 1859:940–50. doi: 10.1016/j.bbabio.2018.05.019
14. Bartel K, Pein H, Popper B, Schmitt S, Janaki-Raman S, Schulze A, et al. Connecting lysosomes and mitochondria - a novel role for lipid metabolism in cancer cell death. *Cell Commun Signal.* (2019) 17:87. doi: 10.1186/s12964-019-0399-2
15. D'Souza K, Nzirorera C, Kienesberger PC. Lipid metabolism and signaling in cardiac lipotoxicity. *Biochim Biophys Acta.* (2016) 1861:1513–24. doi: 10.1016/j.bbalip.2016.02.016
16. Begriche K, Massart J, Robin MA, Borgne-Sanchez A, Fromenty B. Drug-induced toxicity on mitochondria and lipid metabolism: mechanistic diversity and deleterious consequences for the liver. *J Hepatol.* (2011) 54:773–94. doi: 10.1016/j.jhep.2010.11.006
17. Kolmychkova KI, Zhelankin AV, Karagodin VP, Orekhov AN. Mitochondria and inflammation. *Patol Fiziol Eksp Ter.* (2016) 60:114–21.
18. Bugger H, Pfeil K. Mitochondrial ROS in myocardial ischemia reperfusion and remodeling. *Biochim Biophys Acta Mol Basis Dis.* (2020) 1866:165768. doi: 10.1016/j.bbadis.2020.165768
19. Hoppins S, Lackner L, Nunnari J. The machines that divide and fuse mitochondria. *Annu Rev Biochem.* (2007) 76:751–80. doi: 10.1146/annurev.biochem.76.071905.090048
20. Busch KB, Bereiter-Hahn J, Wittig I, Schagger H, Jendrach M. Mitochondrial dynamics generate equal distribution but patchwork localization of respiratory Complex I. *Mol Membr Biol.* (2006) 23:509–20. doi: 10.1080/09687860600877292
21. Dimmer KS, Scorrano L. (De)constructing mitochondria: what for? *Physiology.* (2006) 21:233–41. doi: 10.1152/physiol.00010.2006
22. Twig G, Hyde B, Shirihai OS. Mitochondrial fusion, fission and autophagy as a quality control axis: the bioenergetic view. *Biochim Biophys Acta.* (2008) 1777:1092–7. doi: 10.1016/j.bbabio.2008.05.001
23. Kuzmicic J, Del Campo A, López-Crisosto C, Morales PE, Pennanen C, Bravo-Sagua R, et al. [Mitochondrial dynamics: a potential new therapeutic target for heart failure]. *Rev Esp Cardiol.* (2011) 64:916–23. doi: 10.1016/j.rec.2011.05.022
24. Balaban RS. Domestication of the cardiac mitochondrion for energy conversion. *J Mol Cell Cardiol.* (2009) 46:832–41. doi: 10.1016/j.yjmcc.2009.02.018
25. Solaini G, Harris DA. Biochemical dysfunction in heart mitochondria exposed to ischaemia and reperfusion. *Biochem J.* (2005) 390:377–94. doi: 10.1042/BJ20042006
26. Lejay A, Fang F, John R, Van JA, Barr M, Thaveau F, et al. Ischemia reperfusion injury, ischemic conditioning and diabetes mellitus. *J Mol Cell Cardiol.* (2016) 91:11–22. doi: 10.1016/j.yjmcc.2015.12.020
27. Halestrap AP, Brenner C. The adenine nucleotide translocase: a central component of the mitochondrial permeability transition pore and key player in cell death. *Curr Med Chem.* (2003) 10:1507–25. doi: 10.2174/0929867033457278
28. Kwong JQ, Davis J, Baines CP, Sargent MA, Karch J, Wang X, et al. Genetic deletion of the mitochondrial phosphate carrier desensitizes the mitochondrial permeability transition pore and causes cardiomyopathy. *Cell Death Differ.* (2014) 21:1209–17. doi: 10.1038/cdd.2014.36
29. Baines CP, Kaiser RA, Sheiko T, Craigen WJ, Molkentin JD. Voltage-dependent anion channels are dispensable for mitochondrial-dependent cell death. *Nat Cell Biol.* (2007) 9:550–5. doi: 10.1038/ncb1575
30. Halestrap AP. Mitochondrial permeability: dual role for the ADP/ATP translocator? *Nature.* (2004) 430:983. doi: 10.1038/nature02816
31. Davies KM, Anselmi C, Wittig I, Faraldo-Gómez JD, Kühlbrandt W. Structure of the yeast F1Fo-ATP synthase dimer and its role in shaping the mitochondrial cristae. *Proc Natl Acad Sci USA.* (2012) 109:13602–7. doi: 10.1073/pnas.1204593109
32. Davies KM, Daum B, Gold VA, Mühleip AW, Brandt T, Blum TB, et al. Visualization of ATP synthase dimers in mitochondria by electron cryo-tomography. *J Vis Exp.* (2014) 14:51228. doi: 10.3791/51228
33. He J, Carroll J, Ding S, Fearnley IM, Walker JE. Permeability transition in human mitochondria persists in the absence of peripheral stalk subunits of ATP synthase. *Proc Natl Acad Sci USA.* (2017) 114:9086–91. doi: 10.1073/pnas.1711201114
34. He J, Ford HC, Carroll J, Ding S, Fearnley IM, Walker JE. Persistence of the mitochondrial permeability transition in the absence of subunit c of human ATP synthase. *Proc Natl Acad Sci USA.* (2017) 114:3409–14. doi: 10.1073/pnas.1702357114
35. Bonora M, Bononi A, De Marchi E, Giorgi C, Lebiedzinska M, Marchi S, et al. Role of the c subunit of the FO ATP synthase in mitochondrial permeability transition. *Cell Cycle.* (2013) 12:674–83. doi: 10.4161/cc.23599
36. Azarashvili T, Odinokova I, Bakunts A, Ternovsky V, Krestinina O, Tyynelä J, et al. Potential role of subunit c of F0F1-ATPase and subunit c of storage body in the mitochondrial permeability transition. effect of the phosphorylation status of subunit c on pore opening. *Cell Calcium.* (2014) 55:69–77. doi: 10.1016/j.ceca.2013.12.002
37. Mannella CA, Lederer WJ, Jafri MS. The connection between inner membrane topology and mitochondrial function. *J Mol Cell Cardiol.* (2013) 62:51–7. doi: 10.1016/j.yjmcc.2013.05.001
38. Daum B, Walter A, Horst A, Osiewacz HD, Kühlbrandt W. Age-dependent dissociation of ATP synthase dimers and loss of inner-membrane cristae in mitochondria. *Proc Natl Acad Sci USA.* (2013) 110:15301–6. doi: 10.1073/pnas.1305462110
39. Mnatsakanyan N, Llaguno MC, Yang Y, Yan Y, Weber J, Sigworth FJ, et al. A mitochondrial megachannel resides in monomeric F(1)F(O) ATP synthase. *Nat Commun.* (2019) 10:5823. doi: 10.1038/s41467-019-13766-2
40. Luptak I, Balschi JA, Xing Y, Leone TC, Kelly DP, Tian R. Decreased contractile and metabolic reserve in peroxisome proliferator-activated receptor-alpha-null hearts can be rescued by increasing glucose transport and utilization. *Circulation.* (2005) 112:2339–46. doi: 10.1161/CIRCULATIONAHA.105.534594
41. Neglia D, De Caterina A, Marraccini P, Natali A, Ciardetti M, Vecoli C, et al. Impaired myocardial metabolic reserve and substrate selection flexibility during stress in patients with idiopathic dilated cardiomyopathy. *Am J Physiol Heart Circ Physiol.* (2007) 293:H3270–8. doi: 10.1152/ajpheart.00887.2007
42. Kolwicz SC, Jr., Tian R. Glucose metabolism and cardiac hypertrophy. *Cardiovasc Res.* (2011) 90:194–201. doi: 10.1093/cvr/cvr071
43. Nediani C, Raimondi L, Borchi E, Cerbai E. Nitric oxide/reactive oxygen species generation and nitroso/redox imbalance in heart failure: from molecular mechanisms to therapeutic implications. *Antioxid Redox Signal.* (2011) 14:289–331. doi: 10.1089/ars.2010.3198
44. Yoo SM, Jung YK. A molecular approach to mitophagy and mitochondrial dynamics. *Mol Cells.* (2018) 41:18–26. doi: 10.14348/molcells.2018.2277
45. Bravo-San Pedro JM, Kroemer G, Galluzzi L. Autophagy and mitophagy in cardiovascular disease. *Circ Res.* (2017) 120:1812–24. doi: 10.1161/CIRCRESAHA.117.311082
46. Pickrell AM, Youle RJ. The roles of PINK1, parkin, and mitochondrial fidelity in Parkinson's disease. *Neuron.* (2015) 85:257–73. doi: 10.1016/j.neuron.2014.12.007
47. Matsuda N, Sato S, Shiba K, Okatsu K, Saisho K, Gautier CA, et al. PINK1 stabilized by mitochondrial depolarization recruits Parkin to damaged mitochondria and activates latent Parkin for mitophagy. *J Cell Biol.* (2010) 189:211–21. doi: 10.1083/jcb.200910140
48. Narendra D, Tanaka A, Suen DF, Youle RJ. Parkin is recruited selectively to impaired mitochondria and promotes their autophagy. *J Cell Biol.* (2008) 183:795–803. doi: 10.1083/jcb.200809125
49. Harper JW, Ordureau A, Heo JM. Building and decoding ubiquitin chains for mitophagy. *Nat Rev Mol Cell Biol.* (2018) 19:93–108. doi: 10.1038/nrm.2017.129
50. Sekine S, Youle RJ. PINK1 import regulation; a fine system to convey mitochondrial stress to the cytosol. *BMC Biol.* (2018) 16:2. doi: 10.1186/s12915-017-0470-7
51. Pickles S, Vigié P, Youle RJ. Mitophagy and quality control mechanisms in mitochondrial maintenance. *Curr Biol.* (2018) 28:R170–85. doi: 10.1016/j.cub.2018.01.004

52. Aguirre JD, Dunkerley KM, Mercier P, Shaw GS. Structure of phosphorylated UBL domain and insights into PINK1-orchestrated parkin activation. *Proc Natl Acad Sci USA*. (2017) 114:298–303. doi: 10.1073/pnas.1613040114
53. Ordureau A, Sarraf SA, Duda DM, Heo JM, Jedrychowski MP, Sviderskiy VO, et al. Quantitative proteomics reveal a feedforward mechanism for mitochondrial PARKIN translocation and ubiquitin chain synthesis. *Mol Cell*. (2014) 56:360–75. doi: 10.1016/j.molcel.2014.09.007
54. Chan NC, Salazar AM, Pham AH, Sweredoski MJ, Kolawa NJ, Graham RL, et al. Broad activation of the ubiquitin-proteasome system by Parkin is critical for mitophagy. *Hum Mol Genet*. (2011) 20:1726–37. doi: 10.1093/hmg/ddr048
55. Tanaka A, Cleland MM, Xu S, Narendra DP, Suen DF, Karbowski M, et al. Proteasome and p97 mediate mitophagy and degradation of mitofusins induced by Parkin. *J Cell Biol*. (2010) 191:1367–80. doi: 10.1083/jcb.201007013
56. Santulli G, Lewis DR, Marks AR. Physiology and pathophysiology of excitation-contraction coupling: the functional role of ryanodine receptor. *J Muscle Res Cell Motil*. (2017) 38:37–45. doi: 10.1007/s10974-017-9470-z
57. Ikeda Y, Shirakabe A, Maejima Y, Zhai P, Sciarretta S, Toli J, et al. Endogenous Drp1 mediates mitochondrial autophagy and protects the heart against energy stress. *Circ Res*. (2015) 116:264–78. doi: 10.1161/CIRCRESAHA.116.303356
58. Otera H, Miyata N, Kuge O, Mihara K. Drp1-dependent mitochondrial fission via MiD49/51 is essential for apoptotic cristae remodeling. *J Cell Biol*. (2016) 212:531–44. doi: 10.1083/jcb.201508099
59. Zhou H, Zhang Y, Hu S, Shi C, Zhu P, Ma Q, et al. Melatonin protects cardiac microvasculature against ischemia/reperfusion injury via suppression of mitochondrial fission-VDAC1-HK2-mPTP-mitophagy axis. *J Pineal Res*. (2017) 63:e12413. doi: 10.1111/jpi.12413
60. Song M, Gong G, Burelle Y, Gustafsson ÅB, Kitsis RN, Matkovich SJ, et al. Interdependence of parkin-mediated mitophagy and mitochondrial fission in adult mouse hearts. *Circ Res*. (2015) 117:346–51. doi: 10.1161/CIRCRESAHA.117.306859
61. Zhou H, Wang J, Zhu P, Zhu H, Toan S, Hu S, et al. NR4A1 aggravates the cardiac microvascular ischemia reperfusion injury through suppressing FUNDC1-mediated mitophagy and promoting Mff-required mitochondrial fission by CK2α. *Basic Res Cardiol*. (2018) 113:23. doi: 10.1007/s00395-018-0682-1
62. Frezza C, Cipolat S, Martins de Brito O, Micaroni M, Beznoussenko GV, Rudka T, et al. OPA1 controls apoptotic cristae remodeling independently from mitochondrial fusion. *Cell*. (2006) 126:177–89. doi: 10.1016/j.cell.2006.06.025
63. Chen L, Gong Q, Stice JP, Knowlton AA. Mitochondrial OPA1, apoptosis, heart failure. *Cardiovasc Res*. (2009) 84:91–9. doi: 10.1093/cvr/cvp181
64. Shen T, Zheng M, Cao C, Chen C, Tang J, Zhang W, et al. Mitofusin-2 is a major determinant of oxidative stress-mediated heart muscle cell apoptosis. *J Biol Chem*. (2007) 282:23354–61. doi: 10.1074/jbc.M702657200
65. Xin T, Lu C. Irisin activates Opa1-induced mitophagy to protect cardiomyocytes against apoptosis following myocardial infarction. *Aging*. (2020) 12:4474–88. doi: 10.18632/aging.102899
66. Zhang Y, Wang Y, Xu J, Tian F, Hu S, Chen Y, et al. Melatonin attenuates myocardial ischemia-reperfusion injury via improving mitochondrial fusion/mitophagy and activating the AMPK-OPA1 signaling pathways. *J Pineal Res*. (2019) 66:e12542. doi: 10.1111/jpi.12542
67. Guan L, Che Z, Meng X, Yu Y, Li M, Yu Z, et al. MCU Up-regulation contributes to myocardial ischemia-reperfusion Injury through calpain/OPA-1-mediated mitochondrial fusion/mitophagy Inhibition. *J Cell Mol Med*. (2019) 23:7830–43. doi: 10.1111/jcmm.14662
68. Li G, Yang J, Yang C, Zhu M, Jin Y, McNutt MA, et al. PTENα regulates mitophagy and maintains mitochondrial quality control. *Autophagy*. (2018) 14:1742–60. doi: 10.1080/15548627.2018.1489477
69. Feng Y, Zhao J, Hou H, Zhang H, Jiao Y, Wang J, et al. WDR26 promotes mitophagy of cardiomyocytes induced by hypoxia through Parkin translocation. *Acta Biochim Biophys Sin*. (2016) 48:1075–84. doi: 10.1093/abbs/gmw104
70. Das S, Mitrovsky G, Vasanthi HR, Das DK. Antiaging properties of a grape-derived antioxidant are regulated by mitochondrial balance of fusion and fission leading to mitophagy triggered by a signaling network of Sirt1-Sirt3-Foxo3-PINK1-PARKIN. *Oxid Med Cell Longev*. (2014) 2014:345105. doi: 10.1155/2014/345105
71. Wang Y, Lu X, Zhao P, Jiang J, Yao L. [Overexpression of PPENK reduces myocardial ischemia reperfusion injury by promoting mitophagy in rats]. *Xi Bao Yu Fen Zi Mian Yi Xue Za Zhi*. (2017) 33:1335–40.
72. Bian X, Teng T, Zhao H, Qin J, Qiao Z, Sun Y, et al. Zinc prevents mitochondrial superoxide generation by inducing mitophagy in the setting of hypoxia/reoxygenation in cardiac cells. *Free Radic Res*. (2018) 52:80–91. doi: 10.1080/10715762.2017.1414949
73. Yang M, Linn BS, Zhang Y, Ren J. Mitophagy and mitochondrial integrity in cardiac ischemia-reperfusion injury. *Biochim Biophys Acta Mol Basis Dis*. (2019) 1865:2293–302. doi: 10.1016/j.bbadis.2019.05.007
74. Yu W, Xu M, Zhang T, Zhang Q, Zou C. Mst1 promotes cardiac ischemia-reperfusion injury by inhibiting the ERK-CREB pathway and repressing FUNDC1-mediated mitophagy. *J Physiol Sci*. (2019) 69:113–27. doi: 10.1007/s12576-018-0627-3
75. Zhang W, Chen C, Wang J, Liu L, He Y, Chen Q. Mitophagy in cardiomyocytes and in platelets: a major mechanism of cardioprotection against ischemia/reperfusion injury. *Physiology*. (2018) 33:86–98. doi: 10.1152/physiol.00030.2017
76. Zhang W, Siraj S, Zhang R, Chen Q. Mitophagy receptor FUNDC1 regulates mitochondrial homeostasis and protects the heart from I/R injury. *Autophagy*. (2017) 13:1080–1. doi: 10.1080/15548627.2017.1300224
77. Zhang W, Ren H, Xu C, Zhu C, Wu H, Liu D, et al. Hypoxic mitophagy regulates mitochondrial quality and platelet activation and determines severity of I/R heart injury. *Elife*. (2016) 5:e21407. doi: 10.7554/eLife.21407
78. Fu M, St-Pierre P, Shankar J, Wang PT, Joshi B, Nabi IR. Regulation of mitophagy by the Gp78 E3 ubiquitin ligase. *Mol Biol Cell*. (2013) 24:1153–62. doi: 10.1091/mbc.e12-08-0607
79. Szargel R, Shani V, Abd Elghani F, Mekies LN, Liani E, Rott R, et al. The PINK1, synphilin-1 and SIAH-1 complex constitutes a novel mitophagy pathway. *Hum Mol Genet*. (2016) 25:3476–90. doi: 10.1093/hmg/ddw189
80. Heo JM, Ordureau A, Paulo JA, Rinehart J, Harper JW. The PINK1-PARKIN mitochondrial ubiquitylation pathway drives a program of OPTN/NDP52 recruitment and TBK1 activation to promote mitophagy. *Mol Cell*. (2015) 60:7–20. doi: 10.1016/j.molcel.2015.08.016
81. Moore AS, Holzbaur EL. Dynamic recruitment and activation of ALS-associated TBK1 with its target optineurin are required for efficient mitophagy. *Proc Natl Acad Sci USA*. (2016) 113:E3349–58. doi: 10.1073/pnas.1523810113
82. Richter B, Sliter DA, Herhaus L, Stolz A, Wang C, Beli P, et al. Phosphorylation of OPTN by TBK1 enhances its binding to Ub chains and promotes selective autophagy of damaged mitochondria. *Proc Natl Acad Sci USA*. (2016) 113:4039–44. doi: 10.1073/pnas.1523926113
83. Choong CJ, Okuno T, Ikenaka K, Baba K, Hayakawa H, Koike M, et al. Alternative mitochondrial quality control mediated by extracellular release. *Autophagy*. (2020) 17:2962–74. doi: 10.1080/15548627.2020.1848130
84. Gordon S. Phagocytosis: an immunobiologic process. *Immunity*. (2016) 44:463–75. doi: 10.1016/j.immuni.2016.02.026
85. Nicolás-Ávila JA, Lechuga-Vieco AV, Esteban-Martínez L, Sánchez-Díaz M, Díaz-García E, Santiago DJ, et al. A network of macrophages supports mitochondrial homeostasis in the heart. *Cell*. (2020) 183:94–109.e23. doi: 10.1016/j.cell.2020.08.031
86. Porter KE, Turner NA. Cardiac fibroblasts: at the heart of myocardial remodeling. *Pharmacol Ther*. (2009) 123:255–78. doi: 10.1016/j.pharmthera.2009.05.002
87. Diwan A, Krenz M, Syed FM, Wansapura J, Ren X, Koesters AG, et al. Inhibition of ischemic cardiomyocyte apoptosis through targeted ablation of Bnip3 restrains postinfarction remodeling in mice. *J Clin Invest*. (2007) 117:2825–33. doi: 10.1172/JCI32490
88. Dorn GW II. Mitochondrial pruning by Nix and BNip3: an essential function for cardiac-expressed death factors. *J Cardiovasc Transl Res*. (2010) 3:374–83. doi: 10.1007/s12265-010-9174-x
89. Zhu P, Wan K, Yin M, Hu P, Que Y, Zhou X, et al. RIPK3 induces cardiomyocyte necroptosis via inhibition of AMPK-parkin-mitophagy in cardiac remodelling after myocardial infarction. *Oxid Med Cell Longev*. (2021) 2021:6635955. doi: 10.1155/2021/6635955

90. Song M, Mihara K, Chen Y, Scorrano L, Dorn GW II. Mitochondrial fission and fusion factors reciprocally orchestrate mitophagic culling in mouse hearts and cultured fibroblasts. *Cell Metab*. (2015) 21:273–86. doi: 10.1016/j.cmet.2014.12.011
91. Finkel T. Signal transduction by reactive oxygen species. *J Cell Biol*. (2011) 194:7–15. doi: 10.1083/jcb.201102095
92. D'Autréaux B, Toledano MB. ROS as signalling molecules: mechanisms that generate specificity in ROS homeostasis. *Nat Rev Mol Cell Biol*. (2007) 8:813–24. doi: 10.1038/nrm2256
93. Duchen MR. Mitochondria in health and disease: perspectives on a new mitochondrial biology. *Mol Aspects Med*. (2004) 25:365–451. doi: 10.1016/j.mam.2004.03.001
94. Dougherty CJ, Kubasiak LA, Frazier DP, Li H, Xiong WC, Bishopric NH, et al. Mitochondrial signals initiate the activation of c-Jun N-terminal kinase (JNK) by hypoxia-reoxygenation. *Faseb j*. (2004) 18:1060–70. doi: 10.1096/fj.04-1505com
95. Halestrap AP, Clarke SJ, Khaliulin I. The role of mitochondria in protection of the heart by preconditioning. *Biochim Biophys Acta*. (2007) 1767:1007–31. doi: 10.1016/j.bbabio.2007.05.008
96. Frazier DP, Wilson A, Dougherty CJ, Li H, Bishopric NH, Webster KA. PKC-alpha and TAK-1 are intermediates in the activation of c-Jun NH2-terminal kinase by hypoxia-reoxygenation. *Am J Physiol Heart Circ Physiol*. (2007) 292:H1675–84. doi: 10.1152/ajpheart.01132.2006
97. Zorov DB, Filburn CR, Klotz LO, Zweier JL, Sollott SJ. Reactive oxygen species (ROS)-induced ROS release: a new phenomenon accompanying induction of the mitochondrial permeability transition in cardiac myocytes. *J Exp Med*. (2000) 192:1001–14. doi: 10.1084/jem.192.7.1001
98. Aon MA, Cortassa S, Marbán E, O'Rourke B. Synchronized whole cell oscillations in mitochondrial metabolism triggered by a local release of reactive oxygen species in cardiac myocytes. *J Biol Chem*. (2003) 278:44735–44. doi: 10.1074/jbc.M302673200
99. Braunersreuther V, Montecucco F, Asrih M, Pelli G, Galan K, Frias M, et al. Role of NADPH oxidase isoforms NOX1, NOX2 and NOX4 in myocardial ischemia/reperfusion injury. *J Mol Cell Cardiol*. (2013) 64:99–107. doi: 10.1016/j.yjmcc.2013.09.007
100. Matsushima S, Kuroda J, Ago T, Zhai P, Ikeda Y, Oka S, et al. Broad suppression of NADPH oxidase activity exacerbates ischemia/reperfusion injury through inadvertent downregulation of hypoxia-inducible factor-1α and upregulation of peroxisome proliferator-activated receptor-α. *Circ Res*. (2013) 112:1135–49. doi: 10.1161/CIRCRESAHA.111.300171
101. Pagliaro P, Penna C. Redox signalling and cardioprotection: translatability and mechanism. *Br J Pharmacol*. (2015) 172:1974–95. doi: 10.1111/bph.12975
102. Heusch G. Molecular basis of cardioprotection: signal transduction in ischemic pre-, post-, remote conditioning. *Circ Res*. (2015) 116:674–99. doi: 10.1161/CIRCRESAHA.116.305348
103. Semenza GL. Oxygen-dependent regulation of mitochondrial respiration by hypoxia-inducible factor 1. *Biochem J*. (2007) 405:1–9. doi: 10.1042/BJ20070389
104. Semenza GL. Regulation of oxygen homeostasis by hypoxia-inducible factor 1. *Physiology*. (2009) 24:97–106. doi: 10.1152/physiol.00045.2008
105. Kim JW, Tchernyshyov I, Semenza GL, Dang CV. HIF-1-mediated expression of pyruvate dehydrogenase kinase: a metabolic switch required for cellular adaptation to hypoxia. *Cell Metab*. (2006) 3:177–85. doi: 10.1016/j.cmet.2006.02.002
106. Xu B, Zhang J, Strom J, Lee S, Chen QM. Myocardial ischemic reperfusion induces de novo Nrf2 protein translation. *Biochim Biophys Acta*. (2014) 1842:1638–47. doi: 10.1016/j.bbadis.2014.06.002
107. Itoh K, Chiba T, Takahashi S, Ishii T, Igarashi K, Katoh Y, et al. An Nrf2/small Maf heterodimer mediates the induction of phase II detoxifying enzyme genes through antioxidant response elements. *Biochem Biophys Res Commun*. (1997) 236:313–22. doi: 10.1006/bbrc.1997.6943
108. Kaludercic N, Mialet-Perez J, Paolocci N, Parini A, Di Lisa F. Monoamine oxidases as sources of oxidants in the heart. *J Mol Cell Cardiol*. (2014) 73:34–42. doi: 10.1016/j.yjmcc.2013.12.032
109. Bianchi P, Kunduzova O, Masini E, Cambon C, Bani D, Raimondi L, et al. Oxidative stress by monoamine oxidase mediates receptor-independent cardiomyocyte apoptosis by serotonin and postischemic myocardial injury. *Circulation*. (2005) 112:3297–305. doi: 10.1161/CIRCULATIONAHA.104.528133
110. Carpi A, Menabò R, Kaludercic N, Pelicci P, Di Lisa F, Giorgio M. The cardioprotective effects elicited by p66(Shc) ablation demonstrate the crucial role of mitochondrial ROS formation in ischemia/reperfusion injury. *Biochim Biophys Acta*. (2009) 1787:774–80. doi: 10.1016/j.bbabio.2009.04.001
111. Cohn JN, Ferrari R, Sharpe N. Cardiac remodeling–concepts and clinical implications: a consensus paper from an international forum on cardiac remodeling. behalf of an international forum on cardiac remodeling. *J Am Coll Cardiol*. (2000) 35:569–82. doi: 10.1016/S0735-1097(99)00630-0
112. Ma Y, Iyer RP, Jung M, Czubryt MP, Lindsey ML. Cardiac fibroblast activation post-myocardial infarction: current knowledge gaps. *Trends Pharmacol Sci*. (2017) 38:448–58. doi: 10.1016/j.tips.2017.03.001
113. Siwik DA, Colucci WS. Regulation of matrix metalloproteinases by cytokines and reactive oxygen/nitrogen species in the myocardium. *Heart Fail Rev*. (2004) 9:43–51. doi: 10.1023/B:HREV.0000011393.40674.13
114. Hori M, Nishida K. Oxidative stress and left ventricular remodelling after myocardial infarction. *Cardiovasc Res*. (2009) 81:457–64. doi: 10.1093/cvr/cvn335
115. Siwik DA, Pagano PJ, Colucci WS. Oxidative stress regulates collagen synthesis and matrix metalloproteinase activity in cardiac fibroblasts. *Am J Physiol Cell Physiol*. (2001) 280:C53–60. doi: 10.1152/ajpcell.2001.280.1.C53
116. Tyagi SC, Ratajska A, Weber KT. Myocardial matrix metalloproteinase(s): localization and activation. *Mol Cell Biochem*. (1993) 126:49–59. doi: 10.1007/BF01772207
117. Kinugawa S, Tsutsui H, Hayashidani S, Ide T, Suematsu N, Satoh S, et al. Treatment with dimethylthiourea prevents left ventricular remodeling and failure after experimental myocardial infarction in mice: role of oxidative stress. *Circ Res*. (2000) 87:392–8. doi: 10.1161/01.RES.87.5.392
118. Lacerda D, Ortiz V, Türck P, Campos-Carraro C, Zimmer A, Teixeira R, et al. Stilbenoid pterostilbene complexed with cyclodextrin preserves left ventricular function after myocardial infarction in rats: possible involvement of thiol proteins and modulation of phosphorylated GSK-3β. *Free Radic Res*. (2018) 52:988–99. doi: 10.1080/10715762.2018.1506115
119. Shiomi T, Tsutsui H, Matsusaka H, Murakami K, Hayashidani S, Ikeuchi M, et al. Overexpression of glutathione peroxidase prevents left ventricular remodeling and failure after myocardial infarction in mice. *Circulation*. (2004) 109:544–9. doi: 10.1161/01.CIR.0000109701.77059.E9
120. Matsushima S, Ide T, Yamato M, Matsusaka H, Hattori F, Ikeuchi M, et al. Overexpression of mitochondrial peroxiredoxin-3 prevents left ventricular remodeling and failure after myocardial infarction in mice. *Circulation*. (2006) 113:1779–86. doi: 10.1161/CIRCULATIONAHA.105.582239
121. Dai W, Shi J, Gupta RC, Sabbah HN, Hale SL, Kloner RA. Bendavia, a mitochondria-targeting peptide, improves postinfarction cardiac function, prevents adverse left ventricular remodeling, and restores mitochondria-related gene expression in rats. *J Cardiovasc Pharmacol*. (2014) 64:543–53. doi: 10.1097/FJC.0000000000000155
122. Hill MF, Singal PK. Right and left myocardial antioxidant responses during heart failure subsequent to myocardial infarction. *Circulation*. (1997) 96:2414–20. doi: 10.1161/01.CIR.96.7.2414
123. Nahrendorf M, Pittet MJ, Swirski FK. Monocytes: protagonists of infarct inflammation and repair after myocardial infarction. *Circulation*. (2010) 121:2437–45. doi: 10.1161/CIRCULATIONAHA.109.916346
124. Swirski FK, Nahrendorf M. Leukocyte behavior in atherosclerosis, myocardial infarction, heart failure. *Science*. (2013) 339:161–6. doi: 10.1126/science.1230719
125. Zhou R, Yazdi AS, Menu P, Tschopp J. A role for mitochondria in NLRP3 inflammasome activation. *Nature*. (2011) 469:221–5. doi: 10.1038/nature09663
126. Ip WK, Medzhitov R. Macrophages monitor tissue osmolarity and induce inflammatory response through NLRP3 and NLRC4 inflammasome activation. *Nat Commun*. (2015) 6:6931. doi: 10.1038/ncomms7931
127. Collins LV, Hajizadeh S, Holme E, Jonsson IM, Tarkowski A. Endogenously oxidized mitochondrial DNA induces in vivo and in vitro inflammatory responses. *J Leukoc Biol*. (2004) 75:995–1000. doi: 10.1189/jlb.0703328
128. Nakahira K, Haspel JA, Rathinam VA, Lee SJ, Dolinay T, Lam HC, et al. Autophagy proteins regulate innate immune responses by inhibiting the

release of mitochondrial DNA mediated by the NALP3 inflammasome. *Nat Immunol.* (2011) 12:222–30. doi: 10.1038/ni.1980
129. Lee GS, Subramanian N, Kim AI, Aksentijevich I, Goldbach-Mansky R, Sacks DB, et al. The calcium-sensing receptor regulates the NLRP3 inflammasome through Ca2+ and cAMP. *Nature.* (2012) 492:123–7. doi: 10.1038/nature11588
130. West AP, Khoury-Hanold W, Staron M, Tal MC, Pineda CM, Lang SM, et al. Mitochondrial DNA stress primes the antiviral innate immune response. *Nature.* (2015) 520:553–7. doi: 10.1038/nature14156
131. Palmieri EM, Menga A, Martín-Pérez R, Quinto A, Riera-Domingo C, De Tullio G, et al. Pharmacologic or genetic targeting of glutamine synthetase skews macrophages toward an m1-like phenotype and inhibits tumor metastasis. *Cell Rep.* (2017) 20:1654–66. doi: 10.1016/j.celrep.2017.07.054
132. Yurdagul A, Jr., Subramanian M, Wang X, Crown SB, Ilkayeva OR, et al. Macrophage metabolism of apoptotic cell-derived arginine promotes continual efferocytosis and resolution of injury. *Cell Metab.* (2020) 31:518–33.e10. doi: 10.1016/j.cmet.2020.01.001
133. Ryan DG, O'Neill LAJ. Krebs cycle rewired for macrophage and dendritic cell effector functions. *FEBS Lett.* (2017) 591:2992–3006. doi: 10.1002/1873-3468.12744
134. Mills EL, Kelly B, Logan A, Costa ASH, Varma M, Bryant CE, et al. Succinate dehydrogenase supports metabolic repurposing of mitochondria to drive inflammatory macrophages. *Cell.* (2016) 167:457–70.e13. doi: 10.1016/j.cell.2016.08.064
135. Liu PS, Wang H, Li X, Chao T, Teav T, Christen S, et al. α-ketoglutarate orchestrates macrophage activation through metabolic and epigenetic reprogramming. *Nat Immunol.* (2017) 18:985–94. doi: 10.1038/ni.3796
136. Zhang S, Weinberg S, DeBerge M, Gainullina A, Schipma M, Kinchen JM, et al. Efferocytosis fuels requirements of fatty acid oxidation and the electron transport chain to polarize macrophages for tissue repair. *Cell Metab.* (2019) 29:443–56.e5. doi: 10.1016/j.cmet.2018.12.004
137. Xu J, Chi F, Guo T, Punj V, Lee WN, French SW, et al. NOTCH reprograms mitochondrial metabolism for proinflammatory macrophage activation. *J Clin Invest.* (2015) 125:1579–90. doi: 10.1172/JCI76468
138. Zhang J, Zhang F. Suppressor of ras val-2 promotes inflammation-mediated oxidative stress and cell apoptosis in cardiomyocytes through activating Mst1-mROS signaling pathway. *J Recept Signal Transduct Res.* (2020) 40:224–30. doi: 10.1080/10799893.2020.1726953
139. Li Y, Chen B, Yang X, Zhang C, Jiao Y, Li P, et al. S100a8/a9 signaling causes mitochondrial dysfunction and cardiomyocyte death in response to ischemic/reperfusion injury. *Circulation.* (2019) 140:751–64. doi: 10.1161/CIRCULATIONAHA.118.039262
140. Grotenbreg G, Ploegh H. Chemical biology: dressed-up proteins. *Nature.* (2007) 446:993–5. doi: 10.1038/446993a
141. Geiss-Friedlander R, Melchior F. Concepts in sumoylation: a decade on. *Nat Rev Mol Cell Biol.* (2007) 8:947–56. doi: 10.1038/nrm2293
142. Fukuda H, Sano N, Muto S, Horikoshi M. Simple histone acetylation plays a complex role in the regulation of gene expression. *Brief Funct Genomic Proteomic.* (2006) 5:190–208. doi: 10.1093/bfgp/ell032
143. Chu S, Ferro TJ. Sp1: regulation of gene expression by phosphorylation. *Gene.* (2005) 348:1–11. doi: 10.1016/j.gene.2005.01.013
144. Fukushima A, Lopaschuk GD. Acetylation control of cardiac fatty acid β-oxidation and energy metabolism in obesity, diabetes, heart failure. *Biochim Biophys Acta.* (2016) 1862:2211–20. doi: 10.1016/j.bbadis.2016.07.020
145. Parry TL, Willis MS. Cardiac ubiquitin ligases: their role in cardiac metabolism, autophagy, cardioprotection and therapeutic potential. *Biochim Biophys Acta.* (2016) 1862:2259–69. doi: 10.1016/j.bbadis.2016.07.002
146. Nan J, Zhu W, Rahman MS, Liu M, Li D, Su S, et al. Molecular regulation of mitochondrial dynamics in cardiac disease. *Biochim Biophys Acta Mol Cell Res.* (2017) 1864:1260–73. doi: 10.1016/j.bbamcr.2017.03.006
147. Fang JK, Prabu SK, Sepuri NB, Raza H, Anandatheerthavarada HK, Galati D, et al. Site specific phosphorylation of cytochrome c oxidase subunits I, IVi1 and Vb in rabbit hearts subjected to ischemia/reperfusion. *FEBS Lett.* (2007) 581:1302–10. doi: 10.1016/j.febslet.2007.02.042
148. Prabu SK, Anandatheerthavarada HK, Raza H, Srinivasan S, Spear JF, Avadhani NG. Protein kinase A-mediated phosphorylation modulates cytochrome c oxidase function and augments hypoxia and myocardial ischemia-related injury. *J Biol Chem.* (2006) 281:2061–70. doi: 10.1074/jbc.M507741200
149. Wegrzyn J, Potla R, Chwae YJ, Sepuri NB, Zhang Q, Koeck T, et al. Function of mitochondrial Stat3 in cellular respiration. *Science.* (2009) 323:793–7. doi: 10.1126/science.1164551
150. Heusch G, Musiolik J, Gedik N, Skyschally A. Mitochondrial STAT3 activation and cardioprotection by ischemic postconditioning in pigs with regional myocardial ischemia/reperfusion. *Circ Res.* (2011) 109:1302–8. doi: 10.1161/CIRCRESAHA.111.255604
151. Boengler K, Hilfiker-Kleiner D, Drexler H, Heusch G, Schulz R. The myocardial JAK/STAT pathway: from protection to failure. *Pharmacol Ther.* (2008) 120:172–85. doi: 10.1016/j.pharmthera.2008.08.002
152. Nandi D, Tahiliani P, Kumar A, Chandu D. The ubiquitin-proteasome system. *J Biosci.* (2006) 31:137–55. doi: 10.1007/BF02705243
153. Schmidt M, Finley D. Regulation of proteasome activity in health and disease. *Biochim Biophys Acta.* (2014) 1843:13–25. doi: 10.1016/j.bbamcr.2013.08.012
154. Sun T, Ding W, Xu T, Ao X, Yu T, Li M, et al. Parkin regulates programmed necrosis and myocardial ischemia/reperfusion injury by targeting Cyclophilin-D. *Antioxid Redox Signal.* (2019) 31:1177–93. doi: 10.1089/ars.2019.7734
155. Dalal S, Daniels CR, Li Y, Wright GL, Singh M, Singh K. Exogenous ubiquitin attenuates hypoxia/reoxygenation-induced cardiac myocyte apoptosis via the involvement of CXCR4 and modulation of mitochondrial homeostasis. *Biochem Cell Biol.* (2020) 98:492–501. doi: 10.1139/bcb-2019-0339
156. Yang F, Wu R, Jiang Z, Chen J, Nan J, Su S, et al. Leptin increases mitochondrial OPA1 via GSK3-mediated OMA1 ubiquitination to enhance therapeutic effects of mesenchymal stem cell transplantation. *Cell Death Dis.* (2018) 9:556. doi: 10.1038/s41419-018-0579-9
157. Yeh ET. SUMOylation and De-SUMOylation: wrestling with life's processes. *J Biol Chem.* (2009) 284:8223–7. doi: 10.1074/jbc.R800050200
158. Bian X, Xu J, Zhao H, Zheng Q, Xiao X, Ma X, et al. Zinc-induced SUMOylation of dynamin-related protein 1 protects the heart against ischemia-reperfusion injury. *Oxid Med Cell Longev.* (2019) 2019:1232146. doi: 10.1155/2019/1232146
159. Gao L, Zhao Y, He J, Yan Y, Xu L, Lin N, et al. The desumoylating enzyme sentrin-specific protease 3 contributes to myocardial ischemia reperfusion injury. *J Genet Genomics.* (2018) 45:125–35. doi: 10.1016/j.jgg.2017.12.002
160. Hafner AV, Dai J, Gomes AP, Xiao CY, Palmeira CM, Rosenzweig A, et al. Regulation of the mPTP by SIRT3-mediated deacetylation of CypD at lysine 166 suppresses age-related cardiac hypertrophy. *Aging.* (2010) 2:914–23. doi: 10.18632/aging.100252
161. Parodi-Rullán RM, Chapa-Dubocq X, Rullán PJ, Jang S, Javadov S. High sensitivity of SIRT3 deficient hearts to ischemia-reperfusion is associated with mitochondrial abnormalities. *Front Pharmacol.* (2017) 8:275. doi: 10.3389/fphar.2017.00275
162. Porter GA, Urciuoli WR, Brookes PS, Nadtochiy SM. SIRT3 deficiency exacerbates ischemia-reperfusion injury: implication for aged hearts. *Am J Physiol Heart Circ Physiol.* (2014) 306:H1602–9. doi: 10.1152/ajpheart.00027.2014
163. Lu Y, Feng Y, Liu D, Zhang Z, Gao K, Zhang W, et al. Thymoquinone attenuates myocardial ischemia/reperfusion injury through activation of SIRT1 signaling. *Cell Physiol Biochem.* (2018) 47:1193–206. doi: 10.1159/000490216
164. Zhao TC, Cheng G, Zhang LX, Tseng YT, Padbury JF. Inhibition of histone deacetylases triggers pharmacologic preconditioning effects against myocardial ischemic injury. *Cardiovasc Res.* (2007) 76:473–81. doi: 10.1016/j.cardiores.2007.08.010
165. Boylston JA, Sun J, Chen Y, Gucek M, Sack MN, Murphy E. Characterization of the cardiac succinylome and its role in ischemia-reperfusion injury. *J Mol Cell Cardiol.* (2015) 88:73–81. doi: 10.1016/j.yjmcc.2015.09.005
166. Duarte FV, Palmeira CM, Rolo AP. The emerging role of MitomiRs in the pathophysiology of human disease. *Adv Exp Med Biol.* (2015) 888:123–54. doi: 10.1007/978-3-319-22671-2_8
167. Bandiera S, Rüberg S, Girard M, Cagnard N, Hanein S, Chrétien D, et al. Nuclear outsourcing of RNA interference components to human mitochondria. *PLoS One.* (2011) 6:e20746. doi: 10.1371/journal.pone.0020746

168. Baradan R, Hollander JM, Das S. Mitochondrial miRNAs in diabetes: just the tip of the iceberg. *Can J Physiol Pharmacol.* (2017) 95:1156–62. doi: 10.1139/cjpp-2016-0580
169. Fang G, Qi J, Huang L, Zhao X. LncRNA MRAK048635_P1 is critical for vascular smooth muscle cell function and phenotypic switching in essential hypertension. *Biosci Rep.* (2019) 39:BSR20182229. doi: 10.1042/BSR20182229
170. Bostjancic E, Zidar N, Stajner D, Glavac D. MicroRNA miR-1 is up-regulated in remote myocardium in patients with myocardial infarction. *Folia Biol.* (2010) 56:27–31.
171. Yan K, An T, Zhai M, Huang Y, Wang Q, Wang Y, et al. Mitochondrial miR-762 regulates apoptosis and myocardial infarction by impairing ND2. *Cell Death Dis.* (2019) 10:500. doi: 10.1038/s41419-019-1734-7
172. Devaux Y, Zangrando J, Schroen B, Creemers EE, Pedrazzini T, Chang CP, et al. Long noncoding RNAs in cardiac development and ageing. *Nat Rev Cardiol.* (2015) 12:415–25. doi: 10.1038/nrcardio.2015.55
173. Gomes CPC, Spencer H, Ford KL, Michel LYM, Baker AH, Emanueli C, et al. The function and therapeutic potential of long non-coding RNAs in cardiovascular development and disease. *Mol Ther Nucleic Acids.* (2017) 8:494–507. doi: 10.1016/j.omtn.2017.07.014
174. Dong Y, Yoshitomi T, Hu JF, Cui J. Long noncoding RNAs coordinate functions between mitochondria and the nucleus. *Epigenetics Chromatin.* (2017) 10:41. doi: 10.1186/s13072-017-0149-x
175. Kumarswamy R, Bauters C, Volkmann I, Maury F, Fetisch J, Holzmann A, et al. Circulating long noncoding RNA, LIPCAR, predicts survival in patients with heart failure. *Circ Res.* (2014) 114:1569–75. doi: 10.1161/CIRCRESAHA.114.303915
176. Li HJ, Sun XM, Li ZK, Yin QW, Pang H, Pan JJ, et al. LncRNA UCA1 promotes mitochondrial function of bladder cancer via the MiR-195/ARL2 signaling pathway. *Cell Physiol Biochem.* (2017) 43:2548–61. doi: 10.1159/000484507
177. Wang K, Gan TY, Li N, Liu CY, Zhou LY, Gao JN, et al. Circular RNA mediates cardiomyocyte death via miRNA-dependent upregulation of MTP18 expression. *Cell Death Differ.* (2017) 24:1111–20. doi: 10.1038/cdd.2017.61
178. Adlam VJ, Harrison JC, Porteous CM, James AM, Smith RA, Murphy MP, et al. Targeting an antioxidant to mitochondria decreases cardiac ischemia-reperfusion injury. *Faseb J.* (2005) 19:1088–95. doi: 10.1096/fj.05-3718com
179. Zhao K, Zhao GM, Wu D, Soong Y, Birk AV, Schiller PW, et al. Cell-permeable peptide antioxidants targeted to inner mitochondrial membrane inhibit mitochondrial swelling, oxidative cell death, reperfusion injury. *J Biol Chem.* (2004) 279:34682–90. doi: 10.1074/jbc.M402999200
180. Szeto HH. Mitochondria-targeted cytoprotective peptides for ischemia-reperfusion injury. *Antioxid Redox Signal.* (2008) 10:601–19. doi: 10.1089/ars.2007.1892
181. Cassarino DS, Parks JK, Parker WD, Jr., Bennett JP Jr. The parkinsonian neurotoxin MPP+ opens the mitochondrial permeability transition pore and releases cytochrome c in isolated mitochondria via an oxidative mechanism. *Biochim Biophys Acta.* (1999) 1453:49–62. doi: 10.1016/S0925-4439(98)00083-0
182. Cho J, Won K, Wu D, Soong Y, Liu S, Szeto HH, et al. Potent mitochondria-targeted peptides reduce myocardial infarction in rats. *Coron Artery Dis.* (2007) 18:215–20. doi: 10.1097/01.mca.0000236285.71683.b6
183. Sloan RC, Moukdar F, Frasier CR, Patel HD, Bostian PA, Lust RM, et al. Mitochondrial permeability transition in the diabetic heart: contributions of thiol redox state and mitochondrial calcium to augmented reperfusion injury. *J Mol Cell Cardiol.* (2012) 52:1009–18. doi: 10.1016/j.yjmcc.2012.02.009
184. Iranzo O. Manganese complexes displaying superoxide dismutase activity: a balance between different factors. *Bioorg Chem.* (2011) 39:73–87. doi: 10.1016/j.bioorg.2011.02.001
185. Daubert MA, Yow E, Dunn G, Marchev S, Barnhart H, Douglas PS, et al. Novel mitochondria-targeting peptide in heart failure treatment: a randomized, placebo-controlled trial of elamipretide. *Circ Heart Fail.* (2017) 10:e004389. doi: 10.1161/CIRCHEARTFAILURE.117.004389
186. Gibson CM, Giugliano RP, Kloner RA, Bode C, Tendera M, Jánosi A, et al. EMBRACE STEMI study: a Phase 2a trial to evaluate the safety, tolerability, and efficacy of intravenous MTP-131 on reperfusion injury in patients undergoing primary percutaneous coronary intervention. *Eur Heart J.* (2016) 37:1296–303. doi: 10.1093/eurheartj/ehv597
187. Cerrato CP, Pirisinu M, Vlachos EN, Langel Ü. Novel cell-penetrating peptide targeting mitochondria. *Faseb J.* (2015) 29:4589–99. doi: 10.1096/fj.14-269225
188. Cerrato CP, Langel Ü. Effect of a fusion peptide by covalent conjugation of a mitochondrial cell-penetrating peptide and a glutathione analog peptide. *Mol Ther Methods Clin Dev.* (2017) 5:221–31. doi: 10.1016/j.omtm.2017.04.010
189. Gomes KM, Campos JC, Bechara LR, Queliconi B, Lima VM, Disatnik MH, et al. Aldehyde dehydrogenase 2 activation in heart failure restores mitochondrial function and improves ventricular function and remodelling. *Cardiovasc Res.* (2014) 103:498–508. doi: 10.1093/cvr/cvu125
190. Piot C, Croisille P, Staat P, Thibault H, Rioufol G, Mewton N, et al. Effect of cyclosporine on reperfusion injury in acute myocardial infarction. *N Engl J Med.* (2008) 359:473–81. doi: 10.1056/NEJMoa071142
191. LaRocca TJ, Henson GD, Thorburn A, Sindler AL, Pierce GL, Seals DR. Translational evidence that impaired autophagy contributes to arterial ageing. *J Physiol.* (2012) 590:3305–16. doi: 10.1113/jphysiol.2012.229690
192. Sciarretta S, Yee D, Nagarajan N, Bianchi F, Saito T, Valenti V, et al. Trehalose-induced activation of autophagy improves cardiac remodeling after myocardial infarction. *J Am Coll Cardiol.* (2018) 71:1999–2010. doi: 10.1016/j.jacc.2018.02.066
193. Eisenberg T, Abdellatif M, Schroeder S, Primessnig U, Stekovic S, Pendl T, et al. Cardioprotection and lifespan extension by the natural polyamine spermidine. *Nat Med.* (2016) 22:1428–1438. doi: 10.1038/nm.4222
194. Yan J, Yan JY, Wang YX, Ling YN, Song XD, Wang SY, et al. Spermidine-enhanced autophagic flux improves cardiac dysfunction following myocardial infarction by targeting the AMPK/mTOR signalling pathway. *Br J Pharmacol.* (2019) 176:3126–42. doi: 10.1111/bph.14706
195. Ding M, Dong Q, Liu Z, Liu Z, Qu Y, Li X, et al. Inhibition of dynamin-related protein 1 protects against myocardial ischemia-reperfusion injury in diabetic mice. *Cardiovasc Diabetol.* (2017) 16:19. doi: 10.1186/s12933-017-0501-2
196. Veeranki S, Tyagi SC. Mdivi-1 induced acute changes in the angiogenic profile after ischemia-reperfusion injury in female mice. *Physiol Rep.* (2017) 5:e13298. doi: 10.14814/phy2.13298
197. Wang YT, Lim Y, McCall MN, Huang KT, Haynes CM, Nehrke K, et al. Cardioprotection by the mitochondrial unfolded protein response requires ATF5. *Am J Physiol Heart Circ Physiol.* (2019) 317:H472–78. doi: 10.1152/ajpheart.00244.2019
198. Sanders MJ, Ali ZS, Hegarty BD, Heath R, Snowden MA, Carling D. Defining the mechanism of activation of AMP-activated protein kinase by the small molecule A-769662, a member of the thienopyridone family. *J Biol Chem.* (2007) 282:32539–48. doi: 10.1074/jbc.M706543200
199. Song T, Lv LY, Xu J, Tian ZY, Cui WY, Wang QS, et al. Diet-induced obesity suppresses sevoflurane preconditioning against myocardial ischemia-reperfusion injury: role of AMP-activated protein kinase pathway. *Exp Biol Med.* (2011) 236:1427–36. doi: 10.1258/ebm.2011.011165
200. Diebold S, Moellmann J, Kahles F, Haj-Yehia E, Liehn EA, Nickel A, et al. Myocardial infarction is sufficient to increase GLP-1 secretion, leading to improved left ventricular contractility and mitochondrial respiratory capacity. *Diabetes Obes Metab.* (2018) 20:2911–18. doi: 10.1111/dom.13472
201. Wang X, Ding Z, Yang F, Dai Y, Chen P, Theus S, et al. Modulation of myocardial injury and collagen deposition following ischaemia-reperfusion by linagliptin and liraglutide, both together. *Clin Sci.* (2016) 130:1353–62. doi: 10.1042/CS20160061
202. McDonagh TA, Metra M, Adamo M, Gardner RS, Baumbach A, Böhm M, et al. 2021 ESC Guidelines for the diagnosis and treatment of acute and chronic heart failure. *Eur Heart J.* (2021) 42:3599–726. doi: 10.1093/eurheartj/ehab368
203. Shao Q, Meng L, Lee S, Tse G, Gong M, Zhang Z, et al. Empagliflozin, a sodium glucose co-transporter-2 inhibitor, alleviates atrial remodeling and improves mitochondrial function in high-fat diet/streptozotocin-induced diabetic rats. *Cardiovasc Diabetol.* (2019) 18:165. doi: 10.1186/s12933-019-0964-4
204. Hu Z, Ju F, Du L, Abbott GW. Empagliflozin protects the heart against ischemia/reperfusion-induced sudden cardiac death. *Cardiovasc Diabetol.* (2021) 20:199. doi: 10.1186/s12933-021-01392-6

205. Palee S, Higgins L, Leech T, Chattipakorn SC, Chattipakorn N. Acute metformin treatment provides cardioprotection via improved mitochondrial function in cardiac ischemia / reperfusion injury. *Biomed Pharmacother.* (2020) 130:110604. doi: 10.1016/j.biopha.2020.110604
206. Thummasorn S, Shinlapawittayatorn K, Chattipakorn SC, Chattipakorn N. High-dose Humanin analogue applied during ischemia exerts cardioprotection against ischemia/reperfusion injury by reducing mitochondrial dysfunction. *Cardiovasc Ther.* (2017) 35. doi: 10.1111/1755-5922.12289
207. Shanmugam K, Ravindran S, Kurian GA, Rajesh M. Fisetin confers cardioprotection against myocardial ischemia reperfusion injury by suppressing mitochondrial oxidative stress and mitochondrial dysfunction and inhibiting glycogen synthase kinase 3β activity. *Oxid Med Cell Longev.* (2018) 2018:9173436. doi: 10.1155/2018/9173436
208. Yang Y, Zhang Y, Liu X, Zuo J, Wang K, Liu W, et al. Exogenous taurine attenuates mitochondrial oxidative stress and endoplasmic reticulum stress in rat cardiomyocytes. *Acta Biochim Biophys Sin.* (2013) 45:359–67. doi: 10.1093/abbs/gmt034

Conflict of Interest: The authors declare that the research was conducted in the absence of any commercial or financial relationships that could be construed as a potential conflict of interest.

Publisher's Note: All claims expressed in this article are solely those of the authors and do not necessarily represent those of their affiliated organizations, or those of the publisher, the editors and the reviewers. Any product that may be evaluated in this article, or claim that may be made by its manufacturer, is not guaranteed or endorsed by the publisher.

Copyright © 2021 Xin, Zhang, Li, Gao, Li, Li, Hu and Li. This is an open-access article distributed under the terms of the Creative Commons Attribution License (CC BY). The use, distribution or reproduction in other forums is permitted, provided the original author(s) and the copyright owner(s) are credited and that the original publication in this journal is cited, in accordance with accepted academic practice. No use, distribution or reproduction is permitted which does not comply with these terms.

GLOSSARY

ALDH2, Aldehyde dehydrogenase 2; ANT, adenosine nucleotide translocase; AMPK, Adenosine 5′-monophosphate (AMP)-activated protein kinase; AMI, Acute Myocardial Infarction; ARE, Antioxidant response elements; ASC, Apoptosis-associated speck-like protein; α-KG, α-ketoglutarate; ATP, Adenosine triphosphate; BNIP3, BCL2 Interacting Protein 3; cGAS, GMP-AMP synthase; circRNA, covalently closed, single-stranded RNA; CNC, Cap "n" collar; CREB, cAMP-response element binding protein; CypD, Cyclophilin D; DAMP3, Danger signalling molecules 3; DPP4, Dipeptidyl peptidase-4; Drp1, Dynamin-related protein1; ECM, Extracellular matrix; ETC, electron transport chain; ERK, Extracellular signal-regulated kinas; FAO, Fatty acid β-oxidation; FUNDC1, FUN14 Domain Containing 1; GLP1, Glucagon-like peptide 1; Gpx, Glutathione peroxidase; GSK3, Glycogen synthase kinase-3; GTPase, Guanosine triphosphatases; HDAC, Histone deacetylases; HF, Heart failure; HIF, Hypoxia-inducible factor; hMSC, Human mesenchymal stem cells; IHD, Ischemic heart disease; IL-1β, Interleukin-1β; IRI, Ischemia reperfusion injury; LC3, Microtubule- associated protein1 light chain 3; lncRNA, Long noncoding RNAs; MAO, Monoamine oxidases; MAPK, Mitogen - activated protein kinase; MCU, Mitochondrial Calcium Uniporter; MFACR, Mitochondrial fission and apoptosis-related circRNA; Mfn1/2, Mitofusin 1/2; miRNA, MicroRNA; mitomiRs, Mitochondria miRNAs; MMP, Matrix processing peptidases; MPP, Matrix metalloproteinases; mPTP, Mitochondrial permeability transition pore; mRNA, Messenger RNA; Mst1, Mammalian STE20-like protein kinase 1; mTOR, Mammalian target of rapamycin; NAPDH, Nicotinamide adenine dinucleotide phosphate; NLRP3, Nucleotide-binding oligomerization domain-like receptor family pyrin domain containing 3; Nox, NADPH oxidases; NR4A1, Nuclear receptor subfamily 4 group A member 1; OMM, Outer mitochondrial membrane; OPA, Optica atrophy protein 1; OXPHOS, Oxidative phosphorylation; PAMP, Pathogen-associated molecular patterns; PCI, Percutaneous coronary intervention; PINK, PTEN-induced putative kinase 1; PTM, Post-translational modification; RIPK3, Receptor-interacting protein 3; ROS, Reactive oxygen species; SDH, Succinate dehydrogenase; SENP3, Sentrin-specific protease 3; SGLT2, Sodium-glucose cotransporter 2; SIRT, Sirtuin; SIAH1, Siah E3 ubiquitin protein ligase 1; SMURF1, Smad ubiquitination regulatory factor-1; SOD, Superoxide dismutase; SRV, Suppressor of ras val-2; STAT3, Signal transducer and activator of transcription 3; STING, Stimulator of interferon genes; SUMO, Small ubiquitin-like modifier; TBK1, TANK-binding kinase 1; TCA, Tricarboxylic acid cycle; TNF-α, Tumour necrosis factor α; UPR^{mt}, Mitochondrial unfolded protein response; UPS, Ubiquitin-proteasome system; UTR, untranslated region; VDAC1, Voltage-dependent anion-selective channel protein 1; WDR26, WD repeat domain 26.

frontiers in Cardiovascular Medicine

REVIEW
published: 07 December 2021
doi: 10.3389/fcvm.2021.789458

Ketone Body Metabolism in the Ischemic Heart

*Stephen C. Kolwicz Jr**

Heart and Muscle Metabolism Laboratory, Department of Health and Exercise Physiology, Ursinus College, Collegeville, PA, United States

Ketone bodies have been identified as an important, alternative fuel source in heart failure. In addition, the use of ketone bodies as a fuel source has been suggested to be a potential ergogenic aid for endurance exercise performance. These findings have certainly renewed interest in the use of ketogenic diets and exogenous supplementation in an effort to improve overall health and disease. However, given the prevalence of ischemic heart disease and myocardial infarctions, these strategies may not be ideal for individuals with coronary artery disease. Although research studies have clearly defined changes in fatty acid and glucose metabolism during ischemia and reperfusion, the role of ketone body metabolism in the ischemic and reperfused myocardium is less clear. This review will provide an overview of ketone body metabolism, including the induction of ketosis via physiological or nutritional strategies. In addition, the contribution of ketone body metabolism in healthy and diseased states, with a particular emphasis on ischemia-reperfusion (I-R) injury will be discussed.

Keywords: ischemia, reperfusion, hypoxia, beta-hydroxybutyrate, ketosis

OPEN ACCESS

Edited by:
Haiyang Tang,
University of Arizona, United States

Reviewed by:
Christopher Q. Rogers,
University of South Florida,
United States
Rami Al Batran,
Université de Montréal, Canada

***Correspondence:**
Stephen C. Kolwicz Jr
skolwicz@ursinus.edu

Specialty section:
This article was submitted to Cardiovascular Metabolism, a section of the journal Frontiers in Cardiovascular Medicine

Received: *04 October 2021*
Accepted: *16 November 2021*
Published: *07 December 2021*

Citation:
Kolwicz SC Jr (2021) Ketone Body Metabolism in the Ischemic Heart. Front. Cardiovasc. Med. 8:789458. doi: 10.3389/fcvm.2021.789458

INTRODUCTION

Ketone body metabolism has become an important topic in the scientific and medical communities over the last several years. The identification of elevated ketone body oxidation in hypertrophied and failing hearts (1, 2) and the potential of exogenous ketone body supplements to promote exercise performance (3) have been a critical driver in research. Since ketone bodies are suggested to be more energy efficient than glucose or fatty acids (4, 5), the utilization of ketone bodies as an energy source may be advantageous for failing myocardium or exercising skeletal muscle. Certainly, the therapeutic and ergogenic potential of nutritional or pharmacological strategies that promote cardiac and muscular ketone body metabolism are of increased interest.

Ketogenic diets (KD) are high fat, low carbohydrates that were originally developed for the treatment of epilepsy (6). KDs can also be an effective treatment for inherited metabolic disorders of glucose metabolism (7). Although KDs appear to be effective strategies for weight loss, at least in the short-term, their ability to promote exercise performance appears to be limited (8). The use of exogenous ketone body supplementation has been of increased interest in exercise and sport performance, but the effectiveness of supplements remains controversial (9, 10). Although the KD or supplementation strategies appear to be recognized as plausible treatments in models of cardiac dysfunction and failure (11), there is less discussion regarding the role of ketone body metabolism in ischemic heart disease.

Research studies have uncovered critical changes in cardiac substrate metabolism under conditions of stress, especially in pathological hypertrophy (12, 13), heart failure (14, 15), ischemia-reperfusion (16–18), and obesity/diabetes (19, 20). Although the importance of ketone body

metabolism to the hypertrophied and failing heart has been well-discussed, the contribution of ketone body oxidation to the myocardium following ischemia has received less attention. In this review, ketone body metabolism in the healthy and diseased myocardium will be discussed, with a particular focus on the impact of ketone body metabolism in the functional recovery from ischemic injury.

METABOLIC PATHWAYS OF KETONE BODIES

Ketone bodies are 4-carbon molecules that are synthesized through the process known as ketogenesis and broken down and utilized within tissues via the ketolysis pathway (also referred to as ketone body oxidation). Three ketone bodies exist: acetone, acetoacetate, and beta-hydroxybutyrate (β-OHB). β-OHB is the ketone body which is in highest concentration in the blood and is typically measured in many commercially available assay kits or handheld meters used in the research setting. The liver is the primary site of ketogenesis (**Figure 1**), which generates acetyl-CoA via beta-oxidation of fatty acids. The acetyl-CoA is ultimately converted into acetoacetone or β-OHB via reactions that require several enzymes, namely mitochondrial acetyl-CoA acetyltransferase 1 (Acat1, commonly referred to as thiolase), 3-hydroxy-3-methylglutaryl-CoA synthase (Hmgcs2), HMGC-CoA lyase (Hmgcl), and mitochondrial beta-hydroxybutyrate dehydrogenase (Bdh1). Of note, acetoacetone is generated as a result of the Hmgcl reaction and can be converted to β-OHB via Bdh1. Once β-OHB enters peripheral tissues via monocarboxylate transporters, MCT1 (encoded by the Slc16a1 gene) or MCT2 (encoded by the Slc16a7 gene) (21), the ketolytic process commences (**Figure 1**). Acetyl CoA is produced through rapid oxidation of β-OHB by Bdh1, succinyl-CoA:3-oxoacid-CoA transferase (Scot, encoded by the Oxct1 gene), and Acat1, which then is available for entry into the tricarboxylic acid (TCA) cycle. These ketolytic enzymes are present in the heart and the reactions are primarily based on the substrate availability. However, the Scot reaction is also dependent upon the availability of succinyl CoA.

Older texts often discussed the presence of ketone bodies as negative consequences of abnormal metabolic processes (22, 23). However, since serum ketone bodies are measurable in the fed and fasted condition of healthy humans and animals, there must be some metabolic value. In fact, the use of ketone bodies as a metabolic fuel is suggested to be more energy efficient (4, 5). However, the total ATP yield per carbon atom for ketone bodies is slightly above glucose (∼5.4 vs. ∼5.2), while both substrates lag behind fatty acids (∼6.7) (24, 25). In terms of ATP per oxygen (i.e., P/O ratio), ketone bodies are slightly lower than glucose (∼2.50 vs. ∼2.58), with both yielding higher ratios than fatty acids (∼2.33) (24, 25). Based on these values, ketone bodies would rank second on both scales in relation to glucose and fatty acids. However, in isolated perfused heart experiments in rodents, the presence of ketone bodies in the perfusate increased cardiac efficiency (26, 27) and ATP production (28). Therefore, the relationship of ketone bodies to overall cardiac metabolism may require more intricate examination.

PHYSIOLOGICAL AND NUTRITIONAL KETOSIS

Ketosis is defined as a physiological condition where serum ketone body concentrations are elevated acutely. Studies in humans and rodents commonly report serum ketone body concentrations in the range of ∼0.1 to 0.5 mM, so ketosis is generally identified as serum concentrations above 0.5 mM. Conditions that result in nutrient deprivation or low glucose availability, such as fasting/starvation and exercise (29, 30), are commonly associated with elevated serum ketone body concentrations, which is termed "physiological ketosis." Diabetics, particularly Type I diabetics, may also exhibit elevated serum ketone body levels (31, 32). However, when in the 3.8–25.0 mM range and accompanied by low arterial pH values, the term "ketoacidosis" is used to reflect a potentially dangerous pathological state (33–35). More recently, the term "nutritional ketosis" has been used to better identify a state where ketosis was induced by nutritional or supplementation strategies (36–38). The use of these specific terms could help differentiate between the physiological/pathological and/or intentional/unintentional causes of ketosis.

In our recent study, we explored physiological ketosis in response to both fasting and endurance exercise (29). Female mice fasted up to 8 h, demonstrated gradual increases in serum ketone body concentrations, which peaked at ∼ 0.8 mM (29). Our unpublished data showed that male mice respond similarly, with peak serum ketone body concentrations of ∼0.7 mM. In response to endurance exercise of up to 2.5 h, serum ketone body levels rose to ∼1.2 mM in female mice (29). Interestingly, this "exercise-induced ketosis" was blunted in fasted female mice (29). These values of physiological ketosis related to fasting or exercise are fairly consistent across the literature in both humans (39–41) and rodents (30, 42, 43). However, whether physiological ketosis is consistent between the sexes is relatively unexplored.

To induce nutritional ketosis, one strategy involves the consumption of the ketogenic diet (KD), a diet that is typically low in carbohydrates with high fat and adequate protein. The KD was originally used as a treatment for individuals with diabetes, epilepsy, and other neurological conditions approximately 100 years ago (6, 44, 45). This classical KD called for a fat to protein plus carbohydrate ratio of 4:1 (46), which typically results in a dietary intake of 80-90% of calories from fat, 10-15% calories from protein, and < 5% of calories from carbohydrate sources (5). Although the use of the KD in research has increased significantly over the last several years, the dietary composition can deviate quite substantially from the classical KD. In some human studies, dietary regimens referred to as low-carbohydrate KD (LCKD) or very low-carbohydrate KDs (VLCKD) are used with carbohydrates ranges from ∼10% to 45% of total calories (47–50). Despite the varied ranges of carbohydrate intake, all of these diets tend to be included in the KD category. Therefore,

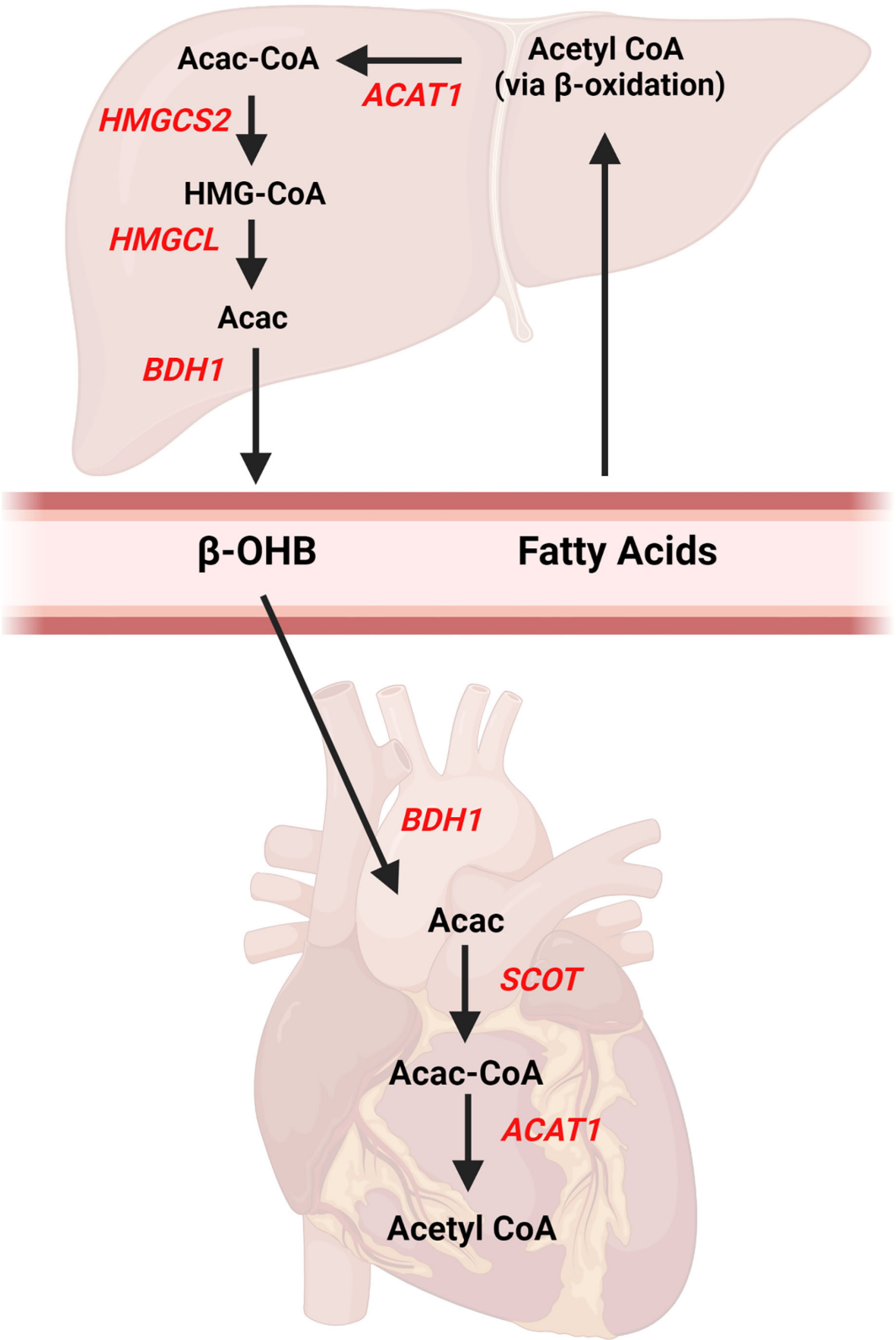

FIGURE 1 | Ketone body pathways in the liver and heart. Ketogenesis occurs primarily in the liver from fatty acids obtained from the blood. Acetyl CoA is formed from hepatic beta-oxidation and ultimately converted to beta-hydroxybutyrate (β-OHB) via multiple enzymatic reactions. Once β-OHB enters the heart, a series of reactions

(Continued)

FIGURE 1 | forms Acetyl CoA for entry into Kreb's Cycle. AcAc, acetoacetate; Acac CoA, acetoacetyl CoA; ACAT1, acetyl-coenzyme A acetyltransferase 1, βOHB, beta-hydroxybutyrate; BDH1, mitochondrial beta-hydroxybutyrate dehydrogenase; HMGCS2, 3-hydroxy-3-methylglutaryl-CoA synthase 2; HMGCL, HMGC-CoA lyase; SCOT, succinyl-CoA:3-oxoacid-CoA transferase. Created with BioRender.com.

careful attention to the details of the dietary composition is needed to adequately interpret experimental findings.

Although the KD has been successful for weight reduction in mice (30, 51) and humans (52, 53), the high fat and low carbohydrate intake may be problematic for long-term adherence. Moreover, KDs are associated with negative consequences such as abnormal glucose homeostasis (54–56), hyperlipidemia (29, 54, 57, 58), and liver steatosis (29, 55). Therefore, another strategy to induce nutritional ketosis has been developed, which involves exogenous ingestion of ketone bodies as a nutritional supplement. These ketone body supplements are now commercially available and have been tested in several studies evaluating the potential ergogenic aid on exercise performance (3, 59–63). However, special attention must be paid to the exact formulation of these supplements as they are available in ketone salts (KS) or ketone esters (KE). Although more readily available and inexpensive, the use of KS supplements can be problematic, depending on the exact formulation, which may include β-OHB or 1,3-butandeniol (BD). In the salt form, β-OHB is present in both the active (D) and non-metabolizable (L) form, which may result in a less effective increase in serum ketone bodies (64, 65). KS supplements that contain BD may also be a less desirable method to induce ketosis since dehydrogenase enzymes in the liver are required to create β-OHB (64, 66). Although several formulations of KE supplements are available, the (R)-3-hydroxybutyl (R)-3-hydroxybutyrate ketone monoester, which converts to D-β-OHB and BD (67) has become the most commonly used. This KE, when combined with carbohydrates, elicited an increase in exercise performance in trained cyclists (3). Of note, other studies using KE supplementation have not consistently shown an increase in exercise performance (61–63).

KETONE BODY METABOLISM IN THE HEALTHY HEART

The term, metabolic flexibility, has become synonymous with the cardiometabolic profile of the healthy heart. Due to the enormous requirement for continual replenishment of energy stores, the heart must possess an ability to utilize any carbon-based substrate available. To this end, the heart can metabolize the exogenous substrates fatty acids, glucose, lactate, amino acids, and ketone bodies to produce energy. Research suggests that the normal healthy heart generates approximately 60-80% of its energy requirements from fatty acids, with approximately 10-20% from glucose (68–70). Lactate can also be an important fuel, particularly during instances of increased workload, such as exercise (71, 72). The contribution of amino acids to cardiac energy metabolism is reported to be low, ∼1-3% (73, 74). However, this low contribution to oxidative metabolism should not be interpreted as insignificant as disruption of amino acid catabolism in genetic models can be detrimental, particularly in stressed conditions (75).

Although previously considered to be a relatively minor substrate, ketone body oxidation is reported to contribute ∼10-20% to cardiac energy metabolism (28, 43). Interestingly, ketone body oxidation may not be essential to the healthy myocardium as cardiac-specific deletion of Bdh1 (76) or Scot (Oxct1) (77) virtually eliminates ketone body oxidation with no myocardial phenotype in unstressed conditions. In contrast, cardiomyocyte overexpression of Bdh1 increases ketone body oxidation by approximately 70% without negatively affecting cardiac function (78). These studies in transgenic mice would suggest that low or high ketone body oxidation is relatively inconsequential to the heart in unchallenged situations. However, a potential concern is the effect of changes in ketone body availability and delivery on the usage of other fuels, particularly glucose and fatty acids, on cardiac metabolism. Indeed, increased delivery of β-OHB suppresses fatty acid oxidation but does not significantly affect glucose oxidation in animal models (30, 76, 79). Increased ketone bodies also decreased myocardial glucose uptake in humans (80). However, increasing β-OHB concentrations in working heart preparation in mice did not affect fatty acid oxidation and tended to enhance glucose oxidation (28). In relation to this, increasing glucose uptake via overexpression of glucose transporter 4 (Glut4) suppressed ketone body oxidation in isolated perfused mouse hearts (81). These seemingly discrepant findings are likely due to differences in the experimental logistics, particularly in the concentrations of ketone bodies employed. However, the influence of changes in ketone body oxidation on oxidation of other substrates appears to be essentially meaningless, as cardiac function remains relatively normal in these situations, thus highlighting the metabolic flexibility of the heart under normal, baseline conditions.

KETONE BODY METABOLISM IN THE OBESE AND DIABETIC HEART

The discussion of ketone bodies in settings of obesity and diabetes are traditionally thought to represent a pathophysiological state due to the condition of diabetic ketoacidosis (DKA) that can result in serious clinical complications (33–35). Indeed, Type 1 diabetic (T1D) patients without insulin therapy quickly develop ketonemia within 5 h (32). Therefore, the American Diabetes Association recommends regular monitoring of both glucose and ketone bodies for T1D (82). However, blood levels of ketone bodies are also increased in Type 2 diabetics (T2D) patients (31), indicating that systemic disruptions in glucose homeostasis, either via insulin deficiency or insulin resistance, result in changes in systemic ketone body concentrations. Whether the elevation in ketone body availability contributes directly to the

cardiac dysfunction often associated with the obese and diabetic heart is not known.

The cardiometabolic profile of the diabetic and obese heart has been generally described as increased reliance on fatty acid oxidation with a concomitant reduction in glucose oxidation (83), which in is contrast to the hypertrophied and failing heart discussed in the next section. However, studies conducted over the last several years also demonstrate alterations in cardiac ketone body metabolism in diabetes. In T2D patients, myocardial uptake of the ketone bodies, β-OHB and acetoacetate were higher than non-diabetic controls, inferring a possible increase of ketone body oxidation in human hearts (84). However, ketone body oxidation was shown to be reduced in isolated hearts from diabetic (*db/db*) mice (20). Consistent with this, T1D, induced by streptozotocin (STZ), or T2D, induced by 12-weeks of high fat diet, was associated with reduced mRNA expression and protein level of myocardial Bdh1 (81). Moreover, STZ hearts demonstrated accumulation of cardiac β-OHB with a tendency for reduced myocardial β-OHB oxidation (81). One potential interpretation of these animal studies is that the reduction in ketone body oxidation is a hallmark of the diabetic heart, which might serve as a therapeutic target. In support of this, a recent study demonstrated improved systolic and diastolic function as well as increased expression of ketone body oxidation enzymes in *db/db* mice fed a diet supplemented with KE (85). Future research can help to clarify the impact of enhanced ketone body metabolism in the obese and diabetic myocardium.

KETONE BODY METABOLISM IN HYPERTROPHY AND FAILURE

Over the last 5 years, the importance of cardiac ketone body metabolism in the pathological setting has gained great attention (1). Although the metabolic derangements that occur in the hypertrophied and failing heart, including significant decreases in fatty acid oxidation concomitant with increased glycolysis, are well established (14, 69, 86), the role of ketone body oxidation previously received little focus. However, seminal studies in humans (87) and mice (88) have underscored the contribution of ketone body metabolism to cardiac pathologies, particularly in heart failure. These publications have led to a host of recent studies that have examined the role of ketone body metabolism in cardiac disease (28, 76, 78, 85, 89, 90).

Findings from recent studies have indicated that the hypertrophied and failing heart demonstrates elevated ketone body oxidation (76, 87, 88), which provides an alternative fuel source to maintain cardiac function. These studies have provided the framework for targeting ketone body metabolism as a potential therapeutic treatment for cardiac dysfunction. Indeed, cardiac-specific deletion of Bdh1 in mice exacerbates cardiac dysfunction and remodeling in a heart failure model (76), while overexpression of Bdh1 protects against cardiac dysfunction and adverse myocardial remodeling (78). These provocative findings could support the use of the KD as a nutritional strategy to treat heart failure. In support of this idea, mice fed a KD of ∼80% fat, ∼20% protein, ∼0% carbohydrates for 4-weeks had reduced pathological remodeling in a combined pressure-overload/myocardial infarction heart failure model (76). However, long term KD treatment (i.e., 62 weeks) may worsen diabetic cardiomyopathy in rats (89). Considering the high fat content of KDs, this may not be a suitable long-term strategy so ketone body supplementation might offer a better alternative. In agreement with this notion, a diet supplemented with KEs improved cardiac function, in part by increased mitochondrial oxygen consumption, in type 2 diabetic mice (85). However, although β-OHB infusion has been reported to increase cardiac function in failing canine hearts (76), provision of β-OHB in the perfusate to hypertrophied and/or failing mouse hearts in isolated heart experiments may not improve cardiac efficiency (28) or myocardial energetics (90). Certainly, experimental conditions, including *in-vivo* vs. *ex-vivo* situation and the concentration of ketone bodies used, are a concern.

KETONE BODY METABOLISM DURING ISCHEMIA AND REPERFUSION

Consistent with the cardiac metabolic profile in hypertrophied and failing hearts, the research literature has clearly defined changes that occur during ischemia-reperfusion (I-R). During reperfusion following ischemia, excessive rates of fatty acid oxidation (16, 18) and uncoupling of glycolysis from glucose oxidation (17, 91) have been reported, which may contribute to the reduced functional recovery from ischemic injury. In support, stimulation of glucose oxidation (18, 92, 93) or inhibition of fatty acid oxidation (94–96) improves functional recovery after cardiac ischemia. Oxidation of ketone bodies is suggested to supplant fatty acid oxidation (30, 76, 79), and as a result, upregulation of ketone body metabolism may decrease reliance on fatty acid oxidation and/or improve the coupling of glycolysis to glucose oxidation. Therefore, investigations examining the relationship of the ketogenic diet, ketone body metabolism, and functional recovery from ischemia are needed.

Although the role of ketone body metabolism in heart failure has gained significant attention in the research and medical communities as a therapeutic intervention (2, 97), the role of ketone body metabolism in the ischemia and post-ischemic heart has been less discussed. However, a recent publication identified that circulating ketone bodies were significantly elevated in patients presenting with ST-Segment Elevation Myocardial Infarction (STEMI) (98). Interestingly, elevations in ketone body concentrations 24 h after percutaneous coronary intervention (PCI) were independently associated with greater infarct size and lower LV ejection fraction after 4-months (98). β-OHB concentrations were higher in blood from acute MI patients and mice following left anterior descending (LAD) ligation surgery, which was negatively associated with left ventricular ejection fraction in both models (99). Ketone bodies, particularly β-OHB, was associated with higher odds ratios for myocardial infarction and ischemic stroke (100). Increased ketone body concentrations have also been reported in heart failure patients (87, 101, 102), after fasting and exercise (29, 30), and diabetes

(31, 32). Therefore, speculation could arise as to whether elevations in serum ketone body concentrations are a hallmark of metabolic stress.

Since ischemia represents a condition with low oxygen and nutrient availability, the likelihood that ketone bodies contribute to metabolic processes would be quite low. Consistent with this, a recent report demonstrated that ketone body utilization was suppressed by myocardial ischemia in patients presenting with chest pain (103). However, β-OHB has been shown to accumulate in rat hearts exposed to low-flow ischemia (104), and since the perfusate was devoid of ketone bodies, this suggests that ketogenesis was active in the ischemic heart. Supporting this, inhibition of Hmgcs2 decreased β-OHB accumulation and improved functional recovery during reperfusion (104). This reported finding is somewhat curious, as extrahepatic tissues have been considered incapable of ketogenesis. Interestingly, recent studies have reported changes in gene and/or protein levels of Hmgcs2 in the hearts of mice and human patients (81, 87, 88). However, the role of Hmgcs2 in the normal heart or in the pathogenesis of cardiac disease is relatively unknown. In terms of ischemia-reperfusion injury, whether improvements in recovery are due to changes in ketone body oxidation or changes in oxidation of glucose or fatty acids is not clear and requires more extensive research.

Several studies from the same laboratory evaluated the effects of a low-carbohydrate diet (LCD) on tolerance to myocardial ischemia (105–108). The LCD diet consisted of 60% of the total calories from fat, 30% of total calories from protein, and 10% of the total calories from carbohydrates. Consumption of LCD was shown to induce a mild nutritional ketosis (108). Isolated hearts from lean and obese rats fed the diet for 2 weeks showed decreased recovery from low flow ischemia (105, 108). The 2-week LCD strategy also resulted in poor function, decreased survival, and increased arrhythmias in rats exposed to left anterior descending (LAD) ligation (107). One potential critique of these studies is the relatively short duration of the dietary intervention as the adaptation to KDs is purported to require 4–6 weeks (8). Since ketosis was relatively mild (∼0.6 mM), perhaps, greater concentrations of serum ketone bodies would be required to cause positive adaptations. However, increasing the ketone body concentration to 1.2 mM did not improve the poor recovery in these animals (106, 108). Surprisingly, increasing ketone body concentrations in the perfusate did not appear to alter myocardial ketone body oxidation either in baseline or I-R conditions; however, there was a mild positive correlation between ketone body oxidation and recovery in all groups (106). Overall, these studies would suggest that a short-term (i.e., 2 weeks) diet of high fat and low carbohydrates would render the heart vulnerable to ischemic stress.

A recent study also evaluated the effectiveness of a KD on cardiac function following MI in mice (99). In this study, mice were fed a KD consisting of ∼94% calories from fat and ∼2% calories from carbohydrates for 4 weeks and then were subjected to LAD ligation. Four weeks following LAD ligation, infarct size was significantly greater and fractional shortening (FS) was significantly lower in mice fed the KD (99). MI hearts fed the KD also had lower protein content of glucose transporter 1 (Glut1) and hypoxia-inducible factor 1 alpha (HIF-*1α*) (99). The findings of this study suggest that elevations in serum ketone bodies have the potential to suppress glucose utilization in the ischemic heart, which may enhance myocardial injury.

In contrast to the above studies, fasting-induced ketosis (109) or long term LCKD (110) were associated with improved responses to ischemia in rats. Extreme fasting of 72 h increased β-OHB nearly 15-fold, which reduced infarct size and ventricular arrhythmias in Wistar rats subjected to occlusion of the LAD (109). Wistar rats fed a LCKD for 19-weeks demonstrated improved recovery following global ischemia compared to a control or high carbohydrate diet, which could be due to maintenance of mitochondrial number (110). Infusion of β-OHB to fed rats for 60 min prior to left coronary artery occlusion did not improve infarct size or functional recovery; however, β-OHB in rats fasted for 84 h led to reduced infarct size and higher functional recovery (111). Although the findings are promising, the severity of the fasting period or duration of the dietary intervention could be a bit impractical. Therefore, alternative methods of elevating ketone bodies may offer a more realistic treatment option.

Exogenous delivery of ketone bodies, especially β-OHB, may represent a suitable cardioprotective strategy for ischemia. Rat hearts reperfused with a glucose buffer containing a 5 mM ketone body concentration had improved LV contractility following 10 min of ischemia (27). Isolated mouse hearts provided with 3 mM β-OHB in the perfusate during reperfusion led to a significant improvement in functional recovery following 30 min of ischemia (112). These studies certainly highlight the potential of acute administration of β-OHB in supraphysiologic levels to improve recovery from ischemia. Mice implanted with an osmotic mini-pump with continuous delivery of β-OHB prior to reperfusion had reduced infarct size and preserved cardiac function (113). KE supplemented to rats, either immediately after or 2 weeks post, left coronary artery ligation resulted in an attenuation of pathological cardiac remodeling and improved ejection fraction compared to chow fed rats (114). Overall, the action of β-OHB or KE in the reperfused myocardium or ischemic myocardium may function via improved mitochondrial energetics (27, 114), reduced inflammation (112), and protection against oxidative stress (113). Certainly, additional investigations are required to further evaluate the therapeutic potential of ketone bodies from ischemic injury. In addition, studies examining long-term treatments would be more practical.

Recently, the use of sodium-glucose co-transporter 2 (SGLT2) inhibitors have been of increased interest in medicine and research due to decreased cardiovascular mortality and heart failure in diabetic patients (115). Although a variety of mechanisms have been proposed regarding the benefits of SGLT2 inhibitor on the heart (116), some studies suggest that SGLT2 inhibitors promote ketone body utilization (117, 118). In animal models, SGLT2 inhibitors are associated with beneficial outcomes in the non-diabetic ischemic heart (117–119). Administration of the SGLT2 inhibitor, dapagliflozin, prior to the onset of ischemia was associated with reduced infarct size and improved recovery in a rat model of

in-vivo ischemia-reperfusion injury (119). Rats treated with empagliflozin for 10 weeks after MI induced by coronary artery ligation had improved cardiac function, an effect that was observed if treatment occurred 2 days prior to or 2 weeks after the surgical procedure (118). Of note, the positive functional outcomes with empagliflozin treatment were associated with elevated serum ketone bodies, upregulation of Bdh1 and Scot (Oxct1), and higher cardiac ATP content, suggesting that enhanced cardiac ketone body utilization was involved (118). In non-diabetic pigs, 2 months of empagliflozin treatment improved cardiac remodeling and LV function after proximal LAD occlusion, which was also associated with increased protein content of Bdh1 and Scot in the myocardium (117). Although these studies in animals are promising and appear to indicate that enhanced cardiac ketone body metabolism is mediating the response, additional work is clearly needed to evaluate the efficacy of SGLT2 inhibitors in ischemic heart disease.

CONCLUSIONS AND PERSPECTIVES

Despite an increase in the number of studies focused on cardiac ketone body metabolism in pathological hypertrophy and heart failure, there seems to be a paucity of research elucidating the role of ketone body metabolism in the ischemic myocardium. Given the reported potential of ketone bodies to affect the use of fatty acids and glucose in the healthy myocardium, their delivery to the heart following bouts of ischemia could influence functional recovery. A summary of the findings from various strategies to enhance ketone body metabolism in models of

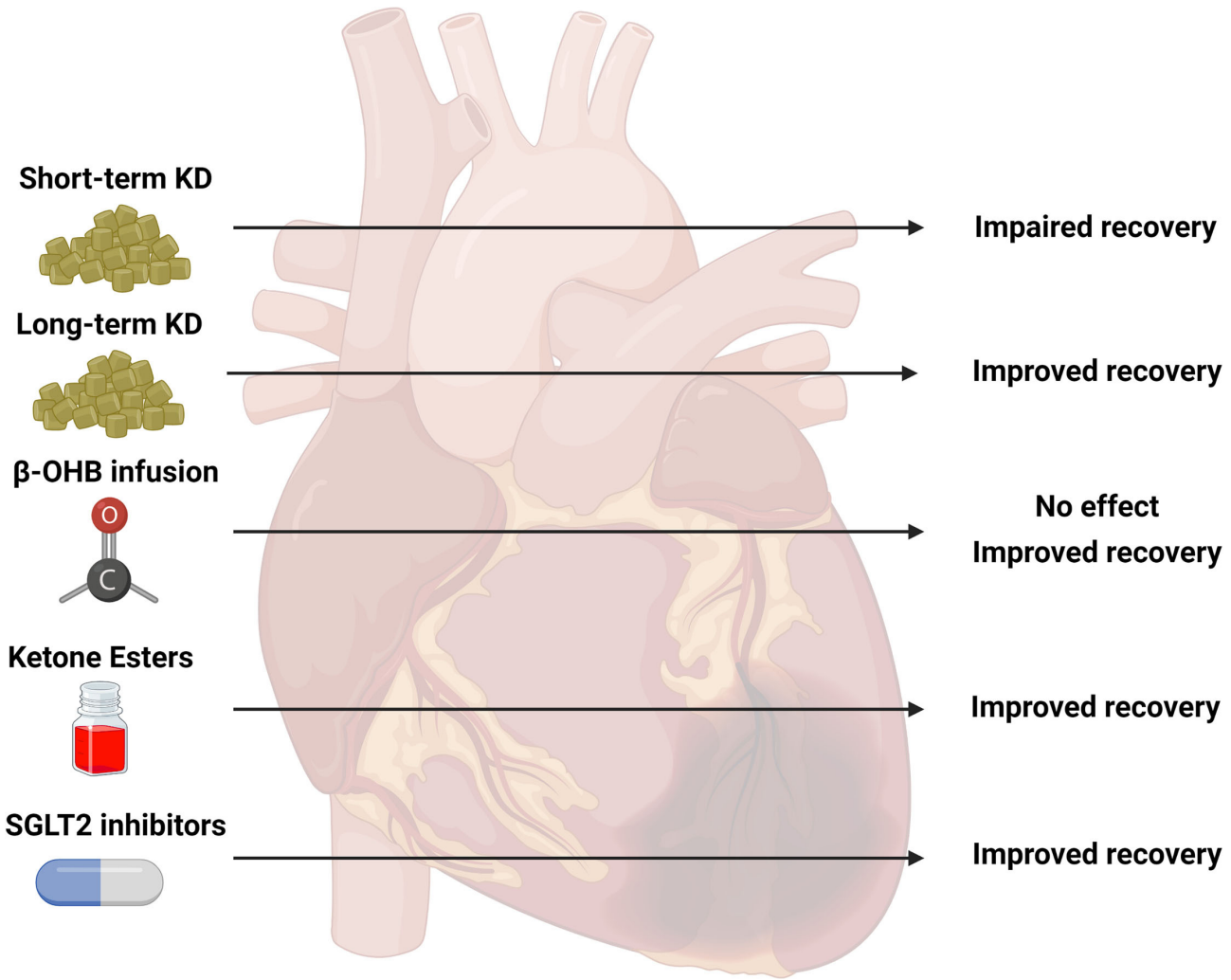

FIGURE 2 | Summary of studies investigating ketone body metabolism in the ischemic heart. Various strategies to target ketone body metabolism in models of cardiac ischemia have been attempted including short-term ketogenic diets (KD, 2–4 weeks), long-term KD (19 weeks), infusion of beta-hydroxybutyrate (β-OHB), ketone ester (KE) supplementation, and sodium-glucose co-transporter 2 (SGLT2) inhibitors. The observed outcomes of these various interventions are presented as impaired, improved, or no effect. The current literature is limited on the effectiveness of these specific strategies: short-term KD (five studies), long-term KD (1 study), β-OHB infusion (four studies), KE supplementation (1 study), SGLT2 inhibitors (three studies). Created with BioRender.com.

ischemia are presented in **Figure 2**. Unfortunately, the current literature does not allow for definitive conclusions to be drawn, due to the relatively low number of studies in animal models. Studies investigating the effects of nutritional ketosis on recovery from ischemia appear to suggest that this strategy is detrimental. However, most of these studies are limited to short-term interventions. Physiological ketosis induced by fasting appears to be promising, but these animal studies seem impractical with fasting of 3 days or more. Delivery of exogenous ketone bodies (i.e., β-OHB) in *ex-vivo* perfused heart preparations have positive reports, but the concentrations used in these studies may be unrealistic compared to the *in-vivo* situation. Although the use of continuous β-OHB delivery via osmotic mini-pumps in mice demonstrates positive effects on functional recovery, the recent report that demonstrated an association between poor outcomes and high ketone body concentrations in humans following MI are equivocal. The use of SGLT2 inhibitors in non-diabetic hearts also appear to be promising. However, additional investigations to further evaluate all of these treatment strategies are warranted. For studies in animal models, careful attention should be paid to the concentrations used either in *in-vivo* or *ex-vivo* experimental conditions to ensure that the ranges of ketone bodies are within achievable concentrations consistent with nutritional or physiological ketosis. In human studies, a focus on the specific etiology of the disease (i.e., ischemic vs. non-ischemic) could help to delineate important contributions of ketone body metabolism to cardiac pathologies.

AUTHOR CONTRIBUTIONS

The author confirms being the sole contributor of this work and has approved it for publication.

FUNDING

This work was supported by an AHA Institutional Research Enhancement Award from the American Heart Association (Grant Number: 20AIREA35080151).

REFERENCES

1. Kolwicz SC, Jr., Airhart S, Tian R. Ketones step to the plate: a game changer for metabolic remodeling in heart failure? *Circulation.* (2016) 133:689–91. doi: 10.1161/CIRCULATIONAHA.116.021230
2. Lopaschuk GD, Karwi QG, Ho KL, Pherwani S, Ketema EB. Ketone metabolism in the failing heart. *Biochim Biophys Acta Mol Cell Biol Lipids.* (2020) 1865:158813. doi: 10.1016/j.bbalip.2020.158813
3. Cox PJ, Kirk T, Ashmore T, Willerton K, Evans R, Smith A, et al. Nutritional ketosis alters fuel preference and thereby endurance performance in athletes. *Cell Metab.* (2016) 24:256–68. doi: 10.1016/j.cmet.2016.07.010
4. Cotter DG, Schugar RC, Crawford PA. Ketone body metabolism and cardiovascular disease. *Am J Physiol Heart Circ Physiol.* (2013) 304:H1060–76. doi: 10.1152/ajpheart.00646.2012
5. Veech RL. The therapeutic implications of ketone bodies: the effects of ketone bodies in pathological conditions: ketosis, ketogenic diet, redox states, insulin resistance, and mitochondrial metabolism. *Prostaglandins Leukot Essent Fatty Acids.* (2004) 70:309–19. doi: 10.1016/j.plefa.2003.09.007
6. Wheless JW. History of the ketogenic diet. *Epilepsia.* (2008) 49 Suppl 8:3–5. doi: 10.1111/j.1528-1167.2008.01821.x
7. Scholl-Burgi S, Holler A, Pichler K, Michel M, Haberlandt E, Karall D. Ketogenic diets in patients with inherited metabolic disorders. *J Inherit Metab Dis.* (2015) 38:765–73. doi: 10.1007/s10545-015-9872-2
8. Harvey KL, Holcomb LE, Kolwicz SC Jr. Ketogenic diets and exercise performance. *Nutrients.* (2019) 11:2296. doi: 10.3390/nu11102296
9. Valenzuela PL, Morales JS, Castillo-Garcia A, Lucia A. Acute ketone supplementation and exercise performance: a systematic review and meta-analysis of randomized controlled trials. *Int J Sports Physiol Perform.* (2020) 1–11. doi: 10.1123/ijspp.2019-0918
10. Yao A, Li Z, Lyu J, Yu L, Wei S, Xue L, et al. On the nutritional and therapeutic effects of ketone body D-beta-hydroxybutyrate. *Appl Microbiol Biotechnol.* (2021) 105:6229–43. doi: 10.1007/s00253-021-11482-w
11. Abdul Kadir A, Clarke K, Evans RD. Cardiac ketone body metabolism. *Biochim Biophys Acta Mol Basis Dis.* (2020) 1866:165739. doi: 10.1016/j.bbadis.2020.165739
12. Choi YS, de Mattos AB, Shao D, Li T, Nabben M, Kim M, et al. Preservation of myocardial fatty acid oxidation prevents diastolic dysfunction in mice subjected to angiotensin II infusion. *J Mol Cell Cardiol.* (2016) 100:64–71. doi: 10.1016/j.yjmcc.2016.09.001
13. Kolwicz SC, Jr., Olson DP, Marney LC, Garcia-Menendez L, Synovec RE, et al. Cardiac-specific deletion of acetyl CoA carboxylase 2 prevents metabolic remodeling during pressure-overload hypertrophy. *Circ Res.* (2012) 111:728–38. doi: 10.1161/CIRCRESAHA.112.268128
14. Fillmore N, Levasseur JL, Fukushima A, Wagg CS, Wang W, Dyck JRB, et al. Uncoupling of glycolysis from glucose oxidation accompanies the development of heart failure with preserved ejection fraction. *Mol Med.* (2018) 24:3. doi: 10.1186/s10020-018-0005-x
15. Lahey R, Wang X, Carley AN, Lewandowski ED. Dietary fat supply to failing hearts determines dynamic lipid signaling for nuclear receptor activation and oxidation of stored triglyceride. *Circulation.* (2014) 130:1790–9. doi: 10.1161/CIRCULATIONAHA.114.011687
16. Kudo N, Barr AJ, Barr RL, Desai S, Lopaschuk GD. High rates of fatty acid oxidation during reperfusion of ischemic hearts are associated with a decrease in malonyl-CoA levels due to an increase in 5'-AMP-activated protein kinase inhibition of acetyl-CoA carboxylase. *J Biol Chem.* (1995) 270:17513–20. doi: 10.1074/jbc.270.29.17513
17. Liu B, el Alaoui-Talibi Z, Clanachan AS, Schulz R, Lopaschuk GD. Uncoupling of contractile function from mitochondrial TCA cycle activity and MVO2 during reperfusion of ischemic hearts. *Am J Physiol.* (1996) 270(1 Pt 2):H72–80. doi: 10.1152/ajpheart.1996.270.1.H72
18. Liu Q, Docherty JC, Rendell JC, Clanachan AS, Lopaschuk GD. High levels of fatty acids delay the recovery of intracellular pH and cardiac efficiency in post-ischemic hearts by inhibiting glucose oxidation. *J Am Coll Cardiol.* (2002) 39:718–25. doi: 10.1016/S0735-1097(01)01803-4
19. Ussher JR, Koves TR, Jaswal JS, Zhang L, Ilkayeva O, Dyck JR, et al. Insulin-stimulated cardiac glucose oxidation is increased in high-fat diet-induced obese mice lacking malonyl CoA decarboxylase. *Diabetes.* (2009) 58:1766–75. doi: 10.2337/db09-0011
20. Verma S, Rawat S, Ho KL, Wagg CS, Zhang L, Teoh H, et al. Empagliflozin increases cardiac energy production in diabetes: novel translational insights into the heart failure benefits of SGLT2 inhibitors. *JACC Basic Transl Sci.* (2018) 3:575–87. doi: 10.1016/j.jacbts.2018.07.006
21. Halestrap AP, Wilson MC. The monocarboxylate transporter family–role and regulation. *IUBMB Life.* (2012) 64:109–19. doi: 10.1002/iub.572
22. Peters JP, Van Slyke DD. *Quantitative Clinical Chemistry*. 2d ed. Baltimore: Williams & Wilkins (1946).
23. Salway JG. *Metabolism at a Glance*. 3rd ed. Malden, Mass: Blackwell Pub. (2004). p. 125.
24. Karwi QG, Uddin GM, Ho KL, Lopaschuk GD. Loss of Metabolic Flexibility in the Failing Heart. *Front Cardiovasc Med.* (2018) 5:68. doi: 10.3389/fcvm.2018.00068
25. Opie LH. *Heart Physiology: From Cell to Circulation*. 4th ed. Philadelphia: Lippincott Williams & Wilkins; 2004. p. xix, 648.
26. Kashiwaya Y, King MT, Veech RL. Substrate signaling by insulin: a ketone bodies ratio mimics insulin action in heart. *Am J Cardiol.* (1997) 80**:** 50A−64A. doi: 10.1016/S0002-9149(97)00458-X

27. Sato K, Kashiwaya Y, Keon CA, Tsuchiya N, King MT, Radda GK, et al. Insulin, ketone bodies, and mitochondrial energy transduction. *FASEB J.* (1995) 9:651–8. doi: 10.1096/fasebj.9.8.7768357
28. Ho KL, Zhang L, Wagg C, Al Batran R, Gopal K, Levasseur J, et al. Increased ketone body oxidation provides additional energy for the failing heart without improving cardiac efficiency. *Cardiovasc Res.* (2019) 115:1606–16. doi: 10.1093/cvr/cvz045
29. Holcomb LE, O'Neill CC, DeWitt EA, Kolwicz SC Jr. The effects of fasting or ketogenic diet on endurance exercise performance and metabolism in female mice. *Metabolites*. (2021) 11:397. doi: 10.3390/metabo11060397
30. Wentz AE, d'Avignon DA, Weber ML, Cotter DG, Doherty JM, Kerns R, et al. Adaptation of myocardial substrate metabolism to a ketogenic nutrient environment. *J Biol Chem.* (2010) 285:24447–56. doi: 10.1074/jbc.M110.100651
31. Avogaro A, Crepaldi C, Miola M, Maran A, Pengo V, Tiengo A, et al. High blood ketone body concentration in type 2 non-insulin dependent diabetic patients. *J Endocrinol Invest.* (1996) 19:99–105. doi: 10.1007/BF03349844
32. Guerci B, Benichou M, Floriot M, Bohme P, Fougnot S, Franck P, et al. Accuracy of an electrochemical sensor for measuring capillary blood ketones by fingerstick samples during metabolic deterioration after continuous subcutaneous insulin infusion interruption in type 1 diabetic patients. *Diabetes Care.* (2003) 26:1137–41. doi: 10.2337/diacare.26.4.1137
33. Gosmanov AR, Gosmanova EO, Dillard-Cannon E. Management of adult diabetic ketoacidosis. *Diabetes Metab Syndr Obes.* (2014) 7:255–64. doi: 10.2147/DMSO.S50516
34. Kanikarla-Marie P, Jain SK. Hyperketonemia and ketosis increase the risk of complications in type 1 diabetes. *Free Radic Biol Med.* (2016) 95:268–77. doi: 10.1016/j.freeradbiomed.2016.03.020
35. Lebovitz HE. Diabetic ketoacidosis. *Lancet.* (1995) 345:767–72. doi: 10.1016/S0140-6736(95)90645-2
36. Gershuni VM, Yan SL, Medici V. Nutritional ketosis for weight management and reversal of metabolic syndrome. *Curr Nutr Rep.* (2018) 7:97–106. doi: 10.1007/s13668-018-0235-0
37. Poff AM, Koutnik AP, Egan B. Nutritional ketosis with ketogenic diets or exogenous ketones: features, convergence, and divergence. *Curr Sports Med Rep.* (2020) 19:251–9. doi: 10.1249/JSR.0000000000000732
38. Roberts MD, Holland AM, Kephart WC, Mobley CB, Mumford PW, Lowery RP, et al. A putative low-carbohydrate ketogenic diet elicits mild nutritional ketosis but does not impair the acute or chronic hypertrophic responses to resistance exercise in rodents. *J Appl Physiol.* (1985) (2016) 120**:**1173–85. doi: 10.1152/japplphysiol.00837.2015
39. Evans M, Cogan KE, Egan B. Metabolism of ketone bodies during exercise and training: physiological basis for exogenous supplementation. *J Physiol.* (2017) 595:2857–71. doi: 10.1113/JP273185
40. Reichard GA Jr, Owen OE, Haff AC, Paul P, Bortz WM. Ketone-body production and oxidation in fasting obese humans. *J Clin Invest.* (1974) 53:508–15. doi: 10.1172/JCI107584
41. Volek JS, Freidenreich DJ, Saenz C, Kunces LJ, Creighton BC, Bartley JM, et al. Metabolic characteristics of keto-adapted ultra-endurance runners. *Metabolism.* (2016) 65:100–10. doi: 10.1016/j.metabol.2015.10.028
42. Kennedy AR, Pissios P, Otu H, Roberson R, Xue B, Asakura K, et al. A high-fat, ketogenic diet induces a unique metabolic state in mice. *Am J Physiol Endocrinol Metab.* (2007) 292:E1724–39. doi: 10.1152/ajpendo.00717.2006
43. Yan J, Young ME, Cui L, Lopaschuk GD, Liao R, Tian R. Increased glucose uptake and oxidation in mouse hearts prevent high fatty acid oxidation but cause cardiac dysfunction in diet-induced obesity. *Circulation.* (2009) 119:2818–28. doi: 10.1161/CIRCULATIONAHA.108.832915
44. Wilder R. The effect of ketonemia on the course of epilepsy. *Mayo Clin Bull.* (1921) 2:307–8.
45. Woodyatt R. Objects and methods of diet adjustment in diabetics. *Arch Intern Med.* (1921) 28:125–41. doi: 10.1001/archinte.1921.00100140002001
46. Peterman M. The ketogenic diet in epilepsy. *JAMA.* (1925) 84:1979–83. doi: 10.1001/jama.1925.02660520007003
47. de Souza RJ, Bray GA, Carey VJ, Hall KD, LeBoff MS, Loria CM, et al. Effects of 4 weight-loss diets differing in fat, protein, and carbohydrate on fat mass, lean mass, visceral adipose tissue, and hepatic fat: results from the POUNDS LOST trial. *Am J Clin Nutr.* (2012) 95:614–25. doi: 10.3945/ajcn.111.026328
48. Shai I, Schwarzfuchs D, Henkin Y, Shahar DR, Witkow S, Greenberg I, et al. Weight loss with a low-carbohydrate, Mediterranean, or low-fat diet. *N Engl J Med.* (2008) 359:229–41. doi: 10.1056/NEJMoa0708681
49. Sondike SB, Copperman N, Jacobson MS. Effects of a low-carbohydrate diet on weight loss and cardiovascular risk factor in overweight adolescents. *J Pediatr.* (2003) 142:253–8. doi: 10.1067/mpd.2003.4
50. Sacks FM, Bray GA, Carey VJ, Smith SR, Ryan DH, Anton SD, et al. Comparison of weight-loss diets with different compositions of fat, protein, and carbohydrates. *N Engl J Med.* (2009) 360:859–73. doi: 10.1056/NEJMoa0804748
51. Badman MK, Kennedy AR, Adams AC, Pissios P, Maratos-Flier E. A very low carbohydrate ketogenic diet improves glucose tolerance in ob/ob mice independently of weight loss. *Am J Physiol Endocrinol Metab.* (2009) 297:E1197–204. doi: 10.1152/ajpendo.00357.2009
52. Partsalaki I, Karvela A, Spiliotis BE. Metabolic impact of a ketogenic diet compared to a hypocaloric diet in obese children and adolescents. *J Pediatr Endocrinol Metab.* (2012) 25:697–704. doi: 10.1515/jpem-2012-0131
53. Samaha FF, Iqbal N, Seshadri P, Chicano KL, Daily DA, McGrory J, et al. A low-carbohydrate as compared with a low-fat diet in severe obesity. *N Engl J Med.* (2003) 348:2074–81. doi: 10.1056/NEJMoa022637
54. Ellenbroek JH, van Dijck L, Tons HA, Rabelink TJ, Carlotti F, Ballieux BE, et al. Long-term ketogenic diet causes glucose intolerance and reduced beta- and alpha-cell mass but no weight loss in mice. *Am J Physiol Endocrinol Metab.* (2014) 306:E552–8. doi: 10.1152/ajpendo.00453.2013
55. Garbow JR, Doherty JM, Schugar RC, Travers S, Weber ML, Wentz AE, et al. Hepatic steatosis, inflammation, and ER stress in mice maintained long term on a very low-carbohydrate ketogenic diet. *Am J Physiol Gastrointest Liver Physiol.* (2011) 300:G956–67. doi: 10.1152/ajpgi.00539.2010
56. Kinzig KP, Honors MA, Hargrave SL. Insulin sensitivity and glucose tolerance are altered by maintenance on a ketogenic diet. *Endocrinology.* (2010) 151:3105–14. doi: 10.1210/en.2010-0175
57. Dashti HM, Al-Zaid NS, Mathew TC, Al-Mousawi M, Talib H, Asfar SK, et al. Long term effects of ketogenic diet in obese subjects with high cholesterol level. *Mol Cell Biochem.* (2006) 286:1–9. doi: 10.1007/s11010-005-9001-x
58. Nilsson J, Ericsson M, Joibari MM, Anderson F, Carlsson L, Nilsson SK, et al. A low-carbohydrate high-fat diet decreases lean mass and impairs cardiac function in pair-fed female C57BL/6J mice. *Nutr Metab.* (2016) 13:79. doi: 10.1186/s12986-016-0132-8
59. Scott BE, Laursen PB, James LJ, Boxer B, Chandler Z, Lam E, et al. The effect of 1,3-butanediol and carbohydrate supplementation on running performance. *J Sci Med Sport.* (2019) 22:702–6. doi: 10.1016/j.jsams.2018.11.027
60. DC Harvey CJ, Schofield GM, Williden M, McQuillan JA. The Effect of Medium Chain Triglycerides on Time to Nutritional Ketosis and Symptoms of Keto-Induction in Healthy Adults: A Randomised Controlled Clinical Trial. *J Nutr Metab.* (2018) 2018:2630565. doi: 10.1155/2018/2630565
61. Dearlove DJ, Faull OK, Rolls E, Clarke K, Cox PJ. Nutritional Ketoacidosis During Incremental Exercise in Healthy Athletes. *Front Physiol.* (2019) 10:290. doi: 10.3389/fphys.2019.00290
62. Evans M, Egan B. Intermittent Running and Cognitive Performance after Ketone Ester Ingestion. *Med Sci Sports Exerc.* (2018) 50:2330–8. doi: 10.1249/MSS.0000000000001700
63. Leckey JJ, Ross ML, Quod M, Hawley JA, Burke LM. Ketone Diester Ingestion Impairs Time-Trial Performance in Professional Cyclists. *Front Physiol.* (2017) 8:806. doi: 10.3389/fphys.2017.00806
64. Kesl SL, Poff AM, Ward NP, Fiorelli TN, Ari C, Van Putten AJ, et al. Effects of exogenous ketone supplementation on blood ketone, glucose, triglyceride, and lipoprotein levels in Sprague-Dawley rats. *Nutr Metab.* (2016) 13:9. doi: 10.1186/s12986-016-0069-y
65. Stubbs BJ, Cox PJ, Evans RD, Santer P, Miller JJ, Faull OK, et al. On the Metabolism of Exogenous Ketones in Humans. *Front Physiol.* (2017) 8:848. doi: 10.3389/fphys.2017.00848
66. Tate RL, Mehlman MA, Tobin RB. Metabolic fate of 1,3-butanediol in the rat: conversion to -hydroxybutyrate. *J Nutr.* (1971) 101:1719–26. doi: 10.1093/jn/101.12.1719
67. Clarke K, Tchabanenko K, Pawlosky R, Carter E, Todd King M, Musa-Veloso K, et al. Kinetics, safety and tolerability of (R)-3-hydroxybutyl (R)-3-

hydroxybutyrate in healthy adult subjects. *Regul Toxicol Pharmacol.* (2012) 63:401–8. doi: 10.1016/j.yrtph.2012.04.008
68. Kolwicz SC, Jr., Purohit S, Tian R. Cardiac metabolism and its interactions with contraction, growth, and survival of cardiomyocytes. *Circ Res.* (2013) 113:603–16. doi: 10.1161/CIRCRESAHA.113.302095
69. Kolwicz SC, Jr., Tian R. Glucose metabolism and cardiac hypertrophy. *Cardiovasc Res.* (2011) 90:194–201. doi: 10.1093/cvr/cvr071
70. Lopaschuk GD, Ussher JR. Evolving Concepts of Myocardial Energy Metabolism: More Than Just Fats and Carbohydrates. *Circ Res.* (2016) 119:1173–6. doi: 10.1161/CIRCRESAHA.116.310078
71. Goodwin GW, Taegtmeyer H. Improved energy homeostasis of the heart in the metabolic state of exercise. *Am J Physiol Heart Circ Physiol.* (2000) 279:H1490–501. doi: 10.1152/ajpheart.2000.279.4.H1490
72. Kaijser L, Berglund B. Myocardial lactate extraction and release at rest and during heavy exercise in healthy men. *Acta Physiol Scand.* (1992) 144:39–45. doi: 10.1111/j.1748-1716.1992.tb09265.x
73. Fillmore N, Wagg CS, Zhang L, Fukushima A, Lopaschuk GD. Cardiac branched-chain amino acid oxidation is reduced during insulin resistance in the heart. *Am J Physiol Endocrinol Metab.* (2018) 315:E1046–E52. doi: 10.1152/ajpendo.00097.2018
74. Ichihara K, Neely JR, Siehl DL, Morgan HE. Utilization of leucine by working rat heart. *Am J Physiol.* (1980) 239:E430–6. doi: 10.1152/ajpendo.1980.239.6.E430
75. Li T, Zhang Z, Kolwicz SC, Jr., Abell L, Roe ND, et al. Defective Branched-Chain Amino Acid Catabolism Disrupts Glucose Metabolism and Sensitizes the Heart to Ischemia-Reperfusion Injury. *Cell Metab.* (2017) 25:374–85. doi: 10.1016/j.cmet.2016.11.005
76. Horton JL, Davidson MT, Kurishima C, Vega RB, Powers JC, Matsuura TR, et al. The failing heart utilizes 3-hydroxybutyrate as a metabolic stress defense. *JCI Insight.* (2019) 4:e124079. doi: 10.1172/jci.insight.124079
77. Schugar RC, Moll AR, Andre d'Avignon D, Weinheimer CJ, Kovacs A, Crawford PA. Cardiomyocyte-specific deficiency of ketone body metabolism promotes accelerated pathological remodeling. *Mol Metab.* (2014) 3:754–69. doi: 10.1016/j.molmet.2014.07.010
78. Uchihashi M, Hoshino A, Okawa Y, Ariyoshi M, Kaimoto S, Tateishi S, et al. Cardiac-specific Bdh1 overexpression ameliorates oxidative stress and cardiac remodeling in pressure overload-induced heart failure. *Circ Heart Fail.* (2017) 10:e004417. doi: 10.1161/CIRCHEARTFAILURE.117.004417
79. Stanley WC, Meadows SR, Kivilo KM, Roth BA, Lopaschuk GD. Beta-Hydroxybutyrate inhibits myocardial fatty acid oxidation *in vivo* independent of changes in malonyl-CoA content. *Am J Physiol Heart Circ Physiol.* (2003) 285:H1626–31. doi: 10.1152/ajpheart.00332.2003
80. Gormsen LC, Svart M, Thomsen HH, Sondergaard E, Vendelbo MH, Christensen N, et al. Ketone body infusion with 3-hydroxybutyrate reduces myocardial glucose uptake and increases blood flow in humans: a positron emission tomography study. *J Am Heart Assoc.* (2017) 6:e005066. doi: 10.1161/JAHA.116.005066
81. Brahma MK, Ha CM, Pepin ME, Mia S, Sun Z, Chatham JC, et al. Increased glucose availability attenuates myocardial ketone body utilization. *J Am Heart Assoc.* (2020) 9:e013039. doi: 10.1161/JAHA.119.013039
82. Chiang JL, Kirkman MS, Laffel LM, Peters AL, Type 1 Diabetes Sourcebook A. Type 1 diabetes through the life span: a position statement of the American Diabetes Association. *Diabetes Care.* (2014) 37:2034–54. doi: 10.2337/dc14-1140
83. Sowton AP, Griffin JL, Murray AJ. Metabolic profiling of the diabetic heart: toward a richer picture. *Front Physiol.* (2019) 10:639. doi: 10.3389/fphys.2019.00639
84. Mizuno Y, Harada E, Nakagawa H, Morikawa Y, Shono M, Kugimiya F, et al. The diabetic heart utilizes ketone bodies as an energy source. *Metabolism.* (2017) 77:65–72. doi: 10.1016/j.metabol.2017.08.005
85. Thai PN, Miller CV, King MT, Schaefer S, Veech RL, Chiamvimonvat N, et al. Ketone ester D-beta-hydroxybutyrate-(r)-1,3 butanediol prevents decline in cardiac function in type 2 diabetic mice. *J Am Heart Assoc.* (2021) 10:e020729. doi: 10.1161/JAHA.120.020729
86. Arnett DK, Blumenthal RS, Albert MA, Buroker AB, Goldberger ZD, Hahn EJ, et al. 2019 ACC/AHA Guideline on the Primary Prevention of Cardiovascular Disease. *Circulation.* (2019) 140:e596–e646. doi: 10.1161/CIR.0000000000000678
87. Bedi KC Jr., Snyder NW, Brandimarto J, Aziz M, Mesaros C, et al. Evidence for intramyocardial disruption of lipid metabolism and increased myocardial ketone utilization in advanced human heart failure. *Circulation.* (2016) 133:706–16. doi: 10.1161/CIRCULATIONAHA.115.017545
88. Aubert G, Martin OJ, Horton JL, Lai L, Vega RB, Leone TC, et al. The failing heart relies on ketone bodies as a fuel. *Circulation.* (2016) 133:698–705. doi: 10.1161/CIRCULATIONAHA.115.017355
89. Abdurrachim D, Teo XQ, Woo CC, Chan WX, Lalic J, Lam CSP, et al. Empagliflozin reduces myocardial ketone utilization while preserving glucose utilization in diabetic hypertensive heart disease: A hyperpolarized (13) C magnetic resonance spectroscopy study. *Diabetes Obes Metab.* (2019) 21:357–65. doi: 10.1111/dom.13536
90. Carley AN, Maurya SK, Fasano M, Wang Y, Selzman CH, Drakos SG, et al. Short-chain fatty acids outpace ketone oxidation in the failing heart. *Circulation.* (2021) 143:1797–808. doi: 10.1161/CIRCULATIONAHA.120.052671
91. Lopaschuk GD, Wambolt RB, Barr RL. An imbalance between glycolysis and glucose oxidation is a possible explanation for the detrimental effects of high levels of fatty acids during aerobic reperfusion of ischemic hearts. *J Pharmacol Exp Ther.* (1993) 264:135–44.
92. Hafstad AD, Khalid AM, How OJ, Larsen TS, Aasum E. Glucose and insulin improve cardiac efficiency and postischemic functional recovery in perfused hearts from type 2 diabetic (db/db) mice. *Am J Physiol Endocrinol Metab.* (2007) 292:E1288–94. doi: 10.1152/ajpendo.00504.2006
93. Ussher JR, Wang W, Gandhi M, Keung W, Samokhvalov V, Oka T, et al. Stimulation of glucose oxidation protects against acute myocardial infarction and reperfusion injury. *Cardiovasc Res.* (2012) 94:359–69. doi: 10.1093/cvr/cvs129
94. Dyck JR, Cheng JF, Stanley WC, Barr R, Chandler MP, Brown S, et al. Malonyl coenzyme a decarboxylase inhibition protects the ischemic heart by inhibiting fatty acid oxidation and stimulating glucose oxidation. *Circ Res.* (2004) 94:e78–84. doi: 10.1161/01.RES.0000129255.19569.8f
95. Dyck JR, Hopkins TA, Bonnet S, Michelakis ED, Young ME, Watanabe M, et al. Absence of malonyl coenzyme A decarboxylase in mice increases cardiac glucose oxidation and protects the heart from ischemic injury. *Circulation.* (2006) 114:1721–8. doi: 10.1161/CIRCULATIONAHA.106.642009
96. Lopaschuk GD, Barr R, Thomas PD, Dyck JR. Beneficial effects of trimetazidine in *ex vivo* working ischemic hearts are due to a stimulation of glucose oxidation secondary to inhibition of long-chain 3-ketoacyl coenzyme a thiolase. *Circ Res.* (2003) 93:e33–7. doi: 10.1161/01.RES.0000086964.07404.A5
97. Yurista SR, Chong CR, Badimon JJ, Kelly DP, de Boer RA, Westenbrink BD. Therapeutic potential of ketone bodies for patients with cardiovascular disease: JACC state-of-the-art review. *J Am Coll Cardiol.* (2021) 77:1660–9. doi: 10.1016/j.jacc.2020.12.065
98. de Koning MLY, Westenbrink BD, Assa S, Garcia E, Connelly MA, van Veldhuisen DJ, et al. Association of circulating ketone bodies with functional outcomes after ST-Segment elevation myocardial infarction. *J Am Coll Cardiol.* (2021) 78:1421–32. doi: 10.1016/j.jacc.2021.07.054
99. Ma X, Dong Z, Liu J, Ma L, Sun X, Gao R, et al. Beta-Hydroxybutyrate exacerbates hypoxic injury by inhibiting HIF-1alpha-dependent glycolysis in cardiomyocytes-adding fuel to the fire? *Cardiovasc Drugs Ther.* (2021). doi: 10.1007/s10557-021-07267-y
100. Holmes MV, Millwood IY, Kartsonaki C, Hill MR, Bennett DA, Boxall R, et al. Lipids, lipoproteins, and metabolites and risk of myocardial infarction and stroke. *J Am Coll Cardiol.* (2018) 71:620–32. doi: 10.1016/j.jacc.2017.12.006
101. Du Z, Shen A, Huang Y, Su L, Lai W, Wang P, et al. 1H-NMR-based metabolic analysis of human serum reveals novel markers of myocardial energy expenditure in heart failure patients. *PLoS ONE.* (2014) 9:e88102. doi: 10.1371/journal.pone.0088102
102. Lommi J, Kupari M, Koskinen P, Naveri H, Leinonen H, Pulkki K, et al. Blood ketone bodies in congestive heart failure. *J Am Coll Cardiol.* (1996) 28:665–72. doi: 10.1016/0735-1097(96)00214-8
103. Arima Y, Izumiya Y, Ishida T, Takashio S, Ishii M, Sueta D, et al. Myocardial ischemia suppresses ketone body utilization. *J Am Coll Cardiol.* (2019) 73:246–7. doi: 10.1016/j.jacc.2018.10.040

104. Lindsay RT, Dieckmann S, Krzyzanska D, Manetta-Jones D, West JA, Castro C, et al. Beta-hydroxybutyrate accumulates in the rat heart during low-flow ischaemia with implications for functional recovery. *Elife.* (2021) 10:e71270. doi: 10.7554/eLife.71270
105. Liu J, Lloyd SG. High-fat, low-carbohydrate diet alters myocardial oxidative stress and impairs recovery of cardiac function after ischemia and reperfusion in obese rats. *Nutr Res.* (2013) 33:311–21. doi: 10.1016/j.nutres.2013.02.005
106. Liu J, Wang P, Douglas SL, Tate JM, Sham S, Lloyd SG. Impact of high-fat, low-carbohydrate diet on myocardial substrate oxidation, insulin sensitivity, and cardiac function after ischemia-reperfusion. *Am J Physiol Heart Circ Physiol.* (2016) 311:H1–H10. doi: 10.1152/ajpheart.00809.2015
107. Liu J, Wang P, Zou L, Qu J, Litovsky S, Umeda P, et al. High-fat, low-carbohydrate diet promotes arrhythmic death and increases myocardial ischemia-reperfusion injury in rats. *Am J Physiol Heart Circ Physiol.* (2014) 307:H598–608. doi: 10.1152/ajpheart.00058.2014
108. Wang P, Tate JM, Lloyd SG. Low carbohydrate diet decreases myocardial insulin signaling and increases susceptibility to myocardial ischemia. *Life Sci.* (2008) 83:836–44. doi: 10.1016/j.lfs.2008.09.024
109. Snorek M, Hodyc D, Sedivy V, Durisova J, Skoumalova A, Wilhelm J, et al. Short-term fasting reduces the extent of myocardial infarction and incidence of reperfusion arrhythmias in rats. *Physiol Res.* (2012) 61:567–74. doi: 10.33549/physiolres.932338
110. Al-Zaid NS, Dashti HM, Mathew TC, Juggi JS. Low carbohydrate ketogenic diet enhances cardiac tolerance to global ischaemia. *Acta Cardiol.* (2007) 62:381–9. doi: 10.2143/AC.62.4.2022282
111. Zou Z, Sasaguri S, Rajesh KG, Suzuki R. dl-3-Hydroxybutyrate administration prevents myocardial damage after coronary occlusion in rat hearts. *Am J Physiol Heart Circ Physiol.* (2002) 283:H1968–74. doi: 10.1152/ajpheart.00250.2002
112. Byrne NJ, Soni S, Takahara S, Ferdaoussi M, Al Batran R, Darwesh AM, et al. Chronically elevating circulating ketones can reduce cardiac inflammation and blunt the development of heart failure. *Circ Heart Fail.* (2020) 13:e006573. doi: 10.1161/CIRCHEARTFAILURE.119.006573
113. Yu Y, Yu Y, Zhang Y, Zhang Z, An W, Zhao X. Treatment with D-beta-hydroxybutyrate protects heart from ischemia/reperfusion injury in mice. *Eur J Pharmacol.* (2018) 829:121–8. doi: 10.1016/j.ejphar.2018.04.019
114. Yurista SR, Matsuura TR, Sillje HHW, Nijholt KT, McDaid KS, Shewale SV, et al. Ketone ester treatment improves cardiac function and reduces pathologic remodeling in preclinical models of heart failure. *Circ Heart Fail.* (2021) 14:e007684. doi: 10.1161/CIRCHEARTFAILURE.120.007684
115. Zinman B, Wanner C, Lachin JM, Fitchett D, Bluhmki E, Hantel S, et al. Empagliflozin, cardiovascular outcomes, and mortality in type 2 diabetes. *N Engl J Med.* (2015) 373:2117–28. doi: 10.1056/NEJMoa1504720
116. Lopaschuk GD, Verma S. Mechanisms of cardiovascular benefits of sodium glucose co-transporter 2 (SGLT2) inhibitors: a state-of-the-art review. *JACC Basic Transl Sci.* (2020) 5:632–44. doi: 10.1016/j.jacbts.2020.02.004
117. Santos-Gallego CG, Requena-Ibanez JA, San Antonio R, Ishikawa K, Watanabe S, Picatoste B, et al. Empagliflozin ameliorates adverse left ventricular remodeling in nondiabetic heart failure by enhancing myocardial energetics. *J Am Coll Cardiol.* (2019) 73:1931–44. doi: 10.1016/j.jacc.2019.01.056
118. Yurista SR, Sillje HHW, Oberdorf-Maass SU, Schouten EM, Pavez Giani MG, Hillebrands JL, et al. Sodium-glucose co-transporter 2 inhibition with empagliflozin improves cardiac function in non-diabetic rats with left ventricular dysfunction after myocardial infarction. *Eur J Heart Fail.* (2019) 21:862–73. doi: 10.1002/ejhf.1473
119. Lahnwong S, Palee S, Apaijai N, Sriwichaiin S, Kerdphoo S, Jaiwongkam T, et al. Acute dapagliflozin administration exerts cardioprotective effects in rats with cardiac ischemia/reperfusion injury. *Cardiovasc Diabetol.* (2020) 19:91. doi: 10.1186/s12933-020-01066-9

Conflict of Interest: The author declares that the research was conducted in the absence of any commercial or financial relationships that could be construed as a potential conflict of interest.

Publisher's Note: All claims expressed in this article are solely those of the authors and do not necessarily represent those of their affiliated organizations, or those of the publisher, the editors and the reviewers. Any product that may be evaluated in this article, or claim that may be made by its manufacturer, is not guaranteed or endorsed by the publisher.

Copyright © 2021 Kolwicz. This is an open-access article distributed under the terms of the Creative Commons Attribution License (CC BY). The use, distribution or reproduction in other forums is permitted, provided the original author(s) and the copyright owner(s) are credited and that the original publication in this journal is cited, in accordance with accepted academic practice. No use, distribution or reproduction is permitted which does not comply with these terms.

frontiers in Cardiovascular Medicine

REVIEW
published: 09 December 2021
doi: 10.3389/fcvm.2021.789267

Mitochondrial Metabolism in Myocardial Remodeling and Mechanical Unloading: Implications for Ischemic Heart Disease

Min Jiang[1,2,3], *Xiaoye Xie*[1,3,4], *Feng Cao*[1,3]* and *Yabin Wang*[1,3]*

[1] Department of Cardiology, National Clinical Research Center for Geriatric Disease, The Second Medical Center, Chinese People's Liberation Army General Hospital, Beijing, China, [2] College of Pulmonary and Critical Care Medicine, Chinese People's Liberation Army General Hospital, Beijing, China, [3] Medical School of Chinese People's Liberation Army, Chinese People's Liberation Army General Hospital, Beijing, China, [4] Department of Cadre Ward, The 960 Hospital of Chinese People's Liberation Army, Jinan, China

Ischemic heart disease refers to myocardial degeneration, necrosis, and fibrosis caused by coronary artery disease. It can lead to severe left ventricular dysfunction (LVEF $\leq$ 35–40%) and is a major cause of heart failure (HF). In each contraction, myocardium is subjected to a variety of mechanical forces, such as stretch, afterload, and shear stress, and these mechanical stresses are clinically associated with myocardial remodeling and, eventually, cardiac outcomes. Mitochondria produce 90% of ATP in the heart and participate in metabolic pathways that regulate the balance of glucose and fatty acid oxidative phosphorylation. However, altered energetics and metabolic reprogramming are proved to aggravate HF development and progression by disturbing substrate utilization. This review briefly summarizes the current insights into the adaptations of cardiomyocytes to mechanical stimuli and underlying mechanisms in ischemic heart disease, with focusing on mitochondrial metabolism. We also discuss how mechanical circulatory support (MCS) alters myocardial energy metabolism and affects the detrimental metabolic adaptations of the dysfunctional myocardium.

Keywords: ischemic heart disease, heart failure, mitochondrial metabolism, veno-arterial ECMO, mechanical unloading, left ventricular assist device

OPEN ACCESS

Edited by:
Shijun Wang,
Fudan University, China

Reviewed by:
Xiaoqiang Tang,
Sichuan University, China
Rui Zhang,
Tongji University, China

****Correspondence:***
Yabin Wang
wyb8202@163.com
Feng Cao
fengcao8828@163.com

Specialty section:
This article was submitted to Cardiovascular Metabolism, a section of the journal Frontiers in Cardiovascular Medicine

Received: *04 October 2021*
Accepted: *04 November 2021*
Published: *09 December 2021*

Citation:
Jiang M, Xie X, Cao F and Wang Y (2021) Mitochondrial Metabolism in Myocardial Remodeling and Mechanical Unloading: Implications for Ischemic Heart Disease. Front. Cardiovasc. Med. 8:789267. doi: 10.3389/fcvm.2021.789267

INTRODUCTION

As estimated by World Health Organization (WHO), ischemic heart disease (IHD) is the leading cause of death worldwide (1). IHD stands for disease syndromes caused by myocardial ischemia due to disproportionate supply and demand of oxygenated blood perfusion in the heart (2). The insufficient oxygen, decreased nutrient levels, as well as deficient substrates and metabolites, are all pathophysiological contributors for IHD. Myocardial ischemia is usually induced by diminished coronary blood flow due to atherosclerosis-induced coronary artery occlusion, clinically manifesting as coronary heart disease or coronary artery disease.

IHD affects cardiac metabolism and function in different stages, ranging from angina to acute myocardial infarction (AMI) and HF. In myocardium, mitochondria produce 90% of ATP, making mitochondrial oxidative phosphorylation (OXPHOS) the primary energy source for the heart. Besides, mitochondria also participate in metabolic pathways that regulate the balance of glucose and fatty acid oxidative phosphorylation. Under physiological conditions, mitochondria keep a

dynamic and homeostatic state in regulating metabolic pathways and cellular ions, which lay foundation for normal cellular functioning. Any deviation from this homeostatic state will lead to mitochondrial dysfunction, including elevated mitochondrial Ca^{2+}, damage of mitochondria membranes and enzymes and defects of electron transport chain (ETC), all of which are contributing factors for cellular apoptosis and necrosis (3).

In terms of interventions, options for IHD mainly focus on reestablishing the oxygen supply-demand imbalance, which is pivotal for clinical prognosis for patients with IHD. Recently, although related approaches have advanced by leaps and bounds, there are still certain numbers of patients who are refractory to conventional treatment, and some of them develop heart failure (HF) after IHD interventions. As heart is a metabolically active organ, metabolism modulation is promising in the treatment of IHD as energy metabolism is closely related with disease progression.

MITOCHONDRIAL METABOLISM IN NORMAL HEART

As a circulatory pump, heart requires cardiomyocytes to generate enormous quantities of ATP to sustain the uninterrupted and orderly coordinated systolic and diastolic function. The main fuels of the myocardium are fatty acids (FAs), glucose, pyruvate, lactate, ketone, and amino acids, which are acquired from the blood continuously for the cardiomyocytes cannot store these energy substrates. As previously reported, the majority of energy (60–90%) required for myocardial activity is derived from free FAs, and the remaining 10–40% originates from carbohydrates and amino acids (4). The myocardial energy metabolism mainly includes substrate utilization, oxidative phosphorylation, and ATP transfer and utilization. Firstly, acetyl-CoA derived from β-oxidation of FAs and glycolysis is synthesized in mitochondria and enters the tricarboxylic acid (TCA) cycle. Under various physiological processes, the healthy heart is metabolically flexible in shifting between substrates to maintain energy production. Then, oxidative phosphorylation is completed in the mitochondria through the respiratory chain and generates the direct energy source ATP. Finally, through the creatine phosphate energy shuttle, creatine kinase (CK) in the mitochondria catalyzes ATP and creatine and generates phosphocreatine (PCr) and adenosine diphosphate (ADP). The generated PCr immediately transfers from mitochondria to myofibrils, where it interacts with ADP and synthesizes ATP and creatine under the catalyzation of myocardial CK so that cardiomyocytes can use ATP for contraction and relaxation and maintain the energy-consuming activity of the heart.

MITOCHONDRIAL METABOLISM IN IHD

The energy metabolism dysfunction caused by IHD includes alterations of substrate utilization, dysfunction of OXPHOS, impairment of ATP synthesis, and mitochondrial dysfunction. Under physiological conditions, fatty acid oxidation (FAO) generates more ATP than glucose oxidation per molecule oxidized at the expense of greater O_2 consumption. In IHD and HF, the O_2 supply to the myocardium is insufficient due to reduced tissue perfusion. Accordingly, both FAO and carbohydrate oxidation decline, and production of ATP is disrupted. To compensate the reduced O_2 shortage, the ATP production in the myocardium switches from aerobic to anaerobic mode, and glycolysis becomes a more predominant source of energy as it yields 11–13% more ATP per unit of consumed O_2 than β-oxidation (5). Besides, under ischemic and hypoxic conditions, large quantities of activated long-chain FAs produced by fat mobilization accumulate in cells and mitochondrial membranes due to decreased or stopped β-oxidation of FAs. These long-chain FAs can result in cardiomyocyte damage and death, and suppress the activity of pyruvate dehydrogenase (PDH), thereby limiting the aerobic oxidation of glucose, reducing the ATP production efficiency, increasing the content of intracellular lactate and hydrogen ions, and, finally, disrupting the myocardial contractility (3, 6).

Oxygen Consumption

It has been increasingly apparent that ischemia and reperfusion (IR)-induced alterations in the kinetics of O_2 supply-to-demand equilibrium depend seriously on the duration and severity of IR. The effects of ischemia exist from short, beneficial ischemia (<10 min) to moderate, reversible ischemia (10–20 min) to severe, irreversible ischemia (>20 min). In reversible ischemia, recovery of overall oxidative metabolism recovers much slower to a preischemic level and couples to contractile function (7). However, in irreversible ischemia, the recovery of oxygen consumption and metabolism is fast, and the mechanical function is severely damaged (8). The IR-induced increases in Ca^{2+} partially explain the rapid recovery of metabolism at early reperfusion in irreversible ischemia, whereas the increased glycolytic rate from exogenous glucose induced by IR results in slower recovery of O_2 consumption-to-demand balance at late reperfusion (9). The concentration of free Ca^{2+} is implicated in regulating several intramitochondrial enzymes, including the PDH, the isocitrate dehydrogenase, and the oxoglutarate dehydrogenase, thus leading to elevated carbohydrate oxidation during early reperfusion (10). This supports the notion that the mitochondrion is the first organelle to display signs of injury under irreversible ischemia, and that regulating mitochondrial energetics within the cell is an early protective strategy of reversible ischemia (9). Moreover, the rapid metabolic recovery uncoupled from mechanical function is a surrogate for poor prognosis of IR injury. Therefore, interventions aiming at attenuating reperfusion blood flow or inhibiting mitochondrial function are considered beneficial (11, 12). In the reperfusion stage following ischemia, FAO generates ATP as a primary energy source at the cost of glucose oxidation negatively impacts the cardiac function in the isolated hearts and in patients with coronary artery disease (6, 13).

Glucose Metabolism

Glucose metabolism mainly includes anaerobic glycolysis, aerobic oxidation, pentose phosphate pathway (PPP), uronic acid pathway, glycogen synthesis and decomposition,

gluconeogenesis, and hexose metabolism, etc. As mentioned above, under hypoxia and ischemia, the aerobic oxidation of FAs is diminished and glycolysis increases and glucose becomes the main energy substrate for myocardial energy metabolism. The uptake of glucose depends on glucose transporters (GLUTs) on sarcolemma of cardiomyocytes, and GLUT1 and GLUT4 are two major isoforms in cardiomyocytes. GLUT1 dominates during fetal and early postnatal life, whereas GLUT4 is the main isoform in adult cardiomyocytes. GLUT4 has a higher affinity for glucose than GLUT1, which makes GLUT4 functioning as the major glucose transporter in adult heart (14). Upon ischemia and hypoxia, GLUT4 translocates to cell membrane from the intracellular vesicles and then augments glucose intake (**Figure 1A**), exhibiting a protective role during cardiac ischemia in neonatal or adult mouse (15–17). Besides, GLUT4 depletion represses glucose use during ischemia and facilitates progression of irreversible cardiac dysfunction associated with blunted ATP generation during IR injury (18). After being transported into cytosol, glucose is phosphorylated by hexokinase, generating glucose 6-phosphate (G6P). Then, G6P is converted into pyruvate by glycolytic enzymes, including phosphofructokinase 1 (PFK1), PFK2, and pyruvate kinase (PK), and the pyruvate can either be metabolized to lactate or be transported into the mitochondrial matrix through the mitochondrial pyruvate carrier (MPC) for oxidation. Under ischemia, the accumulation of 5'-AMP leads to activation of AMP-activated protein kinase (AMPK), which phosphorylates and activates phosphofructokinase-2 (PFK-2) to promote glycolysis (19, 20). Recently, elevated MPC1 and MPC2 have been found in the surviving tissue of the heart subjected to IR injury, indicating a compensatory mechanism that enhances mitochondrial pyruvate uptake to limit intracellular acidosis (21). Upon transportation into mitochondria, pyruvate is converted to acetyl-CoA by pyruvate dehydrogenase (PDH) and further metabolized in the TCA cycle. During ischemia, glucose oxidation is completely shuttled down (**Figure 1A**), and the recovery of it is regulated by FA oxidation as FA competes with glucose for oxidation.

During myocardial reperfusion, the level of O_2 and substrates are restored, whereas glycolysis still remains high, because lactate and inorganic phosphoric acid are washed away which diminish the inhibition of glycolysis, and dysfunctional mitochondria cannot use O_2 effectively. However, glucose oxidation is inhibited during the early stage of reperfusion. As mentioned above, AMPK is activated during ischemia and the accumulated AMPK inactivates ACC at the early stage of reperfusion (8). The decreased ACC activity, in combination with malonyl-CoA degradation leads to decreased malonyl-CoA levels during reperfusion, relieving inhibition of CPT1 and, finally, resulting in upregulated FA oxidation (22, 23). Increased FA oxidation generates high levels of acetyl-CoA and $NADH/NAD^+$, which inhibits the enzyme activity of PDH through activating PDK4 and therefore inhibits pyruvate oxidation (8). The excessive fatty acids β-oxidation facilitates the accumulation of intermediates from the TCA cycle and efflux of citrate to cytosol *via* the mitochondrial citrate carrier (CIC)/SLC25A1, and high levels of cytosolic citrate can suppress PFK-1/2 and pyruvate kinase (PK) activities, and thus diminish glycolysis, pyruvate generation, and oxidation (24, 25). However, as demonstrated before, the Ca^{2+} overload during reperfusion may conquer this inhibition by activating PDH and then increasing glucose oxidation (10, 26). Above all, glucose oxidation is inhibited at an early stage of reperfusion after moderate ischemia, while may increase following more severe or prolonged ischemia (27, 28).

Data from *in vivo* and *ex vivo* studies suggested that promoting glucose oxidation during perfusion is closely correlated with reduced IR injury and improved cardiac function. In *ex vivo* studies, interventions increasing glucose oxidation target the PDH flux, including boosting PDH activity with dichloroacetate, supplementing pyruvate or facilitating glucose uptake by applying high glucose/insulin or overexpressing GLUT1 transporter (29–31). Simultaneously, repressing FAs uptake or FAO also relieves inhibition of glucose oxidation (32, 33). As the improved function observed in the short reperfusion period mostly indicates the accelerated recovery of mechanical function and enhanced re-energization, the long-term post-ischemic myocardial salvage is to be assessed. Therefore, *in vivo* studies administrating glucose oxidation-stimulating substances, such as dichloroacetate, phosphonate compounds, or high-density lipoproteins (HDL) prior to reperfusion reduced infarct size several days after reperfusion (34–36).

Although increased glycolysis only marginally increases ATP production, it promotes flux into the metabolic pathways branching from glycolysis, such as polyol and hexosamine biosynthetic pathways that could independently activate signaling pathways responsible for myocardial remodeling (37, 38). Besides, it has been suggested that glycolysis is intrinsically linked to the redox state of cell (39). Glucose metabolized through glycolysis and the branching PPP in the cytosol feeds the TCA cycle in the mitochondria and produces major reductant e.g., NADH, NADPH for thiol-dependent antioxidant defense. Activation of PPP results in upregulated $NADPH/NADP^+$ and GSH/GSSG couples and an improved redox state, which relieved acute IR injury in cultured cardiomyocytes and mouse hearts (40).

Fatty Acid Oxidation

After uptake into cardiomyocytes, FAs are esterified to fatty acyl-CoA in cytosol and then transferred to carnitines by carnitine palmitoyl transferase 1 (CPT1), which localizes in the inner surface of mitochondrial outer membrane (41). The acylcarnitines are transferred into mitochondrial matrix by carnitine acylcarnitine translocase (CAT) and then converted back into fatty acyl-CoA by CPT2. The fatty acyl-CoA is catalyzed to acetyl-CoA for β-oxidation in mitochondria.

Fatty acids metabolism dysfunction includes FAs and carnitine transport disorder, CoA dehydrogenase deficiency, impairment of enzymes, ketones production disorder, etc. CPT-1 is the rate-limiting enzyme for β-oxidation and is inhibited by Malonyl-CoA, which is synthesized by acetyl-CoA carboxylase (ACC) from acetyl-CoA using biotin and ATP as cofactors. The level of malonyl-CoA in the heart is regulated both by its synthesis and degradation, and AMPK, ACC, and malonyl-CoA decarboxylase (MCD) are extremely important. AMPK phosphorylates and inhibits ACC, which reduces the production

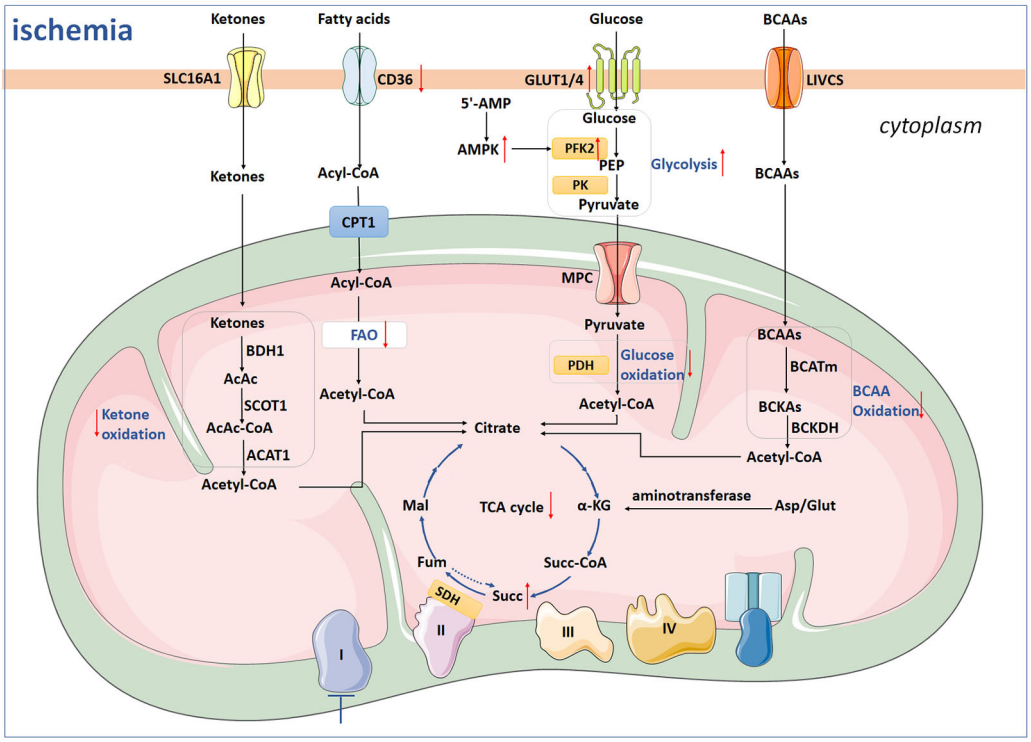

FIGURE 1 | The scheme depicts ketone oxidation, glycolysis, glucose oxidation, fatty acid oxidation, BCAA oxidation, and succinate metabolism under ischemia **(A)** and reperfusion **(B)**. **(A)** Under ischemia, GLUT4-mediated glucose uptake and glycolysis are increased by AMPK-induced PFK-2 activation, whereas glucose

(Continued)

FIGURE 1 | oxidation is shuttled down. The CD36 on sarcolemma, FAs uptake, and FAO are inhibited. Besides, BCAAs and ketones oxidation are also inhibited during ischemia. The TCA cycle and Complex I are inhibited, while the succinate is accumulated from existing metabolites of TCA with mitochondrial Complex II reversal and aminotransferase anaplerosis. **(B)** During reperfusion, CD36 remains low, while FAO returns to the pre-ischemic level. High levels of NADH, acetyl-CoA, and ATP in mitochondria generated from increased FAO inhibit activated PDH *via* activating PDK4 and, therefore, inhibit glycolysis and pyruvate oxidation. The glycolysis still remains high, while glucose oxidation is inhibited. Ketones utilization is increased, while the level of BCAAs oxidation remains to be clarified in the future. Two-thirds of succinate enters into perfusate, and the remaining one-third of succinate is oxidized *via* SDH, driving ROS burst. SLC16A1, Solute carrier (SLC) 16A1/monocarboxylate transporter 1 (MCT1); β-OHB, β-hydroxybutyrate; AcAc, acetoacetate; BDH1, β-hydroxybutyrate dehydrogenase 1; SCOT, succinyl-CoA:3 oxoacid-CoA transferase; AcAc-CoA, catalyze acetoacetyl-CoA; ACAT1, acetyl-CoA acetyltransferase 1; CPT1, carnitine palmitoyl transferase 1; FAO, fatty acids oxidation; GLUT1/4, glucose transporter 1/4; PEP, phosphoenolpyruvate; PK, pyruvate kinase; MPC, mitochondrial pyruvate carrier; PDH, pyruvate dehydrogenase; BCAAs, branched chain amino acids; LIVCS, Leu, Ile, Val: cation symporter; BCKAs, α-keto-acids; BCATm, mitochondrial branched chain aminotransaminase; BCKDH, branched chain α-keto acid dehydrogenase; α-KG, α-ketoglutarate; Fum, fumarate; Mal, malate; Succ, succinate; Succ-CoA, succinyl-CoA; SDH, succinate dehydrogenase; Asp, aspartate; Glut, glutamine. The arrow facing up represents an increase, and down indicates a decrease. Blue lines with a T shape represent inhibition.

of malonyl-CoA and phosphorylates as well as activates MCD, promoting the reverse reaction and converting malonyl-CoA into acetyl-CoA (42). As demonstrated before, AMPK was rapidly activated as an energy sensor to regulate FFAs uptake and oxidation under pathophysiological conditions of hypoxia and ischemia. In cardiomyocytes, AMPK promotes long-chain-FAs uptake through FA translocase (CD36) (43). AMPK activation and relative increase of MCD decrease myocardial malonyl CoA content, which then alleviates inhibition of CPT1 and subsequently facilitates FAO as increased fatty acyl CoA moieties enters into the mitochondrial matrix (44). During mild ischemia, this facilitates fatty acid β-oxidation to be the primary and continuous contributor for oxidative ATP generation, which leads to a decreased level of glucose oxidation, despite increased glycolysis (45). Besides, lactate production by LDH from pyruvate and an increased level of NAD^+ from NADH are also promoted in order to sustain anaerobic glycolysis. The uncoupling of glycolysis and glucose oxidation leads to an accumulation of lactate and H^+, aggravating the ionic disturbance induced by ischemia. However, it should be noted that the accumulated lactate and H^+ are immediately eliminated from the cardiomyocyte under conditions of hypoxia and mild ischemia.

With total ischemia, the FAO is inhibited due to the accumulated reducing equivalents and disturbance of acyl CoA dehydrogenase and 3-hydroxyacyl CoA dehydrogenase enzyme reactions (**Figure 1A**). CD36 on sarcolemma is downregulated by 32%, and the FAO rate decreases by 95% (46). The inhibition of fatty acid β-oxidation inevitably leads to accumulation of metabolic intermediates in various cell compartments. Fatty acyl carnitines accumulate in cytosol and the mitochondrial matrix, while fatty acyl-CoA mainly deposits in mitochondrial matrix because the CoA pool does not exchange with the small cytoplasmic CoA pool (47). The excessive amounts of acylcarnitine accelerate ROS production and increase the probability of mitochondrial permeability transition pore (mPTP) opening, and excessive cytosolic acyl-CoA causes loss of $\Delta\Psi m$ from outside of mitochondria (47, 48). This inhibits the formation of amorphous intramitochondrial densities and disrupts mitochondrial cristae, both of which may eventually induce mitochondrial dysfunction (49). Therefore, the approaches aiming at regulating FA metabolism for cardioprotection in IR injury should first evaluate the potential impact on overall energy homeostasis and possible cardiotoxicity carefully. Recently, studies have shown that inhibition of FAO reduces damage induced by IR using inhibitors, which limit FA transport and metabolism pathways (32, 50–54).

In the stage of perfusion, the activation of AMPK and increased MCD activity still persist, leading to marked decrease of malonyl CoA content. Therefore, the rates of FAO rapidly return to its pre-ischemic level during reperfusion at the expense of glucose oxidation with the CD36 level remained low (**Figure 1B**) (46), whereas the myocardial contraction is still depressed. However, this causes the uncoupling of glucose metabolism and thus deteriorates intracellular acidosis, which increases the risk of cardiac arrhythmias and decreases the contractility because the response between contractile proteins and Ca^{2+} is repressed (55). Therefore, the myocardial recovery is hindered despite the restoration of coronary perfusion.

Ketone Body Oxidation

Ketone bodies [acetoacetate, acetone, and β-hydroxybutyrate (β-OHB)] are synthesized in the liver using acetyl CoA that predominately derived from FAO. They are increasingly being recognized as an important energy substrate of the myocardium, especially in HF (38, 56). After entering mitochondria, they rapidly form acetyl-CoA *via* β-OHB dehydrogenase (BDH1), succinyl-CoA:3-oxoacid-CoA transferase (SCOT) and mitochondrial acetyl-CoA acetyltransferase 1 (ACAT1) (38). The predominant ketone body oxidized in heart is β-OHB. In terms of O_2 consumption for ATP generation, ketones are much more efficient than FAs but less efficient than glucose (4).

Increasing ketone oxidation rates in failing hearts increases overall energy production without compromising glucose or fatty acid metabolism, albeit without increasing cardiac efficiency (57). Previous studies showed that short-term fasting reduces infarct size and limits the duration of ventricular tachycardia occurring at early reperfusion, and this is correlated with increased concentration of β-OHB and β-OHB/acetoacetate ratio (58). However, whether ketonemia induced by fasting in mice after IR injury protect or deteriorates myocardial injury is conflicting (59, 60). Furthermore, *in vivo* studies suggested that the effect of ketonemia may be boosted by exogenous ketone therapy: fasting with ketone infusion led to the least myocardial damage compared with fasting without ketone infusion or a fed state with ketone infusion in rat hearts after coronary occlusion (61).

As β-OHB conferred substantial protection against oxidative stress in multiple organs (62, 63), further mechanism study also confirmed that reduced mitochondrial ROS, enhanced ATP generation, attenuated mitochondrial swelling, and partly restored mPTP in myocardium account for the cardio protection against IR injury (64). To determine ketones utilization under ischemic condition in humans, the concentrations of coronary and systemic serum lactate and β-OHB were measured in 171 consecutive patients with angina (65). The results showed that increased lactate production was associated with decreased myocardial β-OHB consumption, demonstrating suppressed utilization of ketone bodies under ischemia in the coronary circulation (**Figure 1A**) (65).

HF is the next stage of myocardial infarction. A mouse model of progressive HF induced by transverse aortic constriction (TAC)/myocardial infarction exhibited upregulated BDH1 along with upregulated genes encoding ketone body transporters (MCT1 and MCT2) and increased 13C-BHB use on the basis of nuclear magnetic resonance studies (66). Cardiac-specific BDH1 knockout mice exhibit more severe ventricular remodeling and dysfunction after TAC/myocardial infarction (66), whereas BDH1 overexpression attenuates cardiac remodeling and DNA damage in a pressure-overloaded model (67). Increased availability of 3-OHB significantly reduced ventricular remodeling and improved mitochondrial energetics caused by TAC/myocardial infarction in wild-type mice compared with mice-fed normal chow (68). Except for pathway manipulation and ketone supplementation, the cardioprotective effects of SGLT2 inhibitors on infarcted hearts can also be attributed to increased myocardial ketone utilization (69, 70).

BCAA Metabolism

Branched chain amino acids oxidation is also an origin of ATP generation by the heart (71). In mitochondria, leucine, isoleucine, and valine are firstly transaminated to branched chain α-keto-acids (BCKAs) by the mitochondrial branched chain aminotransaminase (BCATm), and then decarboxylated to form CoA compounds by the mitochondrial branched chain α-keto acid dehydrogenase (BCKDH). The products of BCKDH will then generate acetyl-CoA, which fuels for the TCA cycle.

High levels of circulating BCAA and its derivative BCKAs are correlated with increased incidence of cardiovascular disease (72, 73). Previous studies revealed that plasma and cardiac levels of BCAA and BCKAs increase in the rodent model of myocardial IR injury (74, 75). Impaired cardiac BCAA oxidation exacerbates cardiac insulin resistance and directly contributes to cardiac dysfunction and remodeling post AMI (74, 76), while BCAA supplementation aggravates cardiac dysfunction and increases infarct size following coronary artery ligation-induced myocardial infarction (74). As BCAA oxidation rates in heart only supply 1–2% of the total cardiac ATP (75), it is impossible that interventions increasing BCAA catabolism itself have substantial impact on cardiac ATP generation. Recently, BCAA and their intermediates have been recognized to affect glucose and FA metabolism (76–78). In the heart, chronic accumulation of BCAA inhibits PDH activity through suppressing protein O-linked-N-acetylglucosamine (O-GlcNAc) modification, leading to significantly reduced glucose oxidation, and, therefore, rendering the heart vulnerable to IR injury (76). Dietary or genetic factors-induced BCAA accumulation enhances cardiac FAO levels *via* upregulating PPAR-α expression transcriptionally, thereby triggering lipid peroxidation toxicity and rendering the heart vulnerable to IR injury (78). As BCKAs have been shown to trigger ROS formation (79), promoting oxidative decarboxylation of BCKAs through PPC2m overexpression reduces the oxidative stress and eventually alleviates myocardial IR injury (80). However, in contrast with this, another study found that BCKAs attenuate acute IR injury in hearts by inhibiting oxidative stress-induced cell death and protecting mitochondria and energy production (81). The discrepancy may be attributed to the manner of BCKAs exposure and the severity of injury/stress. Moreover, it has been proved that blockade of mitochondria ETC at different complexes inhibits cardiac IR injury (23, 82). BCKAs repress activity of complex I in cardiac mitochondria (83), which capacitate its function as mitochondrial targets for cardioprotection.

Succinate Metabolism

When exposed to ischemia, succinate, a metabolite of the TCA cycle, accumulates and is oxidized by succinate dehydrogenase (SDH) which drives enormous ROS production by mitochondrial complex I (84). Previous study by Zhang and colleagues found that succinate mainly originates from TCA cycle using existing metabolites, such as fumarate, malate, oxaloacetate, citrate, and aconitate, with only trivial contributions from mitochondrial complex II reversal and aminotransferase anaplerosis during heart ischemia (**Figure 1A**) (85). Glucose derived from glycogen also seems to play a part in ischemia induced-succinate accumulation without the requirement of mitochondrial pyruvate entry, suggesting that glucose is not the main source of carbohydrates (85). The α-ketoglutarate (α-KG)-derived succinate is protective at the first few minutes of ischemia as it contains GTP generation through phosphorylating succinyl-CoA synthetase at the substrate level, which defers ischemia-induced ATP exhaustion in cardiomyocytes (86).

Not all succinate that accumulates during ischemia is oxidized by SDH, with approximately two-thirds of them release into the perfusate *via* MCT1 under low pH conditions during early reperfusion (87). The remaining one-third succinate are quickly oxidized within a few minutes of reperfusion, which diminishes the CoQ pool and also hyperpolarizes the inner membrane of mitochondria (84). Together, these alterations drive reverse electron transport (RET) at complex I, which produces ROS dramatically (**Figure 1B**) (84, 88). Besides, succinate oxidation induces generation and secretion of pro-inflammatory factors, such as IL-1β, and simultaneously inhibits production of anti-inflammatory factors (89).

Clinically, the succinate concentration in arterial, coronary sinus, and peripheral venous blood of patients with STEMI is higher than that in patients with non-STEMI or stable angina, and the release of cardiac succinate in STEMI is correlated with the severity of acute myocardial injury (90). The emerging therapeutic and cardioprotective strategy targeting

succinate metabolism *via* SDH inhibition includes preventing its accumulation during ischemia (less oxidizable succinate during reperfusion) and directly depressing its oxidation during reperfusion (91). The TCA cycle intermediate malate and the succinate competitor malonate are known SDH inhibitors (86). SDH inhibition with malonate before ischemia or at the onset of reperfusion reduces infarct size in isolated mice hearts through inhibiting ROS generation and mPTP opening (84, 92). The discovery that one third of accumulated succinate during ischemia is oxidized within the first 5 min of reperfusion (and 59% of which is within the 1st min) suggests that early reperfusion is a critical time window for therapeutic targeting of complex II (85). Furthermore, SDH inhibition by malonate administration at 1-week post-MI facilitates adult cardiomyocyte proliferation, revascularization of the infarct zone, and myocardial regeneration following infarction (93). Above all, succinate represents a promising biomarker for evaluating severity of AMI, and inhibition of SDH proposes a key metabolic target to render protection following infarction.

Epigenetic Aspects of Metabolic Signaling

Most of the previously described substrate utilization and the metabolic process are a result of gene transcription. During the last decades, epigenetics, including DNA modification and posttranslational modification of proteins, are increasingly studied to delineate how metabolites regulate gene expression. Lysine acetylation, one of the posttranslational modifications, can regulate many non-histone proteins, which are involved in gene transcription, mRNA splicing, signal transduction, cell metabolism and survival (94). Sirtuins (SIRT1-7) are Class III histone deacetylases (HDACs), which participate in IR injury *via* regulating mitochondrial metabolism. In the heart mitochondria of SIRT5 knockout mice, mass spectrometry suggests that lysine succinylation is increased and the substrate of SIRT5 includes proteins that participate in FA metabolism, TCA cycle and OXPHOS (95). Compared with wild-type littermates, SIRT5 knockout exacerbates infarction, and this is reversed by pretreatment of malonate, implicating SIRT5 modulates protein succinylation in IR injury. SIRT3 is the primary mitochondrial lysine deacetylase; its knockdown significantly aggravates the extent of IR injury compared to wild-type hearts (96). The enhanced mitochondrial protein acetylation, which is closely correlated with the inhibited activity of complex I and MnSOD, is the underlying mechanism. In the sepsis model, depletion of SIRT3 also induces excessive acetylation of enzymes in the TCA cycle and production of lactate and NADH, which accordingly deteriorate sepsis-induced cardiac dysfunction (97). However, recently, a dual knockout mouse model targeting carnitine acetyltransferase and SIRT3 resulted in a dramatically proteome-wide upregulation of lysine acetylation in heart mitochondria, which exhibited a ∼86% overlap with characteristics of HF, while this has no or minimal impact on mitochondrial function, such as dehydrogenase activity, respiration, redox state and OXPHOS (98). Therefore, clinical and mechanistic studies are to be done to determine protein acetylation in mitochondrial metabolism and its actual contribution to IR injury.

Except for acetylation and succinylation, new acylation mediated by metabolites themselves is founded to participate in epigenetic regulation of gene expression and enzymatic activity. In an HFpEF (HF with preserved ejection fraction) mice model, by partly activating citrate synthase through lysine β-hydroxybutyrylation and inhibiting FA uptake, β-OHB limits the acetyl-CoA pool and thus inhibits mitochondrial acetylation (99). Besides, the crotonylation of histone also regulates gene transcription and metabolism. In hypertrophic cardiomyopathy, Enoyl Coenzyme A Hydratase1 (ECHS1), the enzyme in the second step of fatty acids β-oxidation, reduces the intracellular crotonyl-CoA level and inhibits cardiomyocytes hypertrophy *via* repressing H3K18cr and H2BK12cr and NFATc3 expression (100). Recently, Zhang et al. have discovered that lactate, the product of glycolysis, can stimulate histone lactylation, which participates in M1 macrophage polarization by inducing *Arg1* expression (101). The histone lactylation is later found to regulate tissue repair and cancer progression (101–103). As macrophage phenotype and inflammation are closely correlated with prognosis of IHD and HF (104, 105), the role of this "lactate clock" in cardiovascular system is to be clarified to develop novel therapeutics.

MECHANICAL CIRCULATORY SUPPORT ON MYOCARDIAL MITOCHONDRIAL METABOLISM

In spite of timely perfusion, over 1/4 of patients suffering the first-time AMI develop HF within 1 year (106). For every 5% increase in the myocardial infarct size, the 1-year HF hospitalization and 1-year mortality will increase by 20% (107). The reason for the poor prognosis of patients with AMI is that reperfusion paradoxically worsens myocardial injury. Upon reperfusion, the ischemic myocardium is subjected to abrupt biochemical and metabolic alterations, including mitochondrial re-energization, ROS burst, intracellular and mitochondrial Ca^{2+} overload, rapid pH correction and inflammation (108). These alterations can lead necrosis of endothelial cells and cardiomyocytes *via* opening of mPTP and hypercontraction. The mPTP is a non-selective channel on inner membrane of mitochondria, and its opening disrupts the mitochondrial membrane potential, which uncouples OXPHOS, exhausts ATP, and induces cell death. During ischemia, mPTP is closed, while the reperfusion-induced ROS burst, Ca^{2+} overload, and rapid pH fluctuation cause mPTP opening (109). Therefore, mitochondria, acting as a signaling hub, are an important target for cardioprotection. Improved and more efficient strategies are in urgent demand to limit myocardial injury by inhibiting deleterious response and inducing a cardioprotective mechanism prior to reperfusion of the infarct-related arteries so as to prevent the development of patients with HF after MI. Recently, increasing numbers of mechanical circulatory support (MCS) devices have been applied in clinical practice as they can enhance systemic mean arterial pressure and concurrently reduce left ventricular (LV) wall stress and stroke work, which may be beneficial for myocardial oxygen supply-demand equilibrium (110–112).

Mechanical Loading on Mitochondrial Metabolism of Myocardium

Normally, cardiomyocytes are subjected to three types of mechanical loading, including cyclic stretch imposed by every heartbeat, shear stress generated by flowing blood, and static stretching due to blood pressure. Cardiomyocytes are sensitive to mechanical stress, which are transduced to molecular signaling by biomechanical sensors. The sensors and transduction pathways have been studied for several years in the hope of preventing development and progression of cardiovascular diseases by shutting down mechanotransduction.

Emerging evidence has shown that excessive mechanical loading can disturb mitochondrial homeostasis, including dynamics, metabolism, Ca^{2+} homeostasis and redox state (113, 114). Ca^{2+} leak is the earliest alteration observed under mechanical loading, and during myocardial systole, the duration and amount of Ca^{2+} leak determine the contractile force of myocardium (115). Ca^{2+} is a versatile signaling molecule, which regulates numerous cellular processes, including cell metabolism, and the mitochondrial Ca^{2+} homeostasis is determine by equilibrium between Ca^{2+} influx and efflux, which are regulated by Ca^{2+} channels, transporters, exchangers and subcellular organelles (116, 117). Ca^{2+} affects metabolic processes such as the TCA cycle through allosteric regulation of enzymes or indirectly *via* regulating phosphatases and kinases (118, 119). In addition, Ca^{2+} channels, transporters and exchangers are also reported to be responsible for metabolism (120–122). The Ca^{2+} release-activated Ca^{2+} (CRAC) channel, which imports Ca^{2+} from endoplasmic reticulum and extracellular space, is involved in FA metabolism (119). Piezo1, which is discovered in 2010 by Coste et al. and forms cationic non-specific channels, also participates in mechanotransduction by transducing ionic current and Ca^{2+} influx (123). In cardiovascular system, Piezo1 expresses in endothelial cells, smooth muscle cells, cardiomyocytes, and cardiac fibroblasts and can be activated by cyclic stretch and shear stress. In endothelial cells, Piezo1 couples shear stress-provoked Ca^{2+} entry and endothelial cell organization and alignment *via* Ca^{2+}-activated proteolytic enzyme calpain (124). However, data on the presence and function of Piezo1 in cardiomyocytes are limited. Liang et al. found that the mRNA and the protein level of Piezo1 were upregulated in HF after myocardial infarction (125). In another *in vitro* model, Piezo1 was reported to participate in sensing cyclic stretch and can activate the mechanical low-density lipoprotein (LDL) receptor-related protein 6 (LRP6)/β-catenin signaling pathway (126). Clinically, the increased Piezo1 mRNA level was observed on monocytes of patients with aortic valve stenosis, which increases shear stress on circulating blood cells, and transcatheter aortic valve implantation (TAVI) significantly decreased the mRNA level on monocytes (127). Further *in vitro* mechanistic study suggests that Piezo1-mediated Ca^{2+} influx from intracellular stores, as well as the extracellular environment, was involved in monocyte activation. Apart from Ca^{2+} homeostasis, Piezo1 constitutes a regulator of the Hippo-Yes-associated protein (YAP)/PDZ-binding motif (TAZ) pathway (128, 129), which is involved in converting mechanical stress into biochemical signal and has been well-studied (130). With regular mechanical stress, the activated Hippo proteins phosphorylate YAP/TAZ and thus confine them to cytoplasm. Upon excessive mechanical loading, Hippo is inhibited and YAP/TAZ enters into nucleus where it interacts with the TEAD1 family to induce gene transcription. YAP and TAZ can regulate metabolism of various substrates and mitochondrial function, which has been reviewed in detail previously (131). However, the direct evidence that Piezo1 regulates mitochondrial metabolism is lacking.

LV Unloading by LV-To-Aorta Circulatory Support

Over the past decades, preclinical studies have demonstrated that, compared with reperfusion alone, mechanical unloading of the left ventricle prior to coronary reperfusion can reduce IR injury and myocardial infarct size in AMI (132, 133). Latterly, preclinical studies also indicated that LV unloading and delayed reperfusion by 30 min can initiate cardioprotective changes, including upregulated SDF-1a/CXCR4 expression, increased cardioprotective signaling, and reduced apoptosis (133, 134). Compared with reperfusion alone, 30 min of LV mechanical unloading before reperfusion was adequate to diminish LV infarct size, improve cardiac function, and downregulate biomarkers related to undesirable remodeling and HF 28 days post AMI, thus promoting recovery of myocardial function 30 days after AMI (135). Furthermore, mechanical unloading increased collateral coronary flow and myocardial microvascular perfusion by reducing the LV-end diastolic wall stress (136, 137). In order to determine the safety and feasibility of LV unloading and delayed reperfusion of patients with STEMI, the DTU-STEMI pilot trial (Door-To-Unload in STEMI Pilot Trial) randomly assigns 50 patients with anterior STEMI to LV unloading with immediate reperfusion or LV unloading followed by 30-min delay before reperfusion (138). The results of the trial suggested that, despite delayed reperfusion, LV unloading does not increase the infarct size, which lays a good foundation for a future pivotal trial. In addition, in patients with large anterior STEMIs, which is defined as a sum of precordial ST-segment elevation STE $\geq$ 6 mm, LV unloading reduces infarct size normalized to the area at risk compared with reperfusion alone (138). In patients with LAD occlusion and STE $\geq$ 7 mm, LV unloading also diminishes the infarct size quantified by cardiac magnetic resonance at 3- to 5-day post-MI compared with that in the perfusion-alone group (139).

LV Unloading on Myocardial Mitochondrial Metabolism

Recently, studies focusing on mitochondrial integrity and function under LV unloading have been increasing. The improvement of mitochondrial dysfunction is firstly reported in patients with HF supported with long-term left ventricular assist device (LVAD) therapy (140). To elucidate the mechanisms of the clinical benefit brought by LVAD, tissue specimens were harvested from the explanted hearts at the time of transplantation or LVAD implantation. Mechanical unloading supported by LVAD increased the respiratory rate and efficiency of mitochondrial respiration on TCA cycle-derived substrates in isolated mitochondria, suggesting that mitochondrial

metabolism is involved in the cardioprotective effect of LVAD (140). In failing human myocardium, decreased oxidation and increased accumulation of long-chain FAs in the hypertrophic heart are accompanied by increased acyl-derived intermediates, including lipotoxic ceramides that curtail cardiac function. Mechanical unloading *via* LVAD implantation increased the content of acyl CoA, facilitating the lipid trafficking and amelioration of the lipotoxicity (141–143). Besides, by decreasing LV afterload, LVAD reduces acyl chains required for energy production of the myocardium, which, therefore, restores the upstream acyl CoA pool (143). In the IR injury model, compared with pure reperfusion, LV unloading for 30 min prior to reperfusion upregulates genes associated with mitochondrial function and respiration, and maintains the integrity of mitochondria in the infarct zone (135). And tissue samples from the infarct zone with or without LV unloading following perfusion were analyzed using untargeted metabolomics. Compared with the sham control group, IR significantly reduces the levels of key metabolites related to glycolysis, glucose oxidation, fatty acid transport and oxidation, and amino acid use, while LV unloading preserves the levels of these metabolites (139). Pathway analysis also showed that, compared with reperfusion alone, LV unloading remarkably altered various pathways involved in glycolysis, the TCA cycle, and ETC function, suggesting that LV unloading preserves substrate levels for OXPHOS (139). Further functional studies showed that, compared with IR, LV unloading retains intact mitochondrial structure, including cardiolipin content and activity of ETC, including mitochondrial Complex I, and reduces oxidative stress in mitochondria isolated from the infarct zone. In conclusion, by reestablishing the oxygen supply-consumption balance, the primary clinical prognosis determinant of patients with IHD, LV mechanical unloading preserves myocardial energetics and mitochondrial function, and, therefore, limits the infarct size and improves cardiac function after AMI (**Figure 2**). Nevertheless, more preclinical and human studies concerning LV mechanical unloading require to be done since the panorama of substrate utilization and mitochondrial metabolism is incomplete.

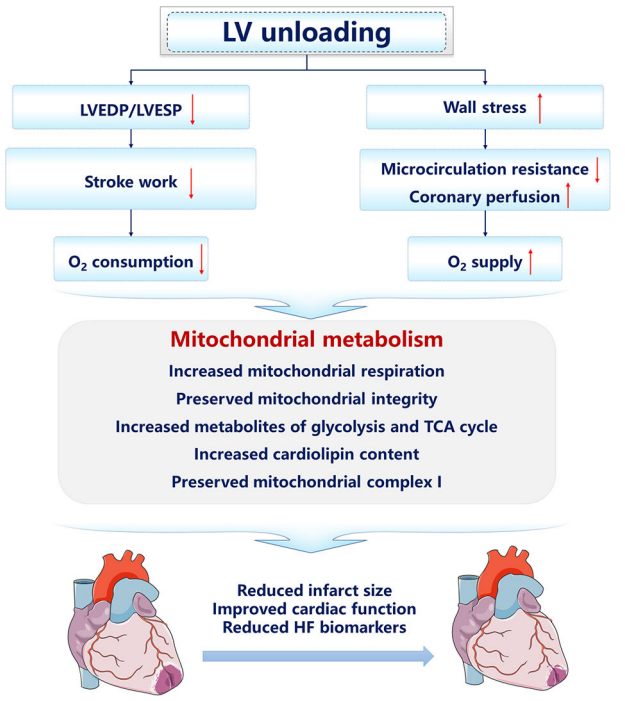

FIGURE 2 | The cardioprotective mechanisms of left ventricular unloading. The arrow facing up represents an increase, and down indicates a decrease.

Metabolic Biomarkers of Myocardial Recovery Under LV Unloading

Recently, the effects of mechanical unloading on mitochondrial metabolism in patients with progressive HF, including ischemic and non-ischemic cardiomyopathy, have increasingly investigated to identify whether progression and improvement of HF are correlated with altered myocardial energetics and the metabolic process induced by mechanical unloading. In the ischemic myocardium, altered distribution of CK isoenzyme may disrupt energy transfer between mitochondria and the contractile apparatus. Cardiolipin is the characteristic phospholipid of the mitochondrial inner membrane whose functional status is a determinant for efficient mitochondrial coupling. Previous studies have shown that LVAD support can improve mitochondrial coupling in ischemic cardiomyopathy (ICM) hearts, and the improvement is associated with the normalization of cardiolipin composition (140, 144).

In normal hearts, lactate can be converted to pyruvate by lactate dehydrogenase (LDH) to enter the TCA cycle and generate ATP, and concurrent lactate production balances the lactate consumption (145). During HF, this balance is disturbed, with an increased glycolytic pyruvate-derived lactate and a simultaneous decrease in lactate utilization (146). Diakos et al. demonstrated that glycolytic metabolites are increased in patients with post-LVAD HF without a corresponding increase of early TCA cycle intermediates, which may be attributed to poor recovery of mitochondrial oxidative capacity and volume density post-LVAD (146). Besides, the subsequent intermediates after succinyl CoA anaplerotic access and amino acids levels are increased post LVAD unloading, representing a complementary energy source that could fuel the TCA cycle and building blocks for protein synthesis (146). Especially, they revealed that patients with better myocardial recovery post LVAD seem to have improved mitochondrial function and structure with LVAD unloading. This is verified in subsequent study showing that MPC1 was lower in myocardial tissue samples of patients with HF than those of non-failing donors (147). The MPC transports pyruvate into the mitochondria for the TCA cycle and is an important modulating point, which determines whether pyruvate is oxidized or converted to lactate (148). In these patients with chronic HF, increased MPC1 abundance post-LVAD is observed in responders (patients with significantly improved myocardial function after LVAD unloading) but not non-responders, suggesting defective mitochondrial pyruvate metabolism may be a primary factor contributing to their HF.

Further animal models and *in vitro* cardiomyocyte models proved that inhibited mitochondrial pyruvate oxidation is closely correlated with cardiomyocyte hypertrophy.

Except for glucose oxidation, the metabolites of glycolysis may be channeled to accessory pathways of glycolysis. Clinically, LVAD implantation enhances levels of glucose and glucose-6-phosphate in patients with ICM (149). Compared with post-LVAD non-responders, rate-limiting enzymes of PPP and one-carbon metabolism, which protect myocardium through producing NADPH to promote biosynthesis and antagonizing oxidative stress, are significantly increased in post-LVAD responders (150). The responders also have improved mitochondrial density and increased expression of α-dystroglycan that maintains the extracellular matrix and cytoskeletal integrity (150).Therefore, the deleterious mitochondrial or related metabolism pathway may be underlying etiology for the cardiac response to LVAD, and specific metabolites may be utilized as cardiac prognostic biomarkers of LVAD implantation. However, concerning LVAD study on HF that includes patients with ischemic and non-ischemic cardiomyopathy, caution should be made when interpreting these results as studies have shown that metabolic processes can be used to distinguish non-ischemic dilated cardiomyopathy from ICM (151).

Hemodynamics of VA-ECMO

Cardiac arrest or cardiogenic shock (CS) occurs in ∼3–10% of patients with AMI and is associated with about 30–50% in-hospital mortality (152, 153). Therefore, percutaneous circulatory support, particularly venoarterial extracorporeal membrane oxygenation (VA-ECMO), which belongs to RA-To-Aterial circulatory support, is increasingly used to provide hemodynamic support for the management of AMI. Since VA-ECMO transfers blood from venous reservoir to the arterial system, the afterload is increased due to the retrograde flow. Thus, the volume status and native ventricular function of the patients will affect LV volume. In patients with low volume in the venous system, VA-ECMO initiation reduces the total cardiac preload and therefore LV volume (154). However, as VA-ECMO is usually applied to CS patients with venous congestion, the pressurized arterial system will increase systemic blood pressure. When the original LV function is retained, the increase in LV systolic pressure will overcome the LV afterload to enable blood ejection *via* aortic valve, and the increased flow and LV systolic blood pressure will not come at the cost of LV diastolic blood pressure when the LV contractility is preserved (154). In patients with LV dysfunction compromised by extensive anterior wall MI, the diminished stroke volume results in increased LV systolic and diastolic pressures because the dysfunctional LV cannot pump blood effectively to resist increased afterload and the pressurized arterial tree (110). The elevated LV afterload increases wall stress of LV and left atrial and therefore increases oxygen demand, which finally hinders myocardial recovery (155). The extra LV afterload and insufficient LV mechanical unloading under VA-ECMO may lead to severe complications, including LV stasis, thrombosis, pulmonary edema, and ventricular dilatation-induced ischemia, all of which increase mortality (156, 157). Particularly, ECMO can reduce both LV end diastolic volume and LV systolic wall stress of the normal hearts but increase LV wall stress in ischemic hearts (158).

To decompress the LV and attenuate increased afterload *via* elevating forward flow, the VA-ECMO is combined with other mechanical devices in clinical practices (159). In a retrospective cohort from America, almost 60% of AMI admissions had a second temporary MCS device besides ECMO, and 30.3% of them were placed concomitantly (160). Previous meta-analysis suggests that ECMO + IABP strategy achieves lower mortality compared with ECMO alone in CS of AMI (161). Compared with that of patients with VA-ECMO alone, the mortality was lower in patients with combined Impella and VA-ECMO (162, 163). Besides, LV unloading done early (within 12 h) seems to be correlated with an increased rate of successful weaning and decreased short-term mortality (164). Recent studies have suggested that combined utilization of Impella to decompress the LV with ECMO reduced the mortality rate of CS (154). However, as VA-ECMO support systemic perfusion at the risk of increasing LV load, available data on VA-ECMO utilization in AMI are limited, and most of them are retrospective. There is an urgent need to conduct randomized controlled trials (RCT) to investigate the application of VA-ECMO in AMI and its effects on infarct size as well as long-term prognosis.

VA-ECMO on Mitochondrial Metabolism of Normal Hearts

As recovery of myocardial function is the primary prerequisite for weaning from the ECMO circuit, it is necessary to fully clarify the effects of changing energy equilibrium and substrate utilization of the heart under ECMO support. Of all these factors, hemodynamics of the heart during ECMO cause changes in substrate metabolism. Even if no direct myocardial damage has occurred before, ECMO can cause cardiac arrest. Therefore, the previously uninjured and unenlarged heart is used to define the effect of ECMO on substrate use and myocardial energetics to exclude the interferences of hypoxia, ischemia, or reperfusion. In infants, systemic studies have shown that ECMO promotes the leucine oxidation and, at the same time, increases the protein degradation rate, leading to negative protein balance and related skeletal muscle atrophy (165). The BCAA undergoes catabolism instead of being incorporated into protein synthesis, providing a carbon substrate for oxidation in the TCA cycle (166). However, evidence concerning heart-specific adaptions in the metabolic process is rare. In an immature swine model, ECMO shifts myocardial metabolic processes toward positive protein balance by preserving BCAA for protein synthesis instead of promoting their oxidation (167). Because ECMO significantly reduces myocardial oxygen consumption, the overall LV leucine oxidation rate is reduced compared with the increase observed in the whole-body-infant study. Besides, pyruvate utilization seems to prevent insulin resistance, further preserving BCAA from oxidation. Simultaneously, ECMO promotes the oxidation of long chain FAs oxidation and inhibits lactate oxidation (168). This metabolic shift during ECMO appears to be explained by rapid

upregulation of PDH kinase-4 (PDK4) protein. As demonstrated by Randle et al. (169), PDH is phosphorylated and inhibited by PDK4, thereby reciprocally increasing FAO *via* acyl-CoA dehydrogenases. ECMO also increased the relative flux from lactate to alanine, further supporting the inhibitory effect of PDK4 on PDH (168). In a VA-ECMO immature piglet model, weaning from ECMO circuits induces a sudden increase in cardiac work and myocardial oxygen consumption, which is associated with shifts in substrate utilization and pathways contribution. The exogenous pyruvate is favored vs. those derived from glycolysis, and acetyl-CoA is generated from endogenous substrate, presumably fatty acids and ketones rather than pyruvate decarboxylation (170). In conclusion, in normal hearts, ECMO preserved positive protein balance *via* promoting the FAO and pyruvate oxidation, and successful weaning will not increase the oxidation of amino acids, nor will it adversely affect the rate of protein synthesis.

VA-ECMO on Mitochondrial Metabolism of Ischemic Hearts

To determine whether VA-ECMO protects the ischemic heart through ameliorating metabolic abnormalities induced by IR, metabolites of neonatal piglets that undergo coronary occlusion for 30 min, followed by ECMO support, have been analyzed (170). The ratio of phosphocreatine to adenosine triphosphate (PCr/ATP) is analyzed as a surrogate for mitochondrial oxidative capacity (171), and it falls when ATP demand nears or exceeds the maximal ATP production rate. Files demonstrated that, compared with the preischemic level, IR significantly decreased the PCr/ATP by $> 50\%$, and ECMO after injury returns the PCr/ATP to near preischemic levels, yet this effect is lost during weaning (172). This suggests that mitochondrial ATP synthesis operates near maximal capacity, as weaning ECMO elevates the energy requirement and disrupts the PCr/ATP. Along with the impaired mitochondrial respiration, IR significantly expanded the intracellular pyruvate pool, and shifted pyruvate from oxidation toward anaerobic glycolysis, indicting by reducing pyruvate decarboxylation (PDC) relative to citric acid cycle (CAC) flux (172). ECMO significantly increased the pyruvate fractional contribution, while weaning followed a similar pattern (172). Besides, the CAC flux is also impaired after ischemia and during reloading. IR did not alter the level of citrate and α-KG but did substantially expand the pools of distal CAC intermediates succinate, fumarate, and malate. The accumulation of succinate is induced by forward flux from α-KG with partial inhibition of SDH within mitochondrial complex II. The high concentrations of succinate might readjust activity of dehydrogenase and produce fumarate and malate at a higher concentration. Alternatively, metabolic analysis suggests that the expansion of oxaloacetate and malate was partially through the anaplerotic entry of pyruvate. As demonstrated previously, IR can promote the carboxylation of anaplerotic pyruvate, which is converted to oxaloacetate by its carboxylase or converted to malate by malic enzyme (173, 174). The metabolic impairments, including the reduced PDC rate and accumulated succinate, also recurred with ECMO weaning, implying that limited OXPHOS due to insufficient acetyl-CoA and disrupted cycling of CAC impaired weaning.

In another adult swine model subjected to LAD occlusion, VA-ECMO was activated followed with 180-min LAD reperfusion, and the hemodynamic parameters were detected. Compared with the group of IR injury, ECMO initiation reduces right atrial RA pressure and LV stroke work but increases the infarct area normalized to the risk area and the infarct area normalized to the total LV area (139). Metabolic data based on unbiased and blinded analysis show that LV unloading by ECMO before reperfusion does not improve the use of myocardial energy substrates, nor can it preserve mitochondrial structure, including cardiolipin content induced by IR injury. Further functional analysis of the mitochondria of infarct zone showed that reperfusion that followed ECMO support also has impaired ETC, including mitochondrial Complexes I, II, and III, and increased oxidative stress with IR. Therefore, despite the fact that ECMO does reduce LV stroke work, it increases the infarct area and fails to protect myocardial mitochondrial and energy metabolism. It should be noted that, except for the hemodynamic effects, the large surface areas of extracorporeal circuits can activate neutrophils, which has already been demonstrated in patients with CS, and the increased circulating neutrophils can mediate reperfusion injury (175). In addition, the data that bypass the left atrium to the femoral artery without an oxygenator can reduce LV stroke work and infarct size also proves this point (133).

In addition to immune alterations, the discrepancies of the two preclinical studies may be attributed to differences between experimental models, such as animal maturity, duration and severity of ischemia, timing of ECMO initiation, flow of ECMO, timing of sampling, etc. Besides, the native cardiac volume and hemodynamic parameters are to be continuously monitored, since they are also correlated with tissue perfusion. As successful weaning of ECMO is based on end-organ function and myocardial recovery, which includes myocardial energetics and substrate utilization, metabolic pathways may be promising therapeutic targets in future clinical practices. Moreover, combined with profound hemodynamic monitoring, metabolites may be used as biomarkers to develop more comprehensive and superior algorithms or models for evaluating myocardial functional recovery.

CONCLUSION

This study summarizes substrate use and metabolic alterations during the process of IHD, with an emphasis on IR injury and HF. Although numerous metabolic processes outlined here are ideal drug targets for IR injury, further pieces of research are still needed to gain full insights into the underlying mechanism. Particularly, by unloading the ischemic heart and establishing the oxygen supply-demand balance, MCS is

promising in reducing IR injury and improving cardiac function. However, their effects on mitochondrial metabolism and cardiac improvement, especially VA-ECMO, still vary under different conditions. Therefore, more studies are needed to elucidate whether MCS has a beneficial impact on cardiac function and long-term prognosis.

AUTHOR CONTRIBUTIONS

MJ wrote the draft of the manuscript and prepared the figures. XX reviewed the manuscript. FC and YW proposed the original idea and reviewed the manuscript. All the authors read and approved the final submitted version of the manuscript.

FUNDING

This work was supported by Beijing Municipal Natural Science Foundation (7202189), Project of National Clinical Research Center for Geriatric Disease (NCRCG-PLAGH-2019024), The National Key Research Program of China (2018YFC0116305), The National Natural Science Foundation of China (grant nos. 91939303 and 81820108019), and Major Program of Central Health Committee (2020ZD05).

REFERENCES

1. Nowbar AN, Gitto M, Howard JP, Francis DP, Al-Lamee R. Mortality from ischemic heart disease. *Circulation*. (2019) 12:5375. doi: 10.1161/CIRCOUTCOMES.118.005375
2. Kaski J, Crea F, Gersh BJ, Camici PG. Reappraisal of ischemic heart disease. *Circulation.* (2018) 138:1463–80. doi: 10.1161/CIRCULATIONAHA.118.031373
3. Lee L. Metabolic manipulation in ischaemic heart disease, a novel approach to treatment. *Eur Heart J.* (2004) 25:634–41. doi: 10.1016/j.ehj.2004.02.018
4. Lopaschuk GD, Karwi QG, Tian R, Wende AR, Abel ED. Cardiac energy metabolism in heart failure. *Circ Res.* (2021) 128:1487–513. doi: 10.1161/CIRCRESAHA.121.318241
5. Faadielessop M, Opie L. Metabolic therapy for heart failure. *Eur Heart J.* (2004) 25:1765–8. doi: 10.1016/j.ehj.2004.08.019
6. Lopaschuk GD, Ussher JR, Folmes CDL, Jaswal JS, Stanley WC. Myocardial fatty acid metabolism in health and disease. *Physiol Rev.* (2010) 90:207–58. doi: 10.1152/physrev.00015.2009
7. Gorge G, Chatelain P, Schaper J, Lerch R. Effect of increasing degrees of ischemic injury on myocardial oxidative metabolism early after reperfusion in isolated rat hearts. *Circ Res.* (1991) 68:1681–92. doi: 10.1161/01.RES.68.6.1681
8. Zuurbier CJ, Bertrand L, Beauloye CR, Andreadou I, Ruiz-Meana M, Jespersen NR, et al. Cardiac metabolism as a driver and therapeutic target of myocardial infarction. *J Cell Mol Med.* (2020) 24:5937–54. doi: 10.1111/jcmm.15180
9. Zuurbier CJ, Ince C. Post-ischaemic changes in the response time of oxygen consumption to demand in the isolated rat heart are mediated partly by calcium and glycolysis. *Pflugers Arch.* (2002) 443:908–16. doi: 10.1007/s00424-001-0744-2
10. Benzi RH, Lerch R. Dissociation between contractile function and oxidative metabolism in postischemic myocardium. Attenuation by ruthenium red administered during reperfusion. *Circ Res.* (1992) 71:567–76. doi: 10.1161/01.RES.71.3.567
11. Stanley WC, Lopaschuk GD, Hall JL, Mccormack JG. Regulation of myocardial carbohydrate metabolism under normal and ischaemic conditions. Potential for pharmacological interventions. *Cardiovasc Res.* (1997) 33:243–57. doi: 10.1016/S0008-6363(96)00245-3
12. Tanaka-Esposito C, Chen Q, Lesnefsky EJ. Blockade of electron transport before ischemia protects mitochondria and decreases myocardial injury during reperfusion in aged rat hearts. *Transl Res.* (2012) 160:207–16. doi: 10.1016/j.trsl.2012.01.024
13. Turer AT, Stevens RD, Bain JR, Muehlbauer MJ, van der Westhuizen J, Mathew JP, et al. Metabolomic profiling reveals distinct patterns of myocardial substrate use in humans with coronary artery disease or left ventricular dysfunction during surgical Ischemia/Reperfusion. *Circulation.* (2009) 119:1736–46. doi: 10.1161/CIRCULATIONAHA.108.816116
14. Montessuit C, Lerch R. Regulation and dysregulation of glucose transport in cardiomyocytes. *Biochimica Biophysica Acta.* (2013) 1833:848–56. doi: 10.1016/j.bbamcr.2012.08.009
15. Shi T, Papay RS, Perez DM. Alpha1A-Adrenergic receptor prevents cardiac ischemic damage through PKCdelta/GLUT1/4-mediated glucose uptake. *J Recept Signal Transduct Res.* (2016) 36:261–70. doi: 10.3109/10799893.2015.1091475
16. Li X, Liu Y, Ma H, Guan Y, Cao Y, Tian Y, et al. Enhancement of glucose metabolism via PGC-1α participates in the cardioprotection of chronic intermittent hypobaric hypoxia. *Front Physiol.* (2016) 7:219. doi: 10.3389/fphys.2016.00219
17. Liu X, Zeng J, Yang Y, Qi C, Xiong T, Wu G, et al. DRD4 mitigates myocardial Ischemia/Reperfusion injury in association with PI3K/AKT mediated glucose metabolism. *Front Pharmacol.* (2021) 11:619426. doi: 10.3389/fphar.2020.619426
18. Tian R, Abel ED. Responses of GLUT4-deficient hearts to ischemia underscore the importance of glycolysis. *Circulation.* (2001) 103:2961–6. doi: 10.1161/01.CIR.103.24.2961
19. Omar MA, Verma S, Clanachan AS. Adenosine-mediated inhibition of 5′-AMP-activated protein kinase and p38 mitogen-activated protein kinase during reperfusion enhances recovery of left ventricular mechanical function. *J Mol Cell Cardiol.* (2012) 52:1308–18. doi: 10.1016/j.yjmcc.2012.03.014
20. Heidrich F, Schotola H, Popov AF, Sohns C, Schuenemann J, Friedrich M, et al. AMPK - activated protein kinase and its role in energy metabolism of the heart. *Curr Cardiol Rev.* (2010) 6:337–42. doi: 10.2174/157340310793566073
21. Fernández-Caggiano M, Prysyazhna O, Barallobre-Barreiro J, Calviñosantos R, Aldama López G, Generosa Crespo-Leiro M, et al. Analysis of mitochondrial proteins in the surviving myocardium after ischemia identifies mitochondrial pyruvate carrier expression as possible mediator of tissue viability. *Mol Cell Proteomics.* (2016) 15:246–55. doi: 10.1074/mcp.M115.051862
22. Kudo N, Barr AJ, Barr RL, Desai S, Lopaschuk GD. High rates of fatty acid oxidation during reperfusion of ischemic hearts are associated with a decrease in malonyl-CoA levels due to an increase in 5'-AMP-activated protein kinase inhibition of acetyl-CoA carboxylase. *J Biol Chem.* (1995) 270:17513–20. doi: 10.1074/jbc.270.29.17513
23. Chouchani ET, Methner C, Nadtochiy SM, Logan A, Pell VR, Ding S, et al. Cardioprotection by S-nitrosation of a cysteine switch on mitochondrial complex I. *Nat Med.* (2013) 19:753–9. doi: 10.1038/nm.3212
24. Garland PB, Randle PJ, Newsholme EA. Citrate as an intermediary in the inhibition of phosphofructokinase in rat heart muscle by fatty acids, ketone bodies, pyruvate, diabetes, and starvation. *Nature.* (1963) 200:169–70. doi: 10.1038/200169a0
25. Heather LC, Clarke K. Metabolism, hypoxia and the diabetic heart. *J Mol Cell Cardiol.* (2011) 50:598–605. doi: 10.1016/j.yjmcc.2011.01.007

26. Lopaschuk GD, Spafford MA, Davies NJ, Wall SR. Glucose and palmitate oxidation in isolated working rat hearts reperfused after a period of transient global ischemia. *Circ Res.* (1990) 66:546–53. doi: 10.1161/01.RES.66.2.546
27. Terrand J, Papageorgiou I, Rosenblatt-Velin N, Lerch R. Calcium-mediated activation of pyruvate dehydrogenase in severely injured postischemic myocardium. *Am J Physiol Heart Circ Physiol.* (2001) 281:H722–30. doi: 10.1152/ajpheart.2001.281.2.H722
28. Lerch R, Tamm C, Papageorgiou I, Benzi RH. Myocardial fatty acid oxidation during ischemia and reperfusion. *Mol Cell Biochem.* (1992) 116:103–9. doi: 10.1007/BF01270576
29. Lewandowski ED, White LT. Pyruvate dehydrogenase influences postischemic heart function. *Circulation.* (1995) 91:2071–9. doi: 10.1161/01.CIR.91.7.2071
30. Wang P, Lloyd SG, Chatham JC. Impact of high glucose/high insulin and dichloroacetate treatment on carbohydrate oxidation and functional recovery after low-flow ischemia and reperfusion in the isolated perfused rat heart. *Circulation.* (2005) 111:2066–72. doi: 10.1161/01.CIR.0000162466.06150.D4
31. Luptak I, Yan J, Cui L, Jain M, Liao R, Tian R. Long-term effects of increased glucose entry on mouse hearts during normal aging and ischemic stress. *Circulation.* (2007) 116:901–9. doi: 10.1161/CIRCULATIONAHA.107.691253
32. Mansor LS, Sousa FM, Yea G, Coumans WA, West JA, Kerr M, et al. Inhibition of sarcolemmal FAT/CD36 by sulfo-N-succinimidyl oleate rapidly corrects metabolism and restores function in the diabetic heart following hypoxia/reoxygenation. *Cardiovasc Res.* (2017) 113:737–48. doi: 10.1093/cvr/cvx045
33. Mccormack JG, Barr RL, Wolff AA, Lopaschuk GD. Ranolazine stimulates glucose oxidation in normoxic, ischemic, and reperfused ischemic rat hearts. *Circulation.* (1996) 93:135–42. doi: 10.1161/01.CIR.93.1.135
34. Ussher JR, Wang W, Gandhi M, Keung W, Samokhvalov V, Oka T, et al. Stimulation of glucose oxidation protects against acute myocardial infarction and reperfusion injury. *Cardiovasc Res.* (2012) 94:359–69. doi: 10.1093/cvr/cvs129
35. Pham V, Zhang W, Chen V, Whitney T, Yao J, Froese D, et al. Design and synthesis of novel pyridoxine 5'-phosphonates as potential antiischemic agents. *J Med Chem.* (2003) 46:3680–7. doi: 10.1021/jm0300678
36. Heywood SE, Richart AL, Henstridge DC, Alt K, Kiriazis H, Zammit C, et al. High-density lipoprotein delivered after myocardial infarction increases cardiac glucose uptake and function in mice. *Sci Transl Med.* (2017) 9:aam6084. doi: 10.1126/scitranslmed.aam6084
37. Doenst T, Nguyen TD, Abel ED. Cardiac metabolism in heart failure. *Circ Res.* (2013) 113:709–24. doi: 10.1161/CIRCRESAHA.113.300376
38. Ritterhoff J, Tian R. Metabolism in cardiomyopathy: every substrate matters. *Cardiovasc Res.* (2017) 113:411–21. doi: 10.1093/cvr/cvx017
39. Griffiths HR, Gao D, Pararasa C. Redox regulation in metabolic programming and inflammation. *Redox Biol.* (2017) 12:50–7. doi: 10.1016/j.redox.2017.01.023
40. Ou W, Liang Y, Qing Y, Wu W, Xie M, Zhang Y, et al. Hypoxic acclimation improves cardiac redox homeostasis and protects heart against ischemia-reperfusion injury through upregulation of O-GlcNAcylation. *Redox Biol.* (2021) 43:101994. doi: 10.1016/j.redox.2021.101994
41. Ellis JM, Frahm JL Li LO, Coleman RA. Acyl-coenzyme a synthetases in metabolic control. *CurrOpinLipidol.* (2010) 21:212–7. doi: 10.1097/MOL.0b013e32833884bb
42. Hopkins TA, Dyck JRB, Lopaschuk GD. AMP-activated protein kinase regulation of fatty acid oxidation in the ischaemic heart. *Biochem Soc T.* (2003) 31:207. doi: 10.1042/bst0310207
43. Shu H, Peng Y, Hang W, Nie J, Zhou N, Wang DW. The role of CD36 in cardiovascular disease. *Cardiovasc Res.* (2020) 2020:cvaa319. doi: 10.1093/cvr/cvaa319
44. Ussher JR, Lopaschuk GD. The malonyl CoA axis as a potential target for treating ischaemic heart disease. *Cardiovasc Res.* (2008) 79:259–68. doi: 10.1093/cvr/cvn130
45. Folmes CDL, Sowah D, Clanachan AS, Lopaschuk GD. High rates of residual fatty acid oxidation during mild ischemia decrease cardiac work and efficiency. *J Mol Cell Cardiol.* (2009) 47:142–8. doi: 10.1016/j.yjmcc.2009.03.005
46. Heather LC, Pates KM, Atherton HJ, Cole MA, Ball DR, Evans RD, et al. Differential translocation of the fatty acid transporter, FAT/CD36, and the glucose transporter, GLUT4, coordinates changes in cardiac substrate metabolism during ischemia and reperfusion. *Circulation.* (2013) 6:1058–66. doi: 10.1161/CIRCHEARTFAILURE.112.000342
47. Tominaga H, Katoh H, Odagiri K, Takeuchi Y, Kawashima H, Saotome M, et al. Different effects of palmitoyl-l-carnitine and palmitoyl-CoA on mitochondrial function in rat ventricular myocytes. *Am J Physiol-Heart C.* (2008) 295:H105–12. doi: 10.1152/ajpheart.01307.2007
48. Liepinsh E, Makrecka-Kuka M, Volska K, Kuka J, Makarova E, Antone U, et al. Long-chain acylcarnitines determine ischaemia/reperfusion-induced damage in heart mitochondria. *Biochem J.* (2016) 473:1191–202. doi: 10.1042/BCJ20160164
49. Tomanek RJ. Myocardial ischemia and infarction. In: Tomanek RJ, editor, *Coronary Vasculature: Development, Structure-Function, and Adaptations*. Boston, MA: Springer US (2013). p. 189–220. doi: 10.1007/978-1-4614-4887-7_10
50. Wang W, Zhang L, Battiprolu PK, Fukushima A, Nguyen K, Milner K, et al. Malonyl CoA decarboxylase inhibition improves cardiac function Post-Myocardial infarction. *JACC.* (2019) 4:385–400. doi: 10.1016/j.jacbts.2019.02.003
51. Dyck JRB, Cheng J, Stanley WC, Barr R, Chandler MP, Brown S, et al. Malonyl coenzyme a decarboxylase inhibition protects the ischemic heart by inhibiting fatty acid oxidation and stimulating glucose oxidation. *Circ Res.* (2004) 94:19569. doi: 10.1161/01.RES.0000129255.19569.8f
52. Liepinsh E, Makrecka-Kuka M, Kuka J, Vilskersts R, Makarova E, Cirule H, et al. Inhibition of L-carnitine biosynthesis and transport by methyl-γ-butyrobetaine decreases fatty acid oxidation and protects against myocardial infarction. *Brit J Pharmacol.* (2015) 172:1319–32. doi: 10.1111/bph.13004
53. Liu Z, Chen J, Huang H, Kuznicki M, Zheng S, Sun W, et al. The protective effect of trimetazidine on myocardial ischemia/reperfusion injury through activating AMPK and ERK signaling pathway. *Metabolism.* (2016) 65:122–30. doi: 10.1016/j.metabol.2015.10.022
54. Hu H, Li X, Ren D, Tan Y, Chen J, Yang L, et al. The cardioprotective effects of carvedilol on ischemia and reperfusion injury by AMPK signaling pathway. *Biomed Pharmacother.* (2019) 117:109106. doi: 10.1016/j.biopha.2019.109106
55. Liu Q, Docherty JC, Rendell JCT, Clanachan AS, Lopaschuk GD. High levels of fatty acids delay the recovery of intracellular pH and cardiac efficiency in post-ischemic hearts by inhibiting glucose oxidation. *J Am Coll Cardiol.* (2002) 39:718–25. doi: 10.1016/S0735-1097(01)01803-4
56. Cotter DG, Schugar RC, Crawford PA. Ketone body metabolism and cardiovascular disease. *Am J Physiol-Heart C.* (2013) 304:H1060–76. doi: 10.1152/ajpheart.00646.2012
57. Ho KL, Zhang L, Wagg C, Al Batran R, Gopal K, Levasseur J, et al. Increased ketone body oxidation provides additional energy for the failing heart without improving cardiac efficiency. *Cardiovasc Res.* (2019) 115:1606–16. doi: 10.1093/cvr/cvz045
58. Anorek M, Hodyc D, Aedivý V, Durišová J, Skoumalová A, Wilhelm J, et al. Short-term fasting reduces the extent of myocardial infarction and incidence of reperfusion arrhythmias in rats. *Physiol Res.* (2012) 2012:567–74. doi: 10.33549/physiolres.932338
59. Al-Zaid NS, Dashti HM, Mathew TC, Juggi JS. Low carbohydrate ketogenic diet enhances cardiac tolerance to global ischaemia. *Acta Cardiol.* (2007) 62:381–9. doi: 10.2143/AC.62.4.2022282
60. Wang P, Tate JM, Lloyd SG. Low carbohydrate diet decreases myocardial insulin signaling and increases susceptibility to myocardial ischemia. *Life Sci.* (2008) 83:836–44. doi: 10.1016/j.lfs.2008.09.024
61. Zou Z, Sasaguri S, Rajesh KG, Suzuki R. Dl-3-Hydroxybutyrate administration prevents myocardial damage after coronary occlusion in rat hearts. *Am J Physiol-Heart C.* (2002) 283:H1968–74. doi: 10.1152/ajpheart.00250.2002
62. Shimazu T, Hirschey MD, Newman J, He W, Shirakawa K, Le Moan N, et al. Suppression of oxidative stress by -Hydroxybutyrate, an endogenous histone deacetylase inhibitor. *Science.* (2013) 339:211–4. doi: 10.1126/science.1227166

63. Puchalska P, Crawford PA. Multi-dimensional roles of ketone bodies in fuel metabolism, signaling, and therapeutics. *Cell Metab.* (2017) 25:262–84. doi: 10.1016/j.cmet.2016.12.022
64. Yu Y, Yu Y, Zhang Y, Zhang Z, An W, Zhao X. Treatment with D-β-hydroxybutyrate protects heart from ischemia/reperfusion injury in mice. *Eur J Pharmacol.* (2018) 829:121–8. doi: 10.1016/j.ejphar.2018.04.019
65. Arima Y, Izumiya Y, Ishida T, Takashio S, Ishii M, Sueta D, et al. Myocardial ischemia suppresses ketone body utilization. *J Am Coll Cardiol.* (2019) 73:246–7. doi: 10.1016/j.jacc.2018.10.040
66. Aubert G, Martin OJ, Horton JL, Lai L, Vega RB, Leone TC, et al. The failing heart relies on ketone bodies as a fuel. *Circulation.* (2016) 133:698–705. doi: 10.1161/CIRCULATIONAHA.115.017355
67. Uchihashi M, Hoshino A, Okawa Y, Ariyoshi M, Kaimoto S, Tateishi S, et al. Cardiac-Specific bdh1 overexpression ameliorates oxidative stress and cardiac remodeling in pressure overload–induced heart failure. *Circulation.* (2017) 10:4417. doi: 10.1161/CIRCHEARTFAILURE.117.004417
68. Horton JL, Davidson MT, Kurishima C, Vega RB, Powers JC, Matsuura TR, et al. The failing heart utilizes 3-hydroxybutyrate as a metabolic stress defense. *JCI Insight.* (2019) 4:124079. doi: 10.1172/jci.insight.124079
69. Yurista SR, Silljé HHW, Oberdorf Maass SU, Schouten EM, Pavez Giani MG, Hillebrands JL, et al. Sodium–glucose co-transporter 2 inhibition with empagliflozin improves cardiac function in non-diabetic rats with left ventricular dysfunction after myocardial infarction. *Eur J Heart Fail.* (2019) 21:862–73. doi: 10.1002/ejhf.1473
70. Selvaraj S, Kelly DP, Margulies KB. Implications of altered ketone metabolism and therapeutic ketosis in heart failure. *Circulation.* (2020) 141:1800–12. doi: 10.1161/CIRCULATIONAHA.119.045033
71. Huang Y, Zhou M, Sun H, Wang Y. Branched-chain amino acid metabolism in heart disease: an epiphenomenon or a real culprit? *Cardiovasc Res.* (2011) 90:220–3. doi: 10.1093/cvr/cvr070
72. Bhattacharya S, Granger CB, Craig D, Haynes C, Bain J, Stevens RD, et al. Validation of the association between a branched chain amino acid metabolite profile and extremes of coronary artery disease in patients referred for cardiac catheterization. *Atherosclerosis.* (2014) 232:191–6. doi: 10.1016/j.atherosclerosis.2013.10.036
73. Santos-Gallego CG, Requena-Ibanez JA, San Antonio R, Ishikawa K, Watanabe S, Picatoste B, et al. Empagliflozin ameliorates adverse left ventricular remodeling in nondiabetic heart failure by enhancing myocardial energetics. *J Am Coll Cardiol.* (2019) 73:1931–44. doi: 10.1016/j.jacc.2019.01.056
74. Wang W, Zhang F, Xia Y, Zhao S, Yan W, Wang H, et al. Defective branched chain amino acid catabolism contributes to cardiac dysfunction and remodeling following myocardial infarction. *Am J Physiol-Heart C.* (2016) 311:H1160–9. doi: 10.1152/ajpheart.00114.2016
75. Karwi QG, Zhang L, Wagg CS, Wang W, Ghandi M, Thai D, et al. Targeting the glucagon receptor improves cardiac function and enhances insulin sensitivity following a myocardial infarction. *Cardiovasc Diabetol.* (2019) 18:4. doi: 10.1186/s12933-019-0806-4
76. Li T, Zhang Z, Kolwicz SC, Abell L, Roe ND, Kim M, et al. Defective Branched-Chain amino acid catabolism disrupts glucose metabolism and sensitizes the heart to Ischemia-Reperfusion injury. *Cell Metab.* (2017) 25:374–85. doi: 10.1016/j.cmet.2016.11.005
77. Jang C, Oh SF, Wada S, Rowe GC, Liu L, Chan MC, et al. A branched-chain amino acid metabolite drives vascular fatty acid transport and causes insulin resistance. *Nat Med.* (2016) 22:421–6. doi: 10.1038/nm.4057
78. Li Y, Xiong Z, Yan W, Gao E, Cheng H, Wu G, et al. Branched chain amino acids exacerbate myocardial ischemia/reperfusion vulnerability *via* enhancing GCN2/ATF6/PPAR-α pathway-dependent fatty acid oxidation. *Theranostics.* (2020) 10:5623–40. doi: 10.7150/thno.44836
79. Lu G, Sun H, She P, Youn J, Warburton S, Ping P, et al. Protein phosphatase 2Cm is a critical regulator of branched-chain amino acid catabolism in mice and cultured cells. *J Clin Invest.* (2009) 119:1678–87. doi: 10.1172/JCI38151
80. Lian K, Guo X, Wang Q, Liu Y, Wang RT, Gao C, et al. PP2Cm overexpression alleviates MI/R injury mediated by a BCAA catabolism defect and oxidative stress in diabetic mice. *Eur J Pharmacol.* (2020) 866:172796. doi: 10.1016/j.ejphar.2019.172796
81. Dong W, Zhou M, Dong M, Pan B, Liu Y, Shao J, et al. Keto acid metabolites of branched-chain amino acids inhibit oxidative stress-induced necrosis and attenuate myocardial ischemia-reperfusion injury. *J Mol Cell Cardiol.* (2016) 101:90–8. doi: 10.1016/j.yjmcc.2016.11.002
82. Lesnefsky EJ, Chen Q, Moghaddas S, Hassan MO, Tandler B, Hoppel CL. Blockade of electron transport during ischemia protects cardiac mitochondria. *J Biol Chem.* (2004) 279:47961–7. doi: 10.1074/jbc.M409720200
83. Sun H, Olson KC, Gao C, Prosdocimo DA, Zhou M, Wang Z, et al. Catabolic defect of Branched-Chain amino acids promotes heart failure. *Circulation.* (2016) 133:2038–49. doi: 10.1161/CIRCULATIONAHA.115.020226
84. Chouchani ET, Pell VR, Gaude E, Aksentijević D, Sundier SY, Robb EL, et al. Ischaemic accumulation of succinate controls reperfusion injury through mitochondrial ROS. *Nature (London).* (2014) 515:431–5. doi: 10.1038/nature13909
85. Zhang J, Wang YT, Miller JH, Day MM, Munger JC, Brookes PS. Accumulation of succinate in cardiac ischemia primarily occurs via canonical krebs cycle activity. *Cell Rep.* (2018) 23:2617–28. doi: 10.1016/j.celrep.2018.04.104
86. Dambrova M, Zuurbier CJ, Borutaite V, Liepinsh E, Makrecka-Kuka M. Energy substrate metabolism and mitochondrial oxidative stress in cardiac ischemia/reperfusion injury. *Free Radical Bio Med.* (2021) 165:24–37. doi: 10.1016/j.freeradbiomed.2021.01.036
87. Andrienko TN, Pasdois P, Pereira GC, Ovens MJ, Halestrap AP. The role of succinate and ROS in reperfusion injury - a critical appraisal. *J Mol Cell Cardiol.* (2017) 110:1–14. doi: 10.1016/j.yjmcc.2017.06.016
88. Chouchani ET, Pell VR, James AM, Work LM, Saeb-Parsy K, Frezza C, et al. Unifying mechanism for mitochondrial superoxide production during ischemia-reperfusion injury. *Cell Metab.* (2016) 23:254–63. doi: 10.1016/j.cmet.2015.12.009
89. Mills EL, Pierce KA, Jedrychowski MP, Garrity R, Winther S, Vidoni S, et al. Accumulation of succinate controls activation of adipose tissue thermogenesis. *Nature.* (2018) 560:102–6. doi: 10.1038/s41586-018-0353-2
90. Kohlhauer M, Dawkins S, Costa ASH, Lee R, Young T, Pell VR, et al. Metabolomic profiling in acute ST-segment–elevation myocardial infarction identifies succinate as an early marker of human ischemia–reperfusion injury. *J Am Heart Assoc.* (2018) 7:7546. doi: 10.1161/JAHA.117.007546
91. Kula-Alwar D, Prag HA, Krieg T. Targeting succinate metabolism in Ischemia/Reperfusion injury. *Circulation.* (2019) 140:1968–70. doi: 10.1161/CIRCULATIONAHA.119.042791
92. Valls-Lacalle L, Barba I, Miró-Casas E, Alburquerque-Béjar JJ, Ruiz-Meana M, Fuertes-Agudo M, et al. Succinate dehydrogenase inhibition with malonate during reperfusion reduces infarct size by preventing mitochondrial permeability transition. *Cardiovasc Res.* (2016) 109:374–84. doi: 10.1093/cvr/cvv279
93. Bae J, Salamon RJ, Brandt EB, Paltzer WG, Zhang Z, Britt EC, et al. Malonate promotes adult cardiomyocyte proliferation and heart regeneration. *Circulation.* (2021) 143:1973–86. doi: 10.1161/CIRCULATIONAHA.120.049952
94. Li P, Ge J, Li H. Lysine acetyltransferases and lysine deacetylases as targets for cardiovascular disease. *Nat Rev Cardiol.* (2020) 17:96–115. doi: 10.1038/s41569-019-0235-9
95. Boylston JA, Sun J, Chen Y, Gucek M, Sack MN, Murphy E. Characterization of the cardiac succinylome and its role in ischemia–reperfusion injury. *J Mol Cell Cardiol.* (2015) 88:73–81. doi: 10.1016/j.yjmcc.2015.09.005
96. Porter GA, Urciuoli WR, Brookes PS, Nadtochiy SM. SIRT3 deficiency exacerbates ischemia-reperfusion injury: implication for aged hearts. *Am J Physiol Heart Circulat Physiol.* (2014) 306:H1602–9. doi: 10.1152/ajpheart.00027.2014
97. Xu Y, Zhang S, Rong J, Lin Y, Du L, Wang Y, et al. Sirt3 is a novel target to treat sepsis induced myocardial dysfunction by acetylated modulation of critical enzymes within cardiac tricarboxylic acid cycle. *Pharmacol Res.* (2020) 159:104887. doi: 10.1016/j.phrs.2020.104887
98. Davidson MT, Grimsrud PA, Lai L, Draper JA, Fisher-Wellman KH, Narowski TM, et al. Extreme acetylation of the cardiac mitochondrial proteome does not promote heart failure. *Circ Res.* (2020) 127:1094–108. doi: 10.1161/CIRCRESAHA.120.317293

99. Deng Y, Xie M, Li Q, Xu X, Ou W, Zhang Y, et al. Targeting mitochondria-inflammation circuit by β-hydroxybutyrate mitigates HFpEF. *Circ Res.* (2021) 128:232–45. doi: 10.1161/CIRCRESAHA.120.317933
100. Tang X, Chen X, Sun X, Xu P, Zhao X, Tong Y, et al. Short-Chain Enoyl-CoA hydratase mediates histone crotonylation and contributes to cardiac homeostasis. *Circulation.* (2021) 143:1066–9. doi: 10.1161/CIRCULATIONAHA.120.049438
101. Zhang D, Tang Z, Huang H, Zhou G, Cui C, Weng Y, et al. Metabolic regulation of gene expression by histone lactylation. *Nature.* (2019) 574:575–80. doi: 10.1038/s41586-019-1678-1
102. Irizarry-Caro RA, Mcdaniel MM, Overcast GR, Jain VG, Troutman TD, Pasare C, et al. signaling adapter BCAP regulates inflammatory to reparatory macrophage transition by promoting histone lactylation. *Proc Nat Acad Sci USA.* (2020) 117:30628–38. doi: 10.1073/pnas.2009778117
103. Dai X, Lv X, Thompson EK, Ostrikov KK. Histone lactylation: epigenetic mark of glycolytic switch. *Trends Genet.* (2021) 9:9. doi: 10.1016/j.tig.2021.09.009
104. Wang H, Jiang M, Li X, Zhao Y, Shao J, Liu Z, et al. Anti-inflammatory therapies for coronary heart disease: a systematic review and meta-analysis. *Front Cardiovasc Med.* (2021) 8:726341. doi: 10.3389/fcvm.2021.726341
105. Swirski FK, Nahrendorf M. Cardioimmunology: the immune system in cardiac homeostasis and disease. *Nat Rev Immunol.* (2018) 18:733–44. doi: 10.1038/s41577-018-0065-8
106. Virani SS, Alonso A, Benjamin EJ, Bittencourt MS, Callaway CW, Carson AP, et al. Heart disease and stroke statistics—2020 update: a report from the American heart association. *Circulation.* (2020) 141:746. doi: 10.1161/CIR.0000000000000746
107. Stone GWM, Selker HPM, Thiele HM, Patel MRM, Udelson JEM, Ohman EMM, et al. Relationship between infarct size and outcomes following primary PCI. *J Am Coll Cardiol.* (2016) 67:1674–83. doi: 10.1016/j.jacc.2016.01.069
108. Yellon DM, Hausenloy DJ. Myocardial reperfusion injury. *N Engl J Med.* (2007) 357:1121–35. doi: 10.1056/NEJMra071667
109. Ramachandra CJA, Hernandez-Resendiz S, Crespo-Avilan GE, Lin Y, Hausenloy DJ. Mitochondria in acute myocardial infarction and cardioprotection. *Ebiomedicine.* (2020) 57:102884. doi: 10.1016/j.ebiom.2020.102884
110. Burkhoff DMP, Sayer GM, Doshi DM, Uriel NM. Hemodynamics of mechanical circulatory support. *J Am Coll Cardiol.* (2015) 66:2663–74. doi: 10.1016/j.jacc.2015.10.017
111. Kapur NK, Paruchuri V, Pham DT, Reyelt L, Murphy B, Beale C, et al. Hemodynamic effects of left atrial or left ventricular cannulation for acute circulatory support in a bovine model of left heart injury. *ASAIO J.* (2015) 61:301–6. doi: 10.1097/MAT.0000000000000195
112. Curran J, Burkhoff D, Kloner RA. Beyond reperfusion: acute ventricular unloading and cardioprotection during myocardial infarction. *J Cardiovasc Transl.* (2019) 12:95–106. doi: 10.1007/s12265-019-9863-z
113. Koo JH, Guan K. Interplay between YAP/TAZ and metabolism. *Cell Metab.* (2018) 28:196–206. doi: 10.1016/j.cmet.2018.07.010
114. Liao H, Qi Y, Ye Y, Yue P, Zhang D, Li Y. Mechanotranduction pathways in the regulation of mitochondrial homeostasis in cardiomyocytes. *Front Cell Dev Biol.* (2021) 8:625089. doi: 10.3389/fcell.2020.625089
115. Zhang Y, Qi Y, Li JJ, He WJ, Gao XH, Zhang Y, et al. Stretch-induced sarcoplasmic reticulum calcium leak is causatively associated with atrial fibrillation in pressure-overloaded hearts. *Cardiovasc Res.* (2021) 117:1091–102. doi: 10.1093/cvr/cvaa163
116. Berridge MJ. Calcium signallingremodelling and disease. *Biochem Soc Trans.* (2012) 40:297–309. doi: 10.1042/BST20110766
117. Boyman L, Karbowski M, Lederer WJ. Regulation of mitochondrial ATP production: Ca(2+) signaling and quality control. *Trends Mol Med.* (2020) 26:21–39. doi: 10.1016/j.molmed.2019.10.007
118. Schaeffer PJ, Wende AR, Magee CJ, Neilson JR, Leone TC, Chen F, et al. Calcineurin and Calcium/Calmodulin-dependent protein kinase activate distinct metabolic gene regulatory programs in cardiac muscle. *J Biol Chem.* (2004) 279:39593–603. doi: 10.1074/jbc.M403649200
119. Hajnoczky G, Robb-Gaspers LD, Seitz MB, Thomas AP. Decoding of cytosolic calcium oscillations in the mitochondria. *Cell.* (1995) 82:415–24. doi: 10.1016/0092-8674(95)90430-1
120. Kohlhaas M, Maack C. Adverse bioenergetic consequences of na+ -Ca2+ exchanger–mediated ca2+ influx in cardiac myocytes. *Circulation.* (2010) 122:2273–80. doi: 10.1161/CIRCULATIONAHA.110.968057
121. Maus M, Cuk M, Patel B, Lian J, Ouimet M, Kaufmann U, et al. Store-operated ca^{2+} entry controls induction of lipolysis and the transcriptional reprogramming to lipid metabolism. *Cell Metab.* (2017) 25:698–712. doi: 10.1016/j.cmet.2016.12.021
122. Ashrafi G, de Juan-Sanz J, Farrell RJ, Ryan TA. Molecular tuning of the axonal mitochondrial ca^{2+} uniporter ensures metabolic flexibility of neurotransmission. *Neuron.* (2020) 105:678–87. doi: 10.1016/j.neuron.2019.11.020
123. Coste B, Mathur J, Schmidt M, Earley TJ, Ranade S, Petrus MJ, et al. Piezo1 and piezo2 are essential components of distinct mechanically activated cation channels. *Science.* (2010) 330:55–60. doi: 10.1126/science.1193270
124. Li J, Hou B, Tumova S, Muraki K, Bruns A, Ludlow MJ, et al. Piezo1 integration of vascular architecture with physiological force. *Nature.* (2014) 515:279–82. doi: 10.1038/nature13701
125. Liang J, Huang B, Yuan G, Chen Y, Liang F, Zeng H, et al. Stretch-activated channel Piezo1 is up-regulated in failure heart and cardiomyocyte stimulated by AngII. *Am J Transl Res.* (2017) 9:2945–55.
126. Wong T, Juang W, Tsai C, Tseng C, Lee W, Chang S, et al. Mechanical stretching simulates cardiac physiology and pathology through mechanosensor piezo1. *J Clin Med.* (2018) 7:410. doi: 10.3390/jcm7110410
127. Baratchi S, Zaldivia MTK, Wallert M, Loseff-Silver J, Al-Aryahi S, Zamani J, et al. Transcatheter aortic valve implantation represents an anti-inflammatory therapy *via* reduction of shear stress–induced, piezo-1–mediated monocyte activation. *Circulation.* (2020) 142:1092–105. doi: 10.1161/CIRCULATIONAHA.120.045536
128. Duchemin A, Vignes H, Vermot J. Mechanically activated piezo channels modulate outflow tract valve development through the Yap1 and Klf2-Notch signaling axis. *Elife.* (2019) 8:44706. doi: 10.7554/eLife.44706
129. Yang Y, Wang D, Zhang C, Yang W, Li C, Gao Z, et al. Piezo1 mediates endothelial atherogenic inflammatory responses *via* regulation of YAP/TAZ activation. *Hum Cell.* (2021). doi: 10.1007/s13577-021-00600-5
130. Meng Z, Qiu Y, Lin KC, Kumar A, Placone JK, Fang C, et al. RAP2 mediates mechanoresponses of the Hippo pathway. *Nature.* (2018) 560:655–60. doi: 10.1038/s41586-018-0444-0
131. Kashihara T, Sadoshima J. Role of YAP/TAZ in energy metabolism in the heart. *J Cardiovasc Pharm.* (2019) 74:483–90. doi: 10.1097/FJC.0000000000000736
132. Saku K, Kakino T, Arimura T, Sunagawa G, Nishikawa T, Sakamoto T, et al. Left ventricular mechanical unloading by total support of impella in myocardial infarction reduces infarct size, preserves left ventricular function, and prevents subsequent heart failure in dogs. *Circulation.* (2018) 11:4397. doi: 10.1161/CIRCHEARTFAILURE.117.004397
133. Kapur NK, Paruchuri V, Urbano-Morales JA, Mackey EE, Daly GH, Qiao X, et al. Mechanically unloading the left ventricle before coronary reperfusion reduces left ventricular wall stress and myocardial infarct size. *Circulation.* (2013) 128:328–36. doi: 10.1161/CIRCULATIONAHA.112.000029
134. Kapur NKM, Qiao XP, Paruchuri VM, Morine KJM, Syed WB, Dow SM, et al. Mechanical pre-conditioning with acute circulatory support before reperfusion limits infarct size in acute myocardial infarction. *JACC Heart Failure.* (2015) 3:873–82. doi: 10.1016/j.jchf.2015.06.010
135. Esposito ML, Zhang Y, Qiao X, Reyelt L, Paruchuri V, Schnitzler GR, et al. Left ventricular unloading before reperfusion promotes functional recovery after acute myocardial infarction. *J Am Coll Cardiol.* (2018) 72:501–14. doi: 10.1016/j.jacc.2018.05.034
136. Watanabe S, Fish K, Kovacic JC, Bikou O, Leonardson L, Nomoto K, et al. Left ventricular unloading using an impella CP improves coronary flow and infarct zone perfusion in ischemic heart failure. *J Am Heart Assoc.* (2018) 7:6462. doi: 10.1161/JAHA.117.006462
137. Briceno N, Annamalai SK, Reyelt L, Crowley P, Qiao X, Swain L, et al. Left ventricular unloading increases the coronary collateral flow index before reperfusion and reduces infarct size in a swine model of acute myocardial infarction. *J Am Heart Assoc.* (2019) 8:13586. doi: 10.1161/JAHA.119.013586
138. Kapur NK, Alkhouli MA, Demartini TJ, Faraz H, George ZH, Goodwin MJ, et al. Unloading the left ventricle before reperfusion in patients with

anterior ST-Segment–elevation myocardial infarction. *Circulation.* (2019) 139:337–46. doi: 10.1161/CIRCULATIONAHA.118.038269
139. Swain L, Reyelt L, Bhave S, Qiao X, Thomas CJ, Zweck E, et al. Transvalvular ventricular unloading before reperfusion in acute myocardial infarction. *J Am Coll Cardiol.* (2020) 76:684–99. doi: 10.1016/j.jacc.2020.06.031
140. Lee SH, Doliba N, Osbakken M, Oz M, Mancini D. Improvement of myocardial mitochondrial function after hemodynamic support with left ventricular assist devices in patients with heart failure. *J Thorac Cardiovasc Surg.* (1998) 116:344–9. doi: 10.1016/S0022-5223(98)70136-9
141. Ji R, Akashi H, Drosatos K, Liao X, Jiang H, Kennel PJ, et al. Increased de novo ceramide synthesis and accumulation in failing myocardium. *JCI Insight.* (2017) 2:96203. doi: 10.1172/jci.insight.96203
142. Chokshi A, Drosatos K, Cheema FH, Ji R, Khawaja T, Yu S, et al. Ventricular assist device implantation corrects myocardial lipotoxicity, reverses insulin resistance, and normalizes cardiac metabolism in patients with advanced heart failure. *Circulation.* (2012) 125:2844–53. doi: 10.1161/CIRCULATIONAHA.111.060889
143. Goldenberg JR, Carley AN, Ji R, Zhang X, Fasano M, Schulze PC, et al. Preservation of acyl coenzyme a attenuates pathological and metabolic cardiac remodeling through selective lipid trafficking. *Circulation.* (2019) 139:2765–77. doi: 10.1161/CIRCULATIONAHA.119.039610
144. Heerdt PM, Schlame M, Jehle R, Barbone A, Burkhoff D, Blanck TJ. Disease-specific remodeling of cardiac mitochondria after a left ventricular assist device. *Ann Thorac Surg.* (2002) 73:1216–21. doi: 10.1016/S0003-4975(01)03621-9
145. Hui S, Ghergurovich JM, Morscher RJ, Jang C, Teng X, Lu W, et al. Glucose feeds the TCA cycle via circulating lactate. *Nature.* (2017) 551:115–8. doi: 10.1038/nature24057
146. Diakos NA, Navankasattusas S, Abel ED, Rutter J, Mccreath L, Ferrin P, et al. Evidence of glycolysis up-regulation and pyruvate mitochondrial oxidation mismatch during mechanical unloading of the failing human heart: Implications for cardiac reloading and conditioning. *JACC Basic Transl Sci.* (2016) 1:432–44. doi: 10.1016/j.jacbts.2016.06.009
147. Cluntun AA, Badolia R, Lettlova S, Parnell KM, Shankar TS, Diakos NA, et al. The pyruvate-lactate axis modulates cardiac hypertrophy and heart failure. *Cell Metab.* (2021) 33:629–48. doi: 10.1016/j.cmet.2020.12.003
148. Bricker DK, Taylor EB, Schell JC, Orsak T, Boutron A, Chen Y, et al. A mitochondrial pyruvate carrier required for pyruvate uptake in yeast, drosophila, and humans. *Science.* (2012) 337:96–100. doi: 10.1126/science.1218099
149. Shahinian JH, Rog Zielinska EA, Schlimpert M, Mayer B, Tholen S, Kammerer B, et al. Impact of left ventricular assist device therapy on the cardiac proteome and metabolome composition in ischemic cardiomyopathy. *Artif Organs.* (2020) 44:257–67. doi: 10.1111/aor.13566
150. Badolia R, Ramadurai DKA, Abel ED, Ferrin P, Taleb I, Shankar TS, et al. The role of nonglycolytic glucose metabolism in myocardial recovery upon mechanical unloading and circulatory support in chronic heart failure. *Circulation.* (2020) 142:259–74. doi: 10.1161/CIRCULATIONAHA.119.044452
151. Huang G, Huang Z, Peng Y, Wang Y, Liu W, Xue Y, et al. Metabolic processes are potential biological processes distinguishing nonischemic dilated cardiomyopathy from ischemic cardiomyopathy: a clue from serum proteomics. *Pharmgenomics Pers Med.* (2021) 14:1169–84. doi: 10.2147/PGPM.S323379
152. Scholz KH, Maier SKG, Maier LS, Lengenfelder B, Jacobshagen C, Jung J, et al. Impact of treatment delay on mortality in ST-segment elevation myocardial infarction (STEMI) patients presenting with and without haemodynamic instability: Results from the German prospective, multicentre FITT-STEMI trial. *Eur Heart J.* (2018) 39:1065–74. doi: 10.1093/eurheartj/ehy004
153. Vallabhajosyula S, Dunlay SM, Prasad A, Kashani K, Sakhuja A, Gersh BJ, et al. Acute noncardiac organ failure in acute myocardial infarction with cardiogenic shock. *J Am Coll Cardiol.* (2019) 73:1781–91. doi: 10.1016/j.jacc.2019.01.053
154. Kapur NK, Davila CD, Chweich H. Protecting the vulnerable left ventricle: the art of unloading with VA-ECMO. *Circ Heart Fail.* (2019) 12:e6581. doi: 10.1161/CIRCHEARTFAILURE.119.006581
155. Lüsebrink E, Orban M, Kupka D, Scherer C, Hagl C, Zimmer S, et al. Prevention and treatment of pulmonary congestion in patients undergoing venoarterial extracorporeal membrane oxygenation for cardiogenic shock. *Eur Heart J.* (2020) 41:3753–61. doi: 10.1093/eurheartj/ehaa547
156. Aso S, Matsui H, Fushimi K, Yasunaga H. The effect of intraaortic balloon pumping under venoarterial extracorporeal membrane oxygenation on mortality of cardiogenic patients: an analysis using a nationwide inpatient database. *Crit Care Med.* (2016) 44:1974–9. doi: 10.1097/CCM.0000000000001828
157. Rao P, Khalpey Z, Smith R, Burkhoff D, Kociol RD. Venoarterial extracorporeal membrane oxygenation for cardiogenic shock and cardiac arrest. *Circulation.* (2018) 11:4905. doi: 10.1161/CIRCHEARTFAILURE.118.004905
158. Jugdutt BI. Ischemia/infarction. *Heart Fail Clin.* (2012) 8:43–51. doi: 10.1016/j.hfc.2011.08.006
159. Abrams D, Combes A, Brodie D. Extracorporeal membrane oxygenation in cardiopulmonary disease in adults. *J Am Coll Cardiol.* (2014) 63:2769–78. doi: 10.1016/j.jacc.2014.03.046
160. Vallabhajosyula S, Prasad A, Bell MR, Sandhu GS, Eleid MF, Dunlay SM, et al. Extracorporeal membrane oxygenation use in acute myocardial infarction in the United States, 2000 to 2014. *Circul Heart Failure.* (2019) 12:e5929. doi: 10.1161/CIRCHEARTFAILURE.119.005929
161. Vallabhajosyula S, Horo JC, Antharam P, Ananthaneni S, Vallabhajosyula S, Stulak JM, et al. Concomitant Intra-Aortic balloon pump use in cardiogenic shock requiring Veno-Arterial extracorporeal membrane oxygenation. *Circulation.* (2018) 11:6930. doi: 10.1161/CIRCINTERVENTIONS.118.006930
162. Vallabhajosyula S, Horo JC, Antharam P, Ananthaneni S, Vallabhajosyula S, Stulak JM, et al. Venoarterial extracorporeal membrane oxygenation with concomitant impella versus venoarterial extracorporeal membrane oxygenation for cardiogenic shock. *ASAIO J.* (2020) 66:497–503. doi: 10.1097/MAT.0000000000001039
163. Tongers J, Sieweke J, Kühn C, Napp LC, Flierl U, Röntgen P, et al. Early escalation of mechanical circulatory support stabilizes and potentially rescues patients in refractory cardiogenic shock. *Circulation.* (2020) 13:5853. doi: 10.1161/CIRCHEARTFAILURE.118.005853
164. Al-Fares AA, Randhawa VK, Englesakis M, Mcdonald MA, Nagpal AD, Estep JD, et al. Optimal strategy and timing of left ventricular venting during Veno-Arterial extracorporeal life support for adults in cardiogenic shock. *Circulation.* (2019) 12:6486. doi: 10.1161/CIRCHEARTFAILURE.119.006486
165. Allan CK, Newburger JW, Mcgrath E, Elder J, Psoinos C, Laussen PC, et al. The relationship between inflammatory activation and clinical outcome after infant cardiopulmonary bypass. *Anesthesia Analgesia.* (2010) 111:1244–51. doi: 10.1213/ANE.0b013e3181f333aa
166. Shew SB, Keshen TH, Jahoor F, Jaksic T. The determinants of protein catabolism in neonates on extracorporeal membrane oxygenation. *J Pediatr Surg.* (1999) 34:1086–90. doi: 10.1016/S0022-3468(99)90572-9
167. Priddy CMOK, Kajimoto M, Ledee DR, Bouchard B, Isern N, Olson AK, et al. Myocardial oxidative metabolism and protein synthesis during mechanical circulatory support by extracorporeal membrane oxygenation. *Am J Physiol-Heart C.* (2013) 304:H406–14. doi: 10.1152/ajpheart.00672.2012
168. Kajimoto M, O'Kelly Priddy CM, Ledee DR, Xu C, Isern N, Olson AK, et al. Extracorporeal membrane oxygenation promotes long chain fatty acid oxidation in the immature swine heart in vivo. *J Mol Cell Cardiol.* (2013) 62:144–52. doi: 10.1016/j.yjmcc.2013.05.014
169. Randle PJ, Garland PB, Hales CN, Newsholme EA. The glucose fatty-acid cycle. Its role in insulin sensitivity and the metabolic disturbances of diabetes mellitus. *Lancet.* (1963) 1:785–9. doi: 10.1016/S0140-6736(63)91500-9
170. Kajimoto M, O'Kelly Priddy CM, Ledee DR, Xu C, Isern N, Olson AK, et al. Myocardial reloading after extracorporeal membrane oxygenation alters substrate metabolism while promoting protein synthesis. *J Am Heart Assoc.* (2013) 2:106. doi: 10.1161/JAHA.113.000106
171. Portman MA, Standaert TA, Ning XH. Relation of myocardial oxygen consumption and function to high energy phosphate utilization during graded hypoxia and reoxygenation in sheep

in vivo. *J Clin Invest*. (1995) 95:2134–42. doi: 10.1172/JCI117902
172. Files MD, Kajimoto M, O'Kelly Priddy CM, Ledee DR, Xu C, Des Rosiers C, et al. Triiodothyronine facilitates weaning from extracorporeal membrane oxygenation by improved mitochondrial substrate utilization. *J Am Heart Assoc*. (2014) 3:680. doi: 10.1161/JAHA.113.000680
173. Des Rosiers C, Labarthe F, Lloyd SG, Chatham JC. Cardiac anaplerosis in health and disease: food for thought. *Cardiovasc Res*. (2011) 90:210–9. doi: 10.1093/cvr/cvr055
174. Pound KM, Sorokina N, Ballal K, Berkich DA, Fasano M, Lanoue KF, et al. Substrate-enzyme competition attenuates upregulated anaplerotic flux through malic enzyme in hypertrophied rat heart and restores triacylglyceride content: Attenuating upregulated anaplerosis in hypertrophy. *Circ Res*. (2009) 104:805–12. doi: 10.1161/CIRCRESAHA.108.189951
175. Frerou A, Lesouhaitier M, Gregoire M, Uhel F, Gacouin A, Reizine F, et al. Venoarterial extracorporeal membrane oxygenation induces early immune alterations. *Crit Care*. (2021) 25:3444. doi: 10.1186/s13054-020-03444-x

Conflict of Interest: The authors declare that the research was conducted in the absence of any commercial or financial relationships that could be construed as a potential conflict of interest.

Publisher's Note: All claims expressed in this article are solely those of the authors and do not necessarily represent those of their affiliated organizations, or those of the publisher, the editors and the reviewers. Any product that may be evaluated in this article, or claim that may be made by its manufacturer, is not guaranteed or endorsed by the publisher.

Copyright © 2021 Jiang, Xie, Cao and Wang. This is an open-access article distributed under the terms of the Creative Commons Attribution License (CC BY). The use, distribution or reproduction in other forums is permitted, provided the original author(s) and the copyright owner(s) are credited and that the original publication in this journal is cited, in accordance with accepted academic practice. No use, distribution or reproduction is permitted which does not comply with these terms.

frontiers in Cardiovascular Medicine

ORIGINAL RESEARCH
published: 03 January 2022
doi: 10.3389/fcvm.2021.788270

Cardioprotective Effects of n-3 Polyunsaturated Fatty Acids: Orchestration of mRNA Expression, Protein Phosphorylation, and Lipid Metabolism in Pressure Overload Hearts

Xiang Li[1†], Weijiang Tan[1,2†], Shuang Zheng[1†], Junjie Zhang[3†], Caiyi Zhu[1], Chun Cai[3], Honghua Chen[1], Chenqi Yang[4], Le Kang[5], Zhanhong Pan[1], W. Glen Pyle[6], Peter H. Backx[7,8], Yunzeng Zou[5] and Feng Hua Yang[1]*

[1] Guangdong Laboratory Animals Monitoring Institute, Guangzhou, China, [2] College of Veterinary Medicine, South China Agricultural University, Guangzhou, China, [3] School of Pharmacy, Guangdong Medical University, Dongguan, China, [4] Faculty of Arts and Sciences, University of Toronto, Toronto, ON, Canada, [5] Shanghai Institute of Cardiovascular Diseases, Zhongshan Hospital and Institutes of Biomedical Sciences, Fudan University, Shanghai, China, [6] Department of Biomedical Sciences, University of Guelph, Guelph, ON, Canada, [7] Department of Physiology, University of Toronto, Toronto, ON, Canada, [8] Department of Biology, York University, Toronto, ON, Canada

OPEN ACCESS

Edited by:
Yang Li,
Stanford University, United States

Reviewed by:
Chen Liu,
The First Affiliated Hospital of Sun Yat-sen University, China
Haiyang Tang,
University of Arizona, United States

***Correspondence:**
Feng Hua Yang
fenghua.yang@gdlami.com

[†] These authors have contributed equally to this work

Specialty section:
This article was submitted to Cardiovascular Metabolism, a section of the journal Frontiers in Cardiovascular Medicine

Received: 01 October 2021
Accepted: 08 December 2021
Published: 03 January 2022

Citation:
Li X, Tan W, Zheng S, Zhang J, Zhu C, Cai C, Chen H, Yang C, Kang L, Pan Z, Pyle WG, Backx PH, Zou Y and Yang FH (2022) Cardioprotective Effects of n-3 Polyunsaturated Fatty Acids: Orchestration of mRNA Expression, Protein Phosphorylation, and Lipid Metabolism in Pressure Overload Hearts. Front. Cardiovasc. Med. 8:788270. doi: 10.3389/fcvm.2021.788270

Background: Pressure overload can result in dilated cardiomyopathy. The beneficial effects of n-3 polyunsaturated fatty acids (n-3 PUFAs) on heart disorders have been widely recognized. However, the molecular mechanisms underlying their protective effects against cardiomyopathy remain unclear.

Methods: Pressure overload in mice induced by 8 weeks of transverse aortic constriction was used to induce dilated cardiomyopathy. A transgenic fat-1 mouse model carrying the n-3 fatty acid desaturase gene fat-1 gene from *Caenorhabditis elegans* was used to evaluate the mechanism of n-3 PUFAs in this disease. Echocardiography, transmission electron microscopy, and histopathological analyses were used to evaluate the structural integrity and function in pressure overloaded fat-1 hearts. mRNA sequencing, label-free phosphoprotein quantification, lipidomics, Western blotting, RT-qPCR, and ATP detection were performed to examine the effects of n-3 PUFAs in the heart.

Results: Compared with wild-type hearts, left ventricular ejection fraction was significantly improved (C57BL/6J [32%] vs. fat-1 [53%]), while the internal diameters of the left ventricle at systole and diastole were reduced in the fat-1 pressure overload hearts. mRNA expression, protein phosphorylation and lipid metabolism were remodeled by pressure overload in wild-type and fat-1 hearts. Specifically, elevation of endogenous n-3 PUFAs maintained the phosphorylation states of proteins in the subcellular compartments of sarcomeres, cytoplasm, membranes, sarcoplasmic reticulum, and mitochondria. Moreover, transcriptomic analysis predicted that endogenous n-3 PUFAs restored mitochondrial respiratory chain function that was lost in the dilated hearts, and

this was supported by reductions in detrimental oxylipins and protection of mitochondrial structure, oxidative phosphorylation, and ATP production.

Conclusions: Endogenous n-3 PUFAs prevents dilated cardiomyopathy via orchestrating gene expression, protein phosphorylation, and lipid metabolism. This is the first study provides mechanistic insights into the cardioprotective effects of n-3 PUFAs in dilated cardiomyopathy through integrated multi-omics data analysis.

Keywords: n-3 PUFA, pressure overload, dilated cardiomyopathy cardioprotection, mitochondrial function, multi-omics analysis

INTRODUCTION

Pressure overload can be induced by hypertension or aortic valve stenosis. It has been estimated that 31.1% of adults have hypertension globally (1), whereas the prevalence of severe aortic stenosis in those aged 75 years and older is 3.4% in European countries and North America (2). Long-standing pressure overload leads to hypertrophic remodeling of the heart and can progress to dilated cardiomyopathy (DCM). This advanced stage of heart disease is characterized by dilation of the atria and ventricles as well as reduced systolic and diastolic function (3). Mutations in genes encoding myofilaments [e.g., titin (4), myosin heavy chain (5), and myosin binding protein C (6)], as well as mitochondrial proteins (7) have been frequently reported in studies of inherent DCM. Systematic changes, including activation of the renin angiotensin-aldosterone system (8), metabolic disorder (9), microvascular injury (10), fibrosis and inflammation (11, 12), and activation of intracellular signaling (13, 14) were detected in pressure overload-induced dilated myocardia. Our pervious study demonstrated that myofilament phosphorylation is a crucial regulatory event in failing hearts (15, 16). Treatment strategies involving angiotensin-converting enzyme inhibitors, device therapy, and etiology-based therapies are used to control blood pressure, restore normal heart rhythm, lower inflammation, and prevent blood clot formation in hypertension-associated cardiomyopathy (3). However, effective treatments for cardiomyopathy involving dilated chambers are lacking.

N-3 polyunsaturated fatty acids (n-3 PUFAs) are important components of cellular membranes. The beneficial effects of n-3 PUFAs on cardiovascular disease have been demonstrated in epidemiological and clinical studies (17, 18). However, the human body cannot synthesize n-3 PUFAs with odd numbers of carbon atoms. Supplementation with n-3 PUFAs including eicosatetraenoic acid (EPA) and docosahexaenoic acid (DHA) has long been performed as a simple alternative approach for blood pressure management. N-3 PUFAs can suppress aldosterone secretion, lower systemic vascular resistance, and reduce blood pressure (19). Metabolism of EPA and DHA share the same pathways with arachidonic acid (AA) including cyclooxygenase (COX), 5-lipoxygenase (LOX), and cytochrome P450 monooxygenase (CYP) enzymes (20). Endogenous n-3 PUFA-derived oxygenated metabolites of EPA and DHA exert beneficial roles. Moreover, n-3 PUFAs show potential for improving cardiac function attributed to pressure overload; however, as the treatment of patients with hypertension is often combined with other medications or device intervention, the molecular mechanisms associated with the beneficial effects of these unsaturated fatty acids in cardiomyopathy remain unclear. Here, we investigated molecular signatures including mRNA expression, protein phosphorylation, and lipid metabolism in a murine pressure overload model to aid to our understanding of the effects elicited by n-3 PUFAs against dilated cardiomyopathy. We further explored whether n-3 PUFAs regulate mitochondrial function that were potentially involved in cardioprotection.

MATERIALS AND METHODS

Animals and Experimental Design

Fat-1 mice were developed by the Kang Laboratory (21). These mice expressed the n-3 fatty acid desaturase gene *fat-1* from *Caenorhabditis elegans*, which converts n-6 PUFAs into n-3 PUFAs, resulting in high levels of endogenous n-3 PUFAs in the heart. Wild-type (WT) and transgenic fat-1 littermates (fat-1) aged 3 months were subjected to a transverse aortic constriction (TAC; the surgical procedure is described below) to develop pressure overload. The four groups of animals were named as WT-Sham, Fat1-Sham, WT-TAC, and Fat1-TAC. After the experiments, the cardiac function of the animals was evaluated using echocardiography. The heart tissues were collected for histological examination, transmission electron microscopy (TEM), mRNA sequencing, label-free protein quantification, lipidomics, and western blotting were conducted to explore effects and underlying mechanisms of the elevation of endogenous n-3 PUFAs in dilated cardiomyopathy.

All animal experiments were conducted in accordance with the guidelines of the Institutional Animal Care and Use Committee of the Guangdong Laboratory Animals Monitoring Institute (No. IACUC2017015). The mice were housed in a specific pathogen-free mouse facility. The ambient temperature and humidity of the facility were 24 ± 2°C and 40–60%,

Abbreviations: ALA, alpha lipoic acid; DHET, dihydroxyeicosatrienoic; DiHETE, dihydroxyeicosatetraenoic acid; DiHOME, Dihydroxy octadecenoic acid; DPA, docosapentaenoic acid; EET, epoxyeicosatrienoic acid; GLA, gamma linolenic acid; HDoHE, hydroxydocosahexaenoic acid; HETE, hydroxyeicosatetraenoic acid; HETrE, hydroxy eicosatrienoic acid; HEPE, hydroxyeicosapentaenoic acid; HHT, hydroxyheptadecatrenoic acid; HODE, hydroxy octadecadienoic acid; HOTrE, hydroxyoctadecatrienoic acid; HpODE, hydroperoxylinoleic acids; KETE, ketoeicosatetraenoic acid; KODE, ketooctadecadienoic acid; LA, linoleic acid; LTX, leukotriene X; PGX, prostaglandin X.

respectively, with a 12-h light-dark cycle. The animals were given *ad libitum* access to water and a regular rodent diet (Keao Xieli Feed Co., Beijing, China). The animal facility was accredited by the Association for Assessment and Accreditation of Laboratory Animal Care.

Transverse Aortic Constriction

To introduce pressure overload stress to the heart, TAC was performed in WT and fat-1 mice. After anesthesia, the mice were intubated and connected to a ventilator. Isoflurane (1–2%) was administered to maintain anesthesia. A 1-cm incision was made on the chest midline around the second rib to open the thoracic cavity. After identifying the aortic thoracic segment, a 7-0 suture was installed under the aorta in the brachiocephalic trunk and the left common carotid artery, and a 26G blunt needle was inserted parallel to the aorta. The needle was removed after the surgical knot was tied. The sham groups of WT and fat-1 mice were subjected to the open chest procedure but not aortic constriction.

Echocardiography

An ultrasound system equipped with a high-frequency probe MS-440 (Vevo 2100; VisualSonics, Toronto, ON, Canada) was used to evaluate the structure and function of WT and fat-1 mice with ventricular pressure overload. Horizontal parasternal short axis B-mode and M-mode images of the heart were recorded for each mouse group (WT-Sham, WT-TAC, Fat1-Sham, and Fat1-TAC). B-mode images of the parasternal short axis in the papillary muscle plane were obtained by placing the probe on the chest midline. M-mode images were acquired at the same position as those of the B-mode recording. The echocardiographic indices included interventricular septum thickness at end-systole and diastole (IVS;s and IVS;d), left ventricular posterior wall thickness at end-systole and diastole (LVPW;s and LVPW;d), left ventricular internal dimension at end-systole and diastole (LVID;s and LVID;d), left ventricular ejection fraction (EF), and short axis fractional shortening (FS).

Histological Examination

Pathological examinations were conducted to determine the cardiac structure, fibrosis, vessel morphology, and cardiomyocyte size as previously described (15, 22). Masson's trichrome staining was performed to identify collagen fibers and muscle tissue, whereas wheat germ agglutinin was used to visualize cardiomyocyte plasma membranes and calculate the cardiomyocyte size. Mice from all four groups (WT-Sham, WT-TAC, Fat1-Sham, and Fat1-TAC) were euthanized, after which their hearts were excised, fixed for 12–16 h in 4% (v/v) paraformaldehyde, embedded in paraffin, and sectioned into 3-μm-thick slices. The following chemicals were used for histological examination: 4',6-diamidino-2-phenylindole (No. P36962; Invitrogen, Carlsbad, CA, USA), Bouin's solution (No. HT10132; Millipore, Billerica, MA, USA) and Weigert's hematoxylin (No. HT10132; Millipore), Biebrich scarlet-acid fuchsin solution (No. HT151; Millipore), and Aniline blue (No. B8653; Millipore). Pathological changes in pressure overload hearts were identified microscopically (DM2500; Leica Microsystems, Wetzlar, Germany). Cardiomyocytes were analyzed using ImageJ 1.52a software (NIH, Bethesda, MD, USA).

Transmission Electron Microscopy

TEM was conducted to examine subcellular changes associated with n-3 PUFA expression. Left ventricular tissues were cut into small blocks (∼1 mm^3), fixed with 2.5% glutaraldehyde and 1% OsO_4, dehydrated in ethanol, and embedded in Araldite. The tissue blocks were cut into slices with a thickness of 60 nm using a Leica cryostat system (EM UC7/FC7) and collected on copper grids. The ultrathin sections were double-stained with 3% uranyl acetate and lead citrate. The subcellular structure was observed using a Tecnai G2 Spirit transmission electron microscope (FEI Company, Hillsboro, OR, USA).

mRNA Sequencing

Total RNA was extracted from the whole hearts of the four groups (WT-Sham, WT-TAC, Fat1-Sham, Fat1-TAC) using TRIzol® Reagent (Thermo Fisher Scientific). The RNA concentration and its integrity was assessed using an RNA Nano 6000 Assay Kit (Agilent Technologies, Santa Clara, CA, USA). A NEBNext® Ultra™ RNA Library Prep Kit for Illumina® (New England Biolabs, Ipswich, MA, USA) was used to generate sequencing libraries. Index codes were added, and the samples were clustered with a cBot Cluster Generation System using a TruSeq PE Cluster Kit v3-cBot-HS (Illumina, San Diego, CA, USA). An Illumina HiSeq platform (Illumina) was used to sequence the libraries.

Raw data was preprocessed for quality control, after which the clean reads were mapped to the reference transcriptome. Next, the four groups of processed data were compared in pairs, and the fold-changes between comparisons were log2-transformed. An adjusted P-value <0.1 was set as the cutoff for identifying differentially expressed genes (DEGs). DEGs with fold-changes >1.5 were considered as upregulated, whereas those with values $<1/1.5$ were considered downregulated.

Phosphoproteomic Analysis

Filter-Aid Sample Preparation

The levels of phosphoprotein in the animal hearts (WT-Sham, WT-TAC, Fat1-Sham, and Fat1-TAC) were quantified using label-free quantitative proteomics technology. A filter-aid sample preparation protocol from Mann Laboratory was used to digest proteins and elute the peptides (23, 24). Briefly, total protein was extracted from the heart tissues using lysis buffer containing 4% sodium dodecyl sulfate (SDS), 100 mM Tris-HCl (pH 7.6), and 1 mM dithiothreitol, and the protein concentration was determined using a Pierce BCA Protein assay kit (No. 23225, Thermo Fisher Scientific, Waltham, MA, USA). The samples were desalted using an Empore SPE Cartridge C18 column (No. 98-0604-0198-5, Sigma, St. Louis, MO, USA; bed internal diameter, 7 mm; volume, 3 mL). The proteins were then concentrated and reconstituted in 40 μL of 0.1% formic acid (No. F0507, Sigma). The protein concentration was measured with a UV light a Spectrometer at 280 nm. Sample quality was verified by performing 12.5% SDS-PAGE protein separation and Coomassie Blue staining.

Liquid Chromatography-Tandem Mass Spectrometry

Phosphopeptides were enriched using a High-SelectTM Fe-NTA Phosphopeptides Enrichment Kit according to the manufacturer's instructions (No. A32992, Thermo Fisher Scientific). After lyophilizatoin, the phosphopeptides peptides were resuspended in 20 μL loading buffer (0.1% formic acid). For liquid chromatography-tandem mass spectrometry (LC-MS/MS) analysis, phosphopeptide samples were injected into a C18-reversed phase analytical column (Thermo Fisher Scientific Easy-Spray Column, No. ES900) and separated with a linear gradient over 120 min at a flow rate of 300 nL/min controlled by IntelliFlow technology. Spectra were acquired on a Q-Exactive orbitrap mass spectrometer (Thermo Fisher Scientific) coupled to an Easy-nLC 1200 system (Thermo Fisher Scientific). MS data were acquired from a survey scan (300–1800 m/z) for higher-energy C-trap dissociation fragmentation. The parameters were: automatic gain control 3e6, maximum inject time of 10 ms, and dynamic exclusion duration 40.0 s. Survey scans were acquired at a resolution of 70,000 at m/z 200, and the resolution for higher-energy C-trap dissociation spectra was set to 17,500 at m/z 200 and isolation width was 2 m/z. The normalized collision energy was 30 eV and the underfill ratio, which specifies the minimum percentage of the target value likely to be reached at maximum fill time, was defined as 0.1%. MS/MS spectra were searched using the MaxQuant 1.5.3.17 software for identification and quantitation analysis.

The label-free quantitative data for phosphoproteins from the four groups (WT-Sham, WT-TAC, Fat1-Sham, Fat1-TAC) were compared in pairs, and the fold-changes between comparisons were log2-transformed. A 0.05 cutoff was set for the *P*-value to identify differentially expressed phosphoproteins (DEPs). DEPs with fold-change values >1.5 and <1/1.5 were considered as upregulated and downregulated, respectively.

Bioinformatic Analysis for mRNA and Phosphoprotein Expression

Biological Process Enrichment Analysis and Protein-Protein Interaction Network Construction

The web-accessible tool Metascape (https://metascape.org) was used to enrich biological processes for the datasets of DEGs and DEPs. Significant enrichment was considered as a *P*-value cutoff of 0.01, minimum overlap of 3, minimum enrichment of 1.5, and limiting-network interactome consisting of 3–500 candidate proteins. A high *P*-value (–log10) of the term in a biological process reflected its relatively higher degree of enrichment. Each DEG or DEP in the interaction network was displayed in the modules according to its biological processes.

Metascape was used to construct protein-protein interaction networks for the enrichment biological processes (25). Biological processes with similar functions were clustered, and then these enrichment clusters were connected according to the algorithm MCODE. Diagrams of the protein interaction network were visualized in Cytoscape v. 3.8.1 (http://www.cytoscape.org).

Venn Diagram Analysis for Differentially Expressed Phosphoproteins

To determine the roles of endogenous n-3 PUFAs in pressure overload hearts, each comparison pair was input into the TBtools program (https://omictools.com/tbtools-tool) to generate Venn diagrams (http://jvenn.toulouse.inra.fr). Here, two intersections were obtained: (1) the intersection of upregulated DEPs in the WT-TAC vs. WT-Sham comparison group and downregulated DEPs in the Fat1-TAC vs. WT-TAC comparison group, and (2) the intersection of downregulated DEPs in the WT-TAC vs. WT-Sham comparison group and upregulated DEPs in the Fat1-TAC vs. WT-Sham comparison group. Next, these two intersections further excluded the up-/downregulated DEPs from the Fat1-Sham vs. WT-Sham comparison. Finally, two new sets of DEPs were obtained: (1) upregulated by pressure overload in the WT hearts but downregulated by fat-1 transgene in the pressure overload condition, and (2) downregulated by pressure overload in the WT hearts but upregulated by fat-1 transgene under pressure overload.

Mitochondrial Function Prediction

Venn diagram analysis was also used to identify genes associated with the mitochondrial respiratory chain complexes that were upregulated by pressure overload in WT hearts, but downregulated by fat-1 transgene in the pressure overload condition. Here, a *P*-value <0.05 was set as the cutoff for screening DEGs associated with the mitochondrial respiratory chain function.

Lipidomic Analysis of n-3 and n-6 PUFAs

Reagents

Chemical used in this study included methanol (No.106009; Merck, Darmstadt, Germany), formic acid (No. 5438040; Merck), ethanoic acid (No. US-FLSA-001; Thermo Fisher Scientific), and ethyl acetate (No. E196SK-4, Thermo Fisher Scientific). The isotope internal standards (IS) for quantification of lipid oxylipins were obtained from Cayman Chemical (Ann Arbor, MI, USA), which are listed as follows: prostaglandin (PG) E2-d4 (No. 314010), PGD2-d4 (No. 312010), PGF2α-d4 (No. 10007275), 6-keto-PGF1α-d4 (No. 315210), leukotriene (LT) C4-d5 (No. 10006198), tetranor-PGEM-d6 (No. 314840), LTB4-d4 (No. 320110), 15-hydroxy-eicosatetraenoic acid (HETE)-d8 (No. 31746), 5-HETE-d8 (No. 334230), thromboxane (TX) B2-d4 (No. 319030),12-HETE-d8 (No. 31745), platelet-activating factor (PAF)-d4 (No. 360900), oleoylethanolamide (OEA)-d4 (No. 9000552), eicosapentaenoic acid (EPA)-d5 (No. 10005056), docosahexaenoic acid (DHA)-d5 (No. 10005057), and arachidonic acid (AA)-d8 (No. 390010). These standards were mixed with methanol to obtain a final concentration of 100 ng/mL.

Extraction of n-3 and n-6 Polyunsaturated Fatty Acids and Oxylipins

The hearts from each group of mice (WT-Sham, WT-TAC, Fat1-Sham, and Fat1-TAC, $N = 4$) were collected and snap-frozen in liquid nitrogen. Total lipids were extracted from the heart tissues using a liquid-liquid extraction protocol as described previously with modifications (26), and 100 mg of heart tissue was homogenized by adding 1 L of methanol (2% formic acid and 0.01 mol/L BHT) and IS mixture (10 μL) and processing in an Omni tissue homogenizer (TH02, Kennesaw, GA, USA). The mixtures were centrifuged at 12,000 ×*g* at 4°C for 10 min

to collect the supernatants, which were mixed with 700 mL of ultra-pure water and 1 mL of ethyl acetate. The mixtures were centrifuged again at 4000 ×*g* at 4°C for 10 min, and the upper organic phase was collected. The organic phase was dried using a nitrogen blower.

Ultra-Performance Liquid Chromatography-Tandem Mass Spectrometry

The dried extracts were dissolved in 10% acetonitrile (No. 900686, Sigma), filtered through a 0.45-μm membrane filter (No. HAWP04700; Millipore), and subjected to ultra-performance liquid chromatography-MS/MS analysis. A Shimadzu LCMS-8050 (Kyoto, Japan) equipped with a Phenomenex C18 column (2.1 mm × 150 mm × 2.6 μm; Torrance, CA, USA) was used to determine the n-3 and n-6 PUFAs and their oxylipins in the heart tissue extracts. The column temperature was set at 40°C, and the injection volume was 5 μL. The mobile phase flow rate was 0.6 mL/min. Gradient elution was performed with 0.1% (v/v) formic acid (solvent A) and acetonitrile (solvent B). The gradient of mobile phase B was set as follows: 10% (0 min), 25% (5 min), 35% (10 min), 75% (20 min), 95% (20.1 min), 95% (25 min), 10% (25.1 min), and 10% (30 min).

Quantitative Analysis of Oxylipins

MS/MS analyses were conducted in both positive and negative ion modes using nitrogen as the nebulizer gas, and PUFAs and oxylipins were identified according to multiple reaction monitoring and relative retention time of the species in the same class. The mass spectrometer was operated with MS operating software (lipid mediator version 2 software package, Shimadzu).

The identified lipid oxylipins were quantified by measuring the peak areas of the detected species as previously described (26). Briefly, the peak areas of each individual lipid oxylipin were corrected by those corresponding to the ISs of the same lipid metabolite class, which compensated for the fluctuations in MS intensities observed during different runs. The corrected peak areas of all identified lipid oxylipins were used for in-depth analysis.

Lipidomic analysis was performed as described previously (16). To process the raw data, MetaboAnalyst V5.0 (Montreal, Canada) was used to generate the clustering diagram and SIMCA 14.1 (Umetrics, Umeå, Sweden) was used for principal component analysis, providing an overview of the dataset structure and relationships. A P-value <0.05 was set as the cutoff for identification of the significant changes of oxylipins between groups. Fold-change values >1.5 were considered as upregulated, whereas values $<1/1.5$ were considered as downregulated.

Multi-Omics Data Analysis

To integrate multi-omics data and understand the insights of n-3 PUFA regulation in fat1-TAC hearts, comparison datasets (Fat1-TAC vs. WT-TAC) from RNA-sequencing, phosphoproteomics, or lipidomics were uploaded to MetaboAnalyst V5.0. The top 10 most enriched pathways were selected for further analysis.

Real Time Quantitative Polymerase Chain Reaction

RT-qPCR was used to verify the expression of genes identified by multi-omics data analysis. Briefly, after total RNA extraction, TB Green Premix Ex Taq II (No. RR820; Takara Bio Inc., Shiga, Japan) was used according to manufacturer's instruction. The reaction steps included 95°C for 30 s, 40 cycles of 95°C for 5 s, 60°C for 34 s, and a final extension at 72°C for 10 min. Transcript levels were normalized to the expression of β-actin. The primers in this experiment listed in **Supplementary Table S1**.

Western Blotting

Expression of fission (dynamin-related protein 1, DRP1) and fusion (optic atrophy-1, OPA1) proteins and oxidative phosphorylation markers (electron transport chain complexes) of the mitochondria was determined to evaluate mitochondrial function (27). The hearts were homogenized in cell lysis buffer (#9803, Cell Signaling Technology, Danvers, MA, USA) containing protease inhibitors and 1% Triton X-100. The samples were centrifuged at 12000 ×*g* at 4°C for 15 min, and the supernatants were retained for further use. Cytosolic (40 μg) proteins were separated using 10% SDS-PAGE and transferred to polyvinylidene fluoride blotting membranes (Millipore). After blocking with 5% skim milk, the membranes were incubated with primary antibodies (as listed above) overnight at 4°C before being incubated with species-appropriate secondary antibodies (Cell Signaling Technology). The bands were detected with Immobilon Western Chemiluminescent HRP Substrate (Millipore). Primary antibodies against DRP1 (No. 8570S, Cell Signaling Technology) and OPA1 (No. 67589S, Cell Signaling Technology) were used, along with a total oxidative phosphorylation rodent western blotting antibody cocktail (No. ab110413, Abcam, Cambridge, UK). Band density was analyzed using ImageJ software (NIH).

Adenosine Triphosphate Assay

The whole heart was homogenized and adenosine triphosphate (ATP) was quantitatively determined using an ATP colorimetric assay kit (#A095-1-1, Nanjing Jiancheng Co., Nanjing, China) following the manufacturer's instructions. Briefly, the homogenates of heart tissues (200 mg in 1.8 mL of milli-Q H_2O) were heated to 100°C for 10 min and centrifuged at 1150 ×*g* for 10 min. The amount of phosphorylating glycerol generated from the supernatants was read at 630 nm using a spectrophotometer (Ultrospec 2100, Biochrom, Cambridge, UK).

Statistical Analysis

For echocardiographic and pathological examinations, the data are presented as the mean ± SEM. Raw data for the WT-Sham, WT-TAC, Fat1-Sham, and Fat1-TAC groups were uploaded to GraphPad Prism 8.0 software (GraphPad, Inc., La Jolla, CA, USA). Significant differences among multiple data groups were analyzed by two-way analysis of variance followed by Tukey's multiple comparisons test (GraphPad Prism 8.0). Graphs showing individual data points were plotted. For mRNA sequencing, phosphoproteomics, and lipidomics analyses, t-tests were used to identify significant differences between pairs of means. Statistical significance was set at $P < 0.05$.

RESULTS

Elevation of Endogenous n-3 PUFAs Reduces Cardiac Remodeling and Improves Cardiac Function

We found that the levels of EPA were significantly increased in the hearts of fat-1 mice. After TAC, both the EPA and DHA levels were significantly higher in the myocardium (**Figure 1A**). The total levels of n-3 PUFAs were significantly higher in the fat-1 TAC hearts than in the WT-TAC hearts, whereas the levels of n-6 PUFAs and ratio of n-6/n-3 PUFA were significantly lower in the fat1-TAC hearts than in the WT-TAC hearts (**Figure 1A**). These measurements suggest that the fat-1 transgene increased endogenous n-3 PUFAs and in the normal and pressure overload hearts, as well as lowered the ratio of n-6 to n-3 in pressure overload hearts.

The heart rate did not differ between groups based on echocardiographic recording (**Figure 1B**; **Table 1**). TAC-induced pressure overload significantly increased LVID;s ($P < 0.0001$) and LVID;d ($P < 0.0001$) in WT mice, whereas these two indices were significantly lower in fat-1 mice than in WT mice (**Figures 1B–D**). Correspondingly, pressure overload significantly increased the LV volume at systole ($P < 0.0001$) and diastole ($P < 0.0001$) in WT mice. The corrected LV mass was significantly increased in WT mice but not in Fat-1 mice (**Table 1**). Cardiac contractile function indices, including EF and FS, showed that the function was preserved in the Fat-1 TAC group but not in the WT-TAC group (**Figures 1B,E,F**).

In addition, we found that pressure overload significantly increased the size of cardiomyocytes and fibrosis (**Figures 1G,H**). Fibrosis was significantly reduced in the myocardium, and cardiomyocyte hypertrophy was reduced in the Fat1-TAC group (**Figures 1G,H**).

Endogenous PUFAs Target Phosphorylation Signaling and Restore Protein Phosphorylation States Under Pressure Overload Conditions

Transcriptomic and phosphoproteomic data analysis (**Figure 2A**) revealed the overall expression profiles of mRNAs and phosphoproteins, respectively (**Figures 2B–E**). Fat-1 transgene caused alterations (up- or downregulation) in the expression of mRNA under normal and pressure overload conditions (**Figure 2C**). Furthermore, analysis of the DEPs revealed that fat-1 transgene regulated expression of phosphoproteins during pressure overload. Specifically, compared with the WT hearts, the fat-1 hearts exhibited upregulation of 18 phosphoproteins and downregulation of 57 phosphoproteins. Meanwhile, under pressure overload conditions, fat-1 transgene up- and downregulated 34 and 49 phosphoproteins, respectively (**Figure 2E**).

Gene set enrichment analysis of biological processes revealed that pressure overload significantly upregulated 49 genes (**Figures 3A,B**). Under pressure overload conditions, at the transcriptional level, elevated endogenous PUFAs downregulated these 49 genes enriched in cardiac remodeling (negative regulation of cell adhesion and positive regulation of growth), inflammation (humoral immune response and regulation of inflammatory response), and alterations in ion and cellular homeostasis (multicellular organismal water homeostasis and cellular response to metal ion) (**Figures 3A,C**).

We further analyzed protein post-translational modification using quantitative phosphoproteomics. Through Venn diagram analysis, we identified 21 phosphoproteins that were potentially affected by elevation of endogenous n-3 PUFAs (**Figures 4A,B**). Among them, five proteins were downregulated by pressure overload, but were upregulated by fat-1 transgene under pressure overload conditions, whereas another 16 proteins were upregulated by pressure overload, however, were downregulated by fat-1 transgene under pressure-overload (**Table 2**). Biological process enrichment for these 21 phosphoproteins revealed fat-1 transgene primarily suppressed expressions levels of phosphoproteins associated with cardiac remodeling (muscle cell differentiation, actin cytoskeleton organization, cell junction organization, angiogenesis) and maintained ion and cellular homeostasis (positive regulation of cation channel activity and response to mechanical stimulus) (**Figure 4C**). Moreover, these 21 phosphoproteins were localized within cardiomyocytes, nerves, and vessels in the myocardium, as well as in various subcellular compartments, including the plasma membrane, cytoplasm, sarcoplasmic reticulum, sarcomere, and mitochondria (**Figure 4D**; **Table 2**). Furthermore, phosphorylation of myofilaments was altered in dilated WT hearts (**Figure 4D**). Under pressure overload conditions, compared with WT mice, fat-1 mice showed higher phosphorylation levels of cTnI S6 and lower levels of titin S3784, β-actin capping protein S263, and α-actinin 2 T822 (**Table 2**; **Supplementary Table S2**). In addition, phosphorylation levels of two other Z-line proteins (PDZ and LIM domain protein 5, as well as sorbin and SH3 domain containing protein 2) were also restored by fat-1 transgene in pressure overload hearts. These results demonstrate that the contractile machinery represents one target of endogenous n-3 PUFAs in pressure overload hearts.

Cardioprotection of Endogenous n-3 PUFAs Is Attributed to Suppression of Their Oxylipin Production in Pressure Overload Hearts

We further explored the protective mechanisms of endogenous n-3 PUFAs based on lipidomic analysis. Shifts in the oxylipin profiles were observed in the myocardium with elevated n-3 PUFAs under pressure overload conditions (**Figures 5A–C**). Forty-seven oxylipins were detected, among which 16 belonged to n-3 and 31 belonged to n-6 metabolic pathways (**Figure 5A**). The number of oxylipins altered by pressure overload or fat-1 transgene is displayed in **Figure 5C**.

Analysis of the metabolic pathways (**Figures 5D–G**) showed that in the n-3 metabolic pathway, pressure overload reduced DHA levels but increased oxylipins 8- and 11-HDoHE levels in the hearts of WT mice (**Figure 5D**). Compared with WT hearts, the n-3 PUFA-protected hearts showed higher concentrations of EPA, DHA, and their oxylipins 17,18-DiHETE and 8-HDoHE,

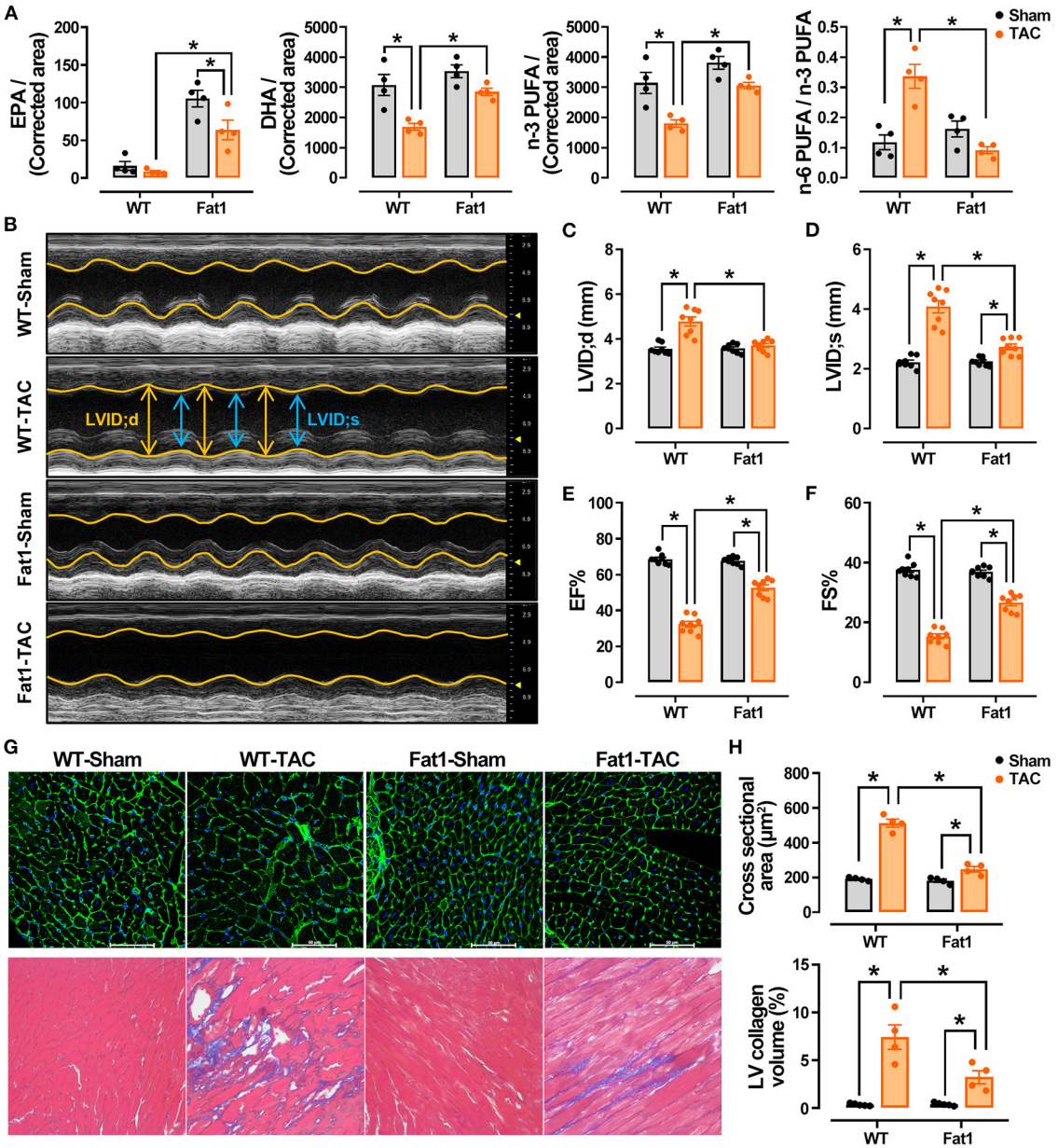

FIGURE 1 | Endogenous n-3 PUFAs and echocardiographic measurements in WT and fat-1 mice with or without pressure overload. Fat-1 transgene increased endogenous n-3 PUFAs in normal and pressure overload hearts and lowered the ratio of n-6 to n-3 PUFAs in pressure overload hearts **(A)**. $N = 4$ for each group. EPA, eicosapentaenoic acid; DHA, docosahexaenoic acid; PUFA, poly unsaturated fatty acid. The M-mode recordings of the four groups are shown in **(B)**. Transverse aortic constriction (TAC)-induced pressure overload significantly increased the internal diameters at diastole **(C)** and systole **(D)** in WT mice, whereas these two indices were lower in fat-1 mice than in WT mice. Cardiac contractile function indices, including EF **(E)** and FS **(F)**, showed that the function was preserved in the fat-1 TAC group. Pressure overload significantly increased the size of cardiomyocytes and fibrosis, which was significantly reduced in the Fat1-TAC group **(G,H)**. $N = 8$ for each group, subjected to echocardiographic analysis, and $N = 4$ for each group subjected to histological observation. LV, left ventricle. All data are presented as the means ± SEM. $^*P < 0.05$ between groups.

whereas lower concentrations of n-3 PUFA oxylipins (12-HEPE, and 7-, 10-, 11-, 13-, and 17-HDoHE) were observed under pressure overload conditions (**Figure 5F**). In the n-6 PUFA metabolic pathway, pressure overload increased the levels of n-6 PUFA oxylipins, including 15-HETrE, 12-keto-LTB4, 9-HETE, 12-HHT, and 6-keto-PGE1α and decreased the levels of the oxylipin 11-beta-PGF2α (**Figure 5E**). Compared to WT hearts, fat-1 hearts exhibited increased levels of n-6 PUFA oxylipins, including 9-HpODE and 15-deoxy-delta-12,14-PGJ2 and decreased levels of oxylipins in the LA-LOX pathway (9-HODE, 9-KODE, and 13-HODE), dihomo-γ-linolenic acid (DGLA)-LOX pathways (15-HETrE), AA-LOX pathways (12-keto-LTB4,

TABLE 1 | Echocardiographic measurements.

Parameters	WT-Sham	WT-TAC	Fat1-Sham	Fat1-TAC
Heart rate (beats/min)	455 ± 6	440 ± 7	467 ± 10	450 ± 11
LV Mass (corrected), mg	102.43 ± 4.11	179.68 ± 16.43*	102.35 ± 4.44#	118.71 ± 5.42#
Interventricular ventricular septum thickness, end-systolic, IVS;s (mm)	1.36 ± 0.01	1.23 ± 0.02	1.34 ± 0.03	1.24 ± 0.03
Interventricular ventricular septum thickness, end-diastolic, IVS;d (mm)	0.89 ± 0.01	0.87 ± 0.02	0.87 ± 0.03	0.89 ± 0.04
Left ventricular posterior wall thickness, end-systolic, LVPW;s (mm)	1.12 ± 0.03	1.05 ± 0.02	1.18 ± 0.02#	1.17 ± 0.02&
Left ventricular posterior wall thickness, end-diastolic, LVPW;d (mm)	0.77 ± 0.02	0.88 ± 0.04*	0.77 ± 0.01#	0.86 ± 0.02
Left ventricular internal dimension, end-systolic, LVID;s (mm)	2.22 ± 0.07	4.08 ± 0.21*	2.24 ± 0.05#	2.74 ± 0.10#
Left ventricular internal dimension, end-diastolic, LVID;d (mm)	3.55 ± 0.08	4.78 ± 0.20*	3.58 ± 0.07#	3.71 ± 0.09#
Ventricular volume at systole (μL)	16.85 ± 1.28	74.91 ± 0.48*	17.53 ± 0.94#	27.99 ± 2.37#
Ventricular volume at diastole (μL)	53.36 ± 3.19	109.26.23 ± 10.37*	54.26.31 ± 0.20#	58.74 ± 3.53#
Ejection fraction, EF (%)	68.58 ± 1.04	32.35 ± 1.66*	67.71 ± 0.76#	52.73 ± 1.67*#&
Short axis fractional shortening, FS (%)	37.57 ± 0.82	15.33 ± 0.83*	36.89 ± 0.59#	26.58 ± 1.01*#&

*All data are presented as the means ± SEM. N = 8. *P < 0.05 vs. WT-Sham, #P < 0.05 vs. WT-TAC, and &P < 0.05 vs. Fat1-Sham (two-way ANOVA, Tukey's multiple comparisons test).*

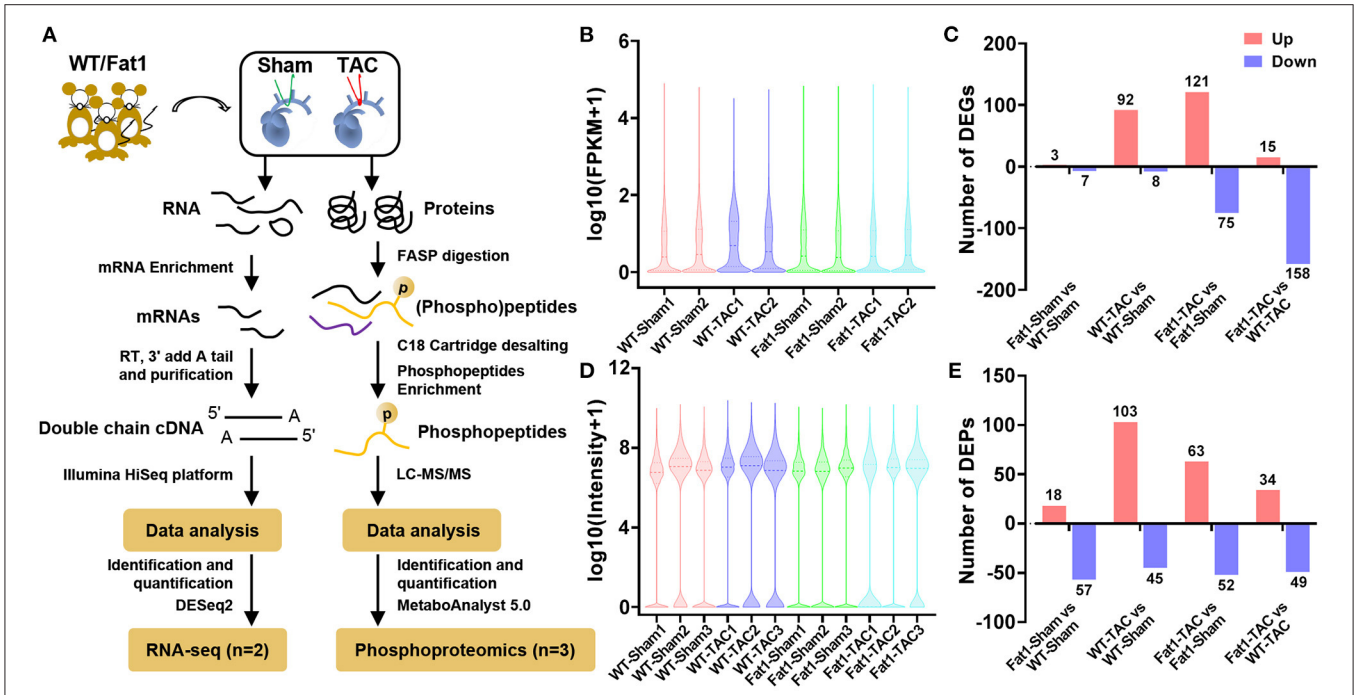

FIGURE 2 | mRNA and phosphoprotein profiles. RNA-sequencing analysis of **(A)** overall mRNA expression profiles **(B)** and differentially expressed genes (DEGs) in pressure overload hearts **(C)**. Quantitative phosphoproteomic analysis **(A)** showed the overall expression profiles of phosphoproteins **(D)** and differentially expressed phosphoproteins (DEPs) in pressure overload hearts **(E)**. *N* = 2 and 3 for RNA-sequencing and phosphoproteomic analysis, respectively.

5-HETE, 5-KETE, 12-HETE, 12-KETE, 8-,9-,11-,15-HETE), AA-CYP pathway (16-HETE), and AA-COX pathway (12-HHT, 6-keto-PGE1α, PGF2α, and 8-iso-15-keto-PGF2α) (**Figure 5G**).

Furthermore, after analyzing differences in oxylipin production within the myocardia (**Figure 6A**), we found that four oxylipins, namely, 12-HHT, 9-HETE, 12-keto-LTB4, and 6-keto-PGF1α were significantly reduced in the pressure overload myocardium protected by n-3 PUFAs (**Figures 6B–E**). The oxylipin profiles in the Fat1-TAC hearts revealed that protective effects of endogenous n-3 PUFAs in pressure overload hearts were attributed to their oxylipins.

Endogenous n-3 PUFAs Protect Mitochondrial Structure and Function Under Pressure Overload Conditions

The results of RNA-sequencing, phosphoprotein quantification, and oxylipin profiling were integrated and analyzed (**Figure 7A**). The top 10 enriched pathways were involved in metabolism (arachidonic acid metabolism, apelin signaling pathway,

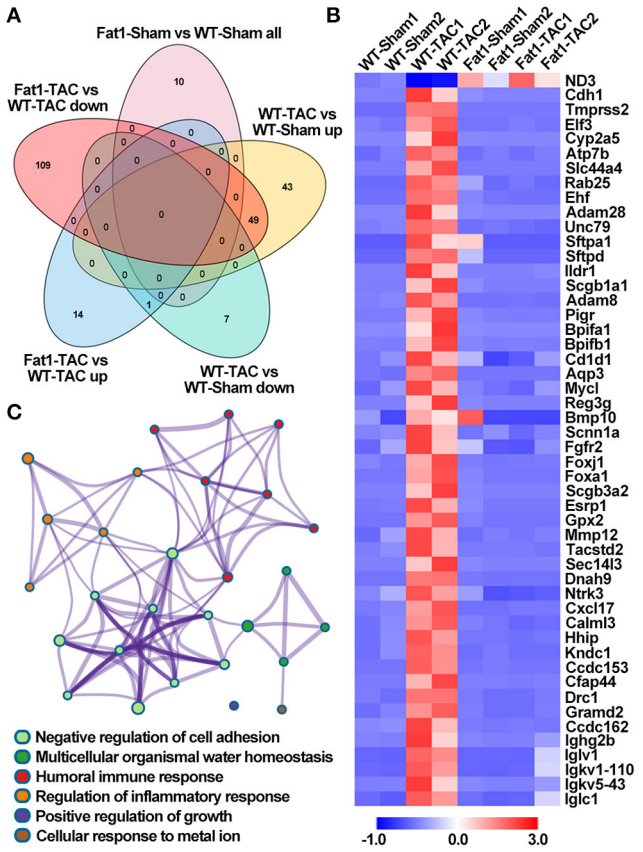

FIGURE 3 | Effects of endogenous N-3 PUFAs on the expression of genes under pressure overload. Gene set enrichment analysis revealed that pressure overload significantly up-/down regulated the biological processes enriched in DEGs, which can be suppressed/restored by fat-1 transgene **(A,B)**. Under pressure overload conditions, elevated endogenous PUFAs downregulated these 49 genes enriched in six biological processes **(C)**. Fat1-Sham vs. WT-Sham all, genes upregulated and downregulated by fat-1 transgene; WT-TAC vs. WT-Sham up, genes upregulated by TAC-induced pressure overload; WT-TAC vs. WT-Sham down, genes downregulated by TAC-induced pressure overload; Fat1-TAC vs. WT-TAC up, genes downregulated by fat-1 transgene under pressure overload conditions; Fat1-TAC vs. WT-TAC down, genes downregulated by fat-1 transgene under pressure overload conditions. $N = 2$ for RNA-sequencing.

peroxisome proliferator-activated receptors (PPAR) signaling pathway, and cGMP-PKG signaling pathway), contractile function (cardiac muscle contraction, adrenergic signaling in cardiomyocytes, cAMP signaling pathway, and calcium signaling pathway), cardiac remodeling (dilated cardiomyopathy and hypertrophic cardiomyopathy). Furthermore, we found that fat-1 transgene altered PPAR signaling pathway, a metabolic pathway links the genes-phosphoproteins-metabolite regulatory network. We compared the profiles of genes, proteins and metalates with PPAR signaling pathway–Mus musculus (mmu03320) of the KEGG database (https://www.genome.jp/kegg-bin), and found that three genes (*Fabp3*, *Pck1*, and *Angptl4*), one phosphoprotein (*Plin5* encoding PDZ and LIM domain protein 5), and two oxylipins (8-HETE, and 13-HODE) matched the pathway (**Figure 7B**). Gene expression verification showed that *Fabp3* was upregulated, but *Pck1* and *Angptl4* were downregulated by fat-1 transgene under pressure overload conditions (**Figures 7C–E**). The KEGG pathway analysis further supported that endogenous n-3 PUFAs protect hearts through regulating gene expression, protein phosphorylation and lipid metabolism.

Mitochondrial function associated RNA-sequencing datasets was examined. Expression of 47 genes encoding oxidative phosphorylation markers, specifically mitochondrial respiratory chain complexes, were significantly downregulated by pressure overload (fold-change > 1.5 and $P < 0.05$). Among them, 23, 1, 7, 8, and 8 genes belonged to complexes I, -II, -III, -IV, and -V, respectively. However, elevation of endogenous n-3 PUFAs restored their expression (**Figure 8A**). Under TEM, the mitochondria were reduced in size and more abundant per square μm in WT-TAC hearts, whereas the mitochondria of Fat1-TAC hearts were normal in terms of shape and size (**Figures 8B–D**). Western blotting analysis further revealed that expression of the fission marker Drp1 was significantly reduced in fat-1 TAC hearts but not in the dilated WT-TAC heart (**Figures 8E,F**). These results confirm that endogenous n-3 PUFAs protected hearts from mitochondrial injury under the pressure overload condition.

Consistent with the protection of mitochondrial structure in fat-1 TAC hearts, the ATP generation was also restored by endogenous n-3 PUFAs under pressure overload conditions (**Figure 8G**). Furthermore, by examining the protein expression of complexes I, -II, -III, and -V, we found that all complexes were downregulated in the dilated WT-TAC hearts. Compared to in the sham hearts, TAC did not suppress the expression of mitochondrial complexes. In contrast, the expression of complex V was significantly upregulated in fat-1 TAC hearts (**Figures 8H,I**). These results demonstrate that endogenous n-3 PUFAs regulate mitochondrial oxidative phosphorylation and ameliorate mitochondrial dysfunction under pressure overload conditions.

DISCUSSION

In the present study, we explored the protective mechanisms of n-3 PUFAs in DCM. This is the first study to employ quantitative phosphoproteomics and multi-omics data analysis to reveal the protective mechanisms provided by endogenous n-3 PUFAs in DCM. Our results reveal that elevated endogenous n-3 PUFAs reduce cardiac remodeling and improve cardiac function. Under pressure overload conditions, n-3 PUFAs target phosphorylation signaling and restore the phosphorylation states of intracellular proteins in the subcellular compartments of sarcomeres, cytoplasm, membranes, sarcoplasmic reticulum, and mitochondria. Further mechanistic studies revealed that endogenous n-3 PUFAs suppress the production of detrimental n-3/n-6 oxylipins and regulate a metabolic associated gene-protein-metabolite pathway. Specifically, the mitochondrial structure, dynamics, oxidative phosphorylation, and function were protected by endogenous n-3 PUFAs in pressure overload hearts. Collectively the results provide insights into the protective mechanisms

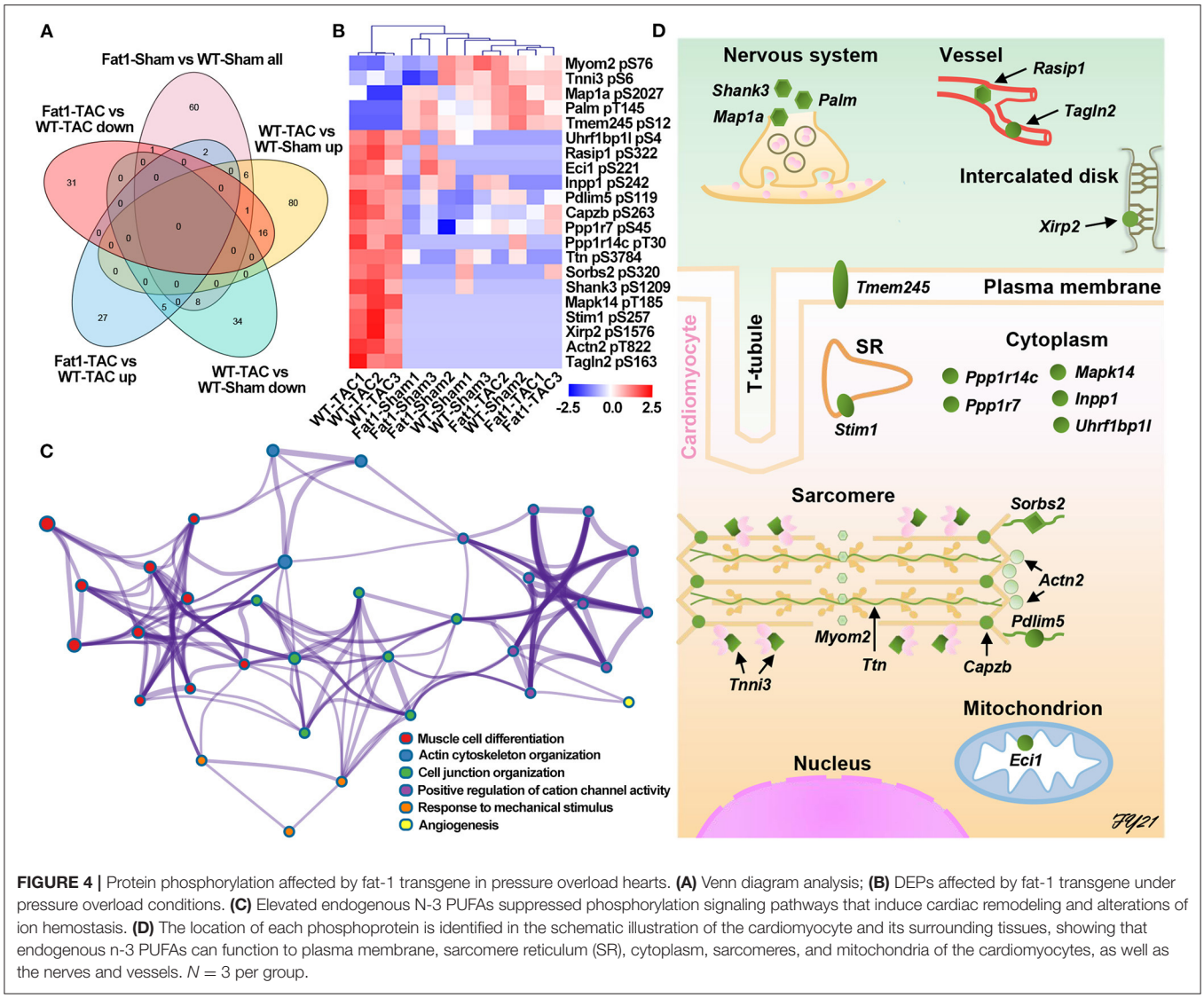

FIGURE 4 | Protein phosphorylation affected by fat-1 transgene in pressure overload hearts. **(A)** Venn diagram analysis; **(B)** DEPs affected by fat-1 transgene under pressure overload conditions. **(C)** Elevated endogenous N-3 PUFAs suppressed phosphorylation signaling pathways that induce cardiac remodeling and alterations of ion hemostasis. **(D)** The location of each phosphoprotein is identified in the schematic illustration of the cardiomyocyte and its surrounding tissues, showing that endogenous n-3 PUFAs can function to plasma membrane, sarcomere reticulum (SR), cytoplasm, sarcomeres, and mitochondria of the cardiomyocytes, as well as the nerves and vessels. $N = 3$ per group.

of n-3 PUFAs in DCM, which involve multiple cellular processes (transcription, post-translational modification, cellular metabolism, mitochondrial oxidative phosphorylation, and mitochondrial dynamics and function) in various cellular compartments. Specifically, our findings demonstrate that mitochondria play a critical role in n-3 PUFA-dependent cardioprotection in DCM.

N-3 PUFAs Maintain Phosphorylation States of Proteins and Prevent Cardiac Remodeling

We employed a transgenic mouse model expressing the *C. elegans* gene fat-1 to explore the protective mechanisms of n-3 PUFAs. Previous studies have employed this transgenic model to reveal that n-3 PUFAs exert anti-inflammatory and anti-apoptotic roles under various conditions (28–30). In addition, n-3 PUFAs reportedly increase phospholipids under hypertensive conditions in postnatal rats (31). Although supplementation with n-3 PUFAs is widely performed by individuals, evidence of the effects of n-3 PUFA treatment from clinical trials is inconsistent, and the molecular mechanisms underlying their effects remain unclear (32). Consistent with the evidence reported by Endo et al. (28), we found that elevated endogenous n-3 PUFAs prevents cardiac remodeling induced by pressure overload. In addition, the structural protection, genes and phosphoproteins enriched in cardiac remodeling were reduced by elevation of endogenous n-3 PUFAs. Activation of multiple phosphorylation signaling pathway is associated with cardiac hypertrophy or dilation. Several kinases such as AMP-activated protein kinase and protein kinase C have been recognized as valuable targets for drug discovery (33, 34). Here, we observed that endogenous n-3 PUFAs induced phosphorylation of proteins in the cardiomyocytes, nerves, and vessels of the heart. Modification of these proteins was centered in the regulation of contractile function. Among the 16 differentially abundant phosphoproteins in the cardiomyocytes, nine interacts with

TABLE 2 | Expression of phosphoproteins regulated by endogenous n-3 PUFAs.

Location	Gene ID	Phosphoprotein	PO	Fat-1
Cardiomyocyte				
Mitochondrion	Eci1	Enoyl-CoA delta isomerase 1, mitochondrial	↑	↓
Sarcomere	Tnni3	Cardiac troponin I	↓	↑
	Myom2	Myomesin 2	↓	↑
	Ttn	Titin	↑	↓
	Capzb	Actin capping protein, beta	↑	↓
	Actn2	Alpha actinin 2	↑	↓
	Pdlim5	PDZ and LIM domain protein 5	↑	↓
	Sorbs2	Sorbin and SH3 domain containing protein 2	↑	↓
Cytoplasm	Ppp1r14c	Protein phosphatase 1, regulatory inhibitor subunit 14C	↑	↓
	Ppp1r7	Protein phosphatase 1, regulatory subunit 7	↑	↓
	Mapk14	Mitogen-activated protein kinase, p38	↑	↓
	Inpp1	Inositol polyphosphate 1-phosphatase	↑	↓
	Uhrf1bp1l	UHRF1 binding protein 1-like	↑	↓
Intercalated disk	Xirp2	Xin actin-binding repeat containing protein 2	↑	↓
Sarcoplasmic reticulum	Stim1	Stromal interaction molecule 1	↑	↓
Plasma membrane	Tmem245	Transmembrane protein 245	↓	↑
Nerve				
	Palm	Paralemmin	↓	↑
	Map1a	Microtubule-associated protein 1A	↓	↑
	Shank3	SH3 and multiple ankyrin repeat domains 3	↑	↓
Vessel				
	Rasip1	Ras interacting protein 1	↑	↓
	Tagln2	Transgelin 2	↑	↓

The phosphoproteins, which had been upregulated (downregulated) by pressure overload, were downregulated (upregulated) by endogenous n-3 PUFAs in pressure overload hearts. N = 3. ↑, upregulated; ↓, downregulated. PO, pressure overload, indicating protein expression affected by pressure overload; Fat-1, fat-1 transgene, indicating protein expression affected by fat-1 transgene under pressure overload condition.

the myofilaments, phospholamban complex, and sarcomeric proteins at the intercalated disks (22, 35, 36), while four cytosolic proteins target either sarcomere or excitation-contraction coupling (37). Previous phosphoproteomic studies have provided insights regarding the roles of myofilament phosphorylation in cardiac contractile function. For instance, cTnI phosphorylated at Ser23/Ser24 regulates the myofilament response to Ca^{2+} (38) and is significantly increased in heart failure. Herein, we found that fat-1 transgene suppresses cTnI S23 phosphorylation in pressure overload hearts (**Supplementary Table S1**). Another phosphorylation site of cTnI, involving the serine 6 (S6) residue may also play a key role in mediating the beneficial effects of n-3 PUFA in fat-1 hearts during DCM. The phosphorylation level of cTnI S6 was downregulated in dilated hearts, and upregulated in fat-1 hearts under pressure overload conditions. Zhang et al. (39) further demonstrated that pseudo-phosphorylation (S6D) in myofilaments depresses the maximum tension of skinned muscle fibers (39). Taken together, elevation of myocardial n-3 PUFA can be a valuable strategy to maintain phosphorylation-dependent regulation of contractile function under pressure overload conditions. However, further studies are needed to clarify the roles of phosphorylation of sarcomeric or cytosolic proteins that are regulated by n-3 PUFAs in DCM.

Post-translational modification of cytosolic proteins involving p38, protein phosphatase type 1, and phosphatidylinositol signaling pathways, contribute to the protective myocardial effect provided by endogenous n-3 PUFAs. These protein kinases and phosphatases influence multiple cardiac activities and are essential for maintaining the hemostasis of cardiomyocytes. For instance, phosphorylation of p38 a key regulator in cardiac development and regeneration (40, 41), while its phosphorylation is decreased in failing human cardiomyocytes (42). Here, we observed an increase in the phosphorylation p38 T185 by pressure overload in WT hearts, and upregulated phosphorylation of p38 T185 in the dilated hearts was restored in fat-1 hearts, suggesting that this residue of p38 can be crucial to functional adaptation for the stressed hearts. In summary, alterations in post-translational modifications of the signaling or structural proteins in the myocardium contribute to the cardioprotective effect of n-3 PUFAs in DCM.

N-3 PUFAs Protect Mitochondrial Structure, Dynamics, and Function

The protection of mitochondria in pressure overload-induced DCM has been observed to involve several processes, including restoration of the expression of mRNAs encoding mitochondrial proteins, preservation of mitochondrial oxidative

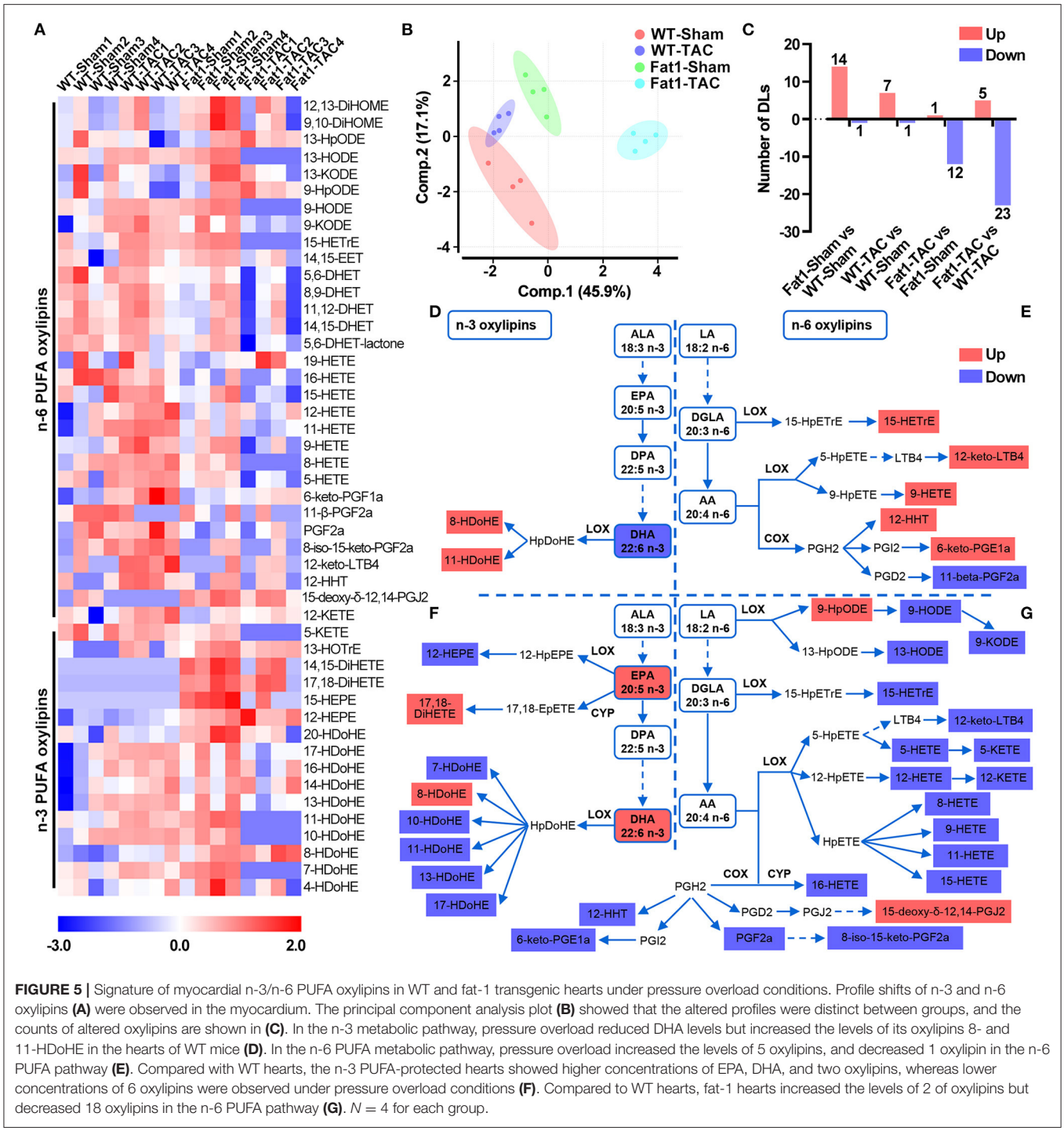

FIGURE 5 | Signature of myocardial n-3/n-6 PUFA oxylipins in WT and fat-1 transgenic hearts under pressure overload conditions. Profile shifts of n-3 and n-6 oxylipins **(A)** were observed in the myocardium. The principal component analysis plot **(B)** showed that the altered profiles were distinct between groups, and the counts of altered oxylipins are shown in **(C)**. In the n-3 metabolic pathway, pressure overload reduced DHA levels but increased the levels of its oxylipins 8- and 11-HDoHE in the hearts of WT mice **(D)**. In the n-6 PUFA metabolic pathway, pressure overload increased the levels of 5 oxylipins, and decreased 1 oxylipin in the n-6 PUFA pathway **(E)**. Compared with WT hearts, the n-3 PUFA-protected hearts showed higher concentrations of EPA, DHA, and two oxylipins, whereas lower concentrations of 6 oxylipins were observed under pressure overload conditions **(F)**. Compared to WT hearts, fat-1 hearts increased the levels of 2 of oxylipins but decreased 18 oxylipins in the n-6 PUFA pathway **(G)**. $N = 4$ for each group.

phosphorylation, maintenance of the mitochondrial structure, control of the phosphorylation levels of mitochondrial proteins, and regulation of mitochondrial dynamics and function. N-3 PUFAs are involved in both enzymatic and non-enzymatic n-3 oxidation pathways (32). In the enzymatic oxidation pathway, phospholipase A2 activates PLA2 and releases EPA or DHA. Next, they are catalyzed by COX, LOX, and CYP enzymes to form a series of oxylipins, including PGs and TXAs. In the non-enzymatic oxidation pathway, reactive oxygen species oxidize EPA and DHA and form lipid peroxides of EPA and DHA, which further metabolize into isoprostanes, isoflurane, alkenes, etc. In this study, we identified several n-3 and n-6 oxylipins that were upregulated in dilated WT hearts. Some of these metabolites are associated with cardiovascular dysfunction. For example,

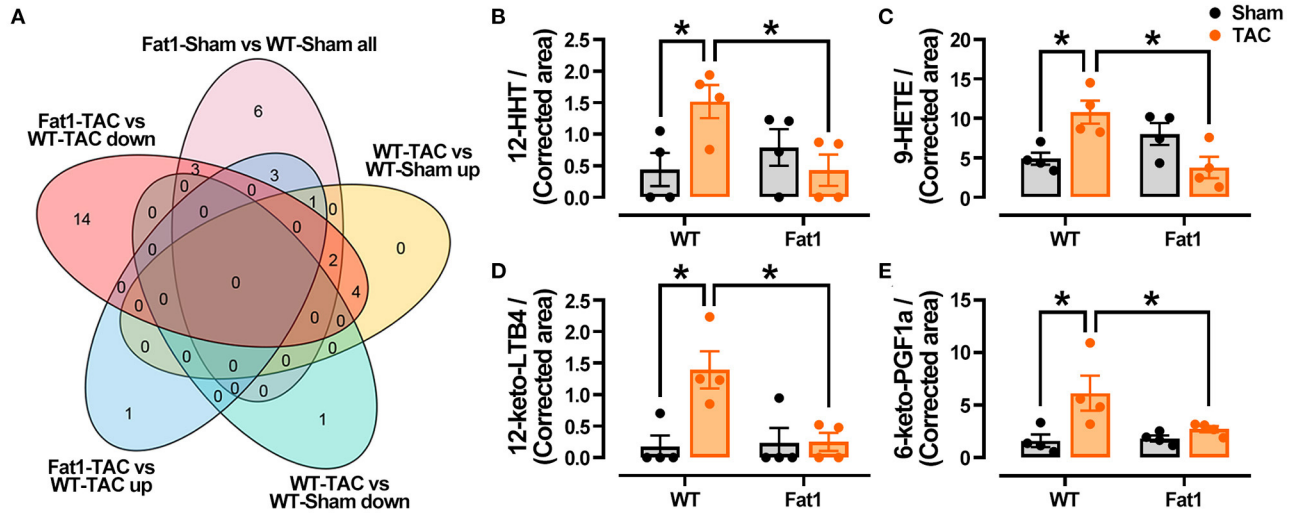

FIGURE 6 | Fat-1 Oxylipin production in pressure overload hearts. **(A)** Venn diagram displaying the oxylipins that were decreased (increased) by pressure overload, were increased (decreased) by fat-1 transgene under pressure overload conditions. Four oxylipins including 12-HHT **(B)**, 9-HETE **(C)**, 12-keto-LTB4 **(D)**, and 6-keto-PGF1a **(E)** were identified via Venn diagram analysis. 12-HHT, 12(S)-hydroxyheptadeca-5Z,8E,10E-trienoic acid; 9-HETE, 9S-hydroxy-5Z,7E,11Z,14Z-eicosatetraenoic acid; 12-keto-LTB4, 12-keto-leukotriene B4; 6-keto-PGF1a, 6-keto-prostaglandin F1alpha. $N = 4$ for each group. * $P < 0.05$ between groups.

plasma HDoHEs, which are oxidative stress indicators, are elevated in hypertensive patients (43). Moreover, plasma HETEs, including 5-, 8-,9-, 11-, 12-, 15-, are upregulated in patients with acute coronary syndrome (44). Meanwhile, mechanistic studies have revealed that 8-HETE and 15-HETE induce hypertrophy in a cardiomyocyte cell line and pulmonary hypertension in rats, respectively (45, 46). Consistent with these findings, we found that the myocardia protected by endogenous n-3 PUFAs exhibited reduced levels of most n-3 (6 in 8 oxylipins) and n-6 oxylipins (18 in 20 oxylipins). Thus, shifts in the metabolic profiles of oxylipins may protect cardiac function by assisting the fat-1 myocardia to resist pressure overload stress.

Furthermore, our integrated multi-omics data revealed that endogenous n-3 PUFAs regulated the expression of various genes and phosphoproteins, as well as the metabolism of oxylipins through the PPAR pathway in pressure overload myocardia. The effectors of oxylipins included PPAR-regulated genes *Fabp3* (upregulated), *Angptl4* (downregulated), and *Pck1* (downregulated) and phosphoprotein perilipin 5. In healthy hearts, PPAR isoforms are activated by fatty acids and act as a master switch in controlling cardiomyocyte metabolism (47). Meanwhile, PPAR agonists are used for treating diabetes and hyperlipidemia, which are risk factors for incident heart failure (48). In this study, we found that fat-1 transgene targeted 8-HETE and 13-HODE and in turn suppressed *Angptl4* and *Pck1* to fine tune lipid and glucose metabolism in the pressure overload hearts. *Angptl4* encodes angiopoietin-like 4 protein, which is a key regulator of lipoprotein lipase, and *Pck1* encodes phosphoenolpyruvate carboxykinase 1, which catalyzes gluconeogenesis. However, the roles of these molecular signals in the stressed heart remain unclear. For example, upregulation of *Angptl4* has been reported in patients with, and an experimental model of, metabolic syndrome (49, 50), whereas activation of cardiac Angptl4 via PPARβ/δ is associated with cardioprotection under lipid overload conditions (51). In addition, We found that phosphorylation of perilipin 5 is associated with the cardiac protective effect in pressure overload fat-1 hearts. Super-resolution microscopy has shown that perilipin 5 is localized at lipid droplet-mitochondria tethering sites (52), suggesting that perilipin 5 is crucial to mitochondrial function. Moreover, activation of perilipin 5 has been shown to protect hearts against oxidative stress and ischemia (53, 54). However, the regulation and function of this gene-metabolite-phosphoprotein signaling network requires further investigation.

Myocardium ATP contents were restored by fat-1 transgene in pressure overload hearts, confirming that n-3 PUFAs protect cardiac metabolic and contractile machinery. Furthermore, we found that mitochondrial oxidative phosphorylation was maintained by fat-1 transgene in pressure overload myocardia. More than 95% of the energy used by cardiomyocytes is produced by oxidative phosphorylation (55) with ∼60–70% of the total ATP produced used to fuel cardiomyocyte contraction, while the remainder is used for various ion pumps including CaATPase in the sarcoplasmic reticulum (56). Reportedly, in heart failure, oxidative phosphorylation levels are reduced (57). Consistent with this finding, we found that pressure overload-induced dilation significantly reduced expression of respiratory chain complexes I–V, whereas myocardia with elevated endogenous n-3 PUFAs resisted the pressure overload and retained the expression of respiratory chain complex I, -II, and -IV. However, in contrast to the above findings, the mRNA profiling of the respiratory chain complex was preserved in the pressure overload fat-1 hearts.

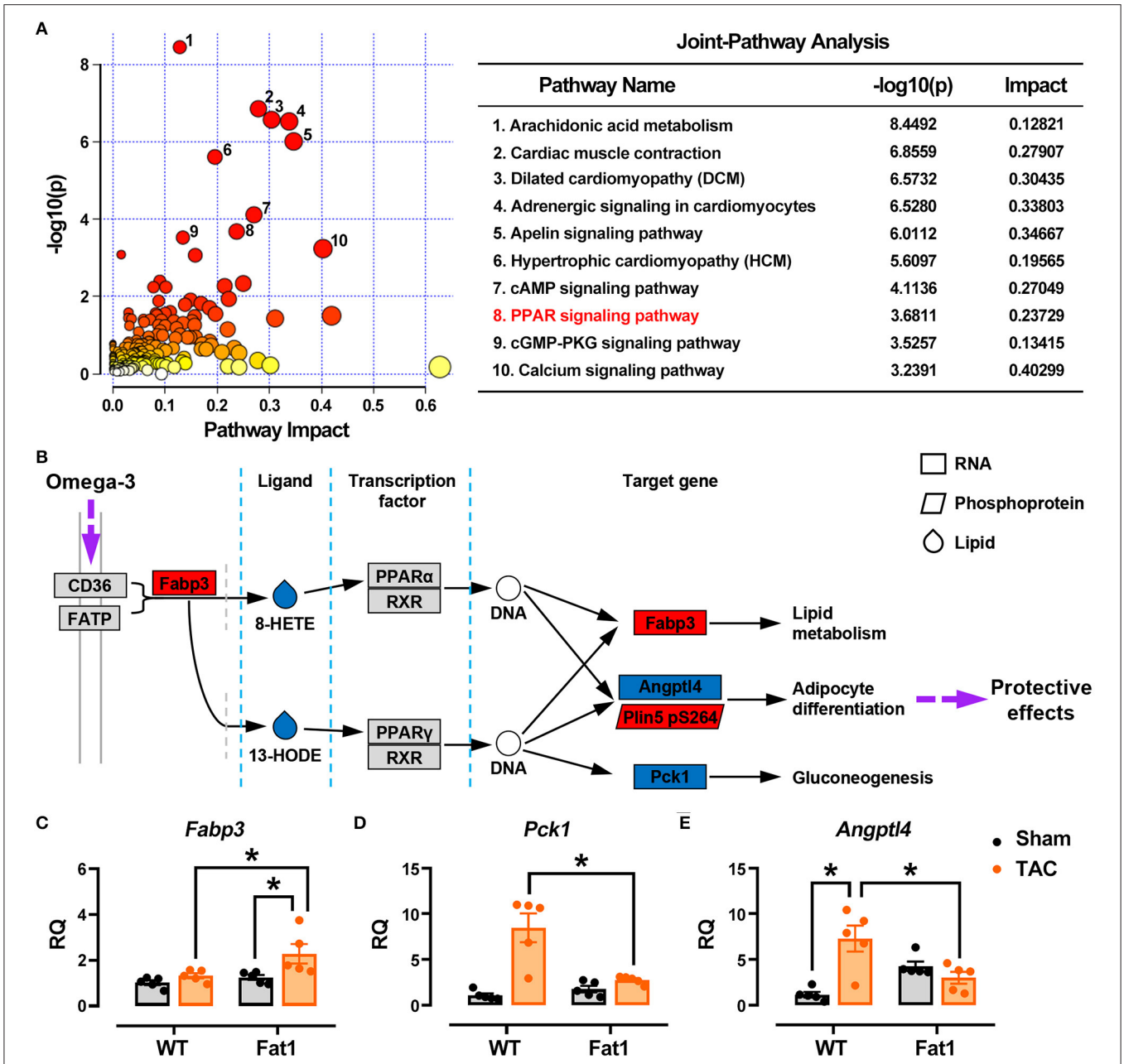

FIGURE 7 | Multi-omics data analysis. The results of RNA-sequencing, phosphoprotein quantification, and oxylipin profiling were integrated and analyzed **(A)**. Top 10 pathways affected by endogenous n-3 PUFAs were selected for analysis, and KEGG pathway analysis was applied to illustrate protective mechanism of n-3 PUFAs in pressure overload hearts **(B)**. Expression of genes identified from multi-omics data analysis has been determined by RT-qPCR **(C–E)**. * $P < 0.05$ between groups.

In conclusion, endogenous n-3 PUFAs prevent dilated cardiomyopathy via orchestrating gene expression, protein phosphorylation, and metabolism. The functional protection of n-3 PUFAs in pressure overload hearts was attributed to preservation of mitochondrial structure, dynamics, and function.

Limitations of the Study

Illustration of the molecular signatures allows us to explore the mechanisms and evaluate therapeutic effects in an unbiased way. However, due to the limitations of research tools, molecular changes detected in unbiased screening of small populations may be difficult to verify in large-scale populations. For example, no commercially available antibodies exist for cTnI T6. In addition, quantitative proteomics indicated that 21 phosphoproteins were mediated by n-3 PUFAs in pressure overload hearts; However, whether these molecules represent specific determinants has not yet been verified, and warrants further investigation to fully elucidate the associated molecular mechanisms.

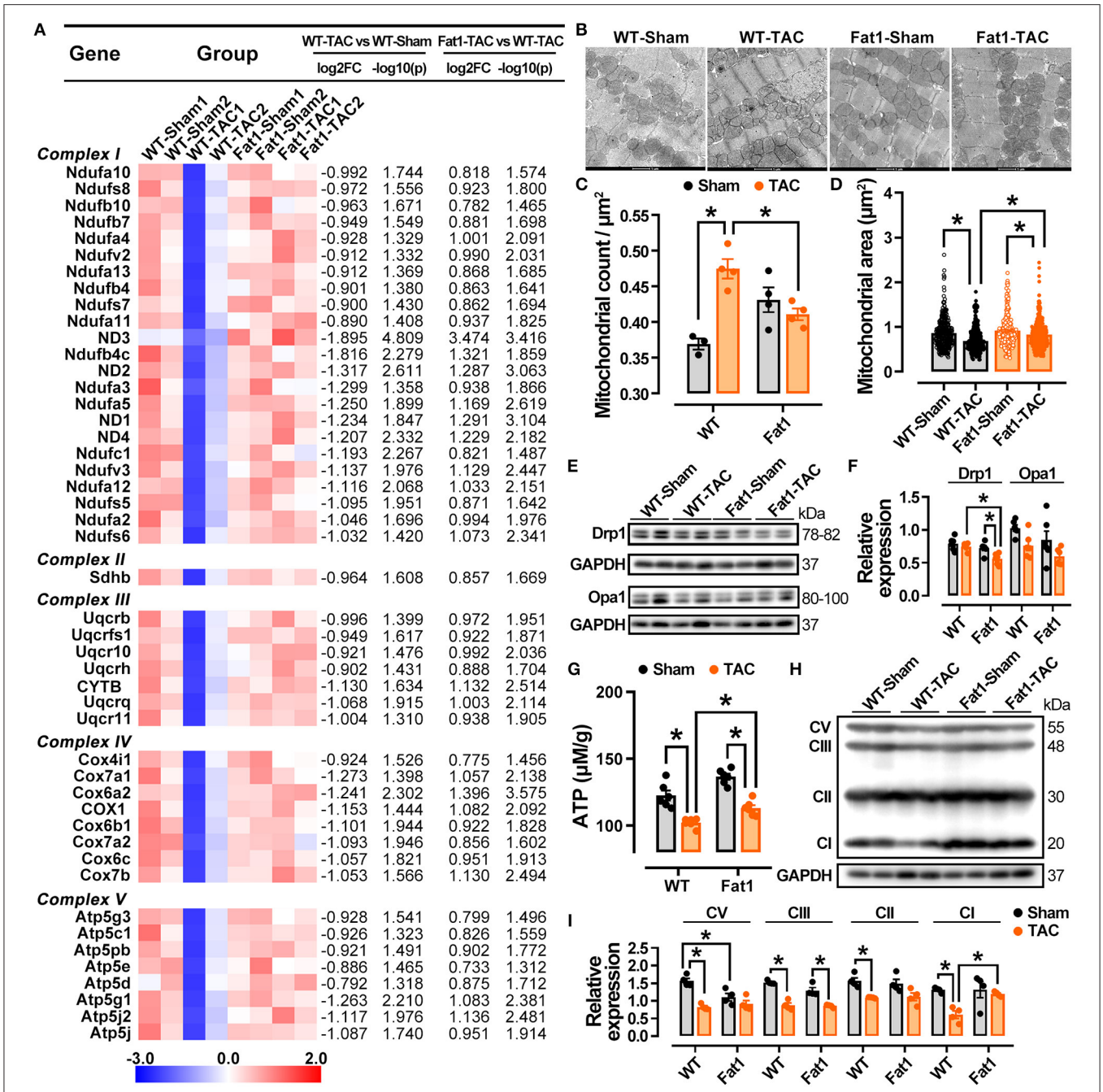

FIGURE 8 | Preservation of mitochondria function by fat-1 transgene in pressure overload hearts. In the RNA-sequencing datasets of experimental groups, 47 genes encoding oxidative phosphorylation markers, mitochondrial respiratory chain complexes were showed **(A)**. Under transmission electron microscopy, the mitochondria display a reduction in size and increase in counts per square μm in WT-TAC hearts, whereas those of Fat1-TAC hearts were not altered by pressure overload **(B–D)**, $N = 300$ mitochondria in the measurement area. The fission marker Drp1 was significantly reduced in Fat-1 TAC hearts but not in the dilated WT-TAC heart **(E,F)**. ATP generation was restored by endogenous n-3 PUFAs under pressure overload conditions **(G)**. The protein expression of respiratory chain complexes was downregulated in the dilated WT-TAC hearts. Compared to the sham hearts, pressure overload did not suppress the expression levels of mitochondrial complexes I, II, V in fat-1 transgenic hearts **(H,I)**. $N = 4$ for each group. $^*P < 0.05$.

DATA AVAILABILITY STATEMENT

The datasets presented in this study can be found in online repositories. The names of the repository/repositories and accession number(s) can be found at: GEO, GSE185686.

ETHICS STATEMENT

The animal study was reviewed and approved by Institutional Animal Care and Use Committee (IACUC) of the Guangdong Laboratory Animals Monitoring Institute (No. IACUC2017015).

AUTHOR CONTRIBUTIONS

FY, XL, and WT designed and initiated the project. WT performed the animal surgery and echocardiographic recording. CC and JZ performed the lipidomic analysis. XL, SZ, HC, CY, LK, and ZP were responsible for western blotting, imaging measurement, pathological examination, or animal care. XL and FY performed the bioinformatics analysis, interpreted the results, and prepared the manuscript. YZ, CZ, WP, and PB provided critical comments during experiment design and manuscript preparation. All authors read and approved the final manuscript.

FUNDING

This work was supported by the Guangzhou Science and Technology Program (201804010206), the Guangdong Science and Technology Program (2018A0303130208, 2019A030317014, and 2008A08003), National Natural Science Foundation of China (31672376, 81941002), and the Guangdong Provincial Key Laboratory of Laboratory Animals (2017B030314171). WP is supported with a Senior Investigator Award for Women's Heart Health from the Heart and Stroke Foundation of Canada.

ACKNOWLEDGMENTS

The authors would like to express our appreciation for the gift of fat-1 transgenic mice from Dr. Jing Xuan Kang at Harvard Medical School, USA.

SUPPLEMENTARY MATERIAL

The Supplementary Material for this article can be found online at: https://www.frontiersin.org/articles/10.3389/fcvm.2021.788270/full#supplementary-material

REFERENCES

1. Mills KT, Bundy JD, Kelly TN, Reed JE, Kearney PM, Reynolds K, et al. Global disparities of hypertension prevalence and control: a systematic analysis of population-based studies from 90 countries. *Circulation.* (2016) 134:441–50. doi: 10.1161/CIRCULATIONAHA.115.018912
2. Osnabrugge RL, Mylotte D, Head SJ, Van Mieghem NM, Nkomo VT, Lereun CM, et al. Aortic stenosis in the elderly: disease prevalence and number of candidates for transcatheter aortic valve replacement: a meta-analysis and modeling study. *J Am Coll Cardiol.* (2013) 62:1002–12. doi: 10.1016/j.jacc.2013.05.015
3. Schultheiss HP, Fairweather D, Caforio ALP, Escher F, Hershberger RE, Lipshultz SE, et al. Dilated cardiomyopathy. *Nat Rev Dis Primers.* (2019) 5:32. doi: 10.1038/s41572-019-0084-1
4. Gerull B, Gramlich M, Atherton J, Mcnabb M, Trombitás K, Sasse-Klaassen S, et al. Mutations of TTN, encoding the giant muscle filament titin, cause familial dilated cardiomyopathy. *Nat Genet.* (2002) 30:201–4. doi: 10.1038/ng815
5. Villard E, Duboscq-Bidot L, Charron P, Benaiche A, Conraads V, Sylvius N, et al. Mutation screening in dilated cardiomyopathy: prominent role of the beta myosin heavy chain gene. *Eur Heart J.* (2005) 26:794–803. doi: 10.1093/eurheartj/ehi193
6. Mcconnell BK, Jones KA, Fatkin D, Arroyo LH, Lee RT, Aristizabal O, et al. Dilated cardiomyopathy in homozygous myosin-binding protein-C mutant mice. *J Clin Invest.* (1999) 104:1235–44. doi: 10.1172/JCI7377
7. Arbustini E, Diegoli M, Fasani R, Grasso M, Morbini P, Banchieri N, et al. Mitochondrial DNA mutations and mitochondrial abnormalities in dilated cardiomyopathy. *Am J Pathol.* (1998) 153:1501–10. doi: 10.1016/S0002-9440(10)65738-0
8. Te Riet L, Van Esch JH, Roks AJ, Van Den Meiracker AH, Danser AH. Hypertension: renin-angiotensin-aldosterone system alterations. *Circ Res.* (2015) 116:960–75. doi: 10.1161/CIRCRESAHA.116.303587
9. Chakraborty S, Mandal J, Yang T, Cheng X, Yeo JY, Mccarthy CG, et al. Metabolites and hypertension: insights into hypertension as a metabolic disorder: 2019 harriet dustan award. *Hypertension.* (2020) 75:1386–96. doi: 10.1161/HYPERTENSIONAHA.120.13896
10. Feihl F, Liaudet L, Levy BI, Waeber B. Hypertension and microvascular remodelling. *Cardiovasc Res.* (2008) 78:274–85. doi: 10.1093/cvr/cvn022
11. Kuwahara F, Kai H, Tokuda K, Takeya M, Takeshita A, Egashira K, et al. Hypertensive myocardial fibrosis and diastolic dysfunction: another model of inflammation? *Hypertension.* (2004) 43:739–45. doi: 10.1161/01.HYP.0000118584.33350.7d
12. Madhur MS, Elijovich F, Alexander MR, Pitzer A, Ishimwe J, Van Beusecum JP, et al. Hypertension: do inflammation and immunity hold the key to solving this epidemic? *Circ Res.* (2021) 128:908–33. doi: 10.1161/CIRCRESAHA.121.318052
13. Sun M, Chen M, Dawood F, Zurawska U, Li JY, Parker T, et al. Tumor necrosis factor-alpha mediates cardiac remodeling and ventricular dysfunction after pressure overload state. *Circulation.* (2007) 115:1398–407. doi: 10.1161/CIRCULATIONAHA.106.643585
14. Ling H, Zhang T, Pereira L, Means CK, Cheng H, Gu Y, et al. Requirement for Ca2+/calmodulin-dependent kinase II in the transition from pressure overload-induced cardiac hypertrophy to heart failure in mice. *J Clin Invest.* (2009) 119:1230–40. doi: 10.1172/JCI38022
15. Tan W, Li X, Zheng S, Li X, Zhang X, Pyle WG, et al. A Porcine model of heart failure with preserved ejection fraction induced by chronic pressure overload characterized by cardiac fibrosis and remodeling. *Front Cardiovasc Med.* (2021) 8:677727. doi: 10.3389/fcvm.2021.677727
16. Zheng S, Tan W, Li X, Li B, Gong B, Pyle WG, et al. Aged monkeys fed a high-fat/high-sugar diet recapitulate metabolic disorders and cardiac contractile dysfunction. *J Cardiovasc Transl Res.* (2021) 14:799–815. doi: 10.1007/s12265-021-10105-z
17. Mori TA. Dietary n-3 PUFA and CVD: a review of the evidence. *Proc Nutr Soc.* (2014) 73:57–64. doi: 10.1017/S0029665113003583
18. Jiang L, Wang J, Xiong K, Xu L, Zhang B, Ma A. Intake of fish and marine n-3 polyunsaturated fatty acids and risk of cardiovascular disease mortality: a meta-analysis of prospective cohort studies. *Nutrients.* (2021) 13:2342. doi: 10.3390/nu13072342
19. Cabo J, Alonso R, Mata P. Omega-3 fatty acids and blood pressure. *Br J Nutr.* (2012) 107(Suppl. 2):S195–200. doi: 10.1017/S0007114512001584
20. Stupin M, Kibel A, Stupin A, Selthofer-Relatić K, Matić A, Mihalj M, et al. The physiological effect of n-3 polyunsaturated fatty acids (n-3 PUFAs) intake and exercise on hemorheology, microvascular function, and physical performance in health and cardiovascular diseases; is there an interaction of exercise and dietary n-3 PUFA intake? *Front Physiol.* (2019) 10:1129. doi: 10.3389/fphys.2019.01129
21. Kang JX, Wang J, Wu L, Kang ZB. Transgenic mice: fat-1 mice convert n-6 to n-3 fatty acids. *Nature.* (2004) 427:504. doi: 10.1038/427504a
22. Li X, Zheng S, Tan W, Chen H, Li X, Wu J, et al. Slit2 Protects Hearts Against Ischemia-Reperfusion Injury by Inhibiting Inflammatory Responses and Maintaining Myofilament Contractile Properties. *Front Physiol.* (2020) 11:228. doi: 10.3389/fphys.2020.00228
23. Wiśniewski JR, Zougman A, Nagaraj N, Mann M. Universal sample preparation method for proteome analysis. *Nat Methods.* (2009) 6:359–62. doi: 10.1038/nmeth.1322
24. Michalski A, Cox J, Mann M. More than 100,000 detectable peptide species elute in single shotgun proteomics runs but the majority is

inaccessible to data-dependent LC-MS/MS. *J Proteome Res.* (2011) 10:1785–93. doi: 10.1021/pr101060v
25. Zhou Y, Zhou B, Pache L, Chang M, Khodabakhshi AH, Tanaseichuk O, et al. Metascape provides a biologist-oriented resource for the analysis of systems-level datasets. *Nat Commun.* (2019) 10:1523. doi: 10.1038/s41467-019-09234-6
26. Zhang LJ, Chen B, Zhang JJ, Li J, Yang Q, Zhong QS, et al. Serum polyunsaturated fatty acid metabolites as useful tool for screening potential biomarker of colorectal cancer. *Prostaglandins Leukot Essent Fatty Acids.* (2017) 120:25–31. doi: 10.1016/j.plefa.2017.04.003
27. Hall AR, Burke N, Dongworth RK, Hausenloy DJ. Mitochondrial fusion and fission proteins: novel therapeutic targets for combating cardiovascular disease. *Br J Pharmacol.* (2014) 171:1890–906. doi: 10.1111/bph.12516
28. Endo J, Sano M, Isobe Y, Fukuda K, Kang JX, Arai H, et al. 18-HEPE, an n-3 fatty acid metabolite released by macrophages, prevents pressure overload-induced maladaptive cardiac remodeling. *J Exp Med.* (2014) 211:1673–87. doi: 10.1084/jem.20132011
29. Ma H, Chen P, Sang C, Huang D, Geng Q, Wang L. Modulation of apoptosis-related microRNAs following myocardial infarction in fat-1 transgenic mice vs. wild-type mice. *J Cell Mol Med.* (2018) 22:5698–707. doi: 10.1111/jcmm.13846
30. Mao S, Ma H, Chen P, Liang Y, Zhang M, Hinek A. Fat-1 transgenic mice rich in endogenous omega-3 fatty acids are protected from lipopolysaccharide-induced cardiac dysfunction. *ESC Heart Fail.* (2021) 8:1966–78. doi: 10.1002/ehf2.13262
31. Novák F, Kolár F, Vocu S, Vecka M, Nováková O. Pressure overload selectively increases n-3 PUFA in myocardial phospholipids during early postnatal period. *Physiol Res.* (2012) 61:S155–163. doi: 10.33549/physiolres.932401
32. Anderson EJ, Taylor DA. Stressing the heart of the matter: re-thinking the mechanisms underlying therapeutic effects of n-3 polyunsaturated fatty acids. *F1000 Med Rep.* (2012) 4:13. doi: 10.3410/M4-13
33. Mochly-Rosen D, Das K, Grimes KV. Protein kinase C, an elusive therapeutic target? *Nat Rev Drug Discov.* (2012) 11:937–57. doi: 10.1038/nrd3871
34. Steinberg GR, Carling D. AMP-activated protein kinase: the current landscape for drug development. *Nat Rev Drug Discov.* (2019) 18:527–51. doi: 10.1038/s41573-019-0019-2
35. Yang FH, Pyle WG. Reduced cardiac CapZ protein protects hearts against acute ischemia-reperfusion injury and enhances preconditioning. *J Mol Cell Cardiol.* (2012) 52:761–72. doi: 10.1016/j.yjmcc.2011.11.013
36. Cacheux M, Strauss B, Raad N, Ilkan Z, Hu J, Benard L, et al. Cardiomyocyte-specific STIM1 (Stromal Interaction Molecule 1) depletion in the adult heart promotes the development of arrhythmogenic discordant alternans. *Circ Arrhythm Electrophysiol.* (2019) 12:e007382. doi: 10.1161/CIRCEP.119.007382
37. Woodcock EA, Wang BH, Arthur JF, Lennard A, Matkovich SJ, Du XJ, et al. Inositol polyphosphate 1-phosphatase is a novel antihypertrophic factor. *J Biol Chem.* (2002) 277:22734–42. doi: 10.1074/jbc.M110405200
38. Solaro RJ, Henze M, Kobayashi T. Integration of troponin I phosphorylation with cardiac regulatory networks. *Circ Res.* (2013) 112:355–66. doi: 10.1161/CIRCRESAHA.112.268672
39. Zhang P, Kirk JA, Ji W, Dos Remedios CG, Kass DA, Van Eyk JE, et al. Multiple reaction monitoring to identify site-specific troponin I phosphorylated residues in the failing human heart. *Circulation.* (2012) 126:1828–37. doi: 10.1161/CIRCULATIONAHA.112.096388
40. Allen M, Svensson L, Roach M, Hambor J, Mcneish J, Gabel CA. Deficiency of the stress kinase p38alpha results in embryonic lethality: characterization of the kinase dependence of stress responses of enzyme-deficient embryonic stem cells. *J Exp Med.* (2000) 191:859–70. doi: 10.1084/jem.191.5.859
41. Romero-Becerra R, Santamans AM, Folgueira C, Sabio G. p38 MAPK pathway in the heart: new insights in health and disease. *Int J Mol Sci.* (2020) 21:7412. doi: 10.3390/ijms21197412
42. Lemke LE, Bloem LJ, Fouts R, Esterman M, Sandusky G, Vlahos CJ. Decreased p38 MAPK activity in end-stage failing human myocardium: p38 MAPK alpha is the predominant isoform expressed in human heart. *J Mol Cell Cardiol.* (2001) 33:1527–40. doi: 10.1006/jmcc.2001.1415
43. Caligiuri SPB, Parikh M, Stamenkovic A, Pierce GN, Aukema HM. Dietary modulation of oxylipins in cardiovascular disease and aging. *Am J Physiol Heart Circ Physiol.* (2017) 313:H903–18. doi: 10.1152/ajpheart.00201.2017
44. Zu L, Guo G, Zhou B, Gao W. Relationship between metabolites of arachidonic acid and prognosis in patients with acute coronary syndrome. *Thromb Res.* (2016) 144:192–201. doi: 10.1016/j.thromres.2016.06.031
45. Maayah ZH, Abdelhamid G, El-Kadi AO. Development of cellular hypertrophy by 8-hydroxyeicosatetraenoic acid in the human ventricular cardiomyocyte, RL-14 cell line, is implicated by MAPK and NF-κB. *Cell Biol Toxicol.* (2015) 31:241–59. doi: 10.1007/s10565-015-9308-7
46. Ruffenach G, O'connor E, Vaillancourt M, Hong J, Cao N, Sarji S, et al. Oral 15-hydroxyeicosatetraenoic acid induces pulmonary hypertension in mice by triggering T cell-dependent endothelial cell apoptosis. *Hypertension.* (2020) 76, 985–996. doi: 10.1161/HYPERTENSIONAHA.120.14697
47. Montaigne D, Butruille L, Staels B. PPAR control of metabolism and cardiovascular functions. *Nat Rev Cardiol.* (2021) 18:809–23. doi: 10.1038/s41569-021-00569-6
48. Pol CJ, Lieu M, Drosatos K. PPARs: protectors or opponents of myocardial function? *PPAR Res.* (2015) 2015:835985. doi: 10.1155/2015/835985
49. Muendlein A, Saely CH, Leiherer A, Fraunberger P, Kinz E, Rein P, et al. Angiopoietin-like protein 4 significantly predicts future cardiovascular events in coronary patients. *Atherosclerosis.* (2014) 237:632–8. doi: 10.1016/j.atherosclerosis.2014.10.028
50. Kesherwani V, Shahshahan HR, Mishra PK. Cardiac transcriptome profiling of diabetic Akita mice using microarray and next generation sequencing. *PLoS ONE.* (2017) 12:e0182828. doi: 10.1371/journal.pone.0182828
51. Georgiadi A, Lichtenstein L, Degenhardt T, Boekschoten MV, Van Bilsen M, Desvergne B, et al. Induction of cardiac Angptl4 by dietary fatty acids is mediated by peroxisome proliferator-activated receptor beta/delta and protects against fatty acid-induced oxidative stress. *Circ Res.* (2010) 106:1712–21. doi: 10.1161/CIRCRESAHA.110.217380
52. Gemmink A, Daemen S, Kuijpers HJH, Schaart G, Duimel H, López-Iglesias C, et al. Super-resolution microscopy localizes perilipin 5 at lipid droplet-mitochondria interaction sites and at lipid droplets juxtaposing to perilipin 2. *Biochim Biophys Acta Mol Cell Biol Lipids.* (2018) 1863:1423–32. doi: 10.1016/j.bbalip.2018.08.016
53. Kuramoto K, Okamura T, Yamaguchi T, Nakamura TY, Wakabayashi S, Morinaga H, et al. Perilipin 5, a lipid droplet-binding protein, protects heart from oxidative burden by sequestering fatty acid from excessive oxidation. *J Biol Chem.* (2012) 287:23852–63. doi: 10.1074/jbc.M111.328708
54. Goldberg IJ, Reue K, Abumrad NA, Bickel PE, Cohen S, Fisher EA, et al. Deciphering the role of lipid droplets in cardiovascular disease: a report from the 2017 National Heart, Lung, and Blood Institute Workshop. *Circulation.* (2018) 138:305–15. doi: 10.1161/CIRCULATIONAHA.118.033704
55. Nolfi-Donegan D, Braganza A, Shiva S. Mitochondrial electron transport chain: oxidative phosphorylation, oxidant production, and methods of measurement. *Redox Biol.* (2020) 37:101674. doi: 10.1016/j.redox.2020.101674
56. Suga H. Ventricular energetics. *Physiol Rev.* (1990) 70:247–77. doi: 10.1152/physrev.1990.70.2.247
57. Rosca MG, Vazquez EJ, Kerner J, Parland W, Chandler MP, Stanley W, et al. Cardiac mitochondria in heart failure: decrease in respirasomes and oxidative phosphorylation. *Cardiovasc Res.* (2008) 80:30–9. doi: 10.1093/cvr/cvn184

Conflict of Interest: The authors declare that the research was conducted in the absence of any commercial or financial relationships that could be construed as a potential conflict of interest.

Publisher's Note: All claims expressed in this article are solely those of the authors and do not necessarily represent those of their affiliated organizations, or those of the publisher, the editors and the reviewers. Any product that may be evaluated in this article, or claim that may be made by its manufacturer, is not guaranteed or endorsed by the publisher.

Copyright © 2022 Li, Tan, Zheng, Zhang, Zhu, Cai, Chen, Yang, Kang, Pan, Pyle, Backx, Zou and Yang. This is an open-access article distributed under the terms of the Creative Commons Attribution License (CC BY). The use, distribution or reproduction in other forums is permitted, provided the original author(s) and the copyright owner(s) are credited and that the original publication in this journal is cited, in accordance with accepted academic practice. No use, distribution or reproduction is permitted which does not comply with these terms.

frontiers in Cardiovascular Medicine

REVIEW
published: 13 January 2022
doi: 10.3389/fcvm.2021.788505

Regulation of Mitochondrial Dynamics by Aerobic Exercise in Cardiovascular Diseases

Changping Gu[1,2,3†], Jie Yan[1†], Liang Zhao[3], Guanghan Wu[1] and Yue-lan Wang[1,2,3]*

[1] Department of Anesthesiology and Perioperative Medicine, The First Affiliated Hospital of Shandong First Medical University, Taian, China, [2] Shandong Provincial Qianfoshan Hospital, Shandong Institute of Anesthesia and Respiratory Critical Medicine, Jinan, China, [3] Department of Anesthesiology and Perioperative Medicine, Shandong Provincial Qianfoshan Hospital, Shandong University, Jinan, China

Mitochondrial dynamics, including continuous biogenesis, fusion, fission, and autophagy, are crucial to maintain mitochondrial integrity, distribution, size, and function, and play an important role in cardiovascular homeostasis. Cardiovascular health improves with aerobic exercise, a well-recognized non-pharmaceutical intervention for both healthy and ill individuals that reduces overall cardiovascular disease (CVD) mortality. Increasing evidence shows that aerobic exercise can effectively regulate the coordinated circulation of mitochondrial dynamics, thus inhibiting CVD development. This review aims to illustrate the benefits of aerobic exercise in prevention and treatment of cardiovascular disease by modulating mitochondrial function.

Keywords: aerobic exercise, mitochondrial dynamics, myocardial mitochondria, cardiovascular disease, mitochondrial fusion, mitochondrial fission

OPEN ACCESS

Edited by:
Lei-Lei Ma,
Fudan University, China

Reviewed by:
Stephen C. Kolwicz Jr.,
Ursinus College, United States
Hyoung Kyu Kim,
Inje University, South Korea

***Correspondence:**
Yue-lan Wang
wyldgf@163.com

† These authors share first authorship

Specialty section:
This article was submitted to Cardiovascular Metabolism, a section of the journal Frontiers in Cardiovascular Medicine

Received: *02 October 2021*
Accepted: *06 December 2021*
Published: *13 January 2022*

Citation:
Gu C, Yan J, Zhao L, Wu G and Wang Y-l (2022) Regulation of Mitochondrial Dynamics by Aerobic Exercise in Cardiovascular Diseases. Front. Cardiovasc. Med. 8:788505. doi: 10.3389/fcvm.2021.788505

INTRODUCTION

Cardiovascular diseases (CVDs) are the leading cause of global mortality and a major contributor to disability worldwide (1). CVD pathogenesis is a complex biological process, but few feasible targets exist to prevent or reverse CVD (2). The American College of Cardiology recently reported significant progress in drug treatment for CVD; however, these drugs always have negative long-term effects, causing a reduction of 10–20% in the left ventricular mass (3). Therefore, it is essential to find effective non-pharmaceutical therapies. Aerobic exercise has many benefits to the cardiovascular system, such as improving the mechanical properties of the heart and enhancing its contractility to reduce the incidence of many CVDs. Some of these improvements may arise from effects on mitochondria.

Mitochondria are the energy factories of cells, producing adenosine triphosphate (ATP), and are the main source of cellular reactive oxygen species (ROS). Dysfunctional mitochondria limit energy production, increase ROS production, and transmit apoptotic signals, leading to tissue damage and organ dysfunction (4). Mitochondrial dynamics, which include mitochondrial biogenesis, fusion, fission, and autophagy, play an important role in maintaining mitochondrial homeostasis and ensuring mitochondrial function (5). Mitochondrial dynamics are particularly important for cells with high energy requirements, such as cardiomyocytes, which continuously require ATP to support heart function (6). Therefore, regulating mitochondrial dynamics through effective interventions is crucial for preventing and treating CVDs (7). In animal models of heart failure, Campos et al. found that aerobic exercise improved the mitochondrial fusion/fission balance and restored cardiac autophagy flux,

thereby improving cardiac function (8). Here, we will address the biological mechanisms of mitochondrial dynamics in CVDs and discuss the mechanism of aerobic exercise in improving cardiovascular diseases, thereby providing valuable clues for CVD prevention and treatment.

MITOCHONDRIAL DYNAMICS AND CVDs

Mitochondria are highly dynamic organelles, constantly undergoing a coordinated cycle of biogenesis, fusion, fission, and degradation (**Figure 1**) (9), and forming a complex network to respond to dynamic changes in energy requirements (10). Maintaining healthy and functional mitochondrial networks is critical for physiological adaptation and coping with stress during development and throughout life (11). Mitochondrial dynamics consist mainly of mitochondrial fusion and fission. Mitochondria are easily damaged by various external stimuli. Damaged mitochondria are cleared by autophagy to maintain the stability of mitochondrial dynamics, which is important to ensuring a healthy mitochondrial network. Defects in this machinery cause a range of diseases especially affecting the cardiovascular system (12). Notably, mounting evidence demonstrates that some of the benefits of aerobic exercise against CVD occur through its effects on three underlying mitochondrial aspects: mitochondrial biogenesis, mitochondrial fusion and fission, and mitochondrial autophagy.

MITOCHONDRIAL BIOGENESIS AND CVDs

Mitochondrial biogenesis requires coordination of nuclear and mitochondrial DNA (12). It is critical to healthy mitochondrial dynamics and further affects myocardial function. Mitochondrial biosynthesis is regulated by the peroxisome proliferator–activated receptor gamma coactivator-1 (PGC-1) family. This includes PGC-1α, PGC-1β, and peroxisome proliferator-activated receptor gamma (PPARγ). PGC-1α plays a vital role in regulating cardiac metabolism. Activation of PGC-1 family transcription factors under conditions of cellular energy requirements, such as cell growth, hypoxia, glucose deprivation, or exercise, enhances mitochondrial remodeling or biosynthesis and restores intracellular energy balance (13). PGC-1 knockdown in mice induces cardiomyopathy *via* fragmentation and elongation of cardiac mitochondria, which is related to changes in mitofusin 1 (MFN1), optic atrophy 1 (OPA1), and dynamin-related protein 1 (DRP1) expression (14).

Multiple transcription factors are found downstream of PGC-1α, and peroxisome proliferator–activated receptors (PPARs), nuclear respiratory factor 1 (NRF1), and mitochondrial transcription factor A (TFAM) are all involved in mitochondrial biogenesis (15). PPARα is a member of the nuclear receptor superfamily of PPARs. PPARs participate in decomposition and metabolism of fatty acids and play a key role in maintaining myocardial energy metabolism (16). Specific knockout of PPARα results in cardiac hypertrophy and fat accumulation in rats, and ultimately heart failure leads to animal death (17, 18). In addition, PPARα can ameliorate cardiac hypertrophy caused by hypertension. The PPARα/NRF2 signaling pathway protects the heart from remodeling induced by stress overload, and up-regulation of PPARα protein expression can improve cardiac hypertrophy (19). NRF1/2 is a key component in regulating nuclear coding of mitochondrial proteins and is closely involved in mitochondrial biogenesis. In models of cardiac hypertrophy and heart failure, gene expression and protein levels of NRF1 and TFAM and protein levels of NRF2 are decreased in the cardiac tissue (20).

AEROBIC EXERCISE IMPROVES CVDs BY REGULATING MITOCHONDRIAL BIOGENESIS

Mitochondrial biogenesis is inhibited in CVDs (21). The number and ATP production of myocardial mitochondria and mitochondrial synthesis regulatory factors increased in rats after an 8-week treadmill test, indicating that aerobic exercise could improve myocardial energy supply and cardiac function by promoting biosynthesis of myocardial mitochondria (22). Treadmill exercise helps improve CVDs; thus, aerobic exercise may exert direct benefit on mitochondrial biogenesis.

In line with this, aerobic exercise can activate the silencing regulatory protein 3 (SIRT3)/PGC-1α/phosphatidylinositol 3 kinase (PI3K)/Akt signaling pathway, resulting in improved mitochondrial biogenesis (23). Such physical activity can also activate the AMPK/PGC-1α pathway in myocardial tissue. PGC-1α can upregulate expression of mitofusin2 (MFN2) protein, which promotes mitochondrial biogenesis and mitochondrial fusion (13). Further, aerobic exercise enhances protein levels of PGC-1α and NRF2, which increases the mRNA levels of *TFAM* and *NRF1* and increases mitochondrial DNA replication. NRF2 promotes expression of various antioxidant enzymes, thus reducing the oxidative stress level of myocardial tissue (24). Thus, aerobic exercise can promote expression of PGC-1α, NRF1, and NRF2, and expression of regulatory factors and induction of mitochondrial biogenesis improve CVDs.

MYOCARDIAL MITOCHONDRIAL FUSION/FISSION AND CVDs

Mitochondria constantly undergo fission and fusion. After mitochondrial fission, offspring mitochondria with higher membrane potential enter the next round of fusion to maintain mitochondrial number and function. These processes are regulated by mitochondrial fusion and fission proteins, and are particularly important for maintaining normal mitochondrial function (25). Mitochondrial fusion proteins include MFN1, MFN2, and OPA1. MFN1 and MFN2 mediate fusion of the outer mitochondrial membrane (OMM), while OPA1 mediates fusion of the inner mitochondrial membrane. DRP1 serves as a critical effector of mitochondrial fission (26).

In CVDs, mitochondrial morphology and fusion-related proteins exhibit alterations. For example, severe mitochondrial fragmentation occurs in myocardial ischemia–reperfusion injury (I/R) models, which significantly inhibits OPA1 expression

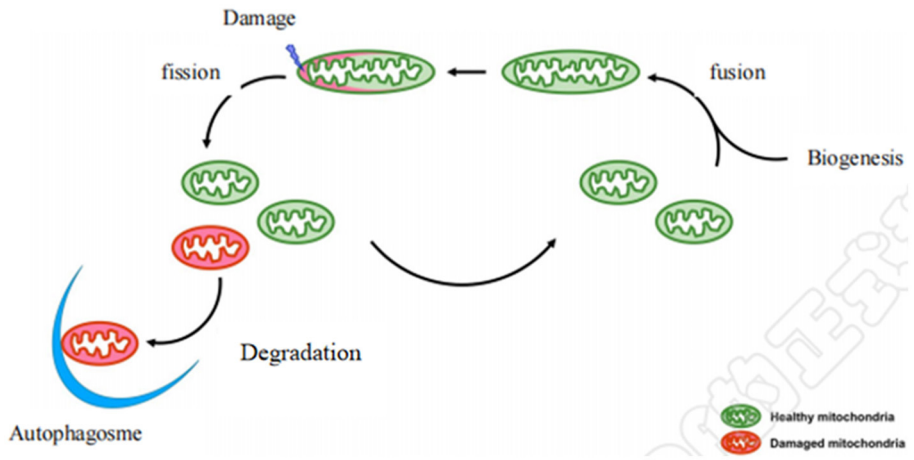

FIGURE 1 | Diagram of mitochondrial dynamics. Mitochondrial biogenesis is the process by which new mitochondria are formed in the cell after mitochondrial fusion. Mitochondrial biogenesis is activated by numerous different signals which can lead to mitochondrial fission and damaged mitochondria are degraded by autophagy.

(27). Further, there is an abnormal increase in myocardial mitochondria, downregulation of mitochondrial biogenesis-related genes, and aggravation of cardiomyopathy after specific deletion of *Mfn1* and *Mfn2* in the mouse myocardium (28). Mitochondrial fission was caused by translocation of phosphorylated DRP1 from the cytoplasm to the mitochondria (26). The use of DRP1 inhibitor reduced DRP1 translocation to the mitochondria, improved the structure and function of the mitochondria, and alleviated myocardial hypertrophy and myocardial fibrosis (29, 30). Besides the positive changes in mitochondrial dynamics in cardiovascular diseases, inhibiting mitochondrial fission may also lead to heart impairment (31, 32). Therefore, both mitochondrial fusion and fission are essential for CVD development. A balanced state of mitochondrial fission and fusion are conducive to disease prevention and improved prognosis.

AEROBIC EXERCISE IMPROVES CVDs BY REGULATING MITOCHONDRIAL FUSION AND FISSION

In CVDs, mitochondria exhibit a high rate of fission and a low rate of fusion, resulting in imbalanced mitochondrial dynamics (12). Notably, aerobic exercise can increase expression of PGC-1α mRNA and protein to improve the level of MFN2 protein and promote mitochondrial fusion (33). Swimming training can downregulate the mir-30B-p53-DRP1 pathway, reduce the contents of p53 and DRP1 proteins in the mouse myocardium, and inhibit myocardial mitochondrial fission (34). The swimming training lasted 8 weeks, 5 days/week. At the beginning, the swimming duration is 30 min. The swimming time was increased by 10 min ever week. Therefore, swimming duration maintained at 90 min after 7–8 weeks. Then, the mice trained twice a day with an interval of 6 h. Aerobic exercise training can induce increased mitochondrial fusion (upregulating the expression of MFN2 and OPA1 proteins) and decreased mitochondrial fission (downregulating the expression of DRP1 protein), and promote mitochondrial kinetic remodeling, effectively alleviating mitochondrial dysfunction in rats with myocardial infarction (MI) (35). After moderate aerobic exercise training, the mRNA levels of *Ppargc1α*, *Opa1*, *Mfn2*, and *Drp1* significantly increased and the diastolic parameters improved in spontaneously hypertensive rats (SHRs) (22). These results suggest that aerobic exercise maintains the balance of mitochondrial fusion and fission in the SHR myocardium and improves mitochondrial function. A comparison of the myocardial mitochondria of animals with heart failure who exercised vs. did not exercise revealed that the number of myocardial mitochondria in the exercise group was decreased and mitochondrial size was increased. Further experiments showed that exercise increased MFN1, MFN2, and DNM1L GTPase activity in the myocardium and reversed the translocation of DNM1L to the mitochondria (8). Therefore, aerobic exercise may have protective effects on the balance of mitochondrial fusion and fission in CVDs.

MYOCARDIAL MITOCHONDRIAL AUTOPHAGY AND CVDs

Mitochondrial autophagy is a selective form of autophagy, which is specialized to remove aging or irreversibly damaged mitochondria and plays a decisive role in control of mitochondrial quality (36). Mitochondrial autophagy and fission can coordinate with each other, and mitochondrial autophagy can remove damaged mitochondrial parts formed by mitochondrial fission and keep mitochondria healthy (37). DRP1 migration and mitochondrial autophagy activation occur almost simultaneously after transverse aortic constriction (TAC) treatment, indicating that

mitochondrial autophagy is closely related to mitochondrial fission (38).

Mitochondrial autophagy may occur through Parkin-dependent or Parkin-independent mechanisms (12). In Parkin-mediated mitotic phagocytosis, PTEN-induced putative kinase 1 (PINK1) recruits Parkin to the outer membrane of mitochondria. Once recruited to the mitochondria, Parkin ubiquitinates several mitochondrial outer membrane proteins, including the mitochondrial fusion proteins MFN1 and MFN2, Miro, Translocase of OMM 20, and voltage-dependent anion channel. Then, the selective autophagy adapter protein P62/Sequestosome 1 is recruited to the mitochondria to interact with LC3 and initiate mitochondrial autophagy (36, 37, 39). Meanwhile, ubiquitination and proteasome degradation of MFN1 and MFN2 results in mitochondrial fission and fragmentation, which further induces mitochondrial autophagy (40). PINK1 and Parkin protein levels are significantly reduced in heart failure models (41). PINK1 knockout mice have a significantly increased number of atherosclerotic lesions (42). Also, Parkin knockout mice show excessive myocardial hypertrophy, myocardial fibrosis, and left ventricular systolic dysfunction in response to TAC (43).

Parkin-independent mitochondrial autophagy occurs independently of Parkin; some autophagy receptor proteins are located in mitochondria and interact with LC3 to recruit autophagosomes to damaged mitochondria. These autophagy receptor proteins include BCL-2/adenovirus E1B19-kDa interacting protein 3 (BNIP3), NIX (also called BNIP3L), and Fun14 Domain–containing 1 (FUNDC1) (36, 44, 45). Lowering of BNIP3 protein levels impairs mitochondrial function, which in turn leads to impaired myocardial cell function (46); also, *FUNDC1* gene knockout exacerbates I/R injury (47).

Mitochondrial autophagy has a significant protective effect on the heart, and autophagy activation is observed in the boundary region of the subacute stage of MI (1 week after MI) (48). Enhancement of autophagy with rapamycin 2 weeks after coronary artery ligation ameliorates cardiac dysfunction and maladaptive remodeling, whereas inhibition of autophagy by buffamycin A1 worsens cardiac dysfunction (49). In conclusion, insufficient mitochondrial autophagy is closely related to CVD development.

AEROBIC EXERCISE IMPROVES CVDs BY REGULATING MITOCHONDRIAL AUTOPHAGY

CVD pathology is associated with weakening of mitochondrial autophagy. Yet, 8 weeks of aerobic exercise on a treadmill can increase the LC3II/LC3I ratio, and thus upregulate Beclin1, LC3, and BNIP3 in the rat myocardium to promote myocardial autophagy (50). For treadmill excise study, rats were trained on a treadmill with an exercise intensity and schedule set at 70% of maximum aerobic capacity. The training group run for 60 min/day, 5 days per week at 10 m/min speed for 8 weeks. After the treadmill excise training, PINK1, Parkin, ubiquitin, P62, and LC3 levels were significantly increased in the rat skeletal muscle (51). Consistent with this finding, exercise improves the oxidative capacity of myocardial mitochondria in animals with heart failure, and this improvement in oxidative capacity is related to reconstruction of autophagy flux. Exercise stimulates mitochondrial autophagy flux by increasing Parkin recruitment in myocardial mitochondria (8). Notably, aerobic exercise training enhances the PINK1/Parkin signaling pathway, thus inducing mitochondrial autophagy (52). This physical activity also upregulates SIRT3 expression, enhances the antioxidant capacity of the body, improves the quality of mitochondria, and helps alleviate cardiac dysfunction in mice after MI (53). These studies suggested that aerobic exercise induces mitochondrial autophagy and improves

TABLE 1 | Comparison of different exercise training programs.

	Treadmill				Swimming
Time	60 min/day	10 or 60 min/day	20–60 min/day	60 min/day	20–60 min/day
Frequency	5 days/week	6 days/week	Every day	Every day	5 days/week
Period	8 weeks	8 weeks	11 weeks	4 weeks	8 weeks
Protocol	Ran on a treadmill at 60–70% VO_2max intensity for 60 minutes.	In the first 4 weeks, 10 m/min, 0% slope, 10 min/day. Then 20 m/min, 5% slope, 60 min/day for 4 weeks.	The speed and incline of the treadmill gradually increased. Starting with low workloads (25 min, 35% Vmax and 0% gradient), to the end of high workloads (60 min, 70%Vmax and 25% gradient).	The rats initially ran 30 min daily at a speed of 10 m/min and gradually increased by 10 min in duration and 2 m/min in speed each day until reaching 60 min per day at a speed of 16 m/min.	Training time was increased by 10 min per week.
Influence on mitochondrial dynamics	Promoted fusion and inhibited fission (expression of MFN2, PGC-1α and OPA1 increased, expression of DRP1 decreased).	Promoted biogenesis (expression of PGC-1α and NRF2 increased).	Promoted autophagy (expression of LC3II and P62 increased).	Promoted biogenesis (SIRT1/PGC-1α signaling pathway was activated).	Promoted fusion and inhibited fission (expression of MFN1, MFN2, and OPA1 increased, expression of DRP1 decreased).

CVDs by increasing the expression of autophagy-related and mitochondrial autophagy–related proteins.

CONCLUSIONS AND PERSPECTIVES

Abundant evidence illustrates the key role of mitochondrial dynamics in cardiac homeostasis. Imbalanced mitochondrial fusion and fission, insufficient mitochondrial autophagy, and weakened mitochondrial biogenesis are the pathological factors leading to CVD occurrence and development. Regular aerobic exercise is a simple and effective way to balance mitochondrial dynamics and improve mitochondrial function, which can build human health. MFN2 and OPA1, which are beneficial to mitochondrial fusion and biogenesis, can be elevated by aerobic exercise. DRP1-induced mitochondrial fission can be inhibited by aerobic exercise in cardiovascular diseases. PINK1/parkin signaling is still the main targeting pathway that induces mitochondrial autophagy following aerobic exercise in cardiovascular diseases. However, one study indicated that acute exercise had no effect on the proteins involved in mitochondrial dynamics. Indeed, after exercise training, the proteins involved in mitochondrial dynamics changed significantly in normotensive control rats, but remained unchanged in spontaneously hypertensive rats (22). This finding aligned with another study finding that myocardial mitochondrial dynamics-related proteins did not change after acute exercise in rats (54).

Aerobic exercise can prevent or alleviate CVD development by regulating proteins involved in mitochondrial dynamics. Exercise can reduce mitochondrial fission, enhance mitochondrial fusion and improve mitochondrial autophagy or biogenesis. Regarding to the type of exercise, we compared some excise programs of treadmill training with swimming, and also summarized the influence of different exercise programs on mitochondrial dynamics (**Table 1**). Treadmill training seems to have a greater effect on modulation of the cardiac proteome than swimming (55). While we can control the intensity and duration of treadmill training to calculate the amount of exercise, swimming training is more difficult to control. Some animals do not exhibit continuous swimming behavior, but rather tend to dive or swing, which results in intermittent hypoxia and may affect interpretation of the results.

Mitochondrial dynamics, including mitochondrial biogenesis, mitochondrial fusion or fission, and mitochondrial autophagy, can be used as disease prevention and treatment targets under exercise intervention. Moreover, the balance between mitochondrial dynamics may be a key factor in disease occurrence or development. However, the mechanism of aerobic exercise intervention in mitochondrial dynamics is complex and needs further long-term research due to its gradual effects and individual differences. Improper exercise can also lead to arthritis, decreased immunity, etc. Therefore, verified and reasonable individualized exercise prescription has important guiding significance for health. It is important to carry out long-term and proper exercise intervention.

The concept of aerobic exercise for disease prevention is increasingly popular, while the number of subhealthy people and older adults is increasing every year. Reasonable exercise prescription intervention for these populations or people with a tendency for organ disease development can significantly reduce disease occurrence. Further studies are needed to explore this idea.

AUTHOR CONTRIBUTIONS

Y-lW: conceptualization and methodology. CG: data curation and writing—original draft preparation. JY: writing—reviewing and editing. LZ: visualization and investigation. GW: software. All authors contributed to the article and approved the submitted version.

REFERENCES

1. Roth GA, Mensah GA, Johnson CO, Addolorato G, Ammirati E, Baddour LM, et al. Global burden of cardiovascular diseases and risk factors, 1990-2019: update from the GBD 2019 Study. *J Am Coll Cardiol.* (2020) 76:2982–3021. doi: 10.1016/j.jacc.2020.11.010
2. Sedding DG, Boyle EC, Demandt J, Sluimer JC, Dutzmann J, Haverich A, et al. Vasa vasorum angiogenesis: key player in the initiation and progression of atherosclerosis and potential target for the treatment of cardiovascular disease. *Front Immunol.* (2018) 9:706. doi: 10.3389/fimmu.2018.00706
3. Whelton PK, Carey RM, Aronow WS, Casey DE, Jr, Collins KJ, Dennison Himmelfarb C, et al. 2017 ACC/AHA/AAPA/ABC/ACPM/AGS/APhA/ASH/ASPC/NMA/PCNA guideline for the prevention, detection, evaluation, and management of high blood pressure in adults: executive summary: a report of the American College of Cardiology/American Heart Association Task Force on Clinical Practice Guidelines. *Hypertension (Dallas, Tex.: 1979).* (2018) 71:1269–324. doi: 10.1161/HYP.0000000000000075
4. Sorrentino V, Menzies KJ, Auwerx J. Repairing mitochondrial dysfunction in disease. *Annu Rev Pharmacol Toxicol.* (2018) 58:353–89. doi: 10.1146/annurev-pharmtox-010716-104908
5. Dorn GW, III. Evolving concepts of mitochondrial dynamics. *Ann Rev Physiol.* (2019) 81:1–17. doi: 10.1146/annurev-physiol-020518-114358
6. Tahrir FG, Langford D, Amini S, Mohseni Ahooyi T, Khalili K. Mitochondrial quality control in cardiac cells: mechanisms and role in cardiac cell injury and disease. *J Cell Physiol.* (2019) 234:8122–33. doi: 10.1002/jcp.27597
7. Crisafulli A, Pagliaro P, Roberto S, Cugusi L, Mercuro G, Lazou A, et al. Diabetic Cardiomyopathy and ischemic heart disease: prevention and therapy by exercise and conditioning. *Int J Mol Sci.* (2020) 21:2896. doi: 10.3390/ijms21082896
8. Campos JC, Queliconi BB, Bozi L, Bechara L, Dourado P, Andres AM, et al. Exercise reestablishes autophagic flux and mitochondrial quality control in heart failure. *Autophagy.* (2017) 13:1304–17. doi: 10.1080/15548627.2017.1325062
9. Kiriyama Y, Nochi H. Intra- and intercellular quality control mechanisms of mitochondria. *Cells.* (2017) 7:1. doi: 10.3390/cells7010001
10. Xie LL, Shi F, Tan Z, Li Y, Bode AM, Cao Y. Mitochondrial network structure homeostasis and cell death. *Cancer Sci.* (2018) 109:3686–94. doi: 10.1111/cas.13830
11. Pickles S, Vigié P, Youle RJ. Mitophagy and quality control mechanisms in mitochondrial maintenance. *Curr Biol.* (2018) 28:R170–85. doi: 10.1016/j.cub.2018.01.004

12. Forte M, Schirone L, Ameri P, Basso C, Catalucci D, Modica J, et al. The role of mitochondrial dynamics in cardiovascular diseases. *Br J Pharmacol.* (2021) 178:2060–76. doi: 10.1111/bph.15068
13. Martin OJ, Lai L, Soundarapandian MM, Leone TC, Zorzano A, Keller MP, et al. A role for peroxisome proliferator-activated receptor γ coactivator-1 in the control of mitochondrial dynamics during postnatal cardiac growth. *Circ Res.* (2014) 114:626–36. doi: 10.1161/CIRCRESAHA.114.302562
14. Kulikova TG, Stepanova OV, Voronova AD, Valikhov MP, Sirotkin VN, Zhirov IV, et al. Pathological remodeling of the myocardium in chronic heart failure: role of PGC-1α. *Bull Exp Biol Med.* (2018) 164:794–7. doi: 10.1007/s10517-018-4082-1
15. Jiang Q, Ji A, Li D, Shi L, Gao M, Lv N, et al. Mitochondria damage in ambient particulate matter induced cardiotoxicity: roles of PPAR alpha/PGC-1 alpha signaling. *Environ Poll (Barking, Essex: 1987).* (2021) 288:117792. doi: 10.1016/j.envpol.2021.117792
16. Yin Z, Zhao Y, He M, Li H, Fan J, Nie X, et al. MiR-30c/PGC-1β protects against diabetic cardiomyopathy *via* PPARα. *Cardiovasc Diabetol.* (2019) 18:7. doi: 10.1186/s12933-019-0811-7
17. Zhu ZY, Gao T, Huang Y, Xue J, Xie ML. Apigenin ameliorates hypertension-induced cardiac hypertrophy and down-regulates cardiac hypoxia inducible factor-lα in rats. *Food Funct.* (2016) 7:1992–8. doi: 10.1039/C5FO01464F
18. Warren JS, Tracy CM, Miller MR, Makaju A, Szulik MW, Oka SI, et al. Histone methyltransferase Smyd1 regulates mitochondrial energetics in the heart. *Proc Natl Acad Sci USA.* (2018) 115:E7871–80. doi: 10.1073/pnas.1800680115
19. Wu QQ, Deng W, Xiao Y, Chen JJ, Liu C, Wang J, et al. The 5-lipoxygenase inhibitor zileuton protects pressure overload-induced cardiac remodeling *via* activating PPARα. *Oxid Med Cell Longev.* (2019) 2019:7536803. doi: 10.1155/2019/7536803
20. Nomura S, Satoh M, Fujita T, Higo T, Sumida T, Ko T, et al. Cardiomyocyte gene programs encoding morphological and functional signatures in cardiac hypertrophy and failure. *Nat Commun.* (2018) 9:4435. doi: 10.1038/s41467-018-06639-7
21. Tan Y, Lei C, Tang H, Zhu X, Yi G. The hippo pathway orchestrates mitochondrial quality control: a novel focus on cardiovascular diseases. *DNA Cell Biol.* (2020) 39:1494–505. doi: 10.1089/dna.2019.5348
22. Quiroga C, Mancilla G, Oyarzun I, Tapia A, Caballero M, Gabrielli LA, et al. Moderate exercise in spontaneously hypertensive rats is unable to activate the expression of genes linked to mitochondrial dynamics and biogenesis in cardiomyocytes. *Front Endocrinol.* (2020) 11:546. doi: 10.3389/fendo.2020.00546
23. Jia D, Hou L, Lv Y, Xi L, Tian Z. Postinfarction exercise training alleviates cardiac dysfunction and adverse remodeling *via* mitochondrial biogenesis and SIRT1/PGC-1α/PI3K/Akt signaling. *J Cell Physiol.* (2019) 234:23705–18. doi: 10.1002/jcp.28939
24. Sun M, Huang C, Wang C, Zheng J, Zhang P, Xu Y, et al. Ginsenoside Rg3 improves cardiac mitochondrial population quality: mimetic exercise training. *Biochem Biophys Res Commun.* (2013) 441:169–74. doi: 10.1016/j.bbrc.2013.10.039
25. Sabouny R, Shutt TE. Reciprocal regulation of mitochondrial fission and fusion. *Trends Biochem Sci.* (2020) 45:564–77. doi: 10.1016/j.tibs.2020.03.009
26. Jin JY, Wei XX, Zhi XL, Wang XH, Meng D. Drp1-dependent mitochondrial fission in cardiovascular disease. *Acta Pharmacol Sin.* (2021) 42:655–64. doi: 10.1038/s41401-020-00518-y
27. Zhang Y, Wang Y, Xu J, Tian F, Hu S, Chen Y, et al. Melatonin attenuates myocardial ischemia-reperfusion injury *via* improving mitochondrial fusion/mitophagy and activating the AMPK-OPA1 signaling pathways. *J Pineal Res.* (2019) 66:e12542. doi: 10.1111/jpi.12542
28. Papanicolaou KN, Kikuchi R, Ngoh GA, Coughlan KA, Dominguez I, Stanley WC, et al. Mitofusins 1 and 2 are essential for postnatal metabolic remodeling in heart. *Circ Res.* (2012) 111:1012–26. doi: 10.1161/CIRCRESAHA.112.274142
29. Tian L, Neuber-Hess M, Mewburn J, Dasgupta A, Dunham-Snary K, Wu D, et al. Ischemia-induced Drp1 and Fis1-mediated mitochondrial fission and right ventricular dysfunction in pulmonary hypertension. *J Mol Med (Berlin, Germany).* (2017) 95:381–93. doi: 10.1007/s00109-017-1522-8
30. Hasan P, Saotome M, Ikoma T, Iguchi K, Kawasaki H, Iwashita T, et al. Mitochondrial fission protein, dynamin-related protein 1, contributes to the promotion of hypertensive cardiac hypertrophy and fibrosis in Dahl-salt sensitive rats. *J Mol Cell Cardiol.* (2018) 121:103–6. doi: 10.1016/j.yjmcc.2018.07.004
31. Ikeda Y, Shirakabe A, Maejima Y, Zhai P, Sciarretta S, Toli J, et al. Endogenous Drp1 mediates mitochondrial autophagy and protects the heart against energy stress. *Circ Res.* (2015) 116:264–78. doi: 10.1161/CIRCRESAHA.116.303356
32. Coronado M, Fajardo G, Nguyen K, Zhao M, Kooiker K, Jung G, et al. Physiological mitochondrial fragmentation is a normal cardiac adaptation to increased energy demand. *Circ Res.* (2018) 122:282–95. doi: 10.1161/CIRCRESAHA.117.310725
33. Moore TM, Zhou Z, Cohn W, Norheim F, Lin AJ, Kalajian N, et al. The impact of exercise on mitochondrial dynamics and the role of Drp1 in exercise performance and training adaptations in skeletal muscle. *Mol Metab.* (2019) 21:51–67. doi: 10.1016/j.molmet.2018.11.012
34. Zhao Y, Ma Z. Swimming training affects apoptosis-related microRNAs and reduces cardiac apoptosis in mice. *Gen Physiol Biophys.* (2016) 35:443–50. doi: 10.4149/gpb_2016012
35. Jiang HK, Wang YH, Sun L, He X, Zhao M, Feng ZH, et al. Aerobic interval training attenuates mitochondrial dysfunction in rats post-myocardial infarction: roles of mitochondrial network dynamics. *Int J Mol Sci.* (2014) 15:5304–22. doi: 10.3390/ijms15045304
36. Ni HM, Williams JA, Ding WX. Mitochondrial dynamics and mitochondrial quality control. *Redox Biol.* (2015) 4:6–13. doi: 10.1016/j.redox.2014.11.006
37. Sciarretta S, Maejima Y, Zablocki D, Sadoshima J. The role of autophagy in the heart. *Annu Rev Physiol.* (2018) 80:1–26. doi: 10.1146/annurev-physiol-021317-121427
38. Shirakabe A, Zhai P, Ikeda Y, Saito T, Maejima Y, Hsu CP, et al. Response by shirakabe et al. to letter regarding article, "Drp1-dependent mitochondrial autophagy plays a protective role against pressure overload-induced mitochondrial dysfunction and heart failure". *Circulation.* (2016) 134:e75–6. doi: 10.1161/CIRCULATIONAHA.116.023667
39. Dikic I, Bremm A. DUBs counteract parkin for efficient mitophagy. *EMBO J.* (2014) 33:2442–3. doi: 10.15252/embj.201490101
40. Basso V, Marchesan E, Peggion C, Chakraborty J, von Stockum S, Giacomello M, et al. Regulation of ER-mitochondria contacts by Parkin *via* Mfn2. *Pharmacol Res.* (2018) 138:43–56. doi: 10.1016/j.phrs.2018.09.006
41. Wang B, Xu M, Li W, Li X, Zheng Q, Niu X. Aerobic exercise protects against pressure overload-induced cardiac dysfunction and hypertrophy *via* β3-AR-nNOS-NO activation. *PLoS ONE.* (2017) 12:e0179648. doi: 10.1371/journal.pone.0179648
42. He L, Zhou Q, Huang Z, Xu J, Zhou H, Lv D, et al. PINK1/Parkin-mediated mitophagy promotes apelin-13-induced vascular smooth muscle cell proliferation by AMPKα and exacerbates atherosclerotic lesions. *J Cell Physiol.* (2019) 234:8668–82. doi: 10.1002/jcp.27527
43. Han K, Hassanzadeh S, Singh K, Menazza S, Nguyen TT, Stevens MV, et al. Parkin regulation of CHOP modulates susceptibility to cardiac endoplasmic reticulum stress. *Sci Rep.* (2017) 7:2093. doi: 10.1038/s41598-017-02339-2
44. Fu R, Deng Q, Zhang H, Hu X, Li Y, Liu Y, et al. A novel autophagy inhibitor berbamine blocks SNARE-mediated autophagosome-lysosome fusion through upregulation of BNIP3. *Cell Death Dis.* (2018) 9:243. doi: 10.1038/s41419-018-0276-8
45. Lampert MA, Orogo AM, Najor RH, Hammerling BC, Leon LJ, Wang BJ, et al. BNIP3L/NIX and FUNDC1-mediated mitophagy is required for mitochondrial network remodeling during cardiac progenitor cell differentiation. *Autophagy.* (2019) 15:1182–98. doi: 10.1080/15548627.2019.1580095
46. Li E, Li X, Huang J, Xu C, Liang Q, Ren K, et al. BMAL1 regulates mitochondrial fission and mitophagy through mitochondrial protein BNIP3 and is critical in the development of dilated cardiomyopathy. *Protein Cell.* (2020) 11:661–79. doi: 10.1007/s13238-020-00713-x
47. Zhang W, Siraj S, Zhang R, Chen Q. Mitophagy receptor FUNDC1 regulates mitochondrial homeostasis and protects the heart from I/R injury. *Autophagy.* (2017) 13:1080–1. doi: 10.1080/15548627.2017.1300224
48. Yu W, Sun S, Xu H, Li C, Ren J, Zhang Y. TBC1D15/RAB7-regulated mitochondria-lysosome interaction confers cardioprotection against acute myocardial infarction-induced cardiac injury. *Theranostics.* (2020) 10:11244–63. doi: 10.7150/thno.46883
49. Wang Z, Zhang H, Liu Z, Ma Z, An D, Xu D. Apigenin attenuates myocardial infarction-induced cardiomyocyte injury by modulating

Parkin-mediated mitochondrial autophagy. *J Biosci.* (2020) 45:75. doi: 10.1007/s12038-020-00047-0
50. Li H, Miao W, Ma J, Xv Z, Bo H, Li J, et al. Acute exercise-induced mitochondrial stress triggers an inflammatory response in the myocardium *via* NLRP3 inflammasome activation with mitophagy. *Oxid Med Cell Longev.* (2016) 2016:1987149. doi: 10.1155/2016/1987149
51. Shang H, Xia Z, Bai S, Zhang HE, Gu B, Wang R. Downhill running acutely elicits mitophagy in rat soleus muscle. *Med Sci Sports Exerc.* (2019) 51:1396–403. doi: 10.1249/MSS.0000000000001906
52. Fiuza-Luces C, Delmiro A, Soares-Miranda L, González-Murillo Á, Martínez-Palacios J, Ramírez M, et al. Exercise training can induce cardiac autophagy at end-stage chronic conditions: insights from a graft-versus-host-disease mouse model. *Brain Behav Immun.* (2014) 39:56–60. doi: 10.1016/j.bbi.2013.11.007
53. Zhao D, Sun Y, Tan Y, Zhang Z, Hou Z, Gao C, et al. Short-duration swimming exercise after myocardial infarction attenuates cardiac dysfunction and regulates mitochondrial quality control in aged mice. *Oxid Med Cell Longev.* (2018) 2018:4079041. doi: 10.1155/2018/4079041
54. Yoo SZ, No MH, Heo JW, Park DH, Kang JH, Kim JH, et al. Effects of acute exercise on mitochondrial function, dynamics, and mitophagy in rat cardiac and skeletal muscles. *Int Neurourol J.* (2019) 23(Suppl. 1):S22–31. doi: 10.5213/inj.1938038.019
55. Ferreira R, Moreira-Gonçalves D, Azevedo AL, Duarte JA, Amado F, Vitorino R. Unraveling the exercise-related proteome signature in heart. *Basic Res Cardiol.* (2015) 110:454. doi: 10.1007/s00395-014-0454-5

Conflict of Interest: The authors declare that the research was conducted in the absence of any commercial or financial relationships that could be construed as a potential conflict of interest.

Publisher's Note: All claims expressed in this article are solely those of the authors and do not necessarily represent those of their affiliated organizations, or those of the publisher, the editors and the reviewers. Any product that may be evaluated in this article, or claim that may be made by its manufacturer, is not guaranteed or endorsed by the publisher.

Copyright © 2022 Gu, Yan, Zhao, Wu and Wang. This is an open-access article distributed under the terms of the Creative Commons Attribution License (CC BY). The use, distribution or reproduction in other forums is permitted, provided the original author(s) and the copyright owner(s) are credited and that the original publication in this journal is cited, in accordance with accepted academic practice. No use, distribution or reproduction is permitted which does not comply with these terms.

frontiers in Cardiovascular Medicine

REVIEW
published: 18 January 2022
doi: 10.3389/fcvm.2021.822969

Mitochondria in Pathological Cardiac Hypertrophy Research and Therapy

Dan Yang[1,2†], Han-Qing Liu[3†], Fang-Yuan Liu[1,2], Zhen Guo[1,2], Peng An[1,2], Ming-Yu Wang[1,2], Zheng Yang[1,2], Di Fan[1,2] and Qi-Zhu Tang[1,2*]*

[1] Department of Cardiology, Renmin Hospital of Wuhan University, Wuhan, China, [2] Hubei Key Laboratory of Metabolic and Chronic Diseases, Wuhan, China, [3] Department of Thyroid and Breast, Renmin Hospital of Wuhan University, Wuhan, China

Cardiac hypertrophy, a stereotypic cardiac response to increased workload, ultimately progresses to severe contractile dysfunction and uncompensated heart failure without appropriate intervention. Sustained cardiac overload inevitably results in high energy consumption, thus breaking the balance between mitochondrial energy supply and cardiac energy demand. In recent years, accumulating evidence has indicated that mitochondrial dysfunction is implicated in pathological cardiac hypertrophy. The significant alterations in mitochondrial energetics and mitochondrial proteome composition, as well as the altered expression of transcripts that have an impact on mitochondrial structure and function, may contribute to the initiation and progression of cardiac hypertrophy. This article presents a summary review of the morphological and functional changes of mitochondria during the hypertrophic response, followed by an overview of the latest research progress on the significant modulatory roles of mitochondria in cardiac hypertrophy. Our article is also to summarize the strategies of mitochondria-targeting as therapeutic targets to treat cardiac hypertrophy.

Keywords: mitochondria, cardiac hypertrophy, regulatory mechanisms, therapeutic strategies, mitophagy

OPEN ACCESS

Edited by:
Shijun Wang,
Fudan University, China

Reviewed by:
Lu Gao,
The First Affiliated Hospital of Zhengzhou University, China
Jiawei Liao,
Dalian Medical University, China

****Correspondence:***
Di Fan
drfanti@yeah.net
Qi-Zhu Tang
qztang@whu.edu.cn

† These authors have contributed equally to this work

Specialty section:
This article was submitted to Cardiovascular Metabolism, a section of the journal Frontiers in Cardiovascular Medicine

Received: *26 November 2021*
Accepted: *23 December 2021*
Published: *18 January 2022*

Citation:
Yang D, Liu H-Q, Liu F-Y, Guo Z, An P, Wang M-Y, Yang Z, Fan D and Tang Q-Z (2022) Mitochondria in Pathological Cardiac Hypertrophy Research and Therapy. Front. Cardiovasc. Med. 8:822969. doi: 10.3389/fcvm.2021.822969

INTRODUCTION

Cardiomyocytes (CMs) are one of the most important cell types which become terminally differentiated once after birth. Therefore, in adult hearts, CMs have no capability of proliferating in response to prolonged pressure/volume overload; instead, they exhibit morphological enlargement to continuously pump blood to provide oxygen and nutrients to the body, thus leading to the increased heart wall thickness and heart mass, and eventually cardiac hypertrophy (1). Cardiac hypertrophy can be generally divided into physiological and pathological hypertrophy. Physiological hypertrophy, which usually occurs during pregnancy and exercise, is characterize with a coordinated increase in ventricular volume and wall thickness, most importantly, it is reversible once the stimulus was relieved (2). In contrast, pathological hypertrophy, a decompensated stage with complex network of cellular and molecular regulation, usually observed in patients with long-term cardiovascular disorders, is accompanied by cardiac systolic/diastolic dysfunction and the enlargement of CMs is often irreversible (3, 4). Pressure/volume overload, Angiotensin II (Ang II), oxidants, activation of α/β adrenergic receptors, hypoxia, aging, and high-glucose are efficient inducers of pathological cardiac hypertrophy (5). It is well established that pathological cardiac hypertrophy has become an independent risk factor for the development of heart failure (HF), a major and growing public health problem globally with increasing morbidity, high mortality, and heavy economic burdens (6).

Over the past few decades,extensive studies have established that previously unrecognized mechanisms, including epigenetic modifications, immunomodulation, impaired protein quality control, aberrant Ca2+ handling, metabolic reprogramming, and cell-to-cell interactions, are involved in the initiation and progression of cardiac hypertrophy (5). With the continuous deepening of research and updating of knowledge, energy metabolism has shown an increasingly compelling role in cardiac hypertrophy. It is widely accepted that mitochondria serve as the power-house of cells and mitochondrial dysfunction often highly correlates with cell pathology, especially in cells requiring high-energy supply such as CMs. Morphometry analysis has demonstrated that the contents of mitochondria occupy 22.0-37.0% of the CMs' mass in various species, and most importantly, the volume densities of mitochondria are closely related to heart rate and cardiac oxygen consumption rate (7). It is also estimated that 60–90% of the energy adult hearts required is originated from the oxidation of fatty acid in mitochondria (8). Therefore, mitochondria serve as the central organelle responsible for coordinating the energy transduction and maintaining the contractile performance of CMs. The critical roles of mitochondria in cardiac ischemia-reperfusion injury, acute myocardial infarction, atherosclerosis, and cardiac aging have recently been reviewed detailedly (9–12). During hypertrophy, mitochondria exhibit extensive alterations in morphology, biogenesis, dynamics and bioenergetics, and mitochondria also participate in the modulation of hypertrophic response and contribute to the transition to decompensated heart failure (13). Mitochondrial abnormalities and myocardial hypertrophy are intimately linked and deserve attention.

In this review, we will summarize the morphological and functional changes of mitochondrial that occur in the hypertrophic hearts, followed by an overview of the critical modulatory roles of mitochondria in response to hypertrophic stimuli, and finally, we will present and discuss the potential therapeutic strategies to prevent or reverse cardiac hypertrophy.

MITOCHONDRIAL ALTERATIONS THROUGH THE TRANSITION FROM CARDIAC HYPERTROPHY TO FAILURE

In hearts of Ang II-induced left ventricular hypertrophy mice, reactive oxygen species (ROS) production, mitochondrial protein carbonyls, mitochondrial DNA damage, signaling related to mitochondrial biogenesis, and autophagy show a dramatic increase (14). Furthermore, in right ventricular cardiac hypertrophy and HF, mitochondrial morphology, fusion/fission balance, Ca^{2+} kinetics, and supercomplex activity are markedly altered, and the dysfunction of mitochondria is mainly attributed to the dysfunction of complex I (15). Increasing lines of evidence demonstrate that during the hypertrophic response, mitochondria display extensive alterations in both morphology and function, which, in turn, directly or indirectly influence the progression of pathological hypertrophy (5, 16). In this section, we will give a summary of the most recent research progress on mitochondrial changes, mainly morphologically and functionally, in response to cardiac hypertrophy.

Mitochondrial Morphological Alterations

Mitochondria play a central role in both cellular physiology and pathology. The morphology of mitochondria is highly plastic, which to some extent is delicately regulated by mitochondrial biogenesis, fission and fusion (17). Biogenesis is usually provoked by preexisting abnormal mitochondria, and it is a complex process during which the mitochondria undergo growth and division with changes in mitochondrial number, size and mass (18). Mitochondrial fission and fusion are collectively termed "mitochondrial dynamism," and genetic interruption of either triggers an accumulation of damaged mitochondria and results in severe cardiomyopathy (19).

Mitochondria in healthy hearts are relatively rich and intact, with complete membrane structures and clear cristae structures; while in hypertrophic hearts, the mitochondria become seriously swollen and deformed, with blurred and ruptured membrane and cristae structures (20). Besides, mitochondria in normal CMs appear to be columnar/ovate in shape, but become filamentous/elongated under stress (20). The morphometric parameters indicated that persistent overload could elevate the area, diameter and perimeter of mitochondria and decrease mitochondrial volume density (21). Utilizing confocal and electron microscopy, researchers have also revealed that in rat models of HF, there exists an increase in small and fragmented mitochondria, which is consistent with an imbalance between mitochondria fusion and fission (22). Mitochondrial cristae, the true bioenergetic components of cells, display prominent morphological changes in the process of cardiac hypertrophy. A recent study has demonstrated that abundant fragmented and lysed cristae was observed in palmitate-treated neonatal rat cardiomyocytes (NRCMs), accompanied by decreased mitochondrial network and complex expression, and elevated ROS levels, which ultimately contribute to NRCM enlargement; and adenovirus-mediated mitofilin overexpression promisingly restored cristae shape and cardiac hypertrophy (23). Therapeutic strategies targeting cristae remodeling may represent an effective way to protect against cardiac hypertrophy.

Interestingly, immunofluorescence staining illustrated a preferred perinuclear localization of mitochondria in normal NRCMs, while in NRCMs stimulated with PE, mitochondria were more dispersed and extensively distributed in the cytoplasm of the cell (24). Gene array analysis suggested that kinesin family member 5b (Kif5b), a kinesin motor protein, was differentially expressed under PE stimulatory conditions. Depletion of Kif5b through specific siRNA targeting Kif5b prevented the peripheral mitochondrial localization in NRCMs as well as reverted PE-induced hypertrophy (24).

Abbreviations: CMs, Cardiomyocytes; NRCMs, normal neonatal rat cardiomyocytes; NF, non-failing; HFrEF, reduced ejection fraction; MMP, mitochondrial membrane potential; SDH, succinate dehydrogenase; Mfn, mitofusin; VDAC2, Voltage-dependent anion channel 2; DCM, dilated cardiomyopathy; TEM, Transmission electron microscopy; MICU1, Mitochondrial calcium uptake 1; TRPC3, Transient receptor potential channel canonical 3; ISO, isoproterenol; Sirt, Sirtuins; Mtus1, mitochondrial tumor suppressor 1.

Taken together, the data support significant changes in mitochondrial morphology under the stimulation of cardiac hypertrophy.

Mitochondrial Functional Alterations

Luo and colleagues have systematically analyzed the cellular and molecular transcriptomic landscape in non-failing (NF) and heart failure with reduced ejection fraction (HFrEF) human hearts. Ingenuity Pathway Analysis (IPA) revealed extensive transcriptional and signaling changes in HFrEF tissues. Notably, the left ventricles (LV) of the failing hearts displayed prominently altered mRNA transcripts related to mitochondrial permeability and mitochondrial biogenesis, including *BCL2L1, CAV2, COX10, DNAJA3, HSPA5, KRT8*, *PRDX3*, *PTCD2*, and etc. (25). These dramatic HFrEF-related transcriptional alterations in the left heart suggested a reciprocal relationship between mitochondrial dysfunction and cardiac pathology.

In the early stage of the development of pathological cardiac hypertrophy, remarkable cardiac insulin-resistance, decreased mitochondrial complex V activity and significantly impaired mitochondrial energy metabolism were observed, which implied that early mitochondrial dysfunction and energy deficit may contribute to the transition from adaptive to maladaptive cardiac hypertrophy (26). Similarly, by combining the transcriptome of individual CMs with cellular morphology, epigenomic characteristics and cardiac function, Nomura et al. successfully reconstructed the trajectory of cardiac hypertrophy and failure, and they demonstrated that in the early stage of cardiac hypertrophy, a number of genes encoding proteins which function in mitochondrial translation/metabolism were significantly activated in CMs (27). Additionally, mitochondria's ability to produce ATP is significantly impaired in response to cardiac hypertrophy. *In vivo* experimental data showed that the activities of NADH dehydrogenase, succinate dehydrogenase (SDH), and mitochondrial membrane potential (MMP) were significantly reduced after hypertrophic insults (21). *In vitro* experiments also suggested that H9c2 cells treated with isoproterenol (ISO) exhibited ROS overload, NO/ROS imbalance, and reduced MMP (28).

The metabolic and transcriptional profiles of hypertrophic murine hearts induced by TAC contribute to a better understanding of the metabolic alterations during maladaptive hypertrophy. By performing microarray analysis, Frey' group have revealed that, in the hearts 6 weeks after TAC surgery, genes involved in mitochondrial beta-oxidation were markedly downregulated, in addition, the expression of certain key enzymes implicated in oxidative phosphorylation and citrate cycle also showed a significant decrease, indicating disturbed mitochondrial function during transition to heart failure (29). And notably, transgenic mice overexpressing catalase in the mitochondria, instead of peroxisomes, were protected from pathological cardiac hypertrophy induced by Ang II stimulation, suggesting that ROS produced in mitochondria plays a central role in mitochondrial energetic failure during decompensated hypertrophy (14).

In summary, it's reasonable to conclude that mitochondrial dysfunction occurs in the early stage of compensatory cardiac hypertrophy, and the functional alteration of mitochondria may represent one essential pathophysiological process that contributes to the transition from compensatory cardiac hypertrophy to decompensated heart failure (**Table 1**).

MECHANISMS LINKING MITOCHONDRIA AND PATHOLOGICAL CARDIAC HYPERTROPHY

Mitochondrial Dynamics

As a dynamic organelle, the mitochondria constantly remodel and exchange contents during periodic fission and fusion. The homeostasis of mitochondrial dynamics is accurately regulated by mitochondrial fission and fusion factors (30). Previous studies have established that the ablation of mitofusin (Mfn) 2 interrupted mitochondrial fusion and caused an accumulation of mitochondria with morphological and functional abnormalities, eventually resulting in progressive cardiac hypertrophy (31). Disruption of mitochondrial fission mediated by Dynamin-related protein1 (Drp1), a pro-fission protein that opposes Mfn2 in mitochondrial dynamics, led to elongated mitochondria, elevated mitochondrial contents, mitochondrial dysfunction, and perturbed mitophagy; furthermore, Drp1-deficient mice developed cardiac pathology and displayed worsened cardiac function (32, 33). Notably, interruption of Mfn1/Mfn2-mediated mitochondrial fusion or Drp1-mediated mitochondrial fission in adult murine hearts was related to rapid lethality (32, 34). Utilizing cardiac-specific deletion of Mfn1/Mfn2 and Drp1 to simultaneously eliminate mitochondrial fission and fusion in the hearts of adult mice, researchers revealed that Mfn1/Mfn2/Drp1 cardiac TKO (triple knockout) mice had a longer survival time and developed a unique form of pathological cardiac hypertrophy compared with fusion-defective Mfn1/Mfn2 cKO or fission-defective Drp1 cKO mice, and provided evidence that cardiac pathology was attributed to the imbalance in mitochondrial dynamism (fission and fusion), instead of the absence of either fission or fusion (19). Thus rebalancing mitochondrial dynamics constitutes a therapeutic candidate to ameliorate cardiac cardiomyopathies which were provoked by imbalanced mitochondrial fission/fusion.

Mitochondrial Calcium Uptake

Calcium ion (Ca^{2+}) plays a central role in mitochondrial function in the heart. Mitochondrial Ca^{2+} intake contributes to the generation of ATP and helps to maintain myocardial contractility. Notably, excessive or insufficient mitochondria Ca^{2+} in the CMs leads to mitochondrial dysfunction and cardiac pathology (35, 36). Recent studies have suggested that, by delicately regulating the uptake and release of Ca^{2+} in response to hypertrophic stimuli, mitochondria maintain the Ca^{2+} homeostasis and cardiac function.

Voltage-dependent anion channel 2 (VDAC2), a porin present on the outer mitochondrial membrane, has recently been reported of high importance to control cardiac remodeling

TABLE 1 | Key features of cardiac hypertrophy and the mitochondrial alterations.

	Cardiac homeostasis	Cardiac hypertrophy
Stimuli	None	Cardiac volume/pressure overload, Ang II, oxidants, activation of α/β adrenergic receptors, hypoxia, aging, high-glucose, and etc.
Cardiac structure	Normal	Enlarged cardiomyocytes, increased heart wall thickness and heart mass, interstitial fibrosis, and increased cellular apoptosis
Cardiac function	Normal	Impaired
Mitochondrial structure	Rich and intact, with complete membrane structures and clear cristae structures	Swollen and deformed, with blurred and ruptured membrane and cristae structures
Mitochondrial distribution	Perinuclear	Dispersed, mainly distributed in the cytoplasm of the cell
ATP production	Normal	Impaired
ROS generation	Normal	Increased
Fatty acid oxidation	Normal	Decreased
Mitochondrial membrane potential (MMP)	Normal	Decreased
Ca^{2+}-induced mitochondrial permeability transition pore	Normal	Increased
NADH dehydrogenase activity	Normal	Decreased
Succinate dehydrogenase (SDH) activity	Normal	Decreased
Mitochondrial dynamics	Normal	Imbalance in mitochondrial fission and fusion
Mitochondrial biogenesis	Normal	Insufficient
Mitophagy	Normal	Transiently activated 3–7 days post-TAC, and downregulated thereafter

(37). Shankar and co-workers successfully performed cardiac-specific *Vdac2* knockout mice and demonstrated that, VDAC2-KO mice exhibited progressive deterioration of cardiac function and eventually developed dilated cardiomyopathy (DCM). Gene and protein expression profiles of the hearts from 16-week-old VDAC2-KO mice suggested that calcium signaling and regulation were markedly altered. In addition, impaired calcium cycling, increased cardiac fibrosis, metabolic alterations were observed in KO mice. Transmission electron microscopy (TEM) was also performed and substantial alterations in the distribution and structure of mitochondria were observed; generally, loss of VDAC2 caused prominently smaller, less dense, and disoriented mitochondria compared to control. Promisingly, reintroduction of VDAC2 through injection with AAV9-αMHC-VDAC2-GFP vector aided in cardiac structural and functional improvement in VDAC2-KO mice. Administration of efsevin, a VDAC2 agonist, greatly enhanced contractile force and accelerated relaxation in the failing hearts, thus VDAC2 may constitute a candidate for HF therapy. Mitochondrial calcium uptake 1 (MICU1), a Ca^{2+} binding protein residing in the intermembrane of mitochondria, was proved to be required in the regulation of cardiac hypertrophy. MICU1 was depressed in hypertrophic hearts, and *in vivo* and *in vitro* experimental data suggested that MICU1 ablation aggravated cardiac hypertrophy induced by Ang-II infusion, as evidenced by the worsened cardiac function, increased hypertrophic biomarkers, and cardiac histological alterations; in contrast, cardiac MICU1 supplementation ameliorated CM enlargement and blunted cardiac dysfunction (38). Utilizing transmission electron microscopy, researchers found that MICU1 knockdown was correlated with massive loss of mitochondrial membrane integrity, ambiguous cristae and myofilaments structures, besides, MICU1 deficiency aggravated the increase in mitochondrial mass, the suppression of MMP, and the depression of ATP contents in hypertrophic hearts. However, overexpression of MICU1 rescued mitochondrial morphological and functional abnormalities (38). Transient receptor potential channel, canonical 3(TRPC3), residing in mitochondria, also exerted regulatory roles in high salt-induced cardiac hypertrophy by mediating mitochondrial function. TRPC3 ablation antagonized cardiac hypertrophy induced by high salt intake, which was achieved by restoring the synthesis of ATP and the activity of complex I and II enzyme in mitochondria (39).

Taken together, mitochondrial Ca^{2+} in the heart plays central roles in stimulating ATP production and maintaining cardiac contractile activity in response to cardiac hypertrophy, thus strategies to main calcium homeostasis in the mitochondria are essential to block cardiac hypertrophic response. Despite great efforts, further investigations are still required to discover the cellular and molecular mechanisms underlying mitochondrial calcium homeostasis. Moreover, the real-time dynamic observation of the mitochondrial calcium alterations inside hypertrophic CMs may contribute to a better understanding of the link between mitochondrial Ca^{2+} and cardiac hypertrophy, and helps to develop novel therapeutic approaches to prevent or block pathological cardiac hypertrophy.

Mitophagy

The autophagic clearance of damaged or unnecessary mitochondria in CMs is delicately mediated by a mitochondria-specific form of autophagy, named mitophagy (8). Mitophagy is

regarded as a critical quality control mechanism to remove damaged or dysfunctional mitochondrial and maintain mitochondrial homeostasis in the heart. In mice subjected to TAC, mitophagy was transiently activated (3–7 days post-TAC), and downregulated below physiological levels thereafter. Importantly, depletion of Drp1 abolished mitophagy and accelerated cardiac hypertrophy and mitochondrial dysfunction induced by overload, however, restoration of mitophagy by Tat-Beclin 1 partially rescued mitophagy and attenuated mitochondrial dysfunction and cardiac hypertrophy during pressure overload (40). The essential regulatory roles of mitophagy in diabetic cardiomyopathy, which is characterized by cardiac hypertrophy, diastolic dysfunction and lipotoxicity, have been investigated. Results from immunofluorescence suggested that the localization of LC3 in mitochondria exhibited a significant increase in CMs isolated from mice receiving high-fat diet (HFD), indicating that HFD consumption notably upregulated mitophagy in the heart. Moreover, in Atg7- or Parkin-deficient HFD mice, cardiac hypertrophy, diastolic dysfunction and lipid accumulation deteriorated and mitophagy was dramatically impaired, suggesting that mitophagy may serve as an adaptive mechanism to protect against diabetic cardiomyopathy in an Atg7- or Parkin-dependent manner. Importantly, treatment with TAT-Beclin1, an activator of mitophagy, effectively restored mitochondrial dysfunction and prevented the development of diabetic cardiomyopathy (41). Another study has reported that PTENα, the first identified PTEN isoform, may function as an important mitochondrial quality controller, and the deficiency of PTENα may contribute to impaired mitochondrial clearance by mitophagy in the heart (42). The ablation of PTENα in mice led to an accumulation of structurally and functionally abnormal cardiac mitochondria; meanwhile, PTENα-depleted mice were more susceptible to ISO-induced cardiac injuries (42).

Collectively, in response to various pathological stresses, CMs selectively remove the dysfunctional mitochondria, reduce ROS production and restore cardiac function through the regulation of mitophagy. Exploring the roles of mitophagy in cardiac hypertrophy exists as an area of great interest.

Enzymes in Mitochondria

Mitochondria contain thousands of different proteins, of which enzymes are an important component. In recent years, increasing lines of evidence support that mitochondrial enzymes, especially those involved in mitochondrial metabolism, have profound effects on cardiac hypertrophy and remodeling (43–48).

NADH: ubiquinone oxidoreductase core subunit S1 (Ndusf1), the prominent component of complex I, has gained particular attention in the regulation of cardiac hypertrophy. A recent study found that Ndusf1 was downregulated in TAC mouse models. Further gain- and loss-of-function analysis revealed that Ndusf1 deficiency deteriorated cardiac hypertrophic response (44). *In vitro* mechanistic exploration showed that the mitochondrial DNA content in CMs was significantly decreased after Ndusf1 deletion, consistently, loss of Ndusf1 dramatically elevated ROS production in CMs. Additionally, results from fluorescent staining illustrated that mitochondrial mass and mitochondrial membrane potential (MMP) were markedly repressed in CMs lack of Ndusf1. Ndusf1 overexpression, in turn, attenuated cardiac hypertrophy and mitochondrial dysfunction. A novel role of mitochondrial GTPases 1 (MTG1), which was known to participate in mitochondrial ribosome assembly and translation, in pathological cardiac hypertrophy has recently been revealed. MTG1 exhibited a significant increase in the heart tissue of both heart failure patients and mice subjected to AB surgery. Further loss- and gain-of-function studies showed that MTG1 depletion worsened AB-induced hypertrophy, whereas MTG1 overexpression mitigated cardiac hypertrophy and dysfunction after the onset of AB. The cardio-protective potentials of MTG1 deficiency were attributed to the improved activity of the mitochondrial respiratory chain complex and subsequently reduced ROS production (43). Mitochondrial Rho GTPase (Miro2), a well-known outer mitochondrial membrane protein mediating intracellular mitochondrial transport, was proved to be effective in the modulation of cardiac inter-mitochondrial communication during cardiac hypertrophy (45). In TAC-induced hypertrophic mouse hearts, downregulated Miro2 expression was detected, along with disrupted inter-mitochondrial communications. And promisingly, the Miro2 transgenic mice were protected from TAC-induced cardiac dysfunction, which was obtained by improving the communications between adjacent mitochondria and attenuating mitochondrial dysfunction (45). *In vivo* and *in vitro* experimental data also demonstrated that endonuclease G (Endog) loss-of-function may serve as a novel determinant of decompensated cardiac hypertrophy and impaired cardiac function. Importantly, in the hearts of Endog-deficient mice, there existed a dramatic increase in mitochondrial depletion and ROS generation, suggesting a previously unappreciated link between mitochondrial dysfunction and maladaptive cardiac hypertrophy (48). Mitochondrial NADP (+)-dependent isocitrate dehydrogenase (IDH2) has been well-known to mediate the balance of mitochondrial redox and help to maintain mitochondrial homeostasis. Notably, studies have also suggested that mitochondria isolated from the hearts of IDH2-deficient mice lost IDH2 activity and $IDH2^{-/-}$ mice rapidly developed uncompensated HF, with increased hypertrophy and mitochondrial dysfunction, which was proved to be caused by the disturbance of the redox homeostasis (46). Glutaredoxin 2 (GRX2), a glutathione-dependent oxidoreductase in mitochondria, was essential in maintaining mitochondrial homeostasis and preserving cardiac structure and function. Based on the genetic and histopathological databases, researchers showed that relatively row expression of GRX2 indicated an increased incidence of human cardiac pathologies, including cardiac hypertrophy, fibrosis and infarct. Loss-of-function analysis also revealed that the absence of GRX2 was highly relevant with impaired mitochondrial dynamics, ultrastructure and energetics in both heart tissue and primary CMs (47).

In summary, the above results provide new insights into the possible molecular mechanisms underlying pathological cardiac hypertrophy, and further suggest that mitochondrial enzymes may represent potential therapeutic targets to alleviate cardiac hypertrophy and dysfunction.

Sirtuin Family

Sirtuins (Sirt), consist of seven identified homologs (Sirt1-7), are a family of class III nicotinamide adenine dinucleotide (NAD+)-dependent deacetylase, among which Sirt3-5 are mainly resident in mitochondria. It has been well established that sirtuins exert protective effects on a variety of aging-related diseases by regulating some important cellular processes in the nucleus, cytoplasm as well as mitochondria to keep a balance of energy metabolism within the cell (49). In this section, we will give an overview of the critical roles of sirtuins, especially mitochondrial sirtuins, in pathological cardiac hypertrophy.

In mice with cardiac-specific *SIRT2* overexpression, Ang II-induced cardiac hypertrophy was repressed and cardiac dysfunction was rescued, whereas cardiac-specific depletion of Sirt2 dramatically aggravated hypertrophic response to Ang II stimulation. Furthermore, the authors showed that SIRT2 could directly bound to and interacted with LKB1, and the deacetylation of LKB1 participated in SIRT2-mediated suppression of stress-induced hypertrophic response (50). Sirt3, another important number of the sirtuin family, exhibited remarkable upregulation in the nuclear under ISO treatment. And adenovirus-mediated exogenous Sirt3 supplementation prevented PE- and ISO-induced hypertrophic response via deacetylating PARP-1 and inhibiting its activity (51). In HFD-induced cardiac hypertrophy and dysfunction, the absence of Sirt3 led to increased ROS generation and aggravated heart function compared with the WT mice, suggesting the significance of Sirt3 in preserving mitochondrial hemostasis and cardiac function during obesity-induced pathological hypertrophy (52). Sirt4, a sirtuin mainly present in mitochondria, plays an essential role in the progression of cardiac hypertrophy. Strictly, loss of Sirt4 protected the mice from Ang II-induced cardiac hypertrophy, whereas cardiac overexpression of Sirt4 accelerated cardiac maladaptation in response to Ang II treatment. Mechanistically, Sirt4 promoted the production of ROS by blunting Sirt3-mediated MnSOD activation, thereby enhancing cardiac decompensation upon Ang II infusion; and application of 4-benzoic acid to mimic MnSOD activity could eliminate Sirt4-mediated hypertrophic alterations (53). This research provided a novel link between mitochondrial oxidative stress and cardiac hypertrophy. Genetic ablation of Sirt5 accelerated cardiac dysfunction and increased mortality in the TAC mice. By performing MS-based proteomics and metabolomics analyses of heart tissues isolated from Sirt5-KO and WT mice, researchers observed an overall decrease in fatty acid oxidation, glucose oxidation and mitochondrial NAD+/NADH (54). Sirt7, the most recently identified sirtuin in mammals, has been proven to protect against TAC-induced cardiac hypertrophy. Additionally, SIRT6 served as a negative modulator of cardiac hypertrophy through interacting with c-Jun and suppressing IGF-Akt signaling (55). In cardiac-specific Sirt7-depletion mice, hypertrophic response was significantly augmented, as evidenced by increased heart weight/tibial length, larger CM cross-sectional area, and deteriorated heart function compared to WT mice receiving TAC operation, and further mechanism investigation indicated that The anti-hypertrophic roles of Sirt7 may be attributed to the deacetylation of GATA4 (56).

The beneficial effects of the sirtuin family on lipid metabolism, glucose oxidation, and ROS production in cardiac hypertrophy are at the pre-clinical level.

Other Mitochondrial Proteins

By performing genome-wide exon array analysis in hypertrophic murine hearts induced by TAC surgery, Ito and colleagues successfully identified Mtus1A, one of the splice variants of mitochondrial tumor suppressor 1 (Mtus1), as a central modulator in hemodynamic stress-induced cardiac hypertrophy. In cardiac-specific Mtus1A transgenic mice, the hypertrophic response was remarkably mitigated, and *in vitro* experimental results revealed that Mtus1A overexpression alleviated the production of ROS and subsequent phosphorylation of ERK, contributing to a decrease in cell hypertrophy and protein synthesis (57). Translocase of inner membrane 50 (TIM50) was downregulated in the failing hearts, *in vivo* and *in vitro* loss- and gain-of-function analysis revealed that TIM50 acted as a novel repressor in cardiac hypertrophy. Overexpression of TIM50 significantly attenuated the increased cell size, oxidative stress and cellular apoptosis induced by Ang II (58). Miro1, a mitochondrial outer membrane protein, also played a central role in modulating mitochondrial dynamics and metabolism in cardiac hypertrophy. In NRCMs, PE stimulation provoked hypertrophic response as well as mitochondrial fission pattern, which were reversed when Miro1 was ablated (59). Inhibition of Dynamin-related protein1 (Drp1), a protein that regulates mitochondrial fission, with specific inhibitors exerted protective effects against ventricular hypertrophy induced by high salt intake, meanwhile, the ROS generation, as well as CaMKII expression were suppressed in Drp1-depleted rats (60). These studies illustrate that some proteins residing inside mitochondria are of great importance to maintain cardiac hemostasis, little changes in these proteins may trigger prominent mitochondrial dysfunction, imbalance in energy production, and pathological cardiac hypertrophy.

MicroRNAs

Although the roles of microRNAs (miRs) in life activities have been widely investigated, there to date exist only a few studies revealing the functions of miRs in mitochondrial structure and function during cardiac hypertrophic response. A very recent study has identified miR-153-3p as a trigger of abnormal mitochondrial fission and hypertrophic response, mainly through the inhibition of Mfn1 translation, and both *in vivo* and *in vitro* experiments confirmed that the ablation of miR-153-3p could dramatically avoid mitochondrial fission as well as cardiac hypertrophy (61). Depletion of miR-106a almost entirely reversed AngII-induced hypertrophic phenotypes. Notably, Mfn2, a well-known mitochondrial fusion protein, was identified as a direct target for miR-106a. Silence of Mfn2 eliminated the anti-hypertrophic effects of miR-106a inhibitors, while Mfn2 overexpression abolished the pro-hypertrophic property of miR-106a. Additionally, miR-106a inhibition or Mfn2 overexpression significantly reversed mitochondrial cristae defects, depolarization of the mitochondrial membrane, and increased ROS generation caused

by sustained cardiac overload (62). Similarly, miR-376b-3p attenuated mitochondrial fragmentation and hypertrophic response in noradrenaline-treated CMs, which was obtained by its direct interactions with mitochondrial fission factor (MFF) to modulate mitochondrial morphology and function (63). Another study has also shown that, in cultured CMs with PE treatment, miR-485-5p overexpression could diminish mitochondrial fragmentation and hypertrophic response by decreasing the level of MAPL expression and upregulating Mfn2 expression (64). In addition, miRs also appear to be effective during hypertrophic response. The latest research progress by Li's group suggested that miR-27b-3p deficiency remarkably reduced cardiac hypertrophy, fibrosis, and inflammation in both TAC and Angiotensin II (Ang II) perfusion-induced murine models; surprisingly, inhibition of endogenous miR-27b-3p could significantly enhance mitochondrial oxidative phosphorylation (OXPHOS) through activating PGC1α/β (65). Overexpression of miR-142-3p reversed MMP, mitochondrial density and effectively abolished hypertrophic response in CMs stimulated by Ang II, which was obtained by suppressing the expression of *SH2B1* (66). These results show that microRNAs are key regulators in mitochondrial function in the heart. The critical roles of microRNAs provide a new perspective on developing new diagnostic and therapeutic tools to block or reverse pathological cardiac hypertrophy.

Regulators Outside Mitochondria

The mechanisms underlying mitochondrial dysfunction and cardiac hypertrophy are multifactorial and likely involve nuclear-encoded regulatory factors, residing outside the mitochondria, that directly or indirectly impact mitochondrial function and contribute to the progression of pathological cardiac hypertrophy. As such, manipulation of these critical regulators might fulfill a double role by suppressing mitochondrial abnormalities and improving cardiac function.

Nuclear factor of activated T cells, cytoplasmic 4 (NFATc4) overexpression aggravated phenylephrine (PE)-induced perturbations in mitochondrial genesis, membrane potential, and mitochondrial respiration; in contrast, NFATc4 deletion mitigated PE-induced mitochondrial dysfunction as well as cardiac hypertrophy (67). Mitochondrial dysfunction induced by Nlrp3 inflammasome also appears to play a regulatory role in Ang II-induced cardiomyopathy. The mitochondria in the hypertrophic heart tissue were swollen and fragmented, but these morphological alterations were significantly reversed in the NLRP3$^{-/-}$ group. In addition to mitochondrial morphological alterations, cardiac hypertrophy also led to mitochondrial dysfunction, which was accompanied by insufficient mitochondrial biogenesis, damaged mtDNA, disordered intracellular ATP synthesis, and low levels of TFAM and PGC1a. Surprisingly, Nlrp3 depletion remarkably reversed the decreased expression of PGC1a and TFAM, abnormal mtDNA and ATP synthase in the hypertrophic heart caused by Ang II infusion (68). Polycystic kidney disease 2-like 1 (PKD2L1), known to serve as an important sour sensor in taste cells, played possible roles in cardiac hypertrophy. *In vitro* and *in vivo* experiments showed that hypertrophic stress (including high salt intake and Ang II infusion) significantly increased the expression of PKD2L1 in mitochondria. PKD2L1-deficient mice exhibited aggravated pathological cardiac hypertrophy caused by a high salt diet, at the same time, less O2 consumption, reduced heat production and a decreased respiratory exchange ratio were also observed in mice with PKD2L1 mutation. Further mechanical investigation illustrated that PKD2L1 was capable of controlling the deteriorated mitochondrial Ca^{2+} overload mediated by NCX1, via restricting p300-mediated histone acetylation on the NCX1 promoter (69). The Grb2-associated binder 1 (Gab1), a key mediator of growth factor receptor signaling, also participated in the regulation of cardiac hypertrophy induced by pressure overload. The levels of Gab1 were diminished in both human and mouse DCM hearts. Cardiac-specific Gab1 knockout mice rapidly developed severe DCM and heart failure after the onset of cardiac hemodynamic stress, furthermore, gene microarray analysis revealed the upregulation of several pro-apoptotic genes and downregulation of some key anti-apoptotic genes. Further analysis of mitochondrial function and caspase activity demonstrated that under hemodynamic stress conditions, Gab1 deficiency caused severe damage to both mitochondrial ultrastructure and function and triggered massive activation of caspase, consequently leading to CM apoptosis and heart failure (70).

In a word, these latest studies provide new mechanistic insights into the link between mitochondria and cardiac hypertrophy (**Figure 1**). In-depth exploration of mitochondria-mediated cellular and molecular regulation would provide a better understanding of the etiology and progression of cardiac hypertrophy and support the discovery of novel biomarkers in diseases and therapeutic targets to fight against cardiomyopathies.

POTENTIAL THERAPEUTIC APPROACHES TARGETING MITOCHONDRIA TO PREVENT OR REVERSE CARDIAC HYPERTROPHY

Phytochemicals

An attractive pharmacological tool for the treatment of cardiac hypertrophy is the traditional phytochemicals. A growing number of studies have proved that phytochemicals are capable of mitigating cardiac hypertrophy in cell and animal models via modulating mitochondrial function and maintaining mitochondrial hemostasis. Wei's recent findings suggest that T89, a traditional Chinese medicine, may be a potential therapeutic approach to treat ISO-induced cardiac hypertrophy, and the underlying mechanisms mainly lay on the regulation of metabolic pathways (71). By performing quantitative proteomics, the group revealed that T_{89} could inhibit glycolysis, accelerate fatty acid oxidation and restore mitochondrial OXPHOS, thereby attenuating energy metabolism disorders and alleviating ISO-induced cardiac injury. Bawei Chenxiang Wan (BCW), another well-known traditional Chinese medicine, was approved to be effective in ISO-induced rat hypertrophic models. Moreover, a number of mitochondrial DNA-encoded genes, such as *ND1*, *Cyt*

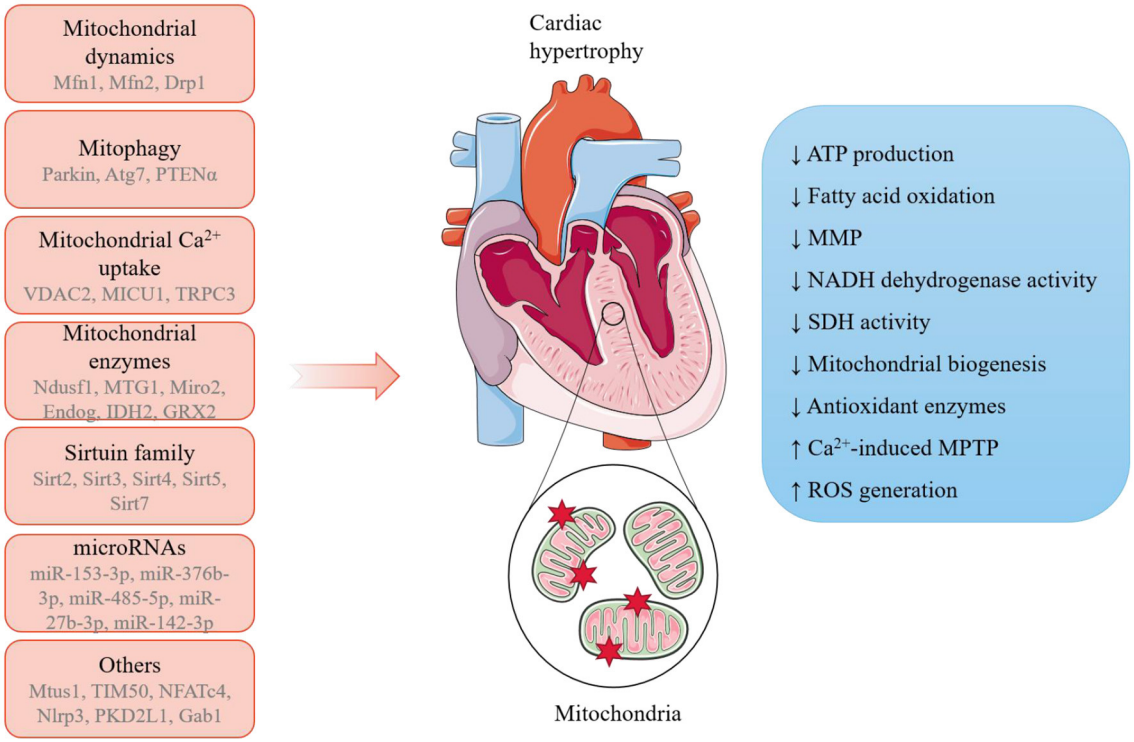

FIGURE 1 | A summary of the potential mechanisms linking mitochondria and pathological cardiac hypertrophy. A range of mitochondria-dependent and -independent regulators have been reported to participate in the initiation and progression of pathological cardiac hypertrophy, during which mitochondria undergo remarkable morphological and functions alterations.

b, ATP 5β, and *mt-coI* were downregulated in ISO-treated rats, but restored when administrated with BCW, indicating that the anti-hypertrophic roles of BCW were obtained by modulating mitochondria function and oxidative phosphorylation (72). Mitophagy may exist as another important target. Berberine has recently been verified to improve heart function in cardiac hypertrophy murine models, which was exactly achieved by the activation of mitophagy via the PINK1/Parkin/Ubiquitination signaling pathway (73). Similarly, the pretreatment of baicalein significantly attenuated cardiac hypertrophy and restored cardiac function in experimental *in vivo/vitro* models by activating mitophagy (74). As a natural bisphenol compound extracted from the magnolia bark, Honokiol (HKL) exerted cardio-protective properties in pathological cardiac hypertrophy. Interestingly, HKL administration substantially decreased the acetylation levels of mitochondrial proteins via directly binding to and activating mitochondrial SIRT3 (75). Similarly, Emodin, as the main component of rhubarb, could effectively block ISO- and TAC-induced cardiac hypertrophy through Sirt3-dependent mitochondrial protection (76).

Antioxidants

In view of the extensive ROS production and severe oxidative stress after the onset of cardiac overload, treatment with antioxidants may represent an efficient approach to attenuate mitochondrial dysfunction and block cardiac hypertrophy. Recent research has found that the application of mitoTEMPO (an antioxidant targeting mitochondrial ROS) or resveratrol (a sirtuin agonist) fulfilled a protective role against nicotine-induced cardiac hypertrophy, fibrosis and inflammation and dysfunction in rats (77). Alpha-lipoic acid (α-LA), another well-known antioxidant, was also proved to protect against TAC-induced adverse cardiac hypertrophy, cardiac dysfunction and mitochondrial dysfunction via ALDH2-dependent activation of a novel mitophagy receptor protein FUNDC1 (78). Similarly, pretreatment with NaHS abolished hypertrophic response, mitochondrial ultrastructure impairment, mitochondrial depletion and oxidative stress during cardiac pressure overload in a Sirt3-dependent way (79). Additionally, lactoferrin seemed to be an effective agent against pathological cardiac hypertrophy in aged mice. After lactoferrin intake, the aged mice showed remarkable improvement of cardiac hypertrophy and dysfunction, which were partly attributed to mitochondrial dynamic rearrangement and the control of mitochondrial-lysosomal axis-related detrimental regulators (80). Interestingly, researchers have recently illustrated the relationship between aerobic exercise and hypertrophy, and they illustrated that in the mice persisting in aerobic exercise, cardiac hypertrophy and dysfunction were greatly improved. Mechanistically, mitochondria from the aerobic exercise group exhibited decreased excessive mitochondrial fission and mitochondrial autophagy, thus restoring mitochondrial

TABLE 2 | A summary of therapeutic approaches targeting mitochondria to treat cardiac hypertrophy.

Potential therapy	Models	Observations	Mechanisms
T89 (71)	ISO-induced rat cardiac hypertrophy	Attenuated cardiac dysfunction and energy metabolism disorders	inhibiting glycolysis, accelerating fatty acid oxidation and restoring mitochondrial OXPHOS
Bawei Chenxiang Wan (72)	ISO-induced rat hypertrophic models	Alleviated cardiac injury and restored mitochondrial DNA-encoded genes	modulating mitochondria function and oxidative phosphorylation
Berberine (73)	TAC-induced murine cardiac hypertrophy	Improved heart function	Activating mitophagy via the PINK1/Parkin/Ubiquitination signaling pathway
Baicalein (74)	ISO-induced murine cardiac hypertrophy	Attenuated cardiac hypertrophy and cardiac function	Activating mitophagy
Honokiol (75)	TAC/ISO-induced murine cardiac hypertrophy	Attenuated cardiac hypertrophy and cardiac function	Decreasing mitochondrial protein acetylation via regulating SIRT3
Emodin (76)	TAC/ISO-induced murine cardiac hypertrophy	Improved ISO- and TAC-induced cardiac hypertrophy	Regulating SIRT3 signaling pathway
Alpha-lipoic acid (78)	TAC-induced murine cardiac hypertrophy	Improved cardiac hypertrophy and function	ALDH2-dependent activation of a novel mitophagy receptor protein FUNDC1
NaHS (79)	TAC-induced murine cardiac hypertrophy	Improved hypertrophic response and mitochondrial function	In a Sirt3-dependent way
Lactoferrin (80)	Aging-related cardiac hypertrophy	Improved cardiac hypertrophy and function	Improving mitochondrial dynamics and mitochondrial-lysosomal axis
aerobic exercise (81)	TAC-induced murine cardiac hypertrophy	Improved cardiac hypertrophy and function	Decreasing excessive mitochondrial fission and mitochondrial autophagy
alpha-ketoglutarate (82)	TAC-induced murine cardiac hypertrophy	Improved cardiac hypertrophy and function	Promoting mitophagy
Allyl Methyl Sulfide (83)	TAC-induced rat cardiac hypertrophy	Improved cardiac hypertrophy and function	Improving mitochondrial energy metabolism
Diazoxide (84)	ISO-induced murine cardiac hypertrophy	Attenuated cardiac hypertrophy	Opening mitoKATP, improving MnSOD activity and decreasing H_2O_2 production

ultrastructure and function in response to hypertrophic insults (81).

Other Mitochondria-Targeted Molecules

A very recent study has found that external supplementation of alpha-ketoglutarate (AKG), an intermediate metabolite of the tricarboxylic acid cycle, effectively suppressed transverse aortic constriction (TAC)-induced cardiac hypertrophy and improved heart function (82). The cardio-protective roles of AKG may be achieved by promoting mitophagy, which helped to remove damaged mitochondria and reduce ROS production (82). Allyl Methyl Sulfide (AMS) intervention also exerted protective effects on TAC-induced cardiac hypertrophy. Mechanistically, PCR array experiments showed that AMS could improve mitochondrial energy metabolism-related genes compared to vehicle control; AMS pre-treatment also restored mitochondrial oxygen consumption rate, MMP and ROS production in CMs stimulated by ISO, mitochondria fusion and fission were also balanced after AMS intervention (83). Pharmacological intervention targeting ATP-sensitive K^+ channels in mitochondria (mitoKATP) may act as a potential therapeutic approach to alleviate cardiac hypertrophy. Treatment with diazoxide in ISO-induced cardiac hypertrophy mice to open mitoKATP significantly improved MnSOD activity and decreased H_2O_2 production, and it went the opposite when treated with 5-hydroxydecanoate or glibenclamide (mitoKATP blockers), indicating that mitoKATP opening seems promising to block oxidative stress and ameliorate cardiac hypertrophy (84). Interestingly, the administration of choline protected against abdominal aorta banding (AAB) and Ang II-induced cardiac hypertrophy and dysfunction. In hypertrophic groups pre-treated with choline, the mito-nuclear protein imbalance was reversed and the unfolded protein response of mitochondria (UPRmt) was greatly activated, thus mitochondrial ultrastructure and function were restored to normal (21).

CONCLUSIONS

Mitochondria are the prominent organelle for the energy supply of CMs, and a large number of researches have demonstrated that mitochondria are highly susceptible to pathological stimuli, including sustained and repeated cardiac overload (5, 16). Pathological cardiac hypertrophy results in functionally and structurally damaged mitochondria, and in turn, the abnormal mitochondria may also mediate cardiac hypertrophic response via regulatory pathways inside and outside mitochondria. It is widely accepted that balanced regulation of mitochondrial energy supply and the cardiac energy consumption is extremely delicate. Thus, efficient cardiac therapies targeting mitochondrial lesions and dysfunction may constitute a new strategy to inhibit the

high susceptibility to pro-hypertrophic stimuli and attenuate pathological cardiac hypertrophy (**Table 2**).

Despite great progress has been made in elucidating the potential regulatory mechanisms underlying cardiac hypertrophy, there are still some issues that remain to be solved. Growing studies have provided evidence that mitochondria exert the regulatory roles on cardiac hypertrophy via countless modulators or signaling pathways, meanwhile, one particular regulator may have multiple effects related or unrelated to hypertrophy, thus identifying the prioritized mechanisms altered and essential in humans is clinically significant and should be highly valued. Selectively suppressing the specific signaling mechanisms is of significant importance in enhancing heart function in patients suffering from cardiac hypertrophy. Moreover, in recent years, increasing studies have revealed the potential protective roles of some agents against cardiac hypertrophy via impacting mitochondrial function, however, these possibilities are mainly verified in animal experiments but are poorly characterized in clinical trials. Future work should also be directed on improving their specificity and efficacy as well as avoiding the potential cytotoxicity.

Another vagueness lies on the causal link between mitochondrial abnormalities and cardiac hypertrophy. It seems that during the hypertrophic response, notable mitochondrial damage was detected, in addition, mitochondria-mediated signaling pathways contribute to the initiation and progression of pathological hypertrophy. It is hard to determine whether structural and functional alterations in mitochondria are the primary cause or secondary effects in pathological cardiac hypertrophy. A detailed time-course study in hypertrophy models may help to explain the issues.

AUTHOR CONTRIBUTIONS

DY, DF, and Q-ZT contributed to the conception and design of the review. The draft of the manuscript was written by DY and H-QL, F-YL, ZG, PA, and M-YW performed the literature search. ZY, DF, and Q-ZT critically revised the manuscript. All authors contributed to the article and approved the submitted version.

FUNDING

This work was supported by grants from the National Natural Science Foundation of China (81900219, 81800216). The funds received are used for open access publication fees.

REFERENCES

1. Shimizu I, Minamino T. Physiological and pathological cardiac hypertrophy. *J Mol Cell Cardiol.* (2016) 97:245–62. doi: 10.1016/j.yjmcc.2016.06.001
2. Gibb AA, Epstein PN, Uchida S, Zheng Y, McNally LA, Obal D, et al. Exercise-induced changes in glucose metabolism promote physiological cardiac growth. *Circulation.* (2017) 136:2144–57. doi: 10.1161/CIRCULATIONAHA.117.028274
3. Yang D, Liu HQ, Liu FY, Tang N, Guo Z, Ma SQ, et al. The roles of noncardiomyocytes in cardiac remodeling. *Int J Biol Sci.* (2020) 16:2414–29. doi: 10.7150/ijbs.47180
4. Yang D, Liu HQ, Liu FY, Tang N, Guo Z, Ma SQ, et al. Critical roles of macrophages in pressure overload-induced cardiac remodeling. *J Mol Med (Berl).* (2021) 99:33–46. doi: 10.1007/s00109-020-02002-w
5. Nakamura M, Sadoshima J. Mechanisms of physiological and pathological cardiac hypertrophy. *Nat Rev Cardiol.* (2018) 15:387–407. doi: 10.1038/s41569-018-0007-y
6. Braunwald E. The war against heart failure: the Lancet lecture. *Lancet.* (2015) 385:812–24. doi: 10.1016/S0140-6736(14)61889-4
7. Barth E, Stämmler G, Speiser B, Schaper J. Ultrastructural quantitation of mitochondria and myofilaments in cardiac muscle from 10 different animal species including man. *J Mol Cell Cardiol.* (1992) 24:669–81. doi: 10.1016/0022-2828(92)93381-S
8. Tong M, Sadoshima J. Mitochondrial autophagy in cardiomyopathy. *Curr Opin Genet Dev.* (2016) 38:8–15. doi: 10.1016/j.gde.2016.02.006
9. Ramachandra CJA, Hernandez-Resendiz S, Crespo-Avilan GE, Lin YH, Hausenloy DJ. Mitochondria in acute myocardial infarction and cardioprotection. *EBioMed.* (2020) 57:102884. doi: 10.1016/j.ebiom.2020.102884
10. Picca A, Mankowski RT, Burman JL, Donisi L, Kim JS, Marzetti E, et al. Mitochondrial quality control mechanisms as molecular targets in cardiac ageing. *Nat Rev Cardiol.* (2018) 15:543–54. doi: 10.1038/s41569-018-0059-z
11. Marin W, Marin D, Ao X, Liu Y. Mitochondria as a therapeutic target for cardiac ischemia-reperfusion injury (Review). *Int J Mol Med.* (2021) 47:485–99. doi: 10.3892/ijmm.2020.4823
12. Peng W, Cai G, Xia Y, Chen J, Wu P, Wang Z, et al. Mitochondrial Dysfunction in Atherosclerosis. *DNA Cell Biol.* (2019) 38:597–606. doi: 10.1089/dna.2018.4552
13. Abel ED, Doenst T. Mitochondrial adaptations to physiological vs. pathological cardiac hypertrophy. *Cardiovasc Res.* (2011) 90:234–42. doi: 10.1093/cvr/cvr015
14. Dai DF, Johnson SC, Villarin JJ, Chin MT, Nieves-Cintrón M, Chen T, et al. Mitochondrial oxidative stress mediates angiotensin II-induced cardiac hypertrophy and Galphaq overexpression-induced heart failure. *Circ Res.* (2011) 108:837–46. doi: 10.1161/CIRCRESAHA.110.232306
15. Wüst RC, de Vries HJ, Wintjes LT, Rodenburg RJ, Niessen HW, Stienen GJ. Mitochondrial complex I dysfunction and altered NAD(P)H kinetics in rat myocardium in cardiac right ventricular hypertrophy and failure. *Cardiovasc Res.* (2016) 111:362–72. doi: 10.1093/cvr/cvw176
16. Facundo H, Brainard RE, Caldas FRL, Lucas AMB. Mitochondria and cardiac hypertrophy. *Adv Exp Med Biol.* (2017) 982:203–26. doi: 10.1007/978-3-319-55330-6_11
17. Heine KB, Hood WR. Mitochondrial behaviour, morphology, and animal performance. *Biol Rev Camb Philos Soc.* (2020) 95:730–7. doi: 10.1111/brv.12584
18. Dorn GW 2nd, Vega RB, Kelly DP. Mitochondrial biogenesis and dynamics in the developing and diseased heart. *Genes Dev.* (2015) 29:1981–91. doi: 10.1101/gad.269894.115
19. Song M, Franco A, Fleischer JA, Zhang L, Dorn GW 2nd. Abrogating mitochondrial dynamics in mouse hearts accelerates mitochondrial senescence. *Cell Metabol.* (2017) 26:872–83.e5. doi: 10.1016/j.cmet.2017.09.023
20. Gao S, Li G, Shao Y, Wei Z, Huang S, Qi F, et al. FABP5 deficiency impairs mitochondrial function and aggravates pathological cardiac remodeling and dysfunction. *Cardiovasc Toxicol.* (2021) 21:619–29. doi: 10.1007/s12012-021-09653-2
21. Xu M, Xue RQ, Lu Y, Yong SY, Wu Q, Cui YL, et al. Choline ameliorates cardiac hypertrophy by regulating metabolic remodelling and UPRmt through SIRT3-AMPK pathway. *Cardiovasc Res.* (2019) 115:530–45. doi: 10.1093/cvr/cvy217

22. Chen L, Gong Q, Stice JP, Knowlton AA. Mitochondrial OPA1, apoptosis, and heart failure. *Cardiovasc Res.* (2009) 84:91–9. doi: 10.1093/cvr/cvp181
23. Xue RQ, Zhao M, Wu Q, Yang S, Cui YL Yu XJ, et al. Regulation of mitochondrial cristae remodelling by acetylcholine alleviates palmitate-induced cardiomyocyte hypertrophy. *Free Radic Biol Med.* (2019) 145:103–17. doi: 10.1016/j.freeradbiomed.2019.09.025
24. Tigchelaar W, de Jong AM, Bloks VW, van Gilst WH, de Boer RA, Silljé HH. Hypertrophy induced KIF5B controls mitochondrial localization and function in neonatal rat cardiomyocytes. *J Mol Cell Cardiol.* (2016) 97:70–81. doi: 10.1016/j.yjmcc.2016.04.005
25. Luo X, Yin J, Dwyer D, Yamawaki T, Zhou H, Ge H, et al. Chamber-enriched gene expression profiles in failing human hearts with reduced ejection fraction. *Sci Rep.* (2021) 11:11839. doi: 10.1038/s41598-021-91214-2
26. Zhang L, Jaswal JS, Ussher JR, Sankaralingam S, Wagg C, Zaugg M, et al. Cardiac insulin-resistance and decreased mitochondrial energy production precede the development of systolic heart failure after pressure-overload hypertrophy. *Circ Heart Fail.* (2013) 6:1039–48. doi: 10.1161/CIRCHEARTFAILURE.112.000228
27. Nomura S, Satoh M, Fujita T, Higo T, Sumida T, Ko T, et al. Cardiomyocyte gene programs encoding morphological and functional signatures in cardiac hypertrophy and failure. *Nat Commun.* (2018) 9:4435. doi: 10.1038/s41467-018-06639-7
28. Su H, Pistolozzi M, Shi X, Sun X, Tan W. Alterations in NO/ROS ratio and expression of Trx1 and Prdx2 in isoproterenol-induced cardiac hypertrophy. *Acta Biochim Biophys Sin (Shanghai).* (2017) 49:1022–8. doi: 10.1093/abbs/gmx102
29. Müller OJ, Heckmann MB, Ding L, Rapti K, Rangrez AY, Gerken T, et al. Comprehensive plasma and tissue profiling reveals systemic metabolic alterations in cardiac hypertrophy and failure. *Cardiovasc Res.* (2019) 115:1296–305. doi: 10.1093/cvr/cvy274
30. Lee H, Yoon Y. Mitochondrial fission and fusion. *Biochem Soc Trans.* (2016) 44:1725–35. doi: 10.1042/BST20160129
31. Chen Y, Dorn GW 2nd. PINK1-phosphorylated mitofusin 2 is a Parkin receptor for culling damaged mitochondria. *Science.* (2013) 340:471–5. doi: 10.1126/science.1231031
32. Song M, Mihara K, Chen Y, Scorrano L, Dorn GW 2nd. Mitochondrial fission and fusion factors reciprocally orchestrate mitophagic culling in mouse hearts and cultured fibroblasts. *Cell Metabol.* (2015) 21:273–86. doi: 10.1016/j.cmet.2014.12.011
33. Ikeda Y, Shirakabe A, Maejima Y, Zhai P, Sciarretta S, Toli J, et al. Endogenous Drp1 mediates mitochondrial autophagy and protects the heart against energy stress. *Circ Res.* (2015) 116:264–78. doi: 10.1161/CIRCRESAHA.116.303356
34. Chen Y, Liu Y, Dorn GW 2nd. Mitochondrial fusion is essential for organelle function and cardiac homeostasis. *Circ Res.* (2011) 109:1327–31. doi: 10.1161/CIRCRESAHA.111.258723
35. Luczak ED, Wu Y, Granger JM, Joiner MA, Wilson NR, Gupta A, et al. Mitochondrial CaMKII causes adverse metabolic reprogramming and dilated cardiomyopathy. *Nat Commun.* (2020) 11:4416. doi: 10.1038/s41467-020-18165-6
36. Dia M, Gomez L, Thibault H, Tessier N, Leon C, Chouabe C, et al. Reduced reticulum-mitochondria Ca(2+) transfer is an early and reversible trigger of mitochondrial dysfunctions in diabetic cardiomyopathy. *Basic Res Cardiol.* (2020) 115:74. doi: 10.1007/s00395-020-00835-7
37. Shankar TS, Ramadurai DKA, Steinhorst K, Sommakia S, Badolia R, Thodou Krokidi A, et al. Cardiac-specific deletion of voltage dependent anion channel 2 leads to dilated cardiomyopathy by altering calcium homeostasis. *Nat Commun.* (2021) 12:4583. doi: 10.1038/s41467-021-24869-0
38. Yang Y, Du J, Xu R, Shen Y, Yang D, Li D, et al. Melatonin alleviates angiotensin-II-induced cardiac hypertrophy via activating MICU1 pathway. *Aging.* (2020) 13:493–515. doi: 10.18632/aging.202159
39. Ma T, Lin S, Wang B, Wang Q, Xia W, Zhang H, et al. TRPC3 deficiency attenuates high salt-induced cardiac hypertrophy by alleviating cardiac mitochondrial dysfunction. *Biochem Biophys Res Commun.* (2019) 519:674–81. doi: 10.1016/j.bbrc.2019.09.018
40. Shirakabe A, Zhai P, Ikeda Y, Saito T, Maejima Y, Hsu CP, et al. Drp1-dependent mitochondrial autophagy plays a protective role against pressure overload-induced mitochondrial dysfunction and heart failure. *Circulation.* (2016) 133:1249–63. doi: 10.1161/CIRCULATIONAHA.115.020502
41. Tong M, Saito T, Zhai P, Oka SI, Mizushima W, Nakamura M, et al. Mitophagy is essential for maintaining cardiac function during high fat diet-induced diabetic cardiomyopathy. *Circ Res.* (2019) 124:1360–71. doi: 10.1161/CIRCRESAHA.118.314607
42. Li G, Yang J, Yang C, Zhu M, Jin Y, McNutt MA, et al. PTENα regulates mitophagy and maintains mitochondrial quality control. *Autophagy.* (2018) 14:1742–60. doi: 10.1080/15548627.2018.1489477
43. Xu D, Zhao Y, Weng X, Lu Y, Li W, Tang K, et al. Novel role of mitochondrial GTPases 1 in pathological cardiac hypertrophy. *J Mol Cell Cardiol.* (2019) 128:105–16. doi: 10.1016/j.yjmcc.2019.01.025
44. Zou R, Tao J, Qiu J, Shi W, Zou M, Chen W, et al. Ndufs1 deficiency aggravates the mitochondrial membrane potential dysfunction in pressure overload-induced myocardial hypertrophy. *Oxid Med Cell Longev.* (2021) 2021:5545261. doi: 10.1155/2021/5545261
45. Cao Y, Xu C, Ye J, He Q, Zhang X, Jia S, et al. Miro2 regulates inter-mitochondrial communication in the heart and protects against TAC-induced cardiac dysfunction. *Circ Res.* (2019) 125:728–43. doi: 10.1161/CIRCRESAHA.119.315432
46. Ku HJ, Ahn Y, Lee JH, Park KM, Park JW. IDH2 deficiency promotes mitochondrial dysfunction and cardiac hypertrophy in mice. *Free Radic Biol Med.* (2015) 80:84–92. doi: 10.1016/j.freeradbiomed.2014.12.018
47. Kanaan GN, Ichim B, Gharibeh L, Maharsy W, Patten DA, Xuan JY, et al. Glutaredoxin-2 controls cardiac mitochondrial dynamics and energetics in mice, and protects against human cardiac pathologies. *Redox Biol.* (2018) 14:509–21. doi: 10.1016/j.redox.2017.10.019
48. McDermott-Roe C, Ye J, Ahmed R, Sun XM, Serafín A, Ware J, et al. Endonuclease G is a novel determinant of cardiac hypertrophy and mitochondrial function. *Nature.* (2011) 478:114–8. doi: 10.1038/nature10490
49. Winnik S, Auwerx J, Sinclair DA, Matter CM. Protective effects of sirtuins in cardiovascular diseases: from bench to bedside. *Eur Heart J.* (2015) 36:3404–12. doi: 10.1093/eurheartj/ehv290
50. Tang X, Chen XF, Wang NY, Wang XM, Liang ST, Zheng W, et al. SIRT2 Acts as a cardioprotective deacetylase in pathological cardiac hypertrophy. *Circulation.* (2017) 136:2051–67. doi: 10.1161/CIRCULATIONAHA.117.028728
51. Feng X, Wang Y, Chen W, Xu S, Li L, Geng Y, et al. SIRT3 inhibits cardiac hypertrophy by regulating PARP-1 activity. *Aging.* (2020) 12:4178–92. doi: 10.18632/aging.102862
52. Zeng H, Vaka VR, He X, Booz GW, Chen JX. High-fat diet induces cardiac remodelling and dysfunction: assessment of the role played by SIRT3 loss. *J Cell Mol Med.* (2015) 19:1847–56. doi: 10.1111/jcmm.12556
53. Luo YX, Tang X, An XZ, Xie XM, Chen XF, Zhao X, et al. SIRT4 accelerates Ang II-induced pathological cardiac hypertrophy by inhibiting manganese superoxide dismutase activity. *Eur Heart J.* (2017) 38:1389–98. doi: 10.1093/eurheartj/ehw138
54. Hershberger KA, Abraham DM, Martin AS, Mao L, Liu J, Gu H, et al. Sirtuin 5 is required for mouse survival in response to cardiac pressure overload. *J Biol Chem.* (2017) 292:19767–81. doi: 10.1074/jbc.M117.809897
55. Sundaresan NR, Vasudevan P, Zhong L, Kim G, Samant S, Parekh V, et al. The sirtuin SIRT6 blocks IGF-Akt signaling and development of cardiac hypertrophy by targeting c-Jun. *Nat Med.* (2012) 18:1643–50. doi: 10.1038/nm.2961
56. Yamamura S, Izumiya Y, Araki S, Nakamura T, Kimura Y, Hanatani S, et al. Cardiomyocyte Sirt (Sirtuin) 7 Ameliorates Stress-Induced Cardiac Hypertrophy by Interacting With and Deacetylating GATA4. *Hypertension.* (2020) 75:98–108. doi: 10.1161/HYPERTENSIONAHA.119.13357
57. Ito S, Asakura M, Liao Y, Min KD, Takahashi A, Shindo K, et al. Identification of the Mtus1 splice variant as a novel inhibitory factor against cardiac hypertrophy. *J Am Heart Assoc.* (2016) 5:e003521. doi: 10.1161/JAHA.116.003521
58. Tang K, Zhao Y, Li H, Zhu M, Li W, Liu W, et al. Translocase of inner membrane 50 functions as a novel protective regulator of pathological cardiac hypertrophy. *J Am Heart Assoc.* (2017) 6:e004346. doi: 10.1161/JAHA.116.004346
59. Conejeros C, Parra V, Sanchez G, Pedrozo Z, Olmedo I. Miro1 as a novel regulator of hypertrophy in neonatal rat cardiomyocytes. *J Mol Cell Cardiol.* (2020) 141:65–9. doi: 10.1016/j.yjmcc.2020.03.014

60. Hasan P, Saotome M, Ikoma T, Iguchi K, Kawasaki H, Iwashita T, et al. Mitochondrial fission protein, dynamin-related protein 1, contributes to the promotion of hypertensive cardiac hypertrophy and fibrosis in Dahl-salt sensitive rats. *J Mol Cell Cardiol.* (2018) 121:103–6. doi: 10.1016/j.yjmcc.2018.07.004
61. Wang T, Zhai M, Xu S, Ponnusamy M, Huang Y, Liu CY, et al. NFATc3-dependent expression of miR-153-3p promotes mitochondrial fragmentation in cardiac hypertrophy by impairing mitofusin-1 expression. *Theranostics.* (2020) 10:553–66. doi: 10.7150/thno.37181
62. Guan X, Wang L, Liu Z, Guo X, Jiang Y, Lu Y, et al. miR-106a promotes cardiac hypertrophy by targeting mitofusin 2. *J Mol Cell Cardiol.* (2016) 99:207–17. doi: 10.1016/j.yjmcc.2016.08.016
63. Sun YL, Li SH, Yang L, Wang Y. miR-376b-3p attenuates mitochondrial fission and cardiac hypertrophy by targeting mitochondrial fission factor. *Clin Exp Pharmacol Physiol.* (2018) 45:779–87. doi: 10.1111/1440-1681.12938
64. Zhao Y, Ponnusamy M, Liu C, Tian J, Dong Y, Gao J, et al. MiR-485-5p modulates mitochondrial fission through targeting mitochondrial anchored protein ligase in cardiac hypertrophy. *Mol Basis Dis.* (2017) 1863:2871–81. doi: 10.1016/j.bbadis.2017.07.034
65. Li G, Shao Y, Guo HC, Zhi Y, Qiao B, Ma K, et al. MicroRNA-27b-3p downregulates FGF1 and aggravates pathological cardiac remodelling. *Cardiovasc Res.* (2021) cvab248. doi: 10.1093/cvr/cvab248
66. Liu BL, Cheng M, Hu S, Wang S, Wang L, Tu X, et al. Overexpression of miR-142-3p improves mitochondrial function in cardiac hypertrophy. *Biomed Pharmacother.* (2018) 108:1347–56. doi: 10.1016/j.biopha.2018.09.146
67. Liu X, Gao S, Gao H, Jiang X, Wei Q. Mitochondrial disruption is involved in the effect of nuclear factor of activated t cells, cytoplasmic 4 on aggravating cardiomyocyte hypertrophy. *J Cardiovasc Pharmacol.* (2021) 77:557–69. doi: 10.1097/FJC.0000000000000986
68. Chen Y, Zeng M, Zhang Y, Guo H, Ding W, Sun T. Nlrp3 deficiency alleviates angiotensin ii-induced cardiomyopathy by inhibiting mitochondrial dysfunction. *Oxid Med Cell Longev.* (2021) 2021:6679100. doi: 10.1155/2021/6679100
69. Lu Z, Cui Y, Wei X, Gao P, Zhang H, Wei X, et al. Deficiency of PKD2L1 (TRPP3) exacerbates pathological cardiac hypertrophy by augmenting NCX1-mediated mitochondrial calcium overload. *Cell Rep.* (2018) 24:1639–52. doi: 10.1016/j.celrep.2018.07.022
70. Zhao J, Yin M, Deng H, Jin FQ, Xu S, Lu Y, et al. Cardiac Gab1 deletion leads to dilated cardiomyopathy associated with mitochondrial damage and cardiomyocyte apoptosis. *Cell Death Differ.* (2016) 23:695–706. doi: 10.1038/cdd.2015.143
71. Wei XH, Guo X, Pan CS, Li H, Cui YC, Yan L, et al. Quantitative proteomics reveal that metabolic improvement contributes to the cardioprotective effect of T(89) on isoproterenol-induced cardiac injury. *Front Physiol.* (2021) 12:653349. doi: 10.3389/fphys.2021.653349
72. Zhang X, Zhang Z, Wang P, Han Y, Liu L, Li J, et al. Bawei chenxiang wan ameliorates cardiac hypertrophy by activating AMPK/PPAR-α signaling pathway improving energy metabolism. *Front Pharmacol.* (2021) 12:653901. doi: 10.3389/fphar.2021.653901
73. Abudureyimu M, Yu W, Cao RY, Zhang Y, Liu H, Zheng H. Berberine promotes cardiac function by upregulating PINK1/Parkin-mediated mitophagy in heart failure. *Front Physiol.* (2020) 11:565751. doi: 10.3389/fphys.2020.565751
74. Liu BY, Li L, Liu GL, Ding W, Chang WG, Xu T, et al. Baicalein attenuates cardiac hypertrophy in mice via suppressing oxidative stress and activating autophagy in cardiomyocytes. *Acta Pharmacol Sin.* (2021) 42:701–14. doi: 10.1038/s41401-020-0496-1
75. Pillai VB, Samant S, Sundaresan NR, Raghuraman H, Kim G, Bonner MY, et al. Honokiol blocks and reverses cardiac hypertrophy in mice by activating mitochondrial Sirt3. *Nat Commun.* (2015) 6:6656. doi: 10.1038/ncomms7656
76. Gao J, Zhang K, Wang Y, Guo R, Liu H, Jia C, et al. A machine learning-driven study indicates emodin improves cardiac hypertrophy by modulation of mitochondrial SIRT3 signaling. *Pharmacol Res.* (2020) 155:104739. doi: 10.1016/j.phrs.2020.104739
77. Ramalingam A, Budin SB, Mohd Fauzi N, Ritchie RH, Zainalabidin S. Targeting mitochondrial reactive oxygen species-mediated oxidative stress attenuates nicotine-induced cardiac remodeling and dysfunction. *Sci Rep.* (2021) 11:13845. doi: 10.1038/s41598-021-93234-4
78. Li W, Yin L, Sun X, Wu J, Dong Z, Hu K, et al. Alpha-lipoic acid protects against pressure overload-induced heart failure via ALDH2-dependent Nrf1-FUNDC1 signaling. *Cell Death Dis.* (2020) 11:599. doi: 10.1038/s41419-020-02805-2
79. Meng G, Liu J, Liu S, Song Q, Liu L, Xie L, et al. Hydrogen sulfide pretreatment improves mitochondrial function in myocardial hypertrophy via a SIRT3-dependent manner. *Br J Pharmacol.* (2018) 175:1126–45. doi: 10.1111/bph.13861
80. Huang L, Chen R, Liu L, Zhou Y, Chen Z. Lactoferrin ameliorates pathological cardiac hypertrophy related to mitochondrial quality control in aged mice. *Food Funct.* (2021) 12:7514–26. doi: 10.1039/D0FO03346D
81. Ma M, Chen W, Hua Y, Jia H, Song Y, Wang Y. Aerobic exercise ameliorates cardiac hypertrophy by regulating mitochondrial quality control and endoplasmic reticulum stress through M(2) AChR. *J Cell Physiol.* (2021) 236:6581–96. doi: 10.1002/jcp.30342
82. An D, Zeng Q, Zhang P, Ma Z, Zhang H, Liu Z, et al. Alpha-ketoglutarate ameliorates pressure overload-induced chronic cardiac dysfunction in mice. *Redox Biol.* (2021) 46:102088. doi: 10.1016/j.redox.2021.102088
83. Mohammed SA, Paramesha B, Meghwani H, Kumar Reddy MP, Arava SK, Banerjee SK. Allyl methyl sulfide preserved pressure overload-induced heart failure via modulation of mitochondrial function. *Biomed Pharmacother.* (2021) 138:111316. doi: 10.1016/j.biopha.2021.111316
84. Lucas AMB, de Lacerda Alexandre JV, Araújo MTS, David CEB, Ponte Viana YI, Coelho BN, et al. Diazoxide modulates cardiac hypertrophy by targeting H2O2 generation and mitochondrial superoxide dismutase activity. *Curr Mol Pharmacol.* (2020) 13:76–83. doi: 10.2174/1874467212666190723144006

Conflict of Interest: The authors declare that the research was conducted in the absence of any commercial or financial relationships that could be construed as a potential conflict of interest.

Publisher's Note: All claims expressed in this article are solely those of the authors and do not necessarily represent those of their affiliated organizations, or those of the publisher, the editors and the reviewers. Any product that may be evaluated in this article, or claim that may be made by its manufacturer, is not guaranteed or endorsed by the publisher.

Copyright © 2022 Yang, Liu, Liu, Guo, An, Wang, Yang, Fan and Tang. This is an open-access article distributed under the terms of the Creative Commons Attribution License (CC BY). The use, distribution or reproduction in other forums is permitted, provided the original author(s) and the copyright owner(s) are credited and that the original publication in this journal is cited, in accordance with accepted academic practice. No use, distribution or reproduction is permitted which does not comply with these terms.

frontiers in Cardiovascular Medicine

REVIEW
published: 14 February 2022
doi: 10.3389/fcvm.2021.808115

Mitochondrial DNA Depletion Syndrome and Its Associated Cardiac Disease

Haiying Wang[1], Yijun Han[2], Shenwei Li[3], Yunan Chen[3], Yafen Chen[3], Jing Wang[4], Yuqing Zhang[3], Yawen Zhang[3], Jingsuo Wang[3], Yong Xia[5] and Jinxiang Yuan[6]**

[1] Department of Physiology, Institute of Basic Medical College, Jining Medical University, Jining, China, [2] Clinical Medical College, Jining Medical University, Jining, China, [3] Institute of Basic Medical College, Jining Medical University, Jining, China, [4] Dongying Fifth People's Hospital, Dongying, China, [5] Key Laboratory of Precision Oncology of Shandong Higher Education, Institute of Precision Medicine, Jining Medical University, Jining, China, [6] The Collaborative Innovation Center, Jining Medical University, Jining, China

Mitochondria is a ubiquitous, energy-supplying (ATP-based) organelle found in nearly all eukaryotes. It acts as a "power plant" by producing ATP through oxidative phosphorylation, providing energy for the cell. The bioenergetic functions of mitochondria are regulated by nuclear genes (nDNA). Mitochondrial DNA (mtDNA) and respiratory enzymes lose normal structure and function when nuclear genes encoding the related mitochondrial factors are impaired, resulting in deficiency in energy production. Massive generation of reactive oxygen species and calcium overload are common causes of mitochondrial diseases. The mitochondrial depletion syndrome (MDS) is associated with the mutations of mitochondrial genes in the nucleus. It is a heterogeneous group of progressive disorders characterized by the low mtDNA copy number. *TK2*, *FBXL4*, *TYPM*, and *AGK* are genes known to be related to MDS. More recent studies identified new mutation loci associated with this disease. Herein, we first summarize the structure and function of mitochondria, and then discuss the characteristics of various types of MDS and its association with cardiac diseases.

Keywords: mitochondrial DNA depletion syndrome, nuclear gene mutation, mtDNA, cardiac disease, ATP

OPEN ACCESS

Edited by:
Jian Wu,
Fudan University, China

Reviewed by:
Jinxi Wang,
The University of Iowa, United States
Pan Gao,
Fudan University, China

Correspondence:
Jinxiang Yuan
yuanjinxiang18@163.com
Yong Xia
xiayong@mail.jnmc.edu.cn

Specialty section:
This article was submitted to Cardiovascular Metabolism, a section of the journal Frontiers in Cardiovascular Medicine

Received: *03 November 2021*
Accepted: *23 December 2021*
Published: *14 February 2022*

Citation:
Wang H, Han Y, Li S, Chen Y, Chen Y, Wang J, Zhang Y, Zhang Y, Wang J, Xia Y and Yuan J (2022) Mitochondrial DNA Depletion Syndrome and Its Associated Cardiac Disease. Front. Cardiovasc. Med. 8:808115. doi: 10.3389/fcvm.2021.808115

STRUCTURE AND FUNCTION OF MITOCHONDRIA

Mitochondrial Structure

The mitochondrion is a double membraned organelle commonly found in eukaryotic cells. It consists of four compartments: an outer mitochondrial membrane (OMM), an inner mitochondrial membrane (IMM), a mitochondrial intermembrane space (IMS), and membrane matrix. The OMM is smooth and contains plenty of pore-forming components. The IMM curves inward and folds into a crest containing a large number of enzymes. It is the site of biological oxidation, a process involving respiratory chain complex (CI-IV) and ATP synthase (CV) (1). IMS, located between the OMM and IMM, contains cytochrome c (Cyt-c), ADP/ATP carrier (AAC), and biotic factors and enzyme proteins including apoptosis-inducing factor (AIF) and pro-caspase 2, 3, 9. Mitochondrial permeability transition pores (MPTP) exist at the OMM-IMM contact site. The opening of MPTPs is related to mitochondrial membrane permeability and is subjected to regulation by lipometabolism, mitochondrial membrane potential change, oxidative stress, and other factors (2). Membrane matrix is a single continuous space containing reactive enzymes,

mitochondrial genome, mitochondrial DNA (mtDNA), ribosomal RNA (rRNA), and transfer RNA (tRNA), which have functional roles in biotransformation and synthesis. Mitochondria are semi-autonomous organelles that are strongly dependent on the biological function of nuclear genes. In mammals, mtDNA consists of 37 genes, including 22 tRNA genes, 13 genes encoding mitochondrial respiratory chain and oxidative phosphorylation-related protein subunits that assemble respiratory chain complex I-IV(CI-CIV), and 2 rRNA genes (12S and 16S) (3). The majority of mitochondrial proteins are encoded by nucleic genes which first synthesize precursor proteins, and then process in the mitochondria to form mature proteins (4). Mitochondria are the "power workshops" of cells. They provide energy for cellular activities and perform biological functions such as signal transduction and biological oxidation.

Mitochondrial Function

ATP Production by Oxidative Phosphorylation

Mitochondria is the metabolic center of cellular activities. ATP is often called "energy currency" of the cell, and the breakage of high energy phosphate bonds by hydrolysis can provide energy for cellular activities. ATP synthesis is indispensable of oxidative phosphorylation (OXPHOS). OXPHOS is closely related to material energy metabolism (5), electron transfer of the mitochondrial respiratory chain and the enzymatic reaction of a series of protease complexes. OXPHOS contributes to ninety percent of the energy production in eukaryotic cells. On the lipid double layers embedded in IMM, electrons are transmitted to O_2 by compound I-IV on the respiratory chain, while simultaneously releasing energy for ATP production in coupling with F0/F1-ATP synthase (complex V) (6) (**Figure 1**). ATP synthesis is impaired when mitochondrial phosphorylation function becomes dysregulated.

Changes in the Mitochondrial Membrane Potential ($\Delta\psi$) via Electron Transfer in the Mitochondrial Respiratory Chain

The transmission of mitochondrial respiratory chain is indispensable of electronic transfer. Therefore, the process is known as the electron transport chain (ETC). Mitochondria pass through complexes I (CI or NADH: ubiquinone oxidoreductase or NADH dehydrogenase), II (CII, succinic acid: ubiquinone oxidoreductase), III (CIII, ubiquinone: Ferric cytochrome C reductase) and IV (CIV, cytochrome C oxidoreductase), transfer electrons to O_2, and release energy which couples with complex V (CV, ATP synthase) to form ATP (7). In mammals, CI is the largest mitochondrial complex composed of 45 subunits, of which 7 are encoded by mitochondrial DNA, namely ND1, ND2, ND3, ND4, ND4L, ND5, and ND6, and the remaining 38 subunits are encoded by nuclear genes. NADH: ubiquinone oxidoreductase subunit AB1 (NDUFAB1), or known as mitochondrial acyl carrier protein, is an important subunit of CI, which can mediate cardioprotective mechanisms and improve mitochondrial bioenergy (8). CIV consists of 13 subunits, of which the largest three subunits (COX I, COX II and COX III) are encoded by mtDNA and can form the core of the cascade reaction, while the remaining 10 subunits (COIV, Va, Vb, VIa-c, VIIa-c, and VIII) are encoded by nDNA. Moreover, the activity of CIV is highly relevant to muscle OXPHOS, followed by CII. CIIIis the most critical mitochondrial respiratory chain enzyme, consisting of 11 different subunits, of which only Cytb is encoded by mtDNA, and Cytb forms a dimer with Cyt C_1 and iron-sulfur protein (Fe-S) (9). CIII transfers electrons from panthenol (reductive coenzyme Q or CoQ) to cytochrome C (Cyt C) through a catalytic mechanism, while protons are transferred from the mitochondrial matrix to the IMS (10) (**Figure 1**). In the process of electron transfer, the complexes interact with each other to form an advanced supramolecular structure known as the supercomplex (SCs) and respiratory corules (11). SCs can improve the efficiency of electron flux through substrate channels or enhanced catalysis, thus promoting electron transport, isolating reaction intermediates and preventing reactive oxygen species (ROS) generation (12).

Mitochondrial and Reactive Oxygen Species

During ATP generation, ETC, and Krebs cycle inevitably lead to electron leakage, causing incomplete reduction of O_2 and formation of free radicals in a form of superoxide anion (O^{2-}). At this point, if the muscle remains in a long-term contraction state, the content of ATP generated by oxidative phosphorylation of respiratory chain increases, and electrons overflow into ETC to generate ROS (13). Furthermore, a low level of ROS can act as signaling molecules that maintain normal cell signal transduction. In contrast, a high level of ROS produced more than endogenous scavenging capacity can trigger cascade reactions that damage cellular macromolecules, such as DNA and proteins. Excessive ROS can also reduce the Ca^{2+}sensitivity of myofibril and damage the contractile function of muscle, possibly through enzyme complexes i and iii (Ci, Ciii)-dependent and/or reduced nicotinamide adenine dinucleotide (NADPH) oxidase-dependent pathways. Alternatively, α-ketoglutaric acid in succinyl-coenzyme A can be oxidized indirectly through mitochondria dehydrogenase to generate NADH, which is responsible for ROS overproduction (14). It has been shown that ROS produced by ETC can damage mtDNA. In the absence of proper repair, DNA damage accumulates, causing a series of mitochondrial-related diseases (15).

Role of Oxygen in Mitochondrial Function

Oxygen is key to the functionality of mitochondria. Oxygen affects normal structure and function of the mitochondria. In the third stage of aerobic respiration, mitochondria use NADH, a product of glycolysis and Tricarboxylic Acid Cycle (TCA), reduced flavin adenosine dinucleotide, $FADH_2$ and other high-energy molecules to reduce oxygen, thereby releasing energy to synthesize ATP. The content of oxygen in the environment is closely related to normal oxidative phosphorylation function of mitochondria (16, 17). In mammals, hypoxic signaling protein (HIF) determines the cellular response to hypoxia. Stable HIF protein controls the expression of glycolysis-related target genes at an appropriate level and maintains ROS production at a low, physiological level by changing the structure of CI, II and IV ETC complexes and reducing the enzyme activity of the complex (18). The morphology of fetal cardiac mitochondria at birth is associated with hypoxia signaling.

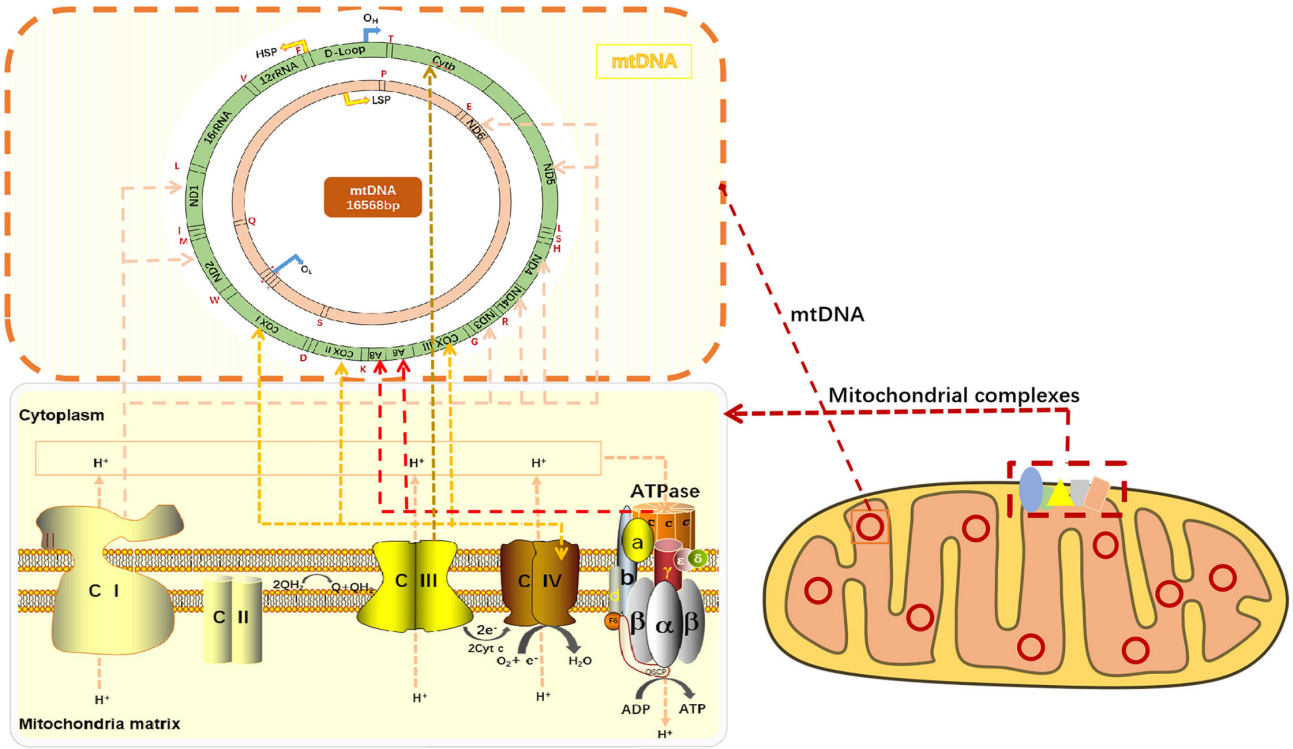

FIGURE 1 | mtDNA encodes respiratory chain complexes for electron transport. Mitochondrial respiratory chain complex I (NADH oxidase) and mitochondrial respiratory chain complex II (succinate dehydrogenase) are the major components of electron entry into mitochondrial electron transport chain (ETC). Complexes I and II catalyze NADH oxidation and succinic acid oxidation to fumaric acid, respectively. Next, coenzyme Q (Q) forms coenzyme (QH2), leading to a decrease in oxygen (the final electron receptor). Mitochondrial respiratory chain complex III (cytochrome c oxidoreductase) is the gatekeeper of the mitochondrial respiratory chain and the main source of reactive oxygen species III, which transfers electrons from panthepanol (reduced coenzyme Q or CoQ) to cytochrome c (cyt c) through a catalytic mechanism of the Q cycle. The mitochondrial respiratory chain complex IV (cytochrome c oxidase) is the final electron acceptor of the mitochondrial ETC, which converts oxygen into water through the oxidation of cyt c, a process associated with ATP synthesis in the mitochondrial membrane. Mitochondrial respiratory chain complex V, also known as F1F0-ATPASE or ATP synthase, works with the four complexes to complete oxidative phosphorylation for ATP production. CI or NADH: Ubiquinone oxidoreductase or NADH encoded by ND1, ND2, ND3, ND4, ND4L, ND5, and ND6 on mtDNA, respectively; CII: dehydrogenase succinic acid, ubiquinone oxidoreductase; CIII: Ubiquinone and ferricytochrome C reducing enzyme encoded by Cytb part on mtDNA, respectively; CIV: CIV, cytochrome c oxidoreductase encoded by COXI, COXII, and COXIII on mtDNA, respectively; The red letters T, F, V, L, I, M, W, D, K, G, R, H, S, L, A, N, C, Y, S, E, P, and Q all indicate tRNA.

Downregulation of mitochondrial HIF pathway after birth leads to increased respiratory capacity and oxidative phosphorylation. Neary et al. found that HIF signal transduction was maintained under normoxic conditions in mouse heart. The α-subunit proline residues of HIF-α are continuously hydroxylated by Prolyl Hydroxylase (PHD) under normoxic conditions. Hypoxia inhibits PHD, which stabilizes HIF-α and promotes its migration to the nucleus where it dimers with the β subunit and binds to the promoters or enhancers through the hypoxia response elements (HRE) to initiate gene transcription (19, 20). Mitochondria are the main oxygen consumers in the heart. When cardiomyocytes are hypoxic, anaerobic glycolysis increases whereas both mitochondrial oxygen consumption and respiration rate decrease. Ambrose et al. have established a cell model of cardiac hypoxia by using HL-1 cardiomyocytes cells highly related to adult cardiac metabolism. The investigators found that the number of mitochondria increased with a simultaneous decrease in CIV activity after 24 h of hypoxia, suggesting that mitochondria keep their total content fairly consistent during remodeling (21).

Mitochondria and Cell Metabolism

Mitochondria achieve metabolic functions mainly by oxidative phosphorylation, ATP production, NADH oxidation, glycolysis and $FADH_2$ production, TCA cycle, and β–oxidation of fatty acids (22). Meanwhile, mitochondria regulate their fusion, fission, biosynthesis, and degradation through metabolism.

Metabolism-Related Biochemical Reactions

Metabolism is fundamental to cellular activities. It represents distinct processes by which human body converts the nutrients, including sugars, lipids and proteins, into small molecules for absorption and consumption. Fatty acid β -oxidation (FAO) is a major process of long-chain fatty acid metabolism. It produces acetyl coenzyme A (acetyl-CoA), NADH, and $FADH_2$ (23). The TCA, also known as the Krebs cycle, is the hub that links

the metabolism of three nutrients. Acetyl-CoA is a common end product of nutrient metabolism, which eventually enters TCA in the form of citrate for thorough oxidation (24). Acetyl CoA is decomposed into CO_2 and H. H is delivered to flavin adenine dinucleotide (FAD) and oxidized nicotinamide adenine dinucleotide (NAD+) to generate $FADH_2$ and NADH (25). Metabolism and energy homeostasis are maintained through the activities of various enzymes including AMP-activated protein kinase (AMPK), a conserved protein present in all eukaryotes. AMPK is involved in the metabolism of lipids and carbohydrates. AMPK is activated when the intracellular AMP concentration increases or the skeletal muscle contracts. The activity of AMPK is also regulated by hormones, cytokines, and ROS (26).

Metabolic Regulation of Mitochondrial Dynamics

Mitochondria are highly dynamic organelles. Mitochondrial dynamics is a physiological process in which mitochondria undergo continuous cycles of fusion and division, resulting in changes in the shape, size and position of mitochondria. Mitochondrial dynamics is often determined by the dynamic balances between fission and fusion as well as between biogenesis and degradation such as mitochondrial phagocytosis (27). Mitochondrial fission and fusion are of great importance in the growth and redistribution of mitochondria and the maintenance of a healthy mitochondrial network (28, 29). Through continuous fusion and fission, mitochondria can exchange the damaged mitochondrial DNA and protein lipids with normal counterparts, thus maintaining the stability of mitochondrial structure and function (30). During this process, the core proteins that mediate mitochondrial division and fusion are membrane remodeling mechanochemical enzymes, such as dynein-related protein-like 1 (Drp1/DLP1), optic nerve atrophy 1 (OPA1), and mitochondrial protein (Mfn). Drp1 regulate fission, while OPA1 and Mfn modulate the fusion of IMM and OMM, respectively (31). It is likely that the processes of mitochondrial fission and fusion are asymmetric in the formation of daughter mitochondria. It has been found that the dynamic changes in mitochondria and CR structure formed by endointimal folding have a significant impact on the integrity of mtDNA. CR distortion often leads to mtDNA loss (32). Genetic loss of mitochondrial fusion can result in inadequate mitochondrial mixing, which links to great heterogeneity of mitochondrial proteins, DNA, and membrane potentials. A function of fission is to identify dysfunctional offspring mitochondria, which are subsequently removed by mitochondrial phagocytosis and coordinate for inhibition of mitochondrial fusion (33). Normal mitochondrial biogenesis depends not only on the action of nDNA and mtDNA, but also on the coordination of mitochondrial DNA replication and fusion with division. Environmental factors, such as oxidative stress, exercise, temperature stress (cold or heat), cell division, regeneration and differentiation, can promote mitochondrial biogenesis. Inhibition of mitochondrial dynamics has some effects on the elimination of irreparable mtDNA damage and transmission of mtDNA mutations (34).

Ca^{2+} Storage

Accumulation of Ca^{2+} in the mitochondrial matrix regulates aerobic metabolism by activating enzymes in the metabolic reactions. Under physiological conditions, Ca^{2+} actively regulates the key dehydrogenase in the TCA response, which is conducive to the regulation of Ca^{2+}-dependent functions in the cytoplasm. Under pathological conditions, high Ca^{2+} concentration can promote the opening of mitochondrial permeability transition pore (MPTP) and induce apoptotic death (35, 36). Excessive deposition of Ca^{2+} often leads to decreased ATP synthesis and increased ROS production, thus aggravating oxidative stress responses. Ca^{2+} overload is often associated with intracellular Ca^{2+} leakage. Sarcoplasmic reticulum (SR) Ca^{2+} leakage mainly occurs through type 2 Ryanodine receptor (RyR2). It plays a fundamental role in Ca^{2+} pathophysiology. RyR2 regulates the level of Ca^{2+} by influencing cardiac excitation-contraction (E-C) coupling (37). Ca^{2+} concentration in mitochondria is also regulated by genes encoding Ca^{2+} unidirectional complexes, including mitochondrial calcium uniporter (MCU) and its regulator Ca^{2+} uptake protein 1 located in the IMM (38). Ca^{2+} absorption is dependent on the energy transfer of the respiratory chain. Due to the restriction of IMM on MCU, a high level of Ca^{2+} is required for MCU to enter the mitochondrial matrix, thus, Ca^{2+} absorption is relatively easy in the vicinity of Ca^{2+} release reservoirs, such as the endoplasmic reticulum (ER). Mitochondria-associated endoplasmic reticulum membrane (MAM) has been found to transport Ca^{2+}. Ca^{2+} can be directly transferred to mitochondria *via* ER membrane where it controls the relevant mitochondrial functions (39).

Mitochondrial Genome Regulation of Its Function

The mitochondrial genome consists of 37 genes, including 22 tRNA genes, 13 genes that encode the subunits of mitochondrial respiratory chain and oxidative phosphorylation-related proteins snd 2 rRNA genes (12S and 16S). Nuclear genes encode about 1,500 mitochondrial proteins, which comprise the majority of mitochondrial respiratory chain polypeptides (40). Additionally, mtDNA also encodes 13 core catalytic peptides, including oxidative phosphorylation complexes i, iii, and iv (41).

It appears that mtDNA depends on mitochondrial nDNA to complete its replication, transcription, translation as well as other processes. Therefore, both nDNA and mtDNA have the regulatory effects on mitochondria, and they jointly ensure the normal function of the mitochondria (42). Given that mtDNA encodes subunits of the respiratory chain complex, mutations in mtDNA can damage the enzymatic activity of oxidative phosphorylation reaction complex, in particular CI, affecting mitochondrial biogenesis (43). The level of mtDNA correlates to mitochondrial fusion. In skeletal muscle, the association between fusion and enzymatic activity in OXPHOS may limit mtDNA defects to the local regions of muscle fibers, which are often associated with mitochondrial myopathy (44). Altogether, mitochondria regulate cell metabolism, growth, senescence, and apoptosis through the coordinated actions of nDNA and mtDNA.

MITOCHONDRIAL DNA DEPLETION SYNDROME

As an autosomal recessive disease, mitochondrial DNA depletion syndrome (MDS) is characterized by severe reduction in mtDNA content in the affected tissues and organs (45). Because mtDNA is controlled by nDNA, the copy number of mitochondria may be reduced when the nuclear gene mutations destroy deoxyribonucleotide metabolism in the affected tissues. The production of key subunits of mitochondrial respiratory chain complex and energy production require a sufficient amount of mtDNA. Deletion of mtDNA can lead to organ dysfunction as a result of insufficient synthesis of respiratory chain components (46–48). Commonly mutated genes include *TK2*, *FBXL4*, *TYPM*, *AGK*, and others. MDS is classified as four forms, which are myopathic form, encephalomyopathic form, hepatocerebral form, and neurogastrointestinal form (49). MDS is usually involved in multiple systems with muscle-related symptoms, such as dystonia and muscle atrophy (50, 51).

Myopathic Mitochondrial DNA Depletion Syndrome

Myopathic MDS, also known as mitochondrial DNA depletion syndrome 2 (MTDPS2) or *TK2* deficiency, is characterized by the reduction of mtDNA content in the affected tissues. It is often associated with severe progressive muscle weakness. Dysphagia mainly involves the respiratory system with other clinical manifestations (52). Some patients have clinical symptoms of hypertrophic cardiomyopathy (53). This type of MDS is usually caused by mutation of *TK2* gene. It occurs in early childhood and presents in the form of myopathy, mostly accompanied by mtDNA deletion/depletion and increased serum level of creatine kinase (CK) (54, 55). *TK2*, located on chromosome 16Q21, encodes a mitochondrial enzyme, thymidine kinase 2 (*TK2*). *TK2* is a rate-limiting enzyme which mediates deoxypyrimidine phosphorylation (56). In non-replicating cells, *TK2* is also involved in the maintenance of dNTP (57). In clinical and molecular genetics, myopathic MDS can be further divided into three different subtypes, namely, paroxysmal myopathy in infants with severe depletion of mtDNA, paroxysmal myopathy in childhood, and delayed myopathy, among which delayed myopathy is the rarest. In addition to muscle weakness, delayed myopathy can also progress to respiratory insufficiency. Different from the previous two, in addition to muscle weakness, respiratory insufficiency can also be developed at the onset and after 12 years old. Muscle mtDNA can show myopathy with deletion, multiple deletion, or both (58).

Encephalomyopathic Mitochondrial DNA Depletion Syndrome

Encephalomyopathic is a relatively common form of MDS, in particular among adults who have progressive external eye muscle paralysis (adPEO). adPEO manifests by ptosis and severe limitation of eye movement. It may also lead to ataxia and cataract (59). Mitochondrial DNA depletion syndrome 13 (MTDPS 13), also known as *FBXL4*-related encephalopathy, is a form of MDS manifested by early lactic acidosis, hypotonia, developmental delay, and feeding difficulty (60). In some cases, encephalopathic MDS accompanies liver disease to form hepatocerebral MDS (59). Mitochondrial DNA depletion syndrome 9 (MTDPS 9) can also occur in patients with cerebromyopathic MDS. Lu et al. reported a case of infantile encephalomyopathic MDS associated with *SUCLG 1* (succinic acid A ligase α subunit) gene in 2017. The case is manifested by neuromyopathy-like symptoms including muscular hypotonia, psychomotor retardation, brain atrophy, developmental delay, and increased levels of methylmalonic acid and its metabolite (61). Encephalomyopathy can be caused by single gene or polygenic mutations with similar effects. These genes may have synergistic effect on the development of MDS (45).

Hepatocerebral Mitochondrial DNA Depletion Syndrome

Hepatocerebral MDS is one of the most common MDS diseases, and at least 50 kinds of related gene mutations have been discovered (62). This disease may occur in newborns within 6 months after birth, as characterized by vomiting, developmental delay, serious progressive liver failure, hypotonia, hyperreflexia, irritability, and hypoglycemia. Patients often die within a year after the onset of symptoms (63). Hyperlactatemia and 3-methylglutaric aciduria are the well-known characteristics of patients with hepatic encephalopathy, while some patients are accompanied by nephrolithiasis or mild ventricular hypertrophy (64). The liver biopsy can show varying degrees of steatosis, bile duct hyperplasia, fibrosis, lobular collapse, and other symptoms. Studies have shown that most patients presented a pattern of fibrosis with neovascularization following diffuse necrosis (65). Reduction of cytochrome-C oxidase (COX) and combined defects of mitochondrial respiratory chain complex may also be detected in infants' livers (66). Clinically, the identified liver-brain type mutations include *POLG1*, *DGUOK*, *C10orf2*, and *MPV17*, among which *MPV17* is relatively rare (67).

Neurogastrointestinal Mitochondrial DNA Depletion Syndrome

Mitochondrial neurogastrointestinal mitochondrial DNA depletion disease (MNGIE) is a rare metabolic disease caused by *TYMP* gene mutation encodes thymidine phosphorylase (TP). Patients with inherited, autosomal recessive *TYMP* mutations show clinical symptoms between 10 and 50 years old, most of which appear before 20 years old (68). In MNGIE, a loss of TP activity leads to the accumulation of deoxyuridine (dUrd) and thymidine (Thd), which infiltrate through the mitochondrial pyrimidine remedy pathway, leading to an imbalance of deoxyuridine triphosphate pool (dNTP). This damages mtDNA, resulting in mitochondrial depletion and ultimately cell death (69). The clinical manifestations of MNGIE include gastrointestinal motility disorders, cachexia, ptosis, ophthalmoplegia, peripheral neuropathy, and related encephalopathy, which often lead to death in adulthood (70). The detection of hypoxia inducible factor-1α (HIF-1α) and vascular endothelial growth factor (VEGF) protein

expression proved that MNGIE patients were accompanied by gastrointestinal vascular diseases (71). Currently, hemodialysis can temporarily eliminate the toxic effects of Thd and dUrd in patients. However, permanent TP replacement therapy with AHSCT is required for more effective treatments of MNGIE (69). The correlation between MNGIE vascular changes and neuromuscular abnormalities provides a new strategy for the treatment of this disease (72). Carrier erythrocyte entrapped thymidine phosphorylase therapy and allogeneic hematopoietic stem cell transplantation are currently available clinical therapeutic options for MNGIE (71).

MDS AND ITS ASSOCIATION WITH CARDIAC DISEASE

Highly energy-consuming organs including heart requires a proper function of mitochondria. Cardiac energy is primarily provided through mitochondrial OXPHOS (73). Cardiomyocytes are prone to hypoxia. There are two mitochondrial populations in cardiomyocytes, namely, interfibrous mitochondria and submyomembrane mitochondria. The interstitial mitochondria are arranged longitudinally and in parallel. The cristae are mainly arranged in tubular shape. Subsarcolemmal mitochondria gather beneath the sarcolemma in the direction of lamellar ridge (74). Mitochondria are vital for the development and maintenance of heart muscle, the largest energy user in the human body. Mitochondria are not only a source of ATP energy, but also generators of ROS, which can both regulate physiological processes, such as the transition from hyperplastic growth to hypertrophic growth after birth, and cause oxidative damage. Excessive ROS production and oxidative damage are associated with cardiac pathology (75). In addition to lowering bioenergy efficiency, damaged mitochondria also produce more reactive oxygen species, resulting in harmful functional and structural consequences in the cardiovascular system (76). The increased production of ROS leads to vascular inflammation, endothelial cell damage and deposition of oxidized low density protein (oxLDL) in the arterial wall (77). In cardiomyocytes, two mitochondrial populations are electrically coupled to each other, providing electrical conduction from one to the other (78). Dysfunctional mitochondria can impair electronic transfer chain activity, cause ATP depletion, increase oxidative stress, and activate intrinsic apoptosis, leading to myocardial cell death (79). Metabolism is not only crucial for regulating the pump function of the heart, but also for maintaining the functional balance and cellular senescence of cardiomyocytes (80). The important functions of mitochondria in redox balance, energy metabolism and calcium balance determine its pathogenic role in heart failure (HF) and cardiovascular disease (CVD) (81–83). There is no effective treatment at present (84). Accumulation of evidence on mitochondrial therapy may help to provides new targets for the treatment of MDS-associated heart disease (85).

Mitochondria, as an important energy "power plant" of the human body, are closely related to the function of the heart. The changes in mitochondrial structure and physiological function play important roles in heart development, heart remodeling, heart failure, and ischemia-reperfusion injury (86). Some cardiac diseases, such as cardiomyopathy, are mostly related to mitochondrial dysfunction. Pulmonary hypertension may lead to enlargement of the right ventricle. Persistent pulmonary hypertension of neonatal apical hypertrophic cardiomyopathy has been proven to be a rare manifestation related to mitochondrial dysfunction (87). When mitochondria are dysfunctional, mtDNA is damaged due to an increase in ROS production (88). Studies have found that MDS involves not only the brain, liver, skeletal muscle and other organs, but also the heart. The impaired mitochondrial DNA replication may result in mtDNA depletion, and ultimately leads to heart failure. Accordingly, the number of the protein encoded by mtDNA is also reduced (73). Santorelli et al. found a tissue-specific deletion of cardiac mtDNA in an infant patient with hypertrophic cardiomyopathy and mitochondrial exhaustion syndrome. There is increasing evidence that MDS can cause cardiomyopathy (89). In addition to the increased levels of blood lactic acid and pyruvate, liver injury and abnormal myocardial enzymes are also common in laboratory examination (90). Two out of twelve MDS children were reported to have elevated myocardial enzymes (91).

FBXL4, *ANT1*, *AGK*, and *SLC25A4* have been confirmed to be associated with cardiomyopathy. Wang et al. reported two cases of *AGK* mutation as a serious manifestation in infants with heart failure. Their skeletal muscle biopsy showed severe mtDNA depletion, along with muscle weakness, growth retardation, and other manifestations of muscle disorders. The cases were diagnosed as Sengers syndrome, thus providing strong evidence for the relationship between mitochondrial depletion syndrome and cardiomyopathy (92). Mitochondrial DNA mutation is considered to change the adaptation between bioenergy systems and dietary patterns, affect the cellular response to stimuli, and increase the susceptibility of mutant individuals to cardiometabolic diseases (93–96).

MDS-Related Genes and Their Defects

TK2

TK2 is a 16q21 gene located on chromosome 16, which encodes for thymidine kinase 2. Many *TK2* gene mutations are associated with MDS. Yan et al. demonstrated a mitochondrial DNA depletion syndrome-2 patient caused by *TK2* compound heterozygous mutation. The *TK2* mutation is considered a recessive genetic mutation type (97). In a case series of 18 patients, Cristina Domínguez-González et al. (99) found that nearly 80% of the patients developed MDS before the age of 12, and only 19% of the patients developed after the age of 12. Clinically, *TK2*-related MDS patients share common symptoms, including progressive myopathy, skeletal muscle involvement (e.g., facial and axial neck flexor weakness), respiratory system involvement, and chronic progressive external ophthalmoplegia (CPEO) (98). A previous study found that mtDNA depletion mostly affected the brain and heart tissues of *TK2* H126N knock-in mice (99). Measurements of mitochondrial *TK2* protein by immunoprecipitation found high levels of *TK2* in heart, liver, and spleen. The level of thymidylate synthase (TS) protein was also high in the heart tissue (100). Thymidine Triphosphate (TTP) is

synthesized mainly by *TK2* in the heart. Kamath et al. found that thymidine monophosphate (TMP) could promote the synthesis of TTP independent of *TK2* in the cardiac mitochondria of rats *in vitro*, suggesting a potential therapeutic strategy for *TK2* deficiency-related diseases (101).

SUCLG1

SUCLG1 gene encodes the α-subunit of succinate COA ligases (SUCL, also known as succinyl CoA synthase). *SUCLG1* subunit is widely expressed in human tissues and abundant in the brain, heart, liver and kidney. A double allele mutation in *SUCLG1* gene can promote the deficiency of succinate synthase or ligase activity, resulting in the reduction of mtDNA synthesis and mtDNA depletion (102–104). Several studies have shown that *SUCLG1* mutations may be related to mitochondrial hepatic encephalopathy. Hove et al. reported that a neonatal patient had elevated transaminase and liver failure symptoms within 2 months after birth. The mtDNA content of the patient was also decreased, accompanied by progressive myopathies. Gene sequence analysis demonstrated a homozygous mutation [c.40A>T (p.M14L)] in *SUCLG1* gene (105). Clinical data showed that succinate ligase deficiency was associated with mtDNA depletion. Liu and co-workers reported five new *SUCLG1* mutations, including exon 5 c.550G >A (p.G184S), exon 7 C.751C>T (p.G251S), exon 7 c.809A>C (p.L270W), exon 8 c.961C>G (p.A321P), and exon 9 826-2A>G (splicing), in three Chinese patients with succinate-CoA ligase deficiency (103). The latter two mutations are speculated to be destructive. There are only few case reports linking *SUCLG1* mutation to heart diseases (106). Therefore, it is worth of tracking and evaluating the potential relationship between *SUCLG1* mutation and impairment of cardiac function due to the abundance of *SUCLG1* in the heart (**Figure 2**).

SLC25A4

SLC25A4 gene is located on chromosome 4 and encodes for adenine nucleotide translocase 1 (ANT1), which is widely expressed in the heart and skeletal muscles. ANT1 translocates ADP/ATP across the IMM, provides ADP to the mitochondrial ATPase (Complex V), and plays an important role in ATP/ADP exchange between the cytosol and mitochondrial compartment (107, 108). Many studies have shown that *SLC25A4* is related to mtDNA depletion sign 12. Thompson et al. found that significant indigenous depletion of mtDNA caused severe mitochondrial respiratory chain deficiencies (109). They identified 2 pathogenic mutation sites: c.703C>G (p.Arg235Gly) and c.239G>A (p.Arg80His). *SLC25A4* c.239G>A was found in a case of mitochondrial exhaustion syndrome (MTDPS12) with epileptic encephalopathy. The patient was admitted to hospital due to continuous facial and limb spasm, accompanied by mild respiratory failure (110). A frame-shift null mutation (c.523delC, p.Q175RfsX38) of *SLC25A4* resulted in autosomal recessive myopathy and cardiomyopathy. Ten patients with homozygous mutation (adenine nucleotide transposon $-1^{-/-}$) were followed up for 6 years. These patients displayed continuous adrenergic activation, exercise intolerance, lactic acidosis, hyperalaninemia, and progressive myocardial thickening. Moreover, ECG, echocardiography, and velocity vector imaging analyses indicated the dysregulated left ventricular relaxation, abnormal myocardial repolarization, and abnormal systolic mechanics. Extensive degeneration of cardiomyocytes and structural abnormalities of mitochondria were also evidence in these patients (111). The characteristics of myopathy and cardiomyopathy were also observed in mice lacking the heart/muscle isoform of ANT1 (112).

AGK

Sengers syndrome is an autosomal recessive genetic disease caused by *AGK* mutations. *AGK*, a mitochondrial membrane kinase, is involved in protein biogenesis (112). Besides, intracellular LPA is generated by the phosphorylation of monoacylglycerol by *AGK* (113). Vukotic et al. found that *AGK* belonged to a subunit of the TIM22 complex that facilitates the transport of metabolite carriers into the IMM. ANT1 levels were reduced in the cells of Sengers syndrome patients, suggesting that *AGK* is needed for the efficient insertion of metabolite carriers (e.g., SLC25A24 and ANT1) (114). The main clinical features of Sengers syndrome are hypertrophic cardiomyopathy, bi-sided cataracts, myopathy, and lactic acidosis. Hypertrophic cardiomyopathy can eventually contribute to the development of heart failure (91).

MPV17

MPV17 is a nuclear-encoded IMM protein expressed in the brain, kidneys, liver, spleen, and heart in humans (115). A large number of studies have demonstrated that the deficiency of *MPV17* may cause abnormalities in mitochondrial ROS production flux, ETC complex activity, mitochondrial membrane potential, and pH value (116, 117). Judith R. Alonzo showed that *Mpv17* could transfer dTMP from cytoplasm to mitochondria for mtDNA synthesis (118). *Mpv17* deficiency may cause a depletion of dTMP pool in the mitochondria (119). Loss of *MPV17* protein leads to a notable reduction in liver mtDNA and ultimately liver dysfunction (120). Mutations in *MPV17* gene can result in neurological problems and failure to thrive in pediatric patients (121). The absence of *MPV17* protein does not appear to significantly affect mtDNA quantity and overall function of the heart in normal adult mice. However, cardiac mitochondria from *MPV17* mutant mice displayed severe cristae damage after ischemia/reperfusion (I/R) injury. *MPV17* mutation also disrupted its interactions with ATP synthase, MICOS, Cyclophilin D, and glucose-regulated protein 75 (GRP75). Mitochondrial sensitivity to Ca^{2+} overload was enhanced in I/R mice, thereby promoting mPTP opening and leading to subsequent cardiomyocyte death (117) (**Figure 3**).

POLG

POLG is the only DNA polymerase γ (POLγ) in the mitochondria. This enzyme is a heterologous trimer consisting of three subunits, which are encoded by *POLG* and *POLG2* genes on chromosome 15. *POLG* gene is a common pathogenic gene of MDS, in which hundreds of mutations have been identified (122). When this gene is mutated, mitochrondria lose the ability to maintain the genome, leading to mtDNA depletion.

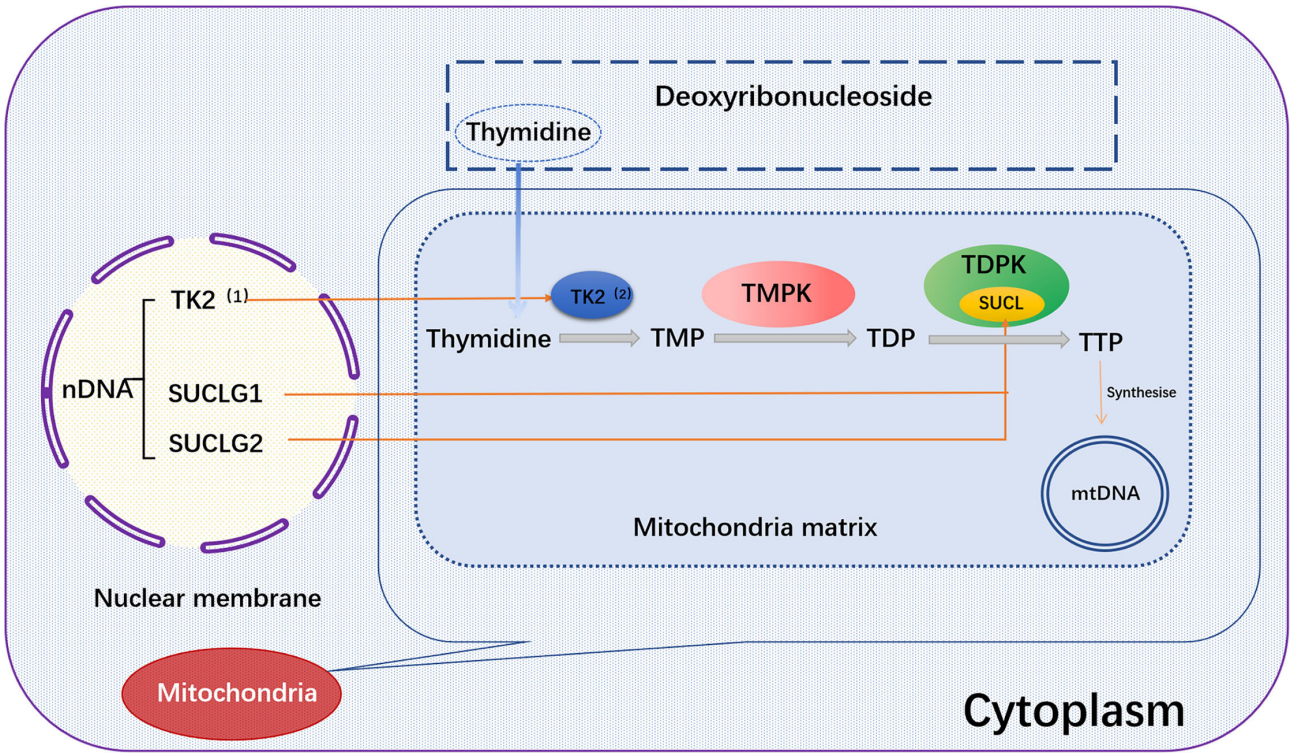

FIGURE 2 | *TK2*, *SUCLG1*, or SUCLG2 regulates mtDNA synthesis. In the salvage pathway, the pre-formed deoxyribothymidine enters the mitochondria. The deoxyribonucleoside is then catalyzed by the thymokinases TMPK and TDPK to phosphorylate the deoxyribonucleoside into the triphosphate form in the subsequent three phosphorylation steps, and further synthesize mtDNA. Among them, *TK2* and TDPK are encoded by the nuclear genes *TK2* and *SUCLG1*/*SUCLG2*, respectively. *TK2*, (1) Thymidine Kinase 2, (2) Thymidine kinase; *SUCLG1*, succinic acid A ligase α subunit; SUCLG2, succinate-CoA ligase GDP-forming β subunit; Thymidine, deoxyribosylthymine; TMPK, Thymidylate kinase; TDPK, Thiamine diphosphokinase; SUCL, Succinyl CoA ligase; TMP, Thymidine monophosphate; TDP, Thymidine diphosphate; TTP, Thymidine 5'-triphosphate.

A large number of mutation sites in *POLG* have been reported, including the homozygous mutation Chr17:62492543 G>A of Chr17 located in *POLG2* gene, which leads to the replacement of R182W in P55. The clinical manifestations of the patient include the reduction in mtDNA content and liver failure, indicative of hepatocerebral MDS. In addition, Hoff et al. showed that the Chr17:62492543 G>A mutation in *POLG*2 and R182W p55 severely damaged the stability of the auxiliary subunit, and was associated with the disease phenotype (123). Recent studies identified a new homozygous mutation [c.2391G>T (p.M797I)] in the C-terminal subdomain of *POLG* in a close family with MNGIE syndrome (124). Heart-specific overexpression of POLγY955C mutant caused dysregulation mtDNA biogenesis, resulting in cardiac dysfunction and eventually premature death. Utilizing transgenic mice expressing human POLγY955C in the heart, William Lewis et al. demonstrated that the mice had defective enzyme machinery for mtDNA replication, which resulted in the phenotype of mtDNA depletion. In addition, the mice also showed the phenotypes of increased mitochondrial oxidative stress, histopathological changes, and abnormal mitochondrial ultrastructure in cardiomyocytes. Moreover, cardiac insufficiency is accompanied by cardiac enlargement, increased ventricular volume, and heart mass (125).

RRM2B

RRM2B (ribonucleotide reductase regulatory TP53 inducible subunit M2B), is located on chromosome 8q22.3, and encodes for ribonucleotide diphosphate reductase subunit M2B and p53-inducible ribonucleotide reductase (RNR) small subunit (p53R2). RNR is responsible for catalyzing free radicals and reducing ribonucleotides, in order to dNTPs to maintain the dNTP library at an appropriate level for DNA synthesis and repair. When this gene is defective, it often leads to the occurrence of mitochondrial diseases. Changes in the structural properties of *RRM2B* protein can also cause mtDNA damage and affect the nervous system (126, 127). Stojanović et al. has reported a missense mutation c.707G>A, p.Cys236Tyr in *RRM2B* gene in the blood cells of a white male. This mutation appears to be associated with congenital deafness and exercise intolerance due to the impairment of nerve conduction (128). Mutations in *RRM2B* gene also cause MNGIE. Two *RRM2B* pathogenic mutations, namely, c.362G>A (p.R121H) and c.329G>A (p.R110H), were identified to be associated with severe mtDNA depletion in a 42-year-old woman. The mutations changed the docking interface of ribonucleoside reductase (RIR2B) homodimeric, thereby affecting the activity of the enzyme (118). In addition, *RRM2B* mutations can also cause

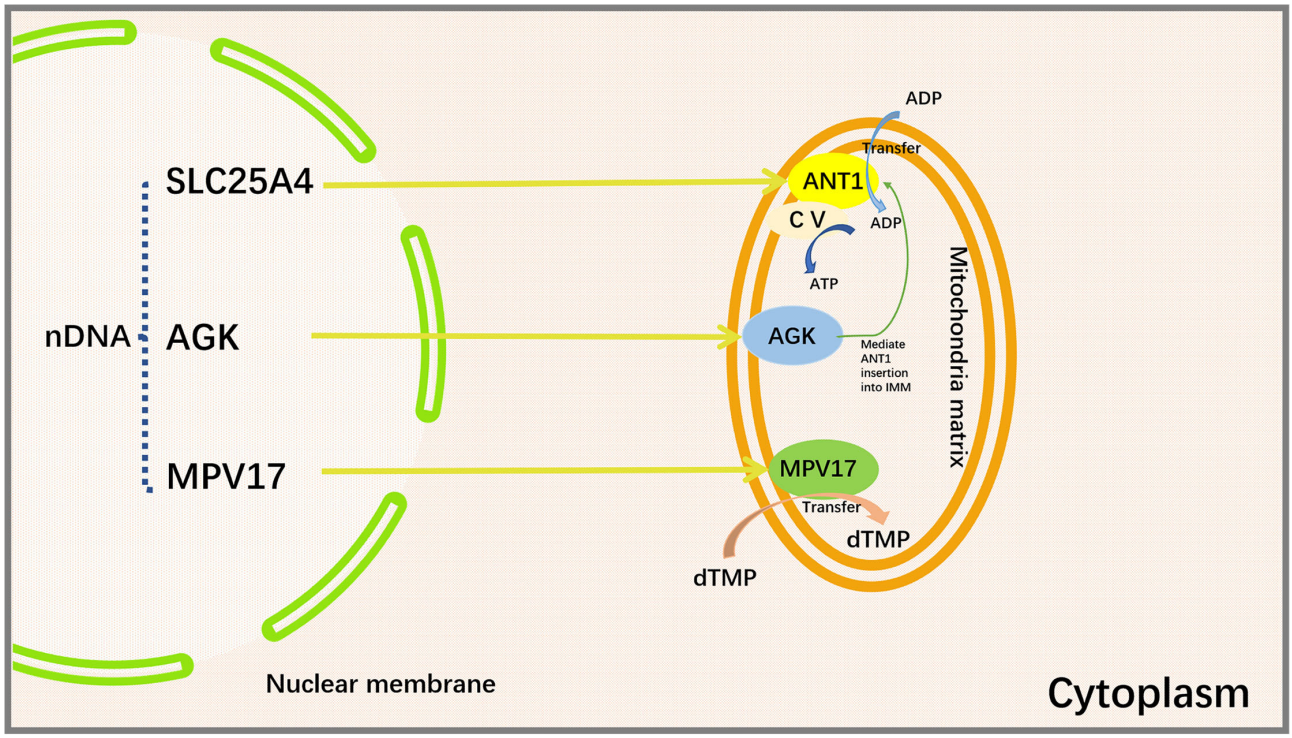

FIGURE 3 | Proteins encoded by *SLC25A4*, *AGK*, and *MPV17* genes and their functions. *SLC25A4*, *AGK* and MPV are important mitochondrial transport proteins. Adenine nucleotide transporter (ANT1) is an ADP/ATP translocator encoded by *SLC25A4* and located on the inner mitochondrial membrane. It mediates the transmembrane exchange of ADP and ATP and provides ADP for mitochondrial ATP synthase. Acylglycerol kinase is a mitochondrial lipid kinase encoded by *AGK* gene. The absence of *AGK* reduces the content of ANT1 in the inner membrane of muscle mitochondria by affecting lipid metabolism. *MPV17* protein is encoded by *MPV17* gene, which is involved in the maintenance of nucleotide homeostasis and transfers dTMP from the cytoplasm to the mitochondria to maintain mtDNA synthesis. *SLC25A4*, Solute Carrier Family 25 Member 4; *AGK*, Acylglycerol Kinase; *MPV17*, Mitochondrial Inner Membrane Protein *MPV17*; ANT1, Adenine nucleotide translocase 1; CV, Complex V, also known as ATP synthase, is one of the mitochondrial respiratory chain electron transport complexes; ADP, Adenosine diphosphate; ATP, Adenosine triphosphate; dTMP, deoxythymidine monophosphate.

cardiovascular disease. In the case report by Albert Z Lim et al. defects in mtDNA maintenance were found in patients with left ventricular hypertrophy, cardiomyopathy and ventricular septal defects (129).

TWNK

Twinkle (*TWNK*, previously designated as C10orf2), is responsible for encoding Twinkle proteins, maintaining mtDNA integrity, and displaying 5′ → 3′ DNA helicase activity when unwinding mitochondrial DNA. Mutations in this gene are associated with mitochondrial DNA depletion syndrome 7 (MTDPS7). Li et al. found that the proband carried two *TWNK* compound heterozygous mutations, of which c.1186C>T (p.Pro396Ser) in exon 1 was inherited from the father, and c.1844G>C (p.Gly615Ala) in exon 5 was inherited from the mother (130). Dominant mutations in *TWNK* cause progressive ophthalmoplegia, mtDNA deletion, and autosomal dominant inheritance 3, while recessive mutations often lead to MTDPS 7 and Perrault syndrome 5. Among them, MTDPS7 is usually manifested by infantile-onset spinocerebellar ataxia (IOSCA). In a report by Kume et al. *TWNK* homozygous mutations could lead to cerebellar ataxia in middle-aged patients (131, 132). Twinkle protein has three main domains: primary enzyme domain, junctional domain, and helical enzyme domain. The entire primary enzyme and connector domains as well as a partial helix enzyme domain are located in exon 1. Exons 2–4 encode the remaining helix enzyme domain. Kume et al. (131) found the amino acid at codon 292 changed from Pro to Thr in IOSCA patients. In addition to homozygous mutations in the helix domain, homozygous mutations in the primary enzyme domain 9 and compound heterozygous mutations in both primary enzyme and helix domain 10 were reported in IOSCA patients (133). Pohjoismäki et al. showed that Twinkle protein encoded by *TWNK* gene may play a direct role in the maintenance of human heart (133). The copy number of myocardial mitochondrial DNA decreased when heart failure occurred, especially after myocardial infarction. Overexpression of Twinkle helicase could greatly increase the copy number of mtDNA, thereby protecting the heart (134). In addition, the overexpression of *TWNK* also decreased the accumulation of ROS-induced mtDNA mutations, thus benefiting cardiomyopathy in Sod2 +/− mice (135).

FBXL4

FBXL4 (F-box and leucine-rich repeat protein 4), located on chromosome 6, is a nDNA that encodes 621-amino-acid F-box protein. *FBXL4* plays vital roles in maintaining mtDNA integrity and stability. It is the first protein family member reported to form Skp1-Cullin-F-box (SCF) (136). In the fibroblasts of patients with *FBXL4* double allele mutations, the dysregulated mitochondrial network, decreased mitochondrial energy metabolism-related enzyme activity and reduced consumption of mtDNA were observed. The mutations can lead to mitochondrial exhaustion syndrome 13 (MTDPS13) of cerebral muscular disease type, which is often manifested as decreased muscle tone, difficulty in eating, delayed nerve development, brain atrophy and other symptoms, accompanied by increased blood lactic acid level (137, 138). Wang et al. found a novel *FBXL4* frameshift mutation (c.993dupA) in a Han Chinese patient, leading to the premature termination of protein synthesis and defects at the protein level (110). Ballout et al. reported the first case of MTDPS13 in Lebanon. Full-exon group sequencing showed that the female patient had a homozygous non-sense mutation c. 1303C>T (p.Arg435*). In addition to the typical clinical manifestations such as encephalopathy and muscle tone reduction, anemia and normal blood ammonia also appeared (139). Emperador et al. reported new *FBXL4* mutations in two patients, which were composite heterozygous mutations c.[858 + 5G>C]; [1510T>C] and homozygous mutation c.[851delC]; [851delC]. Besides, skeletal muscle biopsy showed severe mtDNA depletion (140). In a case reported by Huemer et al. (137) cardiac disease was diagnosed in seven patients with *FBXL4* mutations at an initial visit. Tissue examination and cell staining indicated joint defects in the respiratory chain, reduced production of enzymes related to mitochondrial energy metabolism, and reduced mitochondrial DNA content (136). Antoun et al. reported that *FBXL4* deficiency could result in severe multi-system diseases, including lactic acidosis, cystic white matter disease, cardiomyopathy, arrhythmia, and immunodeficiency (141). A patient with prenatal diagnosis of polyhydramnios and cerebellar atrophy showed mitochondrial encephalomyopathy. This patient suffered from myocardial hypertrophy with ventricular septal defect. Seven of the nine patients (77%) with *FBXL4* deficiency showed abnormal cardiac manifestations, including fallot syndrome (TOF), supraventricular tachycardia (SVT), ventricular septal defect (ASD), and left or right ventricular hypertrophy. These findings imply that cardiac involvement may be one of the most common clinical features of *FBXL4* deficiency (142). It has been reported that two siblings harbor homozygous variants in *FBXL4* gene (c.1750 T>C; p.Cys584Arg). They had symptoms of encephalomyopathy, lactic acidosis and myocardial hypertrophy, which were consistent with the characteristics of mitochondrial injury myopathy caused by *FBXL4* gene mutation. Dichloroacetic acid (DCA) treatment effectively alleviated metabolic acidosis and reversed myocardial hypertrophy in the younger sister (143).

TFAM

The mitochondrial transcription factor A (*TFAM*) gene, located on nuclear chromosome 10q21, is composed of six introns and seven exons. *TFAM* is a member of the HMG box protein family. It contains two HMG box domains, an N-terminal domain and a C-terminal structure. *TFAM* has the ability to maintain mtDNA and initiate mtDNA transcription (144, 145). *TFAM* is a key factor in promoter selection during the initiation of mitochondrial transcription sites. It recognizes the promoter of *POLRMT* and initiates transcription by binding to mtDNA without sequence specificity (146). Stile et al. idenfied a *TFAM* homozygous missense variant (c.533C>T; p. Pro178Leu) among the close relatives of Basque lineage in Colombia. Two siblings showed IUGR, elevated transaminase, preterm infant with hypoglycemia and hyperbilirubinemia progressed to liver failure and death (147). In addition, *TFAM* and mtDNA copy numbers are essential for the control of mitochondrial gene expression; their reduction can lead to poor heart function and aging (148, 149). Heart-specific knockout of *TFAM* induced apoptosis in the heart of a transgenic mouse model. Disruption of *TFAM* in the heart resulted in mtDNA depletion, reduced mitochondrial ATP production rate, and impaired respiratory chain enzyme activities. These defects aggravate heart disease and eventually lead to heart failure (146, 150).

MGME1

Mitochondrial Genome Maintenance Exonuclease 1 (*MGME1* or *DDK1*) belongs to PD-(D/E)XK nuclease superfamily. It is a highly conserved mitochondrial-specific DNA enzyme encoded by *C20orf72 gene*. Mutation of *C20orf72* is associated with exhaustion and rearrangement of mtDNA. Patients with *C20orf72* mutations may have CPEO, myasthenia, respiratory distress and gastrointestinal diseases (151). Mouse studies by Matic et al. suggest that *MGME1* gene product may be a part of the regulatory switch at the end of the D-loop region since it regulates the replication of mtDNA and the termination of H-chain transcription. Lack of *MGME1* may lead to the deletion or depletion of mtDNA in mouse tissue cells (152). *MGME1* may also contribute to cerebellar ataxia since mutation of this gene leads to the occurrence of mtDNA depletion syndrome 11, with a series of clinical manifestations of cerebellar diseases. Recently, Hebbar et al. identified a new code-shift mutation c.359del (p.Pro120Leufs*2) in exon 2 in a child with early progressive cerebellar ataxia. The investigator determined that the mutation was the cause of MTDPS11 (153). A high-throughput mutation screening of 16 patients with dilated or hypertrophic cardiomyopathy indicated that *MGME1* variants are highly associated with the pathogenesis of heart disease (154).

QIL1/MIC13(C19orf70)

MICOS13, also known as *C19orf70*, *MIC13*, or *QIL1* (155, 156), is a component of mitochondrial contact site and cristae tissue system (MICOS) complex. It plays vital roles in maintaining the characteristics of mitochondrial cristae and cellular energy metabolism. *MICOS13* deficiency leads to morphological defects of cristae and cristae junctions and severely impairs the IMM architecture and mitochondrial respiratory function (157). Patients from a consanguineous family were reported to have *MICOS* p.(Gly15Glufs*75) variant, thus resulting in mitochondrial hepato-encephalopathy. Homozygous individuals

displayed syndromes correlated with mitochondrial dysfunction. In addition, multiple organs with high energy demands, including heart, liver and the central nervous system, were damaged (155, 158). It has been reported that two siblings with *QIL1* deficiency exhibited mitochondrial encephalopathy symptom. Loss of *QIL1* in this case showed abnormalities in multiple organs (e.g., liver and muscle), while heart ultrasound indicated mild heart hypertrophy as early as 2 years old (159). Furthermore, *QIL1* point mutation also resulted in cardiac arrhythmia but not cardiac hypertrophy (160).

SUMMARY AND OUTLOOK

MDS is a mitochondrial disease characterized by the reduced amount and/or depletion of mtDNA content. They are caused by mutations in nDNA and can involve two or more organs. In this paper, while discussing the impact of different types of MDS on muscle, brain and nervous system, we explored the potential association between different gene mutations and MDS-associated cardiac diseases, in order to provide guidance for early screening and prevention of these diseases.

AUTHOR CONTRIBUTIONS

JY and YX: conceptualization and resources. HW, YX, and JY: original draft preparation and resources. YH, SL, YuC, YaC, JingW, and YuZ: writing. YH, SL, YuC, YaC, YuZ, YaZ, JingsW, HW, and JY: review and editing. All authors have read and agreed to the published version of the manuscript.

FUNDING

The authors would like to acknowledge funding from the Research Start-up Fund of Jining Medical University (Reference: 600791001), the Foundation of Medical Health Science and Technology Development Program of Shandong Province (Reference: 202002061311), the Research Support Fund for Teachers of Jining Medical University (Reference: JYFC2019KJ013), and the Jining Medical College Student Innovation and Entrepreneurship Training Program Project (Reference: cx2021053).

ACKNOWLEDGMENTS

The authors would like to express their gratitude to EditSprings (https://www.editsprings.com/) for the expert linguistic services. We would also like to acknowledge the support of the research team at Jining Medical University working on the molecular mechanisms and intervention of myocardial infarction.

REFERENCES

1. El-Hattab AW, Craigen WJ, Scaglia F. Mitochondrial DNA maintenance defects. *Biochim Biophys Acta Mol Basis Dis.* (2017) 1863:1539–55. doi: 10.1016/j.bbadis.2017.02.017
2. Kai L, Bingzhen C. Progress on cell apoptosis of mitochondrial regulation. *Biomed Eng Clin.* (2014) 18:501–5. doi: 10.13339/j.cnki.sglc.2014.05.049
3. Thorburn DR, Rahman J, Rahman S. *Mitochondrial DNA-Associated Leigh Syndrome and NARP*. Seattle, WA: University of Washington (1993).
4. Zhou ZD, Saw WT, Tan EK. Mitochondrial CHCHD-Containing proteins: physiologic functions and link with neurodegenerative diseases. *Mol Neurobiol.* (2017) 54:5534–46. doi: 10.1007/s12035-016-0099-5
5. Dogan SA, Cerutti R, Benincá C, Brea-Calvo G, Jacobs HT, Zeviani M, et al. Perturbed redox signaling exacerbates a mitochondrial myopathy. *Cell Metab.* (2018) 28:764–75. doi: 10.1016/j.cmet.2018.07.012
6. Flores-Herrera O, Olvera-Sánchez S, Esparza-Perusquía M, Pardo JP, Rendón JL, Mendoza-Hernández G, et al. Membrane potential regulates mitochondrial ATP-diphosphohydrolase activity but is not involved in progesterone biosynthesis in human syncytiotrophoblast cells. *Biochim Biophys Acta.* (2015) 1847:143–52. doi: 10.1016/j.bbabio.2014.10.002
7. Fernández-Vizarra E, Tiranti V, Zeviani M. Assembly of the oxidative phosphorylation system in humans: what we have learned by studying its defects. *Biochim Biophys Acta.* (2009) 1793:200–11. doi: 10.1016/j.bbamcr.2008.05.028
8. Hou T, Zhang R, Jian C, Wan QD, Wang YR, Shu KL, et al. NDUFAB1 confers cardio-protection by enhancing mitochondrial bioenergetics through coordination of respiratory complex and supercomplex assembly. *Cell Res.* (2019) 29:754–66. doi: 10.1038/s41422-019-0208-x
9. Larsen S, Nielsen J, Hansen CN, Nielesen LB, Wirbrand F, Stride Net, et al. Biomarkers of mitochondrial content in skeletal muscle of healthy young human subjects. *J Physiol.* (2012) 590:3349–60. doi: 10.1113/jphysiol.2012.230185
10. Protasoni M, Pérez-Pérez R, Lobo-Jarne T, Harbour ME, Ding SJ, Peñas A, et al. Respiratory supercomplexes act as a platform for complex III-mediated maturation of human mitochondrial complexes I and IV. *EMBO J.* (2020) 39:e102817. doi: 10.15252/embj.2019102817
11. Teodoro JS, Palmeira CM, Rolo AP. Mitochondrial membrane potential ($\Delta\Psi$) fluctuations associated with the metabolic states of mitochondria. *Methods Mol Biol.* (2018) 1782:109–19. doi: 10.1007/978-1-4939-7831-1_6
12. Acin-Perez R, Enriquez JA. The function of the respiratory supercomplexes: the plasticity model. *Biochim Biophys Acta.* (2014) 1837:444–50. doi: 10.1016/j.bbabio.2013.12.009
13. Ji LL. Redox signaling in skeletal muscle: role of aging and exercise. *Adv Physiol Educ.* (2015) 39:352–9. doi: 10.1152/advan.00106.2014
14. Bouchez C, Devin A. mitochondrial biogenesis and mitochondrial reactive oxygen species (ROS): a complex relationship regulated by the cAMP/PKA signaling pathway. *Cells.* (2019) 8:287. doi: 10.3390/cells8040287
15. Saki M, Prakash A. DNA damage related crosstalk between the nucleus and mitochondria. *Free Radic Biol Med.* (2017) 107:216–27. doi: 10.1016/j.freeradbiomed.2016.11.050
16. Deshpande OA, Mohiuddin SS. *Biochemistry, Oxidative Phosphorylation.* California, CA: StatPearls (2020).
17. Benard G, Bellance N, Jose C, Melser S, Nouette-Gaulain K, Rossignol R. Multi-site control and regulation of mitochondrial energy production. *Biochim Biophys Acta.* (2010) 1797:698–709. doi: 10.1016/j.bbabio.2010.02.030
18. Thomas LW, Staples O, Turmaine M, Ashcroft M. CHCHD4 regulates intracellular oxygenation and perinuclear distribution of mitochondria. *Front Oncol.* (2017) 7:71. doi: 10.3389/fonc.2017.00071
19. Fuhrmann DC, Brüne B. Mitochondrial composition and function under the control of hypoxia. *Redox Biol.* (2017) 12:208–15. doi: 10.1016/j.redox.2017.02.012
20. Neary MT, Ng KE, Ludtmann MH, Hall AR, Piotrowska I, Wang XB, et al. Hypoxia signaling controls postnatal changes in cardiac

mitochondrial morphology and function. *J Mol Cell Cardiol.* (2014) 74:340–52. doi: 10.1016/j.yjmcc.2014.06.013
21. Ambrose LJ, Abd-Jamil AH, Gomes RS, Carter EE, Carr CA, Clarke K, et al. Investigating mitochondrial metabolism in contracting HL-1 cardiomyocytes following hypoxia and pharmacological HIF activation identifies HIF-dependent and independent mechanisms of regulation. *J Cardiovasc Pharmacol Ther.* (2014) 19:574–85. doi: 10.1177/1074248414524480
22. Bhatti JS, Bhatti GK, Reddy PH. Mitochondrial dysfunction and oxidative stress in metabolic disorders - a step towards mitochondria based therapeutic strategies. *Biochim Biophys Acta Mol Basis Dis.* (2017) 1863:1066–77. doi: 10.1016/j.bbadis.2016.11.010
23. Houten SM, Violante S, Ventura FV, Wanders RJA. The biochemistry and physiology of mitochondrial fatty acid β-oxidation and its genetic disorders. *Annu Rev Physiol.* (2016) 78:23–44. doi: 10.1146/annurev-physiol-021115-105045
24. Prasun P. Disorders of pyruvate metabolism and tricarboxylic acid cycle. *Mitochondrial Med.* (2019) 2019:83–95. doi: 10.1016/B978-0-12-817006-9.00015-0
25. Martínez-Reyes I, Chandel NS. Mitochondrial TCA cycle metabolites control physiology and disease. *Nat Commun.* (2020) 11:102. doi: 10.1038/s41467-019-13668-3
26. Dziewulska A, Dobrzyń P, Dobrzyń A. The role of AMP-activated protein kinase in regulation of skeletal muscle metabolism. *Postepy Hig Med Dosw.* (2010) 64:513–21. doi: 10.1677/joe.0.0340273
27. Chen H, Chomyn A, Chan DC. Disruption of fusion results in mitochondrial heterogeneity and dysfunction. *J Biol Chem.* (2005) 280:26185–92. doi: 10.1074/jbc.M503062200
28. Weir HJ, Yao P, Huynh K, Escoubas CC, Goncalves RL, Burkewitz K, et al. Dietary restriction and AMPK increase lifespan *via* mitochondrial network and peroxisome remodeling. *Cell Metab.* (2017) 26:884–96. doi: 10.1016/j.cmet.2017.09.024
29. Gómez-Valadés AG, Gonzalez-Franquesa A, Gama-Perez P, Claret M, Garcia-Roves PM. Emerging concepts in diabetes: mitochondrial dynamics and glucose homeostasis. *Curr Diabetes Rev.* (2017) 13:370–85. doi: 10.2174/1573399812666151012115229
30. Otera H, Ishihara N, Mihara K. New insights into the function and regulation of mitochondrial fission. *Biochim Biophys Acta.* (2013) 1833:1256–68. doi: 10.1016/j.bbamcr.2013.02.002
31. Lee H, Yoon Y. Mitochondrial fission and fusion. *Biochem Soc Trans.* (2016) 44:1725–35. doi: 10.1042/BST20160129
32. Kondadi AK, Anand R, Reichert AS. Functional interplay between cristae biogenesis, mitochondrial dynamics and mitochondrial DNA integrity. *Int J Mol Sci.* (2019) 20:4311. doi: 10.3390/ijms20174311
33. Meyer JN, Leuthner TC, Luz AL. Mitochondrial fusion, fission, and mitochondrial toxicity. *Toxicology.* (2017) 391:42–53. doi: 10.1016/j.tox.2017.07.019
34. Sas K, Szabó E, Vécsei L. Mitochondria, oxidative stress and the kynurenine system, with a focus on ageing and neuroprotection. *Molecules.* (2018) 23:191. doi: 10.3390/molecules23010191
35. Briston T, Roberts M, Lewis S, Powney B, Staddon JM, Szabadkai G, et al. Mitochondrial permeability transition pore: sensitivity to opening and mechanistic dependence on substrate availability. *Sci Rep.* (2017) 7:10492. doi: 10.1038/s41598-017-10673-8
36. Gherardi G, Nogara L, Ciciliot S, Fadini GP, Blaauw B, Braghetta P, et al. Loss of mitochondrial calcium uniporter rewires skeletal muscle metabolism and substrate preference. *Cell Death Differ.* (2019) 26:362–81. doi: 10.1038/s41418-018-0191-7
37. Gherardi G, Monticelli H, Rizzuto R, Mammucari C. The mitochondrial Ca^{2+} uptake and the fine-tuning of aerobic metabolism. *Front Physiol.* (2020) 11:554904. doi: 10.3389/fphys.2020.554904
38. Nemani N, Dong Z, Daw CC, Madaris TR, Ramachandran K, Enslow BT, et al. Mitochondrial pyruvate and fatty acid flux modulate MICU1-dependent control of MCU activity. *Sci Signal.* (2020) 13:eaaz6206. doi: 10.1126/scisignal.aaz6206
39. Gao P, Yan Z, Zhu Z. Mitochondria-Associated endoplasmic reticulum membranes in cardiovascular diseases. *Front Cell Dev Biol.* (2020) 8:604240. doi: 10.3389/fcell.2020.604240
40. Zapico SC, Ubelaker DH. mtDNA mutations and their role in aging, diseases and forensic sciences. *Aging Dis.* (2013) 4:364–80. doi: 10.14336/AD.2013.0400364
41. Kraja AT, Liu C, Fetterman JL, Graff M, Have CT, Gu C, et al. Associations of mitochondrial and nuclear mitochondrial variants and genes with seven metabolic traits. *Am J Hum Genet.* (2019) 104:112–38. doi: 10.1016/j.ajhg.2018.12.001
42. Chaturvedi S, Bala K, Thakur R, Suri V. Mitochondrial encephalomyopathies: advances in understanding. *Med Sci Monit.* (2005) 11:A238–46. doi: 10.1016/j.lfs.2005.02.003
43. Kopinski PK, Janssen KA, Schaefer PM, Trefely S, Perry CE, Potluri P, et al. Regulation of nuclear epigenome by mitochondrial DNA heteroplasmy. *Proc Natl Acad Sci USA.* (2019) 116:16028–35. doi: 10.1073/pnas.1906896116
44. Mishra P, Chan DC. Metabolic regulation of mitochondrial dynamics. *J Cell Biol.* (2016) 212:379–87. doi: 10.1083/jcb.201511036
45. El-Hattab AW, Scaglia F. Mitochondrial DNA depletion syndromes: review and updates of genetic basis, manifestations, and therapeutic options. *Neurotherapeutics.* (2013) 10:186–98. doi: 10.1007/s13311-013-0177-6
46. Moraes CT, Shanske S, Tritschler HJ, Andreetta F, Bonilla E, et al. MtDNA depletion with variable tissue expression: a novel genetic abnormality in mitochondrial diseases. *Am J Hum Genet.* (1991) 48:492–501.
47. Sarzi E, Bourdon A, Chrétien D, Corcos J, Slama A, et al. Mitochondrial DNA depletion is a prevalent cause of multiple respiratory chain deficiency in childhood. *J Pediatr.* (2007) 150:531–4. doi: 10.1016/j.jpeds.2007.01.044
48. Spinazzola A, Invernizzi F, Carrara F,Lamantea E, Donati A, Dirocco M, et al. Clinical and molecular features of mitochondrial DNA depletion syndromes. *J Inherit Metab Dis.* (2009) 32:143–58. doi: 10.1007/s10545-008-1038-z
49. Lin GZ, Qiu JW, Deng M, Lin WX, Guo L, Song YZ. DGUOK-related mitochondrial DNA depletion syndrome: a case report and literature review. *Zhong Guo Dang Dai Er Ke Za Zhi.* (2020) 22:274–9. doi: 10.7499/j.issn.1008-8830.2020.03.017
50. El-Hattab AW, Scaglia F. Hattab AW, Scaglia F. *SUCLG1-Related Mitochondrial DNA Depletion Syndrome, Encephalomyopathic Form With Methylmalonic Aciduria*. GeneReviews® (1993–2021).
51. Wei H, Liu G. Understanding, characteristics and treatment of mitochondrial exhaustion syndrome. *J Pract Diabetol.* (2018) 14:9–10.
52. Blázquez-Bermejo C, Molina-Granada D, Vila-Julià F, Jiménez-Heis D, Zhou X, Torres-Torronteras J, et al. Age-related metabolic changes limit efficacy of deoxynucleoside-based therapy in thymidine kinase 2-deficient mice. *EBio Med.* (2019) 46:342–55. doi: 10.1016/j.ebiom.2019.07.042
53. Wang J, El-Hattab AW, Wong LJC. *TK2-Related Mitochondrial DNA Maintenance Defect, Myopathic Form*. GeneReviews® (1993–2021).
54. Papadimas GK, Vargiami E, Dragoumi P, Van Coster R, Smet J, Seneca S, et al. Mild myopathic phenotype in a patient with homozygous c.416C>T mutation in *TK2* gene. *Acta Myol.* (2020) 39:94–7. doi: 10.36185/2532-1900-012
55. Cámara Y, Carreño-Gago L, Martín MA, Melià MJ, Blázquez A, Delmiro A, et al. Severe *TK2* enzyme activity deficiency in patients with mild forms of myopathy. *Neurology.* (2015) 84:2286–8. doi: 10.1212/WNL.0000000000001644
56. Domínguez-González C, Madruga-Garrido M, Mavillard F, Garone C, Aguirre-Rodríguez FJ, Donati MA, et al. Deoxynucleoside therapy for thymidine kinase 2-deficient myopathy. *Ann Neurol.* (2019) 86:293–303. doi: 10.1002/ana.25506
57. Chanprasert S, Wang J, Weng SW, Enns GM, Boué DR, Wong BL, et al. Molecular and clinical characterization of the myopathic form of mitochondrial DNA depletion syndrome caused by mutations in the thymidine kinase (*TK2*) gene. *Mol Genet Metab.* (2013) 110:153–61. doi: 10.1016/j.ymgme.2013.07.009
58. Garone C, Taylor R W, Nascimento A,Poulton J, Fratter C, Domínguez-González C, et al. Retrospective natural history of thymidine kinase 2 deficiency. *J Med Genet.* (2018) 55:515–21. doi: 10.1136/jmedgenet-2017-105012
59. Lamperti C, Zeviani M. Encephalomyopathies caused by abnormal nuclear-mitochondrial intergenomic cross-talk. *Acta Myol.* (2009) 28:2–11.
60. Köse E, Köse M, Edizer S, Akişin Z, Yilmaz ZB, Sahin A, et al. Different clinical presentation in a patient with two novel

pathogenic variants of the *FBXL4* gene. *Turk J Pediatr.* (2020) 62:652–6. doi: 10.24953/turkjped.2020.04.016
61. Lu X, Li D, Duan F, Li H, Yao X, Ma B, et al. A case of *SUCLG1*-related infantile encephalomyopathy mitochondrial DNA depletion syndrome. *J Clin Pediatr.* (2017) 35:810–4.
62. Mahjoub G, Habibzadeh P, Dastsooz H, Mirzaei M, Kavosi A, Jamali L. Clinical and molecular characterization of three patients with hepatocerebral form of mitochondrial DNA depletion syndrome: a case series. *BMC Med Genet.* (2019) 20:167. doi: 10.1186/s12881-019-0893-9
63. Tadiboyina VT, Rupar A, Atkison P, Feigenbaum A, Kronick J, Wang J et al. Novel mutation in DGUOK in hepatocerebral mitochondrial DNA depletion syndrome associated with cystathioninuria. *Am J Med Genet A.* (2005) 135:289–91. doi: 10.1002/ajmg.a.30748
64. Kishita Y, Shimura M, Kohda M, Akita M, Imai-Okazaki A, Yatsuka Y, et al. A novel homozygous variant in MICOS13/QIL1 causes hepato-encephalopathy with mitochondrial DNA depletion syndrome. *Mol Genet Genomic Med.* (2020) 8:e1427. doi: 10.1002/mgg3.1427
65. Pronicki M, Piekutowska-Abramczuk D, Rokicki D, Iwanicka-Pronicka K, Grajkowska W. Histopathological liver findings in patients with hepatocerebral mitochondrial depletion syndrome with defined molecular basis. *Pol J Pathol.* (2018) 69:292–8. doi: 10.5114/pjp.2018.79549
66. Nogueira C, Almeida LS, Nesti C,Pezzini I, Videira A, Vilarinho L, et al. Syndromes associated with mitochondrial DNA depletion. *Ital J Pediatr.* (2014) 40:34. doi: 10.1186/1824-7288-40-34
67. Kim J, Kang E, Kim Y, Kim JM, Lee BH, Murayama K, et al. *MPV17* mutations in patients with hepatocerebral mitochondrial DNA depletion syndrome. *Mol Genet Metab Rep.* (2016) 8:74–6. doi: 10.1016/j.ymgmr.2016.06.006
68. Yadak R, Breur M, Bugiani M. Gastrointestinal dysmotility in MNGIE: from thymidine phosphorylase enzyme deficiency to altered interstitial cells of cajal. *Orphanet J Rare Dis.* (2019) 14:33. doi: 10.1186/s13023-019-1016-6
69. Hirano M, Garone C, Quinzii C M. CoQ(10) deficiencies and MNGIE: two treatable mitochondrial disorders. *Biochim Biophys Acta.* (2012) 1820:625–31. doi: 10.1016/j.bbagen.2012.01.006
70. Scarpelli M, Todeschini A, Volonghi I, Padovani A, Filosto M. Mitochondrial diseases: advances and issues. *Appl Clin Genet.* (2017) 10:21–6. doi: 10.2147/TACG.S94267
71. Filosto M, Cotti Piccinelli S, Caria F,Gallo Cassarino S, Baldelli E, et al. Mitochondrial neurogastrointestinal encephalomyopathy (MNGIE-MTDPS1). *J Clin Med.* (2018) 7:389. doi: 10.3390/jcm7110389
72. Boschetti E, D'Angelo R, Tardio ML,Costa R, Giordano C, Accarino A, et al. Evidence of enteric angiopathy and neuromuscular hypoxia in patients with mitochondrial neurogastrointestinal encephalomyopathy. *Am J Physiol Gastrointest Liver Physiol.* (2021) 320:G768–G779. doi: 10.1152/ajpgi.00047.2021
73. Chistiakov DA, Shkurat TP, Melnichenko AA, Grechko AV, Orekhov AN. The role of mitochondrial dysfunction in cardiovascular disease: a brief review. *Ann Med.* (2018) 50:121–7. doi: 10.1080/07853890.2017.1417631
74. Riva A, Tandler B, Loffredo F, Vazquez E, Hoppel C. Structural differences in two biochemically defined populations of cardiac mitochondria. *Am J Physiol Heart Circ Physiol.* (2005) 289:H868–72. doi: 10.1152/ajpheart.00866.2004
75. Pohjoismäki JL, Goffart S. The role of mitochondria in cardiac development and protection. *Free Radic Biol Med.* (2017) 106:345–54. doi: 10.1016/j.freeradbiomed.2017.02.032
76. Marzetti E, Csiszar A, Dutta D, Balagopal G, Calvani R, Leeuwenburgh C. Role of mitochondrial dysfunction and altered autophagy in cardiovascular aging and disease: from mechanisms to therapeutics. *Am J Physiol Heart Circ Physiol.* (2013) 305:H459–76. doi: 10.1152/ajpheart.00936.2012
77. Victor VM, Apostolova N, Herance R, Hernandez-Mijares A, Rocha M. Oxidative stress and mitochondrial dysfunction in atherosclerosis: mitochondria-targeted antioxidants as potential therapy. *Curr Med Chem.* (2009) 16:4654–67. doi: 10.2174/092986709789878265
78. Amchenkova AA, Bakeeva LE, Chentsov YS, Skulachev VP, Zorov DB. Coupling membranes as energy-transmitting cables. I. Filamentous mitochondria in fibroblasts and mitochondrial clusters in cardiomyocytes. *J Cell Biol.* (1988) 107:481–95. doi: 10.1083/jcb.107.2.481
79. Green DR, Reed JC. Mitochondria and apoptosis. *Science.* (1998) 281:1309–12. doi: 10.1126/science.281.5381.1309
80. Tang X, Li PH, Chen HZ. Cardiomyocyte senescence and cellular communications within myocardial microenvironments. *Front Endocrinol.* (2020) 11:280. doi: 10.3389/fendo.2020.00280
81. Dey S, DeMazumder D, Sidor A, Foster DB, O'Rourke B. Mitochondrial ROS drive sudden cardiac death and chronic proteome remodeling in heart failure. *Circ Res.* (2018) 123:356–71. doi: 10.1161/CIRCRESAHA.118.312708
82. Dorn GW II, Vega RB, Kelly DP. Mitochondrial biogenesis and dynamics in the developing and diseased heart. *Genes Dev.* (2015) 29:1981–91. doi: 10.1101/gad.269894.115
83. Lee CF, Chavez JD, Garcia-Menendez L, Choi Y, Roe ND, Chiao YA, et al. Normalization of NAD^+ redox balance as a therapy for heart failure. *Circulation.* (2016) 134:883–94. doi: 10.1161/CIRCULATIONAHA.116.022495
84. Nakayama H, Chen X, Baines CP, Klevitsky R, Zhang X, Zhang H, et al. Ca^{2+} and mitochondrial-dependent cardiomyocyte necrosis as a primary mediator of heart failure. *J Clin Invest.* (2007) 117:2431–44. doi: 10.1172/JCI31060
85. Wang W, Karamanlidis G, Tian R. Novel targets for mitochondrial medicine. *Sci Transl Med.* (2016) 8:326rv3. doi: 10.1126/scitranslmed.aac7410
86. Dominic EA, Ramezani A, Anker SD, Verma M, Mehta N, Rao M. Mitochondrial cytopathies and cardiovascular disease. *Heart.* (2014) 100:611–8. doi: 10.1136/heartjnl-2013-304657
87. Behjati M, Sabri MR, Etemadi Far M, Nejati M. Cardiac complications in inherited mitochondrial diseases. *Heart Fail Rev.* (2021) 26:391–403. doi: 10.1007/s10741-020-10009-1
88. Yan Y, Li S, Dong W, Liu C, Wang P, Hou W, et al. Correlation of mitochondrial transcription factor A with coronary heart disease. *J Pract Med.* (2018) 34:2892–5. doi: 10.3969/j.issn.1006-5725.2018.17.018
89. Santorelli FM, Gagliardi MG, Dionisi-Vici C, Parisi F, Tessa A, Carrozzo R, et al. Hypertrophic cardiomyopathy and mtDNA depletion. Successful treatment with heart transplantation. *Neuromuscul Disord.* (2002) 12:56–9. doi: 10.1016/S0960-8966(01)00248-6
90. Fangdai L, Fang F, Liu Z, Shen D, Ding C, Li J, et al. Clinical phenotype and genotypic characteristics of 12 cases of mitochondrial DNA depletion syndrome. *Chin J Pediatr.* (2019) 57:211–6. doi: 10.3760/cma.j.issn.0578-1310.2019.03.011
91. Wang B, Du Z, Shan G, Yan C, Zhang VW, Li Z. Case report: two Chinese infants of sengers syndrome caused by mutations in *AGK* gene. *Front Pediatr.* (2021) 9:639687. doi: 10.3389/fped.2021.639687
92. Dunham-Snary KJ, Ballinger SW. Mitochondrial genetics and obesity: evolutionary adaptation and contemporary disease susceptibility. *Free Radic Biol Med.* (2013) 65:1229–37. doi: 10.1016/j.freeradbiomed.2013.09.007
93. Krzywanski DM, Moellering DR, Fetterman JL, Dunham-Snary KJ, Sammy MJ, Ballinger SW. The mitochondrial paradigm for cardiovascular disease susceptibility and cellular function: a complementary concept to Mendelian genetics. *Lab Invest.* (2011) 91:1122–35. doi: 10.1038/labinvest.2011.95
94. Ruiz-Pesini E, Mishmar D, Brandon M, Procaccio V, Wallace DC. Effects of purifying and adaptive selection on regional variation in human mtDNA. *Science.* (2004) 303:223–6. doi: 10.1126/science.1088434
95. Tian R, Colucci WS, Arany Z, Bachschmid MM, Ballinger SW, Boudina S, et al. Unlocking the secrets of mitochondria in the cardiovascular system: path to a cure in heart failure—a report from the 2018 national heart, lung, and blood institute workshop. *Circulation.* (2019) 140:1205–16. doi: 10.1161/CIRCULATIONAHA.119.040551
96. Yan W, Donghai L, Xingxing Z. Thymidine kinase 2 gene compound heterozygous mutation leads to mitochondrial DNA depletion syndrome-2: a case report. *Chin J Pediatr.* (2018) 56:381–2. doi: 10.3760/cma.j.issn.0578-1310.2018.05.016
97. Domínguez-González C, Hernández-Laín A, Rivas E, Hernández-Voth A, Sayas Catalán J, Fernández-Torrón R, et al. Late-onset thymidine kinase 2 deficiency: a review of 18 cases. *Orphanet J Rare Dis.* (2019) 14:100. doi: 10.1186/s13023-019-1071-z
98. Dorado B, Area E, Akman HO, Hirano M. Onset and organ specificity of *Tk2* deficiency depends on Tk1 down-regulation and transcriptional compensation. *Hum Mol Genet.* (2011) 20:155–64. doi: 10.1093/hmg/ddq453
99. Wang L, Sun R, Eriksson S. Basic biochemical characterization of cytosolic enzymes in thymidine nucleotide synthesis in adult rat tissues: implications for tissue specific mitochondrial DNA depletion

and deoxynucleoside-based therapy for *TK2*-deficiency. *BMC Mol Cell Biol.* (2020) 21:33. doi: 10.1186/s12860-020-00272-3
100. Kamath VG, Hsiung CH, Lizenby ZJ, McKee EE. Heart mitochondrial TTP synthesis and the compartmentalization of TMP. *J Biol Chem.* (2015) 290:2034–41. doi: 10.1074/jbc.M114.624213
101. Landsverk ML, Zhang VW, Wong LC, Andersson HC. A *SUCLG1* mutation in a patient with mitochondrial DNA depletion and congenital anomalies. *Mol Genet Metab Rep.* (2014) 1:451–4. doi: 10.1016/j.ymgmr.2014.09.007
102. Demirbas D, Harris DJ, Arn PH, Huang X, Waisbren SE, Anselm I, et al. Phenotypic variability in deficiency of the α subunit of succinate-CoA ligase. *JIMD Rep.* (2019) 46:63–9. doi: 10.1002/jmd2.12018
103. Rivera H, Merinero B, Martinez-Pardo M, Arroyo I, Ruiz-Sala P, Bornstein B, et al. Marked mitochondrial DNA depletion associated with a novel *SUCLG1* gene mutation resulting in lethal neonatal acidosis, multi-organ failure, and interrupted aortic arch. *Mitochondrion.* (2010) 10:362–8. doi: 10.1016/j.mito.2010.03.003
104. Van Hove JL, Saenz MS, Thomas JA, Gallagher RC, Lovell MA, Fenton LZ, et al. Succinyl-CoA ligase deficiency: a mitochondrial hepatoencephalomyopathy. *Pediatr Res.* (2010) 68:159–64. doi: 10.1203/PDR.0b013e3181e5c3a4
105. Liu Y, Li X, Wang Q, Ding Y, Song J, Yang Y. Five novel *SUCLG1* mutations in three Chinese patients with succinate-CoA ligase deficiency noticed by mild methylmalonic aciduria. *Brain Dev.* (2016) 38:61–7. doi: 10.1016/j.braindev.2015.05.002
106. Körver-Keularts IM, de Visser M, Bakker HD, Wanders RJ, Vansenne F, Scholte HR, et al. Two novel mutations in the *SLC25A4* gene in a patient with mitochondrial myopathy. *JIMD Rep.* (2015) 22:39–45. doi: 10.1007/8904_2015_409
107. Hoshino A, Wang WJ, Wada S, McDermott-Roe C, Evans CS, Gosis B, et al. The ADP/ATP translocase drives mitophagy independent of nucleotide exchange. *Nature.* (2019) 575:375–9. doi: 10.1038/s41586-019-1667-4
108. Thompson K, Majd H, Dallabona C, Reinson K, King MS, Alston CL, et al. Recurrent *de novo* dominant mutations in *SLC25A4* cause severe early-onset mitochondrial disease and loss of mitochondrial DNA copy number. *Am J Hum Genet.* (2016) 99:860–76. doi: 10.1016/j.ajhg.2016.08.014
109. Kashiki T, Kido J, Momosaki K, Kusunoki S, Ozasa S, Nomura K, et al. Mitochondrial DNA depletion syndrome with a mutation in *SLC25A4* developing epileptic encephalopathy: a case report. *Brain Dev.* (2022) 44:56–62. doi: 10.1016/j.braindev.2021.08.005
110. Wang S, Lin L, Wang Y, Wang A, Liu Z, Wu S, et al. Novel homozygous mutation in the *FBXL4* gene is associated with mitochondria DNA depletion syndrome-13. *J Neurol Sci.* (2020) 416:116948. doi: 10.1016/j.jns.2020.116948
111. Guo W, Liu W, Chen Z, Gu Y, Peng S, Shen L, et al. Tyrosine phosphatase SHP2 negatively regulates NLRP3 inflammasome activation *via* ANT1-dependent mitochondrial homeostasis. *Nat Commun.* (2017) 8:2168. doi: 10.1038/s41467-017-02351-0
112. Jackson TD, Hock DH, Fujihara KM, Palmer CS, Frazier AE, Low YC, et al. The TIM22 complex mediates the import of sideroflexins and is required for efficient mitochondrial one-carbon metabolism. *Mol Biol Cell.* (2021) 32:475–91. doi: 10.1091/mbc.E20-06-0390
113. Kalari S, Zhao Y, Spannhake EW, Berdyshev EV, Natarajan V. Role of acylglycerol kinase in LPA-induced IL-8 secretion and transactivation of epidermal growth factor-receptor in human bronchial epithelial cells. *Am J Physiol Lung Cell Mol Physiol.* (2009) 296:L328–36. doi: 10.1152/ajplung.90431.2008
114. Vukotic M, Nolte H, König T, Saita S, Ananjew M, Krüger M, et al. Acylglycerol kinase mutated in sengers syndrome is a subunit of the TIM22 protein translocase in mitochondria. *Mol Cell.* (2017) 67:471–83.e7. doi: 10.1016/j.molcel.2017.06.013
115. Weiher H, Noda T, Gray DA, Sharpe AH Jaenisch R. Transgenic mouse model of kidney disease: insertional inactivation of ubiquitously expressed gene leads to nephrotic syndrome. *Cell.* (1990) 62:425–34. doi: 10.1016/0092-8674(90)90008-3
116. Shvetsova AN, Mennerich D, Keratar JM, Hiltunen JK Kietzmann T. Non-electron transfer chain mitochondrial defects differently regulate HIF-1alpha degradation and transcription. *Redox Biol.* (2017) 12:1052–61. doi: 10.1016/j.redox.2017.05.003
117. Antonenkov VD, Isomursu A, Mennerich D, Vapola MH, Weiher H, Kietzmann T Hiltunen JK. The human mitochondrial DNA depletion syndrome gene *MPV17* encodes a non-selective channel that modulates membrane potential. *J Biol Chem.* (2015) 290:13840–61. doi: 10.1074/jbc.M114.608083
118. Shaibani A, Shchelochkov OA, Zhang S, Katsonis P, Lichtarge O, Wong LJ, et al. Mitochondrial neurogastrointestinal encephalopathy due to mutations in *RRM2B*. *Arch Neurol.* (2009) 66:1028–32. doi: 10.1001/archneurol.2009.139
119. Alonzo JR, Venkataraman C, Field MS, Stover PJ. The mitochondrial inner membrane protein *MPV17* prevents uracil accumulation in mitochondrial DNA. *J Biol Chem.* (2018) 293:20285–94. doi: 10.1074/jbc.RA118.004788
120. Madungwe NB, Feng Y, Imam Aliagan A, Tombo N, Kaya F, Bopassa JC. Inner mitochondrial membrane protein *MPV17* mutant mice display increased myocardial injury after ischemia/reperfusion. *Am J Transl Res.* (2020) 12:3412–28.
121. El-Hattab AW, Wang J, Dai H, Almannai M, Staufner C, Alfadhel M, et al. *MPV17*-relatedmitochondrial DNA maintenance defect: new cases and review of clinical, biochemical, andmolecular aspects. *Hum Mutat.* (2018) 39:461–70. doi: 10.1002/humu.23387
122. Anagnostou ME, Ng YS, Taylor RW, McFarland R. Epilepsy due to mutations in the mitochondrial polymerase gamma (*POLG*) gene: a clinical and molecular genetic review. *Epilepsia.* (2016) 57:1531–45. doi: 10.1111/epi.13508
123. Hoff KE, DeBalsi KL, Sanchez-Quintero MJ, Longley MJ, Hirano M, Naini AB, et al. Characterization of the human homozygous R182W *POLG*2 mutation in mitochondrial DNA depletion syndrome. *PLoS ONE.* (2018) 13:e0203198. doi: 10.1371/journal.pone.0203198
124. Felhi R, Sfaihi L, Charif M, Desquiret-Dumas V, Bris C, Goudenège D, et al. Next generation sequencing in family with MNGIE syndrome associated to optic atrophy: Novel homozygous *POLG* mutation in the C-terminal sub-domain leading to mtDNA depletion. *Clin Chim Acta.* (2019) 488:104–10. doi: 10.1016/j.cca.2018.11.003
125. Lewis W, Day BJ, Kohler JJ, Hosseini SH, Chan SS, Green EC, et al. Decreased mtDNA, oxidative stress, cardiomyopathy, and death from transgenic cardiac targeted human mutant polymerase gamma. *Lab Invest.* (2007) 87:326–35. doi: 10.1038/labinvest.3700523
126. Ait El Cadi C, Krami AM, Charoute H, Elkarhat Z, Sifeddine N, Lakhiari H, et al. Prediction of the impact of deleterious nonsynonymous single nucleotide polymorphisms on the human *RRM2B* gene: a molecular modeling study. *Biomed Res Int.* (2020) 2020:7614634. doi: 10.1155/2020/7614634
127. Tseng YT, Li SW, HuangFu WC, Yen Y, Liu IH. The single nucleotide variant at c.662A>G in human *RRM2B* is a loss-of-function mutation. *Mol Genet Genomic Med.* (2020) 8:e1497. doi: 10.1002/mgg3.1497
128. Stojanovic V, Mayr JA, Sperl W, Barišić N, Doronjski A, Milak G. Infantile peripheral neuropathy, deafness, and proximal tubulopathy associated with a novel mutation of the *RRM2B* gene: case study. *Croat Med J.* (2013) 54:579–84. doi: 10.3325/cmj.2013.54.579
129. Lim AZ, McFarland R, Taylor R W, Gorman GS. *RRM2B Mitochondrial DNA Maintenance Defects.* GeneReviews® (1993–2021).
130. Li X, Li L, Sun Y, Lv F, Zhang G, Liu W, et al. Whole exome sequencing reveals two novel compound heterozygous mutations in *TWNK* as a cause of the hepatocerebral form of mitochondrial DNA depletion syndrome: a case report. *BMC Med Genet.* (2019) 20:146. doi: 10.1186/s12881-019-0875-y
131. Kume K, Morino H, Miyamoto R, Matsuda Y, Ohsawa R, Kanaya Y, et al. Middle-age-onset cerebellar ataxia caused by a homozygous *TWNK* variant: a case report. *BMC Med Genet.* (2020) 21:68. doi: 10.1186/s12881-020-01002-4
132. Jamali F, Ghaedi H, Tafakhori A, Alehabib E, Chapi M, Daftarian N, et al. Homozygous mutation in *TWNK* cases ataxia, sensorineural hearing loss and optic nerve atrophy. *Arch Iran Med.* (2019) 22:728–30.
133. Pohjoismäki JL, Goffart S, Taylor RW, Turnbull DM, Suomalainen A, Jacobs HT, et al. Developmental and pathological changes in the human cardiac muscle mitochondrial DNA organization, replication and copy number. *PLoS ONE.* (2010) 5:e10426. doi: 10.1371/journal.pone.0010426
134. Tanaka A, Ide T, Fujino T, Onitsuka K, Ikeda M, Takehara T, et al. The overexpression of Twinkle helicase ameliorates the progression of cardiac

fibrosis and heart failure in pressure overload model in mice. *PLoS One.* (2013) 8:e67. doi: 10.1371/journal.pone.0067642
135. Pohjoismäki JL, Williams SL, Boettger T, Goffart S, Kim J, Suomalainen A, et al. Overexpression of twinkle-helicase protects cardiomyocytes from genotoxic stress caused by reactive oxygen species. *Proc Natl Acad Sci USA.* (2013) 110:19408–13. doi: 10.1073/pnas.1303046110
136. Strauss KA, DuBiner L, Simon M, Zaragoza M, Sengupta PP, Li P, et al. Severity of cardiomyopathy associated with adenine nucleotide translocator-1 deficiency correlates with mtDNA haplogroup. *Proc Natl Acad Sci USA.* (2013) 110:3453–8. doi: 10.1073/pnas.1300690110
137. Huemer M, Karall D, Schossig A, Abdenur JE, Al Jasmi F, Biagosch C, et al. Clinical, morphological, biochemical, imaging and outcome parameters in 21 individuals with mitochondrial maintenance defect related to *FBXL4* mutations. *J Inherit Metab Dis.* (2015) 38:905–14. doi: 10.1007/s10545-015-9836-6
138. Barøy T, Pedurupillay CR, Bliksrud YT, Rasmussen M, Holmgren A, Vigeland MD, et al. A novel mutation in *FBXL4* in a Norwegian child with encephalomyopathic mitochondrial DNA depletion syndrome 13. *Eur J Med Genet.* (2016) 59:342–6. doi: 10.1016/j.ejmg.2016.05.005
139. Ballout RA, Al Alam C, Bonnen PE, Huemer M, El-Hattab AW, Shbarou R. *FBXL4*-related mitochondrial DNA depletion syndrome 13 (MTDPS13): a case report with a comprehensive mutation review. *Front Genet.* (2019) 10:39. doi: 10.3389/fgene.2019.00039
140. Emperador S, Garrido-Pérez N, Amezcua-Gil J, Gaudó P, Andrés-Sanz JA, Yubero D, et al. Molecular characterization of new *FBXL4* mutations in patients with mtDNA depletion syndrome. *Front Genet.* (2019) 10:1300. doi: 10.3389/fgene.2019.01300
141. Antoun G, McBride S, Vanstone JR, Naas T, Michaud J, Redpath S, et al. Detailed biochemical and bioenergetic characterization of *FBXL4*-related encephalomyopathic mitochondrial DNA depletion. *JIMD Rep.* (2016) 27:1–9. doi: 10.1007/8904_2015_491
142. Dai H, Zhang VW, El-Hattab AW, Ficicioglu C, Shinawi M, Lines M, et al. *FBXL4* defects are common in patients with congenital lactic acidemia and encephalomyopathic mitochondrial DNA depletion syndrome. *Clin Genet.* (2017) 91:634–9. doi: 10.1111/cge.12894
143. Sabouny R, Wong R, Lee-Glover L, Greenway SC, Sinasac DS, Care4Rare Canada, et al. Characterization of the C584R variant in the mtDNA depletion syndrome gene *FBXL4*, reveals a novel role for *FBXL4* as a regulator of mitochondrial fusion. *Biochim Biophys Acta Mol Basis Dis.* (2019) 1865:165536. doi: 10.1016/j.bbadis.2019.165536
144. de Oliveira VC, Gomes Mariano Junior C, Belizário JE, Krieger JE, Fernandes Bressan F, Roballo KCS, et al. Characterization of post-edited cells modified in the *TFAM* gene by CRISPR/Cas9 technology in the bovine model. *PLoS ONE.* (2020) 15:e235856. doi: 10.1371/journal.pone.0235856
145. Zhang J. *SLC26A4, TFAM Gene Polymorphism and Late-Onset Alzheimer's Disease in a Han Chinese Population*. Qingdao: China Ocean University (2013).
146. Bouda E, Stapon A, Garcia-Diaz M. Mechanisms of mammalian mitochondrial transcription. *Protein Sci.* (2019) 28:1594–05. doi: 10.1002/pro.3688
147. Stiles AR, Simon MT, Stover A, Eftekharian S, Khanlou N, Wang HL, et al. Mutations in *TFAM*, encoding mitochondrial transcription factor A, cause neonatal liver failure associated with mtDNA depletion. *Mol Genet Metab.* (2016) 119:91–9. doi: 10.1016/j.ymgme.2016.07.001
148. Bender A, Krishnan KJ, Morris CM, Taylor GA, Reeve AK, Perry RH, et al. High levels of mitochondrial DNA deletions in substantia nigra neurons in aging and Parkinson disease. *Nat Genet.* (2006) 38:515–7. doi: 10.1038/ng1769
149. Hansson A, Hance N, Dufour E, Rantanen A, Hultenby K, Clayton DA, et al. A switch in metabolism precedes increased mitochondrial biogenesis in respiratory chain-deficient mouse hearts. *Proc Natl Acad Sci USA.* (2004) 101:3136–41. doi: 10.1073/pnas.0308710100
150. Li H, Wang J, Wilhelmsson H, Hansson A, Thoren P, Duffy J, et al. Genetic modification of survival in tissue-specific knockout mice with mitochondrial cardiomyopathy. *Proc Natl Acad Sci USA.* (2000) 97:3467–72. doi: 10.1073/pnas.97.7.3467
151. Yang C, Wu R, Liu H, Chen Y, Gao Y, Chen X, et al. Structural insights into DNA degradation by human mitochondrial nuclease *MGME1*. *Nucleic Acids Res.* (2018) 46:11075–88. doi: 10.1093/nar/gky855
152. Matic S, Jiang M, Nicholls TJ, Uhler JP, Dirksen-Schwanenland C, Polosa PL, et al. Mice lacking the mitochondrial exonuclease *MGME1* accumulate mtDNA deletions without developing progeria. *Nat Commun.* (2018) 9:1202. doi: 10.1038/s41467-018-03552-x
153. Hebbar M, Girisha KM, Srivastava A, Bielas S, Shukla A. Homozygous c.359del variant in *MGME1* is associated with early onset cerebellar ataxia. *Eur J Med Genet.* (2017) 60:533–5. doi: 10.1016/j.ejmg.2017.07.010
154. Szabadosova V, Boronova I, Ferenc P, Tothova I, Bernasovska J, Zigova M, et al. Analysis of selected genes associated with cardiomyopathy by next-generation sequencing. *J Clin Lab Anal.* (2018) 32:22254. doi: 10.1002/jcla.22254
155. Zeharia A, Friedman JR, Tobar A, Saada A, Konen O, Fellig Y, et al. Mitochondrial hepato-encephalopathy due to deficiency of QIL1/MIC13 (C19orf70), a MICOS complex subunit. *Eur J Hum Genet.* (2016) 24:1778–82. doi: 10.1038/ejhg.2016.83
156. Zerbes RM, Höß P, Pfanner N, van der Laan M, Bohnert M. Distinct roles of Mic12 and Mic27 in the mitochondrial contact site and cristae organizing system. *Mol Biol.* (2016) 428:1485–92. doi: 10.1016/j.jmb.2016.02.031
157. Guarani V, McNeill EM, Paulo JA, Huttlin EL, Fröhlich F, Gygi SP, et al. QIL1 is a novel mitochondrial protein required for MICOS complex stability and cristae morphology. *Elife.* (2015) 4:e06265. doi: 10.7554/eLife.06265
158. Gödiker J, Grüneberg M, DuChesne I, Reunert J, Rust S, Westermann C, et al. QIL1-dependent assembly of MICOS complex-lethal mutation in C19ORF70 resulting in liver disease and severe neurological retardation. *J Hum Genet.* (2018) 63:707–16. doi: 10.1038/s10038-018-0442-y
159. Guarani V, Jardel C, Chrétien D, Lombès A, Bénit P, Labasse C, et al. QIL1 mutation causes MICOS disassembly and early onset fatal mitochondrial encephalopathy with liver disease. *Elife.* (2016) 5:e17163. doi: 10.7554/eLife.17163
160. Meurs KM, Friedenberg SG, Olby NJ, Condit J, Weidman J, Rosenthal S, et al. A QIL1 variant associated with ventricular arrhythmias and sudden cardiac death in the juvenile rhodesian ridgeback dog. *Genes.* (2019) 10:168. doi: 10.3390/genes10020168

Conflict of Interest: The authors declare that the research was conducted in the absence of any commercial or financial relationships that could be construed as a potential conflict of interest.

Publisher's Note: All claims expressed in this article are solely those of the authors and do not necessarily represent those of their affiliated organizations, or those of the publisher, the editors and the reviewers. Any product that may be evaluated in this article, or claim that may be made by its manufacturer, is not guaranteed or endorsed by the publisher.

Copyright © 2022 Wang, Han, Li, Chen, Chen, Wang, Zhang, Zhang, Wang, Xia and Yuan. This is an open-access article distributed under the terms of the Creative Commons Attribution License (CC BY). The use, distribution or reproduction in other forums is permitted, provided the original author(s) and the copyright owner(s) are credited and that the original publication in this journal is cited, in accordance with accepted academic practice. No use, distribution or reproduction is permitted which does not comply with these terms.

GLOSSARY

Full Name	Abbreviations
Outer Mitochondrial Membrane	OMM
Inner Mitochondrial membrane	IMM
Mitochondrialintermembrane space	IMS
Mitochondrial Respiratory Chain	MRC
Respiratory Chain	RC
Mitochondrial Permeability Transition Pore	MPTP
Mitochondria lDNA	mtDNA
nuclear DNA	nDNA
Ribosomal RNA	rRNA
transfer RNA	tRNA
Mitochondrial DNA depletion syndrome	MDS
Oxidative Phosphorylation	OXPHOS
Electron Transport Chain	ETC
Ubiquinone oxidoreductase subunit AB1	NDUFAB1
cytochrome C	Cyt c
ADP/ATP carrier	AAC
apoptosis-inducing factor	AIF
coenzyme Q10	CoQ10
supercomplex	SCs
Mitochondrial Membrane Potential	MMP
Reactive Oxygen Species	ROS
Nicotinamide Adenine Dinucleotide	NADH
acyl carrier protein	ACP
Tricarboxylic Acid Cycle	TCA
reduced flavin adenosine dinucleotide	FADH2
hypoxia inducible factor	HIF
Prolyl Hydroxylase	PHD
Hypoxia Response Element	HRE
Fatty Acid β-Oxidation	FAO
acetyl Coenzyme A	acetyl-CoA
nicotinamide adenine dinucleotide	NAD+
flavin adenine dinucleotide	FAD
AMP-activated protein kinase	AMPK
mitochondrial protein	Mfn
dynein-related protein-like 1	Drp1 / DLP1
optic nerve atrophy 1	OPA1
Pyruvate Dehydrogen-ase Phosphatase 1	PDP1
Pyruvate Decarboxylase	PDH
α-Ketoglutarate Dehydrogenase	α-KGDH
mitochondrial permeability transition pore	MPTP
Sarcoplasmic Reticulum	SR
type 2 Ryanodine receptor	RyR2
Mitochondrial Calcium Uniporter	MCU
Mitochondrial Calcium Uptake 1	MICU1
Endoplasmic Reticulum	ER
Mitchondria Associated Endoplasmic Reticulum Membrane	MAM
Mitochondrial-Derived Peptide	MDP
mitochondrial DNA depletion syndrome-2	MTDPS2
Creatine Kinase	CK
Thymidine Kinase 2	TK2
Deoxythymidine	dThd
deoxycytidine monophosphate	dCMP
deoxythymidine monophosphate	dTMP
external eye muscle paralysis	adPEO
Mitochondrial Depletion Syndrome 13	MTDPS 13
Mitochondrial Depletion Syndrome 9	MTDPS 9
Cytochrome-C Oxidase	COX
Mitochondrial Neurogastrointestinal Encephalopathy Disease	MNGIE
Thymidine Phosphorylase	TP
vascular endothelial growth factor	VEGF
Thymidine	Thd
Deoxyuridine	dUrd
deoxyuridine triphosphate pool	dNTP
Chronic Progressive External Ophthalmoplegia	CPEO
oxidized low density protein	oxLDL
heart failure	HF
cardiovascular disease	CVD
thymidylate synthase	TS
Thymidine Triphosphate	TTP
Thymidine monophosphate	TMP
Polymerase Gamma	POLG
DNA Polymeraseγ	POLγ
Succinate COA ligases	SUCL
Succinate-CoA Ligase GDP/ADP-Forming Subunit ?	SUCLG 1
Ribonucleotide Reductase Regulatory TP53 Inducible Subunit M2B	RRM2B
Ribonucleotide Reductase	RNR
Ribonucleoside Reductase	RIR2B
Mitochondrial Depletion Syndrome 7	MTDPS 7
Infantile-onset Spinocerebellar Ataxia	IOSCA
Adenine Nucleotide Translocase	ANT1
mitochondrial exhaustion syndrome 12	MTDPS12
Skp1-Cullin-F-box	SCF
Dichloroacetic acid	DCA
mitochondrial transcription factor A	TFAM
mitochondrial contact site and cristae tissue system	MICOS
Mitochondrial Contact Site And Cristae Organizing System Subunit 13	MICOS13
box and leucine-rich repeat protein 4	FBXL4
Twinkle	TWNK
Solute Carrier Family 25 Member 4	SLC25A4
Mitochondrial Inner Membrane Protein MPV17	MPV17
mitochondrial exhaustion syndrome 13	MTDPS13
fallot syndrome	TOF
ventricular septal defect	ASD
supraventricular tachycardia	SVT
glucose-regulated protein 75	GRP75
Mitochondrial Genome Maintenance Exonuclease 1	MGME1
Acylglycerol Kinase	AGK

(Continued)

frontiers in Cardiovascular Medicine

ORIGINAL RESEARCH
published: 21 February 2022
doi: 10.3389/fcvm.2022.808163

Programmed Exercise Attenuates Familial Hypertrophic Cardiomyopathy in Transgenic E22K Mice *via* Inhibition of PKC-α/NFAT Pathway

Haiying Wang[1†], Yuedong Lin[2†], Ran Zhang[3], Yafen Chen[3], Wei Ji[3], Shenwei Li[3], Li Wang[4], Rubin Tan[5*] and Jinxiang Yuan[6*]*

[1] Department of Physiology, Institute of Basic Medical College, Jining Medical University, Jining, China, [2] Cardiac Emergency Department, Affiliated Hospital of Jining Medical University, Jining, China, [3] Institute of Basic Medical College, Jining Medical University, Jining, China, [4] School of Nursing, Medical College, Soochow University, Suzhou, China, [5] Department of Physiology, Basic Medical School, Xuzhou Medical University, Xuzhou, China, [6] The Collaborative Innovation Center, Jining Medical University, Jining, China

OPEN ACCESS

Edited by:
Shijun Wang,
Fudan University, China

Reviewed by:
Alf Mansson,
Linnaeus University, Sweden
Chunkai Huang,
Shanghai Jiao Tong University, China

***Correspondence:**
Li Wang
li-wang-1@suda.edu.cn
Rubin Tan
tanrubin11@126.com
Jinxiang Yuan
yuanjinxiang18@163.com

[†] These authors have contributed equally to this work

Specialty section:
This article was submitted to Cardiovascular Metabolism, a section of the journal Frontiers in Cardiovascular Medicine

Received: 03 November 2021
Accepted: 24 January 2022
Published: 21 February 2022

Citation:
Wang H, Lin Y, Zhang R, Chen Y, Ji W, Li S, Wang L, Tan R and Yuan J (2022) Programmed Exercise Attenuates Familial Hypertrophic Cardiomyopathy in Transgenic E22K Mice via Inhibition of PKC-α/NFAT Pathway. Front. Cardiovasc. Med. 9:808163. doi: 10.3389/fcvm.2022.808163

Familial hypertrophic cardiomyopathy (FHCM), an autosomal dominant disease, is caused by mutations in genes encoding cardiac sarcomeric proteins. E22K, a mutation in the myosin regulatory light chain sarcomere gene, is associated with the development of FHCM. However, the molecular mechanisms by which E22K mutation promotes septal hypertrophy are still elusive. The hypertrophic markers, including beta-myosin heavy chain, atrial natriuretic peptide and B-type natriuretic peptide, were upregulated, as detected by fluorescence quantitative PCR. The gene expression profiles were greatly altered in the left ventricle of E22K mutant mice. Among these genes, nuclear factor of activated T cells (*NFAT*) and protein kinase C-alpha (*PKC*-α) were upregulated, and their protein expression levels were also verified to be elevated. The fibrosis markers, such as phosphorylated Smad and transforming growth factor beta receptor, were also elevated in transgenic E22K mice. After receiving 6 weeks of procedural exercise training, the expression levels of PKC-α and NFAT were reversed in E22K mouse hearts. In addition, the expression levels of several fibrosis-related genes such as transforming growth factor beta receptor 1, Smad4, and alpha smooth muscle actin in E22K mouse hearts were also reversed. Genes that associated with cardiac remodeling such as myocyte enhancer factor 2C, extracellular matrix protein 2 and fibroblast growth factor 12 were reduced after exercising. Taken together, our results indicate that exercise can improve hypertrophy and fibrosis-related indices in transgenic E22K mice *via* PKC-α/NFAT pathway, which provide new insight into the prevention and treatment of familial hypertrophic cardiomyopathy.

Keywords: E22K, PKC-α, NFAT, fibrosis, hypotrophy

INTRODUCTION

Familial hypertrophic cardiomyopathy (FHCM) is an autosomal dominant genetic disease featured by myofibrillar disarray and left ventricle or septal hypertrophy (1, 2). It originates from gene mutations encoding major proteins of myocardial filaments (e.g., myosin) and other related proteins. E22K (glutamic acid to lysine substitution at position 22), a genetic mutation in myosin regulatory light chain (RLC) sarcomeric protein, is located near the Ca^{2+} binding site and RLC phosphorylation site (Ser15) (3). The E22K mutation in RLC gene may cause hypertrophic cardiomyopathy with septal hypertrophy and midventricular obstruction (3), and is closely associated with the eventual formation of FHCM. Previous research has shown that E22K mutation prevents RLC phosphorylation and decreases its affinity for Ca^{2+} binding (3). In transgenic E22K mouse model, the left ventricular systolic and diastolic, ejection or shortening fractions were not affected by E22K mutation, the heart-to-body weight ratio was relatively the same, and the M-mode echo did not show any signs of hypertrophy. However, hematoxylin and eosin staining data showed that 13-month-old E22K mutant mice had the characteristics of enlarged ventricular septa and papillary muscle (2). Other physiological studies indicated that the Ca^{2+} activated force and myofibrillar ATPase activity in E22K mice were increased compared to those in wild-type mice (2).

Protein kinase C (PKC) is a calcium dependent serine/threonine kinase family that can be elicited *via* hydrolysis of membrane phosphatidylinositol and receptor-mediated activation of phospholipase C (PLC) (4). PKC has generally been considered as a master regulator of signal transduction pathway, which regulates various biological functions, including cell growth, differentiation, transformation, apoptosis, tumorigenesis, and so on (5, 6). PKC is a central enzyme that regulates the proliferation and hypertrophy of cardiomyocytes, and plays an essential role in mediating cardiac signal transduction. It has been reported that PKC signaling pathway can be activated by the intracellular events related to circulating hormone response. These events affect different physiological processes of the cardiovascular system, leading to time-varying and force-dependent effects (7). Numerous studies have demonstrated that PKC activation is related to cardiovascular diseases, including heart failure (8–12). The main subtype of PKC expressed in rabbit, mouse and human hearts is PKC-alpha (PKC-α). It has been reported that the activation or overexpression of PKC-α is associated with cardiac hypertrophy, mitogenic stimulation, dilated cardiac myopathy, ischemic injury, myocardial infarction, and human heart failure (13–15). PKC-α triggers the activation of different regulatory proteins, such as the nuclear factor of activated T cells (NFAT) and cyclic adenosine monophosphate (cAMP) response-binding protein (CREB), which are also Ca^{2+} responsive transcription factors (16). The dephosphorylated NFAT can promote the expression of various genes in neurons, cardiac muscle cells, lymphocytes, and skeletal muscle cells (17–19).

Although ventricular hypertrophy caused by E22K mutation has been extensively studied in cell and animal models, the molecular mechanism of myocardial remodeling caused by E22K mutation is still elusive. We hypothesize that the activation of PKC-α/NFAT signaling pathway caused by E22K mutation may lead to cardiomyocyte remodeling. Growing evidence indicates that cardiac rehabilitation is associated with the decreased incidence and mortality of cardiovascular diseases (20, 21). Hypertrophic cardiomyopathy can also be improved by regular exercise, especially aerobic exercise (22). This study aimed to investigate whether the expression levels of genes and proteins related to myocardial remodeling can be reversed in E22K mutant mice after receiving a programmed exercise.

MATERIALS AND METHODS

Mouse Models

Transgenic mice were procured from Dr. Danuta Szczesna-Cordary's laboratory (FL, USA). The transgenic knock-in mice had the expression of myc-tagged human RLCs driven by α-myosin heavy chain promoter. The myc-E22K (Tg-E22K) mutant (2), myc-wild-type (Tg-WT), and non-transgenic (Tg-WT) B6SJL mice were obtained. The animal experiments were approved by the Institutional Animal Care and Use Committee at the Soochow University (reference number: BK20150353), and were performed in compliance with the Guidelines for the Care and Use of Research Animals established by the Soochow University, Suzhou, China. All mice were placed in 12/12 h of dark/bright cycles under specific aseptic (SPF) conditions. They were given unlimited access to water and food throughout the experiment.

Animal Experiments

The Tg-E22K, Tg-WT, and Non-Tg mice (male, 8 weeks old) were randomly assigned to treadmill exercise group (E-Tg-E22K, E-Tg-WT, and E-Non-Tg) and rest (sedentary) control group (R-Tg-E22K, R-Tg-WT, and R-Non-Tg). Mice in the exercise group were introduced to running exercise (4 days per week on a treadmill) for 6 weeks at 20°C. Adaptive training was performed with moderate treadmill running (first ran at 5 m/min for 5 min, and then ran at 10 m/min for another 5 min) 1 day before initiating the exercise program. In the 6-week exercise training, warming-up and cooling-down (5 min running at 5 m/min) were conducted, followed by the running exercise program of 10 min at 10 m/min at week 1, 10 min at 15 m/min week 2, 20 min at 15 m/min at week 3 and 4, and 20 min at 20 m/min at week 5 and 6. Mice in the rest group were placed on the stationary treadmill for 5–10 min for 4 times per week (23). All mice were euthanized

Abbreviations: FHCM, Familial hypertrophic cardiomyopathy; ANP, Atrial natriuretic peptide; BNP, Brain natriuretic peptide; β-MHC, Beta-myosin heavy chain; PKC-α, Protein kinase C-alpha; NFAT, Nuclear factor of activated T cells; MEF2C, Myocyte enhancer factor 2C; Fgf12, Fibroblast growth factor 12; cAMP, Cyclic adenosine monophosphate; CREB, Cyclic adenosine monophosphate response-binding protein; RLC, Regulatory light chain; BSA, Bovine serum albumin; GAPDH, Glyceraldehyde-3-phosphate dehydrogenase; TBST, TBS+Tween; RNA-Seq, RNA Sequencing; DEGs, Differentially expressed genes; TGFβ, Transforming growth factor beta; TGFβR, Transforming growth factor beta receptor; Colq, Collagen-like tail subunit; Myh11, Heavy polypeptide 11; Ecm2, Extracellular matrix protein 2; Creb1, cAMP responsive element binding protein 1; FGFR4, Fibroblast growth factor receptor 4; PLC-γ, Phospholipase C gamma; MyHC, Myosin heavy chain.

TABLE 1 | The primer pairs used for real-time PCR.

Name	q-PCR primer
mGAPDH	F: 5′-CATTTCCTGGTATGACAATGAATACG-3′
	R: 5′-TCCAGGGTTTCTTACTCCTTGGA-3′
β-MHC	F: 5′-TGCAAAGGCTCCAGGTCTGAGGGC-3′
	R: 5′-GCCAACACCAACCTGTCCAAGTTC−3′
ANP	F: 5′-AGGAGAAGATGCCGGTAGAAGA-3′
	R: 5′-GCTTCCTCAGTCTGCTCACTCA-3′
BNP	F: 5′-GTCTTGGCCTTTTGGCTTC-3′
	R: 5′-TTCCTCAGTCTGCTCACTC-3′

by cervical dislocation 3 days after exercise. The heart tissues were collected immediately, and then placed into cold phosphate buffer saline solution to remove any residual blood. All tissue samples were stored in a freezer at −80°C until further analysis.

RNA Sequencing

To reveal the transcriptome changes induced by E22K mutation, TRIzol reagent (Thermo Fisher Scientific, USA) was used to extract total RNA from the heart tissues of mice with different genotypes, including Tg-WT, Tg-E22K, and Non-Tg. The library construction and RNA sequencing were conducted by Novogene Company (Beijing, China).

cDNA Synthesis and Real-Time PCR

Total RNA was extracted from the left ventricular myocardial tissues of three genotypes (Tg-E22K, Tg-WT, and Non-Tg) using Trizol reagent (Thermo Fisher Scientific, Catalog #15596026). After treatment with DNASE-I (New England Biolabs, Catalog #M0303S) to remove genomic DNA, total RNA was cleaned with RNA clean-up Kit (Qiagen, Catalog #74204). cDNA synthesis was conducted with PrimeScript TM RT Master Mix (RR036A, Tkara, China) reaction system according to the manufacturer's instructions. Real-time PCR amplification was conducted by TB Green Premix Ex TaqTM II (RR820A, Tkara, China) reaction system using the primers listed in **Table 1** (24). The $2^{-\Delta\Delta Ct}$ method was used for the relative quantification of gene expression, standardized by glyceraldehyde-3-phosphate dehydrogenase (GAPDH) as the invariant control for the sample, and then compared with the reference sample.

Western Blotting

Total protein of the left ventricular myocardium tissues from three genotype of mice (Tg-E22K, Tg-WT, and Non-Tg) was lysed in 1×RIPA buffer (Bio-Rad). Protein quantification was performed using the BCA protein assay reagent according to manufacturer's instruction. Protein extracts (25 μg/lane) were separated by SDS-PAGE using 10% lab-made Tris-glycine gels, and transferred onto a PVDF membrane. The membranes were blocked with 5% dried milk for 1 h at room temperature, followed by overnight incubation with primary antibody. The primary antibodies were diluted with 1X TBS+Tween (TBST) containing 3% bovine serum albumin (BSA). After washing three times with TBST buffer (10 min/each time), the membranes were incubated with the corresponding secondary antibody in TBST containing 5% dried milk at room temperature for 1 h. Visualization of protein blots was performed using the ECL substrate (Tanon 5200) after three times washing with TBST (10 min/each time). The primary antibodies used were as follows: GAPDH (D16H11, 1:1000, 5174S, Cell Signaling Technology, USA), PKC-α (D7E6E, 1:1000, 59754S, Cell Signaling Technology, USA), NFAT1 (D43B1, 1:1000, 5861S, Cell Signaling Technology, USA), Smad2/3 (D7G7, 1:1000, 8685s, Cell Signaling Technology, USA), Phospho-SMAD2 (Ser465/Ser467, 1:1000, 8685s, Cell Signaling Technology, USA), TGFβ Receptor II (1:1000, 79424s, Cell Signaling Technology, USA). The secondary antibodies used were HRP-linked goat anti-Mouse IgG (1:5000, ZB-2305, ZSGB-Bio, China) and Goat Anti-rabbit IgG (1:5000, ZB-2305, ZSGB-Bio, China). Densitometry analysis was conducted with ImageJ 1.34s software.

Statistical Analysis

Data are presented as mean ± SEM. Unpaired, two-sided Student's *t*-test was used when comparing 2 sets of data as indicated. Meanwhile, unpaired, one-way ANOVA followed by Tukey's *post-hoc* test was used for multiple comparisons. All statistical tests were performed using the GraphPad Prism8 software. $P < 0.05$ was defined as statistical significant.

RESULT

E22K Mutation Induces Ventricular Hypertrophy

To determine the effect of E22K mutation on ventricular hypertrophy, real-time PCR was performed to detect three classic hypertrophic markers in the cardiac tissues of sedentary mice. The hypertrophic markers detected are beta-myosin heavy chain (β-MHC), atrial natriuretic peptide (ANP) and brain natriuretic peptide (BNP). ANP plays an important biological role in inhibiting myocardial hypertrophy and fibrosis, resisting oxidative stress, as well as preventing the development of ischemia/reperfusion injury (25–27). BNP levels are closely related to the degree of left ventricular failure in patients with heart failure (28, 29). β-MHC molecules are important parts of myosin, which play a major role in myocardial contraction (30, 31). It was found that the mRNA levels of β-MHC, ANP, and BNP were upregulated in the cardiac tissues of R-Tg-E22K mice compared to R-Tg-WT mice, indicating that E22K mutation could activate cardiac remodeling (**Figures 1A–C**).

E22K Mutation Affects the Pathological Makers of Cardiac Fibrosis

Fibrosis is often associated with ventricular hypertrophy and impairment of cardiac function. As presented in **Table 2**, fibrosis-related genes such as transforming growth factor beta receptor (*TGFβR*), *Smad*, and *Col1a* were significantly upregulated in E22K mice. TGFβ expression in cardiomyocytes may also responsible for cardiac dysfunction and maladaptive hypertrophy *via* regulation of PKC (32, 33). In cardiac fibroblasts, TGFβ plays a central role in regulating different aspects of fibrosis such as myofibroblast differentiation, inflammatory response,

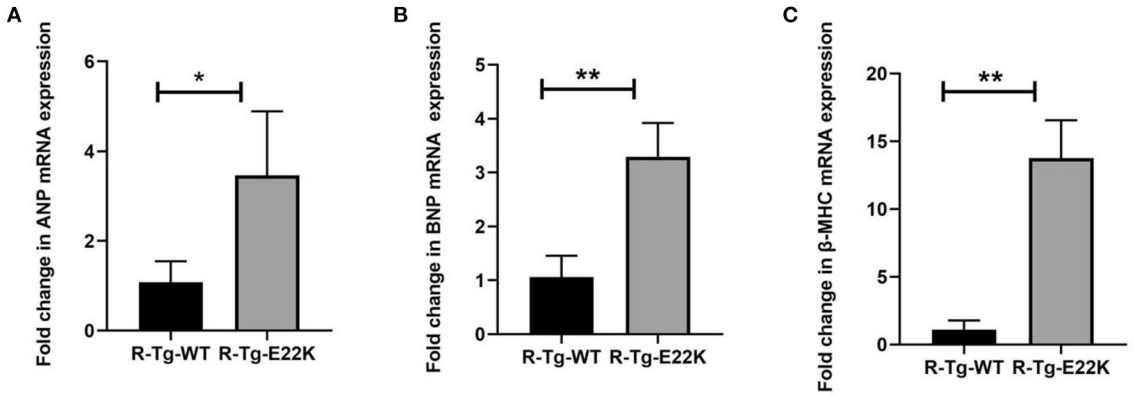

FIGURE 1 | E22K mutation significantly increases the expression levels of ventricular hypertrophy markers. **(A–C)** Real-time PCR analysis was conducted for the R-Tg-E22K and R-Tg-WT mice. The mRNA levels of ANP **(A)**, BNP **(B)**, and β-MHC **(C)** were determined using the delta-delta CT method. Compared to R-Tg-WT mice, the expression levels of these three genes were remarkably upregulated in R-Tg-E22K mice heart tissue. Each sample was repeated three times. Student's *t*-test was employed to assess the differences in abundance levels. $N = 3$, $^{*}p < 0.05$; $^{**}p < 0.01$. R-Tg-WT, wild-type transgenic mice in the rest group; R-Tg-E22K, transgenic E22K mice in the rest group.

extracellular matrix synthesis and gene expression (34–36). TGFβ receptor transmits intracellular signals through Smad proteins, which in turn translocate to the nucleus to control gene transcription (37). The expression levels of TGFβR and p-Smad2 proteins were verified by Western blotting to determine their association with fibrosis in E22K transgenic mouse hearts. Western blot results showed that Smad2 phosphorylation and TGFβR levels were upregulated in R-Tg-E22K mouse heart tissues compared to R-Tg-WT and Non-Tg control mouse heart tissues (**Figures 2A,C**). Quantitative analysis indicated there were significant differences in the protein levels of p-Smad2 and TGFβR ($p < 0.05$, **Figures 2B,D**). Our results indicated that E22K mutation affected the expression of cardiac fibrosis makers in E22K mice heart.

E22K Mutation Remarkably Changes Gene Expression Profiles in the Left Ventricle of Mouse Hearts

To investigate whether RLC site mutation at E22K can affect the gene expression profiles of cardiomyocytes in the left ventricle, RNA sequencing was performed after extraction of total RNA from the heart tissues of mice with three different genotypes in the rest group. In total, 3,136 differentially expressed genes (DEGs) were detected between R-Tg-E22K and R-Tg-WT mice, of which 1,533 were upregulated and 1,603 were downregulated (**Figure 3A**). In addition, 21,317 genes remained unchanged. Similar results were noticed between R-Tg-E22K and R-Non-Tg mice. In this group, 2,907 genes were differentially expressed, of which 1,347 and 1,560 genes were upregulated and downregulated, respectively, and 21,384 genes were not altered (**Figure 3B**). A previous study reported different phenotypes of septal hypertrophy in the hearts of 13-month-old E22K mice *via* histological staining (2). Although echocardiography did not reveal the changes in ejection fraction and shortening fraction between E22K and WT mice (38), our RNA-Seq data indicated three main categories of genes were differentially expressed in the E22K mice heart (**Table 2**). They are myocardial contraction and hypertrophy-related genes (e.g., *Myh6, Myh7b, Mhrt, Nppa,* and *Nppb*), cardiac fibrosis genes (e.g., *Col6a5, Col8a1, Col1a2, Tgfbr1, Tgfb2, Tgfb3, Smad4, and Acta2*) and signaling pathways-associated genes (e.g., *Prkca* and *Nfatc4).*

E22K Mutation Activates PKC-α/NFAT Signaling

As shown in **Table 2**, PKC-α and NFAT were transcriptionally upregulated in R-Tg-E22K mouse hearts compared to those in R-Tg-WT and Non-Tg mouse hearts. Therefore, Western blotting was carried out to detect the protein levels of PKC-α and NFAT. Our results confirmed that, in transgenic E22K mouse heart tissue, the protein expression levels of PKC-α and NFAT transcription factor were significantly enhanced ($p < 0.05$, **Figures 4A–D**).

Exercise Reverses the Protein Expression of PKC-α/NFAT in E22K Mouse Hearts

To test whether the expression of PKC-α/NFAT in E22K mouse hearts can be reversed after receiving an exercise training program, Western blot analysis was carried out. Our results showed that the protein levels of PKC-α (**Figures 5A,B**) and NFAT transcription factor (**Figures 5C,D**) in exercise-trained E22K mice were relatively similar to those in E-Tg-WT and E-Non-Tg control mice. These results imply that exercise can improve PKC-α/NFAT signaling that is dysregulated due to E22K mutation.

Exercise Regulates Cardiac Remodeling Related Genes in the Left Ventricle of Both E22K and WT Mice

To investigate whether exercise can regulate the expression of myocardial function-related genes, all mice were subjected to an

TABLE 2 | Changes in gene expression profiles in the left ventricle of E22K mutant mice.

Gene	Log2FC	*P*-value	P-adj	Gene_description
R-E22K vs. R-WT				
Myh6	−0.760203209	8.73E-14	7.48E-11	Myosin, heavy polypeptide 6, cardiac muscle, alpha
Myh7b	−1.089644008	7.79E-19	1.09E-15	Myosin, heavy chain 7B, cardiac muscle, beta
Mhrt	1.715486122	1.52E-26	5.88E-23	Myosin heavy chain associated RNA transcript
Nppa	2.930583503	0.002454211	0.034356725	Natriuretic peptide type A
Nppb	1.678670308	0.005711738	0.062158281	Natriuretic peptide type B
Col6a5	3.375981869	0.00000577	0.000367596	Collagen, type VI, alpha 5
Col8a1	1.277527091	0.0000159	0.000791111	Collagen, type VIII, alpha 1
Col1a2	0.993288854	0.00086216	0.016063451	Collagen, type I, alpha 2
Tgfbr1	0.594576373	0.002391314	0.033782781	Transforming growth factor, beta receptor I
Tgfb2	1.50076272	1.57E-08	0.00000303	Transforming growth factor, beta 2
Tgfb3	1.186157811	0.000000077	0.000012	Transforming growth factor, beta 3
Smad4	0.329231545	0.001305242	0.021839444	SMAD family member 4
Acta2	1.333706795	0.000000816	0.0000801	alpha smooth muscle actin
Prkca	0.38901659	0.002945265	0.039203284	Protein kinase C, alpha
Nfatc4	0.739779165	0.003460926	0.043890785	Nuclear factor of activated T cells, cytoplasmic, calcineurin dependent 4

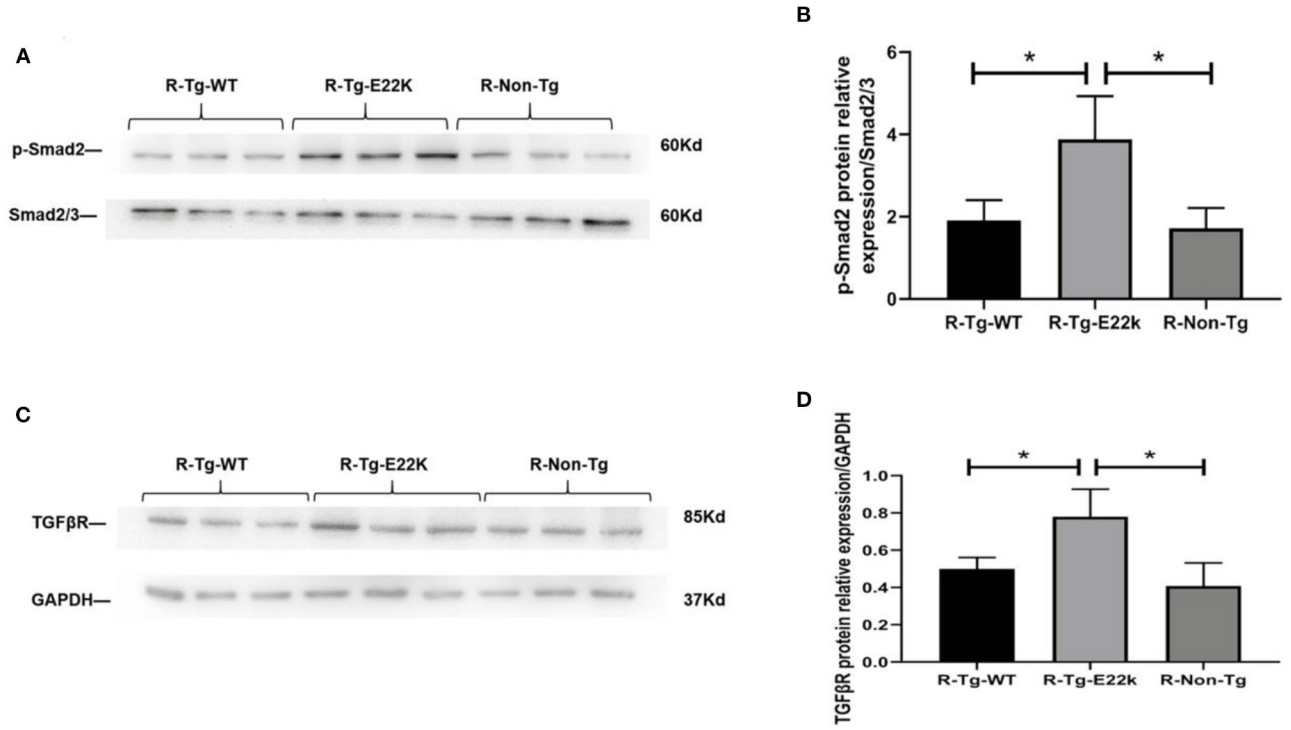

FIGURE 2 | E22K mutation elevates the protein expression of p-Smad2 and TGFβR. Representative Western blot results demonstrated the upregulated expression of TGFβR and increased phosphorylation of Smad2 in R-Tg-E22K mouse hearts compared to those in R-Tg-WT and Non-Tg mouse hearts **(A,C)**. Densitometric analysis of the protein levels of p-Smad2 and TGFβR in each group **(B,D)**. $N = 3$, $^*p < 0.05$. R-Tg-WT, wild-type transgenic mice in the rest group; R-Tg-E22K, transgenic E22K mice in the rest group; R-Non-Tg, non-transgenic wild-type mice in the rest group.

exercise training program for 6 weeks. The mouse hearts were then dissected 3 days after performing the exercise program. RNA sequencing was performed on the left ventricle of both the exercise and sedentary mice. Our results indicated that there were 391 genes with differential expression between R-Tg-E22K and E-Tg-E22K groups, of which 195 and 196 genes were upregulated and downregulated, respectively (**Figure 6A**). Among these genes, the fibrosis-related genes such as fibroblast growth factor

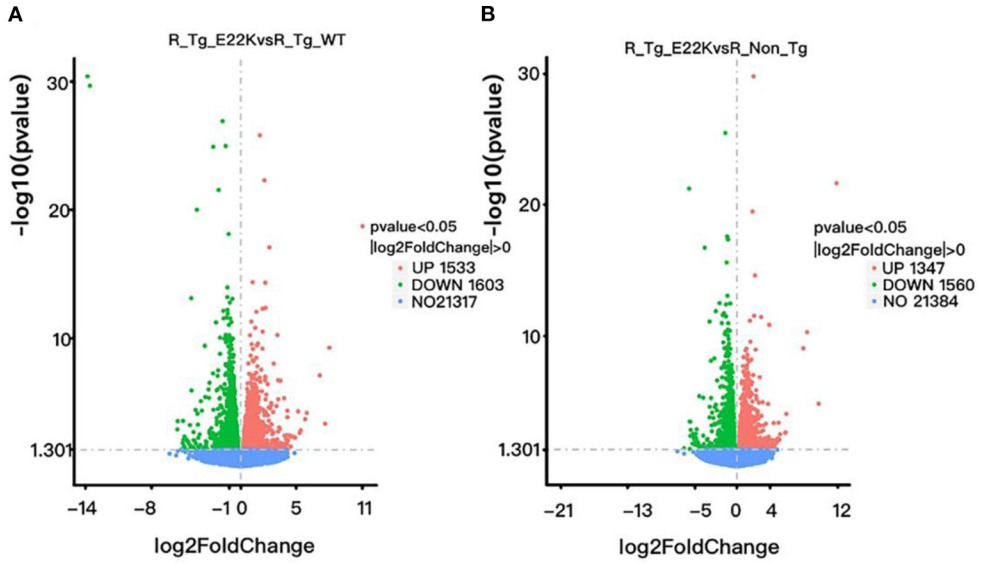

FIGURE 3 | E22K site mutation remarkably changes the gene expression profiles of cardiomyocytes in the left ventricle. Volcano map of DEGs **(A,B)**. There were 3,136 genes differently expressed between R-Tg-E22K and R-Tg-WT groups **(A)**, of which 1,533 and 1,603 genes were upregulated and downregulated, respectively, and 21,317 genes remained unchanged. There were 2,907 genes differently expressed between R-Tg-E22K and R-Non-Tg groups **(B)**, of which 1,347 and 1,560 genes were downregulated and upregulated, respectively, and 21,384 genes were not altered. R-Tg-WT, wild-type transgenic mice in the rest group; R-Tg-E22K, transgenic E22K mice in the rest group; R-Non-Tg, non-transgenic wild-type mice in the rest group.

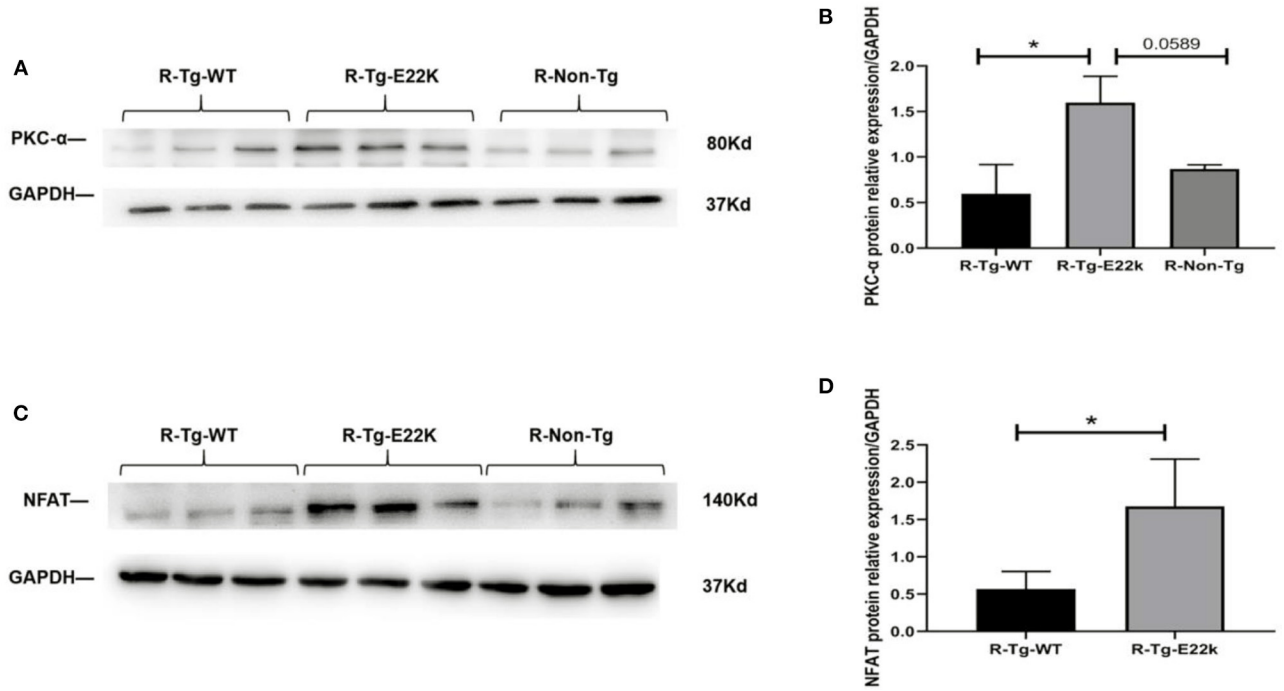

FIGURE 4 | E22K mutation upregulates the protein expression of PKC-α and NFAT. Representative Western blot data showing the upregulated expression levels of PKC-α and NFAT in R-Tg-E22K mouse hearts compared to R-Tg-WT and R-Non-Tg mouse hearts **(A,C)**. Densitometric analysis of the protein levels of PKC-α and NFAT in each group **(B,D)**. $N = 3$, $^*p < 0.05$. R-Tg-WT, wild-type transgenic mice in the rest group; R-Tg-E22K, transgenic E22K mice in the rest group; R-Non-Tg, non-transgenic wild-type mice in the rest group.

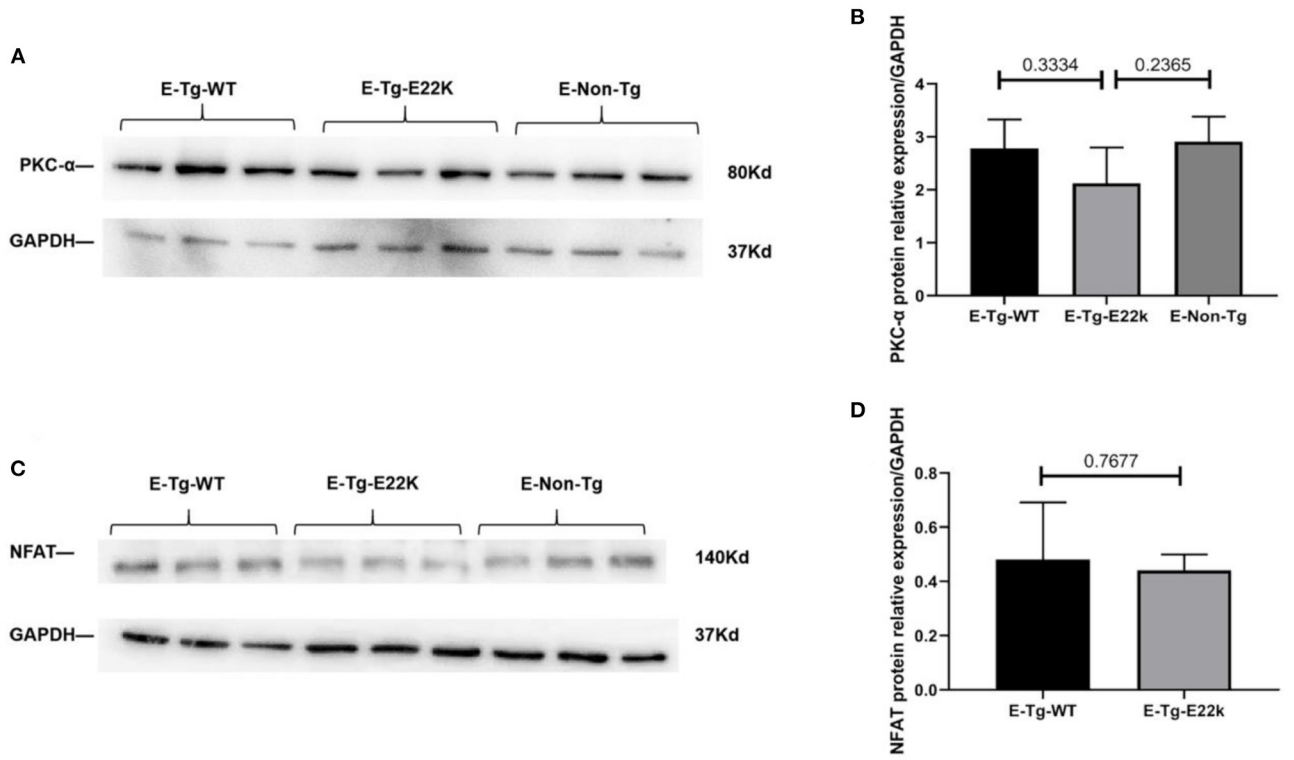

FIGURE 5 | Exercise changes the protein expression of PKC-α/NFAT. Representative Western blot results show that there are no remarkable differences in the expression levels of PKC-α and NFAT between Tg-WT and exercise-trained E22K mice **(A,C)**. Densitometric analysis of the protein levels of PKC-α and NFAT in each group **(B,D)**. $N = 3$, $^*p < 0.05$. E-Tg-WT, wild-type transgenic mice in the exercise group; E-Tg-E22K, transgenic E22K mice in the exercise group; E-Non-Tg, non-transgenic wild-type in the exercise group.

12 (*Fgf12*, Log2FC = −3.71, $p = 0.0009$) and collagen-like tail subunit (*colq*, Log2FC = −0.56, $p = 0.046$), as well as the hypertrophy-related genes such as myocyte enhancer factor 2C (*Mef2*, Log2FC = −0.54, $p = 0.021$), myosin, heavy polypeptide 11 (*Myh11*, LogFC = −0.46, $p = 0.019$), extracellular matrix protein 2 (*Ecm2*, Log2FC = −0.41, $p = 0.005$), cAMP responsive element binding protein 1 (*Creb1*, Log2FC = −0.26, $p = 0.049$), and trans-acting transcription factor 1 (*Sp1*, Log2FC = −0.25, $p = 0.045$) were all downregulated in E22K mice after completing the exercise program (**Table 3**). These results indicated that exercise could reverse the expression patterns of some fibrosis- and hypertrophy-related genes in E22K mutant mice. In addition, there were 456 genes with differential expression between R-Tg-WT and E-Tg-WT groups, of which 294 and 162 genes were upregulated and downregulated, respectively (**Figure 6B**). These data further confirm that exercise can regulate the genes related to cardiac remodeling.

RNA sequencing data indicated that the expression levels of PKC-α and NFAT in E22K mouse hearts did not differ significantly with those in WT mouse hearts after receiving exercise training. This result demonstrates that the dysregulated expression of PKC-α and NFAT in E22K mice is ameliorated after exercise, which is consistent with our Western blot results. In addition, exercise reversed the gene expression of *Tgfbr1, Smad4,* and *Acta2*, which were abnormally elevated in sedentary E22K mice heart (**Table 2** vs. **Table 4**). However, although PKC-α/NFAT and other related genes were remodeled in the hearts of E22K mice, exercise did not modify all hypertrophy-related genes to the same extent as those in WT mouse hearts. The comparative analysis of DEGs in E-Tg-E22K and E-Tg-WT mice showed that most of the hypertrophy- and fibrosis-related genes did not alter following exercise (**Table 4**). These findings suggest that exercise can partially alleviate familial hypertrophic cardiomyopathy in E22K mutant mice.

DISCUSSION

The substitution of glutamic acid to lysine at position 22 (E22K) in RLC gene may cause familial hypertrophic cardiomyopathy (39). A13T, E22K, and P95A are three different RLC mutations that are related to a specific subtype of cardiac hypertrophy characterized by mid-left ventricular obstruction (40). Histological staining revealed the enlarged interventricular and septal papillary muscles in the heart of E22K mutant mice (39).

NFAT and other transcription factors, such as CREB1, are the downstream targets of PKC. Evidence shows that pressure overload-triggered cardiac remodeling is positively correlated

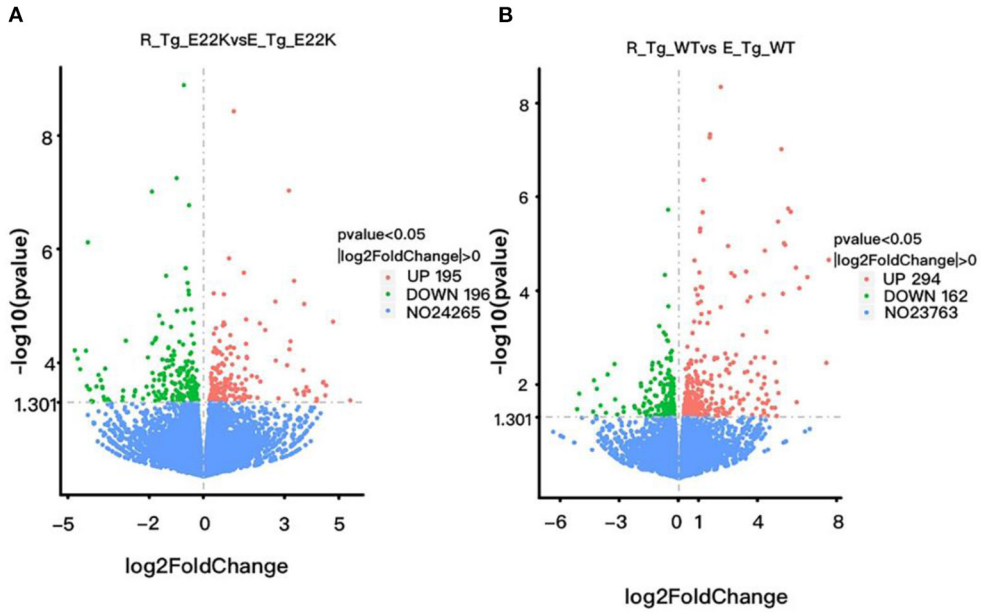

FIGURE 6 | Exercise regulates cardiac remodeling-related genes in mouse hearts. There were 391 genes with differential expression between R-Tg-E22K and E-Tg-E22K groups, of which 195 and 196 genes were upregulated and downregulated, respectively **(A)**. There were 456 genes with differential expression between R-Tg-WT and E-Tg-WT groups, of which 294 and 162 genes were upregulated and downregulated, respectively **(B)**. R-Tg-WT, wild-type transgenic mice in the rest group; R-Tg-E22K, transgenic E22K mice in the rest group; E-Tg-WT, wild-type transgenic mice in the exercise group; E-Tg-E22K, transgenic E22K mice in the exercise group.

TABLE 3 | A list of significant DEGs in E22K mice before and after exercise.

Gene	Log2FC	*P*-value	Padj	Gene_description
E-E22K vs. R-E22K				
Fgf12	−3.711375467	0.000922121	0.999920873	Fibroblast growth factor 12
Colq	−0.558992277	0.045971381	0.999920873	Collagen-like tail subunit
Mef2c	−0.308788186	0.021381395	0.999920873	Myocyte enhancer factor 2C
Myh11	−0.456183295	0.019429391	0.999920873	Myosin, heavy polypeptide 11
Ecm2	−0.412531367	0.00549835	0.999920873	Extracellular matrix protein 2
Creb1	−0.258429962	0.049367256	0.999920873	cAMP responsive element binding protein 1
Sp1	−0.247143887	0.044881631	0.999920873	Trans-acting transcription factor 1

with the sustained activation of NFAT, thus leading to heart failure. Myocardial hypertrophy and fibrosis are common symptoms in patients with chronic kidney disease (41). TGFβ is a crucial modulator of fibrosis, which mediates tissue fibrosis by activating its downstream Smad pathway (42). TGFβ/Smad molecular pathway is involved in the pathogenic differentiation from cardiac fibroblasts to myofibroblasts (43). The activation of both TGFβ/Smad and fibroblast growth factor receptor 4 (FGFR4)/PLC gamma (PLC-γ) signaling cascades can result in the development of fibrosis (42, 44–46). PKC-α is one of the most abundantly PKC subtypes in the myocardium. Growing evidence indicates that the overexpression or activation of PKC-α in transgenic mice decreases Ca^{2+} transients as well as cardiac contractility, which leads to cardiac hypertrophy and ultimately heart failure (47–50). PKC-interacting protein is involved in hypertrophic tissue remolding *via* regulation of calcineurin-NFAT signaling (51). Our study showed that E22K mutation resulted in the upregulated gene expression of hypertrophy and fibrosis markers, and the gene and protein levels of PKC-α and NFAT were significantly elevated in E22K mouse myocardium. In addition, cardiac fibrosis was promoted in E22K mutant mice, as revealed by the increased mRNA and protein expression of fibrosis markers such as p-Smad and TGFβR. Therefore, we speculate that hypertrophy and fibrosis in E22K mouse myocardium may be mediated by PKC-α/NFAT pathway.

Smooth muscle cells (SMC) are one of the important cell types that constitute to the structural and physiological properties of the heart. Vascular smooth muscle cells (VSMC) participate in tissue repair through proliferation, migration and phenotype alteration in response to vascular injury (52). FGF12 has been

TABLE 4 | A list of significant DEGs between E22K and WT mice after exercise.

Gene	Log2FC	*P*-value	Padj	Gene_description
E-E22K vs. E-WT				
Myh7b	−0.737876799	3.76E-06	0.000236149	Myosin, heavy chain 7B, cardiac muscle, beta
Nppa	2.908878667	0.00023003	0.005988536	Natriuretic peptide type A
Nppb	1.353917115	3.37E-08	4.77E-06	Natriuretic peptide type B
Col1a2	1.066315743	2.05E-06	0.000148649	Collagen, type I, alpha 2
Col6a3	0.83315607	1.07E-05	0.000551857	Collagen, type VI, alpha 3
Tgfbr2	0.573306079	0.001080711	0.018510723	Transforming growth factor, beta receptor 2
Tgfb3	1.009221517	3.84E-05	0.001512102	Transforming growth factor, beta 3
Tgfb2	1.784450639	7.85E-11	2.42E-08	Transforming growth factor, beta 2
Smad6	0.532913706	0.001099949	0.018701553	SMAD family member 6
Smad9	−0.679589712	0.022110941	0.141437131	SMAD family member 9

reported to be a key regulator of VSMC phenotype switch (53, 54). In addition, FGFs have been reported to induce cardiac hypertrophy by activating calcineurin/NFAT signaling (55, 56). Our study indicated that *Fgf12* was downregulated in exercise-trained E22K mice compared to rest E22K mice (**Table 3**). Downregulation of *Fgf12* may be related to the improvement of cardiac function. Myocyte enhancer factor 2C (Mef2c) is one of the major cardiac regulators that control both muscle and cardiovascular development (57, 58). It has been reported that the enhanced transcriptional activity of NFAT and MEF2 is associated with pathological myocardial hypertrophy (59, 60). A previous study on HCM mouse models demonstrated that exercise could reduce NFAT, but not MEF2 (22). Our data indicated that *Mef2c* was reduced in E22K mice after completing the exercise program (**Table 3**). This may be due to the different Mef isoforms detected, which function differently. As a highly dynamic non-cellular three-dimensional network, extracellular matrix (ECM) plays crucial roles in modulating cardiac structural homeostasis and cardiac remodeling (61). The abnormal changes in ECM and the structural reconstruction of matrix macromolecules are involved in the pathological process of ventricular hypertrophy, and even heart failure (61). Our data indicated that the expression of *Ecm2* was decreased in E22K mice after performing exercise, indicating a beneficial effect of exercise on cardiac hypertrophy (**Table 3**).

Exercise is a common rehabilitation training method for individuals with muscle atrophy. Exercise can enhance the function of skeletal muscles. However, the gene expression profiles and signaling mechanisms induced by exercise, especially in patients with hypertrophic heart disease, are still elusive. Cardiac hypertrophy is generally an adaptive response to pathological and physiological stimuli. Pathological hypertrophy often develops into myocardium fibrosis, which eventually leads to heart failure. Previous research has shown that cell development, metabolism, non-coding RNA, immune response, translational activation and epigenetic modification can either positively or negatively regulate myocardial hypertrophy. For patients with pathologically hypertrophic heart disease, the mechanisms underlying the positive effect of exercise on cardiac function remain largely unclear. To explore whether physical exercise has a beneficial effect on cardiac physiology at the molecular level in the E22K mice model, a programmed exercise was scheduled for the mice to verify whether exercise can reverse the characteristics of cardiac hypertrophy. Our results showed that the expression levels of PKC-α and NFAT were relatively similar among E-Tg-E22K, E-Tg-WT, and E-Non-Tg mice after receiving the programmed exercise. It has been reported that exercise is beneficial to hypertrophic cardiomyopathy mice harboring MyHC mutations. NFAT is a marker of myocardial hypertrophy (62). Exercise can prevent the activation of NFAT, and even reverse the established heart disease phenotype (22). Our results are consistent with the previous findings. In addition, our study demonstrated that exercise downregulated the cardiac remodeling-related genes (*fgf12*, *colq*, *Mef2C, Ecm2, and Creb1*), and reversed the fibrosis-associated genes (*Tgfbr1, Smad4, and Acta2*), indicating that exercise can improve pathological cardiac remodeling in E22K mutant mice.

CONCLUSION

In this study, we elucidated that the elevated expression of PKC-α and NFAT in E22K mouse myocardium may be a potential mechanism of E22K-induced hypertrophy. Furthermore, we verified that a programmed exercise could downregulate cardiac remodeling-related genes (*fgf12*, *colq*, *Mef2C*, *Ecm2,* and *Creb1*), reverse cardiac fibrosis associated genes (*Tgfbr1*, *Smad4,* and *Acta2*) and inhibit PKC-α/NFAT signaling pathway in the hearts of E22K mutant mice.

Importance and Significance

In this study, the differences in gene expression profiles between E22K mutant and control mice were compared by RNA sequencing, and the molecular mechanisms of hypertrophy and fibrosis were analyzed. Exercise therapy plays a beneficial role in the improvement of cardiac function. Our study indicated that exercise could decrease the expression levels of *fgf12*, *colq*, *Mef2C*, *Ecm2,* and *Creb1*, all of which were related to cardiac remodeling. In addition, cardiac fibrosis-associated genes, such as *Tgfbr1*, *Smad4,* and *Acta2,* could be

reversed by exercise. Furthermore, our results demonstrated that programmed exercise could reverse the upregulated expression of PKC-α and NFAT caused by E22K mutation in E22K mutant mice at both gene and protein levels. Our study highlights the plasticity of PKC-α and NFAT in mouse hearts during pathological hypertrophy. Most importantly, our study may provide clues to novel strategies into the prevention and treatment of familial hypertrophic cardiomyopathy.

DATA AVAILABILITY STATEMENT

The datasets presented in this study can be found in online repositories. The names of the repository/repositories and accession number(s) can be found at: SRA, PRJNA786059.

ETHICS STATEMENT

The animal study was reviewed and approved by Institutional Animal Ethics Guidelines for the Care and Use of Research Animals established by Soochow University, Suzhou, China.

AUTHOR CONTRIBUTIONS

JY, RT, and LW: conceptualization, experimental design, original draft preparation, and data analysis. HW and YL: perform experiments, data collection and analysis, and review and editing. RZ, YC, WJ, and SL: perform of experiments, data analysis, and editing. All authors have read and approved the final version of the manuscript.

FUNDING

The authors would like to acknowledge the Research Start-up Fund of Jining Medical University (Reference: 600791001, JY), the Natural Science Foundation of Jiangsu Province of China (Grant number: BK20150353, LW), the Foundation of Medical Health Science and Technology Development Program of Shandong Province (Reference: 202002061311, HW), the Research Support Fund for Teachers of Jining Medical University (Reference: JYFC2019KJ013, HW), and the Jining Medical College Student Innovation and Entrepreneurship Training Program Project (Reference: cx2021053, HW) for funding this project.

ACKNOWLEDGMENTS

We would like to express our deep gratitude to Prof. Danuta Szczesna-Cordary at University of Miami Miller School of Medicine for providing the transgenic mouse model, which is a great support for our research. We would also like to acknowledge the support of the research team at Jining Medical University working on the molecular mechanisms and intervention of myocardial infarction.

SUPPLEMENTARY MATERIAL

The Supplementary Material for this article can be found online at: https://www.frontiersin.org/articles/10.3389/fcvm.2022.808163/full#supplementary-material

REFERENCES

1. Flavigny J, Richard P, Isnard R, Carrier L, Charron P, Bonne G, et al. Identification of two novel mutations in the ventricular regulatory myosin light chain gene (MYL2) associated with familial and classical forms of hypertrophic cardiomyopathy. *J Mol Med.* (1998) 76:208–14. doi: 10.1007/s001090050210
2. Szczesna-Cordary D, Guzman G, Zhao J, Hernandez O, Wei J, Diaz-Perez Z. The E22K mutation of myosin RLC that causes familial hypertrophic cardiomyopathy increases calcium sensitivity of force and ATPase in transgenic mice. *J Cell Sci.* (2005) 118:3675–83. doi: 10.1242/jcs.02492
3. Szczesna D, Ghosh D, Li Q, Gomes AV, Guzman G, Arana C, et al. Familial hypertrophic cardiomyopathy mutations in the regulatory light chains of myosin affect their structure, Ca^{2+} binding, and phosphorylation. *J Biol Chem.* (2001) 276:7086–92. doi: 10.1074/jbc.M009823200
4. Dempsey EC, Newton AC, Mochly-Rosen D, Fields AP, Reyland ME, Insel PA, et al. Protein kinase C isozymes and the regulation of diverse cell responses. *Am J Phys.* (2000) 279:L429–38. doi: 10.1152/ajplung.2000.279.3.L429
5. Nishizuka Y. The role of protein kinase C in cell surface signal transduction and tumour promotion. *Nature.* (1984) 308:693–8. doi: 10.1038/308693a0
6. Nishizuka Y. Protein kinase C and lipid signaling for sustained cellular responses. *FASEB J.* (1995) 9:484–96.
7. Capogrossi MC, Kaku T, Filburn CR, Pelto DJ, Hansford RG, Spurgeon HA, et al. Phorbol ester and dioctanoylglycerol stimulate membrane association of protein kinase C and have a negative inotropic effect mediated by changes in cytosolic Ca^{2+} in adult rat cardiac myocytes. *Circ Res.* (1990) 66:1143–55. doi: 10.1161/01.res.66.4.1143
8. Glass CK, Witztum JL. Atherosclerosis. The road ahead. *Cell.* (2001) 104:503–16. doi: 10.1016/s0092-8674(01)00238-0
9. Yang X, Cohen MV, Downey JM. Mechanism of cardioprotection by early ischemic preconditioning. *Cardiovasc Drugs Ther.* (2010) 24:225–34. doi: 10.1007/s10557-010-6236-x
10. Sugden PH, Bogoyevitch MA. Intracellular signalling through protein kinases in the heart. *Cardiovasc Res.* (1995) 30:478–92.
11. Ferreira JC, Mochly-Rosen D, Boutjdir M. Regulation of cardiac excitability by protein kinase C isozymes. *Front Biosci.* (2012) 4:532–46. doi: 10.2741/283
12. Palaniyandi SS, Sun L, Ferreira JC, Mochly-Rosen D. Protein kinase C in heart failure: a therapeutic target? *Cardiovasc Res.* (2009) 82:229–39. doi: 10.1093/cvr/cvp001
13. Dorn GW 2nd, Force T. Protein kinase cascades in the regulation of cardiac hypertrophy. *J Clin Invest.* (2005) 115:527–37. doi: 10.1172/JCI 24178
14. Simonis G, Briem SK, Schoen SP, Bock M, Marquetant R, Strasser RH. Protein kinase C in the human heart: differential regulation of the isoforms in aortic stenosis or dilated cardiomyopathy. *Mol Cell Biochem.* (2007) 305:103–11. doi: 10.1007/s11010-007-9533-3
15. Braz JC, Bueno OF, De Windt LJ, Molkentin JD. PKC alpha regulates the hypertrophic growth of cardiomyocytes through extracellular signal-regulated kinase1/2 (ERK1/2). *J Cell Biol.* (2002) 156:905–19. doi: 10.1083/jcb.200108062
16. Gonzalez AA, Liu L, Lara LS, Bourgeois CR, Ibaceta-Gonzalez C, Salinas-Parra N, et al. PKC-α-dependent augmentation of cAMP and CREB phosphorylation mediates the angiotensin II stimulation of renin in the collecting duct. *Am J Physiol Renal Physiol.* (2015) 309:F880–8. doi: 10.1152/ajprenal.00155.2015
17. Hogan PG, Chen L, Nardone J, Rao A. Transcriptional regulation by calcium, calcineurin, and NFAT. *Genes Dev.* (2003) 17:2205–32. doi: 10.1101/gad.1102703

18. Feske S, Okamura H, Hogan PG, Rao A. Ca2+/calcineurin signalling in cells of the immune system. *Biochem Biophys Res Commun.* (2003) 311:1117–32. doi: 10.1016/j.bbrc.2003.09.174
19. De A. Wnt/Ca2+ signaling pathway: a brief overview. *Acta Biochim Biophys Sin.* (2011) 43:745–56. doi: 10.1093/abbs/gmr079
20. Sharma S, Firoozi S, McKenna WJ. Value of exercise testing in assessing clinical state and prognosis in hypertrophic cardiomyopathy. *Cardiol Rev.* (2001) 9:70–6. doi: 10.1097/00045415-200103000-00005
21. Guyatt GH, Devereaux PJ. A review of heart failure treatment. *Mt Sinai J Med.* (2004) 71:47–54.
22. Konhilas JP, Watson PA, Maass A, Boucek DM, Horn T, Stauffer BL, et al. Exercise can prevent and reverse the severity of hypertrophic cardiomyopathy. *Circ Res.* (2006) 98:540–8. doi: 10.1161/01.RES.0000205766.97556.00
23. Chen Z, Li L, Wu W, Liu Z, Huang Y, Yang L, et al. Exercise protects proliferative muscle satellite cells against exhaustion via the Igfbp7-Akt-mTOR axis. *Theranostics.* (2020) 10:6448–66. doi: 10.7150/thno.43577
24. Guo A, Wang Y, Chen B, Wang Y, Yuan J, Zhang L, et al. E-C coupling structural protein junctophilin-2 encodes a stress-adaptive transcription regulator. *Science.* (2018) 362:eaan3303. doi: 10.1126/science.aan3303
25. Forte M, Madonna M, Schiavon S, Valenti V, Versaci F, Zoccai GB, et al. Cardiovascular pleiotropic effects of natriuretic peptides. *Int J Mol Sci.* (2019) 20:3874. doi: 10.3390/ijms20163874
26. Sangawa K, Nakanishi K, Ishino K, Inoue M, Kawada M, Sano S. Atrial natriuretic peptide protects against ischemia-reperfusion injury in the isolated rat heart. *Ann Thorac Surg.* (2004) 77:233–7. doi: 10.1016/s0003-4975(03)01493-0
27. Yamada T, Kotake Y, Nagata H, Takeda J. Atrial natriuretic peptide reduces hepatic ischemia-reperfusion injury in rabbits. *J Anesth.* (2013) 27:901–8. doi: 10.1007/s00540-013-1643-3
28. Gaggin HK, Januzzi JL Jr. Biomarkers and diagnostics in heart failure. *Biochim Biophys Acta.* (2013) 1832:2442–50. doi: 10.1016/j.bbadis.2012.12.014
29. Špinar J, Špinarová L, Vítovec J. Pathophysiology, causes and epidemiology of chronic heart failure. *Vnitr Lek.* (2018) 64:834–8.
30. Maccari S, Pace V, Barbagallo F, Stati T, Ambrosio C, Grò MC, et al. Intermittent β-adrenergic blockade downregulates the gene expression of β-myosin heavy chain in the mouse heart. *Eur J Pharmacol.* (2020) 882:173287. doi: 10.1016/j.ejphar.2020.173287
31. Reda SM, Gollapudi SK, Chandra M. Developmental increase in β-MHC enhances sarcomere length-dependent activation in the myocardium. *J Gen Physiol.* (2019) 151:635–644. doi: 10.1085/jgp.201812183
32. Koitabashi N, Danner T, Zaiman AL, Pinto YM, Rowell J, Mankowski J, et al. Pivotal role of cardiomyocyte TGF-β signaling in the murine pathological response to sustained pressure overload. *J Clin Invest.* (2011) 121:2301–12. doi: 10.1172/JCI44824
33. Wenzel S, Taimor G, Piper HM, Schlüter KD. Redox-sensitive intermediates mediate angiotensin II-induced p38 MAP kinase activation, AP-1 binding activity, and TGF-beta expression in adult ventricular cardiomyocytes. *FASEB J.* (2001) 15:2291–3. doi: 10.1096/fj.00-0827fje
34. Frangogiannis NG. The role of transforming growth factor (TGF)-β in the infarcted myocardium. *J Thorac Dis.* (2017) 9:S52–63. doi: 10.21037/jtd.2016.11.19
35. Biernacka A, Dobaczewski M, Frangogiannis NG. TGF-β signaling in fibrosis. *Growth Factors.* (2011) 29:196–202. doi: 10.3109/08977194.2011.595714
36. Eghbali M, Tomek R, Sukhatme VP, Woods C, Bhambi B. Differential effects of transforming growth factor-beta 1 and phorbol myristate acetate on cardiac fibroblasts. Regulation of fibrillar collagen mRNAs and expression of early transcription factors. *Circ Res.* (1991) 69:483–90. doi: 10.1161/01.res.69.2.483
37. Shi Y, Massagué J. Mechanisms of TGF-beta signaling from cell membrane to the nucleus. *Cell.* (2003) 113:685–700. doi: 10.1016/s0092-8674(03)00432-x
38. Poetter K, Jiang H, Hassanzadeh S, Master SR, Chang A, Dalakas MC, et al. Mutations in either the essential or regulatory light chains of myosin are associated with a rare myopathy in human heart and skeletal muscle. *Nat Genet.* (1996) 13:63–9. doi: 10.1038/ng0596-63
39. Szczesna-Cordary D, Jones M, Moore JR, Watt J, Kerrick WG, Xu Y, et al. Myosin regulatory light chain E22K mutation results in decreased cardiac intracellular calcium and force transients. *FASEB J.* (2007) 21:3974–85. doi: 10.1096/fj.07-8630com
40. Roopnarine O. Mechanical defects of muscle fibers with myosin light chain mutants that cause cardiomyopathy. *Biophys J.* (2003) 84:2440–9. doi: 10.1016/S0006-3495(03)75048-6
41. Uchida L, Tanaka T, Saito H, Sugahara M, Wakashima T, Fukui K, et al. Effects of a prolyl hydroxylase inhibitor on kidney and cardiovascular complications in a rat model of chronic kidney disease. *Am J Physiol Renal Physiol.* (2020) 318:F388–401. doi: 10.1152/ajprenal.00419.2019
42. Yue Y, Meng K, Pu Y, Zhang X. Transforming growth factor beta (TGF-β) mediates cardiac fibrosis and induces diabetic cardiomyopathy. *Diabetes Res Clin Pract.* (2017) 133:124–130. doi: 10.1016/j.diabres.2017.08.018
43. Lu M, Qin Q, Yao J, Sun L, Qin X. Induction of LOX by TGF-β1/Smad/AP-1 signaling aggravates rat myocardial fibrosis and heart failure. *IUBMB Life.* (2019) 71:1729–39. doi: 10.1002/iub.2112
44. Smith ER, Holt SG, Hewitson TD. FGF23 activates injury-primed renal fibroblasts via FGFR4-dependent signalling and enhancement of TGF-β autoinduction. *Int J Biochem Cell Biol.* (2017) 92:63–78. doi: 10.1016/j.biocel.2017.09.009
45. Hao H, Li X, Li Q, Lin H, Chen Z, Xie J, et al. FGF23 promotes myocardial fibrosis in mice through activation of β-catenin. *Oncotarget.* (2016) 7:64649–64. doi: 10.18632/oncotarget.11623
46. Böckmann I, Lischka J, Richter B, Deppe J, Rahn A, Fischer DC, et al. FGF23-mediated activation of local RAAS promotes cardiac hypertrophy and fibrosis. *Int J Mol Sci.* (2019) 20:4634. doi: 10.3390/ijms20184634
47. Braz JC, Gregory K, Pathak A, Zhao W, Sahin B, Klevitsky R, et al. PKC-alpha regulates cardiac contractility and propensity toward heart failure. *Nat Med.* (2004) 10:248–54. doi: 10.1038/nm1000
48. Hambleton M, Hahn H, Pleger ST, Kuhn MC, Klevitsky R, Carr AN, et al. Pharmacological- and gene therapy-based inhibition of protein kinase Calpha/beta enhances cardiac contractility and attenuates heart failure. *Circulation.* (2006) 114:574–82. doi: 10.1161/CIRCULATIONAHA105.592550
49. Hahn HS, Marreez Y, Odley A, Sterbling A, Yussman MG, Hilty KC, et al. Protein kinase Calpha negatively regulates systolic and diastolic function in pathological hypertrophy. *Circ Res.* (2003) 93:1111–9. doi: 10.1161/01.RES.0000105087.79373.17
50. Liu Q, Chen X, Macdonnell SM, Kranias EG, Lorenz JN, Leitges M, et al. Protein kinase C{alpha}, but not PKC{beta} or PKC{gamma}, regulates contractility and heart failure susceptibility: implications for ruboxistaurin as a novel therapeutic approach. *Circ Res.* (2009) 105:194–200. doi: 10.1161/CIRCRESAHA.109.195313
51. Jeong D, Kim JM, Cha H, Oh JG, Park J, Yun SH, et al. PICOT attenuates cardiac hypertrophy by disrupting calcineurin-NFAT signaling. *Circ Res.* (2008) 102:711–9. doi: 10.1161/CIRCRESAHA.107.165985
52. Yeo Y, Yi ES, Kim JM, Jo EK, Seo S, Kim RI, et al. FGF12 (fibroblast growth factor 12) inhibits vascular smooth muscle cell remodeling in pulmonary arterial hypertension. *Hypertension.* (2020) 76:1778–86. doi: 10.1161/HYPERTENSIONAHA.120.15068
53. Song SH, Kim K, Jo EK, Kim YW, Kwon JS, Bae SS, et al. Fibroblast growth factor 12 is a novel regulator of vascular smooth muscle cell plasticity and fate. *Arterioscler Thromb Vasc Biol.* (2016) 36:1928–36. doi: 10.1161/ATVBAHA.116.308017;
54. Nakamura M, Sadoshima J. Mechanisms of physiological and pathological cardiac hypertrophy. *Nat Rev Cardiol.* 2018 15:387–407. doi: 10.1038/s41569-018-0007-y
55. Faul C. Fibroblast growth factor 23 and the heart. *Curr Opin Nephrol Hypertens.* (2012) 21:369–75. doi: 10.1097/MNH.0b013e32835422c4
56. Faul C, Amaral AP, Oskouei B, Hu MC, Sloan A, Isakova T, et al. FGF23 induces left ventricular hypertrophy. *J Clin Invest.* (2011) 121:4393–408. doi: 10.1172/JCI46122
57. Wang L, Huang P, Near D, Ravi K, Xu Y, Liu J, et al. Isoform specific effects of Mef2C during direct cardiac reprogramming. *Cells.* (2020) 9:268. doi: 10.3390/cells9020268

58. Castro V, Grisdale-Helland B, Helland SJ, Torgersen J, Kristensen T, Claireaux G, et al. Cardiac molecular-acclimation mechanisms in response to swimming-induced exercise in Atlantic salmon. *PLoS ONE.* (2013) 8:e55056. doi: 10.1371/journal.pone.0055056
59. Molkentin JD, Lu JR, Antos CL, Markham B, Richardson J, Robbins J, et al. A calcineurin-dependent transcriptional pathway for cardiac hypertrophy. *Cell.* (1998) 93:215–28. doi: 10.1016/s0092-8674(00) 81573-1
60. Passier R, Zeng H, Frey N, Naya FJ, Nicol RL, McKinsey TA, et al. CaM kinase signaling induces cardiac hypertrophy and activates the MEF2 transcription factor *in vivo*. *J Clin Invest.* (2000) 105:1395–406. doi: 10.1172/JCI8551
61. Bonnans C, Chou J, Werb Z. Remodelling the extracellular matrix in development and disease. *Nat Rev Mol Cell Biol.* (2014) 15:786–801. doi: 10.1038/nrm3904
62. Wilkins BJ, Dai YS, Bueno OF, Parsons SA, Xu J, Plank DM, et al. Calcineurin/NFAT coupling participates in pathological, but not physiological, cardiac hypertrophy. *Circ Res.* (2004) 9:110–8. doi: 10.1161/01.RES.0000109415.17511.18

Conflict of Interest: The authors declare that the research was conducted in the absence of any commercial or financial relationships that could be construed as a potential conflict of interest.

Publisher's Note: All claims expressed in this article are solely those of the authors and do not necessarily represent those of their affiliated organizations, or those of the publisher, the editors and the reviewers. Any product that may be evaluated in this article, or claim that may be made by its manufacturer, is not guaranteed or endorsed by the publisher.

Copyright © 2022 Wang, Lin, Zhang, Chen, Ji, Li, Wang, Tan and Yuan. This is an open-access article distributed under the terms of the Creative Commons Attribution License (CC BY). The use, distribution or reproduction in other forums is permitted, provided the original author(s) and the copyright owner(s) are credited and that the original publication in this journal is cited, in accordance with accepted academic practice. No use, distribution or reproduction is permitted which does not comply with these terms.

frontiers in Cardiovascular Medicine

ORIGINAL RESEARCH
published: 25 February 2022
doi: 10.3389/fcvm.2022.803510

Exercise-Generated β-Aminoisobutyric Acid (BAIBA) Reduces Cardiomyocyte Metabolic Stress and Apoptosis Caused by Mitochondrial Dysfunction Through the miR-208b/AMPK Pathway

Yanan Yu[1,2], Wewei Chen[2,3], Ming Yu[2,3], Jinsha Liu[2,3], Huan Sun[2,3] and Ping Yang[2,3]**

[1] Department of Rehabilitation, China-Japan Union Hospital, Changchun, China, [2] Jilin Provincial Engineering Laboratory for Endothelial Function and Genetic Diagnosis of Cardiovascular Disease, Jilin Provincial Cardiovascular Research Center, Changchun, China, [3] Department of Cardiology, China-Japan Union Hospital, Changchun, China

OPEN ACCESS

Edited by:
Jian Wu,
Fudan University, China

Reviewed by:
Wenliang Chen,
York University, Canada
James C. Lo,
Cornell University, United States

***Correspondence:**
Huan Sun
sunhuan0404@jlu.edu.cn
Ping Yang
pyang@jlu.edu.cn

Specialty section:
This article was submitted to Cardiovascular Metabolism, a section of the journal Frontiers in Cardiovascular Medicine

Received: 28 October 2021
Accepted: 31 January 2022
Published: 25 February 2022

Citation:
Yu Y, Chen W, Yu M, Liu J, Sun H and Yang P (2022) Exercise-Generated β-Aminoisobutyric Acid (BAIBA) Reduces Cardiomyocyte Metabolic Stress and Apoptosis Caused by Mitochondrial Dysfunction Through the miR-208b/AMPK Pathway. Front. Cardiovasc. Med. 9:803510. doi: 10.3389/fcvm.2022.803510

Objective: To explore the cardioprotective effects of exercise-derived β-aminoisobutyric (BAIBA) on cardiomyocyte apoptosis and energy metabolism in a rat model of heart failure (HF).

Methods: In male Sprague-Dawley rats (8-week-old), myocardial infarction (MI) was used to induce HF by ligating the left anterior descending branch of the coronary artery. In the Sham group, the coronary artery was threaded but not ligated. After HF development, Sham and HF rats were exercised 60 min daily, 5 days/week on a treadmill for 8 weeks (50–60% maximal intensity) and exercise-induced cardiac remodeling after MI were assessed using echocardiography, hematoxylin and eosin (H&E), Masson's Trichrome, and TUNEL staining for the detection of apoptosis-associated factors in cardiac tissue. High-throughput sequencing and mass spectrometry were used to measure BAIBA production and to explore its cardioprotective effects and molecular actions. To further characterize the cardioprotective effects of BAIBA, an *in vitro* model of apoptosis was generated by applying H_2O_2 to H9C2 cells to induce mitochondrial dysfunction. In addition, cells were transfected with either a miR-208b analog or a miR-208b inhibitor. Apoptosis-related proteins were detected by Western Blotting (WB). ATP production was also assessed by luminometry. After administration of BAIBA and Compound C, the expression of proteins related to apoptosis, mitochondrial function, lipid uptake, and β-oxidative were determined. Changes in the levels of reactive oxygen species (ROS) were assessed by fluorescence microscopy. In addition, alterations in membrane potential ($\delta\psi m$) were obtained by confocal microscopy.

Results: Rats with HF after MI are accompanied by mitochondrial dysfunction, metabolic stress and apoptosis. Reduced expression of apoptosis-related proteins was observed, together with increased ATP production and reduced mitochondrial dysfunction in the exercised compared with the Sham (non-exercised) HF group. Importantly, exercise increased the production of BAIBA, irrespective of the presence of

HF. To assess whether BAIBA had similar effects to exercise in ameliorating HF-induced adverse cardiac remodeling, rats were treated with 75 mg/kg/ day of BAIBA and we found BAIBA had a similar cardioprotective effect. Transcriptomic analyses found that the expression of miR-208b was increased after BAIBA administration, and subsequent transfection with an miR-208b analog ameliorated both the expression of apoptosis-related proteins and energy metabolism in H_2O_2-treated H9C2 cells. In combining transcriptomic with metabolomic analyses, we identified AMPK as a downstream target for BAIBA in attenuating metabolic stress in HF. Further cell experiments confirmed that BAIBA increased AMPK phosphorylation and had a cardioprotective effect on downstream fatty acid uptake, oxidative efficiency, and mitochondrial function, which was prevented by the AMPK inhibitor Compound C.

Conclusion: Exercise-generated BAIBA can reduce cardiomyocyte metabolic stress and apoptosis induced by mitochondrial dysfunction through the miR-208b/AMPK pathway.

Keywords: mitochondrial dysfunction, metabolic stress, exercise, lipid metabolism, heart failure

INTRODUCTION

Metabolic disorders play a key role in the occurrence and progression of heart failure (HF) after myocardial infarction (MI). The restoration of energy homeostasis is important for cardiac function (1). Mitochondria produce ATP and can thus regulate energy metabolism (2), which involves the selection and utilization of substrates, efficient oxidative phosphorylation, and energy shuttling at the mitochondrial level (3). These metabolic processes are closely integrated to maintain the rapid, sustained, and sufficient output of ATP. HF leads to a loss of metabolic substrate flexibility and a decrease in oxidative phosphorylation efficiency, which is accompanied by mitochondrial dysfunction (4, 5). This metabolic dysregulation can occur due to destruction of the mitochondrial complex, mitochondrial uncoupling, crest remodeling and swelling, and changes of mitochondrial membrane potential, leading to reactive oxygen species (ROS) accumulation, insufficient ATP production, apoptosis, and death (6–8). Thus, finding ways to attenuate cardiac metabolic stress and mitochondrial dysfunction in patients with HF is of clinical importance.

Of the known interventions for HF patients, moderate exercise is known to have a beneficial effect on cardiac function in this population (9–14). Indeed, moderate continuous endurance training is known to be a safe, efficient, and well-tolerated intervention by HF patients that it is recommended by the Heart Failure Association (15). Importantly, impairments of cardiac metabolism in HF patients can be partially restored through exercise due to the improved mitochondrial quality control, bioenergetics, and cardiac function (16). Despite the known beneficial effects of exercise in HF patients, many HF patients are exercise intolerant or have a reduced exercise capability (17, 18). Therefore, being able to identify a substance that can mimic the beneficial effects of exercise in improving cardiac function and energy metabolism in patients with HF is necessary. BAIBA is a small molecule (103.6 Da) composed of two enantiomers (L-BAIBA and D-BAIBA) produced by skeletal muscles during exercise, and mediates the beneficial effect of exercise from skeletal muscle to other tissues and organs via the endocrine system (19). In this study, we have focused mainly on L-BAIBA, which is produced by muscle contraction (19) and can effectively improve glucose and lipid metabolism, activate β-oxidation of fatty acids in the liver, and increase AMPK phosphorylation in adipose tissue (20–25). However, whether BAIBA could be used a cardioprotective therapeutic intervention to mimic the effects of exercise in patients with HF has not been studied.

Our study found that exercise-generated BAIBA could effectively improve cardiac function, energy metabolism, and reduce apoptosis in rats with HF after MI. Importantly, oral administration of BAIBA increased the expression of miR-208b, which is a heart-specific miRNA that is encoded on intron 27 of the gene encoding α-MHC and is essential for the expression of genes involved in cardiac contractility and fibrosis. These findings align with previous studies from our group (26), suggesting miR-208b has a protective effect on myocardial apoptosis and mitochondrial dysfunction in rats with MI. Moreover, BAIBA also increased the ratio of p-AMPK/AMPK in HF rats, reducing apoptosis in H_2O_2-induced H9C2 cells and leading to improved mitochondrial function and energy metabolism, suggesting BAIBA reduces cardiomyocyte metabolic stress and apoptosis caused by mitochondrial dysfunction through the miR-208b/AMPK pathway.

MATERIALS AND METHODS

Animal Experiments

Animal experiments were approved by the Ethics Committee of the First Hospital of Jilin University. Male Sprague-Dawley (SD) rats (8 weeks, 250 g) were used to establish. In male Sprague-Dawley rats (8-week-old), myocardial infarction (MI)

was used to induce HF by ligating the left anterior descending branch of the coronary artery (27). In the Sham group, the coronary artery was threaded but not ligated. The procedure was carried out under aseptic conditions and anesthesia induced by inhaling oxygen anesthesia containing 1.5–2.0% isoflurane. After disinfection, the skin of the prothoracic area was cut longitudinally, the chest muscle was separated, the intercostal space was exposed and punctured, and the anterior descending branch of the coronary artery was ligated after separating the pericardium. The soft tissue and skin of the chest was sutured and disinfected with penicillin. Intraperitoneal injections of 160,000 units/day penicillin were administered for a total of seven days. Four weeks after the procedure, the rats were examined by echocardiography and divided into separated groups according to ejection fraction (EF) %. Details of the groups are shown in **Supplementary File 1**. Briefly, for the exercise studies, rats were divided into 4 groups: (i) Sham; (ii) heart failure (HF); (iii) heart failure with exercise (HFE); and (iv) Sham and exercise (ShamE) groups. For the β-aminoisobutyric (BAIBA) studies, rats were divided into 3 groups: (i) Sham; (ii) heart failure (HF); (iii) heart failure with BAIBA(BAIBA) groups. For the exercise groups, rats were exercised daily on a treadmill (Shanghai Ruanlong Technology Co., Ltd. BW-ZHPT) involving 10–20 min acclimation, 0.3–0.6 km/h, and 0% incline. After 3 days' acclimation, the maximum exercise intensity was tested, starting at 0.3 km/h and increasing by 0.3 km/h every 3 min until exhaustion (28). The rats were run on the treadmill for 8 weeks (50 to 60% of maximum intensity), 60 min/day, 5 days/week, and at a 0% incline. For the BAIBA studies, BAIBA (MCE; HY-113380) was administered orally by gavage at a daily dose of 75 mg/kg for 8 weeks (29, 30) to rats with HF. The corresponding dose of BAIBA was dissolved in 1ml ddH2O, and the rats in the Sham group and the HF group were given the same volume of ddH2O orally by gavage. At 12 weeks post-op, rats in each group were examined by echocardiography, and the hearts were quickly removed under deep anesthesia. After the heart was removed, it was washed with cold PBS, dried with sterile medical gauze. Part of the left ventricle was quickly fixed in 4% paraformaldehyde for subsequent histological evaluation, while part of the left ventricle was quickly frozen in liquid nitrogen (or at−80°C) for subsequent transcriptomic, proteomic, and biochemical analysis. All experiments were conducted following the guidelines of animal research institutions and in accordance with the guidelines for the Care and Use of Experimental Animals published by the National Institutes of Health (NIH publ.no.85-23, revised in 1996).

Echocardiography

To non-invasively assess changes in cardiac structure and function, GE VIVId-i was used for the echocardiographic examinations at 4 and 12 weeks post-MI. Rats were anesthetized using the method used for the infarction surgery (described above) and were maintained under anesthesia for the entire echocardiographic examination. The probe (10S; 4.0–11.0 MHz) was placed directly on the shaved chest wall. The left ventricular end diastolic diameter (LVIDd), left ventricular end systolic diameter (LVIDs), interventricular septal thickness (IVDs), ejection fraction (EF) % and fractional shortening (FS) were measured. EF was calculated as stroke volume (SV)/end-diastolic volume (EDV) × 100%. FS was calculated as (LVIDd–LVIDs)/LVIDd × 100%.

H&E Staining

The left ventricular tissue was fixed in 4% paraformaldehyde for 24 h, embedded in paraffin, and sliced into 4 μm sections. The sections were dewaxed with xylene and an ethanol gradient, stained with hematoxylin, washed with 1% (v/v) hydrochloric acid for 30 s, and stained with eosin for 2 min. After gradient ethanol dehydration, permeation, and sealing, photographs were taken under a microscope (OLYMPUS BX53).

Masson's Staining

Paraffin sections were dewaxed into the water, stained with Wiegert's iron hematoxylin solution for 5 min, differentiated with hydrochloric acid alcohol, and washed with tap water. The sections were stained with fuchsin solution for 5 min, molybdophosphoriTUNEL acid solution for 3 min, and toluidine blue-O re-staining for 5 min. The slices were soaked in 1% glacial acetic acid for 1 min before dehydration, permeation, and sealing. Sections were observed and photographed under a microscope (OLYMPUS BX53). Image-Pro Plus 6.0 software (Media Cybernetics, USA) was used to analyze images. Three visual fields at x400 were tested randomly in each sample. The degree of fibrosis was calculated as the percentage of collagen area.

TUNEL Staining

Paraffin sections were dewaxed with xylene, hydrated with an ethanol gradient, and then treated with 20 μg /ml protease KJI without DNase at 37°C for 30 min. After repeated rinsing with PBS, 50 μl TUNEL monitoring solution was added and the sample was incubated at 37°C for 60 min. After washing, the sections were sealed with an anti-fluorescence quenching solution and observed under a fluorescence microscope (Lycra, DL-80, Germany). Nuclei of normal and apoptotic cells appeared light blue and light red after staining, respectively. Three visual fields at x400 were tested randomly in each sample. The apoptotic index value was calculated as the number of apoptotic cells divided by the total number of cells in each field of view (x400).

Transmission Electron Microscopy

Mitochondrial ultrastructure was observed by TEM. Tissue specimens were fixed with 3% glutaraldehyde, then re-fixed in 1% SO4, rinsed with PBS solution, and embedded in Epon resin after ethanol gradient dehydration. Ultra-thin slices (50 nm) were cut using a diamond knife, and the glass slides were fixed onto the copper specimen table with conductive paste. Platinum was sprayed onto the sample for transmission electron microscopic observation (Hitachi H600 Electron Microscope, Hitachi, Japan) and imaging. Magnification is ×1.2k; ×3.0k, and ×8.0k, respectively.

Cell Transfection

Rat cardio myoblast H9C2 cells were cultured until 60–70% confluent and were then transfected using Lipofectamine

2000 (Invitrogen, Carlsbad, CA, USA) with a miR-208b analog (100 nM), a miR-208b inhibitor (100 nM), or a miR-208b negative control (NC) vector (100 nM) in serum-free and Penicillin-Streptomycin-free medium, after 6 h, the cells were changed into complete medium and continued to be cultured for 24 h before incubation with H_2O_2.The miR-208b analog, miR-208b inhibitor, and miR-208b NC were designed by Gene Pharma (Suzhou, China). The sequences were as follows: miR-208b analog; (5′-AUAAGACGAACAAAAGGU-3′ 5′-CUUUUGUUCGUCUUAUUU−3′), miR-208b inhibitor; (5′-ACCUUUUGUUCGUCUUAU-3′), miR208b Negative control (NC); (5′-CAGUACUUUUGUGUAGUACAA-3′).

Cell Experiments

Mitochondrial dysfunction was induced in H9C2 cells by incubation with 200 μM H_2O_2 for 24 h to generate a model of myocardial apoptosis. The cells were divided into the following groups: Control, H_2O_2, BAIBA, miR-208b analog, miR-208b inhibitor, miR-208b NC, and Control, H_2O_2, BAIBA, Compound C. The transfection concentration of miR-208b was 100 nM. The concentrations of BAIBA and Compound C were 30 and 10 μM, respectively.

Western Blotting

H9C2 cells or myocardial tissue were treated with RIPA lysis buffer containing protease and phosphatase inhibitors (Sangon Biotech, Shanghai, China), and total protein concentrations were measured using a BCA protein assay kit (Sangon Biotech, Shanghai, China). After denaturation at 95°C for 5 min in SDS sample buffer, proteins were separated on SDS-PAGE and transferred to PVDF membranes. The membranes were blocked with 5% (w/v) BSA for 1 h, followed by incubation overnight at 4°C with specific antibodies (all from Abcam, Cambridge, UK) against the following proteins: Bax (ab32503), BCL-2 (ab196495), pro-caspase 3(ab184787), cleaved-caspase 3 (ab214430), DRP-1 (ab184247), OPA-1 (ab42364), PGC-1 α (ab106814), SUCLA (ab202582), ACADL (ab129711), CD36 (ab133625), CPT-1 (ab234111), P-ACC (ab68191), ACC (ab45174), p-AMPK (ab133448), AMPK (ab207442), and GAPDH (ab181602). After washing, the membrane was incubated with an HRP-coupled secondary antibody for 60 min, washed again, and finally incubated with enhanced chemiluminescence (ECL) solution (Sigma, USA).

qRT-PCR Analysis

Myocardial tissue samples or H9C2 cell samples were homogenized in TRIzol reagent for RNA extraction and the RNA concentration was evaluated by spectrophotometry. Equal amounts (2 μg) of purified RNA were used as templates, and the First Strand cDNA synthesis kit (Sangon Biotech, Shanghai, China) was used to synthesize cDNA and miRNA. Quantitative RT-PCR analysis was performed on a real-time PCR system (ABI 7500 DX) using SYBR Green Master Mix (Sangon Biotech), cDNA template, and specific primers (miR-208-3p primer 5′-GCGCATAAGACGAACAAAAGGT-3′). GAPDH was used to standardize mRNA expression, while U6 (also known as RNU6) was used to standardize miRNA expression. The relative expression levels of the target genes were determined by the $2^{-\Delta\Delta CT}$ method.

ATP Measurements

An ATP test kit (Beyotime, Shanghai, China) was used according to the manufacturer's instructions. Cell lysates or myocardial tissue lysates were centrifuged at 12 000 x g for 5 min, and the supernatant was retained. One hundred microliters of the supplied ATP solution were added to each of the wells of 96-well plates and allowed to stand at room temperature for 3–5 min. Twenty microliters of the lysate supernatant or standard solutions were then added, mixed quickly, and, after 5 sec, the LUL value (relative light unit, RLU) was determined by chemiluminescence measurement in a luminometer.

Mitochondrial Membrane Potential

JC-1 dye (5,5', 6,6'-tetrachloro-1,1', 3,3'-tetraethyl Benzimidazole carbonyl cyanine iodide) was used to evaluate Δ ψ m. H9C2 cells were incubated with JC-1 staining solution at 37°C for 20 minutes. The cells were then washed with JC-1 buffer and imaged by confocal microscopy (Nikon, A1, Japan). JC-1 can form aggregates in healthy mitochondria and has red fluorescence (Em. 590 nm) at the polarized Δ ψ m. In cells with altered mitochondrial function, JC-1 can only form a monomer with resultant green fluorescence (Em. 527 nm) in the cytoplasm during depolarization. The ratio between red and green fluorescence of H9C2 cells was used for the detection of the mitochondrial membrane potential.

Detection of Intracellular ROS Level

The production of ROS was measured using a ROS assay kit (Beyotime) using the 2-dichlorofluorescein diacetate (H_2-DCFDA) method. H9C2 cells were incubated with 10 μM H_2-DCFDA in the dark at 37°C for 20 min. After washing with PBS, the cells were imaged with fluorescence microscopy (Leica DL-80, Germany).

Non-targeted Metabolomics Sequencing

Rat myocardial tissues were used for non-targeted metabolomics sequencing. The specific location was the anterior wall of the left ventricle (in the BAIBA group, the area around the infarction was used). One milliliter of 90% cold methanol was added to 100 ml of sample, which was then homogenized using an MP homogenizer followed by sonication at low temperature and centrifugation. The supernatant was dried in a vacuum centrifuge. For LC-MS analysis, the samples were re-dissolved in 100 μL acetonitrile/water (1:1, v/v). For HILIC separation, samples were analyzed using a 2.1 x 100 mm ACQUIY UPLC BEH 1.7 μm column (Waters, Ireland). A 2 μL aliquot of each sample was injected. In the MS-only acquisition, the instrument was set to acquire over the m/z range 60–1000 Da. The product ion scan was acquired using information-dependent acquisition (IDA) with selection of the high-sensitivity mode. The raw MS data (wiff.scan files) were converted to MzXML files using ProteoWizard MSConvert before importing into the freely available XCMS software. In the extracted ion features,

only the variables with over 50% of the non-zero measurement values in at least one group were kept. Compound identification of metabolites in the MS/MS spectra was performed with an in-house database established with available authentic standards. After normalization to total peak intensity, the processed data were uploaded before importing into SIMCA-P (version 16.1, Umetrics, Umea, Sweden), where the data were subjected to multivariate data analysis, including Pareto-scaled principal component analysis (PCA) and orthogonal partial least-squares discriminant analysis (OPLS-DA). Seven-fold cross-validation and response permutation testing was used to evaluate the robustness of the model. The variable importance in the projection (VIP) value of each variable in the OPLS-DA model was calculated to measure its contribution to the classification. Metabolites with VIP values >1 was further analyzed for significance using Student's *t*-test at the univariate level, with *p*-values < 0.05 considered as statistically significant.

Transcriptomics Sequencing

Rat myocardial tissues were used for non-targeted metabolomics sequencing. Specifically, the anterior wall of the left ventricle was used; in the BAIBA group the area around the infarction was used). Total RNA was extracted using the TRIzol® reagent. Paired-end libraries were prepared using an ABclonal mRNA-seq Lib Prep Kit (ABclonal, China). Adaptor-ligated cDNAs were used for PCR amplification. The PCR products were purified (AMPure XP system) and library quality was assessed on an Agilent Bioanalyzer 4150 system. Finally, sequencing was performed with an Illumina Novaseq 6000 /MGISEQ-T7 system. The data generated from Illumina/BGI platform were used for bioinformatics analysis. All analyses were performed using an in-house pipeline from Shanghai Applied Protein Technology. In this step, the adapter sequences were removed and low-quality sequences and reads with N ratios > 5% were filtered out to obtain clean reads for subsequent analysis. The clean reads were aligned separately to the reference genome with orientation mode using HISAT2 software to obtain mapped reads. The mapped reads were spliced using Stringtie software, after which Gffcompare software was used to compare them with the reference genome GTF/GFF file to identify the original unannotated transcription region and discover new transcripts and new genes. Feature Counts was used to count the reads numbers mapped to each gene. The FPKM of each gene was calculated based on the length of the gene and reads count mapped to the gene. Differential expression analysis was performed using the DESeq2, and genes with |log2FC|>1 and Padj < 0.05 were considered to be differentially expressed genes.

Joint Analysis of Sequencing Data

Principle component analysis (PCA) was performed with SIMCA Version 14.1 using quantitative data from the two omics analyses. All differentially expressed genes and metabolites were queried and mapped to pathways based on the online Kyoto Encyclopedia of Genes and Genomes (KEGG, http://www.kegg.jp/). Enrichment analysis was also performed. R Version 3.5.1 was used to combine the KEGG annotation and enrichment result of the omics analyses. Venn diagrams and bar plots were drawn. Z-score normalization was performed on the quantitative data of the target differentially modified peptides, and heatmaps were drawn with R Version 3.5.1 (Distance Matrix Computation: Euclidean, Hierarchical Clustering: complete linkage).

Statistical Analysis

GraphPad Prism5 software (GraphPad Software Company, San Diego, CA, USA) was used to determine independent-sample differences between two groups. The differences between multiple groups were tested by one-way ANOVA. *P*-values < 0.05 were considered statistically significant.

RESULTS

Exercise Improves Cardiac Morphology and Function in Rats With Heart Failure After Myocardial Infarction

We established the rat model of HF after myocardial infarction (MI) by ligation of the anterior descending coronary artery. The immediate mortality rate of MI group was 61%, and the delayed mortality rate was 63.9%. It is well-established that MI induces maladaptive changes in the myocardium and extracellular matrix (ECM), which leads to ventricular pathological remodeling (structural and functional) and the occurrence and development of heart failure (HF) (**Figure 1**). Indeed, compared with rats in the Sham group, rats in the HF group showed morphological abnormalities, such as incomplete structure, different size, and disordered arrangement of cardiomyocytes (**Figure 1A**). By contrast, we found that 8 weeks of treadmill exercise (50 to 60% of maximum intensity, 60 min/day, 5 days/week, and at a 0% incline) reduces adverse MI-induced morphological changes. Specifically, despite the presence of a clear ischemic necrotic area in MI compared with the Sham group, the anterior wall of the left ventricle was still able to support and maintain the normal shape of the left ventricle (**Figure 1A**). Moreover, as shown in (**Figures 1B,C**), large collagen deposits were seen in the intercellular spaces, together with damaged cells and red blood cells, among other abnormalities with HF, which was ameliorated with exercise ($P = 0.008$). We further observed the morphology of mitochondria in the peri-infarcted area of rats in each group. Compared with the Sham group, the sarcoplasmic reticulum in the HF group appeared dilated, and the transverse canal (TT) was compressed and deformed (**Figure 1D**). Moreover, the mitochondria were arranged in a disordered fashion, with swollen mitochondrial crests and many absent cristae, and there was significant mitochondrial vacuolation. Surprisingly, exercise reduced mitochondrial vacuolation in the peri-infarcted area of the HFE group, and crest structures appeared relatively regular, suggesting exercise improved cardiac morphological changes and function after MI (**Figure 1D**). Consistent with this contention, echocardiography revealed that compared with the Sham group, LVIDd and LVIDs in HF group had increased, while EF, FS, and IVDs was significantly decreased, which was

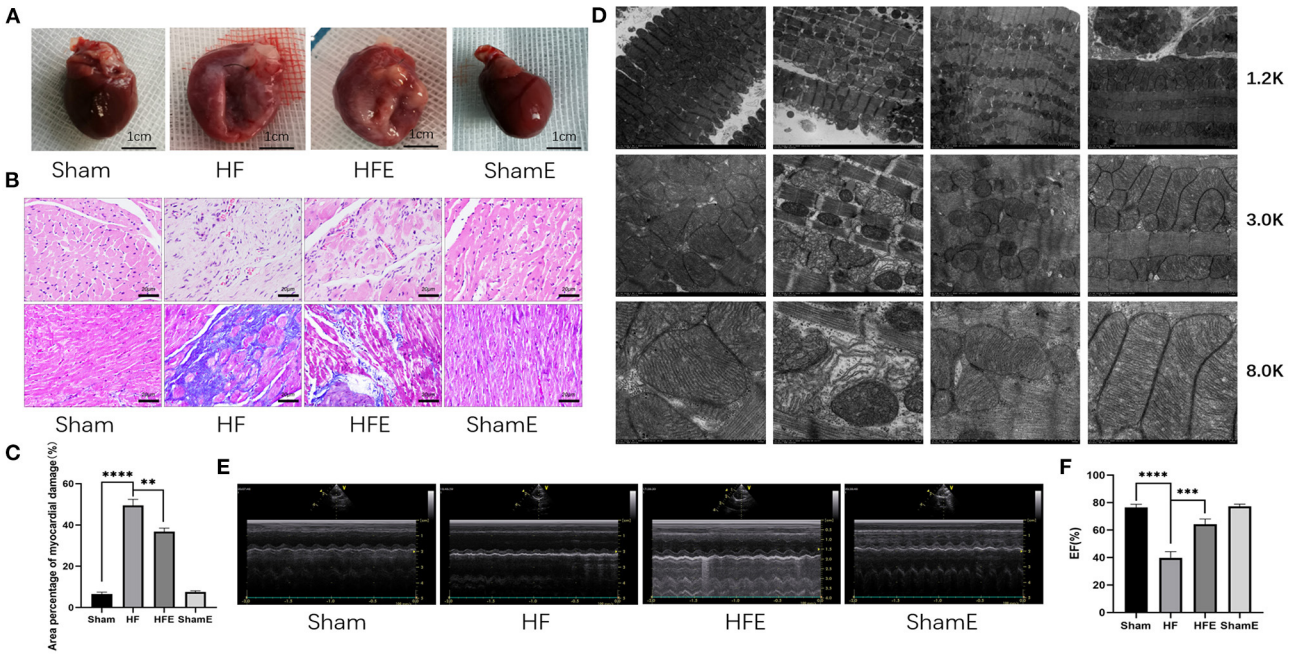

FIGURE 1 | Exercise improves cardiac morphological changes and function in rats after induced myocardial infarction. **(A)** The overall appearance of the hearts of rats from the Sham, HF, HFE, and ShamE groups, scale bar = 1 cm. **(B)** Cardiomyocytes stained by H&E, Scale bar = 20 μm, Mason tricolor-stained cardiac fibrosis, scale bar = 20 μm. **(C)** Quantitative analysis of collagen deposition in the left ventricle; $n = 3$; ****$P < 0.0001$; **$P < 0.01$. **(D)** Electron micrograph (TEM) of mitochondrial morphology in a longitudinal section of ventricular muscle. Magnification, ×12 000; ×30 000, and ×80 000. **(E)** M-mode echocardiography of rats in each group. **(F)** Statistical analysis of left ventricular EF determined by echocardiography. $n = 6$; ****$P < 0.0001$; ***$P < 0.001$.

ameliorated with exercise in the HFE group (**Figures 1E,F**, **Supplementary Files 3A–D**).

Exercise Alleviates Apoptosis in Rats With Heart Failure After Myocardial Infarction

In MI-induced HF, apoptosis is a key mediator of adverse left ventricular remodeling. In addition, alterations in ATP production are thought to play a significant role in apoptosis-induced by mitochondrial dysfunction. As shown in **Figure 2**, TUNEL staining revealed that the number of apoptotic nuclei was increased in the HF group, while exercise effectively decreased ($P = 0.0099$) both the number of apoptotic nuclei and the rate of apoptosis with HF (**Figures 2A,B**). In addition, ATP production was significantly reduced in HF compared to Sham rats, with the decrease in ATP production reversed ($P = 0.0002$) by exercise training (**Figure 2C**). To determine why exercise reduced the rate of apoptosis, we examined the expression of apoptosis-related proteins. As shown in **Figures 2D–F**, WB analysis showed that exercise could regulate the expression of apoptosis-related proteins. Specifically, compared with the Sham group, levels of cleaved/pro- caspase3 were up-regulated, while that of BCL-2/Bax was down-regulated in HF rats, with the pathological changes in apoptosis-related expression attenuated ($P = 0.0177$; $P = 0.0146$) with exercise training in the HFE group (**Figures 2D–F**). Therefore, it is clear that exercise may exert beneficial effects in HF by improving energy metabolism and reducing cellular apoptosis.

Exercise-Generated BAIBA Improves Cardiac Function and Energy Metabolism Disturbance in Rats With Heart Failure

β-aminoisobutyric acid (BAIBA) is a small molecule produced by skeletal muscle during exercise that reaches distant tissues via the bloodstream to exert beneficial physiological functions. As BAIBA appears to mediate is beneficial effects by improving energy metabolism (23, 25, 31). We sought to determine whether it may contribute to the improvements in cardiac structure and function with exercise in HF. As shown in **Figure 3A**, 8 weeks of exercise training increased ($P = \mathbf{0.0263}$) the concentration of BAIBA in the peripheral circulation of both Sham and HF rats (**Figure 3A**). Given these findings, we sought to determine whether we could mimic the beneficial effects of exercise training in HF through BAIBA administration. Thus, we gave BAIBA (75 mg/kg/day) to rats by oral gavage and evaluated the cardiac function 8 weeks later to verify whether oral BAIBA could improve the cardiac structure and function of rats with HF after MI. As shown in **Figure 3B**, we found that 8 weeks of orally administered BAIBA improved the left ventricular morphological abnormalities in rats with HF in comparison with the HF-only group. Specifically, BAIBA was able to alleviate cardiomyocyte lysis and necrosis as well as to reduce the numbers of disordered structures (**Figure 3C**), reduce ($P = 0.0001$) collagen deposition (**Figure 3D**), and increase the EF ($P = 0.001$), FS ($P = 0.0028$) and IVDs ($P = 0.0002$) while decrease the LVIDd ($P = 0.027$) and LVIDs ($P = 0.0001$) (**Figures 3E,F**, **Supplementary Files 3E–H**)

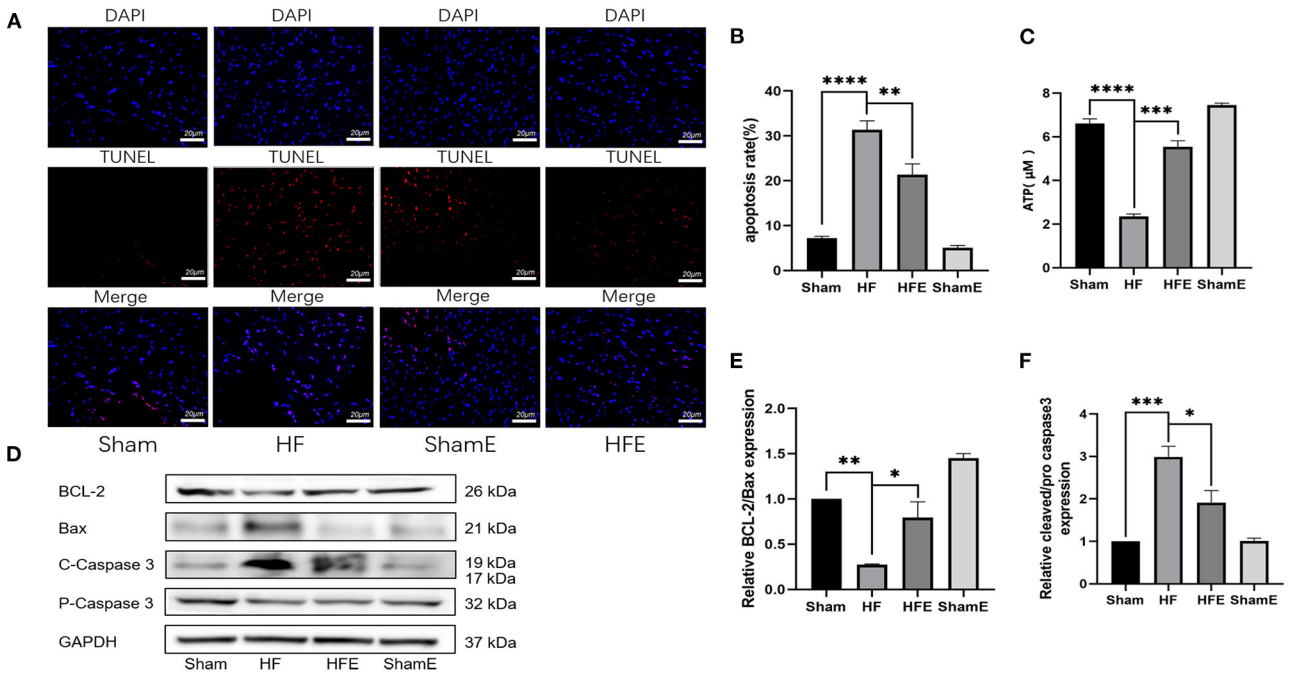

FIGURE 2 | Exercise improves energy metabolism disorders and apoptosis in rats after induced myocardial infarction. **(A)** Representative TUNEL staining from rats in Sham, HF, HFE and ShamE groups, Scale = 20 μm. **(B)** ATP levels in each group; $n = 6$. ****$P < 0.0001$; ***$P < 0.001$. **(C)** Apoptosis rates in each group, ****$P < 0.0001$; **$P < 0.01$. Three random field per rat are shown. **(D)** Representative images of apoptosis-related proteins detected by WB. **(E,F)** Light density assessment of apoptosis-related proteins detected by WB. $n = 3$; ***$P < 0.001$, **$P < 0.01$, *$P < 0.05$.

in rats with HF.TEM showed that oral administration of BAIBA could effectively reverse the morphological destruction of mitochondria caused by HF (**Figure 3G**). Moreover, in assessing cardiomyocyte apoptosis, TUNEL fluorescence staining showed that compared with the HF group, the numbers of apoptotic nuclei in the BAIBA-treated group were decreased ($P = 0.011$) (**Figures 4A,B**). Consistent with reduced apoptosis, BAIBA reversed ($P < 0.0001$) the decreases in ATP production observed with HF (**Figure 4C**). Importantly, WB showed that BAIBA regulated the expression of apoptosis-related proteins (**Figures 4D–F**) and mRNA levels (**Figures 4G–I**) in a similar manner to exercise, indicating that BAIBA reversed the adverse changes in apoptosis-related gene expression caused by HF.

BAIBA Up-Regulated miR-208b to Improve Disordered Energy Metabolism and Apoptosis in Rats With HF

To further understand the mechanism by which BAIBA improves energetics and exerts an anti-apoptotic effect, we next performed transcriptomic sequencing on tissue from the area surrounding the infarct in the anterior wall of the left ventricle in the HF and BAIBA groups. An orthogonal partial least squares discriminant analysis model (OPLS-DA) was used to detect the polymerization and the stability of the method. As shown in **Figure 5A**, the results showed a clear separation in the two groups in terms of gene expression. Specifically, RNA-sequencing revealed that 11 genes were upregulated, and 18 genes were downregulated in the BAIBA group compared to the Sham group (FC > 2.0, $P < 0.05$). Importantly, the volcano plot of differentially expressed mRNAs showed that BAIBA up-regulated the expression of miR-208b (**Figure 5B**), which we have previously shown to have a protective effect on myocardial apoptosis (26). Indeed, consistent with sequencing results, PCR showed alterations in miR-208b levels in response to exercise, regardless of HF or not (**Supplementary File 2A**). The clustering heatmap of DEGs showed differences in myocardial expression of miR-208b between the BAIBA and Sham groups (**Figure 5D**). Importantly, the expression of miR-208b was upregulated by BAIBA in a dose-dependent manner, with higher concentrations of BAIBA (10–30 μM) driving greater relative expression of miR-208b (**Figure 5C**). Moreover, BAIBA administration was found to reverse ($P < 0.0001$) the decrease in ATP concentrations in H9C2 cells caused by H_2O_2 (**Figure 5E**). Interestingly, administration of the miR-208b analog augmented BAIBA-induced cardioprotective effects, which was prevented by treatment with the miR-208b inhibitor (**Figure 5F**). In addition, the alterations in the expression of apoptosis-related proteins caused by H_2O_2 were reversed by treatment with the miR-208b analog, consistent with the effects of BAIBA, while the beneficial directional changers were attenuated by the miR-208b inhibitor (**Figures 5G,H**).

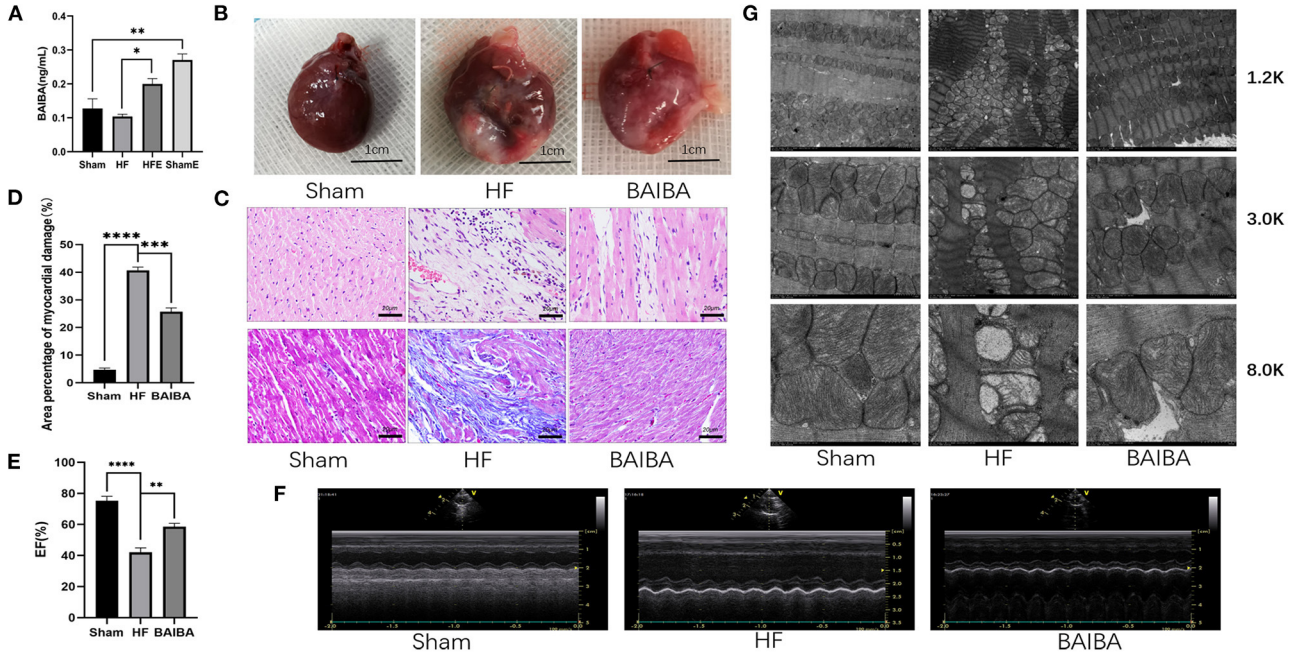

FIGURE 3 | Exercise-generated BAIBA improves morphology and functioning in rats with heart failure. **(A)** BAIBA concentrations in the serum of rats from the Sham, HF, HFE, and ShamE groups; $n = 3$; $^{**}P < 0.01$, $^{*}P < 0.05$. **(B)** The overall appearance of the rat hearts, T scale = 1 cm. **(C)** Cardiomyocytes stained by H&E. Scale bar = 20 μm, Masson tricolor-stained cardiac fibrosis, scale = 20 μm. **(D)** Quantitative analysis of collagen deposition in the left ventricle; $n = 3$; $^{****}P < 0.0001$ $^{***}P < 0.001$. **(E)** Statistical analysis of left ventricular EF determined by echocardiography. $n = 6$; $^{****}P < 0.0001$; $^{**}P < 0.01$. **(F)** M-mode echocardiography of rats in each group. **(G)** Electron micrograph (TEM) of mitochondrial morphology in a longitudinal section of ventricular muscle. Magnification, ×12,000; ×3,000, and ×80,000.

BAIBA Modulates Myocardial Metabolism Through the AMPK Pathway

It is clear from our study that upregulation of BAIBA and, subsequently, miR-208b improved energy metabolism and reduced apoptosis in HF rats. To further determine the specific metabolic targets of miR-208b in cardiomyocytes, a metabolomic profiling analysis was used. As shown in **Figure 6A**, metabolites were identified in both the positive ($n = 183$) and negative ($n = 103$) ion modes, with all metabolites classified and counted according to their chemical taxonomy and attribution. The OPLS-DA showed a clear separation between the two groups in both negative and positive ion modes (**Figure 6B**). Specifically, a total of 40 metabolites were found to be differentially expressed using a strict OPLS-DA Variable Importance for the Projection VIP >1 and P-value < 0.05 as the screening criteria (**Table 1**). The hierarchical clustering heatmap of the differential metabolites in the negative and positive modes is shown in **Figures 6C,D**. Differential abundance scores were used to analyze pathway changes in the metabolites, which showed that the differential metabolites were primarily involved in glycolysis and gluconeogenesis, glyceride metabolism, the pentose phosphate pathway, insulin resistance, purine metabolism, amino acid biosynthesis, and amino acid metabolism, histidine metabolism, arginine biosynthesis, glyoxylic acid, and dicarboxylic acid metabolism, glycine, serine, and threonine metabolism, taurine and low taurine metabolism, alanine, aspartic acid, and glutamic acid metabolism, β-glutamate, arginine and proline metabolism (**Figure 6E**), consistent with a role of BAIBA and miR-208b modulating myocardial metabolism. Importantly, the multi-group analysis showed that the differentially expressed genes and metabolites were mainly enriched in the AMP-activated protein kinase (AMPK) signaling pathway, which is a cellular energy sensor that plays a key role in cell growth, survival, and the maintenance of energy homeostasis. Other pathways that were enriched, to a lesser extent, in the HIF-1 signaling, FoxO signaling, fructose and mannose metabolism, insulin secretion, glucagon signaling, and insulin resistance pathways (**Figure 6F**).

BAIBA Increases AMPK Phosphorylation, Increases Free Fatty Acid Uptake and Oxidation Efficiency, and Improves Mitochondrial Function

Given the prominent enrichment of the differentially expressed in the AMPK pathway, we further interrogated the link between BAIBA administration and downstream changes in the AMPK signaling pathway. In rats with HF, oral administration of BAIBA elevated ($P = 0.0003$) the proportion of phospho-AMPK (p-AMPK) (**Figures 7A,B**), while in H9C2 cardiomyocytes, BAIBA also increased p-AMPK expression in the expression in a dose-dependent manner (**Figures 7C,D**). Transfection of the miR-208b analog amplified ($P = 0.0001$) this effect

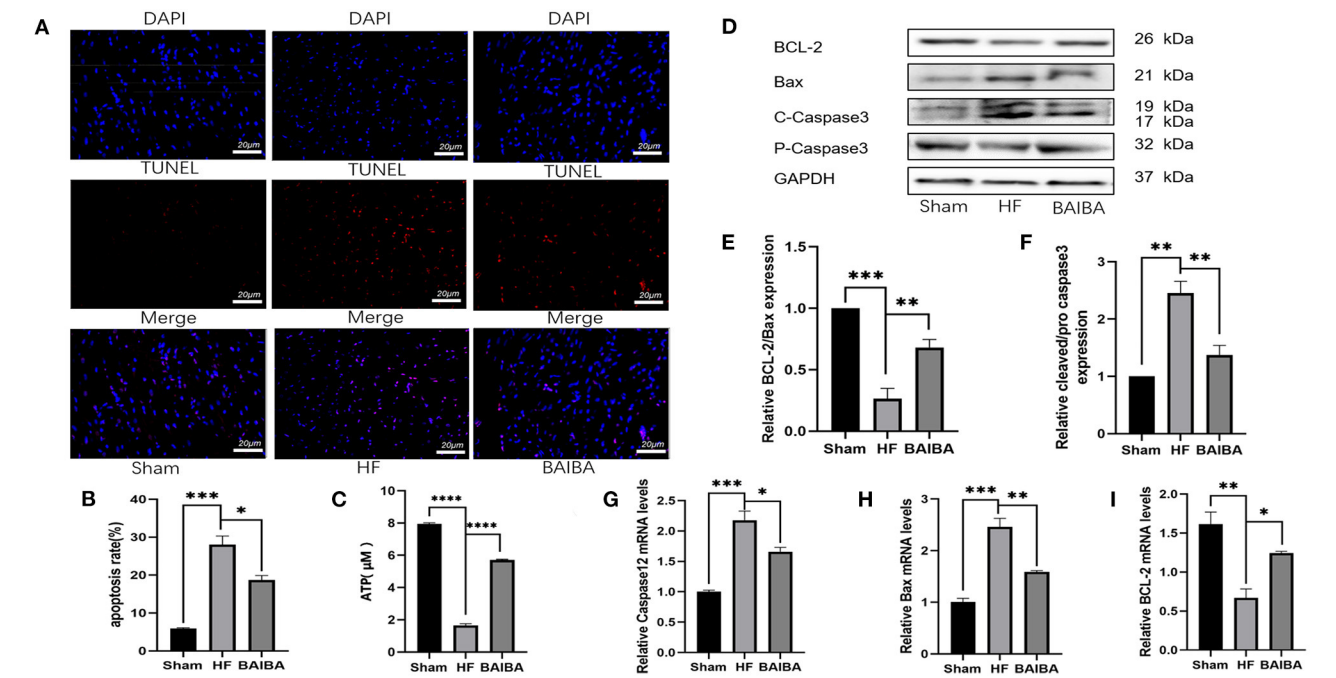

FIGURE 4 | BAIBA improves energy metabolism disorders and apoptosis in rats after induced heart failure. **(A)** Representative TUNEL staining from rats in the Sham, HF and BAIBA groups, scale = 20 μm. **(B)** Apoptosis rates in each group, $^{***}P < 0.001$; $^{*}P < 0.05$. Three random fields per rat are shown. **(C)** ATP levels in each group; $n = 6$. $^{****}P < 0.0001$. **(D)** Representative images of apoptosis-related proteins by WB. **(E,F)** Light density assessment of apoptosis-related proteins detected by WB. $n = 3$; $^{***}P < 0.001$, $^{**}P < 0.01$. **(G–I)** Real-time quantitative PCR analysis of apoptosis-related genes. $n = 3$; $^{***}P < 0.001$, $^{**}P < 0.01$, $^{*}P < 0.05$.

on AMPK phosphorylation, while the miR-208b inhibitor counteracted ($P = 0.0222$) the effect (**Figures 5F,I**). Taken together, these findings suggest that the phosphorylation of AMPK by BAIBA may be mediated by miR-208b. As a main metabolic switch, activated AMPK can increase the flexibility of metabolic substrates and improve mitochondrial function through mitochondrial biogenesis and quality control. Thus, we next performed WB analysis of downstream AMPK proteins in HF rat models. Fatty acids are an important metabolic substrate in the heart, and we therefore assessed changes in a number of these key enzymes in fatty acid oxidation (FAO), including carnitine palmitoyltransferase-1 (CPT-1), acyl-CoA dehydrogenase long chain (ACADL), and acetyl-CoA carboxylase (ACC), using WB (**Figure 7E**). In quantifying changes in these enzymes, compared with the HF group, BAIBA increased ($P = 0.0014$) the expression of the fatty acid uptake-related protein CD36 (**Figure 7F**). Moreover, BAIBA increased the expression of p-ACC ($P < 0.0001$) (**Figure 7G**), CPT-1 ($P < 0.0001$) (**Figure 7H**), and ACADL ($P = 0.0015$) (**Figure 7I**), all of which would increase fatty acid uptake and oxidation efficiency. At the same time, BAIBA also increased the biogenesis of mitochondria and improved their functioning (**Figure 7J**). Mitochondrial fusion and fission form the core of mitochondrial quality control. Our results showed that BAIBA ameliorated ($P = 0.002$; $P = 0.0004$) the reductions in optic nerve atrophy 1 (OPA1) and dynamic protein-associated protein 1 (Drp1) expression, thus improving mitochondrial quality (**Figures 7K,L**). Moreover, BAIBA was found to increase ($P = 0.0288$) the expression of peroxisome proliferator-activated receptor (PPAR) γ coactivator-1 α (PGC-1α), which is a strong activator of cardiac mitochondrial biogenesis (**Figure 7M**). SUCLA2 is a core enzyme of the tricarboxylic acid cycle (TCA), participating in acetyl-CoA oxidation; BAIBA attenuated ($P = 0.0114$) the decreased SUCLA expression in rats in the HF group (**Figure 7N**). Therefore, our findings suggest BAIBA mediates its beneficial effects on cardiac energetics by increasing AMPK phosphorylation, fatty acid intake and oxidation, and improving mitochondrial function.

The Protective Effects of BAIBA on Apoptosis, Disordered Energy Metabolism, Mitochondrial Function, and FA Uptake and Oxidation Are Offset by AMPK Inhibition

Our results suggest that the protective effect of BAIBA was mediated by the AMPK pathway. To further interrogate how activation of this pathway attenuates apoptosis, we began by assessing the impact of BAIBA on ROS production, which is known initiator of cardiomyocyte apoptosis. As shown in **Figure 8A**, ROS production was increase in the H_2O_2-treated group compared with the controls, consistent with a link to myocardial apoptosis. Importantly, treatment with BAIBA reversed this effect by reducing ROS production, while treatment with the AMPK inhibitor, Compound C, counteracted the

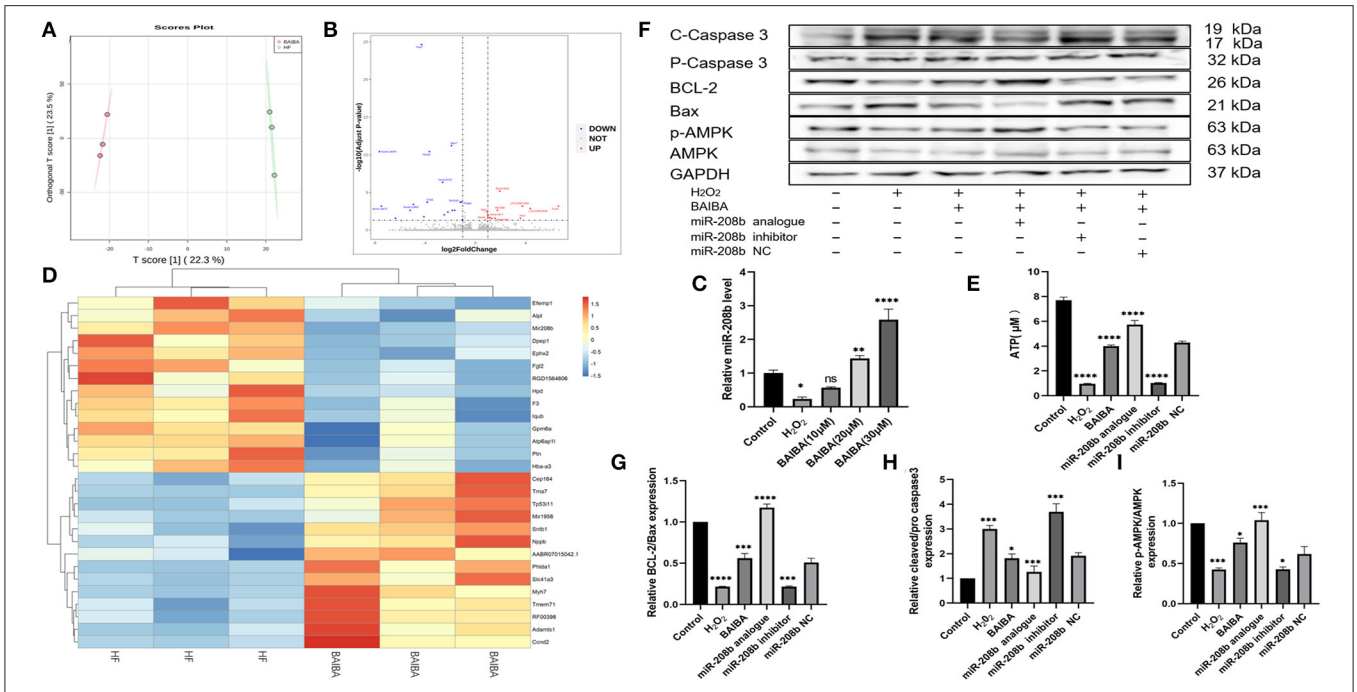

FIGURE 5 | High-throughput sequencing shows that BAIBA plays an anti-apoptotic role through miR-208b. **(A)** OPLS-DA of BAIBA vs. HF group, $n = 3$. **(B)** Volcano plot of differential mRNAs. **(C)** Clustering heatmap of differential mRNA between the BAIBA and Sham groups. **(D)** Representative images of apoptosis-related proteins detected by WB. **(E)** Expression of miR-208b after stimulation with different concentrations of BAIBA vs. H_2O_2 group. $n = 3$, $^{****}P < 0.0001$; $^{**}P < 0.01$; $^{*}P < 0.05$. **(F)** ATP levels in each group, H_2O_2 vs. Control group; BAIBA, miR-208 analog vs. H_2O_2 group; miR-208 inhibitor vs. BAIBA group. $n = 3$. $^{****}P < 0.0001$. **(G,H)** Light density assessment of apoptosis-related proteins detected by WB. H_2O_2 vs. Control group; BAIBA, miR-208 analog vs. H_2O_2 group; miR-208 inhibitor vs. BAIBA group. $n = 3$; $^{****}P < 0.0001$, $^{***}P < 0.001$, $^{*}P < 0.05$. **(I)** Light density assessment of p-AMPK detected by WB. H_2O_2 vs. Control group; BAIBA, miR-208 analog vs. H_2O_2 group; miR-208 inhibitor vs. BAIBA group. $n = 3$; $^{***}P < 0.001$, $^{*}P < 0.05$.

BAIBA-mediated action (**Figure 8A**). Moreover, mitochondrial membrane potential staining showed similar directional changes with our treatment groups. Specifically, BAIBA treatment counteracted the drop in mitochondrial membrane potential caused by H_2O_2, which was counteracted ($P = 0.0002$) by treatment with Compound C (**Figures 8B,C**). Treatment with Compound C also reversed ($P < 0.0001$) the protective effects of BAIBA on ATP production (**Figure 8D**). Consistent with above, the BAIBA-mediated reversal of H_2O_2-induced changes in apoptosis-related protein expression was also offset by the AMPK inhibitor (**Figures 8E–G**). Analysis of the expression of proteins associated with fatty acid uptake and β-oxidation (**Figures 8H–L**) as well as mitochondrial proteins (**Figures 8M–Q**) further confirmed these findings, demonstrating that BAIBA mediates its cardioprotective effects through AMPK and that AMPK inhibition reverses the protective effect of BAIBA on the expression of these proteins.

DISCUSSION

The heart is an energy-consuming organ and requires sufficient ATP to maintain its pump function. Normal cardiomyocytes have metabolic flexibility. Various metabolic substrates including fatty acids, carbohydrates (glucose and lactates), ketones, and amino acids enter the tricarboxylic acid cycle to form ATP, allowing the maintenance of normal cardiac contraction. Mitochondria play important roles in the production of ATP. By contrast, a loss of metabolic substrate flexibility caused by mitochondrial dysfunction may be a key factor in heart failure, leading to metabolic and oxidative stress as well as increased cellular apoptosis, forming a vicious cycle. Our results showed that in rats with HF after MI, the mitochondria were arranged in a disordered fashion, with swollen mitochondrial crests and many absent cristae, and there was significant mitochondrial vacuolation. As a result, the production of ATP decreased, which accelerated the progression of HF. Therefore, mitochondrial function is a crucial therapeutic target for heart failure (2, 32).

Moderate exercise is known to have a beneficial effect on heart function in patients with HF (9). Moderate continuous training is efficient, safe, and well tolerated by HF patients, and it is recommended by the Heart Failure Association Guidelines (15). Cardiac energy metabolism can be partially restored through exercise due to improvements in oxidation ability and by restoring energy transfer. Exercise can also restore cardiac autophagic flux in heart failure. This is related to improved mitochondrial quality control, bioenergetics, and cardiac function (16). Our results showed that in rats with HF after MI, the EF% of the exercise group was superior

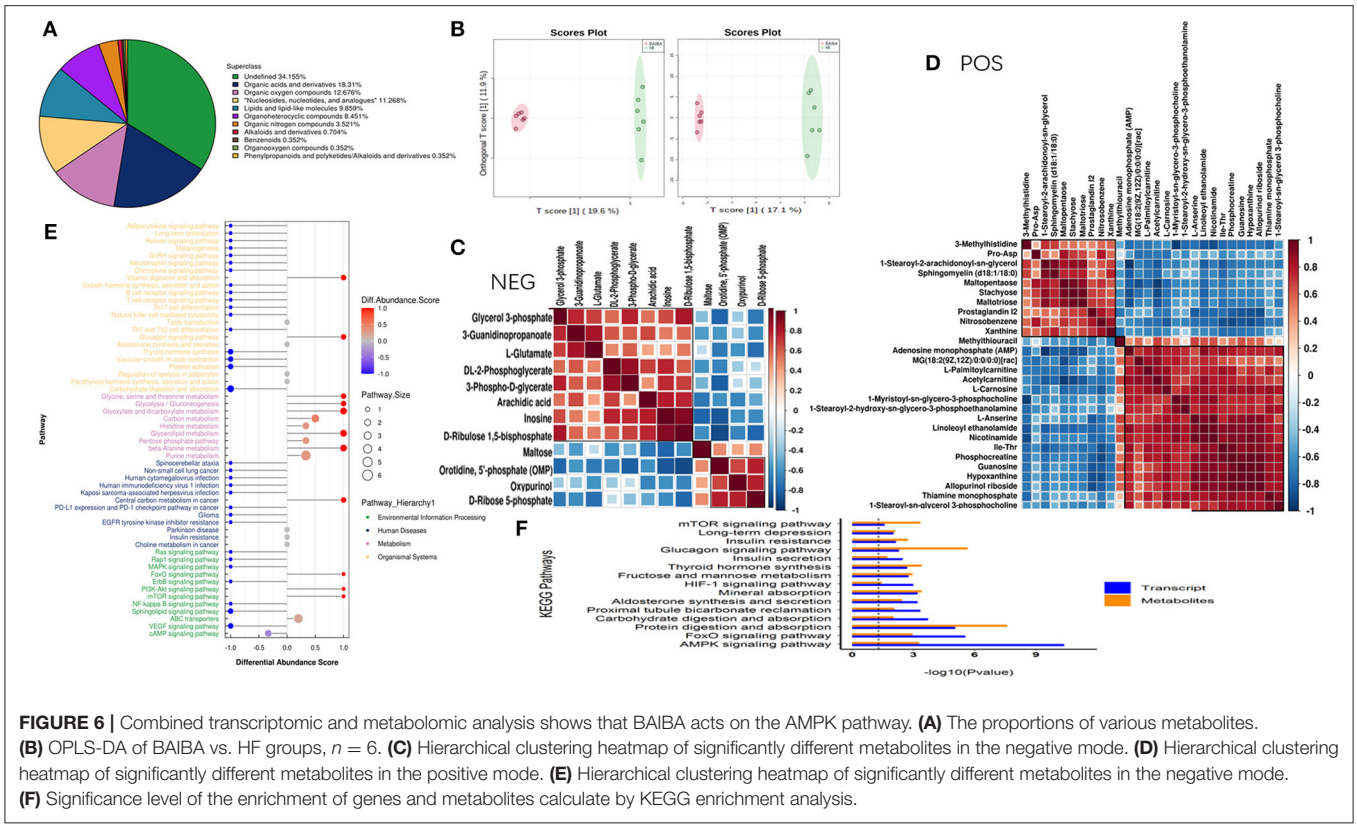

FIGURE 6 | Combined transcriptomic and metabolomic analysis shows that BAIBA acts on the AMPK pathway. **(A)** The proportions of various metabolites. **(B)** OPLS-DA of BAIBA vs. HF groups, $n = 6$. **(C)** Hierarchical clustering heatmap of significantly different metabolites in the negative mode. **(D)** Hierarchical clustering heatmap of significantly different metabolites in the positive mode. **(E)** Hierarchical clustering heatmap of significantly different metabolites in the negative mode. **(F)** Significance level of the enrichment of genes and metabolites calculate by KEGG enrichment analysis.

to that of the HF group. Despite being forced exercise, which may be associated with stress responses (33), 8 weeks of treadmill training alleviated the degree of cardiomyocyte apoptosis surrounding the infarcted region and improved mitochondrial morphology. The protective function of exercise in HF patients undergoing continuous aerobic exercise training is primarily determined by the total energy expenditure, including the training intensity, duration, and frequency of the training program. However, a considerable number of patients with HF are unable to undertake effective exercise due to circulatory disorders and skeletal muscle mitochondrial dysfunction, among other reasons. For these patients, their recovery can potentially be improved by the identification of the targets of exercise-induced protection and using these to find alternative treatments.

BAIBA is a small molecule (103.6 Da) produced by skeletal muscles during exercise and mediates the beneficial effect of exercise from skeletal muscle to other tissues and organs via the endocrine system (19). BAIBA activates the fatty acid β-oxidation pathway in the liver, converts white adipose tissue to brown fat (25), improves insulin resistance and skeletal myositis by the autocrine/paracrine systems, prevents diet-induced obesity (34), and protects against metabolic dysfunction in type 2 diabetes (22). Here, it was found that the production of BAIBA increased after exercise in both the control group and HF rats, which may underlie the cardioprotective effects of exercise in HF. Importantly, we found that 8-weeks of BAIBA administration in rats with HF improved cardiac function, reversed metabolic stress, and reduced apoptosis. Moreover, transcriptomic analyses revealed this protective action of BAIBA was found to be linked to increased expression of miR-208b, which is a heart-specific miRNA encoded on intron 27 of the gene encoding α-MHC that is essential for the expression of genes involved in cardiac contractility and fibrosis. An increased plasma concentration of miR-208b has been linked to myocardial injury and may serve as a biomarker of acute myocardial infarction (35). Nonetheless, previous studies have demonstrated miR-208b may serve a protective role in myocardial fibrosis after infarction through GATA4 signaling (36). Consistent with a cardioprotective role of miR-208b in the current study, we have previously shown that miR-208b has a protective effect on myocardial apoptosis (26). Specifically, our findings confirm that BAIBA increases the expression of miR-208b in a dose-dependent manner, and that the miR-208b analog is a downstream mediator of the protective effects on left ventricular remodeling and function through the reduction of metabolic stress and apoptosis caused by mitochondrial dysfunction in rats with HF. Indeed, metabolomic profiling linked the protective effects to differential regulation of metabolites involved in glycolysis, gluconeogenesis, amino acid biosynthesis, and other metabolic pathways, consistent with the maintenance of mitochondrial energetics being important being a crucial therapeutic target in HF. Importantly, we identified that the protective effect of BAIBA on the heart in HF is linked to the AMPK signaling pathway, with both BAIBA and miR-208b increasing AMPK phosphorylation in a concentration-dependent manner. As

TABLE 1 | Differential metabolites between the BAIBA and Sham groups.

Adduct	Name	VIP	FC	*P*-value	m/z	rt(S)
(M-H)-	Maltose	1.747133102	1.853496517	0.001105606	341.10984	449.316
(M-H)-	Inosine	12.68850649	0.712132158	0.001207444	267.07386	217.6715
(M+CH3COO)-	D-Ribulose 1 5-bisphosphate	1.782550319	0.408627194	0.006806923	369.00044	435.2515
(M-H)-	3-Guanidinopropanoate	2.954725215	0.706925321	0.006926241	130.06213	349.242
(M-H)-	Arachidic acid	1.684319676	0.568914743	0.007538358	311.29604	39.914
(M-H)-	DL-2-Phosphoglycerate	7.329573369	0.381760658	0.020325427	184.98581	470.9
(2M-H)-	3-Phospho-D-glycerate	1.661451592	0.236277794	0.022903901	370.98	470.953
(M-H)-	Orotidine 5′-phosphate (OMP)	1.241131943	2.081168265	0.026892841	367.01093	462.396
(M-H)-	Glycerol 3-phosphate	4.084530216	0.647349896	0.034960137	171.0064	430.0125
(M-H)-	Oxypurinol	3.882881699	2.518632379	0.035085539	151.02612	244.2205
(M+CH3COO)-	D-Ribose 5-phosphate	3.659360842	1.325621035	0.043880746	289.03359	461.66
(M-H)-	L-Glutamate	2.849537956	0.851050259	0.043943848	146.04609	396.561
(M+Na)+	Acetylcarnitine	1.462328082	0.777352931	0.000245574	226.10363	307.7345
(M+H)+	Linoleoyl ethanolamide	1.354137268	0.655316044	0.000279653	324.28769	36.2295
(M+H)+	Phosphocreatine	2.021285259	0.491283479	0.000868958	212.0419	438.9865
(M+H)+	Nicotinamide	10.74306783	0.861527316	0.000943401	123.05523	62.2415
(M+H)+	L-Carnosine	5.421254128	0.405729569	0.000965206	227.11325	422.118
(M+H)+	Hypoxanthine	11.7857247	0.749549435	0.001039384	137.04539	216.9845
(M+H)+	Guanosine	1.89912572	0.675033308	0.001314684	284.09775	262.743
(M+H)+	Ile-Thr	1.15320574	0.437272107	0.001616012	233.14837	50.792
(M+NH4)+	Stachyose	2.154557724	2.41875441	0.001949267	684.25204	488.522
(M+H-H2O)+	MG(18:2(9Z 12Z)/0:0/0:0)[rac]	3.985687426	0.713154762	0.002312178	337.2717	37.0085
(M+H-H2O)+	1-Stearoyl-2-arachidonoyl-sn-glycerol	3.795636092	1.243900004	0.003384257	627.5309	192.458
(M+NH4)+	Maltotriose	3.45554989	1.846746797	0.003497007	522.20034	449.2395
(M+CH3CN+H)+	Nitrosobenzene	1.178848398	3.325302789	0.003873997	149.07237	65.885
(2M+H)+	Allopurinol riboside	3.958330117	0.666746052	0.004621944	537.16584	216.9845
(M+H)+	1-Myristoyl-sn-glycero-3-phosphocholine	1.456332015	0.600830069	0.005324648	468.30597	200.3165
(M+H)+	Xanthine	1.574238507	1.288697953	0.005441952	153.039	219.5835
(M+Na)+	Maltopentaose	1.810989097	3.062600739	0.009029524	851.26122	507.208
(M+H)+	Prostaglandin I2	1.149081762	3.557597818	0.011067474	353.2302	161.7475
(M+H)+	Adenosine monophosphate (AMP)	1.028294798	0.585128158	0.011123783	348.06833	402.638
(M+H)+	3-Methylhistidine	2.088235504	1.488995206	0.011725758	170.09117	432.186
(M+H)+	Thiamine monophosphate	1.534209559	0.789752069	0.014247642	345.07645	490.066
(M+H)+	L-Palmitoylcarnitine	7.742755165	0.572001197	0.014438134	400.34053	175.461
(M+H)+	Sphingomyelin (d18:1/18:0)	2.537052905	1.128875942	0.016585356	731.60242	180.9475
(M+H)+	1-Stearoyl-2-hydroxy-sn-glycero-3-phosphoethanolamine	5.020219423	0.643566288	0.028989733	482.32254	198.3845
(M+H)+	Pro-Asp	1.148515883	1.075266343	0.030657874	231.09604	425.271
(M-2H+3Na)+	1-Stearoyl-sn-glycerol 3-phosphocholine	1.914627352	0.53137472	0.03432785	590.31848	184.124
(M+H-H2O)+	Methylthiouracil	1.291816999	0.788053158	0.036373882	125.01941	354.4835
(M+H)+	L-Anserine	6.031617223	0.28555341	0.04015567	241.12884	416.913

miR-208b analog transfection enhanced AMPK activation by BAIBA, and the miR-208b inhibitor counteracted this effect, our findings suggest a novel cardioprotective signaling cascade in which activation of AMPK by BAIBA may be mediated by miR-208b.

Our *in vivo* findings of a BAIBA-mediated increases in AMPK supports the notion that reducing cardiomyocyte metabolic stress is important for HF treatment and outcomes. As a cellular energy sensor and metabolic switch, AMPK plays a key role not only in cell growth and survival but also in systemic energy homeostasis (37). Moreover, AMPK mediates mitochondrial fission to cope with energy stress, which would be increased in HF. Our findings support a mechanistic framework by which BAIBA reduces cardiomyocyte metabolic stress and apoptosis caused by mitochondrial dysfunction through the miR-208b/AMPK pathway. Indeed, our results showed that BAIBA can not only increase the expression of AMPK, but can effectively improve the expression of proteins related to fatty acid uptake and oxidation, which is known to have beneficial effects in HF models (38, 39). Mechanistically, BAIBA

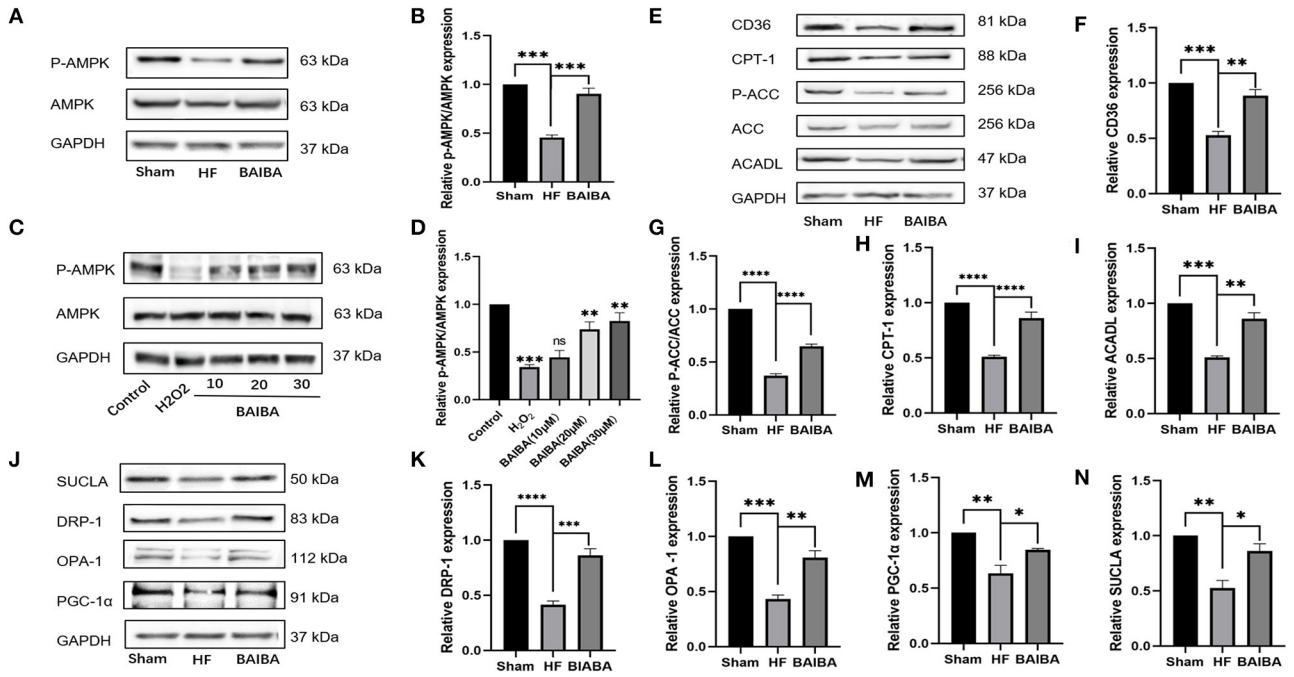

FIGURE 7 | BAIBA increases cardiomyocytes AMPK phosphorylation, fatty acid intake and oxidation, and improves mitochondrial function of Heart Failure Rats. **(A)** Representative images of p-AMPK expression in the Sham, HF, and BAIBA groups detected by WB. **(B)** Light density assessment of p-AMPK expression in the Sham, HF, and BAIBA groups. $n = 3$; $^{***}P < 0.001$. **(C)** Representative images of p-AMPK expression in the Control, H_20_2, BAIBA (10 mM), BAIBA (20 mM), and BAIBA (30 mM) groups detected by WB. **(D)** Light density assessment of p-AMPK expression in the Control, H_20_2, BAIBA (10 mM), BAIBA (20 mM), and BAIBA (30 mM) groups. $n = 3$; $^{***}P < 0.001$, $^{**}P < 0.01$. **(E)** Representative images of fatty acid uptake and oxidation-related protein expression in the Sham, HF, and BAIBA groups detected by WB. **(F–I)** Light density assessment of fatty acid uptake and oxidation-related protein expression in the Sham, HF, and BAIBA groups. $n = 3$; $^{****}P < 0.0001$; $^{***}P < 0.001$; $^{**}P < 0.01$. **(J)** Representative images of mitochondrial protein expression in the Sham, HF, and BAIBA groups detected by WB. **(K–N)** Light density assessment of mitochondrial protein expression in the Sham, HF, and BAIBA groups. $n = 3$; $^{****}P < 0.0001$; $^{***}P < 0.001$; $^{**}P < 0.01$; $^{*}P < 0.05$.

promotes fatty acid uptake by cardiomyocytes by increasing the translocation of the fatty acid transporter CD36 to the membrane (40). In addition, the rate-limiting step of β-oxidation is the CPT1-mediated mitochondrial transmembrane transfer of fatty acids. Moreover, AMPK inhibits the production of malonyl-CoA carboxylase (ACC) by phosphorylation, increases the activity of CPT1, and increases the efficiency of myocardial fatty acid β-oxidation (41). As BAIBA increases CPT-1 levels in the context of heart failure and thereby improves the efficiency of fatty acid oxidation and attenuates metabolic stress (42). Indeed, we found that BAIBA effectively improved the expression of mitochondrial proteins. As the power houses that maintain cardiac energy supply, mitochondrial dysfunction is a prominent mediatory of pathological processes that can drive adverse cardiac remodeling, including redox imbalance, protein modification, ROS signaling, ion homeostasis, and inflammation (43, 44). However, our findings suggest BAIBA may prevent mitochondrial dysfunction by upregulating the expression of OPA1 and Drp1. Mitochondrial fusion and fission are the core of mitochondrial quality control and the fusion of the mitochondrial inner membrane is dependent on OPA1, which maintains closure of the crest junction, preventing cytochrome c release and apoptosis (45). Thus, reduced expression of OPA1 in dysfunctional mitochondria is accompanied by the destruction and loss of the mitochondrial crest and loosening of the mitochondrial junction, leading to apoptosis (46, 47). Moreover, Drp1 is a GTP enzyme that mediates mitochondrial fission (48) which promotes autophagy of damaged mitochondria (49). By contrast, reduced levels of Drp1 results in mitochondrial elongation and accumulation of damaged mitochondria, together with an inhibition of mitochondrial autophagy, leading to mitochondrial dysfunction and cardiomyocyte apoptosis (50). Thus, the improvement in mitochondrial function could increase the stability of the mitochondrial membrane potential and optimize the morphology of the mitochondrial crest, thus avoiding cytochrome c release and ROS accumulation, and ultimately preventing apoptosis. Taken together, our findings suggest that in patients with HF, the pharmacological activation of AMPK with BAIBA could be used as a therapeutic strategy to improve cardiac energy supply. While SGLT2, metformin, statins, and trimetazidine have received significant attention in the treatment of cardiovascular diseases because of their activation of AMPK (51–54), our findings suggest that BAIBA administration could be an alternative therapeutic approach to reduce metabolic stress and mitochondrial dysfunction in HF.

In addition to regulating the metabolism of the failing heart, AMPK can also mediate a variety of physiological signaling

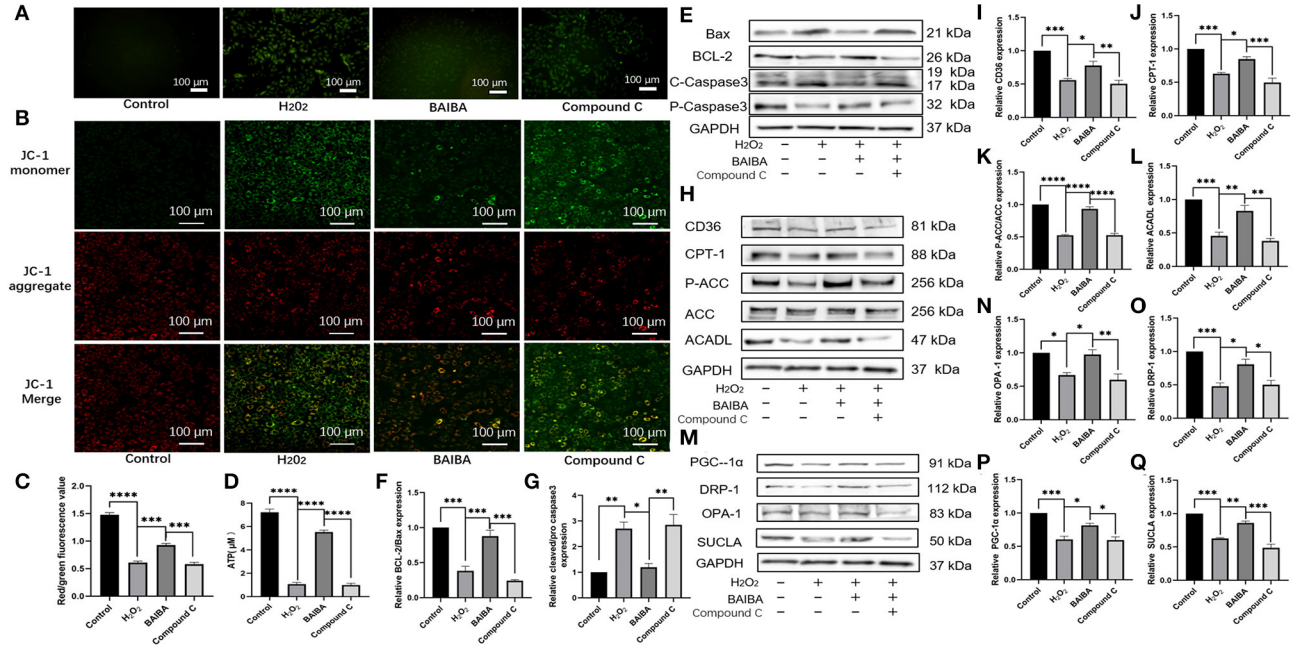

FIGURE 8 | Effects of BAIBA administration on apoptosis, energy metabolism disorders, mitochondrial function, and fatty acid uptake and utilization. **(A)** ROS production in Control, H_2O_2, BAIBA, and Compound C-treated cells, the scale bar in each image is 100 μm. **(B)** Representative $\Delta\Psi$ m staining determined by measuring changes in JC-1-derived fluorescence from red (high potential, J-aggregates) to green (low potential, monomeric) using confocal microscopy; data are representative of three independent experiments. **(C)** Statistical analysis of JC-1 red fluorescence percentage; $n = 5$ wells. $^{***}P < 0.0001$, $^{****}P < 0.0001$; **(D)** ATP levels in each group; $n = 3$. $^{****}P < 0.0001$; **(E)** Representative images of apoptosis-related proteins of each group. **(F,G)** Light density assessment of apoptosis-related protein expression. $n = 3$; $^{***}P < 0.001$, $^{**}P < 0.01$, $^{*}P < 0.05$. **(H)** Representative images of fatty acid uptake and oxidation-related protein expression in each group. **(I–L)** Light density assessment of fatty acid uptake and oxidation-related protein expression. $n = 3$; $^{****}P < 0.0001$; $^{***}P < 0.001$; $^{**}P < 0.01$. $^{*}P < 0.05$. **(M)** Representative images of mitochondria related protein expression of each group. **(N–Q)** Light density assessment of mitochondria related protein expression, $n = 3$; $^{***}P < 0.001$; $^{**}P < 0.01$; $^{*}P < 0.05$.

pathways (55). AMPK promotes autophagy directly through phosphorylation of the Unc-51-like kinase 1 (ULK1) kinase complex (56), and indirectly enhances autophagy through mTORC1 inactivation (57). The inhibition of mTOR affects protein synthesis, reducing the accumulation of unfolded proteins and thus reducing endoplasmic reticulum stress (58). AMPK activation can also reduce inflammation and cell death by inhibiting JNK and NF-κB, thereby protecting cardiomyocytes (59).

Our study is not without limitations. While our findings show the cardioprotective effect of BAIBA is mediated through an miR-208b/AMPK-mediated pathway, we cannot rule out that other pathways may contribute to the protective effect on cardiac structure and function. Moreover, we did not use double staining to indicate which cell type in heart tissue is subjected to apoptosis. Co-staining cardiomyocytes with TUNEL staining would be more convincing for the presentation of the results, though it is well-established that MI models of HF induce cardiomyocyte apoptosis. In addition, we used GAPDH as an internal control for normalizing expression. However, apoptosis caused by mitochondrial dysfunction may be accompanied by changes in glycolysis. To overcome this limitation, we further monitored the relative levels of β-actin in our samples, with our results indicating the relative level of GAPDH is almost equal to that of β-actin (**Supplementary File 2**).

In conclusion, this study confirmed that exercise-generated BAIBA increased AMPK phosphorylation through the expression of miR-208b to reshape the energy metabolism of rats with HF, improving mitochondrial dysfunction and reducing apoptosis. But for patients with heart failure, whether BAIBA can be used as an alternative for exercise therapy still requires more studies.

CONCLUSION

Exercise-generated BAIBA can reduce cardiomyocyte metabolic stress and apoptosis induced by mitochondrial dysfunction through the miR-208b/AMPK pathway.

DATA AVAILABILITY STATEMENT

The data presented in the study are deposited in the MetaboLights repository, accession number MTBLS3927; And GEO repository, accession number GSE193432.

ETHICS STATEMENT

Animal experiments were approved by the Ethics Committee of the First Hospital of Jilin University. The ethics number is 20210710. Written informed consent was obtained from the patient for the publication of this case report and any accompanying images.

AUTHOR CONTRIBUTIONS

PY is the chief investigator, conceived the study, led the proposal, and protocol development. WWC, MY, and JSL contributed to study design. YNY performed experiments, analyzed and interpreted the data, and drafted the manuscript. HS contributed resources, designed research, in supervised the project, and reviewed the manuscript. All authors read and approved the final manuscript.

FUNDING

This work was supported by the National Natural Science Foundation of China, No. 81570360.

SUPPLEMENTARY MATERIAL

The Supplementary Material for this article can be found online at: https://www.frontiersin.org/articles/10.3389/fcvm.2022.803510/full#supplementary-material

REFERENCES

1. He Y, Huang W, Zhang C, Chen L, Xu R, Li N, et al. Energy metabolism disorders and potential therapeutic drugs in heart failure. *Acta Pharm Sin B.* (2021) 11:1098–116. doi: 10.1016/j.apsb.2020.10.007
2. Ramachandra CJA, Hernandez-Resendiz S, Crespo-Avilan GE, Lin YH, Hausenloy DJ. Mitochondria in acute myocardial infarction and cardioprotection. *EBioMedicine.* (2020) 57:102884. doi: 10.1016/j.ebiom.2020.102884
3. Lopaschuk GD, Ussher JR. Evolving concepts of myocardial energy metabolism: more than just fats and carbohydrates. *Circ Res.* (2016) 119:1173–6. doi: 10.1161/CIRCRESAHA.116.310078
4. Karwi QG, Uddin GM, Ho KL, Lopaschuk GD. Loss of metabolic flexibility in the failing heart. *Front Cardiovasc Med.* (2018) 5:68. doi: 10.3389/fcvm.2018.00068
5. Wang ZV, Li DL, Hill JA. Heart failure and loss of metabolic control. *J Cardiovasc Pharmacol.* (2014) 63:302–13. doi: 10.1097/FJC.0000000000000054
6. Zhu H, Toan S, Mui D, Zhou H. Mitochondrial quality surveillance as a therapeutic target in myocardial infarction. *Acta Physiol.* (2021) 231:e13590. doi: 10.1111/apha.13590
7. Chistiakov DA, Shkurat TP, Melnichenko AA, Grechko AV, Orekhov AN. The role of mitochondrial dysfunction in cardiovascular disease: a brief review. *Ann Med.* (2018) 50:121–7. doi: 10.1080/07853890.2017.1417631
8. Aimo A, Borrelli C, Vergaro G, Piepoli MF, Caterina AR, Mirizzi G, et al. Targeting mitochondrial dysfunction in chronic heart failure: current evidence and potential approaches. *Curr Pharm Des.* (2016) 22:4807–22. doi: 10.2174/1381612822666160701075027
9. Cattadori G, Segurini C, Picozzi A, Padeletti L, Anzà C. Exercise and heart failure: an update. *ESC Heart Fail.* (2018) 5:222–32. doi: 10.1002/ehf2.12225
10. Giuliano C, Karahalios A, Neil C, Allen J, Levinger I. The effects of resistance training on muscle strength, quality of life and aerobic capacity in patients with chronic heart failure - a meta-analysis. *Int J Cardiol.* (2017) 227:413–23. doi: 10.1016/j.ijcard.2016.11.023
11. Tucker WJ, Beaudry RI, Liang Y, Clark AM, Tomczak CR, Nelson MD, et al. Meta-analysis of exercise training on left ventricular ejection fraction in heart failure with reduced ejection fraction: a 10-year update. *Prog Cardiovasc Dis.* (2019) 62:163–71. doi: 10.1016/j.pcad.2018.08.006
12. Jiang H, Jia D, Zhang B, Yang W, Dong Z, Sun X, et al. Exercise improves cardiac function and glucose metabolism in mice with experimental myocardial infarction through inhibiting HDAC4 and upregulating GLUT1 expression. *Basic Res Cardiol.* (2020) 115:28. doi: 10.1007/s00395-020-0787-1
13. Stølen T, Shi M, Wohlwend M, Høydal MA, Bathen TF, Ellingsen Ø, et al. Effect of exercise training on cardiac metabolism in rats with heart failure. *Scand Cardiovasc J.* (2020) 54:84–91. doi: 10.1080/14017431.2019.1658893
14. Crimi E, Ignarro LJ, Cacciatore F, Napoli C. Mechanisms by which exercise training benefits patients with heart failure. *Nat Rev Cardiol.* (2009) 6:292–300. doi: 10.1038/nrcardio.2009.8
15. McDonagh TA, Metra M, Adamo M, Gardner RS, Baumbach A, Böhm M, et al. 2021 ESC Guidelines for the diagnosis and treatment of acute and chronic heart failure. *Eur Heart J.* (2021) 42:3599–726.
16. Campos JC, Queliconi BB, Bozi LHM, Bechara LRG, Dourado PMM, Andres AM, et al. Exercise reestablishes autophagic flux and mitochondrial quality control in heart failure. *Autophagy.* (2017) 13:1304–17. doi: 10.1080/15548627.2017.1325062
17. Malhotra R, Bakken K, D'Elia E, Lewis GD. Cardiopulmonary exercise testing in heart failure. *JACC Heart Fail.* (2016) 4:607–16. doi: 10.1016/j.jchf.2016.03.022
18. Lunde PK, Sjaastad I, Schiøtz Thorud HM, Sejersted OM. Skeletal muscle disorders in heart failure. *Acta Physiol Scand.* (2001) 171:277–94. doi: 10.1046/j.1365-201x.2001.00830.x
19. Kitase Y, Vallejo JA, Gutheil W, Vemula H, Jähn K, Yi J, et al. β-aminoisobutyric acid, l-BAIBA, is a muscle-derived osteocyte survival factor. *Cell Rep.* (2018) 22:1531–44. doi: 10.1016/j.celrep.2018.01.041
20. Jung TW, Park HS, Choi GH, Kim D, Lee T. β-aminoisobutyric acid attenuates LPS-induced inflammation and insulin resistance in adipocytes through AMPK-mediated pathway. *J Biomed Sci.* (2018) 25:27. doi: 10.1186/s12929-018-0431-7
21. Tanianskii DA, Jarzebska N, Birkenfeld AL, O'Sullivan JF, Rodionov RN. Beta-aminoisobutyric acid as a novel regulator of carbohydrate and lipid metabolism. *Nutrients.* (2019) 11:524. doi: 10.3390/nu11030524
22. Shi CX, Zhao MX, Shu XD, Xiong XQ, Wang JJ, Gao XY, et al. β-aminoisobutyric acid attenuates hepatic endoplasmic reticulum stress and glucose/lipid metabolic disturbance in mice with type 2 diabetes. *Sci Rep.* (2016) 6:21924. doi: 10.1038/srep21924
23. Barlow JP, Karstoft K, Vigelsø A, Gram M, Helge JW, Dela F, et al. Beta-aminoisobutyric acid is released by contracting human skeletal muscle and lowers insulin release from INS-1 832/3 cells by mediating mitochondrial energy metabolism. *Metabolism open.* (2020) 7:100053. doi: 10.1016/j.metop.2020.100053
24. Stautemas J, Van Kuilenburg ABP, Stroomer L, Vaz F, Blancquaert L, Lefevere FBD, et al. Acute aerobic exercise leads to increased plasma levels of R- and S-β-aminoisobutyric acid in humans. *Front Physiol.* (2019) 10:1240. doi: 10.3389/fphys.2019.01240
25. Roberts LD, Boström P, O'Sullivan JF, Schinzel RT, Lewis GD, Dejam A, et al. β-Aminoisobutyric acid induces browning of white fat and hepatic β-oxidation and is inversely correlated with cardiometabolic risk factors. *Cell Metab.* (2014) 19:96–108. doi: 10.1016/j.cmet.2013.12.003
26. Wang X, Yang C, Liu X, Yang P. Ghrelin alleviates angiotensin II-induced H9c2 apoptosis: impact of the miR-208 family. *Med Sci Monit Int Med J Exp Clin Res.* (2018) 24:6707–16. doi: 10.12659/MSM.908096

27. Muthuramu I, Lox M, Jacobs F, De Geest B. Permanent ligation of the left anterior descending coronary artery in mice: a model of post-myocardial infarction remodelling and heart failure. *J Vis Exp.* (2014) 94:52206. doi: 10.3791/52206
28. Amaral SL, Zorn TM, Michelini LC. Exercise training normalizes wall-to-lumen ratio of the gracilis muscle arterioles and reduces pressure in spontaneously hypertensive rats. *J Hypertens.* (2000) 18:1563–72. doi: 10.1097/00004872-200018110-00006
29. Paula SM, Couto GK, Fontes MT, Costa SK, Negrão CE, Mill JG, et al. Exercise training restores the myogenic response in skeletal muscle resistance arteries and corrects peripheral edema in rats with heart failure. *Am J Physiol Heart Circ Physiol.* (2019) 317:H87–h96. doi: 10.1152/ajpheart.00042.2019
30. Park BS, Tu TH, Lee H, Jeong DY, Yang S, Lee BJ, et al. Beta-aminoisobutyric acid inhibits hypothalamic inflammation by reversing microglia activation. *Cells.* (2019) 8:1609. doi: 10.3390/cells8121609
31. Gonzalez-Gil AM, Elizondo-Montemayor L. The role of exercise in the interplay between myokines, hepatokines, osteokines, adipokines, and modulation of inflammation for energy substrate redistribution and fat mass loss: a review. *Nutrients.* (2020) 12:1899. doi: 10.3390/nu12061899
32. Shin B, Saeed MY, Esch JJ, Guariento A, Blitzer D, Moskowitzova K, et al. A novel biological strategy for myocardial protection by intracoronary delivery of mitochondria: safety and efficacy. *JACC Basic Transl Sci.* (2019) 4:871–88. doi: 10.1016/j.jacbts.2019.08.007
33. Mousavi SR, Jafari M, Rezaei S, Agha-Alinejad H, Sobhani V. Evaluation of the effects of different intensities of forced running wheel exercise on oxidative stress biomarkers in muscle, liver and serum of untrained rats. *Lab Anim.* (2020) 49:119–25. doi: 10.1038/s41684-020-0503-7
34. Jung TW, Hwang HJ, Hong HC, Yoo HJ, Baik SH, Choi KM, et al. attenuates insulin resistance and inflammation induced by palmitate or a high fat diet via an AMPK-PPARδ-dependent pathway in mice. *Diabetologia.* (2015) 58:2096–105. doi: 10.1007/s00125-015-3663-z
35. Lu F, Li SZ, Gao X, Gong YN, Shi PX, Zhang C. Diagnostic value of circulating miR-208b and miR-499 in peripheral blood of patients with acute myocardial infarction. *J Biol Regul Homeost Agents.* (2020) 34:1071–5. doi: 10.23812/20-171-L-2
36. Zhou C, Cui Q, Su G, Guo X, Liu X, Zhang J. MicroRNA-208b Alleviates post-infarction myocardial fibrosis in a rat model by inhibiting GATA4. *Med Sci Monit.* (2016) 22:1808–16. doi: 10.12659/MSM.896428
37. Qi D, Young LH, AMPK. energy sensor and survival mechanism in the ischemic heart. *Trends Endocrinol Metab.* (2015) 26:422–9. doi: 10.1016/j.tem.2015.05.010
38. Gao K, Zhang J, Gao P, Wang Q, Liu Y, Liu J, et al. Qishen granules exerts cardioprotective effects on rats with heart failure via regulating fatty acid and glucose metabolism. *Chin Med.* (2020) 15:21. doi: 10.1186/s13020-020-0299-9
39. Kerr M, Dodd MS, Heather LC. The 'goldilocks zone' of fatty acid metabolism; to ensure that the relationship with cardiac function is just right. *Clin Sci.* (2017) 131:2079–94. doi: 10.1042/CS20160671
40. Huang Y, Zhang K, Jiang M, Ni J, Chen J, Li L, et al. Regulation of energy metabolism by combination therapy attenuates cardiac metabolic remodeling in heart failure. *Int J Biol Sci.* (2020) 16:3133–48. doi: 10.7150/ijbs.49520
41. Dyck JR, Lopaschuk GD. AMPK alterations in cardiac physiology and pathology: enemy or ally? *J Physiol.* (2006) 574:95–112. doi: 10.1113/jphysiol.2006.109389
42. Wolfgang MJ, Kurama T, Dai Y, Suwa A, Asaumi M, Matsumoto S, et al. The brain-specific carnitine palmitoyltransferase-1c regulates energy homeostasis. *Proc Natl Acad Sci U S A.* (2006) 103:7282–7. doi: 10.1073/pnas.0602205103
43. Zhou B, Tian R. Mitochondrial dysfunction in pathophysiology of heart failure. *J Clin Invest.* (2018) 128:3716–26. doi: 10.1172/JCI120849
44. Tian R, Colucci WS, Arany Z, Bachschmid MM, Ballinger SW, Boudina S, et al. Unlocking the secrets of mitochondria in the cardiovascular system: path to a cure in heart failure—a report from the 2018 national heart, lung, and blood institute workshop. *Circulation.* (2019) 140:1205–16. doi: 10.1161/CIRCULATIONAHA.119.040551
45. Colina-Tenorio L, Horten P, Pfanner N, Rampelt H. Shaping the mitochondrial inner membrane in health and disease. *J Intern Med.* (2020) 287:645–64. doi: 10.1111/joim.13031
46. Alaimo A, Gorojod RM, Beauquis J, Muñoz MJ, Saravia F, Kotler ML. Deregulation of mitochondria-shaping proteins Opa-1 and Drp-1 in manganese-induced apoptosis. *PLoS ONE.* (2014) 9:e91848. doi: 10.1371/journal.pone.0091848
47. Chen L, Gong Q, Stice JP, Knowlton AA. Mitochondrial OPA1, apoptosis, and heart failure. *Cardiovasc Res.* (2009) 84:91–9. doi: 10.1093/cvr/cvp181
48. Fonseca TB, Sánchez-Guerrero Á, Milosevic I, Raimundo N. Mitochondrial fission requires DRP1 but not dynamins. *Nature.* (2019) 570:E34–e42. doi: 10.1038/s41586-019-1296-y
49. Tagaya M, Arasaki K. Regulation of mitochondrial dynamics and autophagy by the mitochondria-associated membrane. *Adv Exp Med Biol.* (2017) 997:33–47. doi: 10.1007/978-981-10-4567-7_3
50. Ikeda Y, Shirakabe A, Maejima Y, Zhai P, Sciarretta S, Toli J, et al. Endogenous Drp1 mediates mitochondrial autophagy and protects the heart against energy stress. *Circ Res.* (2015) 116:264–78. doi: 10.1161/CIRCRESAHA.116.303356
51. Lee CC, Chen WT, Chen SY, Lee TM. Dapagliflozin attenuates arrhythmic vulnerabilities by regulating connexin43 expression via the AMPK pathway in post-infarcted rat hearts. *Biochem Pharmacol.* (2021) 192:114674. doi: 10.1016/j.bcp.2021.114674
52. Wang Y, An H, Liu T, Qin C, Sesaki H, Guo S, et al. Metformin improves mitochondrial respiratory activity through activation of AMPK. *Cell Rep.* (2019) 29:1511–23. doi: 10.1016/j.celrep.2019.09.070
53. Sun W, Lee TS, Zhu M, Gu C, Wang Y, Zhu Y, et al. Statins activate AMP-activated protein kinase in vitro and in vivo. *Circulation.* (2006) 114:2655–62. doi: 10.1161/CIRCULATIONAHA.106.630194
54. Liu Z, Chen JM, Huang H, Kuznicki M, Zheng S, Sun W, et al. The protective effect of trimetazidine on myocardial ischemia/reperfusion injury through activating AMPK and ERK signaling pathway. *Metabolism.* (2016) 65:122–30. doi: 10.1016/j.metabol.2015.10.022
55. Li X, Liu J, Lu Q, Ren D, Sun X, Rousselle T, et al. AMPK: a therapeutic target of heart failure-not only metabolism regulation. *Biosci Rep.* (2019) 39. doi: 10.1042/BSR20181767
56. Kim J, Kundu M, Viollet B, Guan KL, AMPK. and mTOR regulate autophagy through direct phosphorylation of Ulk1. *Nat Cell Biol.* (2011) 13:132–41. doi: 10.1038/ncb2152
57. Gwinn DM, Shackelford DB, Egan DF, Mihaylova MM, Mery A, Vasquez DS, et al. AMPK phosphorylation of raptor mediates a metabolic checkpoint. *Mol Cell.* (2008) 30:214–26. doi: 10.1016/j.molcel.2008.03.003
58. Park HW, Park H, Ro SH, Jang I, Semple IA, Kim DN, et al. Hepatoprotective role of Sestrin2 against chronic ER stress. *Nat Commun.* (2014) 5:4233. doi: 10.1038/ncomms5233
59. Chen X, Li X, Zhang W, He J, Xu B, Lei B, et al. Activation of AMPK inhibits inflammatory response during hypoxia and reoxygenation through modulating JNK-mediated NF-κB pathway. *Metabolism.* (2018) 83:256–70. doi: 10.1016/j.metabol.2018.03.004

Conflict of Interest: The authors declare that the research was conducted in the absence of any commercial or financial relationships that could be construed as a potential conflict of interest.

Publisher's Note: All claims expressed in this article are solely those of the authors and do not necessarily represent those of their affiliated organizations, or those of the publisher, the editors and the reviewers. Any product that may be evaluated in this article, or claim that may be made by its manufacturer, is not guaranteed or endorsed by the publisher.

Copyright © 2022 Yu, Chen, Yu, Liu, Sun and Yang. This is an open-access article distributed under the terms of the Creative Commons Attribution License (CC BY). The use, distribution or reproduction in other forums is permitted, provided the original author(s) and the copyright owner(s) are credited and that the original publication in this journal is cited, in accordance with accepted academic practice. No use, distribution or reproduction is permitted which does not comply with these terms.

frontiers in Cardiovascular Medicine

ORIGINAL RESEARCH
published: 04 March 2022
doi: 10.3389/fcvm.2022.783426

Dioscin Alleviates Cardiac Dysfunction in Acute Myocardial Infarction *via* Rescuing Mitochondrial Malfunction

Tianyu Shen[1†], *Dayin Lyu*[2†], *Mengping Zhang*[3], *Hui Shang*[1*] *and Qiulun Lu*[2*]

[1] Department of Orthopaedic, Taihe Hospital, Hubei University of Medicine, Shiyan, China, [2] Key Laboratory of Cardiovascular and Cerebrovascular Medicine, Collaborative Innovation Center for Cardiovascular Disease Translational Medicine, Nanjing Medical University, Nanjing, China, [3] Department of Hematology, Taihe Hospital, Hubei University of Medicine, Shiyan, China

OPEN ACCESS

Edited by:
Haiyang Tang,
University of Arizona, United States

Reviewed by:
Weiming Wang,
Central South University, China
Jun Zou,
Georgia State University,
United States
Stephen C. Kolwicz Jr.,
Ursinus College, United States

***Correspondence:**
Hui Shang
shanghui6340@163.com
Qiulun Lu
qiulunlu@njmu.edu.cn

[†] These authors have contributed equally to this work

Specialty section:
This article was submitted to Cardiovascular Metabolism, a section of the journal Frontiers in Cardiovascular Medicine

Received: 26 September 2021
Accepted: 01 February 2022
Published: 04 March 2022

Citation:
Shen T, Lyu D, Zhang M, Shang H and Lu Q (2022) Dioscin Alleviates Cardiac Dysfunction in Acute Myocardial Infarction via Rescuing Mitochondrial Malfunction. Front. Cardiovasc. Med. 9:783426. doi: 10.3389/fcvm.2022.783426

Myocardial infarction is one of the most severe heart diseases, leading to sudden death. Currently, angiography and stenting are widely performed in clinics, yet more effective treatment is still needed. Herein, we presented that dioscin, a natural product, showed protective effect on infarcted hearts *via* mitochondrial maintenance. Upon dioscin treatment, cardiac dysfunction was alleviated, and remodeling is prevented. Mechanistically, disocin maintains mitochondria function through the maintenance of Kreb's cycle, and suppresion of ROS accumulation. In this way, by targeting mitochondrial dysfunction, dioscin is a potential drug for infarcted hearts.

Keywords: myocardial infarction, dioscin, mitochondrial dysfunction, ROS, KREB'S cycle

INTRODUCTION

Nowadays, it is widely considered that cardiovascular diseases are one of the major causes for human mortality around the world (1). Particularly, myocardial infarction (MI) affects large population in both developing and developed countries (2). It characterized with dysfunction of energy supply and reactive oxygen species (ROS) generation relates to mitochondrial-based disorder, which leads to pathogenesis of MI and even heart failure (3). Therefore, novel drugs of protecting the heart against myocardial infarction are urgently needed.

Mitochondrial dysfunction is associated with the pathogenesis of myocardial infarction (4). Mitochondrial-derived ROS represent a major source of oxidative stress in cardiomyocytes (5). On the other hand, the primary source of energy generating processes is located at mitochondria among the cell, which is severe sensitive to free radical occurrence in cardiomyocytes (6). Taken together, mitochondria maintenance would moderate heart injury after infarction.

Recently, researches indicated that natural productions from some herbals have potential therapeutic effect for the prevention and treatment of cardiovascular diseases (7). The protective effects are associated with mitochondrial function, including alleviating mitochondrial oxidative stress, de-activation of respiratory chain enzymes, postponing mitochondrial Kreb's cycle, and maintenance of mitochondrial membrane potential ($\Delta\psi$) and ATP content (8–10). Dioscin, a natural steroid saponin isolated from the root bark of wild *dioscorea nipponica*, is reported to treat MI by promoting angiogenesis (11). Additionally, it was reported that dioscin maintains mitochondrial dynamics, which rescues silicosis by reducing mitochondrial-dependent apoptosis (12). However, whether dioscin protects cardiac injury against MI by rescuing mitochondrial dysfunction remains unclear.

Here, our work revealed that dioscin attenuates cardiac dysfunction induced by myocardial infarction. Administration of dioscin benefits infarcted hearts could significantly enhance mitochondrial Kreb's cycle and activities of respiratory chain enzymes, reduce ROS by promoting the antioxidant enzyme activities, and suppress the cardiomyocytes apoptosis by rescuing mitochondrial member potential. Taken together, our results showed that dioscin could alleviate MI *via* attenuate mitochondrial malfunction.

MATERIALS AND METHODS

Animal Model and Chemicals

Mice were male and at age of 8 weeks old. All male C57BL/6 were from Jiangsu Animal Experimental for Medical and Pharmaceutical Research Center. The *in vivo* experiments were approval of Institutional Animal Care and Use Committees at the University of Nanjing Medical University (Number: 1912034) and carried out in accordance with the guidelines. Mice were kept with 12 h light/12 h dark cycle at 23 ± 3°C and 30–70% humidity.

Infarction mouse model was generated through ligature of the left anterior descending (LAD) as described previously with male mice (11). Briefly, mice were anesthetized with 1.5–2% isoflurane, and then a left thoracotomy and pericardiotomy was performed. The left anterior descending was completely occluded by a knot with 7–0 non-absorbable surgical suture. After the ribs and skin were closed with 5–0 silk, the mouse remained under anesthesia until succinylcholine was completely metabolized. For the procedure of sham surgery, mice underwent the same procedure without the ligation of the artery.

Dioscin (80 mg/kg/day, Di'ao group, Chengdu, China) was administrated with mice for 2 weeks beginning on the day of operation. Briefly, the dioscin was first dissolved in dimethyl sulphoxide (DMSO) and then added 5% sodium carboxymethyl cellulose (CMC-Na) to make the volume ratio for 1:19. Consequently, the mice were given the dissolution by intragastric administration for continuous 14 days after myocardial infarction 1 day. The treatment groups were given dioscin solution and the control groups were given same volume of 5% CMC-Na vehicle solution. The preparation and application of the drug's dissolution should be completed in 1 day.

Echocardiography

Transthoracic echocardiographic analysis was performed 2 weeks after the sham or MI surgery as previously described (13). Echocardiography on unconscious mice was used with a Vevo 2100 system (VisualSonics). The echocardiography was blinded to the mice in this study.

Histological Analysis

Hematoxylin and eosin and Masson trichrome staining were performed as described previously (14). The whole hearts were collected and fixed in 4% paraformaldehyde, embedded in paraffin, and then cut into 5-μm serial sections. Image analysis and quantification of fibrosis was performed by a blinded investigator using Image J software.

Mitochondrial Isolation

The purification of cardiac mitochondrial fraction from the heart tissues or cultured primary cardiomyocytes was followed as previously described (15), using Mitochondrial Extraction Kit (Solarbio Life Sciences, SM0020) according to the manufacturer's instructions.

Estimation of Reactive Oxygen Species

Dihydroethidium (DHE) staining (Beyotime, China) was performed as described previously (16). Briefly, heart samples were embedded in OCT compound and transverse sectioned at 5 μm thickness to perform staining and then conserved at −80°C. Next, heart sections were set in room temperature for 10 min and then washing by PBS three times for 5 min. Further, the sections were incubated with the DHE (1:1,000) for 30 min in wet box at 37°C. Finally, after washing by PBS three times for 5 min, co-stain with DAPI. The imagines are photographed by confocal, and we use the same intensity of laser.

Estimation of Mitochondrial Enzymatic and Non-enzymatic Antioxidant

The activity of glutathione peroxidase (GPx), superoxide dismutase (SOD), glutathione-S-transferase (GST), catalase (CAT), glutathione (GSH) was determined in cardiac tissues, using Micro Superoxide Dismutase (SOD) Assay Kit (Solarbio Life Sciences, BC0175, BC0205, BC1195, BC0355, and BC1175) according to the manufacturer's instructions.

TCA Cycle Enzyme Activities and Respiratory Chain Enzymes

Effect of dioscin on MI-induced mitochondrial damage was measured by detection of the activities of mitochondrial enzymes such as malate dehydrogenase (MDH), isocitrate dehydrogenase (ICDH), and succinate dehydrogenase (SDH) using Micro Isocitrate Dehydrogenase Mitochondrial (ICDHm) Assay Kit (Solarbio Life Sciences, BC2165), Micro Succinate Dehydrogenase (SDH) Assay Kit (Solarbio Life Sciences, BC0955) and Micro NADP-Malate Dehydrogenase (NAD-MDH) Assay Kit (Solarbio Life Sciences, BC1055) according to the manufacturer's instructions.

The nicotinamide adenine dinucleotide dehydrogenase (NADH) activity was determined in cardiac tissues as reported (17), using Micro Nicotinamide Adenine Dinucleotide Dehydrogenase (NADH) Assay Kit (Solarbio Life Sciences, BC0635) according to the manufacturer's instructions.

The cytochrome c-oxidase (NCR) activity was determined in cardiac tissues, using Micro NADPH-cytochrome C Reductase Assay Kit (Solarbio Life Sciences, BC2725) according to the manufacturer's instructions.

Cell Culture

H9C2 cells were cultured in DMEM (Servicebio) medium with 10% FBS (Gibco, Life Technologies) and 1% penicillin/streptomycin (Beyotime). Final concentration of 100 μM $CoCl_2$ (Sigma-Aldrich) was added to simulate hypoxia condition. After 24 h of treatment, the extraction of mRNA

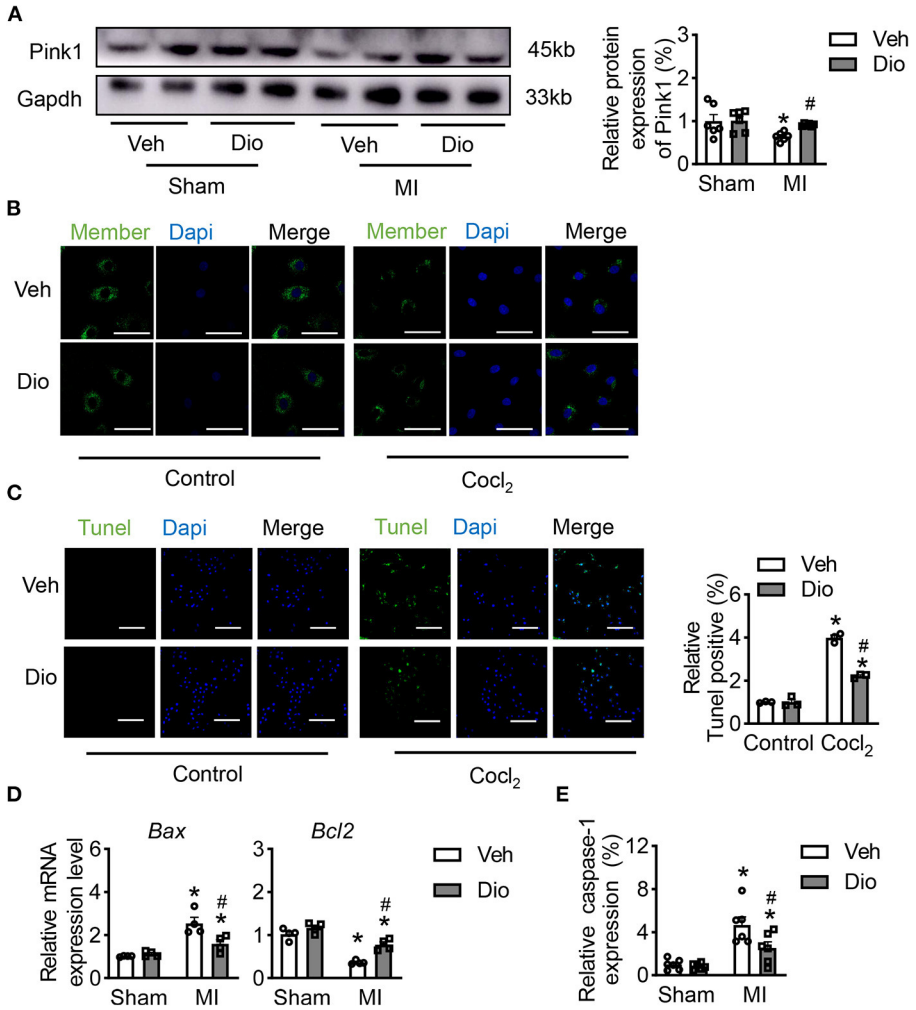

FIGURE 1 | Dioscin alleviates the mitochondrial injury by CoCl2 in H9C2 cells. **(A)** The protein level of Pink1 in heart tissue ($n = 6$). **(B)** Representative images of the active mitochondrial, bar = 20 μm ($n = 3$). **(C)** Representative images of TUNEL staining to detect the anti-apoptosis role of dioscin *in vitro*, bar = 50 μm ($n = 3$). **(D)** The mRNA level of *Bax* and *Bcl2 in vivo* ($n = 4$). **(E)** The measurable of caspase-1 *in vivo* ($n = 6$). Data are mean ± SEM. $^{*}P < 0.05$ vs. sham group, $^{\#}P < 0.05$ vs. MI group.

was performed. And after 48 h, the corresponding staining was performed.

qRT-PCR

Total RNA was extracted using RNeasy Mini Kit (Qiagen). cDNA was generated using HiScript III 1st Strand cDNA Synthesis (Vazyme) and then qPCR was performed using on QuantStudio 5 applied biosystems (Thermo Fisher Scientific) with Hifair III One Step RT-qPCR SYBR Green Kit (Yeasen), all according to the manufacturer's instructions. Actin was regard as control and the data analysis was using 2CT. Obtaining form three independent experiments, and each sample was repeated duplicated in each experiment. Primer sequence are listed below.

For mouse qPCR:

Anp: TTCTTCCTCGTCTTGGCCTTT, GACCTCATCTTC TACCGGCATCT;

Bnp: CACCGCTGGGAGGTCACT, GTGAGGCCTTGGTC CTTCAAGGTCACT;

β-mhc: ATGTGCCGGACCTTGGAA, CCTCGGGTTAGC TGAGAGATCA;

Bax: CCCGAGAGGTCTTTTTCC, GCCTTGAGCACCA GTTTG;

Bcl$_2$: CCTGGCTGTCTCTGAAGACC, CTCACTTGTGGC CCAGGTAT;

Actin: CATCGTCCACCGCAAATG, CACCTTCACCGT TCCAGTT.

Mitochondrial Membrane Potential

Mitochondrial membrane potential was measured by the method of fluorescent probe, using the MitoTracker® Green FM (Yeasen, 40742ES50) according to the manufacturer's instructions.

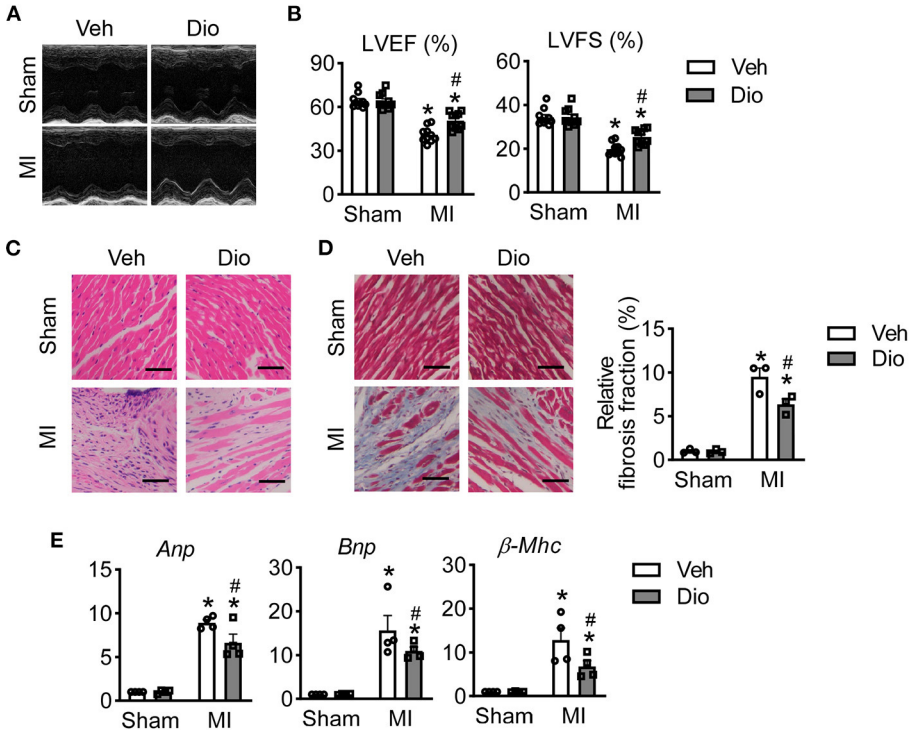

FIGURE 2 | Dioscin protects mice against infarcted injury. **(A)** Representative images of echocardiographic measurement ($n = 10$). **(B)** Echocardiographic parameters for left ventricular ejection fraction (LVEF, %) and left ventricular fractional shortening (LVFS, %) ($n = 10$). **(C)** Representative images of HE staining, bar = 100 μm ($n = 3$). **(D)** Representative images of Masson trichrome stained and its quantification, bar = 100 μm ($n = 3$). **(E)** The mRNA level of heart failure markers for natriuretic peptide A (*Anp*), natriuretic peptide B (*Bnp*) and beta-myosin heavy chain (*β-Mhc*) ($n = 4$). Data are mean ± SEM. $^{*}P < 0.05$ *vs.* sham group, $^{\#}P < 0.05$ *vs.* MI group.

TUNEL Staining

TUNEL staining was performed as previously report (18). The suitable density H9C2 cells were induced to $CoCl_2$ (100 uM, Sigma, 449776) under the condition of treatment with dioscin (5 mg/L) for 48 h, compared to control group. Further, the H9C2 cells were fixed in 4% paraformaldehyde and stained with One Step TUNEL Apoptosis Assay Kit (Beyotime, C1086). TUNEL positive were counted from different images per sample, and the averages were presented.

Estimation of Caspase-1 Activities

The cysteine-requiring aspartate protease 1 (Caspase-1) activity was determined in cardiac tissues, using Caspase-1 Reductase Assay Kit (Hypertime, China) according to the manufacturer's instructions.

Statistical Analysis

Data were presented as mean ± standard error of the mean (SEM) using GraphPad Prism 8. Two-tailed unpaired *t*-test were used to determine the differences between two groups, and two-ANOVA was employed for comparisons of the differences between multiple groups. Statistical significance is indicated by * $p < 0.05$.

RESULTS

Dioscin Alleviates the Mitochondrial Impairment by $CoCl_2$ in H9C2 Cells

Mitochondrial dysfunction is one of the primary causes for cardiac death in response to infarction. Firstly, we performed *in vivo* experiment to assess the mitochondrial injury after dioscin treatment in MI heart tissues. The protein level of Pink1 revealed that dioscin recovered the expression of Pink1 after MI, indicating dioscin has a protective role in mitochondria (**Figure 1A**). Then, the protective effect of dioscin was evaluated on mitochondrial membrane potential. The disturbance of the mitochondrial membrane potential (MMP) caused by $CoCl_2$, and this injury was mitigated by dioscin (**Figure 1B**). Considering the impaired mitochondria could lead to cell death, the dead cells were detected by using TUNEL assay. This showed that dioscin recovered the numbers of H9C2 cells in response to hypoxic condition (**Figure 1C**). Additionally, the mRNA levels of *Bax* and Bcl_2 as apoptotic markers were detected in hypoxic H9C2 cells after dioscin treatment. The results showed that dioscin exerts anti-apoptotic effects and prevents cells from death by downregulating *Bax* expression and increasing Bcl_2 expression (**Figure 1D**). Furthermore, the activities of cysteine-requiring aspartate protease 1 (caspase-1) was repressed in hypoxic cells after dioscin incubation,

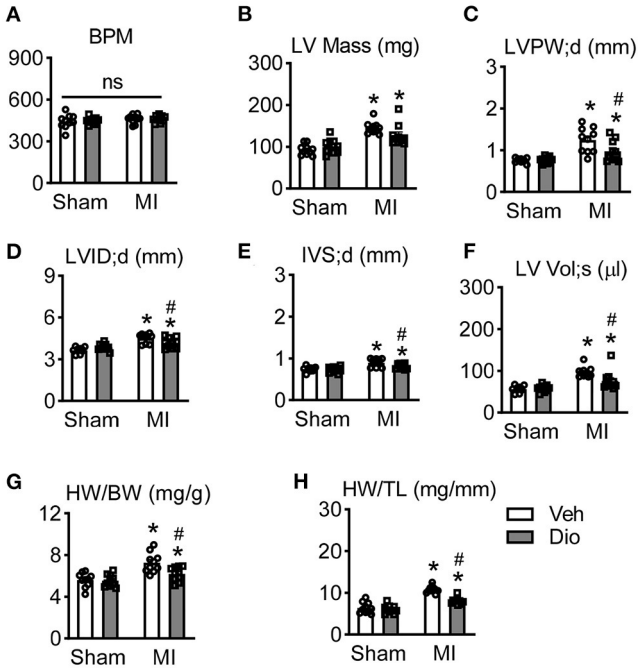

FIGURE 3 | Dioscin prevents cardiac remodeling in response to myocardial infarction. **(A)** The analysis of beat per minute (BPM). Echocardiographic parameters of **(B)** left ventricular mass (LV Mass; mg), **(C)** end-diastolic left ventricular posterior wall (LVPW; d, mm), **(D)** end-diastolic left ventricular inner diameter (LVID; d, mm), **(E)** end-diastolic left ventricular septum (IVS; d, mm), and **(F)** left ventricular end-systolic volume (LV Vol; s, μl). **(G)** The ratio of heart weight to body weight (HW/BW; mg/g). **(H)** The ratio of heart weight to tibia length (HW/TL; mg/mm). $n = 10$ each group. Data are mean ± SEM. $^{*}P < 0.05$ *vs.* sham group, $^{\#}P < 0.05$ *vs.* MI group.

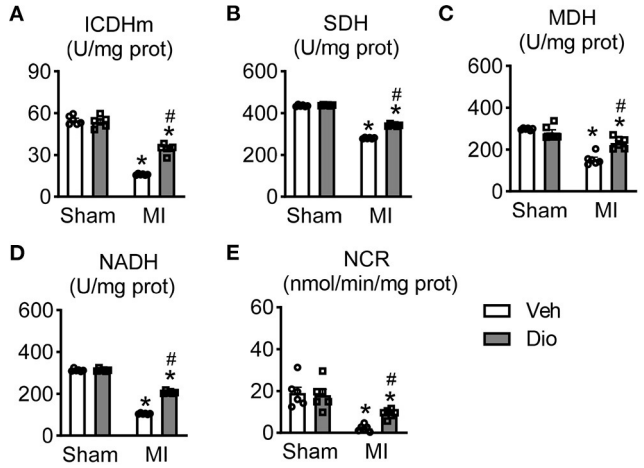

FIGURE 4 | Effect of dioscin on the activities of mitochondrial KREB cycle and respiratory chain enzymes in hearts after MI. The key enzymes of tricarboxylic acid cycle (TCA) of **(A)** isocitrate dehydrogenase (ICDH; U/mg prot), **(B)** succinate dehydrogenase (SDH; U/mg prot), and **(C)** malate dehydrogenase (MDH; U/mg prot). The measureable of respiratory chain enzymes of **(D)** nitotinamide adenine dinucleotide dehydrogenase (the complex I, NADH; U/mg prot) and **(E)** cytochrome c-oxidase (the complex III, NCR; nmol/min/mg prot). $n = 6$. Data are mean ± SEM. $^{*}P < 0.05$ *vs.* sham group, $^{\#}P < 0.05$ *vs.* MI group.

suggesting that dioscin repressed apoptosis caused by hypoxia (**Figure 1E**). These data suggest that dioscin plays protective roles against hypoxia induced mitochondrial injury to mitigate cellular apoptosis.

Dioscin Protects Cardiac Dysfunction Against Myocardial Infarction

To determine the therapeutic role of dioscin *in vivo*, mice were subjected to MI surgery. Two weeks after dioscin administration, the echocardiography was performed to monitor cardiac function. Representative echocardiograph showed that the infarcted mice exhibited left chamber dilation, and dioscin administration alleviated the cardiac deformation (**Figure 2A**). Then, cardiac function analysis showed that the left ventricular ejection fraction (LVEF) and left ventricular fractional shortening (LVFS) were recovered after administration of dioscin in infarcted mice (**Figure 2B**). Additionally, haematoxylin and eosin (HE) staining of heart sections from mice in each group showed that the normal arrangement of cells was destroyed in infarcted heart increased, which could be prevented by dioscin (**Figure 2C**). Representative images exhibited that less collagen deposition after dioscin treatment by the size of blue region compared to MI group, which was decreased about 50% (**Figure 2D**), Suggesting dioscin alleviated cardiac fibrosis in infarcted hearts. Additionally, the expression level of heart failure markers was detected in hearts, including natriuretic peptide A (*Anp*), natriuretic peptide B (*Bnp*) and beta-myosin heavy chain (*β-Mhc*). It showed that the increased levels of *Anp*, *Bnp* and *β-Mhc* mRNA levels in heart tissues from infarcted mice were suppressed by dioscin administration (**Figure 2E**). These results indicate that dioscin administration preserved the cardiac function by alleviating cardiac fibrosis after MI.

Dioscin Prevents Cardiac Remodeling in MI Mouse Model

Considered the recovery of cardiac function occurs in infarcted hearts after disocin administration, cardiac remodeling was measured. There is no significant difference of heart rate among these four groups (**Figure 3A**). It was consistent with previous report that infarction increases left ventricular mass. Such increase was significantly repressed after administration of dioscin (**Figure 3B**). Other cardiac structure parameters, such as left ventricular posterior wall end-diastolic thickness (LVPW; d), left ventricular inner diameter end-diastolic thickness (LVID; d), left ventricular septum (IVS), and left ventricular end-systolic volume (LV Vol; d) were also sufficiently persevered after dioscin administration in infarcted hearts (**Figures 3C–F**). Additionally, mice subjected to MI showed a significant increase in heart weight/body weight (HW/BW) ratio and heart weight/tibia length (HW/TL), which could be ameliorated by dioscin e (**Figures 3G,H**). These results demonstrate that dioscin attenuated MI-induced heart remodeling.

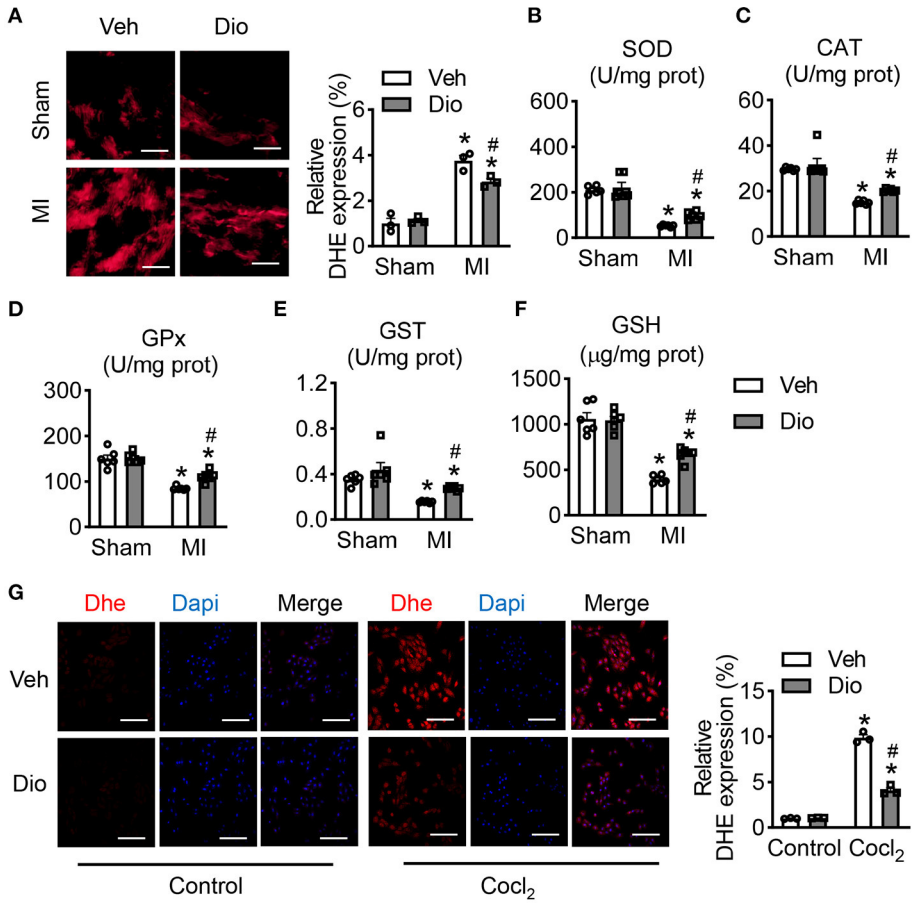

FIGURE 5 | Dioscin modulates mitochondrial antioxidant status. **(A)** Representative images of DHE in heart section and its qualification, bar = 50 μm ($n = 3$). The antioxidant enzymes of **(B)** superoxide dismutase (SOD; U/mg prot), **(C)** catalase (CAT; U/mg prot), **(D)** peroxidase (GPx; U/mg prot), **(E)** glutathione-S-transferase (GST; U/mg prot), and **(F)** glutathione (GSH; U/mg prot) ($n = 6$). **(G)** Representative images of DHE in H9C2 cells and its quantification, bar = 50 μm ($n = 3$). Data are mean ± SEM. $^{*}P < 0.05$ *vs.* sham group, $^{\#}P < 0.05$ *vs.* MI group.

Effect of Dioscin on the Activities of Mitochondrial Kreb's Cycle in Heart After MI

The impaired function of creatine kinase and decreased mitochondrial respiration are often observed in myocardium after pathological injury, including myocardial infarction and hypertrophy (19, 20). In attempt to explore the effect of dioscin in the process of energy metabolism, the activities of mitochondrial enzymes were measured in mice hearts. The activities of isocitrate dehydrogenase (ICDH), succinate dehydrogenase (SDH) and malate dehydrogenase (MDH) in mitochondria were significantly downregulated in the infarcted hearts compared to the sham group (**Figures 4A–C**). The activities of these enzymes were remarkable enhanced by treatment with dioscin in MI group (**Figures 4A–C**). These proved the beneficial role of dioscin on Kreb's cycle enzymes, which are the major source of ATP production in the cells. We further examined the activities of respiratory chain enzyme responsible for the synthesis of ATP. The activities of nicotinamide adenine dinucleotide dehydrogenase (NADH) (the Complex I) and cytochrome c-oxidase (the Complex III) were significantly reduced in the mitochondrial isolated from cardiac tissues obtained from the mice subjected to MI. Conversely, the decline was inhibited by treatment with dioscin (**Figures 4D,E**). Overall, these findings suggest that dioscin promotes the activities of mitochondrial Kreb's cycle in myocardial infarction.

Dioscin Modulates Mitochondrial Antioxidant Status in Heart

In the infarcted hearts, subcellular organelles undergo stress caused by the released of reactive oxygen species (ROS) from mitochondria. Hence, prevention of ROS accumulation in the subcellular compartments are essential for the restoration of the normal cardiomyocyte function. Representative images of dihydroethidium (DHE) staining showed that dioscin attenuated the increase of ROS in response to MI surgery (**Figure 5A**). We further detected the expression of antioxidant enzymes in mitochondria. Consistently, the activities of superoxide

dismutase (SOD), catalase (CAT), glutathione peroxidase (GPx) and glutathione-S-transferase (GST) were declined in the animals subjected to MI, but recovred after dioscin treatment (**Figures 5B–E**). The decrease in the endogenous antioxidant defense enzyme system was corroborated to a diminished glutathione (GSH) content (**Figure 5F**). Similarly, the ROS accumulation was measured in H9C2 cells. Consistent with *in vivo* experiments, dioscin suppressed the enhancement of ROS caused by $CoCl_2$ (**Figure 5G**). These results confirmed that dioscin abrogated the oxidative stress, enhancing the endogenous antioxidant defense system. Taken together, our study demonstrates that dioscin protects heart dysfunction against myocardial infarction by suppressing the oxidative stress.

DISCUSSION

In this study, the activities of antioxidant enzymes were obviously enhanced by treatment of dioscin to further eliminate the production of ROS. Herein, dioscin alleviated cardiac dysfunction in mouse model of MI *via* mitochondrial protection. In detail, dioscin speeds up the Kreb's cycle by up-regulating the activities of enzymes in mitochondrial. Our study further confirmed the therapeutic effect of dioscin in mice infarcted/hypoxic modelshearts and provided the promising administration of dioscin for heart diseases in clinics.

It has been reported that the mitochondrial ROS could be an index of oxidative stress in hearts. Notably, mitochondrial ROS (mtROS) is the main resource of oxidative stress. Previous studies showed dioscin protects against pulmonary injury by inhibition of the mtROS by activating autophagy (12). Dioscin also activates NRF2 and SIRT2 signal pathway to suppress ROS in doxorubicin-induced cardiotoxicity (21). Moreover, dioscin preventing the accumulation of ROS via activating FXR/LKB1 signal in ischemia/reperfusion injury (22). Although dioscin could improve mitochondrial function in pathological condition, whether it is involved in Kreb's cycle of mitochondria remained unclear.

The Kreb's cycle is a series of complex chemical reaction, which is occurred in organisms to generate energy (23). We detected the essential enzyme activities in mitochondrial Kreb's cycle and respiratory chain, which were enhanced after diosicin administration against the infarction/hypoxia injury. The selective accumulation of the citric acid cycle intermediate succinate is a typical metabolic issue after infarction in a range of tissues, responsible for the accumulation of mitochondrial ROS production after reperfusion (23). The i*n vivo* reduction in the activities of Kreb's cycle in infarcted hearts may represent at an early maladaptive phase in the metabolic alterations after MI (24). It has been reported that high-throughput liquid chromatography-mass spectrometry (LC-MS)-based metabolomics demonstrate that dioscin could be associated with gluconeogenesis, Kreb's cycle, and butanoate metabolism (24). Consistently with the previous results, we further confirmed that dioscin is involved with Kreb's cycle. However, the insight underlying mechanism between disocin and Kreb's cycle requires further study.

Many studies showed that dioscin could, prevent infarction/hypoxia-induced apoptosis via down-regulating the *Bax* expression (25). Furthermore, dioscin is presented as a therapeutic nature product to maintain mitochondrial membrane potential (26). Our study suggested that the mitochondrial member potential was protected by dioscin administration in response to infarction/hypoxia, and further suppressed the apoptosis of cardiomyocytes.

In summary, the findings of current study indicate the cardioprotective role of dioscin against cardiac injury by suppressing the production of ROS in mitochondria, enhancing the activities of Kreb's cycle enzymes and respiratory chain complexes, and maintaining the structure and function of mitochondria. Our study could help to better understanding the mechanism underlying the dioscin treatment of infarcted heart diseases.

DATA AVAILABILITY STATEMENT

The original contributions presented in the study are included in the article/supplementary material, further inquiries can be directed to the corresponding authors.

ETHICS STATEMENT

The animal study was reviewed and approved by Institutional Animal Care and Use Committees at the University of Nanjing Medical University (Ethical Approval Number: 1912034).

AUTHOR CONTRIBUTIONS

QL and HS designed the study and revised the manuscript. DL, TS, and MZ carried out the experiments and wrote the manuscript. All authors contributed to the article and approved the submitted version.

FUNDING

This study was supported by the grants from the National Natural Science Foundation of China (81970414 to QL) and the Natural Science Foundation of the Jiangsu Higher Education Institutions of China (19KJA35000 to QL).

REFERENCES

1. Writing Group M, Mozaffarian D, Benjamin EJ, Go AS, Arnett DK, Blaha MJ, et al. Heart disease and stroke statistics-2016 update: a report from the American heart association. *Circulation.* (2016) 133:e38–360. doi: 10.1161/CIR.0000000000000350
2. Othman AI, Elkomy MM, El-Missiry MA, Dardor M. Epigallocatechin-3-gallate prevents cardiac apoptosis by modulating the intrinsic apoptotic

pathway in isoproterenol-induced myocardial infarction. *Eur J Pharmacol.* (2017) 794:27–36. doi: 10.1016/j.ejphar.2016.11.014
3. Anderson S, Bankier AT, Barrell BG, de Bruijn MH, Coulson AR, Drouin J, et al. Sequence and organization of the human mitochondrial genome. *Nature.* (1981) 290:457–65. doi: 10.1038/290457a0
4. Yan K, An T, Zhai M, Huang Y, Wang Q, Wang Y, et al. Mitochondrial miR-762 regulates apoptosis and myocardial infarction by impairing ND2. *Cell Death Dis.* (2019) 10:500. doi: 10.1038/s41419-019-1734-7
5. DeBerardinis RJ, Chandel NS. Fundamentals of cancer metabolism. *Sci Adv.* (2016) 2:e1600200. doi: 10.1126/sciadv.1600200
6. Luczak ED, Wu Y, Granger JM, Joiner MA, Wilson NR, Gupta A, et al. Mitochondrial CaMKII causes adverse metabolic reprogramming and dilated cardiomyopathy. *Nat Commun.* (2020) 11:4416. doi: 10.1038/s41467-020-18165-6
7. Wu L, Li F, Zhao C, Ming Y, Zheng C, Li Y, et al. Effects and mechanisms of traditional Chinese herbal medicine in the treatment of ischemic cardiomyopathy. *Pharmacol Res.* (2020) 151:104488. doi: 10.1016/j.phrs.2019.104488
8. Shanmugam K, Ravindran S, Kurian GA, Rajesh M. Fisetin confers cardioprotection against myocardial ischemia reperfusion injury by suppressing mitochondrial oxidative stress and mitochondrial dysfunction and inhibiting glycogen synthase kinase 3beta activity. *Oxid Med Cell Longev.* (2018) 2018:9173436. doi: 10.1155/2018/9173436
9. Saranya S, Baskaran R, Poornima P, Vijaya Padma V. Berbamine ameliorates isoproterenol-induced myocardial infarction by inhibiting mitochondrial dysfunction and apoptosis in rats. *J Cell Biochem.* (2019) 120:3101–13. doi: 10.1002/jcb.27522
10. Xue W, Wang X, Tang H, Sun F, Zhu H, Huang D, et al. Vitexin attenuates myocardial ischemia/reperfusion injury in rats by regulating mitochondrial dysfunction induced by mitochondrial dynamics imbalance. *Biomed Pharmacother.* (2020) 124:109849. doi: 10.1016/j.biopha.2020.109849
11. Kong C, Lyu D, He C, Li R, Lu Q. Dioscin elevates lncRNA MANTIS in therapeutic angiogenesis for heart diseases. *Aging Cell.* (2021) 20:e13392. doi: 10.1111/acel.13392
12. Du S, Li C, Lu Y, Lei X, Zhang Y, Li S, et al. Dioscin alleviates crystalline silica-induced pulmonary inflammation and fibrosis through promoting alveolar macrophage autophagy. *Theranostics.* (2019) 9:1878–92. doi: 10.7150/thno.29682
13. Du L, Chen J, Wu Y, Xia G, Chen M, Zhao P, et al. Long non-coding RNA N1LR protects against myocardial ischemic/reperfusion injury through regulating the TGF-beta signaling pathway. *Front Cardiovasc Med.* (2021) 8:654969. doi: 10.3389/fcvm.2021.654969
14. Yao Y, Lu Q, Hu Z, Yu Y, Chen Q, Wang QK, et al. non-canonical pathway regulates ER stress signaling and blocks ER stress-induced apoptosis and heart failure. *Nat Commun.* (2017) 8:133. doi: 10.1038/s41467-017-00171-w
15. Xue X, Yang JY, He Y, Wang LR, Liu P, Yu LS, et al. Aggregated single-walled carbon nanotubes attenuate the behavioural and neurochemical effects of methamphetamine in mice. *Nat Nanotechnol.* (2016) 11:613–20. doi: 10.1038/nnano.2016.23
16. Tawarahara K, Kurata C, Okayama K, Watanabe H, Kobayashi A, Yamazaki N. Reversal of perfusion defect on resting thallium-201 emission computed tomography in stunned myocardium and coronary spasm. *Am Heart J.* (1993) 125:1425–7. doi: 10.1016/0002-8703(93)91016-8
17. Yin X, Zhang X, Lv C, Li C, Yu Y, Wang X, et al. Protocatechuic acid ameliorates neurocognitive functions impairment induced by chronic intermittent hypoxia. *Sci Rep.* (2015) 5:14507. doi: 10.1038/srep14507
18. Ding L, Lu S, Zhou Y, Lyu D, Ouyang C, Ma Z, et al. The 3' untranslated region protects the heart from angiotensin II-induced cardiac dysfunction via AGGF1 expression. *Mol Ther.* (2020) 28:1119–32. doi: 10.1016/j.ymthe.2020.02.002
19. Ingwall JS, Kramer MF, Fifer MA, Lorell BH, Shemin R, Grossman W, et al. The creatine kinase system in normal and diseased human myocardium. *N Engl J Med.* (1985) 313:1050–4. doi: 10.1056/NEJM198510243131704
20. Rosca MG, Vazquez EJ, Kerner J, Parland W, Chandler MP, Stanley W, et al. Cardiac mitochondria in heart failure: decrease in respirasomes and oxidative phosphorylation. *Cardiovasc Res.* (2008) 80:30–9. doi: 10.1093/cvr/cvn184
21. Zhao L, Tao X, Qi Y, Xu L, Yin L, Peng J. Protective effect of dioscin against doxorubicin-induced cardiotoxicity via adjusting microRNA-140-5p-mediated myocardial oxidative stress. *Redox Biol.* (2018) 16:189–98. doi: 10.1016/j.redox.2018.02.026
22. Dong L, Yin L, Li R, Xu L, Xu Y, Han X, et al. Dioscin alleviates lung ischemia/reperfusion injury by regulating FXR-mediated oxidative stress, apoptosis, and inflammation. *Eur J Pharmacol.* (2021) 908:174321. doi: 10.1016/j.ejphar.2021.174321
23. Martinez-Reyes I, Chandel NS. Mitochondrial TCA cycle metabolites control physiology and disease. *Nat Commun.* (2020) 11:102. doi: 10.1038/s41467-019-13668-3
24. Wang XX, Yu PC, Li J. High-Throughput metabolomics for identification of metabolic pathways and deciphering the effect mechanism of dioscin on rectal cancer from cell metabolic profiles coupled with chemometrics analysis. *Front Pharmacol.* (2020) 11:68. doi: 10.3389/fphar.2020.00068
25. Si L, Zheng L, Xu L, Yin L, Han X, Qi Y, et al. Dioscin suppresses human laryngeal cancer cells growth via induction of cell-cycle arrest and MAPK-mediated mitochondrial-derived apoptosis and inhibition of tumor invasion. *Eur J Pharmacol.* (2016) 774:105–17. doi: 10.1016/j.ejphar.2016.02.009
26. Qin J, Kang Y, Xu Z, Zang C, Fang B, Liu X. Dioscin prevents the mitochondrial apoptosis and attenuates oxidative stress in cardiac H9c2 cells. *Drug Res.* (2014) 64:47–52. doi: 10.1055/s-0033-1349101

Conflict of Interest: The authors declare that the research was conducted in the absence of any commercial or financial relationships that could be construed as a potential conflict of interest.

Publisher's Note: All claims expressed in this article are solely those of the authors and do not necessarily represent those of their affiliated organizations, or those of the publisher, the editors and the reviewers. Any product that may be evaluated in this article, or claim that may be made by its manufacturer, is not guaranteed or endorsed by the publisher.

Copyright © 2022 Shen, Lyu, Zhang, Shang and Lu. This is an open-access article distributed under the terms of the Creative Commons Attribution License (CC BY). The use, distribution or reproduction in other forums is permitted, provided the original author(s) and the copyright owner(s) are credited and that the original publication in this journal is cited, in accordance with accepted academic practice. No use, distribution or reproduction is permitted which does not comply with these terms.

frontiers in Cardiovascular Medicine

ORIGINAL RESEARCH
published: 23 March 2022
doi: 10.3389/fcvm.2022.789203

Melatonin Engineered Adipose-Derived Biomimetic Nanovesicles Regulate Mitochondrial Functions and Promote Myocardial Repair in Myocardial Infarction

Yang Zhang[1†], Ning Yang[1†], Xu Huang[2], Yan Zhu[1,3], Shan Gao[1], Zhongyang Liu[4], Feng Cao[1] and Yabin Wang[1*]*

[1] Department of Cardiology, The Second Medical Center and National Clinical Research Center for Geriatric Diseases, Chinese People's Liberation Army General Hospital and Medical School of Chinese People's Liberation Army, Beijing, China, [2] Department of Cardiology, Zhongda Hospital, School of Medicine, Southeast University, Nanjing, China, [3] Nankai University School of Medicine, Nankai University, Tianjin, China, [4] Department of Orthopedics, The Fourth Medical Center of Chinese PLA General Hospital, Beijing, China

OPEN ACCESS

Edited by:
Shijun Wang,
Fudan University, China

Reviewed by:
Rita Rezzani,
University of Brescia, Italy
Amanda Jo LeBlanc,
University of Louisville, United States

***Correspondence:**
Yabin Wang
wyb8202@163.com
Feng Cao
fengcao8828@163.com

[†] These authors have contributed equally to this work

Specialty section:
This article was submitted to Cardiovascular Metabolism, a section of the journal Frontiers in Cardiovascular Medicine

Received: 04 October 2021
Accepted: 31 January 2022
Published: 23 March 2022

Citation:
Zhang Y, Yang N, Huang X, Zhu Y, Gao S, Liu Z, Cao F and Wang Y (2022) Melatonin Engineered Adipose-Derived Biomimetic Nanovesicles Regulate Mitochondrial Functions and Promote Myocardial Repair in Myocardial Infarction. Front. Cardiovasc. Med. 9:789203. doi: 10.3389/fcvm.2022.789203

Myocardial infarction (MI), one type of ischemic heart disease, is a major cause of disability and mortality worldwide. Currently, extracellular vesicles (EVs) derived from adipose-derived stem cells (ADSC) have been proven to be a potentially promising therapeutic treatment for MI. However, the inconvenience of isolation, the low productivity, and the high cost of EVs greatly limits their application in clinic. In this study, we constructed novel biomimetic ADSC-derived nanovesicles (ADSC NVs) to achieve cell-free therapy for MI. Here, we firstly developed a novel Mel@NVs delivery system consisting of engineered ADSC NVs with melatonin (Mel). Then, the characterization and properties of Mel@NVs were performed. The effect of Mel@NVs on cellular oxidative stress and myocardial infarction repair was conducted. The results showed that Mel@NVs treatment under ischemia mimic condition reduced cell apoptosis from 42.59 ± 2.69% to 13.88 ± 1.77%. Moreover, this novel engineered Mel@NVs could ameliorate excessive ROS generation, promote microvessel formation, and attenuate cardiac fibrosis, which further alleviates mitochondrial dysfunction and finally enhance myocardial repair. Hence, the engineered NVs show a potential strategy for MI therapy.

Keywords: myocardial infarction, melatonin, biomimetic nanovesicles, mitochondrial function, reactive oxygen species

INTRODUCTION

Myocardial infarction (MI), one type of ischemic heart disease (IHD), is the leading cause of disability and mortality worldwide (1). Myocardial injury is the most important factor which results in MI. Evidence has demonstrated that oxidative stress is an important pathophysiological mechanism of myocardial injury, and the production of excessive reactive oxygen species (ROS) can impair cell function and vitality (2, 3). Therefore, improving the survival rate of cardiomyocytes and inhibiting the production and accumulation of reactive oxygen species may be essential to improve the prognosis of ischemic diseases. Recent studies have shown that the application of antioxidant

drugs could attenuate oxidative stress efficiently. Researchers have revealed that melatonin can resist oxidative stress damage in a variety of ways, including direct detoxification and indirect enzymatic hydrolysis of reactive oxygen species (4–7). In fact, melatonin is an indole heterocyclic compound secreted by the pineal gland (8, 9). For its antioxidative purpose to use in diseases, melatonin was also known as the antioxidant drug because of its efficacy on myocardial injury, which has been verified by several studies (10, 11). However, the half-life of the drug in the body is relatively low, which affects the actual therapeutic effect and causes side effects. Therefore, various nano-delivery carriers have been developed to carry drugs and deliver them to the injured site (12, 13). Unfortunately, the application of nanocarriers for drug delivery is limited due to their immunogenicity and toxicity, low loading capacity, and biodistribution problems (14, 15).

Recently, considerable progress has been concentrated on EVs. EVs are natural microvesicles secreted by many cell types with excellent biocompatibility, low cytotoxicity, immune inertness, and long-term circulation capabilities (16, 17). Due to their nano-scale size and excellent biocompatibility, EVs have been considered as natural carriers used in drug delivery applications (18, 19). Compared with commonly used synthetic carriers, the high biocompatibility of EVs makes them an ideal choice for drug delivery without causing adverse pro-inflammatory and immune responses. In addition to its unique characteristics, EVs are also enriched with specific components such as proteins, mRNAs, and miRNAs from parent cells, thereby playing critical roles in various physiological and pathological processes to transplant the natural biological functions of original cells, for example, cell proliferation, differentiation, and virus spreading, which can be directly used to treat many diseases (20, 21). Moreover, EVs derived from mesenchymal stem cells (MSC), such as bone marrow mesenchymal stem cells (BMMSC) and ADSC, have the capacity to enhance heart function after MI because EVs are rich in miRNAs (22, 23). MSCs derived EVs' miR-143-3p could reduce cardiomyocyte apoptosis by inhibiting chk2-beclin2 pathway to regulate autophagy (24). Meanwhile, ADSC-derived EVs overexpressing in microRNAs were studied to observe whether they have a better protective effect on MI, including miR-126 and miR-146a (25, 26). Therefore, EVs derived from adipose-derived mesenchymal stem cells not only have their own therapeutic effects but also have the advantages of rich sources and convenient access (27). However, the current extraction and purification of EVs and production efficiency have certain limitations, which hinder the possibility of EVs being used in clinical treatment. Recently, EVs mimicking nanovesicles (NVs), which have similar size and composition to EVs, have been harvested by continuously extruding cells through a microfilter (28, 29). EVs obtained by extruding the cells can not only retain the biological factors of the stem cells themselves but also greatly increase the productivity of the vesicles.

In this study, we constructed novel biomimetic ADSC-derived nanovesicles (ADSC NVs) to achieve cell-free therapy for MI. Here, we firstly developed a novel system consisting of engineered ADSC NVs with melatonin (Mel). NVs with controllable dimensions and high yield were harvested by continuously extruding ADSCs through filters with different pore sizes. Then the melatonin was loaded into the NVs by sonication to fabricate melatonin engineered NVs (Mel@NVs). Next, Mel@NVs was conducted to test its cardiac protective effect on cells and MI mice model both *in vitro* and *in vivo*, respectively. The ROS levels, apoptotic rate, histological morphologies, cardiac functions, and neovascularization were analyzed in this study.

MATERIALS AND METHODS

Animals

C57BL/6j male mice (Adult, $n = 40$, 8 weeks old, 22–25 g, specific-pathogen-free) were obtained from SPF Biotechnology Co., Ltd. (Beijing, China). All operations were conducted under the Guidance of National Institutes of Health for the Care and Use of Laboratory Animals and acclaimed by the Ethics Committee of the Chinese People's Liberation Army General Hospital.

Animals Grouping and Myocardial Infarction Model

The total animals were randomly divided into four groups ($n = 10$ each): (i) Sham surgery group (Sham group); (ii) MI + PBS group (MI group); (iii) MI + NVs group (NVs group); (iv) MI+Mel@NVs (Mel@NVs group). The ligation of the left anterior descending (LAD) artery was performed to establish the myocardial infarction (MI) model. Finally, mice were anesthetized by inhalation of isoflurane and received mechanical ventilation. LAD artery was received permanent ligation with a 6-0 silk suture after left thoracotomy. When the left ventricle (LV) had pale discoloration and an elevation of the ST segment on electrocardiographic (ECG) was recorded, it is confirmed that the vessel was successfully occluded. Mice in the sham-operated group were only performed thoracotomy without ligation. Then, NVs and Mel@NVs in 20 μl PBS were injected intramyocardially at three various portions in the area of the infarcted myocardium with a 30-gauge needle. MI group animals were injected with the same volume of PBS for control.

Cell Culture

Adipose-derived stem cells (ADSC) were obtained by the Department of Orthopedics, Peking University People's Hospital (acquired from Cellular Biomedicine Group). ADSCs were cultured in Growth Medium for Human ADSCs (Cyagen Biosciences, Suzhou, China). The H9C2 cell line was obtained from Procell Life Science & Technology (Wuhan, China). This type of cell was cultured in Dulbecco's Modified Eagle's Medium (DMEM, Hyclone, Logan, Utah, USA) added with 10% fetal bovine serum (FBS, Gibco, USA) and 1% antibiotic (Invitrogen, CA). All assays were expressed in a humidified environment full with 5% CO_2 at 37°C.

Establishment of H/SD Cell Models *in vitro*

The hypoxia/serum deprivation (H/SD) cell model was established by hypoxia/serum deprivation. In short, H9C2 cells were cultured in Hanks buffer for 24 h and cultured in a 37°C hypoxic environment (1% O_2, 5% CO_2, and 94% N_2). The

control cells group were normally cultured in 95% air and 5% CO_2 for an equal time.

Characterization of ADSCs

The surface specific markers of ADSC were analyzed by flow cytometry (FACS-Calibur, BD Biosciences, California, USA). The adipogenic, osteogenic, and chondrogenesis differentiation of ADSCs were conducted for confirming ADSCs' multi-cell differentiation ability. The morphologic images of cells were obtained using an optical microscope (Olympus Corporation, Tokyo, Japan).

Preparation of NVs

ADSCs were washed three times with cold PBS and harvested by cell scrapers and then suspended in PBS with a concentration of at least 1×10^6 cells/ml. The cell suspensions were sequentially extruded through 1 μm, 400 nm, and 200 nm polycarbonate membrane (Whatman Inc, USA) using a mini-extruder (Avanti Polar Lipids) five to six times. Here, we defined the extruded vesicles as nanovesicles (NVs). The harvested NVs were diluted in PBS and stored at −80°C.

Characterization of NVs

The zeta-potential, size distribution and concentration of NVs were measured using ZetaView (Particle Metrix, Germany). The morphologic images of NVs were observed via transmission electron microscopy (TEM, JEM-2000EX, Japan). The number of proteins in the NVs was analyzed using total proteins using the BCA Protein Assay Kit (Solarbio, China). The number of specific EV proteins included were observed by western blot.

Melatonin Loading Into NVs

Melatonin was loaded into the NVs (1 mL) and the fluid solution was conducted under ultrasonic treatment (30) (20% amplitude, 7 cycles, 15 s on/off, 180 s duration, 120 s cooling period between each cycle). After sonication, the mixture was then cultured at 37°C for 240 min to allow for recovery of the nanovesicle membrane to form Mel@NVs. Mel@NVs were obtained by ultrafiltration and excessive free melatonin was removed from the supernatant. The loading efficiency of melatonin encapsulated into nanovesicles was measured via high-performance liquid chromatography (HPLC, LC-20AD, Shimadzu, Japan).

Cellular Uptake of Mel@NVs

For observing nanovesicles tracing in H9C2 cells, nanovesicles were labeled with PKH26 (Sigma Aldrich, USA) by dying with the staining applied according to the manufacturer'sinstructions. H9C2 cells incubated in a confocal cell dish were cultured with PKH26-dyed nanovesicles for 4 h and washed with PBS. Then, cells were treated with 4% paraformaldehyde for 10 min and rinsed with PBS. After rinsing, 0.5% triton X-100 was used to permeabilize cells for 300 s, and then PBS was used to wash cells. Cells were subsequently stained with FITC-phalloidin (Solarbio, China) for 30 min and rinsed with PBS. Finally, cells nuclei were labeled with DAPI (Beyotime, China). Cellular uptake of the nanovesicles was obtained by using a confocal microscope (Nikon, Japan).

Detection of Cellular and Mitochondrial ROS

The quantity of cellular ROS production was detected by dihydroethidium (DHE, Beyotime, China) staining in line with the manufacturer's instructions. In brief, cells were cultured with 1 mM DHE probe for 30 min in darkness at 37°C, and then rinsed with PBS three times and subsequently observed. The quantity of mitochondrial ROS production was determined by mitochondrial superoxide indicator (MitoSOX, Invitrogen) corresponding to the instructions. In short, cells were rinsed twice with PBS and loaded with the probes (4 μM) for 10 min in the dark atmosphere at 37°C. Then cells were rinsed twice and stained with DAPI. The images were then captured by a confocal microscope (Nikon, Japan). The fluorescence of DHE or mitoSOX was analyzed according to previous studies (21, 31, 32). In general, these obtained fluorescence images were run and calculated via Image J software.

Cytokines Measurement

Cell supernatant was collected in cold conditions. Enzyme-linked immunosorbent assay (ELISA) was performed in accordance with the manufacturer's instructions to measure the level of anti-inflammatory cytokines (TGF-β and IL-10) and pro-inflammatory cytokines (IL-6 and TNF-α) (Xi-Tang, Shanghai, China).

Western Blot

Cells were rinsed with pre-cooling PBS three times and scraped and then lysed with RIPA (Solarbio, China) containing 1 mM phenylmethylsulfonyl fluoride (PMSF, Beyotime) on ice for 10 min. After centrifugation at 12,000 rpm for 10 min at 4°C, the supernatant was obtained and the quantity of protein was analyzed by BCA Protein Assay Kit (Solarbio, China). The protein extract was separated by 12% SDS-PAGE at 150 V for 60 min then transferred to the PVDF membrane under 200 mA current for 60 min. Under blocking, the membrane was cultured with the primary antibody for 8 h at 4°C, washed with TBST, and treated with a suitable secondary antibody for 60 min at room temperature and rinsed with TBST. The immunoblotting was observed using an ECL substrate kit (Millipore, Germany). The using antibodies included Bax antibody (1:1,000, Cell Signaling Technology (CST), USA), Bcl-2 antibody (1:1,000, CST, USA), and β-actin antibody (1:5,000, Proteintech, USA).

Flow Cytometry Assay

Cells were harvested and blown for 5 min to obtain a single-cell suspension, washed with cold PBS three times. Then, cells were cultured with Annexin V-FITC/binding buffer solution for 30 min in the dark atmosphere. Finally, the mixture was incubated with PI buffer for 10 min in line with the manufacturer's instructions (BD Biosciences, USA). The apoptosis and necrosis rate of cells were analyzed by flow cytometry.

Echocardiogram Detection

All mice were examined by echocardiography 4 weeks after the operation. After the mice were inhalation-anesthetized, heart

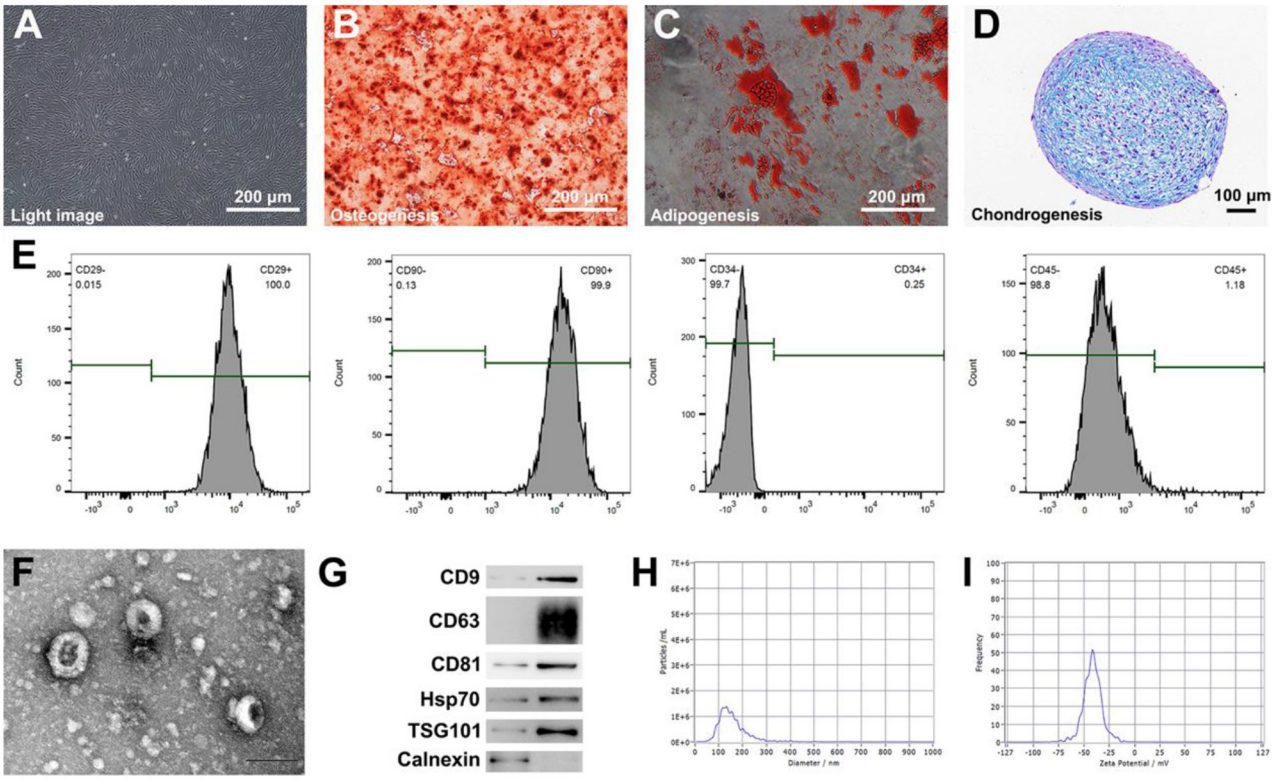

FIGURE 1 | Characterization of ADSCs and ADSC-derived biomimetic nanovesicles. **(A)** The morphology of ADSCs by using a microscope. Scale bar = 200 μm. **(B–D)** Osteogenic, adipogenic, and chondrogenic differentiation of ADSCs. Scale bar = 200 μm. **(E)** Analysis of flow cytometry indicating surface markers of ADSCs. **(F)** The characteristic image of ADSC-derived biomimetic nanovesicles under TEM. Scale bar = 100 nm. **(G)** Western blot analysis of nanovesicles' positive markers including CD9, CD63, CD81, Hsp70, and TSG101. Calnexin was used as the negative control. **(H,I)** Size distribution and zeta potential of nanovesicles.

function was measured by echocardiography. M-mode images and left ventricular ejection fraction (LVEF) were measured. All operations and analyses were performed by an experienced researcher who was unaware of the experimental group.

Heart Tissue Immunofluorescence Staining

The left ventricle including the MI area was embedded in paraffin. Hematoxylin-Eosin (H&E) staining and Masson staining were performed separately. An optical microscope (Olympus, Japan) was used to analyze the morphological changes of the nucleus and cytoplasm around the MI marginal zone in H&E staining. Masson staining observed collagen scar tissue and myocardial fibrosis at 4 weeks postoperatively. Immunofluorescence staining with anti-CD31 antibody (Abcam, USA) was used to examine the formation of new blood vessels in the sections. The density of microvessels was analyzed as the number of vessels per field under microscope according to Lin's previous study (11).

Statistical Analysis

All experimental data were expressed as mean ± SEM. Student's *t*-test was used for comparison between two groups, and one-way ANOVA was performed for multiple comparisons among more than two groups. These data were analyzed and processed by GraphPad Prism 9.0 (GraphPad Software, San Diego, California). When the *P*-value was < 0.05, the differences were considered statistically significant.

RESULTS

Characterization of ADSCs and ADSC-Derived NVs

The morphology of ADSCs was observed using an optical microscope (**Figure 1A**). The multipotential differentiation properties of ADSCs were confirmed through osteogenesis, adipogenesis, and chondrogenesis experiments in response to appropriate inducement (**Figures 1B–D**). To gain further understanding of ADSCs, the immunophenotype of the ADSCs was detected by flow cytometry. The positive markers were CD90 and CD29, meanwhile, the negative markers were CD34 and CD45 (**Figure 1E**); these features confirmed that the cells were ADSCs. Next, we prepared NVs by continuously extruding ADSCs. The morphological image of nanovesicles derived from ADSCs was then observed by TEM, and the obtained nano-vesicles showed a morphology similar to typical exosomes (**Figure 1F**). Western blot analysis demonstrated that NVs expressed exosome-specific markers, namely TSG101, CD9, CD63, CD81, and Hsp70. In contrast, calnexin was not observed

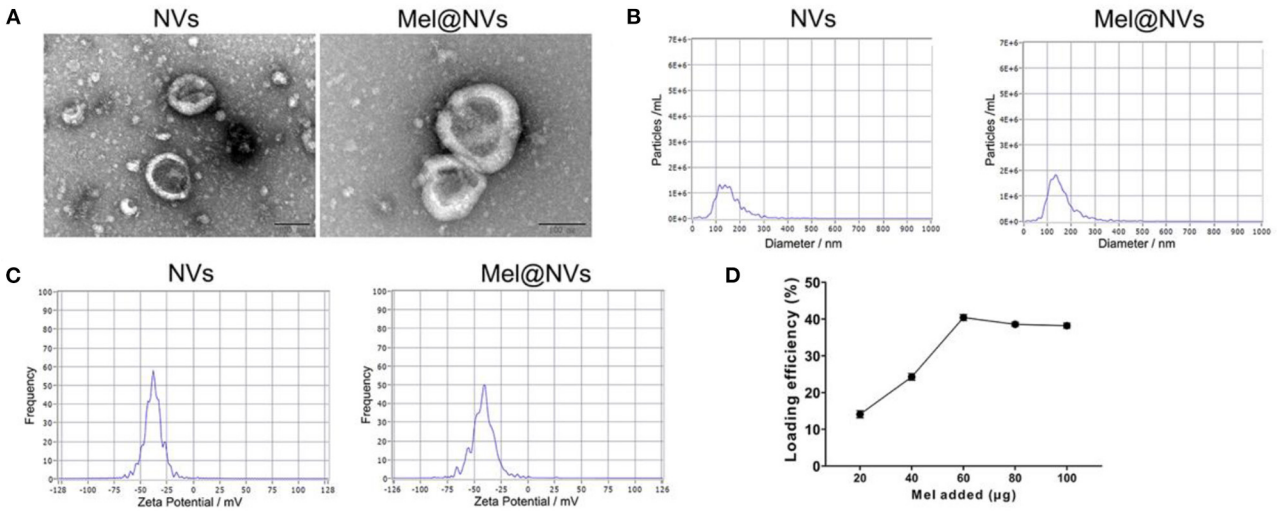

FIGURE 2 | Preparation and characterization of Mel@NVs. **(A)** The characteristic images of NVs and Mel@NVs via TEM. Scale bar = 100 nm. **(B,C)** Size distribution and zeta potential of Mel@NVs. **(D)** HPLC analysis of loading efficiency. A different amount of melatonin was added into NVs (10 μg). The loading was sonicated when 40 μg melatonin was added. The results represented the mean ± standard deviation ($n = 3$).

in isolated exosomes (**Figure 1G**). Moreover, the average size of NVs was 141.7 ± 59.2 nm (**Figure 1H**), and the value of zeta potential in NVs was −41.1 mV (**Figure 1I**).

Preparation and Characterization of Mel@NVs

Next, we loaded melatonin into NVs by sonication. **Figure 2A** showed that the morphology of Mel@NVs was similar to that of NVs, with a characteristic cup-shaped structure. The average size of Mel@NVs was 142.9 ± 60.4 nm, which was compared to that of NVs (144.6 ± 59.3 nm) (**Figure 2B**). Meanwhile, the values of zeta potential (**Figure 2C**) in Mel@NVs and NVs were −41.5 and −37.9 mV, respectively. Moreover, high-performance liquid chromatography (HPLC) analysis showed that the melatonin was loaded successfully, and the loading capacity of Mel was 40.42% (**Figure 2D**). These results indicated that there were no big changes in the surface properties of Mel@NVs after loading melatonin into NVs.

Cellular Uptake and Cardio-Protective Effects of Mel@NVs in H9C2 Cells

In order to observe the uptake of NVs at a cellular level, we labeled NVs and Mel@NVs with red-fluorescent protein PKH26, and labeled the cell cytoskeleton with phalloidin (green color). H9C2 cells were observed under fluorescence microscopy after being incubated PKH26-stained NVs and Mel@NVs (**Figure 3A**). The fluorescence images showed that PKH26-labeled NVs and Mel@NVs were taken up by H9C2 cells and scattered around the nucleus. Even after 24 h of hypoxia treatment, Mel@NVs can still be taken up by cardiomyocytes. Flow cytometry analysis quantitatively detected the rates of apoptosis and necrosis in the four groups. The apoptotic and necrotic rate of cardiomyocytes was significantly reduced in the Mel@NVs treatment group (13.88 ± 1.77%) compared to that in H/SD treatment group (42.59 ± 2.69%) and NVs treatment group (27.56 ± 3.04%). In order to analyze mitochondrial apoptotic effect, western blotting was performed to detect mitochondrial apoptosis-related proteins, such as Bax and Bcl-2. The western blot results demonstrated that Mel@NVs significantly down-regulated pro-apoptotic protein (Bax) and up-regulated anti-apoptotic protein (Bcl-2). Furthermore, the levels of anti-inflammatory factors (such as TGF-β and IL-10) and pro-inflammatory factors (such as IL-6 and TNF-α) were analyzed by ELISA assays. As shown in **Figure 3**, compared with the H/SD group, NVs and Mel@NVs groups both showed higher levels of anti-inflammatory cytokines, but the lower level of pro-inflammatory cytokines, indicating the effective anti-inflammatory properties of Mel@NVs on cardiomyocytes under ischemia mimic condition *in vitro*. These experiments showed that Mel@NVs have a better cytoprotective effect than NVs ascribed to the introduction of melatonin into NVs.

The ROS Scavenge and Mitochondrial Functional Protection of Mel@NVs *in vitro*

To observe whether Mel@NVs play a cardio-protective effect on scavenging ROS, DHE staining was used to detect ROS levels. **Figures 4A–E** showed that the red fluorescence intensity, which represents the level of ROS, was the lowest in the control group, and the highest in H/SD treatment group. The fluorescence intensity in the NVs treatment group was lower than that in H/SD group. Interestingly, Mel@NVs treatment group showed a significantly reduced intensity than NVs addition. Moreover, mitoSOX, a mitochondrial ROS detection probe, was used to observe the production of ROS in mitochondria in different treatment groups. **Figures 4F–J** showed that under H/SD exposure, the level of mitoSOX was the highest compared

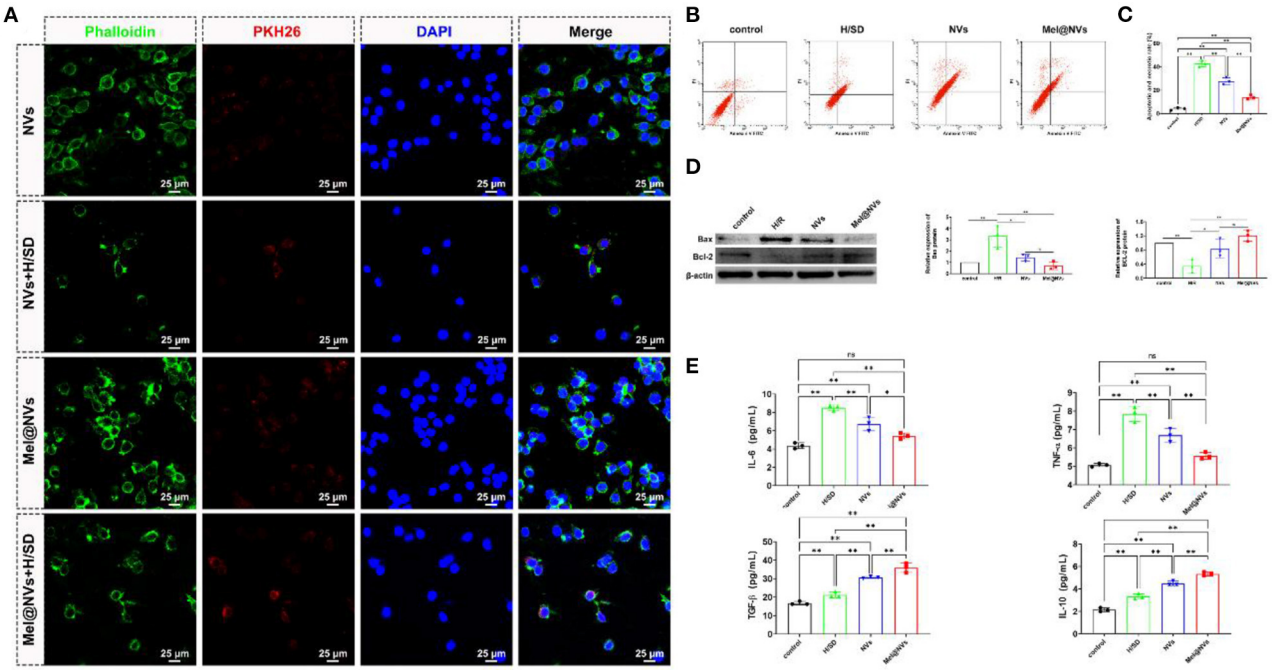

FIGURE 3 | Cellular uptake and cardioprotective effects of Mel@NVs in H9C2 cells. **(A)** Representative images of NVs and Mel@NVs taken up by H9C2 cells in control and H/SD conditions. **(B)** The apoptotic rate of annexin-V/PI staining in different conditions by using flow cytometric detection. **(C)** The analysis of the quantity of apoptotic and necrotic cells by flow cytometry (**$p < 0.01$). **(D)** Detection of apoptosis-related proteins using Western blotting test. **(E)** The amount of anti-inflammatory and pro-inflammatory cytokines using ELISA in H9C2 cells with different treatments (*$p < 0.05$; **$p < 0.01$; ns, not significant. $n = 3$).

to other groups. After the introduction of Mel@NVs, the intensity of ROS was lower than that in the NVs treatment group. All the above data showed that Mel@NVs could reduce cellular and mitochondrial oxidative stress effects, which might be a novel cardioprotective drug platform for MI.

Therapeutic Effects of Mel@NVs in MI Model

In order to evaluate the potential cardioprotective effects of Mel@NVs *in vivo*, NVs and Mel@NVs were micro-injected directly into the myocardium of MI mice model. To confirm whether Mel@NVs inhibited cell apoptosis *in vivo*, TUNEL staining was used. As shown in **Figure 5A**, compared with the MI group, TUNEL-positive cells were significantly reduced in the heart sections of Mel@NVs injected-mice (**Figure 5B**). After 4 weeks, the cardiac function after myocardial infarction was measured by M-mode echocardiography (**Figure 5C**), and EF% and FS% were evaluated (**Figures 5D,E**). Compared with the MI group, the levels of EF% and FS% of mice injected with Mel@NVs increased significantly after MI. In addition, the reduction in myocardial remodeling and fibrosis assessed by H&E staining and Masson staining were observed among groups (**Figures 6A,B**), demonstrating that Mel@NVs treatment could reduce cardiomyocyte fibrosis. In addition, angiogenesis is an important factor that indicates the repair of ischemic myocardium. Therefore, we performed CD31-stained assay to observe the neovascularization. Compared with MI mice, Mel@NVs treatment significantly increased the expression level of CD31 (**Figures 6C,D**). According to the above experiments, Mel@NVs showed effective cardioprotection in infarcted hearts by reversing functional decompensation and pathological remodeling.

DISCUSSION

In this study, we first obtained nanovesicles derived from ADSC by continuous extrusion method, and then successfully constructed melatonin engineering biomimetic nanovesicles after sonication. Both *in vitro* and *in vivo* experiments have illustrated that Mel@NVs could reduce oxidative stress and improve myocardial injury repair effect.

Previous studies have shown that the obstructed vessels were unable to supply blood to the heart and then caused MI, leading to massive death of myocardial cells, followed by inflammation and oxidative stress (33, 34). The infarcted microenvironment full of inflammation and oxidative stress were the main reasons for the low survival rate of cardiomyocytes. The abnormal mitochondrial metabolism caused by excessive reactive oxygen species (ROS) severely affects the health of mitochondria in cardiometabolic diseases such as MI (35). Therefore, inhibiting oxidative stress has been proven to reduce cardiomyocyte apoptosis and alleviate cardiac dysfunction (36).

Melatonin has been reported to reduce cell injury in oxidative stress environments by neutralizing free produced

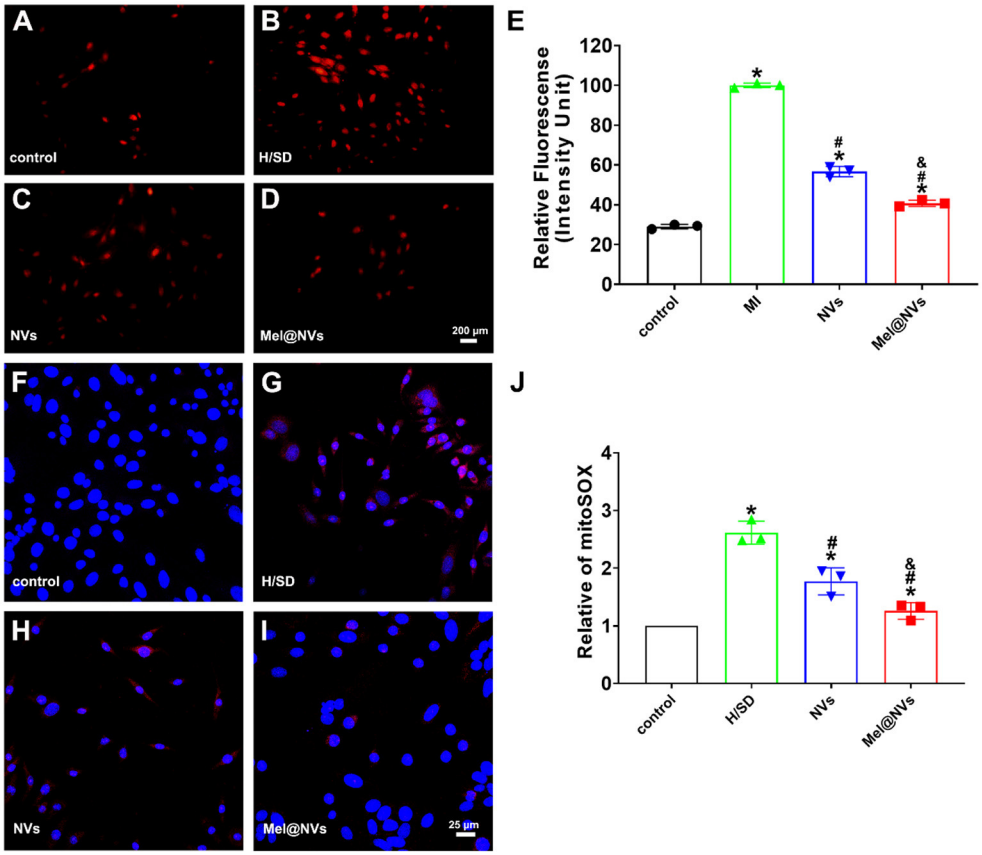

FIGURE 4 | The effect of Mel@NVs on reactive oxygen species levels in H/SD condition. **(A–D)** The ROS levels in cells by using DHE probe and the images were obtained using fluorescence microscopy. Scale bar = 200 μm. **(E)** The quantification of the DHE fluorescence intensity is shown in a bar graph (*$p < 0.05$ v.s. control; #$p < 0.05$ v.s. H/SD treatment; &$p < 0.05$ v.s. NVs treatment). **(F–I)** The oxygen species levels in mitochondria were observed by using a Mito-SOX probe and the images were obtained using confocal laser scanning microscopy. Scale bar = 25 μm. **(J)** The quantification of Mito-SOX fluorescence intensity is detected in different assays (*$p < 0.05$ v.s. control; #$p < 0.05$ v.s. H/SD treatment; &$p < 0.05$ v.s. NVs treatment). The results represented the mean ± standard deviation ($n = 3$).

radicals (37). This drug is anti-apoptotic, anti-inflammatory, and is widely used in many diseases, including ischemic heart disease (38). Previous literature has shown that melatonin can reduce the production and accumulation of ROS, maintain the structural integrity of mitochondria to protect mitochondria from ischemic damage (39). Moreover, melatonin can play a cardioprotective effect with its antioxidant activity and ability to inhibit neutrophils in myocardial tissue (40). However, its application in the treatment of MI has been limited because of the low half-life in the body. In our study, we used a simple but effective strategy to encapsulate melatonin into biomimetic stem cell-derived nanovesicles to fabricate a novel engineered Mel@NVs delivery system.

In recent years, extracellular vesicles (EVs) from various types of cells have been obtained and further applied in many diseases. EVs are natural membrane vesicles that participate in cell-to-cell communication (41). In addition to being loaded with complex cargo from parental cells, including proteins, mRNAs, microRNAs (miRNAs), and additional macromolecules, EVs have become attractive candidates for drug delivery applications for transferring their contents to recipient cells through endogenous uptake (42, 43). However, the current common method for extraction and purification of EVs is complicated and time-consuming, which limits their application in clinic. In this study, a serial-filters extrusion approach was conducted and NVs were obtained which possessed the morphologies and characteristic biomarkers of EVs, in line with previous studies. Next, Mel@NVs were designed by using a method of loading melatonin into nanovesicles via ultrasonic treatment. The results showed that Mel@NVs were successfully fabricated and the productivity of drug-loaded vesicles was higher.

In order to detect the effect of Mel@NVs on ROS, we used a hypoxia and serum deprivation (H/SD) environment, which could represent an oxidative stress condition. Mel@NVs could reverse the apoptotic rate after H/SD treatment, reduce pro-inflammatory factors, and promote anti-inflammatory cytokines, indicating that this novel Mel@NVs system could establish a protective milieu for cardiomyocytes under ischemia mimic condition *in vitro*. In addition, the DHE staining and mitoSOX experiments were performed and the results showed that the

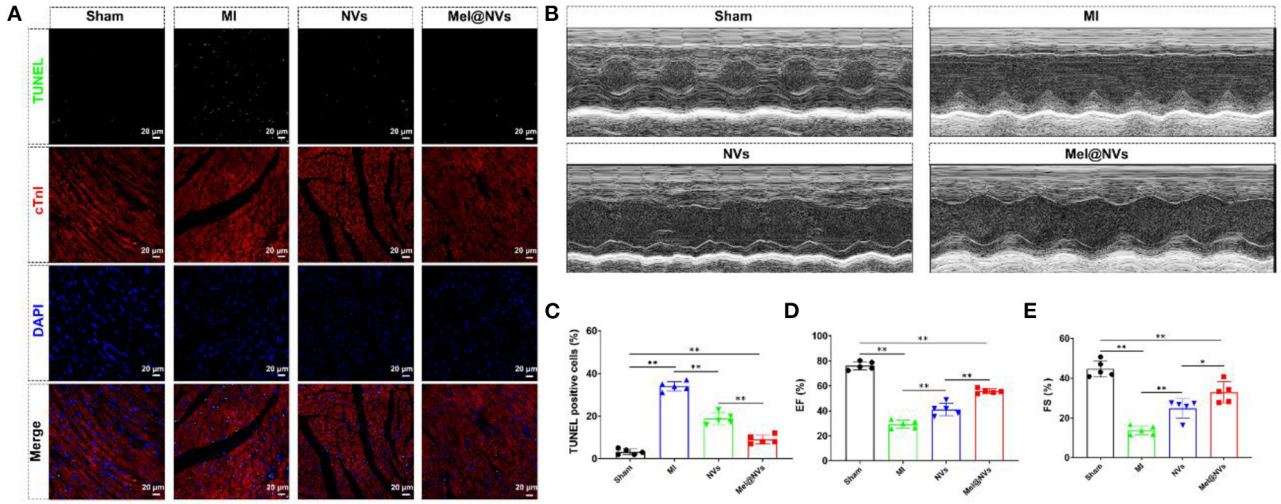

FIGURE 5 | Apoptotic effect and cardiac function at 4 weeks after MI treatment in mice. **(A)** Representative fluorescence images of TUNEL-stained myocardial sections. The images showed TUNEL-positive cells (green color), myocardium stained with monoclonal antibody cTnI (red color), and total nuclei stained with DAPI (blue color). Scale bar = 20 μm. **(B)** M-mode echocardiography for heart function evaluation. **(C)** The quantification of representative TUNEL-positive apoptotic cells (**$p < 0.01$). The results represented the mean ± standard deviation ($n = 5$). **(D)** The ejection fraction rate (EF%) standing for heart function is presented as a bar graph (**$p < 0.01$). The results expressed the mean ± standard deviation ($n = 5$). **(E)** The fractional shortening (FS%) standing for heart function is represented as a bar graph (*$p < 0.05$; **$p < 0.01$). The results represented the mean ± standard deviation ($n = 5$).

levels of ROS in cells and mitochondria were significantly reduced in the Mel@NVs treatment than that in NVs treatment. *In vivo* experiments showed that Mel@NVs treatment was able to reduce cardiomyocyte apoptosis and fibrosis, most importantly, promote the formation of microvessels, and finally improve cardiac functional recovery. Therefore, our strategy of combining melatonin and stem cell-derived NVs can not only inhibit oxidative stress and protect mitochondrial function through melatonin, but also use the vesicle's own protein and other nutritional factors to improve the microenvironment and ameliorate myocardial infarction.

In fact, previous studies have demonstrated that EVs not only possess the function of a drug carrier, but themselves also have anti-apoptotic effects used to treat animals in myocardial infarction inherited from their parental cells including ADSCs. EVs released by human cardiac progenitor cells have cardioprotective effects and improve cardiac function after myocardial infarction to the same extent as their parental cells. EVs derived from cardiac progenitor cells are rich in cardioprotective microRNAs, especially mir-146a-3p (44). MiRNAs are small, non-coding RNAs that regulate gene expression in a sequence-dependent manner (45). They play an important role in cell proliferation, differentiation, and even tumorigenesis and development (46). In recent years, studies have demonstrated that miRNAs are dysregulated in response to ischemic injury of the heart and actively contribute to cardiac remodeling after MI (47). There was a paper published in 2012 indicating that the therapeutic targeting of miR-15 in mice reduces infarct size and cardiac remodeling and enhances cardiac function in response to MI (48). Moreover, EVs of miR-126 overexpressing ADSCs reduce H9C2 cells damage by reducing the expression of inflammatory factors during hypoxia induction. Under hypoxic conditions, they can reduce the expression of fibrosis-related proteins in H9C2 cells and significantly promote the generation and migration of microvessels. It was confirmed that EVs rich in miR-126 can significantly reduce the myocardial injury area of infarction *in vivo* studies. These results demonstrated that ADSC-derived EVs overexpressing miR-126 could prevent myocardial injury by protecting cardiomyocytes from apoptosis, inflammation and fibrosis, and increasing angiogenesis (25). It was confirmed MSC-derived EVs can polarize M1 macrophages to M2 macrophages *in vivo* and *in vitro* experiments. MiRNA sequencing and bioinformatics analysis of MSC EVs suggest that miR-182 is a valuable candidate mediator for macrophage polarization. Reducing mir-182 in MSC EVs could partially weaken its regulation of macrophage polarization. Administration of MSC EVs to mice by intramyocardial injection after myocardial I/R reduced infarct area and alleviated Inflammatory levels in heart and serum. The results showed that MSC EVs changed the polarization state of macrophages through miR-182 and offered a novel method to reduce myocardial I/R injury in mice (49). MiRNAs could not only promote or inhibit cardiomyocyte death but also regulate angiogenesis after ischemia. MiRNAs that possess stem cell or progenitor cell-mediated cardioprotection can regulate cardiac regeneration so that they have great therapeutic potential in the treatment of acute myocardial infarction. For us, it is necessary to further explore the miRNAs that play a protective role against myocardial injury in stem cell-derived EVs and its underlying mechanism in the future.

Besides those above-mentioned EVs containing miRNAs possessing cardioprotection, the application of EVs as

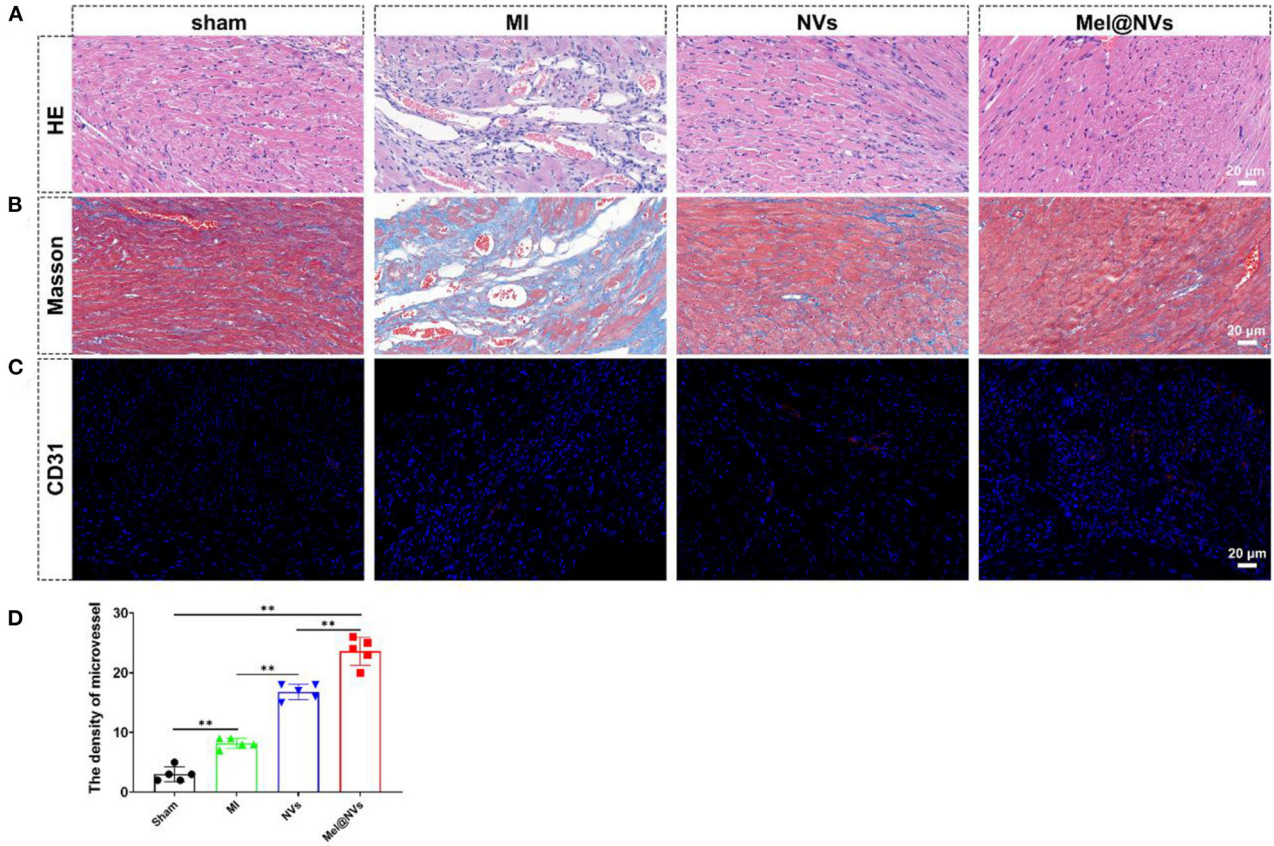

FIGURE 6 | Histological evaluation of the effect of Mel@NVs in MI model at 4 weeks after MI in mice. **(A)** H&E staining in different groups. **(B)** Masson's trichrome staining in different groups. **(C)** Representative immunohistochemical dyed for CD31-positive cells in different groups (red color), and DAPI (blue color). **(D)** Quantitative analysis of micro-vessels in different groups (**$p < 0.01$). The results represented the mean ± standard deviation ($n = 5$).

biomimetic drug carriers has become a significant research hotspot. EVs contain several desirable properties: the inherent ability to carry bioactive substances including proteins; immune tolerance with great biocompatibility; ideal stability in body fluids; natural targeting characteristics of cells; and the ability to cross biological barriers (41, 50). On the other hand, the tiny size of EVs provides favorable benefits for drug delivery, including reducing phagocytosis of circulating monocytes and passive accumulation to diseased tissues through imaged blood vessels (51). The unique characteristics of EVs promote the development of EVs based drug carriers in clinic. So far, no EV based therapies are available on the clinical application. Nevertheless, a few clinical trials were designed to explore the safety of EVs as drug delivery carriers. A phase I clinical trial (nct01294072) is currently being studied to explore the ability of plant-derived exosomes to deliver curcumin to normal and colonic tissues for the treatment of colon cancer. In another ongoing phase II clinical trial (nct01854866), the safety and efficacy of using tumor cell-derived exosomes as chemotherapeutic drug carriers in the treatment of malignant ascites. The above clinical trials have proved that autologous administration based on EVs as drug delivery carriers usually encompass no serious toxicity and adverse side effects, suggesting the safety and feasibility of this method. Biomimetic nanotechnology can create drug delivery systems similar to EVs. Extrusion technology can produce nanovesicles, which have the ability to produce vesicles more efficiently, and this method is highly biomimetic (52–54). In our study, the application of Mel@NVs has a significant therapeutic effect on infarcted myocardium *in vitro* and *in vivo*, further experimental studies are still needed in the future. The obstacle in the clinical application of NVs is the need for scalable EVs separation methods and more effective drug delivery methods for different therapies. Another challenge is to transform NVs from non-specific organ accumulation to targeted accumulation in desired tissues. Therefore, exploring new technological approaches to produce NVs with high targeting efficiency and safety will be our main research direction in the future.

In summary, our results showed that Mel@NVs protected the vitality of myocardial cells *in vitro* by reducing oxidative stress damage and apoptosis, and infarcted myocardial tissue *in vivo*. Through the use of the myocardial infarction model, it has been confirmed that the designed Mel@NVs play a therapeutic role in cardiac repair. Therefore, engineered nanovesicles will provide a potential strategy for the treatment of myocardial infarction.

DATA AVAILABILITY STATEMENT

The original contributions presented in the study are included in the article/supplementary material, further inquiries can be directed to the corresponding author/s.

ETHICS STATEMENT

The animal study was reviewed and approved by The Institutional Animal Care and Use Committee of Chinese PLA General Hospital.

AUTHOR CONTRIBUTIONS

FC and YW conceived and designed the experiments. YZha, XH, and YZhu performed the experiments. YZha, XH, YZhu, SG, and ZL analyzed the data. YW and FC provided financial support and co-wrote the article. YW edited the manuscript. All authors contributed to the article and approved the submitted version.

FUNDING

All authors are grateful to the Beijing Municipal Natural Science Foundation (7202189), National Nature Science Foundation of China (81530058, 81970443, 81671731, 81570272, 81571841, and 91939303), National Key Research Program of China (2016YFB0303303), NSFC Projects of International Cooperation and Exchanges (81820108019), Beijing Tianjin and Hebei Special Foundation (19JCZDJC63900), the Capital Clinical Feature Research Project (Z171100001017158), Big Data Program of Chinese PLA General Hospital (2017MBD-008), and Translational Medicine Program of Chinese PLA general hospital (2017TM- 003).

REFERENCES

1. Miao C, Lei M, Hu W, Han S, Wang Q. A brief review: the therapeutic potential of bone marrow mesenchymal stem cells in myocardial infarction. *Stem Cell Res Ther.* (2017) 8:242. doi: 10.1186/s13287-017-0697-9
2. Hori M, Nishida K. Oxidative stress and left ventricular remodelling after myocardial infarction. *Cardiovasc Res.* (2009) 81:457–64. doi: 10.1093/cvr/cvn335
3. Zorov DB, Juhaszova M, Sollott SJ. Mitochondrial reactive oxygen species (ROS) and ROS-induced ROS release. *Physiol Rev.* (2014) 94:909–50. doi: 10.1152/physrev.00026.2013
4. Ma Z, Xin Z, Di W, Yan X, Li X, Reiter RJ, et al. Melatonin and mitochondrial function during ischemia/reperfusion injury. *Cell Mol Life Sci.* (2017) 74:3989–98. doi: 10.1007/s00018-017-2618-6
5. Reiter RJ, Rosales-Corral S, Tan DX, Jou MJ, Galano A, Xu B. Melatonin as a mitochondria-targeted antioxidant: one of evolution's best ideas. *Cell Mol Life Sci.* (2017) 74:3863–81. doi: 10.1007/s00018-017-2609-7
6. Majidinia M, Reiter RJ, Shakouri SK, Yousefi B. The role of melatonin, a multitasking molecule, in retarding the processes of ageing. *Ageing Res Rev.* (2018) 47:198–213. doi: 10.1016/j.arr.2018.07.010
7. Arnao MB, Hernandez-Ruiz J. Melatonin: a new plant hormone and/or a plant master regulator? *Trends Plant Sci.* (2019) 24:38–48. doi: 10.1016/j.tplants.2018.10.010
8. Boyanova L, Markovska R, Mitov I. Virulence arsenal of the most pathogenic species among the gram-positive anaerobic cocci, *Finegoldia magna*. *Anaerobe.* (2016) 42:145–51. doi: 10.1016/j.anaerobe.2016.10.007
9. Lochner A, Marais E, Huisamen B. Melatonin and cardioprotection against ischaemia/reperfusion injury: what's new? A review. *J Pineal Res.* (2018) 65:e12490. doi: 10.1111/jpi.12490
10. Reiter RJ, Tan DX. Melatonin: a novel protective agent against oxidative injury of the ischemic/reperfused heart. *Cardiovasc Res.* (2003) 58:10–9. doi: 10.1016/S0008-6363(02)00827-1
11. Lin Y, Liu J, Bai R, Shi J, Zhu X, Liu J, et al. Mitochondria-inspired nanoparticles with microenvironment-adapting capacities for on-demand drug delivery after ischemic injury. *ACS Nano.* (2020) 14:11846–59. doi: 10.1021/acsnano.0c04727
12. Couvreur P. Nanoparticles in drug delivery: past, present and future. *Adv Drug Deliv Rev.* (2013) 65:21–3. doi: 10.1016/j.addr.2012.04.010
13. Peng Q, Zhang S, Yang Q, Zhang T, Wei XQ, Jiang L, et al. Preformed albumin corona, a protective coating for nanoparticles based drug delivery system. *Biomaterials.* (2013) 34:8521–30. doi: 10.1016/j.biomaterials.2013.07.102
14. Wang Y, Miao L, Satterlee A, Huang L. Delivery of oligonucleotides with lipid nanoparticles. *Adv Drug Deliv Rev.* (2015) 87:68–80. doi: 10.1016/j.addr.2015.02.007
15. Park JH, Dehaini D, Zhou J, Holay M, Fang RH, Zhang L. Biomimetic nanoparticle technology for cardiovascular disease detection and treatment. *Nanoscale Horiz.* (2020) 5:25–42. doi: 10.1039/C9NH00291J
16. Ela S, Mager I, Breakefield XO, Wood MJ. Extracellular vesicles: biology and emerging therapeutic opportunities. *Nat Rev Drug Discov.* (2013) 12:347–57. doi: 10.1038/nrd3978
17. Kourembanas S. Exosomes: vehicles of intercellular signaling, biomarkers, and vectors of cell therapy. *Annu Rev Physiol.* (2015) 77:13–27. doi: 10.1146/annurev-physiol-021014-071641
18. Armstrong JPK, Stevens MM. Strategic design of extracellular vesicle drug delivery systems. *Adv Drug Deliv Rev.* (2018) 130:12–6. doi: 10.1016/j.addr.2018.06.017
19. Maeki M, Kimura N, Sato Y, Harashima H, Tokeshi M. Advances in microfluidics for lipid nanoparticles and extracellular vesicles and applications in drug delivery systems. *Adv Drug Deliv Rev.* (2018) 128:84–100. doi: 10.1016/j.addr.2018.03.008
20. Kumar S, Michael IJ, Park J, Granick S, Cho YK. Cloaked exosomes: biocompatible, durable, degradable encapsulation. *Small.* (2018) 14:e1802052. doi: 10.1002/smll.201802052
21. Ni D, Wei H, Chen W, Bao Q, Rosenkrans ZT, Barnhart TE, et al. Ceria nanoparticles meet hepatic ischemia-reperfusion injury: the perfect imperfection. *Adv Mater.* (2019) 31:e1902956. doi: 10.1002/adma.201902956
22. Sun L, Zhu W, Zhao P, Zhang J, Lu Y, Zhu Y, et al. Down-regulated exosomal microRNA-221 - 3p derived from senescent mesenchymal stem cells impairs heart repair. *Front Cell Dev Biol.* (2020) 8:263. doi: 10.3389/fcell.2020.00263
23. Yue Y, Wang C, Benedict C, Huang G, Truongcao M, Roy R, et al. Interleukin-10 deficiency alters endothelial progenitor cell-derived exosome reparative effect on myocardial repair via integrin-linked kinase enrichment. *Circ Res.* (2020) 126:315–29. doi: 10.1161/CIRCRESAHA.119.315829
24. Chen G, Wang M, Ruan Z, Zhu L, Tang C. Mesenchymal stem cell-derived exosomal miR-143-3p suppresses myocardial ischemia-reperfusion injury by regulating autophagy. *Life Sci.* (2021) 280:119742. doi: 10.1016/j.lfs.2021.119742
25. Luo Q, Guo D, Liu G, Chen G, Hang M, Jin M. Exosomes from MiR-126-overexpressing adscs are therapeutic in relieving acute myocardial ischaemic injury. *Cell Physiol Biochem.* (2017) 44:2105–16. doi: 10.1159/000485949
26. Pan J, Alimujiang M, Chen Q, Shi H, Luo X. Exosomes derived from miR-146a-modified adipose-derived stem cells attenuate acute myocardial infarction-induced myocardial damage via downregulation of early growth response factor 1. *J Cell Biochem.* (2019) 120:4433–43. doi: 10.1002/jcb.27731
27. Chen J, Ren S, Duscher D, Kang Y, Liu Y, Wang C, et al. Exosomes from human adipose-derived stem cells promote sciatic nerve regeneration

via optimizing Schwann cell function. *J Cell Physiol.* (2019) 234:23097–110. doi: 10.1002/jcp.28873
28. Oh K, Kim SR, Kim DK, Seo MW, Lee C, Lee HM, et al. *In vivo* differentiation of therapeutic insulin-producing cells from bone marrow cells via extracellular vesicle-mimetic nanovesicles. *ACS Nano.* (2015) 9:11718–27. doi: 10.1021/acsnano.5b02997
29. Jo W, Jeong D, Kim J, Park J. Self-renewal of bone marrow stem cells by nanovesicles engineered from embryonic stem cells. *Adv Healthc Mater.* (2016) 5:3148–56. doi: 10.1002/adhm.201600810
30. Kim MS, Haney MJ, Zhao Y, Mahajan V, Deygen I, Klyachko NL, et al. Development of exosome-encapsulated paclitaxel to overcome MDR in cancer cells. *Nanomedicine.* (2016) 12:655–64. doi: 10.1016/j.nano.2015.10.012
31. Ma Q, Yang J, Huang X, Guo W, Li S, Zhou H, et al. Poly(Lactide-Co-Glycolide)-Monomethoxy-Poly-(Polyethylene Glycol) nanoparticles loaded with melatonin protect adipose-derived stem cells transplanted in infarcted heart tissue. *Stem Cells.* (2018) 36:540–50. doi: 10.1002/stem.2777
32. Han D, Wang Y, Chen J, Zhang J, Yu P, Zhang R, et al. Activation of melatonin receptor 2 but not melatonin receptor 1 mediates melatonin-conferred cardioprotection against myocardial ischemia/reperfusion injury. *J Pineal Res.* (2019) 67:e12571. doi: 10.1111/jpi.12571
33. Chouchani ET, Methner C, Nadtochiy SM, Logan A, Pell VR, Ding S, et al. Cardioprotection by S-nitrosation of a cysteine switch on mitochondrial complex I. *Nat Med.* (2013) 19:753–9. doi: 10.1038/nm.3212
34. Ikeda Y, Sciarretta S, Nagarajan N, Rubattu S, Volpe M, Frati G, et al. New insights into the role of mitochondrial dynamics and autophagy during oxidative stress and aging in the heart. *Oxid Med Cell Longev.* (2014) 2014:210934. doi: 10.1155/2014/210934
35. Rabinovich-Nikitin I, Lieberman B, Martino TA, Kirshenbaum LA. Circadian-Regulated cell death in cardiovascular diseases. *Circulation.* (2019) 139:965–80. doi: 10.1161/CIRCULATIONAHA.118.036550
36. Petrie JR, Guzik TJ, Touyz RM. Diabetes, hypertension, and cardiovascular disease: clinical insights and vascular mechanisms. *Can J Cardiol.* (2018) 34:575–84. doi: 10.1016/j.cjca.2017.12.005
37. Han D, Huang W, Li X, Gao L, Su T, Li X, et al. Melatonin facilitates adipose-derived mesenchymal stem cells to repair the murine infarcted heart via the SIRT1 signaling pathway. *J Pineal Res.* (2016) 60:178–92. doi: 10.1111/jpi.12299
38. Yang Y, Sun Y, Yi W, Li Y, Fan C, Xin Z, et al. A review of melatonin as a suitable antioxidant against myocardial ischemia-reperfusion injury and clinical heart diseases. *J Pineal Res.* (2014) 57:357–66. doi: 10.1111/jpi.12175
39. Areti A, Komirishetty P, Akuthota M, Malik RA, Kumar A. Melatonin prevents mitochondrial dysfunction and promotes neuroprotection by inducing autophagy during oxaliplatin-evoked peripheral neuropathy. *J Pineal Res.* (2017) 62. doi: 10.1111/jpi.12393
40. Ciosek J, Drobnik J. Function of the hypothalamo-neurohypophysial system in rats with myocardial infarction is modified by melatonin. *Pharmacol Rep.* (2012) 64:1442–54. doi: 10.1016/S1734-1140(12)70942-8
41. Vader P, Mol EA, Pasterkamp G, Schiffelers RM. Extracellular vesicles for drug delivery. *Adv Drug Deliv Rev.* (2016) 106:148–56. doi: 10.1016/j.addr.2016.02.006
42. Maas SLN, Breakefield XO, Weaver AM. Extracellular vesicles: unique intercellular delivery vehicles. *Trends Cell Biol.* (2017) 27:172–88. doi: 10.1016/j.tcb.2016.11.003
43. Van Niel G, D'angelo G, Raposo G. Shedding light on the cell biology of extracellular vesicles. *Nat Rev Mol Cell Biol.* (2018) 19:213–28. doi: 10.1038/nrm.2017.125
44. Barile L, Moccetti T, Marbán E, Vassalli G. Roles of exosomes in cardioprotection. *Eur Heart J.* (2017) 38:1372–9. doi: 10.1093/eurheartj/ehw304
45. Colombo M, Raposo G, Théry C. Biogenesis, secretion, and intercellular interactions of exosomes and other extracellular vesicles. *Annu Rev Cell Dev Biol.* (2014) 30:255–89. doi: 10.1146/annurev-cellbio-101512-122326
46. Yi M, Xu L, Jiao Y, Luo S, Li A, Wu K. The role of cancer-derived microRNAs in cancer immune escape. *J Hematol Oncol.* (2020) 13:25. doi: 10.1186/s13045-020-00848-8
47. Zhu W, Sun L, Zhao P, Liu Y, Zhang J, Zhang Y, et al. Macrophage migration inhibitory factor facilitates the therapeutic efficacy of mesenchymal stem cells derived exosomes in acute myocardial infarction through upregulating miR-133a-3p. *J Nanobiotechnol.* (2021) 19:61. doi: 10.1186/s12951-021-00808-5
48. Hullinger TG, Montgomery RL, Seto AG, Dickinson BA, Semus HM, Lynch JM, et al. Inhibition of miR-15 protects against cardiac ischemic injury. *Circ Res.* (2012) 110:71–81. doi: 10.1161/circresaha.111.244442
49. Zhao J, Li X, Hu J, Chen F, Qiao S, Sun X, et al. Mesenchymal stromal cell-derived exosomes attenuate myocardial ischaemia-reperfusion injury through miR-182-regulated macrophage polarization. *Cardiovasc Res.* (2019) 115:1205–16. doi: 10.1093/cvr/cvz040
50. Morad G, Carman CV, Hagedorn EJ, Perlin JR, Zon LI, Mustafaoglu N, et al. Tumor-derived extracellular vesicles breach the intact blood-brain barrier via transcytosis. *ACS Nano.* (2019) 13:13853–65. doi: 10.1021/acsnano.9b04397
51. Lu M, Huang Y. Bioinspired exosome-like therapeutics and delivery nanoplatforms. *Biomaterials.* (2020) 242:119925. doi: 10.1016/j.biomaterials.2020.119925
52. Cheng G, Li W, Ha L, Han X, Hao S, Wan Y, et al. Self-assembly of extracellular vesicle-like metal-organic framework nanoparticles for protection and intracellular delivery of biofunctional proteins. *J Am Chem Soc.* (2018) 140:7282–91. doi: 10.1021/jacs.8b03584
53. Xiong F, Ling X, Chen X, Chen J, Tan J, Cao W, et al. Pursuing specific chemotherapy of orthotopic breast cancer with lung metastasis from docking nanoparticles driven by bioinspired exosomes. *Nano Lett.* (2019) 19:3256–66. doi: 10.1021/acs.nanolett.9b00824
54. Lee JR, Park BW, Kim J, Choo YW, Kim HY, Yoon JK. Nanovesicles derived from iron oxide nanoparticles-incorporated mesenchymal stem cells for cardiac repair. *Sci Adv.* (2020) 6:eaaz0952. doi: 10.1126/sciadv.aaz0952

Conflict of Interest: The authors declare that the research was conducted in the absence of any commercial or financial relationships that could be construed as a potential conflict of interest.

Publisher's Note: All claims expressed in this article are solely those of the authors and do not necessarily represent those of their affiliated organizations, or those of the publisher, the editors and the reviewers. Any product that may be evaluated in this article, or claim that may be made by its manufacturer, is not guaranteed or endorsed by the publisher.

Copyright © 2022 Zhang, Yang, Huang, Zhu, Gao, Liu, Cao and Wang. This is an open-access article distributed under the terms of the Creative Commons Attribution License (CC BY). The use, distribution or reproduction in other forums is permitted, provided the original author(s) and the copyright owner(s) are credited and that the original publication in this journal is cited, in accordance with accepted academic practice. No use, distribution or reproduction is permitted which does not comply with these terms.

frontiers | Frontiers in Cardiovascular Medicine

ORIGINAL RESEARCH
published: 11 April 2022
doi: 10.3389/fcvm.2022.781753

Profilin 2 and Endothelial Exosomal Profilin 2 Promote Angiogenesis and Myocardial Infarction Repair in Mice

Zhenkun Li[1,2†], Xueyun Huo[1†], Keyan Chen[3], Fenghua Yang[4], Weijiang Tan[4], Qi Zhang[5], Haixu Yu[5], Changlong Li[1], Deshan Zhou[1], Hao Chen[6], Baoquan Zhao[6], Yuan Wang[5], Zhenwen Chen[1] and Xiaoyan Du[1*]*

[1] School of Basic Medical Sciences, Capital Medical University, Beijing Key Laboratory of Cancer Invasion & Metastasis Research, Beijing, China, [2] Experimental Center, Beijing Friendship Hospital, Capital Medical University, Beijing, China, [3] Department of Laboratory Animal Science, China Medical University, Dalian, China, [4] Guangdong Laboratory Animals Monitoring Institute, Guangdong Provincial Key Laboratory of Laboratory Animals, Guangzhou, China, [5] Beijing Anzhen Hospital, Capital Medical University, Beijing, China, [6] State Key Laboratory of Toxicology and Medical Countermeasures, Institute of Pharmacology and Toxicology, Beijing, China

OPEN ACCESS

Edited by:
Shijun Wang,
Zhongshan Hospital, Fudan University, China

Reviewed by:
Jian Zhang,
Nanjing Medical University, China
Jinxuan Zhao,
Nanjing Drum Tower Hospital, China

***Correspondence:**
Xiaoyan Du
duduyan@ccmu.edu.cn
Zhenwen Chen
czwen@ccmu.edu.cn

† These authors have contributed equally to this work

Specialty section:
This article was submitted to Cardiovascular Metabolism, a section of the journal Frontiers in Cardiovascular Medicine

Received: 23 September 2021
Accepted: 11 January 2022
Published: 11 April 2022

Citation:
Li Z, Huo X, Chen K, Yang F, Tan W, Zhang Q, Yu H, Li C, Zhou D, Chen H, Zhao B, Wang Y, Chen Z and Du X (2022) Profilin 2 and Endothelial Exosomal Profilin 2 Promote Angiogenesis and Myocardial Infarction Repair in Mice. Front. Cardiovasc. Med. 9:781753. doi: 10.3389/fcvm.2022.781753

Cardiovascular diseases (CVD) are the leading cause of death worldwide, wherein myocardial infarction (MI) is the most dangerous one. Promoting angiogenesis is a prospective strategy to alleviate MI. Our previous study indicated that profilin 2 (PFN2) may be a novel target associated with angiogenesis. Further results showed higher levels of serum PFN2 and exosomal PFN2 in patients, mice, and pigs with MI. In this study, we explored whether PFN2 and endothelial cell (EC)-derived exosomal PFN2 could increase angiogenesis and be beneficial for the treatment of MI. Serum PFN2, exosomes, and exosomal PFN2 were elevated in rats with MI. PFN2 and exosomes from PFN2-overexpressing ECs (OE-exo) enhanced EC proliferation, migration, and tube formation ability. OE-exo also significantly increased the vessel number in zebrafish and protected the ECs from inflammatory injury. Moreover, OE-exo-treated mice with MI showed improvement in motor ability, ejection fraction, left ventricular shortening fraction, and left ventricular mass, as well as increased vessel numbers in the MI location, and decreased infarction volume. Mechanistically, PI3K might be the upstream regulator of PFN2, while ERK might be the downstream regulator in the PI3K-PFN2-ERK axis. Taken together, our findings demonstrate that PFN2 and exosomal PFN2 promote EC proliferation, migration, and tube formation through the PI3K-PFN2-ERK axis. Exosomal PFN2 may be a valuable target in the repair of MI injury via angiogenesis.

Keywords: angiogenesis, endothelial cells, exosomes, myocardial infarction, profilin 2

INTRODUCTION

Myocardial infarction (MI) is caused by ischemia, a condition referring lack of oxygen delivery to heart tissues. Ischemic heart disease is responsible for over 9 million deaths in 2016 according to the World Health Organization estimates (1). MI leads to cardiac myocyte death and subsequent necrosis of the tissue in the infarcted area, attracting inflammatory cells that phagocytose dead cells and debris within the infarcted area (2). Infarct size is a major indicator of post-MI remodeling, subsequent heart failure (3), and eventually prognosis (4–6), and in the longer term, inflammation contributes to changes associated with an increased likelihood of heart failure and mortality (7, 8).

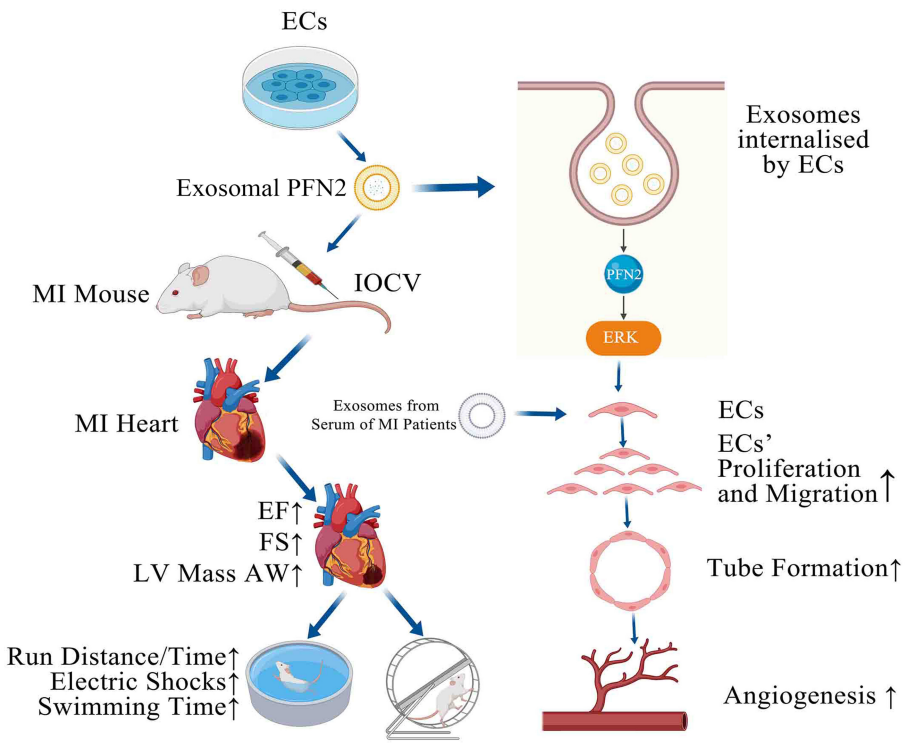

GRAPHICAL ABSTRACT | PFN2-overexpressing ECs (OE-exo) treated MI mice showed improvement in infarction volume, cardiac function and motor ability, and PFN2/ OE-exo significantly enhanced EC proliferation, migration, tube formation ability and angiogenesis.

During MI, cardiomyocytes die as a result of transmural ischemia (9). One of the most important biological processes during myocardial healing after ischemic injury is microvascular angiogenesis, which consists of the development of new blood vessels from pre-existing vasculature (10). Angiogenesis is stimulated by increased levels of vascular endothelial growth factor (VEGF) and basic fibroblast growth factor (bFGF), which are released in response to the infarction. Recent study has shown that the promotion of angiogenesis in the ischemic region is the promising therapeutic strategies for preventing MI (11). Researchers found that irisin exerts a therapeutic effect against myocardial infarction via promoting angiogenesis (12) and a novel Ca^{2+} current blocker promotes angiogenesis and cardiac healing after experimental myocardial infarction in mice (13). Therefore, it is particularly important to explore new molecules and therapy pathways that relieving the adverse effects of inflammation and promoting angiogenesis after myocardial infarction.

Exosomes can deliver a wide range of functional molecules such as proteins, RNAs, and genomic DNA (14–16). Evidence has shown that exosomes deliver bioactive molecules to endothelial cells (ECs) to induce angiogenesis (17), and ECs could also release exosomes to mediate the formation of blood vessels (18). Recent research has highlighted the significant potential of pericardial fluid- and plasma-derived exosomes as therapeutic angiogenesis targets in patients with MI (19, 20). Although exosomes have been shown to play an important role in angiogenesis (21), our knowledge of cardiac repair medicated by vascular EC-derived exosomes post MI is very limited.

Profilin (PFN), a 12–15 kDa actin-binding protein, is ubiquitously expressed and highly conservative (22). PFNs participate in many cellular processes such as cell motility, metabolism, signal transduction and gene transcription (23). Among PFN Isoforms, profilin 2 (PFN2) has been known to play key roles in tumor progression. Zhang H et al. found loss of PFN2 contributes to enhanced epithelial-mesenchymal transition and metastasis of colorectal cancer (24) and Tang et al. reported that PFN2 promoting TGF-β-mediated EMT and increased VEGF expression (25). But the effects of PFN2 on the function of endothelial cells and inflammation after MI have been unknown. Most recently, we found that PFN2 and exosomal PFN2 could promote small cell lung cancer growth and metastasis as well as tumor angiogenesis (26), we speculated that exosomal PFN2 might also promote angiogenesis on cardiac tissue after MI.

In the present study, we hypothesized that MI release exosomes carrying PFN2, which promotes angiogenesis. Therefore, we examined the serum of patients with MI and found that levels PFN2, exosomes, and exosomal PFN2 were increased during angiogenesis phase. We further demonstrated that the beneficial function of PFN2 and endothelial exosomal

PFN2 in the proliferation, migration, and tube formation of ECs. Moreover, exosomal PFN2 derived from ECs has a significant therapeutic effect in mice with myocardial infarction. We also revealed that PFN2 were involved in PI3K -PFN2-ERK axis during angiogenesis.

MATERIALS AND METHODS

MI Patients

According to the period from symptom onset to diagnosis, we divided the samples into 2–10 h of MI group ($n = 30$), 8–15 days after MI group ($n = 30$), and healthy controls group ($n = 24$). All patients provided informed consent and the patient information is listed in **Supplementary Table 1**.

Inclusion Criteria

(1) Meet the diagnostic criteria of acute myocardial infarction;
(2) Patients with unconscious disorder can actively cooperate with medical staff;
(3) Patients who have informed the purpose, method and significance of the study, voluntarily participated in the study and signed the informed consent.

Exclusion Criteria

(1) Complicated with serious organ diseases;
(2) Incomplete clinical data.

Myocardial Infarction Models of Mice, Rats and Pigs

A total of 15 male Wistar rats (230–280 g, 7–8 weeks old) were utilized in the study. The animals were maintained under controlled conditions with a temperature of 24 ± 2°C, humidity of 55–65%, a 12 h light/dark cycle, and *ad libitum* access to standard laboratory diet and water.

Rodent MI Models

Briefly, surgery was performed under isoflurane (2.5%) inhalation anesthesia and mechanical ventilation. The MI model was established by performing a left lateral thoracotomy and ligating the left anterior descending artery (LAD) using a 10-0 suture. The sera were collected before and after surgery at different time points to evaluate the expression of PFN2, exosomes, and exosomal PFN2.

The experimental pigs were anesthetized with ketamine and maintained with isoflurane. kept in the right lateral position, cut open the left rib 3–4, exposed the main coronary artery of the heart, ligated between the second and third branches, and the chest wall was sutured layer by layer after successful myocardial infarction confirmed by electrocardiogram. Serum samples from pigs with MI ($n = 4$) and their corresponding controls ($n = 4$) were collected at different time points after MI.

Reagents

RPMI-1640 medium and phosphate-buffered saline (PBS) were purchased from Hyclone (USA), and Endothelial Cell Medium was from ScienCell (USA). MTT and DMSO were purchased from Beyotime (China). PI3K inhibitor LY-294002 and ERK1/2 inhibitor HY-50846 were from MCE (USA). The various antibodies used in the experiments were obtained from Abcam (UK).

Isolation of Exosomes

Exosomes were isolated by the salting-out method (Serum) and ultracentrifugation (Cells culture medium with exosome-depleted fetal bovine serum). The serum sample was centrifuged at 2,000 × *g* for 20 min at room temperature to remove cells and debris. The supernatant was transferred gently to a new tube and centrifuged again at 10,000 × *g* for 20 min at room temperature to remove debris. The clarified serum was transferred to a new tube and 0.5 volumes of PBS and 0.3 volumes of exosomes isolation reagent were added. The sample was vortexed and centrifuged at 10,000 × *g* for 5 min at room temperature, and the supernatant was aspirated and discarded. Finally, the tube was centrifuged for 30 s at 10,000 × *g*, and the residual supernatant was discarded by careful aspiration. PBS was added, and the exosomes were resuspended by vortex. The cell culture medium was centrifuged at 300 × *g* for 10 min, and the supernatant was centrifuged at 2,000 × *g* for 10 min/ 10,000 × *g* for 30 min/140,000 × *g* for 90 min, PBS was added to the pellet, and the exosomes were resuspended by vortex. Exosomes were identified by transmission electron microscopy (TEM). Exosomes were stored at 4°C within a week or −80°C within 3 months. In cell co-culture experiences, the final concentration of exosomes was 10 μg/ml. In animal experiences, mice were injected with 50 μg exosomes mixed in 100 μl PBS.

Immunofluorescence and Masson's Staining

After functional analysis, 21 mice with MI, with or without exosomes were euthanized, and the heart tissues were fixed in formalin and embedded in paraffin. Immunofluorescence analysis was performed on 4 μm thick myocardial tissue sections. The sections were incubated with primary antibodies against PFN2 (Abcam, ab191054, UK) or $CD31^+$ (Abcam, ab24590, UK). Alexa Fluor 488- or Alexa Fluor 555-conjugated secondary antibodies (Invitrogen) were added and incubated for 1 h. After staining with Hoechst 33342 (Sigma-Aldrich) and sealing with an anti-fade fluorescence mounting medium (Solarbio), the images were captured.

For Masson's staining, the samples were treated with hematoxylin for 5 min, with deionized water for 30 s three times, and with Masson's dye (HT15, Sigma, USA) for 7 min. Then, the sections were treated with 2% glacial acetic acid solution and 10% molybdic acid for 5 min. After aniline blue staining for 5 min and gradient alcohol washing, neutral gum was used to seal the slide, and the sample was observed under a microscope.

Exercise Endurance Capacity

A mouse model of MI was established using 21 mice with 7 animals in each group. The experimental procedure was similar to that of the rat model of MI. On the 5th day after MI, the animals were randomly divided into three groups and injected in the tail vein with profilin 2 overexpressing EC-exosomes (OE-exo), normal EC-exosomes (exo), and saline. After 21 days of

injection, all animals were subjected to physical fitness (YLS-10B) and swimming endurance tests. Cardiac function was evaluated for ejection fraction (EF), fractional shortening (FS), left ventricular (LV) mass AW, and LV volume as detected by type-B ultrasonic test.

Echocardiography

The effects of exosomal PFN2 on the cardiac function of MI mouse were evaluated using a high-frequency ultrasound system Vevo2100 (VisualSonics, Canada) equipped with a linear array transducer (MS250, 13–24 MHz). This transducer is specifically designed for mouse, guinea pigs or other similar sizes of small animals. During image acquisition, mice were anesthetized continuously with 2% isoflurane. All animals were placed in the dorsal recumbent position for ultrasound imaging. Ejection fraction (EF) and fractional shortening (FS) were detected by type-B ultrasonic test.

Transmission Electron Microscopy

For identification of exosomes by TEM, samples were fixed in 0.01 M PBS (pH 7.4) at 4°C overnight. After washing with PBS, the samples were fixed in 1% OsO_4 for 30 min, rinsed with distilled water, precipitated and dehydrated in concentration gradient alcohol, stained with 1% uranyl acetate for 30 min, and finally embedded in TAAb812. After polymerization at 60°C overnight, the precipitate was sliced, and the ultrathin sections were observed under a Tecnai transmission electron microscope (FEI, USA).

PFN2 Overexpression and PFN2 Knockdown Endothelial Cells

Human umbilical vein ECs (HUVECs) were cultured in RPMI-1640 medium (SH30809.01, Hyclone, USA). Rat brain microvascular ECs (RBMECs) were cultured in Endothelial Cell Medium (1001, ScienCell, USA) for the first five generations and then cultured in RPMI-1640 medium.

Lentiviral vectors were used for profilin 2 overexpression (PFN2-OE or OE) and profilin 2-knockdown (PFN2-KD or KD) in endothelial cells. The PFN2-OE cells were generated using pLVX-mCMV-ZsGreen-PGK-Puro vector, and PFN2-KD cells were infected with pLVX-shRNA2-Puro. The sequences of profiling 2 primer and profilin 2-shRNA are listed in **Supplementary Table 2**. HUVECs and RBMECs were transduced for 24 h with recombinant lentivirus and cultured for 72 h. The transduction efficacy was verified by GFP expression as determined by fluorescence microscopy, and subsequently confirmed by qPCR and western blotting.

Quantitative Polymerase Chain Reaction (QPCR) Analysis

A total of 15 gerbils at different developmental stages [embryo (prenatal), brain, and heart (postnatal)] were used for qPCR analysis (3 samples for each time point) of PFN2 levels during development. The expression levels of ECs were also analyzed with qPCR. qPCR was also performed following the earlier described protocol. Cells were resuspended in medium at a density of 2,000 cells/well. Total RNA was extracted from ECs using TRIzol reagent (Tiangen). We synthesized cDNA using FastQuant RT Kit (Tiangen) following manufacturer's instructions. An iQ5 thermal cycler (Bio-Rad, USA) was used to perform qPCR as follows: pre-denaturation at 95°C for 15 min, 40 cycles of denaturation at 95°C for 10 s, annealing and extension at 60°C for 35 s, and 71 cycles of melt curve analysis at 60°C for 10 s. Primer sequences for profilin 2 and other genes are listed in **Supplementary Table 2**.

Vascular Development of Zebrafish

The zebrafish model was established by microinjection of exosomes labeled with the fluorescent carbocyanine dye Dil (red), (Solarbio, D8700-10) into the perivitelline cavity of mp805a zebrafish embryos at 24 h post-fertilization. The embryos were cultured at room temperature, and the distribution of exosomes was observed by fluorescence microscopy from 0 to 48 h after injection. The zebrafish vascular structure and the number of vessels were imaged using a confocal microscope (TCS SP5, Leica).

Inflammatory Models of the Cell

ECs were treated with 1 μg/mL of LPS for 24 h.

Real-Time Cell Analyzer (RTCA) Assay

We used a real-time cell analyzer (RTCA) system (ACEA, USA) to explore the effect of PFN2 on endothelial cell migration and proliferation, as described in our previous report (27). Briefly, cells were seeded in E-plates at a density of 1,000 HUVECs/well and 2,000 RBMECs/well. The E-plates were then transferred to the RTCA-Dual Purpose instrument for automated real-time monitoring under standard incubator conditions. Cell index measurements were collected every 5 min. Cellular migration and invasion were also monitored using the RTCA system on cell invasion-and-migration (CIM)-plates instead of E-plates. Cell migration activity was monitored with the impedance readouts. Migration assays were performed by seeding cells in the upper chambers of the CIM-plates in serum-free medium at a density of 10,000 cells/well. The bottom chambers of the CIM-plates were filled with serum-containing medium to promote migration across the membranes along the serum gradient. Data were collected by real-time readouts.

Enzyme-Linked Immunosorbent Assay (ELISA) and Analysis of Exosomal PFN2

The sera were collected before and after surgery at different time points and PFN2, basic fibroblast growth factor (bFGF), and vascular endothelial growth factor (VEGFA) were detected using ELISA kits. The protein levels in the cell culture supernatant and serum were verified by ELISA. The proteins in the cell culture supernatant were determined using a human PFN2 ELISA kit (Cyagen, USA) and the VEGFA (R&D) kit. The concentrations of PFN2, bFGF, and VEGFA in the serum samples obtained from mouse, patient, pig, and rat with MI were determined using the mouse (Cyagen), human (Cyagen), pig (Cyagen), and rat ELISA kits (Cyagen), respectively. Exosomal PFN2 and VEGFA in the serum were identified using mouse or pig PFN2 and VEGFA kit (Cyagen). All experiments were performed

according to the manufacturer's instructions. The level of rat exosomes in the serum was detected by Overall Exosomes Capture and Quantification (Plasma, Colorimetric) kit (NBP2-49782, Novus, USA).

Endothelial Tube Formation Assay

The *in vitro* effects of PFN2 on HUVEC and RBMEC cell angiogenesis and viability were evaluated by tube formation assay. The tube formation assay was performed using Matrigel® (BD Biosciences), according to the manufacturer's instructions. Matrigel® was thawed overnight at 4°C. The 96-well plate and 100 μl pipette tips were maintained at 4°C overnight. Subsequently, Matrigel® (30 μl/well) was added to the 96-well plate and incubated at 37°C for 1 h. Then, cells were incubated for 24 h at 37°C 5% CO_2. Tube formation was observed using an inverted phase-contrast microscope. The total branching length of the vascular network was determined using ImageJ.

MTT Assay

MTT assay as reported previously (27). Briefly, Target cells were resuspended in medium at a density of 2000 cells/well and were allowed to adhere for 6 hours. Wells containing 100-μL medium alone (without cells) were used as negative controls. MTT assays were performed at 48 h. The results for the negative control were used as a baseline. Each experiment was repeated 3 times, and the results are presented as a percentage of viable cells as calculated by the following equation: (mean absorbance of experimental well/mean absorbance of positive control well) × 100 = percentage of viable cells.

Western Blot Analysis

Protein extraction and western blotting were performed as reported previously (27). The primary antibodies used were as follows: PFN2 (Abcam, ab191054, UK), PI3K (Abcam, ab32089, UK), p-ERK (CST, 4372, USA), VEGFA (Abcam, ab214424, UK), PCNA (Abcam, ab92552, UK), Alix (Abcam, ab186429, UK), and GAPDH (Abcam, ab181602, UK), and were diluted 1:1000. The secondary antibodies were diluted 1:5000. The membranes were washed thoroughly, and protein bands were visualized with enhanced chemiluminescence (ECL) immunoblotting detection reagent (Thermo Fisher Scientific, USA). Semi-quantitative results were normalized to the expression of the housekeeping gene GAPDH, after gray scanning.

Statistical Analysis

Statistical analysis was performed using SPSS 16.0 (SPSS Inc., USA). After the normality test and variance homogeneity test of measured data, comparisons between different groups were performed using Student's *t*-test, one-way ANOVA, or repeated-measures ANOVA (Tukey). Bar charts show the mean ± SEM. A $p \leq 0.05$ indicated a significant difference.

RESULTS

PFN2 and Exosomal PFN2 Levels Increased in the Serum of Post-MI Patients and the MI Animal Models During Angiogenesis Phase

VEGFA and bFGF are well-known markers for the establishment of collateral circulation after MI (28, 29). We measured the PFN2, VEGFA and bFGF levels in the serum of patients with MI and in pig animal model to explore the relationship between serum PFN2 level and angiogenesis after MI. The results showed increased PFN2 levels in the serum of patients with MI, especially in patients after 8–15 days post-MI ($p = 0.021$) compared to their corresponding CTL, consistent with the levels of VEGFA and bFGF (**Figure 1A**). We also observed significantly higher levels of PFN2, VEGFA, and bFGF in pigs with MI compared to healthy CTL on days 7 and 14 post-MI, respectively (**Figure 1B**). These data showed a positive correlation between serum PFN2 levels and markers for the establishment of collateral circulation, which suggested the possible relationship between PFN2 and angiogenesis after MI. Besides, we found that PFN2 was negative associated with creatinine kinase-myocardial band (CK-MB) (Pearson correlation = −0.321, $p = 0.012$) and diastolic blood pressure (DBP) (Pearson correlation = −0.300, $p = 0.020$) (**Supplementary Figure 1**), which both indicated poor prognosis of MI (30, 31).

To examine if PFN2 was delivered intracellularly by exosomes in serum, we isolated exosomes from the serum of patients with MI and, after identification by TEM, tested the exosomal PFN2 level between the CTL and MI groups. The data indicated that exosomes were present in the MI serum (**Figure 1C**). In addition, the exosomal CD31 and PFN2 levels in the MI group were significantly higher than those in the CTL group ($p = 0.035/p = 0.025$) (**Figures 1D,E**), which suggested that elevated PFN2 content might be associated with endothelial cells derived exosomes increasing in MI patients serum.

We established a rat model of MI by coronary artery ligation and then analyzed the dynamic changes in serum PFN2, exosomes, and exosomal PFN2 at different time points after surgery. Intriguingly, serum exosomes, serum exosomal PFN2 levels, and serum PFN2 levels increased significantly after MI on the 3rd day ($p = 0.037$), 9th day ($p = 0.028$), and 18th day ($p = 0.043$), respectively (**Figure 1F**). These data implicate the association of PFN2 as well as exosomal PFN2 with MI.

Exosomal PFN2 Reduces Infarction in Post-MI Mouse Hearts and Enhances Exercise Endurance Capacity in Post-MI Mice

We tested the cardiac function and repair of infarction in mice with MI 30 days after injecting exo, OE-exo, and saline by physical fitness tests and echocardiography. The results showed significantly improved EF and FS (two critical indicators reflecting cardiac function) in the OE-exo-injected group, higher than the exo and saline groups (**Figure 2A**). The running time in exo- and saline-injected mice with MI were lower than in

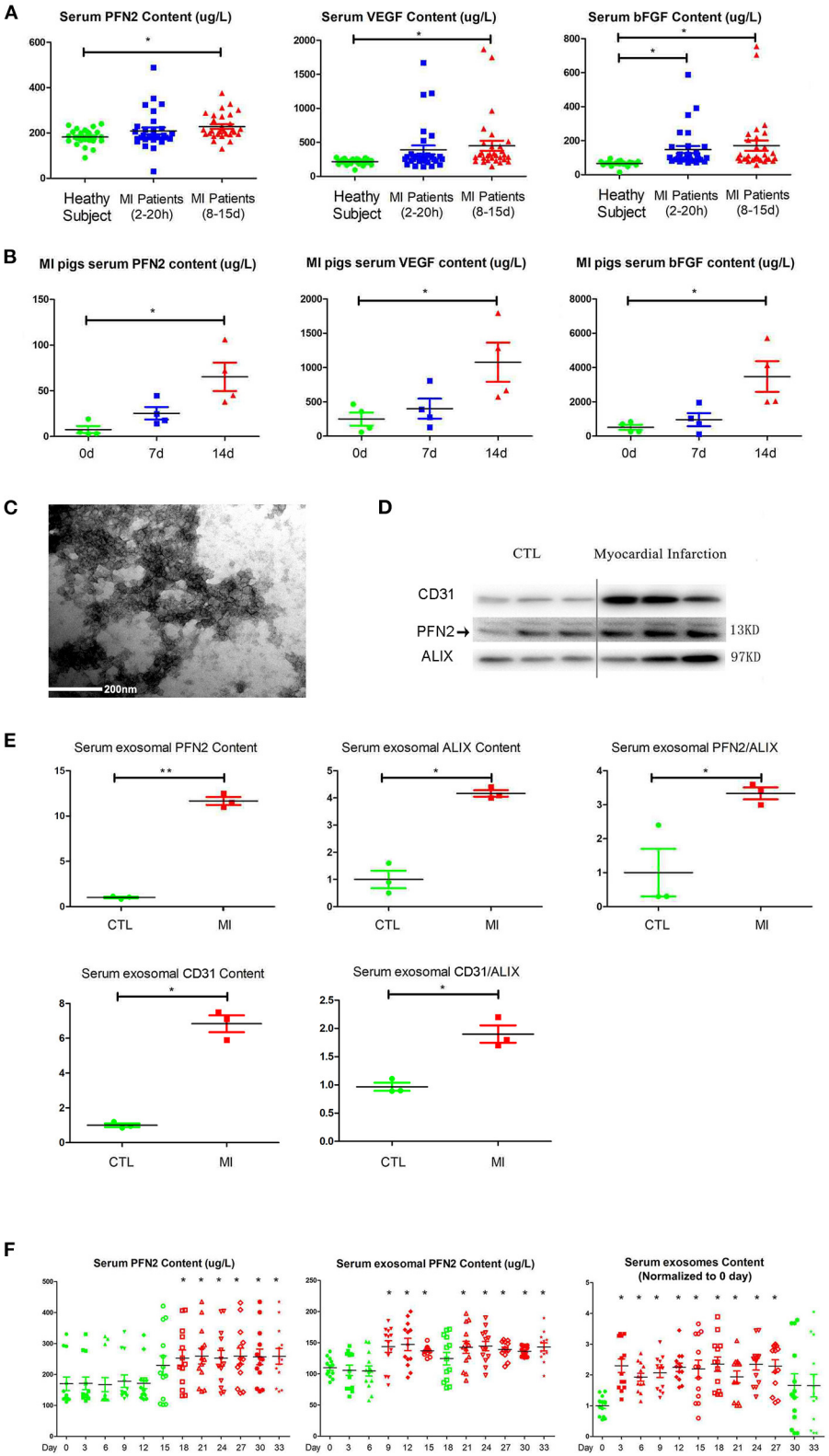

FIGURE 1 | Increased PFN2 and exosomal PFN2 levels in the serum of patients with MI and in animal models. **(A)** Enhanced PFN2 levels, VEGFA and bFGF levels in patients with MI (patients with MI 2–20 h, $n = 30$; MI 8–15 d, $n = 30$; CTL, $n = 24$). **(B)** Enhanced PFN2 levels, VEGFA and bFGF levels in pigs with MI (pigs with MI, $n = 4$; CTL, $n = 4$). **(C)** Identification of serum exosomes in patients with MI by electron microscopy. **(D)** Exosomal PFN2 between CTL ($n = 3$) and MI groups ($n = 3$). **(E)** Exosomal PFN2 levels between CTL ($n = 3$) and MI groups ($n = 3$) (The protein level was normalized to control). **(F)** Serum PFN2 levels, Exosomal PFN2 levels and Exosomes in rats ($n = 13$) before and after MI. $^*p < 0.05$, one-way ANOVA and repeated-measures ANOVA (Tukey).

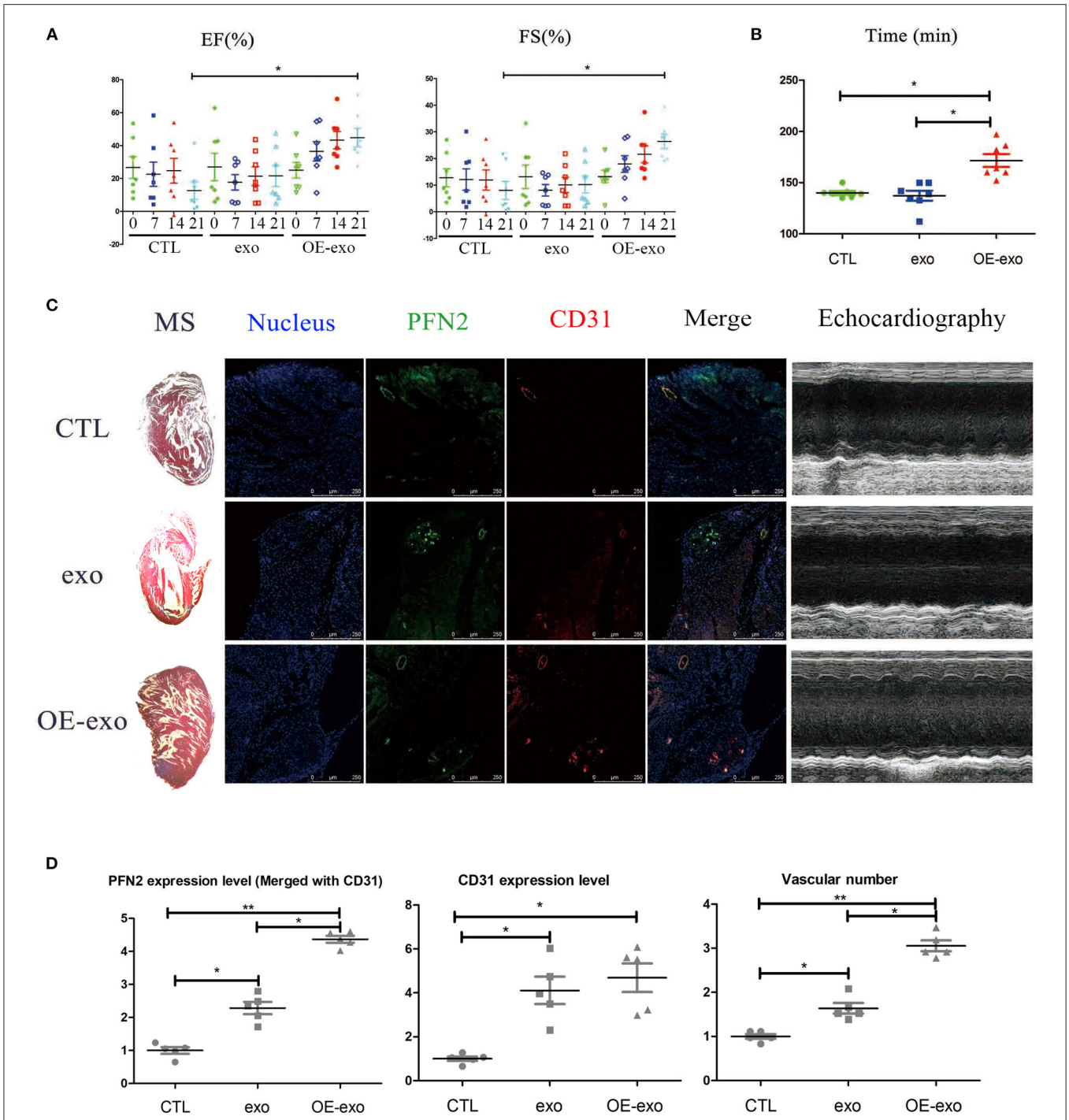

FIGURE 2 | Exosomal PFN2 repairs infarction in mouse with MI and restores cardiac function. **(A)** The cardiac function of mouse with MI as evaluated by type-B ultrasonic test EF and FS after treatment with exosomes demonstrated the benefit to MI impairment. **(B)** Physical fitness was evaluated by fatigue test after treatment with exosomes in mouse with MI which displayed significant improvement of heart function, $n = 7$. **(C)** Infarction volume (Masson's staining) decreased and PFN2 (green)/CD31 (red) staining increased in heart tissue of mouse with MI after treatment with exosomes. **(D)** Statistical results of **(C)**. $n = 3$, normalized to control. $^*p < 0.05$, one-way ANOVA (Tukey).

OE-exo-injected mice (**Figure 2B**). These data indicated that OE-exo injection could improve global cardiac function. Masson's staining, echocardiography and Immunofluorescence staining results showed decreased infarction volume and increased vasculature as well as PFN2 (merged with CD31) levels in the heart vessels of OE-exo-injected mice with MI (**Figures 2C,D**).

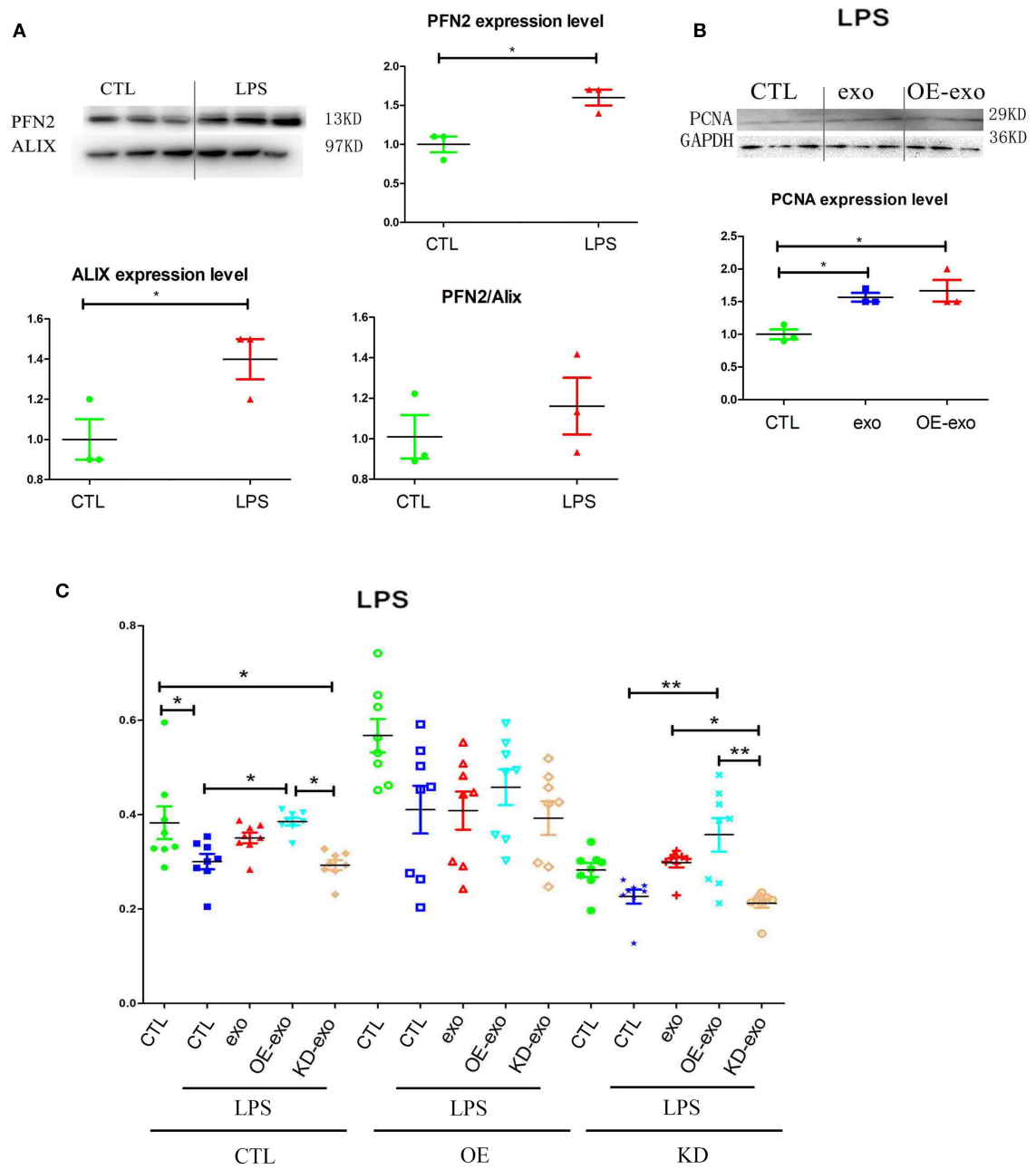

FIGURE 3 | PFN2 protects ECs after LPS treatment. **(A)** PFN2 and Alix expression levels in LPS-treated EC exosomes, $n = 3$, normalized to control. **(B)** PCNA expression levels of ECs under LPS stimulus after treatment with various exosomes, $n = 3$, normalized to control. **(C)** Viability of ECs under LPS stimulation after treatment with various exosomes. $n = 8$. $^*p < 0.05$, one-way ANOVA (Tukey).

Together, these results demonstrate that exosomal PFN2 treatment effectively promotes the recovery of cardiac function.

Exosomal PFN2 Protects Endothelial Cells Against Inflammation

Since PFN2 and exosomal PFN2 enhance the proliferation and migration of ECs, we hypothesized that PFN2 might protect ECs from inflammatory stimulus. First, our results showed that LPS stimulation increased the levels of both PFN2 and the exosomes marker Alix, indicating elevated exosomes secretion by ECs after LPS treatment (**Figure 3A**).

When HUVECs were treated with exo, OE-exo, or KD-exo under LPS stimulus, proliferation of the cells increased in the

OE-exo group compared to that in the exo group (**Figures 3B,C**). Compared to normal cells, LPS could block the proliferation of HUVECs (**Figure 3B**), but this blocking effect could be reduced by exo, especially the exosomes from OE cells, while KD-exo had limited effects. Overexpression of PFN2 could partially prevent the blocking of proliferation induced by LPS treatment in ECs (**Figure 3B**). Taken together, our results suggest that exosomal PFN2 could increase the viability of ECs after LPS treatment.

Exosomal PFN2 Increases Angiogenic Ability *in vitro* and *in vivo*

To determine whether exosomal PFN2 promotes angiogenesis, we first overexpressed the PFN2 in the endothelial cells (**Supplementary Figure 2**) followed by isolation of the exosomes. We labeled OE-exo with Dil (red) and co-cultured them with HUVECs to explore if exosomes could be internalized by ECs. Next, we treated the endothelial cells with the exosomes carrying overexpressed PFN2.

We isolated exosomes from EC culture medium and identified them by TEM and western blotting. We detected the secretion of PFN2-containing exosomes by ECs (**Figures 4A,B**); the exosomes secreted by OE-ECs had significantly higher PFN2 protein levels than the control ECs (**Figure 4B**) ($p = 0.042$). And the results showed internalization of OE-exo into the perinuclear compartment in HUVECs (**Figure 4C**). Then the effect of exosomes isolated from normal ECs (exo), and PFN2-overexpressing ECs (OE-exo) on the proliferation of ECs was investigated. The results showed that the level of PCNA increased in ECs in the OE-exo group ($p = 0.048$) compared to the exo group (**Figure 4D**).

However, when ECs were directly treated with PFN2 protein, it could not increase the proliferation and migration of ECs (**Supplementary Figure 3**), implying that exosomes are crucial for PFN2-induced angiogenic ability in ECs.

Larval zebrafish are commonly used in vascular research because they are transparent, and their vessels can be visualized directly. We explored the effect of OE-exo on angiogenesis in zebrafish. The results showed increased angiogenesis in larval zebrafish after treatment with exosomes, and OE-exo showed the highest effect (**Figure 4E**). These data suggest that transportation of PFN2 by exosomes increases HUVEC proliferation and migration as well as angiogenesis.

Elevation of PFN2 Is Associated With Vascular Development and Promotes the Tube Formation

To understand the relationship between PFN2 and angiogenesis, we explored the role of PFN2 in gerbil embryo development using VEGFA as a positive control. The results showed that both PFN2 and VEGFA reached maximal expression levels on day 10 of the embryo stage (**Figure 5A**). Since day 10 (embryo) is a critical time point for vascular development, this result shows the important association of PFN2 with vascular formation.

To investigate the role of PFN2 in angiogenesis and its influence on the proliferation and migration of both venous and arterial ECs, we established PFN2 overexpression (OE) and knockdown (KD) EC lines using HUVECs (venous ECs) and RBMECs (arterial ECs). PFN2 RNA expression (**Supplementary Figure 2A**) and protein levels (**Supplementary Figure 2B**) increased significantly in OE cells, with a significant decrease in KD cells. We performed experiments using PFN2-OE and PFN2-KD in both HUVECs and RBMECs by RTCA analysis (**Figure 5B**). The results showed that OE-HUVECs exhibited greater proliferation and migration ability ($p = 0.044$; $p = 0.035$), while KD-HUVECs showed reduced proliferation ($p = 0.037$) and migration ($p = 0.030$). Similar results were observed in OE-RBMECs ($p = 0.040$; $p = 0.038$) as well as KD-RBMECs ($p = 0.040$ and $p = 0.029$, respectively). The results of the tube formation test demonstrated that compared to the control and KD-ECs, OE-ECs showed a significantly increased tube length ($p = 0.038$) (**Figure 5C**). These results indicate that PFN2 could significantly increase the proliferation, migration and the angiogenic ability of ECs.

PFN2 Regulates Angiogenesis via the PI3K and ERK Signaling Pathways

We further explored the potential signaling pathways through which PFN2 was involved in angiogenesis. We identified the regulatory relationship between angiogenesis-related proteins and PFN2. When PI3K was inhibited, PFN2 expression level was reduced ($p = 0.024$), while PFN2 overexpression increased the expression of ERK ($p = 0.025$) and its knockdown decreased ERK expression ($p = 0.031$) (**Figures 6A,B**). However, VEGFA had no influence on PFN2 levels in HUVECs. Similarly, PFN2 overexpression or knockdown also had no effect on VEGFA levels in ECs (**Supplementary Figure 4**).

Importantly, we found ERK (merged with PFN2) levels were increased in the post-MI murine hearts treated with OE-exo (**Figures 6C,D**).

These data demonstrate that PFN2 promotes angiogenesis through the PI3K-PFN2-ERK axis, and is not associated with VEGFA. Moreover, we performed a rescue experiment to determine whether the PI3K-PFN2-ERK axis contributed to EC angiogenesis. PI3K or ERK inhibition in OE-EC cells was mimicked by LY294002 or HY-50846, respectively. These data further confirm that PFN2 enhances EC angiogenesis through the PI3K-PFN2-ERK axis (**Graphical Abstract**).

DISCUSSION

The present study, for the first time, demonstrates an increased level of serum PFN2 and exosomal PFN2 in patients and animals with MI, which positively correlated with bFGF and VEGFA levels. PFN2 and exosomal PFN2 impact the angiogenic ability of ECs *in vitro*, and exosomal PFN2 treatment significantly increased the vessel number in zebrafish *in vivo*. More importantly, endothelial exosomal PFN2 dramatically improved cardiac function and physical motion in mice with

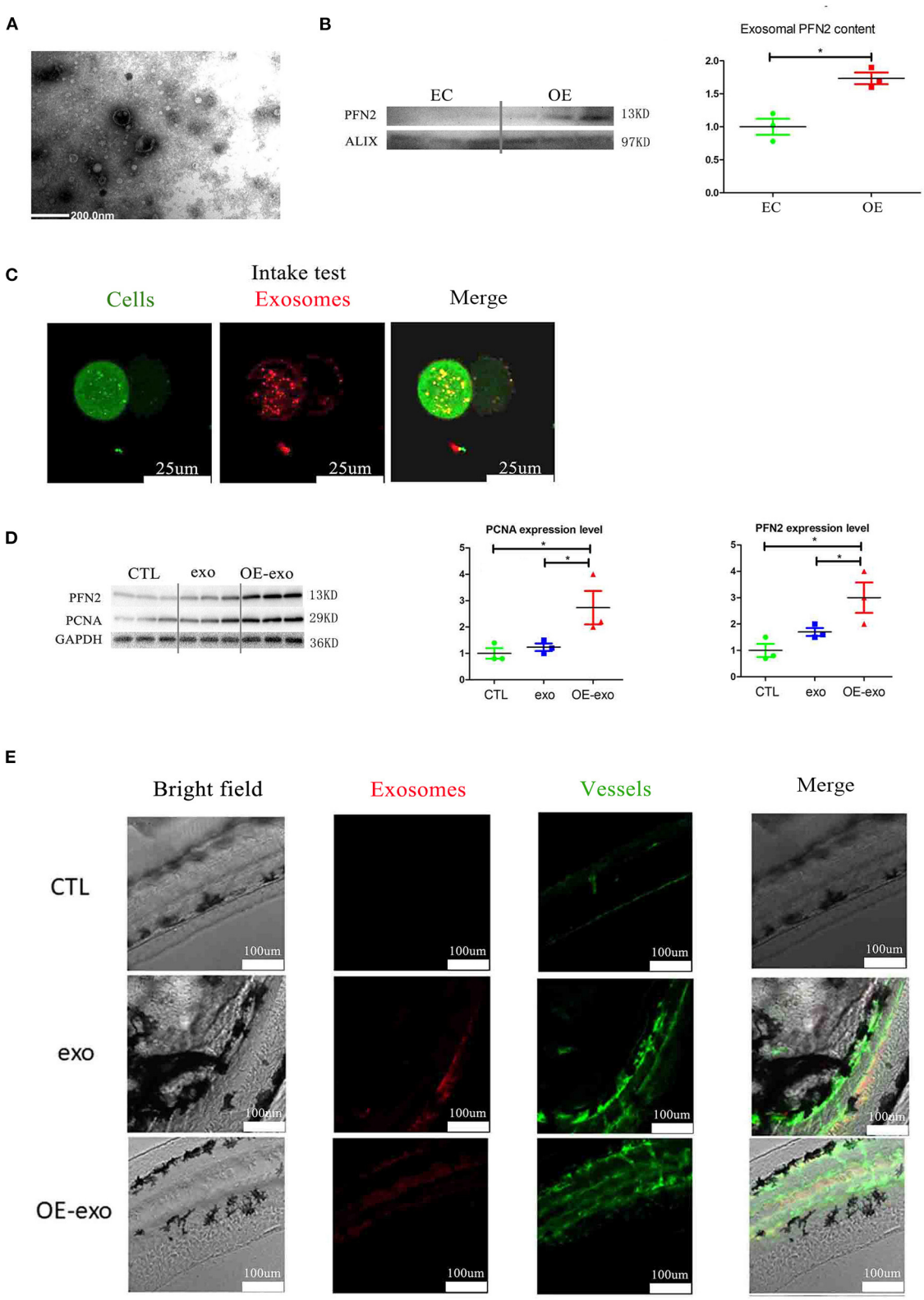

FIGURE 4 | Exosomal PFN2 enhances the proliferation ability of ECs and OE-exo treated zebrafish showed significantly increased vessel number than exo and control. **(A)** The exosomes secreted from ECs were identified by electron microscopy. **(B)** PFN2 expression in exosomes ($n = 3$, the expression levels were normalized

(Continued)

FIGURE 4 | to control). **(C)** Exosomes could be internalized by ECs. **(D)** PFN2 and PCNA expression levels in CTL, exosomes from normal ECs (exo), PFN2-overexpressing ECs (OE-exo), and PFN2 knockdown ECs (KD-exo), $n = 3$, and the expression levels were normalized to control. **(E)** OE-exo-treated zebrafish showed significantly increased vessel number than exo and control. Exo, exosomes from normal ECs; OE-exo, exosomes from PFN2-overexpressing ECs; CTL, PBS as control. $^*p < 0.05$, one-way ANOVA (Tukey).

MI, thereby repairing MI injury. It is known that current clinical treatments for MI aim to alleviate symptoms by surgical interventions and by dissolving arterial blockage by injection of thrombolytic or clot-dissolving drugs. However, due to the patient's clinical condition or limitation of available technology, a significant number of MI cases would be ineligible to receive therapy either by surgical interventions or by clearance of arterial blockage (32). As a result, the development of advanced strategies based on improving angiogenesis in some cases is critical to prevent or decrease MI injury (33, 34). Our results which focus on enhancing the proliferative and migratory ability of ECs by endothelial exosomal PFN2 may be a promising strategy for therapeutic angiogenesis treatment for MI. Since endothelial exosomes are relatively safe, our current strategy is feasible and efficient for future clinical treatment of MI.

PFN2 is a member of the profilin family and shares 80% similarity with PFN1. We selected PFN2 due to its association with variations in the circle of Willis (35). An earlier report described that PFN2 is specifically expressed in neuronal cells and kidney cells (36). Unlike reports on other profilin family members such as PFN1, studies on PFN2 are quite few and are mainly related to tumors (37, 38). Studies on the role of PFN2 in angiogenesis are rare. Very recently, we found that exosomal PFN2 from small cell lung cancer (SCLC) cells could promote the growth of these cells, as well as significantly improve the proliferation, migration, and tube formation of ECs (37). Furthermore, we found that PFN2 reached maximum levels in 10-day gerbil embryos, which is the critical vascular development time point in animals. To explore the effect of PFN2 on angiogenesis, we showed that overexpression of PFN2 enhanced the proliferative, migratory, and tube formation abilities of ECs. Moreover, endothelial exosomal PFN2 ameliorated cardiac function after MI. The effect of PFN2 on angiogenesis explored in the current study is similar to PFN1, which is expected to be a new target for the treatment of MI as reported in a recent study (39). Our current results partly corroborate the findings in this report, but more adequately confirmed that exosomal PFN2 could improve angiogenesis and thereby restore cardiac function. We showed that the PFN2-enriched exosomes from ECs increased the number of vessels in zebrafish, a compelling evidence that PFN2 may be regarded as a novel angiogenic molecule. Moreover, our study revealed that serum PFN2 levels increased in patients, rats, mice, and pigs, with MI accompanied with increased levels of VEGFA and bFGF, well-known growth factors for angiogenesis (28, 29), suggesting that PFN2 might be an effective complementary marker for collateral vessel development in MI. We monitored the dynamic changes in PFN2, exosomes, and exosomal PFN2 after coronary artery occlusion, all of which increased in the serum of rats with MI and reached maximal exosomes numbers earlier than the exosomal PFN2, and PFN2. Thus, we established 7-days post-MI as the time point for injection of OE-exo for maximum exosomal PFN2 expression. The above strategy using OE-exo resulted in a comparable, suitable and efficient therapy for mice with MI.

Several molecular pathways are involved in angiogenesis during MI repair (40, 41). VEGFA is the most common contributor to angiogenesis and manifests cardioprotective effects in the repair of infarcted heart (40, 42). Therefore, we explored whether the angiogenic function of PFN2 was via the VEGFA pathway. However, our results illustrated that overexpression or knockdown of PFN2 in ECs had no impact on the level of VEGFA, and vice versa (**Supplementary Figure 3**). These results showed that PFN2 was involved in angiogenesis independent of the VEGFA pathway in ECs. However, these findings are different from that reported by Tang YN et al. where they observed that PFN2 promoted tumor growth of non-small cell lung cancer by PFN2-SMAD2/3-VEGFA pathway (36). Further, our investigation regarding the molecular mechanism indicated that the PI3K-PFN2-ERK axis is involved in PFN2-mediated angiogenesis. These data are consistent with our work in SCLC which showed that exosomal PFN2 from SCLC cells activated Smad2/3 in these cells and pERK in ECs. Interestingly, Hao P et al. reported significantly higher PFN1 levels in the heart tissues of rats with MI than in control animals, and together with pERK levels positively correlated with the levels of CK-MB, EMP, and others (43). Our present results preliminarily confirm that PFN2 could enhance ERK levels as well as suggests a novel mechanism that affects EC angiogenesis by the PFN2-ERK axis.

As an emerging therapeutic candidate for MI treatment, exosomes have been described to mediate local and distant micro-communication between cardiomyocytes and endothelial cells (44). Todorova et al. reported that exosomes were involved in EC proliferation, migration, sprouting, branching, and tube formation (17). Accumulating literature has proved that the exosomes involved in the repair of MI, as an angiogenic mediator, could be secreted from bone marrow cells (45), cardiomyocytes (46), and endothelial progenitor cells (47). Exosome cargos vary from miRNAs (48), LncRNAs (49), and proteins (19). It has been reported that cardiomyocytes and endothelial cells could interact or communicate with exosomes and promote angiogenesis in ECs (50). Furthermore, targeting endothelial exosomes is beneficial for the prevention of cardiovascular diseases (51). Considering that PFN2 is an intracellular protein, we hypothesized that it may need a medium to be delivered from donor cells to recipient cells. As we expected, PFN2-enriched exosomes (OE-exo) derived from ECs could promote angiogenesis *in vivo* and *in vitro*, repair EC injury under

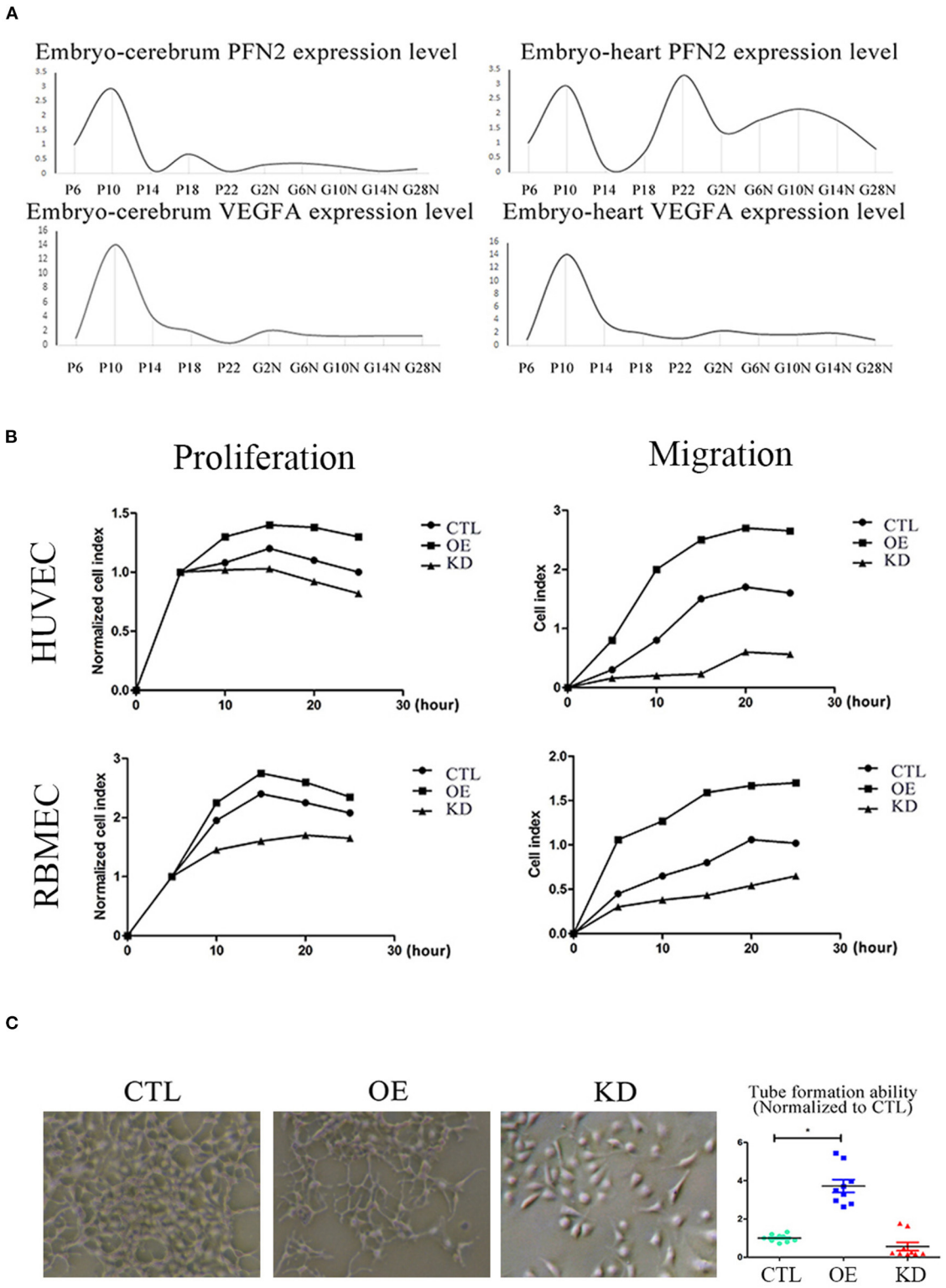

FIGURE 5 | PFN2 promotes proliferation and migration of ECs, as well as tube formation and reaches the maximum level in 10-day embryo. **(A)** The mRNA levels of PFN2 and VEGFA at different developmental stages of gerbils ($n = 15$) embryo (prenatal), brain and heart (postnatal). **(B)** PFN2 significantly promoted proliferation of HUVECs ($n = 3$) and RBMECs ($n = 3$), as well as showed a positive effect on migration of HUVECs ($n = 3$) and RBMECs ($n = 3$). **(C)** The tube length in PFN2-overexpressing ECs (OE) was significantly increased than that in blank CTL and PFN2 knockdown ECs (KD), $n = 3$. $^*p < 0.05$, one-way ANOVA and repeated-measures ANOVA (Tukey).

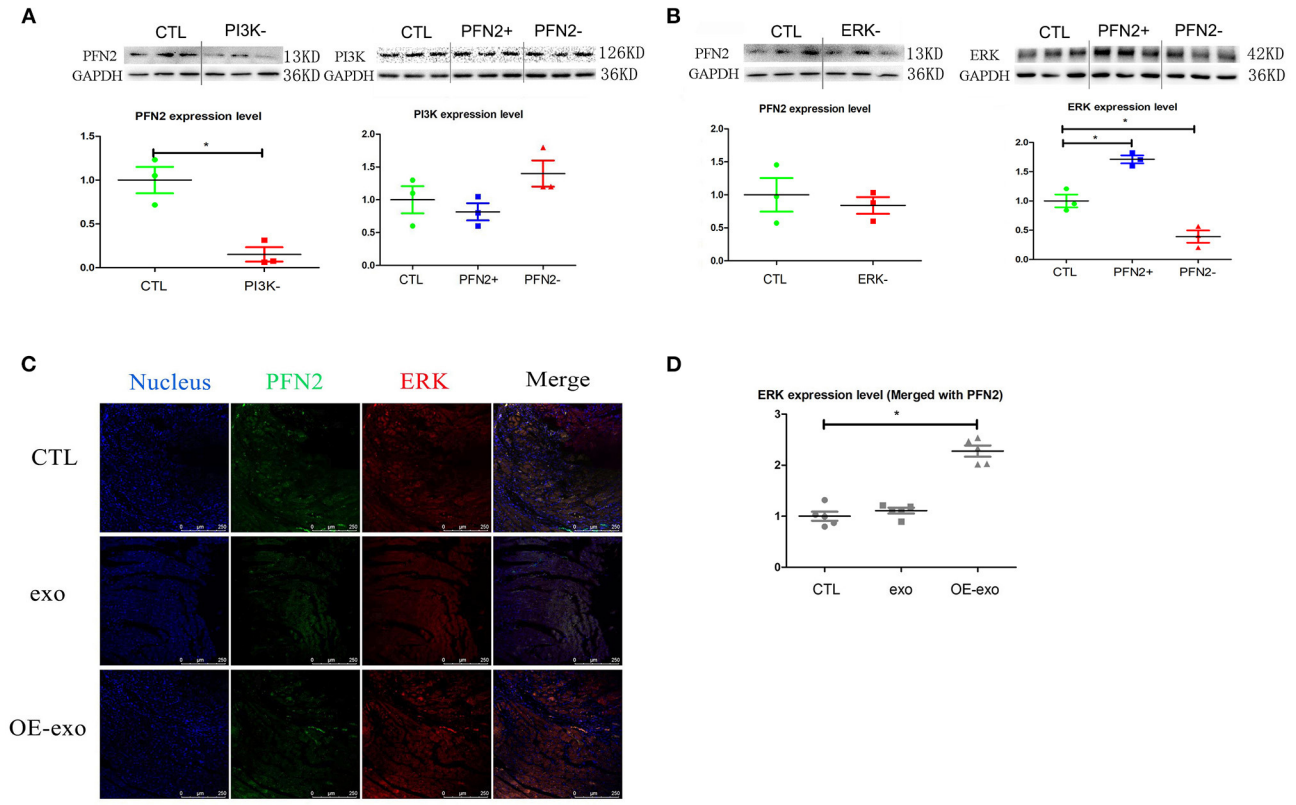

FIGURE 6 | PFN2 involved molecular signaling pathway. **(A)** PFN2 expression level in HUVECs treated with PI3K inhibitor and PI3K expression level in OE and KD, $n = 3$, normalized to control. **(B)** PFN2 expression level in HUVECs treated with ERK inhibitor and ERK expression level in OE and KD, $n = 3$, normalized to control. **(C)** ERK and PFN2 expression levels in the heart tissue of MI mice treated with different exosomes, $n = 3$, normalized to control. **(D)** Statistical result of **(C)**. $^*p < 0.05$, Student's *t*-test and one-way ANOVA (Tukey).

inflammatory stimulus, and significantly attenuate MI injury. However, in contrast to exosomal PFN2, PFN2 protein could not directly increase, even slightly, the viability and migration of ECs (**Supplementary Figure 3**), implying that exosomes are critical mediators for PFN2-mediated angiogenic ability. Recently studies have provided insights into the exosomal cancer-homing behavior of different tumor cell lines, indicating that exosomes have the ability to target their parental cells (52). In the current study, the exosomes we focused on were from the normal human endothelial cell line, which had a higher target efficiency in angiogenesis than other types of cells. Song et al. reported that extracellular vesicles loaded with miRNA-21 isolated from HEK293T cells could effectively inhibit apoptosis of cardiomyocytes and ECs, therefore used for rescue of MI, showing no inflammation with 293T-exosomes (53). Our endothelial cell-derived exosomes might have more biological safety. Moreover, OE-exo from the EC line is available more readily and has less immunological risk than exosomes from explant-derived cardiac stromal cells from heart failure patients and normal donor hearts (54). Taken together, this study provides a new insight into the role of exosomes and for the first time confirms the potential use of endothelial OE-PFN2-exo in treating myocardial infarction (**Graphical Abstract**).

CONCLUSIONS

In summary, PFN2 and endothelial exosomal PFN2 promoted EC angiogenic ability and protected ECs from inflammation, consequently alleviating infarction and enhancing cardiac function in MI, mediated by the PI3K-PFN2-ERK axis. This study, for the first time, showed that PFN2 plays a role in angiogenesis and that endothelial exosomal PFN2 could be a prospective therapeutic strategy for treating MI.

DATA AVAILABILITY STATEMENT

The raw data supporting the conclusions of this article will be made available by the authors, without undue reservation.

ETHICS STATEMENT

The studies involving human participants were reviewed and approved by Ethics Committee of Anzhen Hospital. The patients/participants provided their written informed consent to participate in this study. The animal study was reviewed

and approved by Animal Experiments and Experimental Animal Welfare Committee of Capital Medical University.

AUTHOR CONTRIBUTIONS

ZL, XH, ZC, and XD designed the research studies and wrote the manuscript. ZL, XH, KC, FY, WT, QZ, HY, HC, BZ, and YW conducted the experiments. ZL, XH, KC, and HC acquired the data. ZL and XH analyzed the data. ZL, XH, QZ, HY, and YW collected clinical samples and information. All authors contributed to the article and approved the submitted version.

FUNDING

This study was funded by the National Natural Science Foundation of China (Nos. 32070531, 31970512).

SUPPLEMENTARY MATERIAL

The Supplementary Material for this article can be found online at: https://www.frontiersin.org/articles/10.3389/fcvm.2022.781753/full#supplementary-material

REFERENCES

1. *WHO Global Health Estimates 2016: Deaths by Cause, Age, Sex, by Country and by Region, 2000-2016*. Available online at: http://www.who.int/healthinfo/global_burden_disease/estimates/en/
2. Swirski FK, Nahrendorf M. Leukocyte behavior in atherosclerosis, myocardial infarction, heart failure. *Science.* (2013) 339:161–6. doi: 10.1126/science.1230719
3. Heusch G, Libby P, Gersh B, Yellon D, Böhm M, Lopaschuk G, et al. Cardiovascular remodelling in coronary artery disease and heart failure. *Lancet.* (2014) 383:1933–43. doi: 10.1016/S0140-6736(14)60107-0
4. Eitel I, Desch S, Fuernau G, Hildebrand L, Gutberlet M, Schuler G, et al. Prognostic significance and determinants of myocardial salvage assessed by cardiovascular magnetic resonance in acute reperfused myocardial infarction. *J Am Coll Cardiol.* (2010) 55:2470–9. doi: 10.1016/j.jacc.2010.01.049
5. Miller TD, Hodge DO, Sutton JM, Grines CL, O'Keefe JH, DeWood MA, et al. Usefulness of technetium-99m sestamibi infarct size in predicting posthospital mortality following acute myocardial infarction. *Am J Cardiol.* (1998) 81:1491–3. doi: 10.1016/S0002-9149(98)00220-3
6. Miller TD, Christian TF, Hopfenspirger MR, Hodge DO, Gersh BJ, Gibbons J, et al. Infarct size after acute myocardial infarction measured by quantitative tomographic 99mTc sestamibi imaging predicts subsequent mortality. *Circulation.* (1995) 92:334–41. doi: 10.1161/01.CIR.92.3.334
7. Metra M, Teerlink JR. Heart failure. *Lancet.* (2017) 390:1981–95. doi: 10.1016/S0140-6736(17)31071-1
8. van der Laan AM, Nahrendorf M, Piek JJ. Healing and adverse remodelling after acute myocardial infarction: role of the cellular immune response. *Heart.* (2012) 98:1384–90. doi: 10.1136/heartjnl-2012-301623
9. DeWood MA, Spores J, Notske R, Mouser LT, Burroughs R, Golden MS, et al. Prevalence of total coronary occlusion during the early hours of transmural myocardial infarction. *N Engl J Med.* (1980) 303:897–902. doi: 10.1056/NEJM198010163031601
10. Risau W. Mechanisms of angiogenesis. *Nature.* (1997) 386:671–4. doi: 10.1038/386671a0
11. Zhu JZ, Bao XY, Zheng Q, Tong Q, Zhu PC, Zhuang Z, et al. Buyang Huanwu decoction exerts cardioprotective effects through targeting angiogenesis via Caveolin-1/VEGF signaling pathway in mice with acute myocardial infarction. *Oxid Med Cell Longev.* (2019) 2019:4275984. doi: 10.1155/2019/4275984
12. Liao Q, Qu S, Tang LX, Li LP, He DF, Zeng CY, et al. Irisin exerts a therapeutic effect against myocardial infarction via promoting angiogenesis. *Acta Pharmacol Sin.* (2019) 40:1314–21. doi: 10.1038/s41401-019-0230-z
13. Cui G, Xin Q, Tseng HHL, Hoi MP, Wang Y, Yang B, et al. A novel Ca(2+) current blocker promotes angiogenesis and cardiac healing after experimental myocardial infarction in mice. *Pharmacol Res.* (2018) 134:109–17. doi: 10.1016/j.phrs.2018.06.005
14. Zhang G, Zhu Z, Wang H, Yu Y, Chen W, Waqas A, et al. Exosomes derived from human neural stem cells stimulated by interferon gamma improve therapeutic ability in ischemic stroke model. *J Adv Res.* (2020) 24:435–45. doi: 10.1016/j.jare.2020.05.017
15. Pham TP, Boon RA. Exosomes non-coding RNA. The healers of the heart? *Cardiovasc Res.* (2020) 116:258–9. doi: 10.1093/cvr/cvz190
16. Barile L, Moccetti T, Marbán E, Vassalli G. Roles of exosomes in cardioprotection. *Eur Heart J.* (2017) 38:1372–9. doi: 10.1093/eurheartj/ehw304
17. Todorova D, Simoncini S, Lacroix R, Sabatier F, Dignat-George F. Extracellular vesicles in angiogenesis. *Circ Res.* (2017) 120:1658–73. doi: 10.1161/CIRCRESAHA.117.309681
18. Wang J, Sun X, Zhao J, Yang Y, Cai X, Xu J, et al. Exosomes: a novel strategy for treatment and prevention of diseases. *Front Pharmacol.* (2017) 8:300. doi: 10.3389/fphar.2017.00300
19. Vicencio JM, Yellon DM, Sivaraman V, Das D, Boi-Doku C, Arjun S, et al. Plasma exosomes protect the myocardium from ischemia-reperfusion injury. *J Am Coll Cardiol.* (2015) 65:1525–36. doi: 10.1016/j.jacc.2015.02.026
20. Sahoo S, Mathiyalagan P, Hajjar RJ. Pericardial fluid exosomes: a new material to treat cardiovascular disease. *Mol Therapy.* (2017) 25:568–9. doi: 10.1016/j.ymthe.2017.02.002
21. van Balkom BW, de Jong OG, Smits M, Brummelman J, den Ouden K, de Bree PM, et al. Endothelial cells require miR-214 to secrete exosomes that suppress senescence and induce angiogenesis in human and mouse endothelial cells. *Blood.* (2013) 121:3997–4006, s1–15. doi: 10.1182/blood-2013-02-478925
22. Khadka DK, Liu W, Habas R. Non-redundant roles for Profilin2 and Profilin1 during vertebrate gastrulation. *Dev Biol.* (2009) 332:396–406. doi: 10.1016/j.ydbio.2009.06.008
23. Olson EN, Nordheim A. Linking actin dynamics and gene transcription to drive cellular motile functions. *Nat Rev Mol Cell Biol.* (2010) 11:353–65. doi: 10.1038/nrm2890
24. Zhang H, Yang W, Yan J, Zhou K, Wan B, Shi P, et al. Loss of profilin 2 contributes to enhanced epithelial-mesenchymal transition and metastasis of colorectal cancer. *Int J Oncol.* (2018) 53:1118–28. doi: 10.3892/ijo.2018.4475
25. Tang YN, Ding WQ, Guo XJ, Yuan XW, Wang DM, Song G, et al. Epigenetic regulation of Smad2 and Smad3 by profilin-2 promotes lung cancer growth and metastasis. *Nat Commun.* (2015) 6:8230. doi: 10.1038/ncomms9230
26. Cao Q, Liu Y, Wu Y, Hu C, Sun L, Wang J, et al. Profilin 2 promotes growth, metastasis, and angiogenesis of small cell lung cancer through cancer-derived exosomes. *Aging.* (2020) 12:25981–99. doi: 10.18632/aging.202213
27. Li Z, Wang S, Huo X, Yu H, Lu J, Zhang S, et al. Cystatin C expression is promoted by VEGFA blocking, with inhibitory effects on endothelial cell angiogenic functions including proliferation, migration, and chorioallantoic membrane angiogenesis. *J Am Heart Assoc.* (2018) 7:e009167. doi: 10.1161/JAHA.118.009167
28. Osadnik T, Strzelczyk JK, Lekston A, Reguła R, Bujak K, Fronczek M, et al. The association of functional polymorphisms in genes encoding growth factors for endothelial cells and smooth muscle cells with the severity of coronary artery disease. *BMC Cardiovasc Disord.* (2016) 16:218. doi: 10.1186/s12872-016-0402-4
29. Sellke FW, Wang SY, Stamler A, Lopez JJ, Li J, Li J, et al. Enhanced microvascular relaxations to VEGF and bFGF in chronically ischemic porcine myocardium. *Am J Physiol.* (1996) 271(2 Pt 2):H713–20. doi: 10.1152/ajpheart.1996.271.2.H713
30. Arvanitis M, Qi G, Bhatt DL, Post WS, Chatterjee N, Battle A, et al. Linear and nonlinear Mendelian randomization analyses of the association between diastolic blood pressure and cardiovascular events: the J-curve revisited.

Circulation. (2021) 143:895–906. doi: 10.1161/CIRCULATIONAHA.120.049819
31. Pöyhönen P, Kylmälä M, Vesterinen P, Kivistö S, Holmström M, Lauerma K, et al. Peak CK-MB has a strong association with chronic scar size and wall motion abnormalities after revascularized non-transmural myocardial infarction - a prospective CMR study. *BMC Cardiovasc Disord.* (2018) 18:27. doi: 10.1186/s12872-018-0767-7
32. Lu L, Liu M, Sun R, Zheng Y, Zhang P. Myocardial infarction: symptoms and treatments. *Cell Biochem Biophys.* (2015) 72:865–7. doi: 10.1007/s12013-015-0553-4
33. Lopez JJ, Laham RJ, Stamler A, Pearlman JD, Bunting S, Kaplan A, et al. VEGF administration in chronic myocardial ischemia in pigs. *Cardiovasc Res.* (1998) 40:272–81. doi: 10.1016/S0008-6363(98)00136-9
34. Zhou NQ, Liu N, Li P, Ping S, Peng QS, Shi D, et al. Tert-butylhydroquinone promotes angiogenesis and improves heart functions in rats after myocardial infarction. *Clin Exp Hypertens.* (2017) 39:402–8. doi: 10.1080/10641963.2016.1259322
35. Li Z, Huo X, Zhang S, Lu J, Li C, Guo M, et al. Selection of genes associated with variations in the Circle of Willis in gerbils using suppression subtractive hybridization. *PLoS ONE.* (2015) 10:e0127355. doi: 10.1371/journal.pone.0127355
36. Di Nardo A, Gareus R, Kwiatkowski D, Witke W. Alternative splicing of the mouse profilin II gene generates functionally different profilin isoforms. *J Cell Sci.* (2000) 113(Pt 21):3795–803. doi: 10.1242/jcs.113.21.3795
37. Kim MJ, Lee YS, Han GY, Lee HN, Ahn C, Kim W, et al. Profilin 2 promotes migration, invasion, and stemness of HT29 human colorectal cancer stem cells. *Biosci Biotechnol Biochem.* (2015) 79:1438–46. doi: 10.1080/09168451.2015.1043118
38. Zhou K, Chen J, Wu J, Xu Y, Wu Q, Yue J, et al. Profilin 2 promotes proliferation and metastasis of head and neck cancer cells by regulating PI3K/AKT/β-catenin signaling pathway. *Oncol Res.* (2019) 27:1079–88. doi: 10.3727/096504019X15579146061957
39. Fan Y, Arif A, Gong Y, Jia J, Eswarappa SM, Willard BL, et al. Stimulus-dependent phosphorylation of profilin-1 in angiogenesis. *Nat Cell Biol.* (2012) 14:1046–56. doi: 10.1038/ncb2580
40. Du Y, Ge Y, Xu Z, Aa N, Gu X, Meng H, et al. Hypoxia-inducible factor 1 alpha (HIF-1α)/vascular endothelial growth factor (VEGF) pathway participates in angiogenesis of myocardial infarction in muscone-treated mice: preliminary study. *Med Sci Monit.* (2018) 24:8870–77. doi: 10.12659/MSM.912051
41. Li SN, Li P, Liu WH, Shang JJ, Qiu SL, Zhou MX, et al. Danhong injection enhances angiogenesis after myocardial infarction by activating MiR-126/ERK/VEGF pathway. *Biomed Pharmacother.* (2019) 120:109538. doi: 10.1016/j.biopha.2019.109538
42. Zou J, Fei Q, Xiao H, Wang H, Liu K, Liu M, et al. VEGF-A promotes angiogenesis after acute myocardial infarction through increasing ROS production and enhancing ER stress-mediated autophagy. *J Cell Physiol.* (2019) 234:17690–703. doi: 10.1002/jcp.28395
43. Hao P, Fu K, Wang SP, Ma CY, Xu ZY, Cao FY, et al. Expression of profilin-1 in endothelial cells of rats with acute myocardial infarction. *Eur Rev Med Pharmacol Sci.* (2017) 21:1318–22.
44. Sahoo S, Losordo DW. Exosomes and cardiac repair after myocardial infarction. *Circ Res.* (2014) 114:333–44. doi: 10.1161/CIRCRESAHA.114.300639
45. Huang P, Wang L, Li Q, Xu J, Xu J, Xiong Y, et al. Combinatorial treatment of acute myocardial infarction using stem cells and their derived exosomes resulted in improved heart performance. *Stem Cell Res Therapy.* (2019) 10:300. doi: 10.1186/s13287-019-1353-3
46. Ribeiro-Rodrigues TM, Laundos TL, Pereira-Carvalho R, Batista-Almeida D, Pereira R, Coelho-Santos V, et al. Exosomes secreted by cardiomyocytes subjected to ischaemia promote cardiac angiogenesis. *Cardiovasc Res.* (2017) 113:1338–50. doi: 10.1093/cvr/cvx118
47. Chang TY, Tsai WC, Huang TS, Su SH, Chang CY, Ma HY, et al. Dysregulation of endothelial colony-forming cell function by a negative feedback loop of circulating miR-146a and−146b in cardiovascular disease patients. *PLoS ONE.* (2017) 12:e0181562. doi: 10.1371/journal.pone.0181562
48. Emanueli C, Shearn AI, Angelini GD, Sahoo S. Exosomes and exosomal miRNAs in cardiovascular protection and repair. *Vasc Pharmacol.* (2015) 71:24–30. doi: 10.1016/j.vph.2015.02.008
49. Chang W, Wang J. Exosomes and their noncoding RNA cargo are emerging as new modulators for diabetes mellitus. *Cells.* (2019) 8:853. doi: 10.3390/cells808085350
50. Garcia NA, Ontoria-Oviedo I, González-King H, Diez-Juan A, Sepúlveda P. Glucose starvation in cardiomyocytes enhances exosome secretion and promotes angiogenesis in endothelial cells. *PLoS ONE.* (2015) 10:e0138849. doi: 10.1371/journal.pone.0138849
51. Jia G, Sowers JR. Targeting endothelial exosomes for the prevention of cardiovascular disease. *Biochim Biophys Acta.* (2020) 1866:165833. doi: 10.1016/j.bbadis.2020.165833
52. Qiao L, Hu S, Huang K, Su T, Li Z, Vandergriff A, et al. Tumor cell-derived exosomes home to their cells of origin and can be used as Trojan horses to deliver cancer drugs. *Theranostics.* (2020) 10:3474–87. doi: 10.7150/thno.39434
53. Song Y, Zhang C, Zhang J, Jiao Z, Dong N, Wang G, et al. Localized injection of miRNA-21-enriched extracellular vesicles effectively restores cardiac function after myocardial infarction. *Theranostics.* (2019) 9:2346–60. doi: 10.7150/thno.29945
54. Qiao L, Hu S, Liu S, Zhang H, Ma H, Huang K, et al. microRNA-21-5p dysregulation in exosomes derived from heart failure patients impairs regenerative potential. *J Clin Investig.* (2019) 129:2237–50. doi: 10.1172/JCI123135

Conflict of Interest: The authors declare that the research was conducted in the absence of any commercial or financial relationships that could be construed as a potential conflict of interest.

Publisher's Note: All claims expressed in this article are solely those of the authors and do not necessarily represent those of their affiliated organizations, or those of the publisher, the editors and the reviewers. Any product that may be evaluated in this article, or claim that may be made by its manufacturer, is not guaranteed or endorsed by the publisher.

Copyright © 2022 Li, Huo, Chen, Yang, Tan, Zhang, Yu, Li, Zhou, Chen, Zhao, Wang, Chen and Du. This is an open-access article distributed under the terms of the Creative Commons Attribution License (CC BY). The use, distribution or reproduction in other forums is permitted, provided the original author(s) and the copyright owner(s) are credited and that the original publication in this journal is cited, in accordance with accepted academic practice. No use, distribution or reproduction is permitted which does not comply with these terms.

frontiers | Frontiers in Cardiovascular Medicine

ORIGINAL RESEARCH
published: 25 April 2022
doi: 10.3389/fcvm.2022.821317

NEU1 Regulates Mitochondrial Energy Metabolism and Oxidative Stress Post-myocardial Infarction in Mice *via* the SIRT1/PGC-1 Alpha Axis

Zhen Guo[1,2†], Di Fan[1,2†], Fang-Yuan Liu[1,2†], Shu-Qing Ma[1,2], Peng An[1,2], Dan Yang[1,2], Min-Yu Wang[1,2], Zheng Yang[1,2] and Qi-Zhu Tang[1,2]*

[1] Department of Cardiology, Renmin Hospital of Wuhan University, Wuhan, China, [2] Hubei Key Laboratory of Metabolic and Chronic Diseases, Wuhan, China

OPEN ACCESS

Edited by:
Shijun Wang,
Fudan University, China

Reviewed by:
Jian Cao,
Chinese PLA General Hospital, China
Xiaoping Wang,
Beijing University of Chinese Medicine, China

***Correspondence:**
Qi-Zhu Tang
qztang@whu.edu.cn

[†] These authors have contributed equally to this work

Specialty section:
This article was submitted to Cardiovascular Metabolism, a section of the journal Frontiers in Cardiovascular Medicine

Received: 24 November 2021
Accepted: 22 March 2022
Published: 25 April 2022

Citation:
Guo Z, Fan D, Liu F-Y, Ma S-Q, An P, Yang D, Wang M-Y, Yang Z and Tang Q-Z (2022) NEU1 Regulates Mitochondrial Energy Metabolism and Oxidative Stress Post-myocardial Infarction in Mice via the SIRT1/PGC-1 Alpha Axis. Front. Cardiovasc. Med. 9:821317. doi: 10.3389/fcvm.2022.821317

Objective: Neuraminidase 1 (NEU1) participates in the response to multiple receptor signals and regulates various cellular metabolic behaviors. Importantly, it is closely related to the occurrence and progression of cardiovascular diseases. Because ischemic heart disease is often accompanied by impaired mitochondrial energy metabolism and oxidative stress. The purpose of this study was to investigate the functions and possible mechanisms of NEU1 in myocardial remodeling and mitochondrial metabolism induced by myocardial infarction (MI).

Methods: In this study, the MI-induced mouse mode, hypoxia-treated H9C2 cells model, and hypoxia-treated neonatal rat cardiomyocytes (NRCMs) model were constructed. Echocardiography and histological analysis were adopted to evaluate the morphology and function of the heart at the whole heart level. Western blot was adopted to determine the related expression level of signaling pathway proteins and mitochondria. Mitochondrial energy metabolism and oxidative stress were detected by various testing kits.

Results: Neuraminidase 1 was markedly upregulated in MI cardiac tissue. Cardiomyocyte-specific NEU1 deficiency restored cardiac function, cardiac hypertrophy, and myocardial interstitial fibrosis. What is more, cardiomyocyte-specific NEU1 deficiency inhibited mitochondrial dysfunction and oxidative stress induced by MI. Further experiments found that the sirtuin-1/peroxisome proliferator-activated receptor γ coactivator α (SIRT1/PGC-1α) protein level in MI myocardium was down-regulated, which was closely related to the above-mentioned mitochondrial changes. Cardiomyocyte-specific NEU1 deficiency increased the expression of SIRT1, PGC-1α, and mitochondrial transcription factor A (TFAM); which improved mitochondrial metabolism and oxidative stress. Inhibition of SIRT1 activity or PGC-1α activity eliminated the beneficial effects of cardiomyocyte-specific NEU1 deficiency. PGC-1α knockout mice experiments verified that NEU1 inhibition restored cardiac function induced by MI through SIRT1/PGC-1α signaling pathway.

Conclusion: Cardiomyocyte-specific NEU1 deficiency can alleviate MI-induced myocardial remodeling, oxidative stress, and mitochondrial energy metabolism disorder. In terms of mechanism, the specific deletion of NEU1 may play a role by enhancing the SIRT1/PGC-1α signaling pathway. Therefore, cardiomyocyte-specific NEU1 may provide an alternative treatment strategy for heart failure post-MI.

Keywords: neuraminidase 1, myocardial infarction, mitochondrial metabolism, SIRT1, oxidative stress

INTRODUCTION

Heart failure (HF) is the terminal stage of many cardiovascular diseases (myocardial infarction (MI), arrhythmia), with high morbidity and mortality worldwide, and is a major challenge to human health (1). Despite various treatment strategies such as drug therapy (2), left ventricular assist device (3), artificial heart (4), and heart transplantation (5), the progression of heart failure after MI is still fundamentally irreversible. Among the plethora of mechanisms related to the onset and progression of MI, mitochondria are the most concerned (6–8). Due to the heart's high demand for energy, mitochondria are highly enriched in myocardial tissue, which is essential for the function of the heart (9). Mitochondria plays an important role in ATP production, reactive oxygen formation, cell apoptosis, and signal transduction in the metabolic process of cardiomyocytes. The generation of mitochondrial reactive oxygen species (ROS) is an important early driver of MI damage, but it has been considered to be a non-specific result of the interaction between respiratory chain dysfunction and oxygen in MI (10). In fact, mitochondrial dysfunction is an important predictor of cell death (11). Thus, the involvement of mitochondrial in MI is complex, and a detailed understanding of the pathogenic and reparatory mechanisms triggered by mitochondrial mediators is a prerequisite for the development of mitochondrial-targeted therapies.

Peroxisome proliferator-activated receptor γ coactivator-1α (PGC-1α) is a key booster of mitochondrial function and metabolism. PGC-1α is highly expressed in tissues with high-energy demands (such as heart, and adipose tissue), and regulates downstream signal pathways and mitochondrial oxidative stress-related proteins (such as components of the electron transport system) (12). PGC-1α is abnormally expressed in cardiac hypertrophy, heart failure, chronic cardiomyopathy, etc. (13). The deficiency of PGC-1α promotes mitochondrial dysfunction in the progression of various diseases (14). Mammalian sirtuin 1 (SIRT1) belongs to the sirtuin protein family. It is an enzyme responsible for protein deacetylation in cell regulation. It is closely related to the pathophysiological process of inflammation, mitochondrial biogenesis, cell aging, and subsequent aging (15). Under nutrient-restricted conditions, SIRT1 regulates PGC-1α target genes and is essential in dealing with increased fatty acid oxidation (16). The deficiency of SIRT1 promotes mitochondrial dysfunction and causes dilated cardiomyopathy in mice (17).

The properties of new signal mediators related to MI and mitochondrial function are the key focus for exploring new drug targets to improve clinical outcomes. Neuraminidases (NEUs), also known as sialidase, is a family of enzymes that decompose sialic acid on the cell surface. Four mammalian NEU species (NEU1, NEU2, NEU3, and NEU4) have been identified based on differences in subcellular localization and enzyme properties, of which NEU1 is the most abundant. NEU1 has a catabolic function and participates in the structural and functional regulation of cell receptors (18). Recent research found that neuraminidase 1 (NEU1) colocalizes with some but not all mitochondria within platelets (19). Studies have shown that NEU1 upregulation in infiltrating cardiac monocytes and macrophages leads to heart failure after ischemia-reperfusion by promoting inflammation (20). In addition, plasma neuraminidase activity increased after MI compared with healthy controls (21). NEU1 is a key driver of myocardial hypertrophy, and anti-influenza drugs zanamivir and oseltamivir (viral NEU inhibitors) can significantly alleviate myocardial hypertrophy (22). However, the role of NEU1 in mitochondrial dysfunction in MI remains unknown. Based on limited clues, we hypothesized that NEU1 is involved in mitochondrial function and metabolic changes in MI.

Therefore, this study aims to determine (i) the specific effects (if any) of NEU1 on cardiac function, mitochondrial function, and metabolism post-MI; (ii) what is the mechanism of NEU1 on the changes in cardiac mitochondrial energy metabolism?

METHODS

Animals Experimental Model

All animal management is based on the "Guidelines for the Care and Use of Laboratory Animals" published by the National Institutes of Health (NIH publication number 85–23, revised in 2001), and is supported by the Animal Care and Use Committee of Renmin Hospital of Wuhan University. C57/BL6 mice (8–10 weeks) were purchased from the Institute of Laboratory Animal Science (Beijing, China). After 7 days of adaptation, we use continuous inhalation of 1.5% isoflurane to anesthetize mice, and MI was established as described previous (23). Simply put in order to accurately expose the heart, a left thoracic incision was made in the fifth intercostal space. Permanently ligate the anterior descending branch of the left coronary artery with 6-0 silk thread. In total 4-0 nylon thread is used to suture the skin after ligation, except for ligating the LAD coronary arteries, sham-operated mice used the same procedure. Place these mice in a 37°C constant temperature cage until they recover. According to the manufacturer's manual, 4 weeks before LAD ligation, the adeno-associated virus 9 (AAV9)-targeted to NEU1 and injected directly into the myocardium at three different locations in the ischemic area. The dose was 1×10^{10}

VP (24). Mice were randomized into four groups: Sham + AAV9-shRNA, Sham + AAV9-shNEU1, MI + AAV9-shRNA, and MI + AAV9-shNEU1 groups.

Conditional PGC-1α deletion was generated by crossing PGC-1$\alpha^{flox/flox}$ mice (Cyagen, China) with mice carrying α-MHC-MEM-Cre transgene (Jackson Laboratory, USA). For cardiac specific-knockout of PGC-1α, pharmaceutical-grade tamoxifen dissolved in corn oil was injected into 6-week old mice for five consecutive days (50 mg/kg per day, i.p.). The PCR method was used to identify the genomic DNA of the tail of PGC-1α-cKO mice. Perform functional data and gene expression level analysis in pairs of male a-MHC-PGC-1α-KO (cKO) and male littermates (Cre), PGC-1α knockout male mice (8–10 weeks old) that weighed between 22 and 27g were used in all experiments and maintained a 12/12-h light–dark cycle in a temperature and humidity-controlled room.

Echocardiography

All the mice were anesthetized with 1.5% isoflurane and placed supine on a heating pad (37°C). The echocardiography was performed with MyLab 30CV ultrasound (Biosound Esaote Inc.) with a 10-MHz linear array ultrasound transducer to evaluate the cardiac function of mice after MI or sham treatment (25).

Western Blot

Heart tissues and cultured cardiomyocytes were collected and lysed by RIPA lysis buffer. In a subset of the experiment, the previously described method was used to separate mitochondria and cytoplasmic components in heart tissue samples (26). The same amount of protein was transferred to the PVDF membrane after electrophoresis. The membrane was blocked, and the primary antibody was incubated overnight under 4°C. The primary antibodies used are listed as follows: NEU1(#ab233119; 1:1000, Abcam); Mitofusin 2 (MFN2) (#9482S; 1:1,000, CST); dynamin-related protein 1 (DRP1) (# SC-32898, 1:500, SANTA); SIRT1 (# ab110304, 1:1000, Abcam); PGC-1alpha (# ab191838, 1:1,000, Abcam); transcription factor A, mitochondrial (TFAM) (#7495, 1:1,000, CST); voltage-dependent anion channels (VDAC) (#ab191440, 1:1,000, Abcam);. GAPDH (#2722, 1:1,000, CST). Then incubated with the secondary antibody for 1 h at room temperature. The protein bands were observed using ChemiDoc XRS (Bio-Rad Laboratories, Inc.)+ system with ECL reagents, and the intensity of bands was quantified by using Image J, and the protein abundance was normalized to the levels of GAPDH or VDAC.

Real-Time PCR

Extract total RNA from mouse myocardial tissue or H9C2 cells with TRIzol reagent (Roche, 11667165001). Use 2 μg total RNA and transcript First Stand cDNA Synthesis Kit (Roche, 04897030001) for cDNA synthesis reaction. The LightCycler 480 real-time PCR system (Roche) is used to perform a real-time quantitative PCR reaction with a volume of 20 μl. The gene expression level was normalized to the GAPDH gene expression level, and the relative mRNA level was quantified with the internal control. The primers used are presented as follows: Mice-TGFβ1: 5′-ATCCTGTCCAAACTAAGGCTCG-3′(F), 5′-ACCTCTTTAGCATAGTAGTCCGC-3′(R); Mice-Col1: 5′-CCCAACCCAGAGATCCCATT-3′(F), 5′-GAAGCACAGGAGCAGGTGTAGA-3′(R); Mice-Col3: 5′- GATCAGGCCAGTGGAAATGT-3′(F), 5′-GTGTGTTTCGTGCAACCATC-3′(R);

Mice-GAPDH: 5′- TCATCAACGGGAAGCCCATC-3′(F), 5′- CTCGTGGTTCACACCCATCA-3′(R).

Histological Analysis

Take out the heart and immediately place it in 10% potassium chloride solution, squeeze out the blood in the heart cavity, and place it in 10% formalin. The hearts were dissected into 5 μm slices. Wheat germ agglutinin (WGA) for histopathology to determine the myocyte cross-sectional area (CSA). Picro-Sirius red (PSR) for determining cardiac fibrosis.

Mitochondrial Isolation and Mitochondrial Respiratory Chain Complex Activity

According to the manufacturer's instruction, heart mitochondria was isolated by Tissue Mitochondria Isolation Kit (C3606, Beyotime). The specific activity of complex I (27), complex II (28), complex III (29), and complex IV (30) in myocardial tissues was determined by the methods previously contributed by investigators.

Analysis of Mitochondrial ROS

The MnSOD Assay Kit with WST-8 (Beyotime, S0103) was used to detect the MnSOD activities of fresh heart or NRCMs according to the manufacturer's instructions.

Stain NRCMs with mitochondria-specific superoxide indicator triphenylphosphonium-linked hydroethidium (MitoSOX) (M36008, Thermo Fisher Scientific) to detect the production of mitochondrial superoxide. The mitochondrial subcellular location of MitoSOX was confirmed by co-labeling with 50 nM MitoTracker Green (C1048, Beyotime). ROS production in the fresh heart was assessed by dihydroethidium (DHE) staining (31). A fluorescence microscope (OLYMPUS DX51) and DP2-BSW software (version 2.2) were used to obtain the representative images.

ATP Content

According to the manufacturer's instruction, an ATP content kit (S0026, Beyotime) was used to detect cellular ATP content. ATP level was further normalized to protein content.

Quantification of mtDNA

According to the manufacturer's instructions, use the DNeasy Blood and Tissue Kit (Qiagen, 69504) to collect heart tissue or cells to isolate total DNA. Mitochondrial DNA (mtDNA) was quantified by mitochondrial NADH-ubiquinone oxidoreductase chain 1 (MT-ND1) and nuclear DNA (nDNA) named GAPDH. Mouse primers are presented as follows: MT-ND1: 5′-TCTAATCGCCATAGCCTTCC-3′(F), 5′-GCGTCTGCAAATGGTTGTAA-3′(R); GAPDH: 5′-GTCAAGGCAGAGAACGGGAA-3′(F), 5′-GGTTCACGCCCATCACAAAC-3′(R).

Cell Culture and Treatments

To examine the levels of mitochondrial biogenesis and function *in vitro*, neonatal rat cardiac myocytes (NRCMs) were isolated and cultured in Dulbecco's modified Eagle's/F-12 (11330, Gibco, Grand Island, NY, USA), supplemented with 15% fetal bovine serum (10099, Gibco) as previously described (25). We ordered H9C2 cells from the Cell Bank of the Chinese Academy of Sciences (Shanghai, China) and cultured them in DMEM containing 10% fetal bovine serum and 1% penicillin-streptomycin. There was no mycoplasma contamination in the cells. This study did not use common misidentified cells.

Adenoviral vectors carrying NEU1 small hairpin RNAs (shNEU1) or the scrambled shRNA were used to infect NRCMs or H9C2 cells at an MOI of 100 for 4 h to produce transfected cells with stable NEU1 knockdown expression. NRCMs or H9C2 cells are hypoxic at 1% oxygen concentration to simulate MI injury *in vivo*. To examine the functional role of SIRT1 or PGC-1α *in vitro*, NRCMs or H9C2 cells were treated with SIRT1 inhibitor EX5727 (40 μM, HY-15452, MCE) (32) or PGC-1α inhibitor SR-18292 (10 μM; HY-101491, MCE) (33) was added to the cell medium to determine its inhibitory effects on mitochondrial.

Statistical Analysis

The data were expressed as mean ± SEM. Survival data were analyzed by the Kaplan–Meier method followed by a Mantel–Cox log rank test. Student's unpaired *t*-test was used to compare the two groups. One-way ANOVA followed by Tukey's *post hoc* test was used among multiple groups. $P < 0.05$ indicates that the difference is statistically significant.

RESULTS

NEU1 Expression Was Increased in MI Tissues

First of all, immunoblot showed dramatically elevated NEU1 expression in the mice hearts 3 days after MI, compared with sham-operated controls. Moreover, the NEU1 protein level in infarct area of mouse hearts 3 days after MI increased greater than in the non-infarct area (**Figure 1A**). Similar results were obtained in regard to the effect of MI on mRNA expression of NEU1 (**Figure 1B**). ELISA data further confirmed that MI stimulation increased NEU1 expression in mice hearts (**Figure 1C**). Our finding of elevated NEU1 expression after acute MI model is consistent with previous observations (34). Next, we further investigated confirmed NEU1 expression in the mice hearts 8 weeks after MI. However, for the acute MI model, significant increased NEU1 expression was observed in mice in acutely infarct area, but restore baseline 8 weeks after MI. Western blot, RT-PCR, and ELISA data showed the expression of NEU1 were increased in the non-infarct area of mouse hearts 8 weeks after MI (**Figures 1D–F**). In summary, these data suggested that NEU1 contributed to cardiac ischemic injury at the early stage, as well as chronic pathological after MI. Highly expressing NEU1 accumulate in the non-infarct heart during the chronic phase of MI, suggesting a potential role for NEU1 in regulating cardiac remodeling in an MI setting.

NEU1 Knockdown Improved Survival Rate and Cardiac Function in Mice Post-MI

Next, we hypothesized that the knockdown of NEU1 may exert functional effects on the chronic phase of post-MI. We used small hairpin RNA (shRNA) delivered by cardiotropic adeno-associated virus (AAV) 9 vectors to cardiac region-specific NEU1 knockdown mice. As shown in **Figure 2A**, AAV9-shNEU1#2 significantly inhibited NEU1 mRNA level in mice hearts compared with others. The efficiency of AAV9-shNEU1 is presented in **Figure 2B**. The specific inhibitory expression of NEU1 is achieved in the heart, not in other tissues (lung, liver, etc.) (**Supplementary Figure 1A**). To determine the functional role of NEU1 in MI tissue, mice were subjected to permanent LAD ligation for 4 weeks after AAV9 injection. At 0, 3, 28, and 56 days after MI, the ejection fraction (EF), fractional shortening (FS), end-systolic volume (ESV), and left ventricular diameter (LVIDs) of shNEU1 mice were significantly better than those of shRNA mice. Besides, LV chamber dilation was attenuated in shNEU1 mic 8 weeks post-MI, as demonstrated by a drastic decline in end diastolic volume (EDV), ESV, LV internal diameter at end diastole (LVIDd), and LVIDs (**Supplementary Figure 1B**, **Figure 2C**). Remarkably, knockdown of NEU1 in cardiac robustly improved post-MI survival (**Figure 2D**). Collectively, our data illustrate the beneficial effects of cardiac-specific NEU1 loss on MI.

NEU1 Knockdown Prevented Cardiac Hypertrophy and Fibrosis Post-MI

After MI, the infarcted myocardium increases the workload of the non-infarcted myocardium, leading to hypertrophy and fibrosis (35). WGA stained heart sections showed that NEU1 deficiency reduced the CSA of cardiomyocytes (**Figures 3A,C**). and significantly reduced the heart weight/body weight ratio (HW/BW) (**Figure 3B**) post-MI. PSR data showed that NEU1 deficiency mice significantly attenuated myocardial fibrosis caused by MI compared with mice injected with shRNA (**Figures 3A,D**). Compared with the MI+shRNA group, the hypertrophy genes (ANP, BNP, etc.) RNA level was significantly downregulated in the hearts of MI+shNEU1 group mice (**Figure 3E**). In addition, RT-PCR showed that NEU1 knockdown inhibited MI-induced increases in *Col1a1*, *Col3a1*, and *Ctgf* (**Figure 3F**). Collectively, the improvement in heart function in the MI + shNEU1 group of mice was consistent with alleviated cardiac remodeling as evidenced by suppression of cardiac hypertrophy and fibrosis in infarcted hearts.

NEU1 Knockdown Attenuated Mitochondrial Deficiencies and Enhanced SIRT1/PGC-1α Pathway Activation Post-MI

Mitochondrial dysfunction and structural changes that occur during ischemia are critically implicated in pathophysiology in the infarcted myocardium (36). We measured the respiratory chain enzyme activities. Under basic conditions, the mitochondrial respiratory chain complexes enzyme activities in the Sham group and shNEU1 group did not change significantly, while the enzyme activities of complexes I, III, and IV in the MI group were significantly reduced when compared with

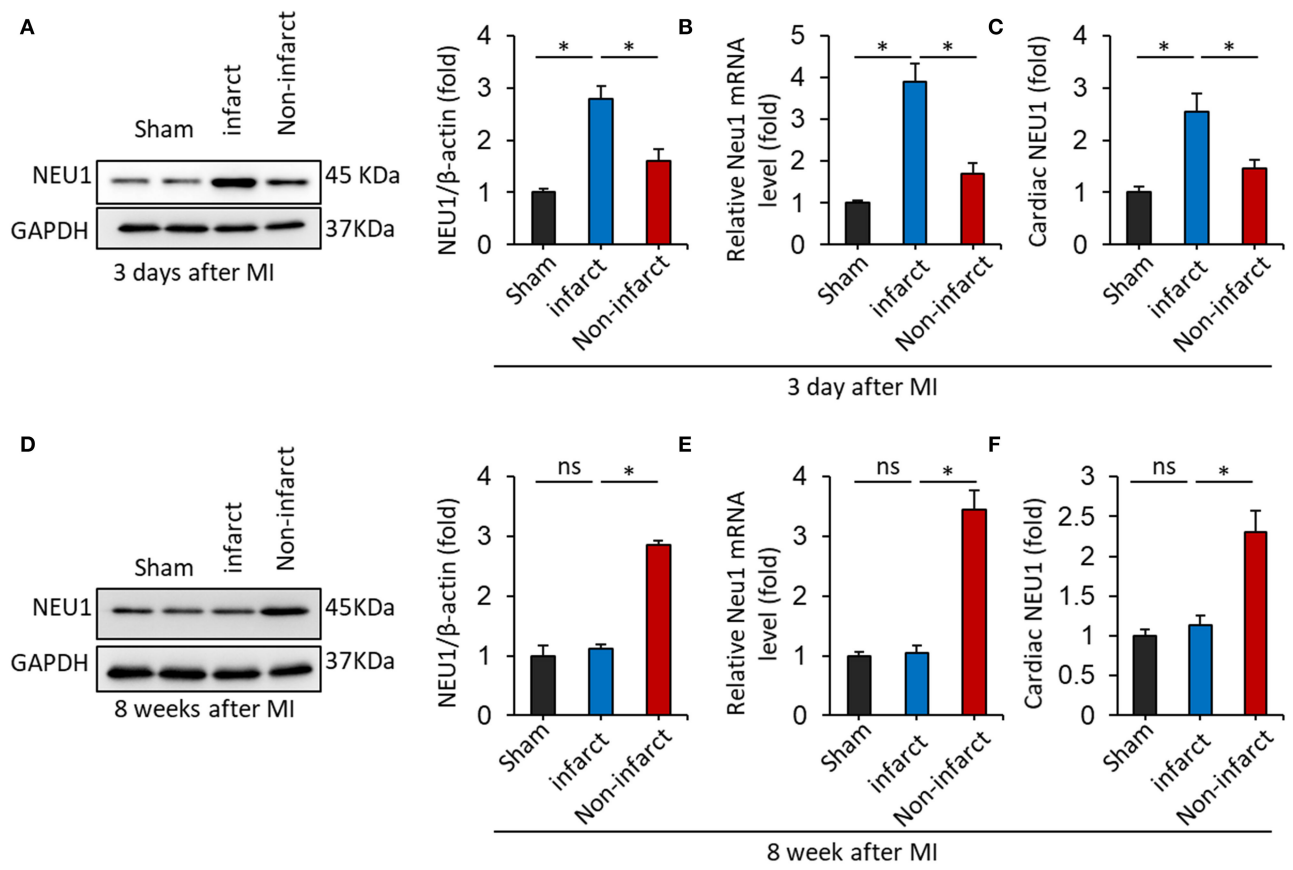

FIGURE 1 | NEU1 expression was increased in mice heart post-MI. **(A)** Immunoblot analysis of NEU1 protein ($n = 6$) in the mouse heart 3 days after LAD surgery. **(B)** RT-PCR analysis of NEU1 mRNA in the mouse heart 3 days after MI. **(C)** Cardiac NEU1 expression detected by ELISA ($n = 6$). **(D)** Immunoblot analysis of NEU1 protein ($n = 6$) in the mouse heart 28 days after LAD surgery. **(E)** RT-PCR analysis of NEU1 mRNA in the mouse heart 28 days after MI. **(F)** Cardiac NEU1 expression detected by ELISA ($n = 6$). $^*p < 0.05$ vs. corresponding group. n.s., non-significant.

the Sham group. Most importantly, the enzyme activity of complex II did not decrease significantly in the shNEU1-MI group because it is only encoded by nuclear DNA (**Figure 4A**). mtDNA copy number data showed that, the mtDNA:nDNA ratio in the MI group was reduced when compared with the Sham group, while the NEU1 knockdown increased the ratio (**Figure 4B**). ATP, as the most important energy molecule, plays an important role in various physiological and pathological processes of cardiomyocytes. The significant decrease in ATP levels of ischemic myocardium indicates impaired or decreased mitochondrial function, and is related to the irreversible changes in myocardial cells because the cells exhaust their energy storage and cannot sustain cellular vital activities (35). ATP content was significantly lower in 8 weeks post-MI mice hearts, and NEU1 knockdown significantly increased the ATP content in the context of MI (**Figure 4C**). Manganese superoxide dismutase (SOD2 or MnSOD) is a mitochondrial matrix antioxidant enzyme responsible for removing free radicals generated locally (37). The activity of MnSOD decreased in 8 weeks post-MI, while NUE1 inhibition can improve the decreased MnSOD activity induced by MI (**Figure 4D**). Mitochondria are responsible for the production of ATP, which can produce a small amount of ROS. Therefore, we determined the mitochondrial ROS production in mice hearts. NEU1 knockdown attenuated oxidative stress in mice hearts with MI surgery (**Figure 4E**).

Transcription factor A plays a vital role in the maintenance of mtDNA and thus, ATP production (38). SIRT1 and PGC-1α are key regulators involved in processes such as myocardial mitochondrial biogenesis and energy metabolism. Western blots showed that SIRT1, PGC-1α, and TFAM expression levels decreased after MI surgery for 8 weeks. Meanwhile, NEU1 knockdown increased cardiac expression of these proteins in MI mice (**Figures 4F,G**). The imbalance between mitochondrial division and fusion is closely related to the pathology of myocardial I/R injury (39). MFN2 and DRP1 are essential mitochondrial protein, which mediates mitochondrial functions. The expression of MFN2 decreased, and the expression of DRP1 increased in MI tissues, however, NEU1 knockdown reversed the above-mentioned protein changes (**Figures 4F,H**). In summary, these findings indicate that NEU1 inhibition alleviated ischemia-associated mitochondrial damage and exerted cardioprotective

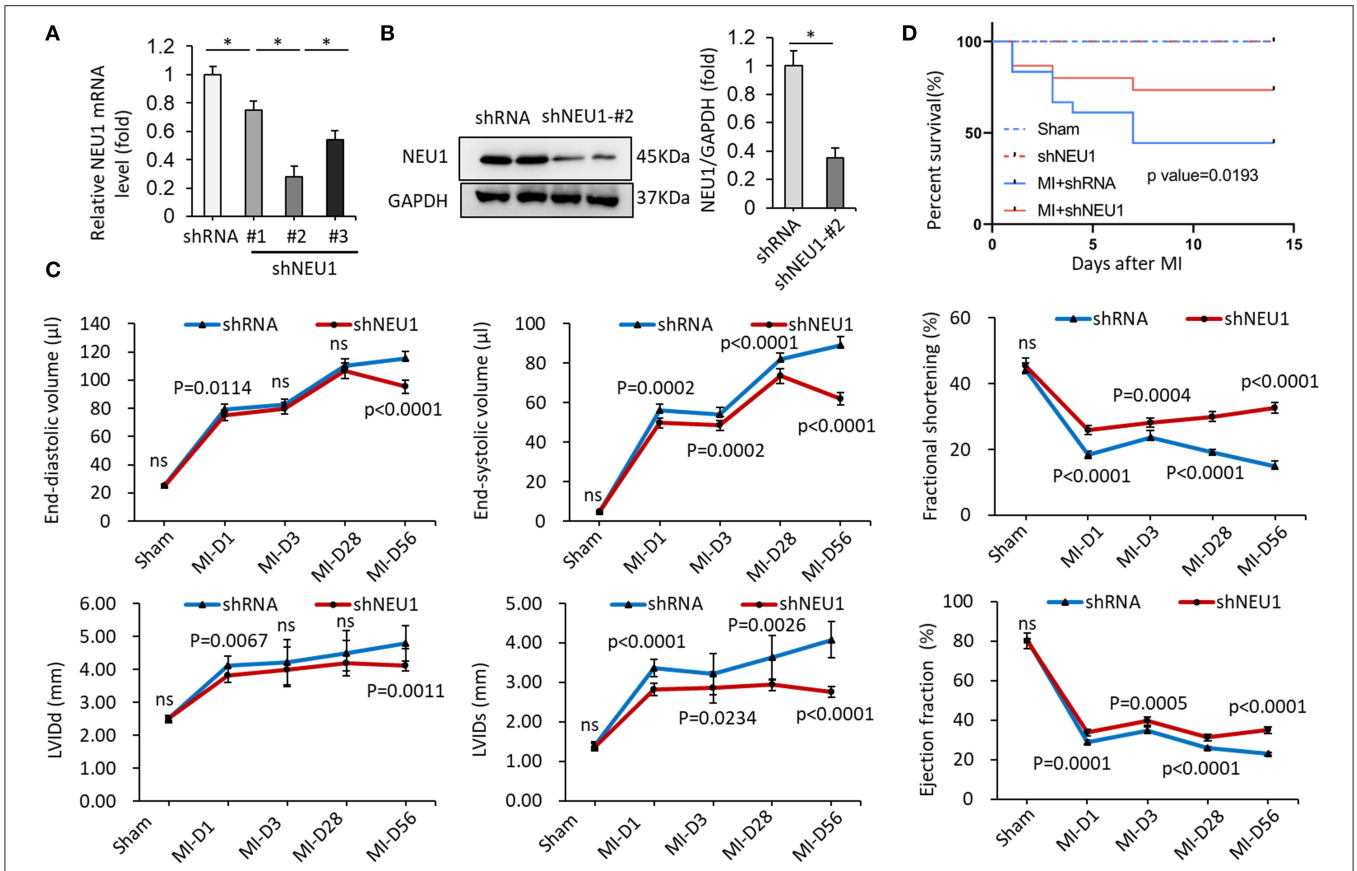

FIGURE 2 | NEU1 knockdown improved survival rates and cardiac function post-MI. **(A)** mRNA levels of NEU1 after AAV9-shRNA or AAV9-shNEU1 injection in mice heart ($n = 6$). **(B)** NEU1 protein expression and quantitative data ($n = 6$). **(C)** Echocardiographic measurements of left ventricular internal diameter at end-systole (LVIDs), left ventricular internal diameter at end-diastole (LVIDd), fractional shortening (FS), ejection fraction (EF), end-diastolic volume (EDV), and end-systolic volume (ESV) in shRNA and shNEU1 hearts after sham operation or 1, 3, 28 and 56 ($n = 12$ per group) days post-MI. **(D)** Kaplan–Meier survival analysis of mice after MI ($n = 12$). $^*p < 0.05$ vs. corresponding group. n.s., non-significant.

effects by enhancing the SIRT1/PGC-1α signaling pathway *in vivo*.

NEU1 Inhibition Attenuated Hopoxia-Induced Mitochondrial Deficiencies and Enhanced SIRT1/PGC-1α Pathway Activation *in vitro*

We transfected NRCMs with shRNA or shNEU1 and then cultured NRCMs in a hypoxia or normoxia environment. There are no significant changes in the enzymatic activity of complex I, II, III, and IV between normxia+shRNA group and normxia+shNEU1 group. Hypoxia treatment significantly decreased the enzymatic activities of complex I, III, and IV, while NEU1 inhibition blocked these enzyme activity changes. Consistent with results *in vivo*, the enzymatic activity of complex II was not altered in either group (**Figure 5A**). mtDNA copy number data showed that compared with the normxia+shRNA group, the mtDNA:nDNA ratio in the hypoxic+shRNA group decreased, while NEU1 knockdown increased the ratio (**Figure 5B**). ATP content and MnSOD activity were significantly decreased by administrated with hypoxia but increased with NEU1 inhibition (**Figures 5C,D**). The fluorescence intensity of the mitoSOX among groups proved that NEU1 knockdown attenuated oxidative stress in NRCMs with hypoxia treatment (**Figure 5E**).

Consistent with *in vivo* experiments, hypoxia treatment significantly decreased SIRT1, PGC-1α, and TFAM protein levels, but increased by adding of shNEU1 in H9C2 cells (**Figures 5F,G**). Hypoxia decreased the MFN2 level and increased the DRP1 level, however, NEU1 knockdown increased the MFN2 level and decreased the DRP1 level in H9C2 cells (**Figures 5F,H**).

SIRT1 or PGC-1α Inhibition Abolished ShNEU1-Mediated Mitochondrial Biogenesis and Function Improvement in Hypoxia-Administrated NRCMs or H9C2 Cells

Use SIRT1 inhibitor EX-527 to verify whether shNEU1-mediated mitochondrial metabolism and functional enhancement are mediated by SIRT1 activation. As shown in **Figures 6A,B**,

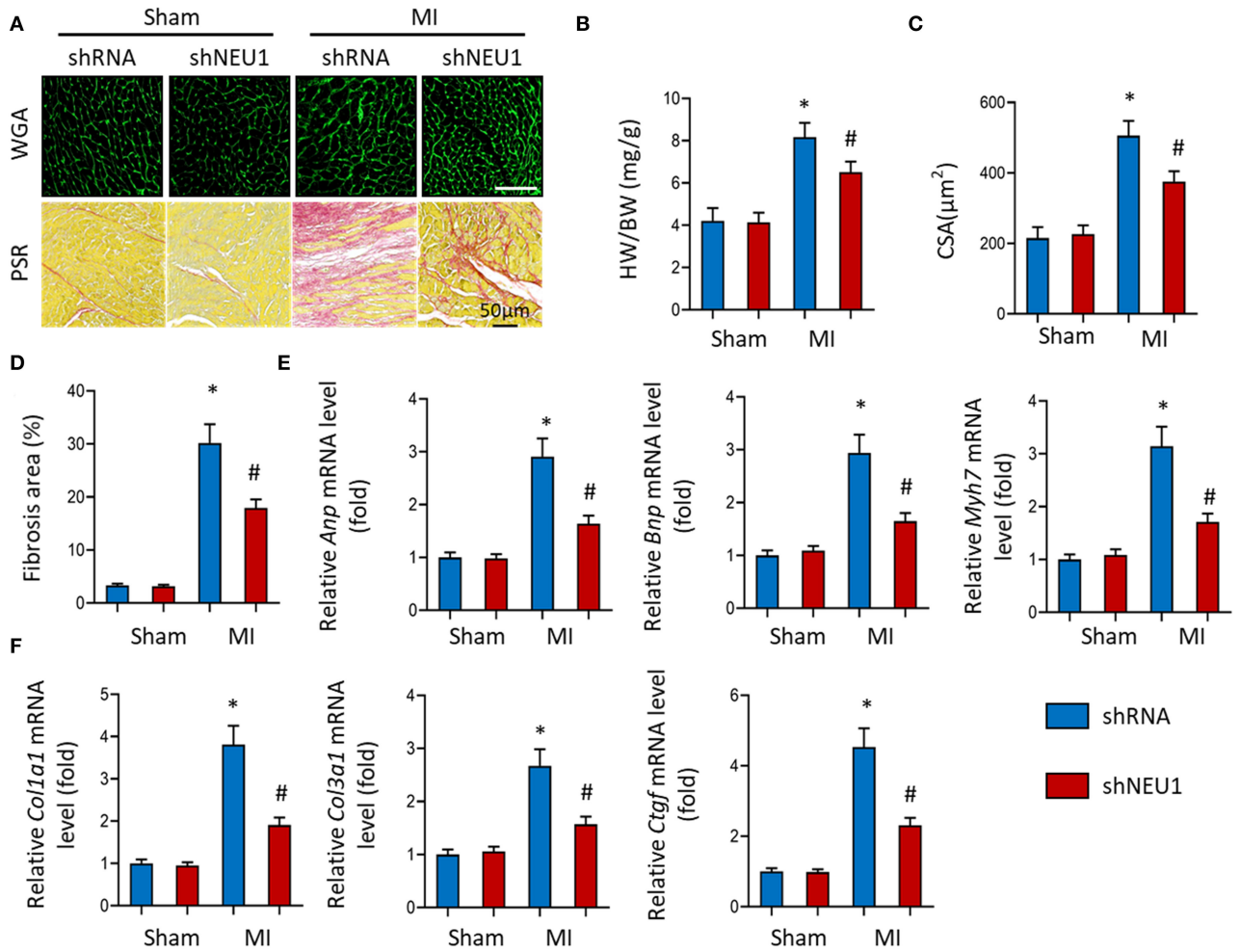

FIGURE 3 | NEU1 knockdown prevented cardiac hypertrophy and fibrosis post-MI. **(A)** WGA staining and PSR staining of shNEU1 and shRNA in mice hearts 8 weeks post MI or sham ($n = 12$). **(B)** Statistical results of heart weight/body weight (HW/BW, $n = 12$). **(C)** Statistical results for the cross-sectional areas of myocytes (CSA, $n = 100$ cells/sample, $n = 6$ per group). **(D)** Quantification of fibrotic areas in mice hearts 8 weeks post-MI. **(E,F)** RT-PCR analyses of fetal gene (*Anp*, *Bnp*, *Myh7*) and fibrotic markers (*Col1a1*, *Col3a1*, *Ctgf*) in each group ($n = 6$). *$p < 0.05$ vs. corresponding group. n.s., non-significant.

shNEU1 enhanced the SIRT1, PGC-1α, and TFAM protein levels in H9C2 cells cultured under a hypoxia environment. Meanwhile, EX527 eliminated the increase in these protein expressions induced by shNEU1. We next detected the mtDNA level, the content of ATP production, complex IV activity, and mitochondrial oxidative stress in NRCMs. We noted that NEU1 inhibition reversed the hypoxia-induced decrease in mtDNA level, ATP levels, complex IV activity, and MnSOD activity, whereas EX527 partly abrogated these effects (**Figures 6C–F**).

Next, to test whether that PGC-1α is a key regulator in shNEU1-mediated mitochondrial biogenesis and functional improvement, we examined the alterations in PGC-1α and TFAM through exposure to the PGC-1α inhibitor SR-18292. Similar to EX-527, the PGC-1α inhibitor abolished the shNEU1-induced increase in protein expressions in H9C2 cells (**Figures 7A,B**). We next detected the expression of mtDNA, the content of ATP production, complex IV activity, and mitochondrial oxidative stress in NRCMs. We noted that NEU1 inhibition reversed the hypoxia-induced decrease in mtDNA level, ATP levels, complex IV activity, and MnSOD activity, whereas SR-18292 partly abrogated these effects (**Figures 7C–F**). These results strongly suggest that shNEU1 relieves MI by activating SIRT1/PGC-1α and enhancing mitochondrial biogenesis, thereby improving cardiomyocyte mitochondrial function.

PGC1α Deficiency Offset the Cardio-Protective Effects of NEU1 Knockdown *in vivo*

To explore its mechanism more deeply, we further used PGC-1α-cKO mice to study the effects of PGC-1α on shNEU1-induced cardioprotection. Consistent with *in vitro* experimental data, we observed that NEU1 inhibition lost the protective effect in PGC-1α-cKO mice, as evidenced by the indistinguishable survival rate between the cKO+MI group and cKO+MI+shNEU1 group

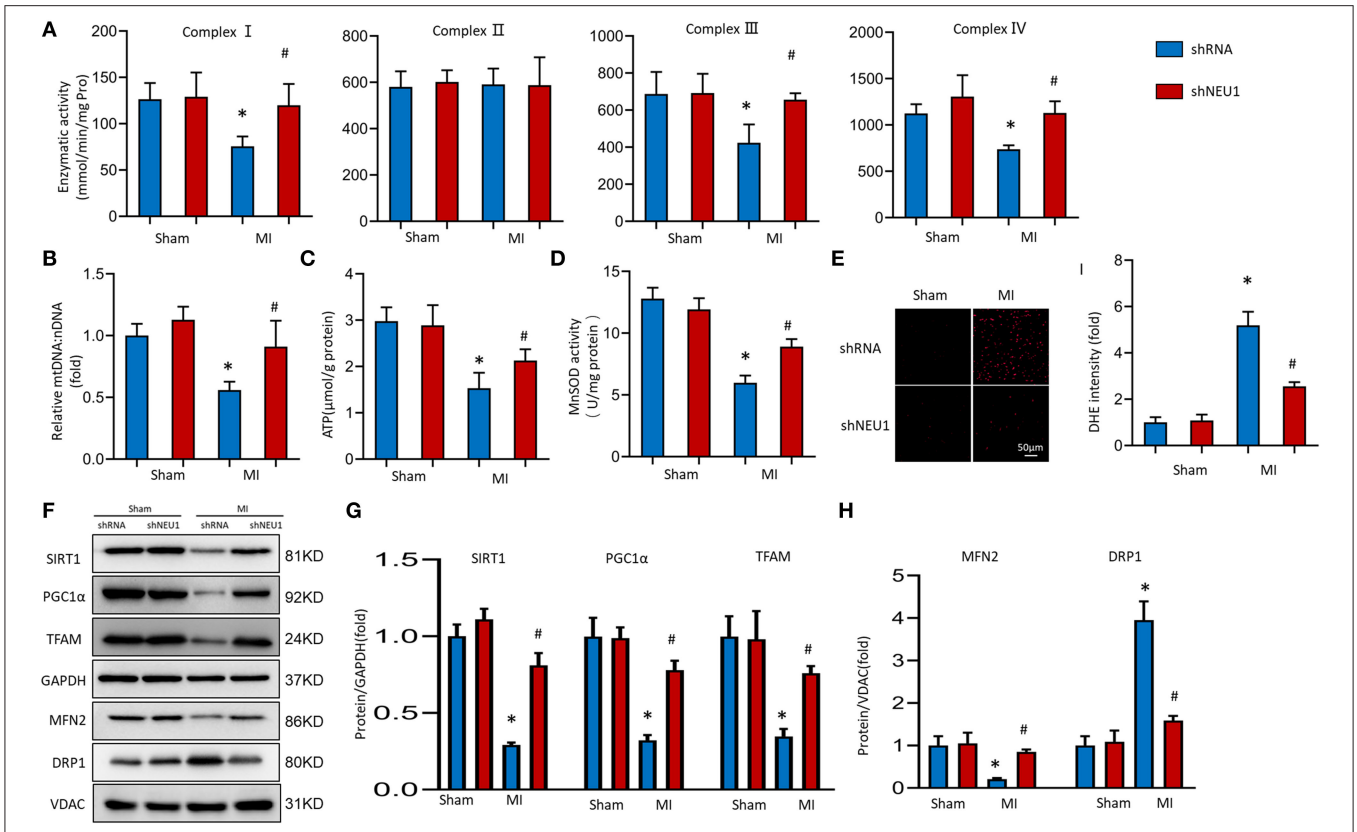

FIGURE 4 | NEU1 knockdown attenuated mitochondrial deficiencies and ROS accumulation post-MI. **(A)** Enzymatic activity of mitochondrial electron transport chain enzymes (I, II, III, and IV) in isolated mitochondria from four groups of mice ($n = 6$). **(B)** Relative mitochondrial DNA content (mtDNA: nDNA) of heart ($n = 6$). **(C)** ATP content of cardiomyocytes in fresh heart ($n = 6$). **(D)** Mitochondrial ROS is assessed by MnSOD activity of fresh heart ($n = 6$). **(E)** ROS production in myocardial detected by DHE in fresh heart tissues. **(F–H)** Western blot image and quantitative results of the SIRT1/PGC1α pathway, the MFN2, and DRP1 of each group *in vivo* ($n = 6$). *$p < 0.05$ vs. Sham+shRNA group, #$p < 0.05$ vs. MI+shRNA group.

(**Figure 8A**). Besides, WGA staining and HW/BW results showed that NEU1 knockdown does not counter myocardial hypertrophy induced by MI in PGC-1α-cKO mice (**Figures 8B–D**). PSR staining results showed that NEU1 inhibition cannot alleviate cardiac fibrosis in consistent with the findings *in vitro*, shNEU1 lost its protective effects on inflammatory response in cKO+MI+shNEU1 group mice (**Figures 8B,E**). Furthermore, the heart function (determined by FS, EF, and LVIDd), showed no significant differences between the cKO+MI group and the cKO+MI+shNEU1 group (**Figures 8F–H**). Collectively, these data indicated that PGC-1α ablation completely eliminated the cardioprotection of NEU1 knockdown.

DISCUSSION

In this study, we demonstrated a novel role for NEU1 in MI. We observed that NEU1 is significantly elevated in mice hearts post-MI. Cardiac region-specific NEU1 inhibition prevented the development of cardiac dysfunction and remodeling in chronic MI hearts, *via* improving mitochondrial energy metabolism and decreasing mitochondrial oxidative stress in myocardial tissue post-MI. Mechanistically, through *in vivo* and *in vitro* experiments, NEU1 knockdown ameliorated cardiomyocytes injury by regulating the SIRT1/PGC-1α signaling pathway, thereby enhancing the biogenesis and function of mitochondria. Together, these data reveal a previously unappreciated mechanism that governs mitochondrial energy metabolism switch and chronic MI-induced cardiac remodeling.

In our study, we found that NEU1 is dramatically elevated in the infarct area of acute ischemic cardiac injury, which is consistent with previous findings (34). However, the increased NEU1 in the infarct area was declined to the baseline during the chronic phase of MI. In the infarcted area, scar tissue was formed during chronic MI, with few viable cardiomyocytes, leading to NEU1 decreasing. While, for the chronic MI model, NEU1 expression was significantly increased in non-infarct areas of mice, suggesting a potential role of NEU1 in regulating MI-induced cardiac remodeling.

As a member of the neuraminidases family, NEU1 is known to participate in multiple cellular processes (26, 40–42) and inherited disease (43). Collectively, NEU1 is closely related to inflammation and promotes the occurrence and development of atherosclerosis and HF (44). In the human hypertrophic cardiomyopathy or rodent myocardial hypertrophy

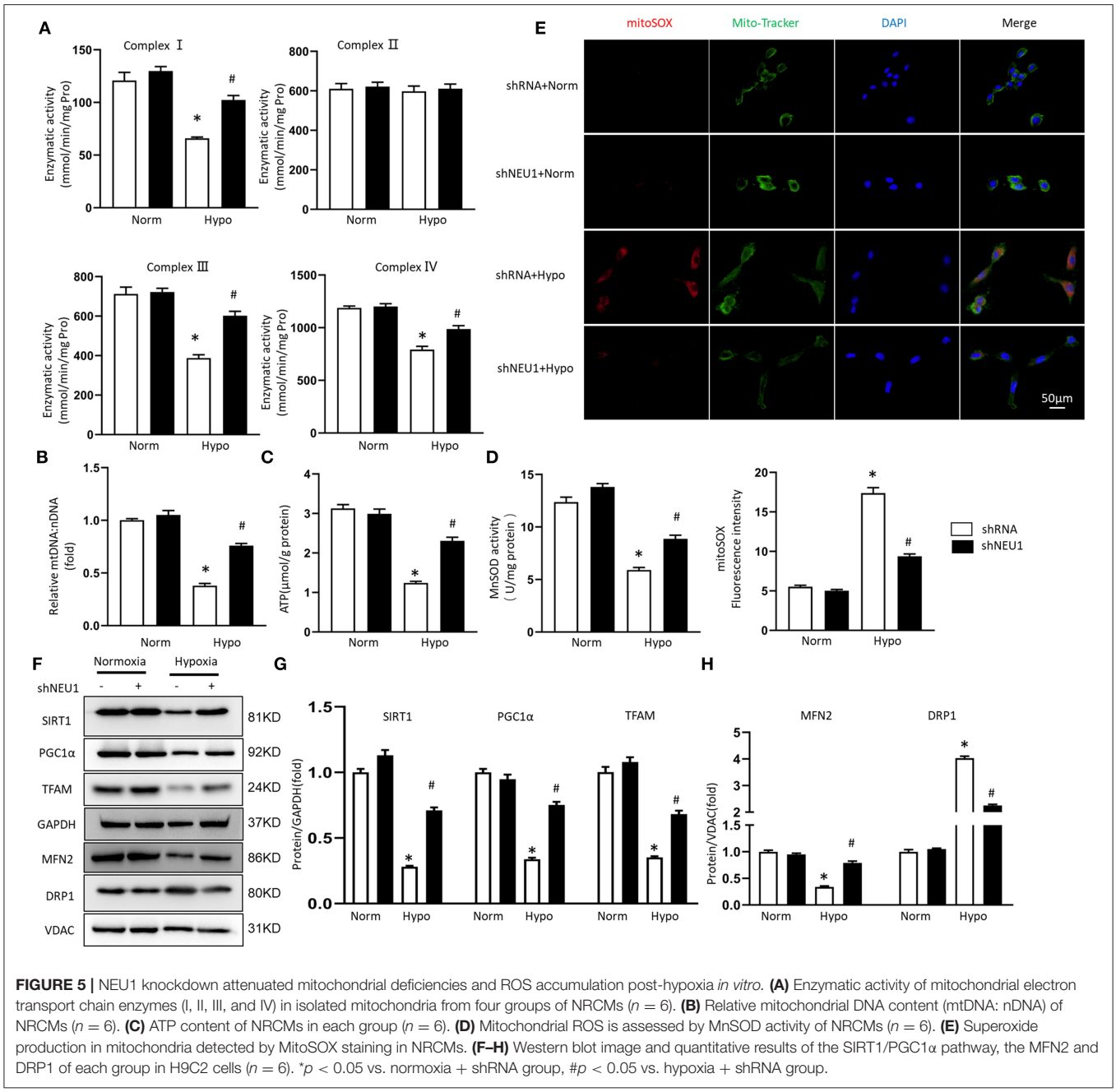

FIGURE 5 | NEU1 knockdown attenuated mitochondrial deficiencies and ROS accumulation post-hypoxia *in vitro*. **(A)** Enzymatic activity of mitochondrial electron transport chain enzymes (I, II, III, and IV) in isolated mitochondria from four groups of NRCMs ($n = 6$). **(B)** Relative mitochondrial DNA content (mtDNA: nDNA) of NRCMs ($n = 6$). **(C)** ATP content of NRCMs in each group ($n = 6$). **(D)** Mitochondrial ROS is assessed by MnSOD activity of NRCMs ($n = 6$). **(E)** Superoxide production in mitochondria detected by MitoSOX staining in NRCMs. **(F–H)** Western blot image and quantitative results of the SIRT1/PGC1α pathway, the MFN2 and DRP1 of each group in H9C2 cells ($n = 6$). *$p < 0.05$ vs. normoxia + shRNA group, #$p < 0.05$ vs. hypoxia + shRNA group.

model, NEU1 was significantly increased, and targeted inhibition of NEU1 expression effectively prevented the development of cardiac hypertrophy and remodeling (22). There was a similar article recently published mentioned that after the myocardium is exposed to I/R, the NEU1 protein level and activity in myocardial cells and infiltrating monocytes increase, and cause inflammation, hypertrophy, and HF. However, systemic inhibition of NEU1 can alleviates myocardial injury and dysfunction after I/R injury (20). Similar to this study, the expression of NEU1 is elevated in myocardial tissue of MI, and NEU1 knockdown can significantly improve cardiac dysfunction and myocardial remodeling. Importantly, the difference and novelty of our work are that, NEU1 knockdown is a protective effect produced by improving cardiac mitochondrial dysfunction and mitochondrial oxidative stress. While the previous research direction is that NEU1 promotes the increased level and duration of monocyte inflammation after reperfusion of an infarcted heart. In our hands, NEU1 level was increased in the ischemic heart while NEU1 inhibition preserved cardiac function and improved myocardial morphology post-MI.

More and more evidence showed that SIRT1 can induce nuclear localization and deacetylation to increase the

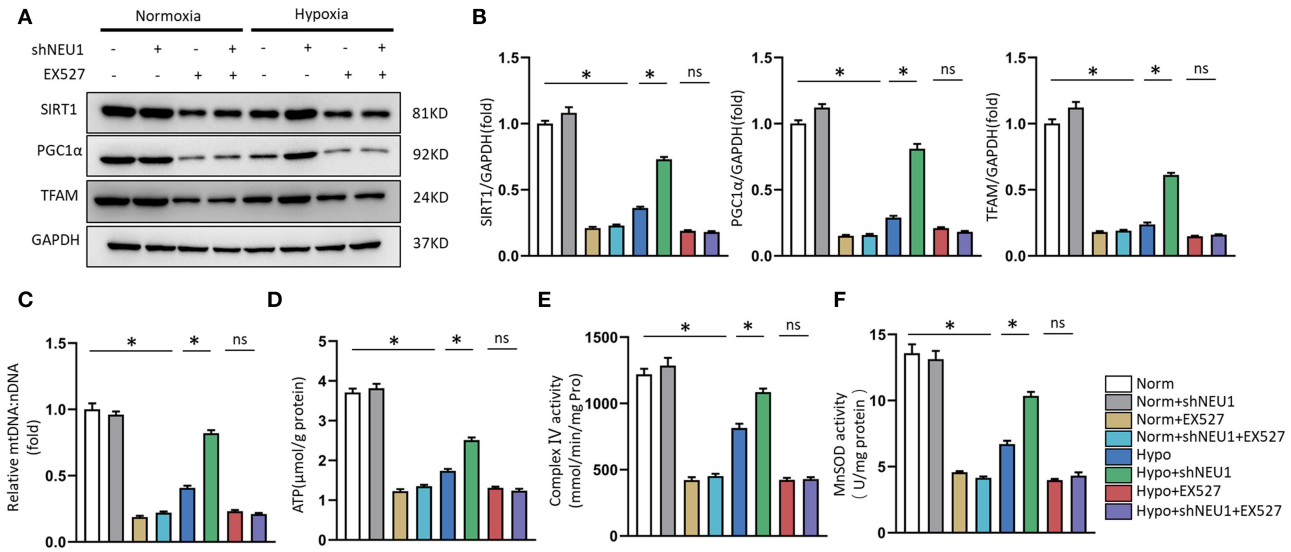

FIGURE 6 | SIRT1 inhibition abolished shNEU1-induced mitochondrial biogenesis and function improvement in hypoxia-administrated NRCMs or H9C2 cells. **(A,B)** Western blot image and quantitative results of SIRT1, PGC1α and TFAM of each group in H9C2 cells ($n = 6$). **(C)** Relative mitochondrial DNA content (mtDNA: nDNA) of NRCMs ($n = 6$). **(D)** ATP content of NRCMs ($n = 6$). **(E)** Enzymatic activity of mitochondrial complex IV in isolated mitochondria from four groups of NRCMs ($n = 6$). **(F)** Mitochondrial ROS is assessed by MnSOD activity of NRCMs ($n = 6$). *$p < 0.05$ vs. corresponding group, n.s., non-significant.

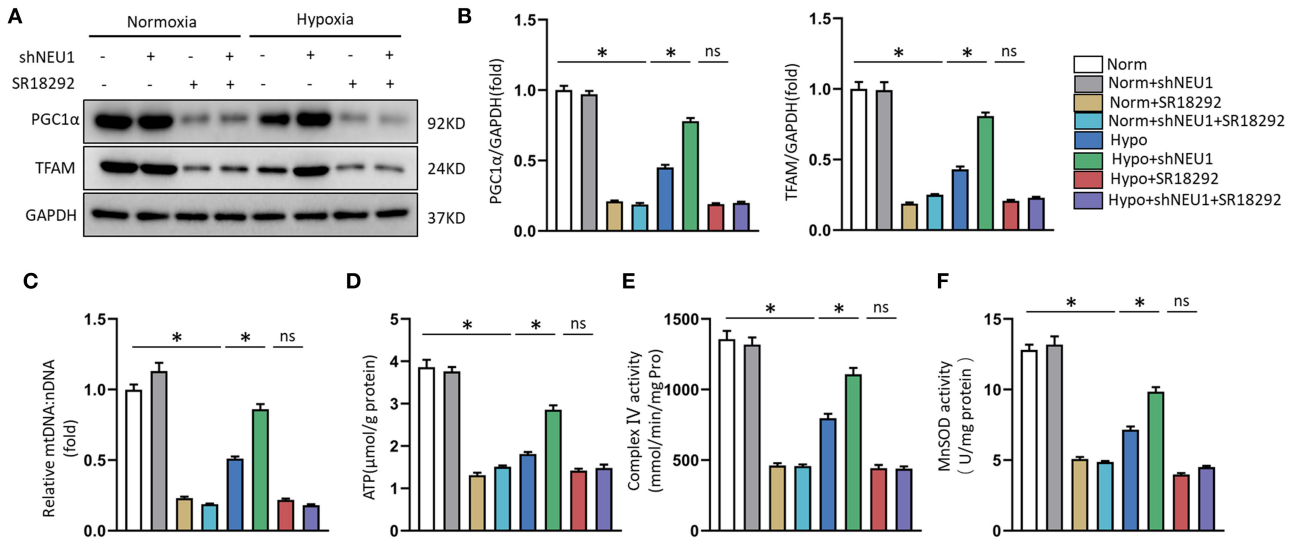

FIGURE 7 | PGC1α inhibition abolished shNEU1-induced mitochondrial biogenesis and function improvement in hypoxia-administrated NRCMs or H9C2 cells. **(A,B)** Western blot image and quantitative results of PGC1α and TFAM of each group in H9C2 cells ($n = 6$). **(C)** Relative mitochondrial DNA content (mtDNA: nDNA) of NRCMs ($n = 6$). **(D)** ATP content of NRCMs ($n = 6$). **(E)** Enzymatic activity of mitochondrial complex IV in isolated mitochondria from four groups of NRCMs ($n = 6$). **(F)** Mitochondrial ROS is assessed by MnSOD activity of NRCMs ($n = 6$). *$p < 0.05$ vs. corresponding group, n.s., non-significant.

transcriptional activity of PGC-1α, and has an important role in promoting the function and structure of mitochondria (45, 46), which is associated with improved metabolic regulation and antioxidant stress (47). PGC-1α is a key regulator of mitochondrial structure and function, which controls the expression of mitochondrial and nuclear-encoding mitochondrial genes, and regulates the transcription of TFAM (48). In fact, overexpression of SIRT1 and subsequent activation of PGC-1α protects against metabolic decline and cardiovascular disease (49, 50). In our work, we found that under MI or hypoxia conditions, the SIRT1, PGC-1α, and TFAM levels downregulated significantly. While NEU1 knockdown prevented the decline of SIRT1/PGC-1α signaling proteins in MI, or in hypoxia-treated H9C2 cells. Since the inhibition of SIRT1/PGC-1α axis protein

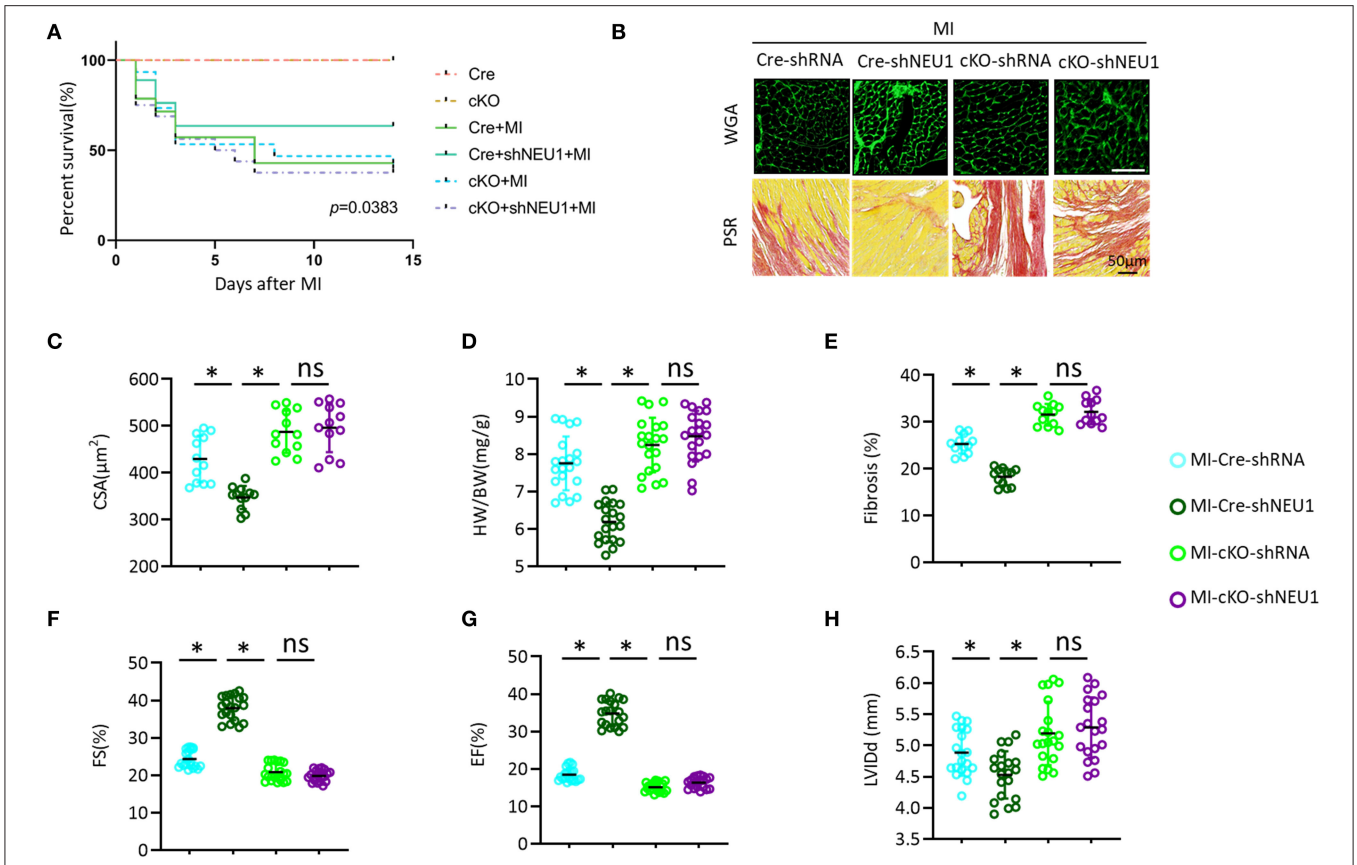

FIGURE 8 | PGC1α deficiency offset the protective effects of shNEU1 *in vivo*. **(A)** Kaplan–Meier survival analysis of each group in 2 weeks after MI ($n = 20$). **(B)** WGA staining and PSR staining of each group mice heart ($n = 12$). **(C)** Statistical results for the cross-sectional areas of myocytes (CSA, n =100 cells/sample, $n = 12$ per group). **(D)** Statistical results of HW/BW ($n = 20$). **(E)** Quantification of fibrotic areas in 8 weeks post-MI ($n = 12$). **(F)** FS of mice in 8 weeks post MI ($n = 20$). **(G)** EF of mice in 8 weeks after MI ($n = 20$). **(H)** LVIDd diameter ($n = 20$). *$P < 0.05$ vs. corresponding group; n.s., non-significant.

by NEU1 was eliminated by independent inhibition of SIRT1 activity (EX527) or PGC-1α expression (SR-18292). Our data show that there is a strong correlation between NEU1 and the mitochondrial biogenesis mediated by the SIRT1/PGC-1α pathway, and it has an important potential impact on myocardial remodeling during MI. Since the effects of NEU1 inhibition on SIRT1/PGC-1α axis protein are eliminated by independently inhibiting SIRT1 activity (EX527) or PGC-1α expression (with SR-18292), our data indicated that there is a strong association between SIRT1/PGC-1α pathway-mediated NEU1 and mitochondrial biogenesis, with important potential implications for HF post-MI.

A large number of reports have revealed the adverse effects of mitochondrial damage in the onset and progression of acute MI (51), which is well-related to our results. Previous studies have shown a close link between mtDNA damage and reduced mitochondrial electron transport complex enzyme activity (52). Because the maintenance of mtDNA is essential for mitochondrial protein expression, the reduction of mtDNA copy number can lead to mitochondrial dysfunction and loss. Evidence shows that mtDNA defects, mitochondrial structural changes and dysfunction promote the occurrence and progression of HF (53). PGC-1α acts on the upstream of TFAM and can increase mtDNA levels in cells and mice (54). Our study showed that the relative amounts of TFAM and mtDNA decreased significantly in the mouse heart failure model after MI, and clearly proved that NEU1 inhibition can limit the decline of mtDNA levels and keep it at a normal level in the heart tissue of MI mice. Consistent with the changes in mtDNA and transcription levels, the activity of complexes I, III, and IV is significantly reduced in the heart after MI because part of it is encoded by the mtDNA gene; while the complex II activity is not affected because it is entirely composed of nuclear DNA coding. Knockdown of NEU1 can significantly improve the adverse changes in the mitochondrial complexes I, III, and IV activity caused by MI or hypoxia. Transgene expression of PGC-1α or the use of peroxisome proliferator-activated receptor agonist benzoate to treat mitochondrial myopathy can promote mitochondrial biogenesis, improve respiration, and prolong lifespan (55). We found that inhibition of NEU1 maintained the ATP levels of cardiomyocytes in MI, and these beneficial outcomes were eliminated independently by EX527 or SR-18292.

The stability of the dynamic balance between mitochondrial fusion and division is very important to maintain the

biological function of mitochondria (56). MFN2 and DRP1 are important proteins regulating mitochondrial fusion and division (56, 57), and MFN2 can participate in cell proliferation and apoptosis and maintains mitochondrial DNA stability by regulating mitochondrial fusion and division and changing the morphology and function of mitochondria (58). Overexpression of DRP1 protein can promote mitochondrial division and damage the mitochondrial network structure. Inhibition of DRP1 promotes mitochondrial fusion, increases network structure, and repairs damaged mitochondria (59). In this study, the MFN2 protein level was decreased and the DRP1 protein level was increased in the pathological state, suggesting that MI-induced decreased release of the mitochondrial fusion protein and increased production of mitotic protein. While NEU1 knockdown blocks undesirable changes in mitochondrial fusion and division proteins, suggesting that NEU1 inhibition may prevent mitochondrial damage by promoting MFN2 expression and inhibiting DRP1 expression, inhibiting the occurrence of mitochondrial division.

This study has some limitations. First, NEU1 was elevated in MI mice hearts, while, we did not explore why and how NEU1 increased. Second, in our work, we mainly used AAV9-NEU1 to verify its effect, and did not use genetically engineered mice related to NEU1. Third, the study only investigated the inhibitory effect of NEU1 but did not study the role of overexpression of NEU1.

In summary, the evidence we provide shows that the expression of NEU1 in the myocardial tissue of MI mice is significantly upregulated, and the biogenesis and function of mitochondria are impaired. At the same time, the signal molecules in the SIRT1/PGC-1α pathway are downregulated. Through *in vivo* and *in vitro* experimental analysis, we proved that NEU1 inhibition promotes the biogenesis and function of mitochondria by enhancing the SIRT1/PGC-1α signaling pathway, thereby improving poor myocardial remodeling after MI. NEU1 inhibition opens up a whole new field of treatment after myocardial infarction. Existing NEU1 inhibitors (antiviral drugs such as zanamivir and oseltamivir) have good safety and pharmacokinetic properties and may be used to ameliorate mitochondrial metabolism and oxidative stress in myocardial infarction or heart failure.

DATA AVAILABILITY STATEMENT

The original contributions presented in the study are included in the article/**Supplementary Materials**, further inquiries can be directed to the corresponding author/s.

ETHICS STATEMENT

The animal study was reviewed and approved by the Animal Care and Use Committee of Renmin Hospital of Wuhan University (IACUC Issue No. WDRM20190803).

AUTHOR CONTRIBUTIONS

ZG, F-YL, and DF performed experiments and analyzed the data. ZG, DF, ZY, and Q-ZT designed experiments, supervised and conceptualized the study, and wrote and edited the manuscript. ZG and DF wrote and edited the manuscript. S-QM, PA, DY, and M-YW assisted with some experiments and discussed the results. ZG and F-YL conducted bioinformatics analysis. All authors contributed to the article and approved the submitted version.

FUNDING

The National Natural Science Foundation of China (81900219).

SUPPLEMENTARY MATERIAL

The Supplementary Material for this article can be found online at: https://www.frontiersin.org/articles/10.3389/fcvm.2022.821317/full#supplementary-material

REFERENCES

1. Benjamin EJ, Virani SS, Callaway CW, Chamberlain AM, Chang AR, Cheng S, et al. Heart disease and stroke statistics-2018 update: a report from the American Heart Association. *Circulation.* (2018) 137:e67–e492. doi: 10.1161/CIR.0000000000000573
2. Owens AT, Brozena SC, Jessup M. New management strategies in heart failure. *Circ Res.* (2016) 118:480–95. doi: 10.1161/CIRCRESAHA.115.306567
3. Braunwald E. The war against heart failure: the Lancet lecture. *Lancet.* (2015) 385:812–24. doi: 10.1016/S0140-6736(14)61889-4
4. Cohn WE, Timms DL, Frazier OH. Total artificial hearts: past, present, and future. *Nat Rev Cardiol.* (2015) 12:609–17. doi: 10.1038/nrcardio.2015.79
5. Yacoub M. Cardiac donation after circulatory death: a time to reflect. *Lancet.* (2015) 385:2554–6. doi: 10.1016/S0140-6736(15)60683-3
6. Del Re DP, Amgalan D, Linkermann A, Liu Q, Kitsis RN. Fundamental mechanisms of regulated cell death and implications for heart disease. *Physiol Rev.* (2019) 99:1765–817. doi: 10.1152/physrev.00022.2018
7. Davidson SM, Adameova A, Barile L, Cabrera-Fuentes HA, Lazou A, Pagliaro P, et al. Mitochondrial and mitochondrial-independent pathways of myocardial cell death during ischaemia and reperfusion injury. *J Cell Mol Med.* (2020) 24:3795–806. doi: 10.1111/jcmm.15127
8. Gibb AA, Hill BG. Metabolic coordination of physiological and pathological cardiac remodeling. *Circ Res.* (2018) 123:107–28. doi: 10.1161/CIRCRESAHA.118.312017
9. Siasos G, Tsigkou V, Kosmopoulos M, Theodosiadis D, Simantiris S, Tagkou NM, et al. Mitochondria and cardiovascular diseases-from pathophysiology to treatment. *Ann Transl Med.* (2018) 6:256. doi: 10.21037/atm.2018.06.21
10. Eltzschig HK, Eckle T. Ischemia and reperfusion–from mechanism to translation. *Nat Med.* (2011) 17:1391–401. doi: 10.1038/nm.2507
11. Newmeyer DD, Ferguson-Miller S. Mitochondria: releasing power for life and unleashing the machineries of death. *Cell.* (2003) 112:481–90. doi: 10.1016/S0092-8674(03)00116-8
12. Choi HI, Kim HJ, Park JS, Kim IJ, Bae EH, Ma SK, et al. PGC-1alpha attenuates hydrogen peroxide-induced apoptotic cell death by upregulating Nrf-2 *via* GSK3beta inactivation mediated by activated p38 in HK-2 Cells. *Sci Rep.* (2017) 7:4319. doi: 10.1038/s41598-017-04593-w
13. McDermott-Roe C, Ye J, Ahmed R, Sun XM, Serafin A, Ware J, et al. Endonuclease G is a novel determinant of cardiac hypertrophy and mitochondrial function. *Nature.* (2011) 478:114–8. doi: 10.1038/nature10490
14. Vina J, Gomez-Cabrera MC, Borras C, Froio T, Sanchis-Gomar F, Martinez-Bello VE, et al. Mitochondrial biogenesis in exercise and in ageing. *Adv Drug Deliv Rev.* (2009) 61:1369–74. doi: 10.1016/j.addr.2009.06.006

15. Gomes AP, Price NL, Ling AJ, Moslehi JJ, Montgomery MK, Rajman L, et al. Declining NAD(+) induces a pseudohypoxic state disrupting nuclear-mitochondrial communication during aging. *Cell.* (2013) 155:1624–38. doi: 10.1016/j.cell.2013.11.037
16. Gerhart-Hines Z, Rodgers JT, Bare O, Lerin C, Kim SH, Mostoslavsky R, et al. Metabolic control of muscle mitochondrial function and fatty acid oxidation through SIRT1/PGC-1alpha. *EMBO J.* (2007) 26:1913–23. doi: 10.1038/sj.emboj.7601633
17. Yuan Y, Cruzat VF, Newsholme P, Cheng J, Chen Y, Lu Y, Regulation of SIRT1 in aging: Roles in mitochondrial function and biogenesis. *Mech Ageing Dev.* (2016) 155:10–21. doi: 10.1016/j.mad.2016.02.003
18. Miyagi T, Yamaguchi K. Mammalian sialidases: physiological and pathological roles in cellular functions. *Glycobiology.* (2012) 22:880–96. doi: 10.1093/glycob/cws057
19. Quach ME, Chen W, Li R. Mechanisms of platelet clearance and translation to improve platelet storage. *Blood.* (2018) 131:1512–21. doi: 10.1182/blood-2017-08-743229
20. Heimerl M, Sieve I, Ricke-Hoch M, Erschow S, Battmer K, Scherr M, et al. Neuraminidase-1 promotes heart failure after ischemia/reperfusion injury by affecting cardiomyocytes and invading monocytes/macrophages. *Basic Res Cardiol.* (2020) 115:62. doi: 10.1007/s00395-020-00821-z
21. Hanson VA, Shettigar UR, Loungani RR, Nadijcka MD. Plasma sialidase activity in acute myocardial infarction. *Am Heart J.* (1987) 114:59–63. doi: 10.1016/0002-8703(87)90307-3
22. Chen QQ, Ma G, Liu JF, Cai YY, Zhang JY, Wei TT, et al. Neuraminidase 1 is a driver of experimental cardiac hypertrophy. *Eur Heart J.* (2021) 42:3770–82. doi: 10.1093/eurheartj/ehab347
23. Gao E, Lei YH, Shang X, Huang ZM, Zuo L, Boucher M, et al. A novel and efficient model of coronary artery ligation and myocardial infarction in the mouse. *Circ Res.* (2010) 107:1445–53. doi: 10.1161/CIRCRESAHA.110.223925
24. Yan W, Lin C, Guo Y, Chen Y, Du Y, Lau WB, et al. N-Cadherin overexpression mobilizes the protective effects of mesenchymal stromal cells against ischemic heart injury through a beta-catenin-dependent manner. *Circ Res.* (2020) 126:857–74. doi: 10.1161/CIRCRESAHA.119.315806
25. Ma SQ, Guo Z, Liu FY, Hasan SG, Yang D, Tang N, et al. 6-Gingerol protects against cardiac remodeling by inhibiting the p38 mitogen-activated protein kinase pathway. *Acta Pharmacol Sin.* (2021) 42:1575–86. doi: 10.1038/s41401-020-00587-z
26. Marcu R, Neeley CK, Karamanlidis G, Hawkins BJ, Multi-parameter measurement of the permeability transition pore opening in isolated mouse heart mitochondria. *J Vis Exp.* (2012) 67. doi: 10.3791/4131
27. Kramer KA, Oglesbee D, Hartman SJ, Huey J, Anderson B, Magera MJ, et al. Automated spectrophotometric analysis of mitochondrial respiratory chain complex enzyme activities in cultured skin fibroblasts. *Clin Chem.* (2005) 51:2110–6. doi: 10.1373/clinchem.2005.050146
28. Miro O, Barrientos A, Alonso JR, Casademont J, Jarreta D, Urbano-Marquez A, et al. Effects of general anaesthetic procedures on mitochondrial function of human skeletal muscle. *Eur J Clin Pharmacol.* (1999) 55:35–41. doi: 10.1007/s002280050589
29. Krahenbuhl S, Talos C, Wiesmann U, Hoppel CL. Development and evaluation of a spectrophotometric assay for complex III in isolated mitochondria, tissues and fibroblasts from rats and humans. *Clin Chim Acta.* (1994) 230:177–87. doi: 10.1016/0009-8981(94)90270-4
30. Veitch K, Hue L. Flunarizine and cinnarizine inhibit mitochondrial complexes I and II: possible implication for parkinsonism. *Mol Pharmacol.* (1994) 45:158–63.
31. Guo Z, Tang N, Liu FY, Yang Z, Ma SQ, An P, et al. TLR9 deficiency alleviates doxorubicin-induced cardiotoxicity *via* the regulation of autophagy. *J Cell Mol Med.* (2020) 24:10913–23. doi: 10.1111/jcmm.15719
32. Wang J, Li S, Wang J, Wu F, Chen Y, Zhang H, et al. Spermidine alleviates cardiac aging by improving mitochondrial biogenesis and function. *Aging.* (2020) 12:650–71. doi: 10.18632/aging.102647
33. Li Y, Feng YF, Liu XT, Li YC, Zhu HM, Sun MR, et al., Songorine promotes cardiac mitochondrial biogenesis *via* Nrf2 induction during sepsis. *Redox Biol.* (2021) 38:101771. doi: 10.1016/j.redox.2020.101771
34. Zhang L, Wei TT Li Y, Li J, Fan Y, Huang FQ, et al. Functional metabolomics characterizes a key role for n-acetylneuraminic acid in coronary artery diseases. *Circulation.* (2018) 137:1374–90. doi: 10.1161/CIRCULATIONAHA.117.031139
35. Frangogiannis NG. Pathophysiology of Myocardial Infarction. *Compr Physiol.* (2015) 5:1841–75. doi: 10.1002/cphy.c150006
36. Ong SB, Gustafsson AB. New roles for mitochondria in cell death in the reperfused myocardium. *Cardiovasc Res.* (2012) 94:190–6. doi: 10.1093/cvr/cvr312
37. Fukai T, Ushio-Fukai M. Superoxide dismutases: role in redox signaling, vascular function, and diseases. *Antioxid Redox Signal.* (2011) 15:1583–606. doi: 10.1089/ars.2011.3999
38. Kang D, Kim SH, Hamasaki N. Mitochondrial transcription factor A (TFAM): roles in maintenance of mtDNA and cellular functions. *Mitochondrion.* (2007) 7:39–44. doi: 10.1016/j.mito.2006.11.017
39. Maneechote C, Palee S, Chattipakorn SC, Chattipakorn N. Roles of mitochondrial dynamics modulators in cardiac ischaemia/reperfusion injury. *J Cell Mol Med.* (2017) 21:2643–53. doi: 10.1111/jcmm.13330
40. Amith SR, Jayanth P, Franchuk S, Finlay T, Seyrantepe V, Beyaert R, et al. NEU1 desialylation of sialyl alpha-2,3-linked beta-galactosyl residues of TOLL-like receptor 4 is essential for receptor activation and cellular signaling. *Cell Signal.* (2010) 22:314–24. doi: 10.1016/j.cellsig.2009.09.038
41. Hinek A, Bodnaruk TD, Bunda S, Wang Y, Liu K. Neuraminidase-1, a subunit of the cell surface elastin receptor, desialylates and functionally inactivates adjacent receptors interacting with the mitogenic growth factors PDGF-BB and IGF-2. *Am J Pathol.* (2008) 173:1042–56. doi: 10.2353/ajpath.2008.071081
42. Dridi L, Seyrantepe V, Fougerat A, Pan X, Bonneil E, Thibault P, et al. Positive regulation of insulin signaling by neuraminidase 1. *Diabetes.* (2013) 62:2338–46. doi: 10.2337/db12-1825
43. Franceschetti S, Canafoglia L. Sialidoses. *Epileptic Disord.* (2016) 18:89–93. doi: 10.1684/epd.2016.0845
44. Yang A, Gyulay G, Mitchell M, White E, Trigatti BL, Igdoura SA. Hypomorphic sialidase expression decreases serum cholesterol by downregulation of VLDL production in mice. *J Lipid Res.* (2012) 53:2573–85. doi: 10.1194/jlr.M027300
45. Little JP, Safdar A, Cermak N, Tarnopolsky MA, Gibala MJ. Acute endurance exercise increases the nuclear abundance of PGC-1alpha in trained human skeletal muscle. *Am J Physiol Regul Integr Comp Physiol.* (2010) 298:R912–7. doi: 10.1152/ajpregu.00409.2009
46. Rodgers JT, Lerin C, Haas W, Gygi SP, Spiegelman BM, Puigserver P. Nutrient control of glucose homeostasis through a complex of PGC-1alpha and SIRT1. *Nature.* (2005) 434:113–8. doi: 10.1038/nature03354
47. Bordone L, Guarente L. Calorie restriction, SIRT1 and metabolism: understanding longevity. *Nat Rev Mol Cell Biol.* (2005) 6:298–305. doi: 10.1038/nrm1616
48. Fernandez-Marcos PJ, Auwerx J, Regulation of PGC-1alpha, a nodal regulator of mitochondrial biogenesis. *Am J Clin Nutr.* (2011) 93:884S−90. doi: 10.3945/ajcn.110.001917
49. Planavila A, Dominguez E, Navarro M, Vinciguerra M, Iglesias R, Giralt M, et al. Dilated cardiomyopathy and mitochondrial dysfunction in Sirt1-deficient mice: a role for Sirt1-Mef2 in adult heart. *J Mol Cell Cardiol.* (2012) 53:521–31. doi: 10.1016/j.yjmcc.2012.07.019
50. Yang Y, Duan W, Li Y, Jin Z, Yan J, Yu S, et al. Novel role of silent information regulator 1 in myocardial ischemia. *Circulation.* (2013) 128:2232–40. doi: 10.1161/CIRCULATIONAHA.113.002480
51. Boengler K, Lochnit G, Schulz R. Mitochondria "THE" target of myocardial conditioning. *Am J Physiol Heart Circ Physiol.* (2018) 315:H1215–31. doi: 10.1152/ajpheart.00124.2018
52. Wallace DC. Mitochondrial diseases in man and mouse. *Science.* (1999) 283:1482–8. doi: 10.1126/science.283.5407.1482
53. Ide T, Tsutsui H, Hayashidani S, Kang D, Suematsu N, Nakamura K, et al. Mitochondrial DNA damage and dysfunction associated with oxidative stress in failing hearts after myocardial infarction. *Circ Res.* (2001) 88:529–35. doi: 10.1161/01.RES.88.5.529
54. Lin J, Wu H, Tarr PT, Zhang CY, Wu Z, Boss O, et al. Transcriptional co-activator PGC-1 alpha drives the formation of slow-twitch muscle fibres. *Nature.* (2002) 418:797–801. doi: 10.1038/nature00904
55. Wenz T, Diaz F, Spiegelman BM, Moraes CT. Activation of the PPAR/PGC-1alpha pathway prevents a bioenergetic deficit and effectively

improves a mitochondrial myopathy phenotype. *Cell Metab.* (2008) 8:249–56. doi: 10.1016/j.cmet.2008.07.006
56. Atkins K, Dasgupta A, Chen KH, Mewburn J, Archer SL. The role of Drp1 adaptor proteins MiD49 and MiD51in mitochondrial fission: implications for human disease. *Clin Sci.* (2016) 130:1861–74. doi: 10.1042/CS20160030
57. Thaher O, Wolf C, Dey PN, Pouya A, Wüllner V, Tenzer S, et al., The thiol switch C684 in Mitofusin-2 mediates redox-induced alterations of mitochondrial shape and respiration. *Neurochem Int.* (2017) 117:167–73. doi: 10.1016/j.neuint.2017.05.009
58. Givvimani S, Pushpakumar S, Veeranki S, Tyagi SC. Dysregulation of Mfn2 and Drp-1 proteins in heart failure. *Can J Physiol Pharmacol.* (2014) 92:583–91. doi: 10.1139/cjpp-2014-0060
59. Li Y, Wang P, Wei J, Fan R, Zuo Y, Shi M, et al., Inhibition of Drp1 by Mdivi-1 attenuates cerebral ischemic injury *via* inhibition of the mitochondria-dependent apoptotic pathway after cardiac arrest. *Neuroscience.* (2015) 311:67–74. doi: 10.1016/j.neuroscience.2015.10.020

Conflict of Interest: The authors declare that the research was conducted in the absence of any commercial or financial relationships that could be construed as a potential conflict of interest.

Publisher's Note: All claims expressed in this article are solely those of the authors and do not necessarily represent those of their affiliated organizations, or those of the publisher, the editors and the reviewers. Any product that may be evaluated in this article, or claim that may be made by its manufacturer, is not guaranteed or endorsed by the publisher.

Copyright © 2022 Guo, Fan, Liu, Ma, An, Yang, Wang, Yang and Tang. This is an open-access article distributed under the terms of the Creative Commons Attribution License (CC BY). The use, distribution or reproduction in other forums is permitted, provided the original author(s) and the copyright owner(s) are credited and that the original publication in this journal is cited, in accordance with accepted academic practice. No use, distribution or reproduction is permitted which does not comply with these terms.

Advantages of publishing in Frontiers

OPEN ACCESS
Articles are free to read for greatest visibility and readership

FAST PUBLICATION
Around 90 days from submission to decision

HIGH QUALITY PEER-REVIEW
Rigorous, collaborative, and constructive peer-review

TRANSPARENT PEER-REVIEW
Editors and reviewers acknowledged by name on published articles

Frontiers
Avenue du Tribunal-Fédéral 34
1005 Lausanne | Switzerland

Visit us: www.frontiersin.org
Contact us: frontiersin.org/about/contact

REPRODUCIBILITY OF RESEARCH
Support open data and methods to enhance research reproducibility

DIGITAL PUBLISHING
Articles designed for optimal readership across devices

FOLLOW US
@frontiersin

IMPACT METRICS
Advanced article metrics track visibility across digital media

EXTENSIVE PROMOTION
Marketing and promotion of impactful research

LOOP RESEARCH NETWORK
Our network increases your article's readership